CHAPTER 3

DESIGN OF STRUCTURES COMPONENTS, EQUIPMENT, AND SYSTEMS

INTENTIONALLY BLANK

CONTENTS

ACRONYMS/ABBREVIATIONS 3-8

3. DESIGN OF STRUCTURES, COMPONENTS, EQUIPMENT, AND SYSTEMS 3-11

3.1 General Design Criteria for ATR 3-11

3.1.1 Overall Requirements 3-12
3.1.2 Protection by Multiple Fission Product Barriers 3-17
3.1.3 Protection and Reactivity Control Systems 3-24
3.1.4 Fluid Systems 3-31
3.1.5 Reactor Confinement 3-38
3.1.6 Fuel and Radioactivity Control 3-43
3.1.7 New Criteria for ATR 3-45

3.2 Classification of Structures, Components, and Systems 3-49

3.2.1 Seismic Classification 3-50
3.2.2 System Quality Group Classification 3-51

3.3 Wind and Tornado Loadings 3-53

3.3.1 Wind Loadings 3-53
3.3.2 Tornado Loadings 3-54

3.4 Water Level (Flood) Design 3-56

3.4.1 Flood Protection 3-56
3.4.2 Analytical and Test Procedures 3-57

3.5 Missile Protection 3-58

3.5.1 Missile Selection and Description 3-58
3.5.2 Structures, Systems, and Components to be Protected from Externally Generated Missiles 3-61
3.5.3 Barrier-Design Procedures 3-61

3.6 Protection Against Dynamic Effects Associated with the Postulated Rupture of Piping 3-64

3.6.1 Plant Design for Protection Against Postulated Piping Failures in Fluid Systems Outside Confinement 3-64
3.6.2 Determination of Rupture Locations and Dynamic Effects Associated with the Postulated Rupture of Piping 3-64

3.7 Seismic Design 3-66

3.7.1 Seismic Design Parameters 3-67
3.7.2 Seismic System Analysis 3-69

3.7.3 Seismic Subsystem Analysis 3-75
3.7.4 Seismic Instrumentation 3-79

3.8 Design of Seismic Category I Structures 3-94

3.8.1 Reactor Building 3-94
3.8.2 Internal Structures 3-102
3.8.3 Other Seismic Category I Structures 3-102
3.8.4 Foundations of Seismic Category I Structures 3-107

3.9 Mechanical Systems and Components 3-123

3.9.1 Special Topics for Mechanical Components 3-123
3.9.2 Dynamic Testing and Analysis 3-125
3.9.3 ASME Code Class 1, 2, and 3 Components, Component Supports, and Core Support Structures 3-127
3.9.4 Reactivity-Control Systems (Control Element Drive Systems) 3-130
3.9.5 Reactor Internals 3-137
3.9.6 Inservice Testing and Pumps and Valves 3-141

3.10 Seismic Qualification of Seismic Category I Instrumentation and Electrical Equipment 3-173

3.10.1 Seismic Qualification Criteria 3-174
3.10.2 Methods and Procedures for Qualifying Electrical Equipment and Instrumentation 3-174
3.10.3 Methods and Procedures of Analysis or Testing of Supports of Electrical Equipment and Instrumentation 3-175
3.10.4 Operating License Review 3-175

3.11 Environmental Design of Mechanical and Electrical Equipment 3-181

3.11.1 Equipment Identification and Environmental Conditions 3-181
3.11.2 Qualification Tests and Analyses 3-183
3.11.3 Loss of Ventilation 3-184
3.11.4 Estimated Chemical and Radiation Environment 3-184

3.12 Effects of Volcanism upon Structures 3-187

3.13 References 3-188

FIGURES

3.2-1. Methodology of ATR safety-related systems. 3-52
3.7-1. Safe Shutdown Earthquake design spectra from Gorman. 3-87
3.7-2. Safe Shutdown Earthquake horizontal design response spectra. 3-88
3.7-3. Safe Shutdown Earthquake vertical design response spectra. 3-89
3.7-4. Alternate damping values for response spectra analysis of Class 1, 2, and 3 piping. 3-90
3.7-5. Cross sections through the Advanced Test Reactor area. 3-91
3.7-6. Map showing the locations of borings prior to construction for the Advanced Test Reactor area. 3-92
3.7-7. Shear moduli versus depth at ETR. 3-93
3.7-8. Shear moduli and damping ratios versus shear strain for sand and gravel. 3-93
3.8-1. Reactor Building elevations, east and south. 3-110
3.8-2. Reactor Building elevations, west and north. 3-111
3.8-3. Confinement area, Section A-A. 3-112
3.8-4. Confinement area, Section B-B. 3-113
3.8-5. Confinement area, Section C-C. 3-114
3.8-6. Confinement area, Section D-D. 3-115
3.8-7. Confinement area, first-floor plan. 3-116
3.8-8. Confinement area, mezzanine plan. 3-117
3.8-9. Confinement area, first-basement plan. 3-118
3.8-10. Confinement area, second-basement plan. 3-119
3.8-11. Confinement area, miscellaneous plans. 3-120
3.8-12. Confinement area, penetration details. 3-121
3.8-13. Confinement area, wall sections. 3-122
3.9-1. Reactivity-control elements within the reactor core. 3-157
3.9-2. Vertical control element drive arrangement. 3-158
3.9-3. Safety-rod assembly. 3-159
3.9-4. Location of safety-rod control drive assemblies. 3-160
3.9-5. Safety-rod drive mechanism. 3-161
3.9-6. Outer shim control cylinder assembly. 3-162
3.9-7. Outer shim control cylinder drive. 3-163
3.9-8. Neck shim and regulating rod drives. 3-164

3.9-9. Vertical reactor internals arrangement. 3-165

3.9-10. Horizontal reactor internals arrangement. 3-166

3.9-11. Reactor vessel coolant flow. 3-167

3.9-12. ATR core internal support structure 3-168

3.9-13. Outlet-flow pipes. 3-169

3.9-14. Neck shim rod housing assembly. 3-170

3.9-15. Center flux trap baffle and N-16 assembly 3-171

3.9-16. Capsule-irradiation tanks arrangement 3-172

TABLES

3.1-1. Comparison of ATR and PWR characteristics 3-47

3.1-2. Piping design and safety limit pressures and temperatures at specific locations 3-47

3.1-3. ATR multiple means of decay heat removal 3-48

3.2-1. ATR systems containing Seismic Category I components and structural elements 3-51

3.3-1. Design wind-pressures requirement 3-55

3.3-2. Wind capacities of ATR structures 3-55

3.3-3. Wind hazard evaluation/probabilities of wind hazards 3-55

3.5-1. Missiles considered in evaluating the ATR building and steel water-storage tank 3-61

3.5-2. Characteristics of airway travel within 20 mi of ATR 3-61

3.5-3. Vortex test flight frequency history 3-62

3.5-4. Aircraft crash results 3-63

3.7-1. Horizontal design spectra for safe shutdown earthquake 3-80

3.7-2. Vertical design spectra for safe shutdown earthquake 3-82

3.7-3. Damping values to be used in dynamic analysis 3-84

3.7-4. ATR superstructure modes of vibration 3-84

3.7-5. Summary of Stress Result for Seismic Analysis of Category I Structures 3-85

3.7-6. ATR response spectra for SSE 3-86

3.7-7. ATR Response Spectra for SSE 3-86

3.8-1. Analysis results of internal pressure of confinement structures 3-107

3.8-2. Calculated stress ratios in ATR building elements 3-108

3.8-3. Allowable stresses for steel and masonry in load combinations A and B 3-109

3.8-4. Materials used in the construction of the ATR reactor building 3-109

3.8-5. Materials used in the raw-water storage tanks 3-109

3.9-1. Transients used in the design and fatigue analysis of the ATR vessel 3-141

3.9-2. General guidelines on ASME allowable stress limits for specified service loading combinations 3-142

3.9-3. Load cases considered in ASME Section 3 analysis of ATR reactor vessel 3-142

3.9-4. Computer programs used in analysis 3-143

3.9-5. Load combinations used in the reactor vessel faulted analysis 3-144

3.9-6. Allowable stress intensities for various portions of the reactor vessel 3-144

3.9-7. Reactor vessel faulted condition: Summary of results for support-condition I 3-145

3.9-8. Reactor vessel faulted condition: Summary of results for support-condition 3-146

3.9-9. Load cases considered in ASME Section III analysis of ATR piping and supports 3-147

3.9-10. ATR safety related active pumps and valves 3-148

3.9-11. Ground-acceleration capacities of ATR structures and equipment 3-149

3.9-12. Performance characteristics of the safety-rod system 3-154

3.9-13. Performance characteristics of the OSCC system 3-155

3.9-14. Summary of loading parameters for reactor internals 3-156

3.10-1. Ground-acceleration capacities of ATR electrical equipment and instrumentation 3-177

3.11-1. NRC Regulatory Guide 1.89 requirements for equipment qualification 3-186

ACRONYMS/ABBREVIATIONS

AEC	U.S. Atomic Energy Commission
ACI	American Concrete Institute
AISC	American Institute of Steel Construction
ANS	American Nuclear Society
ANSI	American National Standards Institute
ASA	American Standards Association
ASCE	American Society of Civil Engineers
ASME	American Society of Mechanical Engineers
ASTM	American Society for Testing and Materials
ATR	Advanced Test Reactor
AVZ	Axial Volcanic Zone
AWS	American Welding Society
AWWA	American Water Works Association
BHFIS	Bottom Head Firewater Injection System
BTP	Branch Technical Position
CAM	continuous air monitor
CFA	Central Facilities Area
CFR	Code of Federal Regulations
CK	check valve
CLOFA	complete loss of flow accident
DBE	design basis earthquake
DG	diesel generator
DHR	decay heat removal
DOE	U.S. Department of Energy
EDF	engineering design file
EFIS	emergency firewater injection system
EG&G Idaho	EG&G Idaho, Inc.
EPRI	Electric Power Research Institute
ESF	engineered safety features
ESRP	Eastern Snake River Plain
ETR	Engineering Test Reactor
FAA	Federal Aviation Administration
FIS	firewater injection system
FMEA	failure mode and effects analysis
FO	fuel oil
ft-msl	feet-mean sea level
FW	firewater
FY	fiscal year
GDC	general design criterion
GIP	Generic Implementation Procedure
GL	Generic Letter

HCLPF	High Confidence Low Probability of Failure
H&V	heating and ventilating
HFIR	High-Flux Isotope Reactor
ICBO	International Conference of Building Officials
ID	inside diameter
IDO	Idaho Operations Office reports (Issued by DOE and its precessors)
IEEE	Institute of Electrical and Electronic Engineers
INEEL	Idaho National Engineering and Environmental Laboratory
INTEC	Idaho Nuclear Technology and Engineering Center
IPT	inpile tube
ISI	inservice inspection
LCR	log countrate system
LDW	low-pressure demineralized water
LMITCO	Lockheed Martin Idaho Technologies Company, Inc.
LOCA	loss of coolant accident
MCC	motor control center
MEB	Management Evaluation Branch
msl	mean sea level
MTR	Materials Test Reactor
MW_{th}	megawatt, thermal
NBS	National Bureau of Standards
NIST	National Institute of Standards and Technology
NMIS	Nuclear Materials Inspection and Storage
NOAA	National Oceanic and Atmospheric Administration
NRC	U.S. Nuclear Regulatory Commission
NSC	Nuclear Services Corporation
OBE	operating basis earthquake
OD	outside diameter
OSCC	outer shim control cylinder
PCRS	primary coolant recycle system
PCS	primary coolant system
PGA	peak ground acceleration
PMF	probable maximum flood
PMP	probable maximum precipitation
PPS	plant protective system
PRA	probabilistic risk assessment
psf	pounds per square foot
PWR	pressurized water reactor
QPP	Quality Program Plan
RDAS	reactor data acquisition system
RDT	Reactor Development and Technology
RG	Regulatory Guide
RMSS	radiation monitoring and seal system

RP	Reactor Programs
RPU	Remote Processing Unit
RSS	reactor shutdown system
SAIC	Science Applications International Corporation
SAR	Safety Analysis Report
SATS	Surveillance and Test System
SDD	system design description
SDRC	Structural Dynamics Research Corporation
SG	switchgear
SMA	strong-motion accelerograph
SV	solenoid valve
SQUG	Seismic Qualification Users Group
SRP	Standard Review Plan
SSC	structures, systems, and components
SSE	safe shutdown earthquake
SSI	soil structure interaction
SSRAP	Senior Seismic Review and Advisory Panel
TRA	Test Reactor Area
TSR	Technical Safety Requirements
UBC	Uniform Building Code
UCW	utility cooling water
UFSAR	Upgraded Final Safety Analysis Report
UPS	uninterruptible power supply
USD	ultimate-stress design
USI	Unresolved Safety Issue
UVFIS	Upper Vessel Firewater Injection System
VVS	Vessel Vent System
WSD	working-stress design

3. DESIGN OF STRUCTURES, COMPONENTS, EQUIPMENT, AND SYSTEMS

The Advanced Test Reactor (ATR) is located at the Test Reactor Area (TRA) within the boundaries of the Idaho National Engineering and Environmental Laboratory (INEEL). ATR, in operation since 1969, is a 250-MW_{th} nuclear reactor designed to study the effects of intense irradiation on samples of reactor materials. A comparison of ATR to a typical commercial pressurized water reactor (PWR) is presented in Table 3.1-1. ATR is significantly different from a PWR, having a smaller core, higher power density, lower primary coolant system (PCS) pressure and temperature, greater ratio of coolant weight to power, and a confinement structure rather than a containment building. The confinement structure is designed to be a barrier to radionuclide release to the atmosphere, similar to a containment building for a PWR; however, the confinement structure has a higher leakage rate and lower overpressurization structural failure limit. Also, the confinement does not require venting during a severe accident because of the low pressure and low power of the ATR (Eide, Khericha, and Thatcher 1991).

3.1 General Design Criteria for ATR

Facility-specific General Design Criteria (GDC) were developed at the start of the Safety Analysis Report (SAR) upgrade in 1989 (Croucher 1989). The facility-specific GDC were developed by adapting the U.S. Nuclear Regulatory Commission (NRC) GDC for water-cooled nuclear power plants in the Code of Federal Regulations (CFR) 10 CFR 50, Appendix A (CFR 1999), to the ATR. While application of 10 CFR 50, Appendix A to ATR was not explicitly required, the CFR was used as guidance in establishing the principle design criteria for the ATR. This approach was consistent with Department of Energy (DOE) Order 5480.6, Safety of Department of Energy-Owned Nuclear Reactors (DOE 1986) which was in effect in 1989.

As described by Croucher (1989), forty-eight of the NRC GDC have been adopted for use by the ATR, the other seven do not apply because of the special nature of this reactor. Of the 48 adopted, 27 were adopted without change, 14 were adopted with only minor changes, and seven were revised to reflect the design of the existing facility. Two new GDC were added: GDC 70, "Experiment Facilities," and GDC 71, "Emergency Response Systems Design," because of the special nature of this reactor.

Information notes have been included to provide explanations for the ATR GDC that have been adopted from the NRC GDC with only minor changes, and for some ATR criteria that have been adopted without change but require further qualification. Basis statements have been included for new ATR GDC and ATR GDC that required significant modification to the corresponding NRC GDC.

The development of facility-specific GDC was completed prior to the release of DOE Order 5480.30, "Nuclear Reactor Safety Design Criteria" (DOE 2001a). This Order establishes nuclear safety design criteria applicable to the design, fabrication, construction, testing, and performance requirements of nuclear reactor facilities and safety class structures, systems, and components (SSC) within these facilities. This Order is applicable to both new and existing reactor facilities. For existing facilities, the SAR prepared per DOE Order 5480.23 is to serve to establish and evaluate the adequacy of the safety bases. This SAR serves that function. Further, the SAR is to demonstrate that the appropriate provisions of Order 5480.30 are compared and evaluated against the safety design basis. This SAR compares the safety design basis to the NRC GDC, but not to the criteria in Order 5480.30. A comparison to the DOE GDC in Order 5480.30 has not been formalized. The DOE Advanced Test Reactor Safety Evaluation Report (DOE 1996b) concludes there would be little value added to reanalyze the ATR GDC against the GDC in DOE Order 5480.30. Modifications to important-to-safety SSC to further address or remove the qualifications on compliance with the facility-specific GDC will be considered in accordance with DOE Order 5480.30 direction for modifications to existing facilities.

The facility-specific GDC establish minimum requirements for new construction and modification of important-to-safety SSC. Additional requirements for new construction and modification of important-to-safety SSC will be considered in accordance with the guidance for backfitting in DOE Orders 5480.4 (DOE 1993), 5480.23 (DOE 1994b), 10 CFR 830 (2002b), and 5480.30 (DOE 2001a).

Some of the terminology used in the previous ATR authorization basis and used in the Upgraded Final Safety Analysis Report (UFSAR) differs from the terminology used in the GDC's. Throughout the UFSAR, historical terminology was used to the extent practical to maintain consistency. Many of the GDC refer to "anticipated operational occurrences." Unless indicated otherwise in the GDC, these are to be interpreted as normal operation or Condition 1. Further discussion on Condition 1 and clarification of Condition 1, 2, 3, and 4 relative to the historical references to normal operation, anticipated faults, unlikely faults, and extremely unlikely faults is provided in Chapter 15 (Accident Analyses).

3.1.1 Overall Requirements[a]

3.1.1.1 Criterion 1—Quality Standards and Records. SSC important to safety shall be designed, fabricated, erected, and tested to quality standards commensurate with the importance of the safety functions to be performed. Where generally recognized codes and standards are used, they shall be identified and evaluated to determine their applicability, adequacy, and sufficiency and shall be supplemented or modified as necessary to assure a quality product in keeping with the required safety function. A quality assurance program shall be established and implemented in order to provide adequate assurance that these SSC will satisfactorily perform their safety functions. Appropriate records of the design, fabrication, erection, and testing of SSC important to safety shall be maintained by or under the control of the operating contractor throughout the life of the unit.

3.1.1.1.1 Information Note—Existing records of the design, fabrication, erection, and testing of SSC important to safety are being maintained by the operating contractor.

---

[a] In the sections that follow, the text of each criterion is presented as it was given by Croucher (1989). When the text is enclosed in quotation marks, Croucher's wording is identical to that in 10 CFR 50, Appendix A (CFR 1999), except for direct substitutions such as "confinement" for "containment." Direct substitutions in otherwise verbatim wording are enclosed in square brackets.

3.1.1.1.2 Discussion—The Contractor's *Quality and Requirements Management* manual meets the requirements of the American Society of Mechanical Engineers (ASME) NQA-1-1997 Edition (ASME 1997), 10 CFR 830.120 (CFR 2002a), and U.S. Department of Energy (DOE) Order 414.1A (DOE 2001b).

3.1.1.2 Criterion 2—Design Bases for Protection Against Natural Phenomena. SSC important to safety shall be designed to withstand the effects of natural phenomena such as earthquakes, tornadoes, and floods without loss of capability to perform their safety functions. The design bases for these SSC shall reflect: (1) appropriate consideration of the most severe of the natural phenomena that have been historically reported for the site and surrounding area, with sufficient margin for the limited accuracy, quantity, and period of time in which the historical data have been accumulated, (2) appropriate combinations of the effects of normal and accident conditions with the effects of the natural phenomena, and (3) the importance of the safety functions to be performed.

3.1.1.2.1 Information Note—Mention of hurricanes, tsunami, and seiches is deleted. These phenomena are not concerns because the ATR Facility is not adjacent to an ocean, inland sea, or lake.

3.1.1.2.2 Discussion—ATR was originally designed before facility-specific design criteria for protection against natural phenomenon were established. Building design conformed with the requirements of the Uniform Building Code (UBC), 1961 edition for Zone 2 locations (ICBO 1961). Natural phenomenon hazards according to these UBC provisions included seismic loads (generally 5% of gravity loads) and wind loads varying from 30 to 40 lb/ft^2, depending on height as specified in the Atomic Energy Commission standards for this area.

Since original construction of ATR, facility-specific seismic design criteria have been developed. These criteria have been revised since first being introduced. In general, each revision has resulted in more stringent acceptance criteria.

As new SSC have been installed, they have typically been shown to meet the seismic design criteria applicable at the time of installation. Some, but not all, original SSC have been reanalyzed as new criteria were introduced. The most notable reanalysis effort was performed in the mid-1970's, immediately following development of the first facility-specific seismic design criteria (Gorman 1972). Seismic analyses for selected SSC (considered at the time to be the most critical) were updated as part of the Seismic Analysis Program Plan (Mousseau 1973). Some modifications were performed as a result of these analyses. Similarly, other analyses performed since original construction have resulted in some additional modifications to reduce seismic fragility.

The result of the periodic changes in seismic design criteria over the operating life of the ATR, and the selective upgrades of SSC to these changed criteria, is that there is a full spectrum of seismic qualification for SSC important to safety. Some have not been qualified, some were qualified to the UBC during original construction, some have been qualified or requalified to criteria in effect after original construction (but no longer in effect), and some are fully qualified to the criteria applicable today.

The most current and comprehensive evaluation of the risks associated with seismic events is documented in the probabilistic risk assessment (PRA) Level 1 report (Eide, Khericha, and Thatcher 1991). The PRA efforts included evaluation of risks associated with external events including seismic, flooding, volcanic activity, and extreme wind. The evaluation included a walkdown of risk-significant SSC to estimate seismic fragility (i.e., the severity of seismic motion that would result in a loss of function for the SSC). The seismic fragility estimates were input to evaluations of the various accident sequences and initiating events to determine risk of fuel damage. The evaluations showed that the risk of fuel damage resulting from seismic events is low. The evaluations also provided a basis for prioritizing upgrades for further risk reduction. The highest priority upgrades have been completed.

3.1.1.2.3 Seismic Analysis—The introduction of facility-specific seismic design criteria in the 1970's resulted in the definition of a Design Basis Earthquake (DBE)/safe shutdown earthquake (SSE) for ATR. The DBE/SSE is the maximum postulated seismic event for which it should be demonstrated that the reactor can be safely shut down and maintained in a safe condition. This DBE/SSE is based on a Richter magnitude 7.3 earthquake occurring in the vicinity of the Howe fault and resulting in a peak ground acceleration of 0.24g at bedrock (Gorman 1989b). The seismic design criteria associated with this DBE/SSE are applied during design and construction of new SSC that are required to be seismically qualified.

The DOE-ID AE Standards (DOE-ID 2002) have been revised to incorporate new seismic design requirements of DOE Standards DOE-STD-1020 (DOE 2002a)and DOE-STD-1021 (DOE 2002b). The TRA site specific Performance Categories PC 1 and PC 2 seismic design criteria use the International Building Code (IBC 2000) spectral accelerations. The TRA site specific PC 3 and PC 4 horizontal and vertical seismic design criteria for rock Design Basis Earthquake/Safe Shutdown Earthquake (DBE/SSE) is available in the DOE-ID Standard (DOE-ID 2002). The TRA site specific PC 3 and PC 4 horizontal and vertical seismic design criteria for soil DBE is under development, and will be incorporated into the AE Standards when completed.

An operating basis earthquake (OBE) is not defined for the ATR. The OBE, typically taken as one-half of the SSE, is defined for commercial nuclear power plants as the seismic event for which seismically-qualified SSC are analyzed to withstand without sustaining damage. An OBE is not applicable since the seismic subsystem of the plant protective system (PPS) is designed to scram the reactor at the onset of a seismic event, ensuring safety rod insertion before damaging seismic motion occurs.

3.1.1.2.4 External Flooding Analysis—Four external flooding scenarios were identified that could result in flooding of the ATR site:

A. Hydraulic failure of the Mackay Dam with the 100-year recurrence interval flood

B. Hydraulic failure of the Mackay Dam with the 500-year recurrence interval flood

C. Overtopping failure of the Mackay Dam caused by the probable maximum flood (PMF)

D. Seismic failure of the Mackay Dam coincident with the 25-year recurrence interval flood.

The overtopping failure caused by the PMF could result in loss of commercial and diesel power (station blackout). The other scenarios affect the ATR through the loss of commercial power.

The PRA results indicate a mean frequency for external flooding event sequences between 1.0×10^{-8} and 8.5×10^{-8} per year. The total mean frequency of all sequences is 1.3×10^{-7} per year (Eide, Khericha, and Thatcher 1991).

3.1.1.2.5 Volcanic Activity Analysis—Design basis criteria for volcanic activity have not been established for the INEEL. Basaltic eruptions are characterized primarily by the quiet extrusion of lava flows that are controlled by topography and will travel downslope. The shortest recurrence intervals (8,000 to 15,000 years), the most recent volcanism (Holocene lava fields), and the most probable areas of future basaltic volcanism and ground deformation are the Axial Volcanic Zone and the Arco Volcanic-Rift Zone. Within this context, the estimated total annual frequency of fuel damage due to lava inundation was 8.4×10^{-8} (Hackett and Khericha 1993).

3.1.1.2.6 Tornado/Extreme Wind Analysis—A tornado/extreme wind analysis, according to the 1985 INEEL Extreme Wind/Tornado Hazard Study (Coats and Murray 1985), was performed for the reactor building and the raw water storage tanks. This analysis included the effects of Site-specific tornados/straight winds as well as tornado-generated missiles (Arendts 1989a, 1989b; Gorman 1989a).

The conclusions from these studies show that the masonry block wall extending from the ATR Critical Facility roof to the highbay (reactor room) roof requires additional protection against wind-borne missiles. However, the PRA does not consider wind-borne missiles a credible concern for the following reasons. First, straight wind dominates the hazard at the INEEL for frequencies of exceedence larger than 10^{-6} per year (i.e., tornados are incredible). Second, the medium perforation wind speed for the given missiles was found to be high enough that the missile damage is judged to be not a concern for stright-wind hazard (Eide, Khericha, and Thatcher 1991). Also, the reactor building reactor room and control room, including adjacent office structures, are capable of resisting wind speeds greater than established hazard values if girt and siding damage are not considered (Arendts 1989a; Gorman 1989a).

The capability of the ATR to perform the safety functions of reactor shutdown, decay heat removal, primary coolant inventory control, and confinement isolation without the ac power system indicates that it could withstand tornado damage (assuming that the Emergency Firewater Injection System (EFIS) remains operational).

The PRA results indicate a mean annual fuel damage frequency for wind-initiated sequences of about 1.15×10^{-6} per year (Atkinson and Thatcher 1994).

A discussion of present site-specific natural phenomena hazards is presented in Chapter 2 (Site Characteristics).

3.1.1.3 Criterion 3—Fire Protection. SSC important to safety shall be designed and located to minimize, consistent with other safety requirements, the probability and effect of fires and explosions. Noncombustible and heat resistant materials shall be used wherever practical throughout the unit, particularly in locations such as the confinement and control room. Fire detection and fighting systems of appropriate capacity and capability shall be provided and designed to minimize the adverse effects of fires on SSC important to safety. Fire fighting systems shall be designed to assure that their rupture or inadvertent operation does not significantly impair the safety capability of these SSC.

3.1.1.3.1 Discussion—Automatic fire suppression systems are provided by wet pipe and preaction sprinkler systems in most areas of the plant. Halon fire suppression systems are provided in some areas. Fire extinguishers and standpipe connections equipped with fire hoses are available in many areas of the plant. Manual fire suppression is provided by the TRA emergency brigade and the INEEL Fire Department located 6 miles from ATR.

Location-dependent equipment vulnerabilities with regard to fire damage are identified in Thatcher (2000a) by identifying the location of safety-related equipment and other equipment relevant to the protection of irradiated reactor or canal fuel that may be vulnerable to fire events. Considering the shared equipment locations, an evaluation of fire-induced Chapter 15 accident initiators and beyond design basis accidents was performed (Thatcher 2000b). This analysis identified the administrative controls and fire protection features necessary to maintain an acceptably low frequency of fire-induced threats to fuel safety. Fire protection equipment is discussed in Chapter 9 (Auxiliary Systems).

3.1.1.4 Criterion 4—Environmental and Dynamic Effects Design Bases. SSC important to safety shall be designed to accommodate the effects of and to be compatible with the environmental conditions associated with normal operation, maintenance, testing, and postulated accidents, including loss-of-coolant accidents. These SSC shall be appropriately protected against dynamic effects, including the effects of missiles, pipe whipping, and discharging fluids, that may result from equipment failures or from events and conditions outside the Facility.

3.1.1.4.1 Discussion—Rotating machinery that could be sources of missiles include the primary coolant pumps and diesel generators. The four primary coolant pumps are aligned parallel to each other in separate pump rooms on the first basement of the reactor building. The primary pump motors, however, are parallel to each other in the same room, and also in the basement. Diesel generators M-42 and M-43 are aligned on a common longitudinal axis in the diesel generator room. The M-6 diesel generator is in a separate diesel building. Potential missiles from rotating machinery have been considered in an evaluation of the PPS (INEEL 2000), and were found to be insignificant hazards.

Wadkins (1988) concludes that the primary system stainless steel piping would fail with small leaks rather than catastrophic blowouts. EG&G Idaho performed pipe tests to failure and correlated the size of the failure with the energy level of the system. Wadkins (1988) shows that for annealed Type 304 stainless steel piping, the smaller the system pressure, the smaller the size of the failure. The conclusion is that a low-pressure system such as ATR will experience a ductile rupture and comparatively small leak rate rather than a complete rupture and high leak rate. Consequently, pipe whip or any similar sudden destructive failures of the PCS are considered extremely low probability accidents. Pipe whip or sudden failure of the higher energy experiment loop piping systems is evaluated in Chapter 10 (Experiment and Irradiation Facilities).

A missile shield plug is secured into the transfer plate to shield the confinement roof against missile projectiles ejected from the vessel from any inpile experiments.

Environmental specifications for the PPS can be found in Chapter 7 (Instrumentation and Controls) and in the PPS System Design Descriptions, SDD-7.7.1 - EFIS, 7.7.2 - RSS, 7.7.4 - RMSS, and 7.1.6 - VVS (EG&G Idaho 1986, 1988b; INEEL 2000, 2003).

3.1.1.5 Criterion 5—Sharing of Structures, Systems, and Components. SSC important to safety shall not be shared with other facilities unless it can be shown that sharing will not significantly impair their ability to perform their safety functions including, in the event of an accident in a shared component or a sharing facility, an orderly shutdown and cooldown of the facility.

3.1.1.5.1 Information Note—In GDC 5, the term "nuclear power units" has been replaced in Criterion 5 by the phrase "shared component or a sharing facility." This is considered a direct substitution.

3.1.1.5.2 Discussion—The SSC important to safety that are shared by the facility with other TRA facilities are the firewater system, the demineralizer system, commercial power, and the M-6 diesel generator. Failures of these shared systems have been analyzed and are discussed in UFSAR Chapter 15 (Accident Analyses). When appropriate, the analyses address failures of the SSC and failures in the TRA facilities that share the SSC. In the cases of the demineralizer system and commercial power, failures that may occur in the shared SSC will not adversely impact the ATR. In the case of the firewater system due to redundancies in the firewater loop, a failure in the firewater system can be isolated without adversely impacting the ability of the EFIS to perform its safety functions. In the case of the M-6 diesel generator, a failure in the sharing facility (utility area via TRA 609) could result in a trip of the generator. However, the diesel can be selected to provide power to ATR only and restarted if needed.

3.1.2 Protection by Multiple Fission Product Barriers

3.1.2.1 Criterion 10—Reactor Design. "The reactor core and associated coolant, control, and protection systems shall be designed with the appropriate margin to assure that Plant Protection Criteria for fuel performance are not exceeded during any condition of normal operation, including the effects of anticipated operational occurrences."

3.1.2.1.1 Discussion—The ATR was designed to ensure adequate safety margins to Plant Protection Criteria for fuel performance during normal operation (Condition 1) and off-normal occurrences (Conditions 2 through 4). Chapter 4 (Reactor) discusses the reactor design, including the design bases, and operating conditions. Chapter 5 (Primary Coolant System) describes the remainder of the PCS. The ATR operates within conditions based on the UFSAR, which are listed in the Technical Safety Requirements (TSR) that ensure adequate safety margins to Plant Protection Criteria for fuel performance. The PPS is composed of the Reactor Shutdown System (RSS), and Engineered Safety Features (ESF). The PPS ensures that safety margins to Plant Protection Criteria for fuel performance are maintained during any credible off-normal plant occurrence. The PPS is discussed in Chapter 7 (Instrumentation and Controls), and the ESF is discussed in Chapter 6 (Engineered Safety Features). The accident analysis that established the basis for the PPS and TSR is discussed in Chapter 15 (Accident Analyses).

3.1.2.2 Criterion 11—Reactor Inherent Protection. "The reactor core and associated coolant systems shall be designed so that in the power operating range the net effect of the prompt inherent nuclear feedback characteristics tends to compensate for a rapid increase in reactivity."

3.1.2.2.1 Discussion—The ATR has strong negative reactivity coefficients for coolant-temperature and coolant-void increases in the fuel element. The reactivity coefficient for fuel temperature increase is only weakly negative. The fuel temperature coefficient results from a decrease in distance between fuel plates caused by the expansion of the fuel with temperature increase. The coolant-temperature and voiding-increase reactivity coefficients in the flux traps and the reflector, however, are positive.

3.1.2.3 Criterion 12—Suppression of Reactor Power Oscillations. "The reactor core and associated coolant, control, and protection systems shall be designed to assure that power oscillations which can result in conditions exceeding Plant Protection Criteria for fuel performance are not possible or can be reliably and readily detected and suppressed."

3.1.2.3.1 Discussion—Potential sources of positive reactivity or power increases are shim drum or shim rod movements, regulating rod movement, rapid cool down of the primary coolant, or experimental loop voiding. The PPS includes two subsystems designed to trip the reactor during reactivity transients. The neutron level subsystem is a two-out-of-three system with a high power Limiting Control Setting of ≤ 1.15 times full power during pressurized operation. The wide range neutron level subsystem is also a two-out-of-three system with a high power Limiting Control Setting of ≤ 1.15 times full power during pressurized operation. The wide range system does not offer continuous period protection. Instead, it monitors reactor period by timing power increase over discrete intervals providing an effective reactor period Limiting Control Setting of ≥ 1.3 seconds. Eleven scram points are provided over the five-decade range protected by the system.

3.1.2.4 Criterion 13—Instrumentation and Control. Instrumentation shall be provided to monitor variables and systems over their anticipated ranges for normal operation, for anticipated operational occurrences, and for accident conditions as appropriate to assure adequate safety, including those variables and systems that can affect the fission process, the integrity of the reactor core, the primary coolant pressure boundary, and the confinement and associated systems. Appropriate controls shall be provided to maintain these variables and systems within prescribed operating ranges.

3.1.2.4.1 Information Note—"Containment" was changed to "confinement." Since ATR is a moderate-pressure, low-temperature facility with a relatively small fission-product inventory and is remotely located, a leak-tight containment structure as required for nuclear power reactors was not provided. A confinement structure provides the required barrier to limit the rate of release of fission products following a postulated accident.

3.1.2.4.2 Discussion—Numerous instrumentation and control systems actuate automatic protective actions and exercise proper control against unsafe and improper reactor operation. The control system provides graded corrective actions to reduce the frequency of protective actions by the PPS. The total reactivity available to the automatic control system and the servo mechanism is less than the delayed neutron fraction. Display instrumentation monitors effectiveness and status of automatic protective actions. The PPS is capable of mitigating any credible control system malfunction.

The PPS is independent from nonsafety-related instrumentation and control systems. No significant system interactions beyond the scope of the PPS design basis have been identified during a review of ATR functional requirements (Buescher 1993).

Lobe powers are not monitored directly over all postulated accident conditions. The lobe powers are obtained from the lobe power calculation and indication system. The system is designed for the operating range and under certain conditions will saturate before lobe power reaches the safety limit. Additionally, the system design does not provide immediate indications of power changes and does not function under rapid transient conditions. Under these conditions, there may not be a direct indication of the maximum power reached. However, there will be ample indication that the power level has exceeded the setting for the nuclear instrumentation based on the control room recorders. Off-normal conditions that result in high lobe powers will require reconstruction of the event to determine the power levels reached.

3.1.2.5 Criterion 14—Primary Coolant Pressure Boundary. "The primary coolant pressure boundary shall be designed, fabricated, erected, and tested so as to have an extremely low probability of abnormal leakage, of rapidly propagating failure, and of gross rupture."

3.1.2.5.1 Discussion—The coolant enters the reactor vessel at ≤ 125°F and approximately 372 psig (measured at the PPS vessel inlet pressure tap). The reactor inlet coolant pressure is regulated by controlling the inventory of coolant. The pressurizing and gland seal pumps discharge into the system and the pressure control valve bleeds from the system to maintain constant pressure. Overpressure protection is provided by two sets of two safety relief valves and the high pressure ESF.

A surge tank air cushion is provided to damp minor pressure fluctuations. The total volume of the surge tank is 1,000 ft^3 of which approximately 50 ft^3 is air when the normal primary system operating pressures and flow are maintained.

The PCS was designed, fabricated, erected, and tested to pertinent codes and standards current at the time of construction. The PCS was subsequently analyzed ASME Section III, Class 2, 1977 Edition (Class I for Seismic) and found to meet the intent of the Section III. PCS construction materials were chosen that are ductile and resistant to erosion, corrosion, intergranular stress-corrosion cracking, and embrittlement.

3.1.2.6 Criterion 15—Primary Coolant System Design. The primary coolant system and associated auxiliary, control, and protection systems shall be designed with sufficient margin to assure that the design conditions of the primary coolant pressure boundary are not exceeded during any condition of normal operation, including anticipated operational occurrences.

3.1.2.6.1 Discussion—The reactor is cooled by circulating pressurized demineralized water in a closed primary loop. Primary coolant flow rate is adjusted to produce a 100 psi differential pressure drop across the reactor core when in the three-pump operating mode. The three primary coolant pumps have a combined capability of 54,000 gpm while retaining the fourth 18,000 gpm pump as a spare. The expected coolant requirement at 250 MW_{th} is 49,000 gpm, yielding an excess coolant capacity of 5,000 gpm. Operation at lower power levels often allows for operation with only two primary coolant pumps, retaining the third and fourth pumps as spares.

Primary coolant vessel inlet temperature is controlled by varying the secondary coolant flow to the primary heat exchanger. PCS pressure control is provided by a surge tank and the degassing and pressurizing subsystem, and is monitored by the PPS.

The piping design and safety limit pressures and temperatures at the specified locations are shown in Table 3.1-2.

Mechanical operations and anticipated transients have been analyzed to be within the pressure and temperature limits established in Table 3.1-2.

3.1.2.7 Criterion 16—Confinement Design. Reactor confinement and associated systems shall be provided to establish a barrier against the uncontrolled release of radioactivity to the environment and to assure that the confinement design conditions important to safety are not exceeded for as long as postulated accident conditions require.

3.1.2.7.1 Information Note—"Containment" was changed to "confinement"; "an essentially leak-tight barrier" was changed to "a barrier." Since ATR is a low-energy facility with a relatively small fission product inventory and is remotely located, a leak-tight containment structure required for nuclear power reactors is not needed. A confinement structure provides a barrier to limit the rate of release of fission products following design-basis accidents.

3.1.2.7.2 Discussion—Unlike commercial nuclear plants, ATR does not have containment purge valves to control the containment pressure or isolation valves to isolate the containment in case of a severe accident. However, ATR uses an interlocked ventilation system, including exhaust and supply fan systems, exhaust stack, roof ventilators, and closure dampers to control confinement atmospheric conditions during normal operation (deBoisblanc, Cohen, and Walker 1966).

The integrity of the confinement system has been verified by a number of studies (Close 1988a, 1988b; Atkinson 1976, 1988). These studies have shown that a loss of coolant accident (LOCA) or a major reactivity excursion will not result in overpressurization of the confinement. Even though the initial leakage rate in the first minutes after a LOCA exceeds the designed leakage rate, the high release rate will not result in an unacceptable amount of radioactive release to the external environment.

3.1.2.8 Criterion 17—Electric Power Systems. An on-site electric power system and an off-site electric power system shall be provided to permit functioning of SSC important to safety. The safety function for each system (assuming the other system is not functioning) shall be to provide sufficient capacity and capability to assure that (1) Plant Protection Criteria for fuel performance and related design conditions of the primary coolant pressure boundary are not exceeded as a result of anticipated operational occurrences, and (2) the core is cooled and confinement integrity and other vital functions are maintained in the event of postulated accidents.

The on-site electric power supplies, including the batteries, and the on-site electric distribution system shall have sufficient independence, redundancy, and testability to assure performance of critical safety functions assuming a single failure of any one of the eight power systems listed below.

Electric power from the transmission network to the on-site electric distribution system shall be supplied by two physically independent circuits (not necessarily on separate rights of way) designed and located so as to minimize to the extent practical the likelihood of their simultaneous failure under operating and postulated accident and environmental conditions. A switchyard common to both circuits is acceptable. Adequate on-site power shall be available in sufficient time following the loss of all off-site electric power, to assure that Plant Protection Criteria for fuel performance and design conditions of the primary coolant pressure boundary are not exceeded. Adequate electric power shall be available in sufficient time following a loss of coolant accident to assure that core cooling, confinement integrity, and other vital safety functions are maintained.

Provisions shall be included to minimize the probability of losing electric power from any remaining supplies as a result of, or coincident with, the loss of power from the transmission network or the loss of power from the on-site electric power supplies.

3.1.2.8.1 Basis—The GDC is written with on-site (power-station generated) power as the primary source. For ATR, off-site power is the primary source. The changes made to the GDC reflect this difference. In GDC 17, sentence 3 of paragraph 3, which reads "Each of these circuits shall be designed to be available in sufficient time following a loss of all on-site alternating current power supplies and the other off-site electric power circuits to assure that...", has been replaced by "Adequate onsite power shall be available in sufficient time following the loss of all offsite electric power to assure that...." Paragraph 3, sentence 4 in GDC 17, "One of these circuits shall be designed to be available within a few seconds following a loss-of-coolant...", has been replaced by "Adequate electric power shall be available in sufficient time following a loss-of-coolant...." In the last paragraph of GDC 17, the following was deleted: "..., the loss of power generated by the nuclear power unit,...."

3.1.2.8.2 Discussion—The electric power system was designed and built before Class 1E design requirements were established for the commercial nuclear power industry. Even though the electric power system has many redundant features, it does not generally meet the current nuclear industry requirements for physical and electrical separation of redundant parts of Class 1E systems.

The electric power system consists of the following eight subsystems:

A. Commercial power (4160 & 480 Vac buses)

B. Diesel power (4160/480 Vac buses)

C. Diesel power (480/208/120 Vac buses)

D. Diesel-commercial power (480 Vac bus)

E. Diesel-commercial power (208/120 Vac buses)

F. Instrument 250 Vdc and 208/120 Vac battery-backed power

G. Utility 250 Vdc and 208/120 Vac battery-backed power

H. PPS 32 Vdc battery-backed power.

The diesel buses are electrically independent from the commercial power buses. Battery E-59, which supplies instrumentation 208/120 Vac, is independent of battery E-58, which supplies utility dc power and 208/120 Vac battery backed power. The four PPS power supply divisions have independent batteries, battery chargers, and distribution panels.

The following redundant features exist in the electric power system:

- Two feeds exist from the offsite grid to the onsite electric power system, one feeding each of two commercial buses.
- Any one of three diesel generators can supply all ac loads normally supplied from diesel bus E-3.

- Motors for the following equipment may be energized from either commercial power or diesel power, as selected manually for each motor:
  - Primary pressurizing pumps M-14 and M-15
  - High pressure demineralized water circulated pumps M-35 and M-36
  - Primary gland seal pumps M-40 and M-41
  - Some of the experiments loop primary pressurized water circulating pumps.
- Diesel-commercial motor control center E-15 has two feeds and can be supplied from either diesel power or commercial power.

Safety-related loads are supplied through uninterruptible battery-backed power supplies as required to ensure that critical safety functions are met. In addition, the RSS and the EFIS (diesel driven pumps are in separate buildings) will function with a loss of commercial and diesel power.

The electrical power and diesel generator support systems were evaluated for dependent and common cause failures for the PRA, including external events. The most vulnerable location for these events was identified as the switchgear room, and several risk-reduction upgrades were recommended and implemented to reduce the risk of a loss of all electrical power (Atkinson and Thatcher 1994). The principal upgrade was the relocation of the Utility Battery-Backed Power System out of the switchgear room. With the completion of the upgrades, no single event (with a significant frequency of occurrence) will result in a total loss of electrical power to power-supported safety systems and no loss-of-power event sequences or seismic event of a SSE magnitude or less will lead to fuel damage with a frequency greater than 1×10^{-6}/yr. Therefore, although the electric power system lacks the degree of redundancy and separation commonly found in commercial power reactors, the redundancy of power sources and separation of battery-backed power systems for the electrical system with the completed upgrades is adequate to support power-supported safety functions (emergency coolant pumps and Vessel Vent System (VVS)).

3.1.2.9 Criterion 18—Inspection and Testing of Electric Power Systems. Electric power systems important to safety shall be designed to permit appropriate periodic inspection and testing of important areas and features, such as wiring, insulation, connections, and switchboards, to assess the continuity of the systems and the condition of their components. The systems shall be designed with a capability to test periodically (1) the operability and functional performance of the components of the systems, such as on-site power sources, relays, switches, and buses and (2) the operability of the systems as a whole and, under conditions as close to design as practical, the full operational sequence that brings the systems into operation.

3.1.2.9.1 Information Note—The details concerning the term "full operational sequence that brings the systems into operation," in GDC 18 have been deleted. The specific systems listed in GDC 18, apply to power reactors and do not all apply to the ATR.

3.1.2.9.2 Discussion—Important electrical-power systems were designed to permit periodic inspection and testing of important areas and features. Examples of such systems are:

- Diesel generators (M-42 and M-43)
- Quick-start diesel generator (M-6)

- Battery banks (utility, instrument, and PPS)
- Utility and instrument uninterruptible power system
- PPS supply.

The electrical systems are inspected and maintained as a part of the maintenance program described in Chapter 14 (Initial Test Program, Inservice Surveillance, and Maintenance). The types of maintenance and the frequency are based on vendor specifications as they are available. Additional requirements for selected electrical sources and systems are found in Chapter 8 (Electric Power). The electrical power requirements imposed by the accident analysis are described in Chapter 16 (Derivation of Technical Safety Requirements).

3.1.2.10 Criterion 19—Control Room. A control room shall be provided from which actions can be taken to operate the ATR safely under normal conditions and to maintain it in a safe condition for Condition 2 and 3 incidents. Reactor controls shall be designed to achieve a safe condition under accident conditions including loss-of-coolant accidents with minimum action prior to a required evacuation; facilities shall be provided to obtain essential safety information about the facility from an alternative habitable location.

3.1.2.10.1 Basis—At the end of sentence one in GDC 19, "...in a safe condition under accident conditions, including loss-of-coolant accidents." is replaced by "...in a safe condition for Condition 2 and 3 incidents." There are some Condition 4 incidents for which the control room will not be habitable.

The remainder of GDC 19 is replaced by the second sentence. The control room is located within the confinement, and the control room is not designed to be habitable during all accident conditions. Under accident conditions, controls are designed to achieve a safe shutdown condition with minimum action prior to a required evacuation.

3.1.2.10.2 Discussion—The control room has been upgraded to meet the human engineering design requirements of NUREG-0737, Supplement 1 (NRC 1982), and NUREG-0700 (NRC 1981a). No deviations exist that could represent a significant safety deficiency. Although the control room is not designed for long-term habitability following a severe accident, this also does not present a serious safety deficiency since only plant depressurization actuated from the control room may be required once the safety rods have been inserted into the reactor. Emergency action planning does not assume post accident habitation following initiation of plant shutdown. If a PCS depressurization is required, this can also be quickly accomplished, by the VVS activated manually before evacuation.

Post accident control room occupancy is not critical to ensure safe shutdown. Safe shutdown can also be accomplished from the Room 101, which is outside the control room and confinement envelope. Shutdown is accomplished by operating the Emergency Scram Backup and Reverse switches, and can be accomplished very quickly. This action will not only insert the safety rods but initiates insertion of all reactivity shim control elements (neck shims and shim cylinders).

The scram inserts the safety rods and assures that the core is subcritical. Depressurization of the PCS by opening the vent valves assures that firewater (the system operates at relatively low pressure) can be added to the PCS if needed to maintain the inventory. The EFIS is an automatic system that does not require operator action beyond assuring the PCS is depressurized. With the reactor subcritical and the EFIS available to maintain inventory, there are no operator actions required to assure a stable configuration for the reactor.

3.1.3 Protection and Reactivity Control Systems

3.1.3.1 Criterion 20—Protection System Functions. "The protection system shall be designed (1) to initiate automatically the operation of the appropriate systems including the reactivity control systems, to assure that Plant Protection Criteria for fuel performance are not exceeded as a result of anticipated operational occurrences and (2) to sense accident conditions and to initiate the operation of systems and components important to safety."

3.1.3.1.1 Discussion—The PPS consists of two major subsystems that perform reactor shutdown and certain ESF functions. The PPS subsystems are the RSS, and the ESF.

The RSS performs the following protective actions:

- Release of the safety rods (reactor scram) when certain plant variables are outside acceptable value ranges
- Actuate certain ESF when certain plant variables are outside acceptable value ranges.

The ESF are the RMSS, the EFIS, the VVS, vessel level alarm indication, the primary pump shutoff system, the pressurizing and gland-seal-pump shutoff system, the LOCA Primary Coolant Pump Shutoff System, and the PCS overpressure relief system. All of these ESF are discussed in detail in Chapter 6 (Engineered Safety Features).

3.1.3.2 Criterion 21—Protection System Reliability and Testability. "The protection system shall be designed for high functional reliability and inservice testability commensurate with the safety functions to be performed. Redundancy and independence designed into the protection system shall be sufficient to assure that (1) no single failure results in loss of the protection function, and (2) removal from service of any components or channel does not result in loss of the required minimum redundancy unless the acceptable reliability of operation of the protection system can be otherwise demonstrated. The protection system shall be designed to permit periodic testing of its functioning when the reactor is in operation, including a capability to test channels independently to determine failures and losses of redundancy that may have occurred."

3.1.3.2.1 Discussion—An automatic surveillance and test system (SATS) has been provided that is used to check the RSS periodically during reactor operation. These checks confirm subsystem operability, check setpoint values, and verify system calibration by protective channel intercomparison. If the SATS is inoperable, its functions will be performed manually.

The RSS is designed to be a completely redundant system. No single failure in the RSS will result in a loss of the protective functions provided by that system. Although the ATR was not designed with strict application of the single failure criterion, there is a high degree of redundancy associated with critical safety systems, and especially with the ESFs. The accident analyses presented in Chapter 15 (Accident Analyses) consider the redundancy and independence of these safety systems in determining the reliability of mitigating equipment and limiting single failures. Therefore, the intent of requirement (1) is met.

Requirement (2) of this GDC is met by limitations placed on the equipment being out of service or otherwise inoperable. The action required when the equipment is inoperable is specified in the TSR. Typically the action is to shutdown the reactor within a specified time period if the component cannot be returned to service.

3.1.3.3 Criterion 22—Protection System Independence. The protection system shall be designed to assure that the effects of natural phenomena, and of normal operating, maintenance, testing, and postulated accident conditions on redundant channels do not result in loss of the protection function, or shall be demonstrated to be acceptable on some other defined basis. Design techniques, such as functional diversity or diversity in component design and principles of operation, shall be used to the extent practical to prevent loss of the protection function.

3.1.3.3.1 Discussion—The reactor has a completely independent PPS that is separate from the normal operational control system. The PPS includes special instruments, and special relays. These safety devices are not used for any operational function except for parameter indication. In addition, the PPS power is supplied from a 32 Vdc distribution system that is independent from other instrumentation power supplies. The updated PPS continues to meet the independence criteria established for the original PPS (Buescher 1993, specifically referring within Buescher's EDF to the December 23, 1988 letter from Vargo to Norin, and the Norin et al. report SAIC-88/1952).

The RSS subsystem of the PPS interfaces with the non-safety SATS. Isolation between these two systems is provided so that a failure of SATS does not affect the ability of the RSS to perform its intended safety function (Durney 1988).

The RSS is designed with three instrument channels (i.e., components performing similar functions located physically separate areas). The signal path from the sensors monitoring plant variables goes to an analog comparator or to a contact-to-logic-level-converter (CLLC) which converts the signal to a logic level compatible with the two-out-of-three logic modules. Each analog comparator and CLLC has four identical outputs. Each output is sent to a two-out-of-three logic module. If any two of the three plant variables exceed the trip point, the comparator or CLLC is tripped, the two out of three modules are tripped and the rod clutch controllers release the safety rods, causing the reactor to shut down. The RSS will trip the reactor on any one of the PPS scram setpoints. Several of the plant conditions (setpoints) that initiate scrams are monitored by at least one primary and one diverse safety-related system. The diversity provided in the RSS subsystems is described in Section 7.1.2.1.7.

The design bases for other less likely natural phenomena, such as extreme wind, external flooding, earthquakes, and volcanic eruptions, were discussed for Criterion 2 - *Design Bases for Protection Against Natural Phenomena*, Section 3.1.1.2 and Criterion 4 - *Environmental and Dynamic Effects Design Bases*, Section 3.1.1.4.

3.1.3.4 Criterion 23—Protection System Failure Modes. The protection system shall be designed to fail into a safe state or into a state demonstrated to be acceptable on some other defined basis if conditions such as disconnection of the system, loss of energy (e.g., electric power, instrument air), or postulated adverse environments (e.g., extreme heat or cold, fire, pressure, water, and radiation) are experienced.

3.1.3.4.1 Discussion—A Failure Mode and Effects Analysis (FMEA) of the ATR RSS was performed in 1975 (INEEL 2000)[a]. The results of this analysis indicated that:

- The RSS design is adequate to accomplish its protective functions given that one failure exists at any point in the system.
- Under the assumption of a postulated single failure and concurrent periodic testing within a redundant portion of the RSS, a number of situations result in which RSS coincidence logic is reduced to 2-out-of-2.

Mean time before failure and mean time to repair for the RSS were estimated in 1975 (INEEL 2000). This analysis indicated that the mean time before failure achieved the System Design Description requirements of 20,000 hours minimum and 5,000 hours minimum for unsafe and safe failures, respectively.

An analysis was conducted in 1975 (INEEL 2000) of the effects on the RSS of accidents and equipment failures occurring in the reactor building (first floor, and first and second basements). Events considered included the following:

- Fire (diesel oil fire, local fire in control area, local fire in PPS room, 480 Vac cable tray fire, local fire in second basement)
- Internal flooding (storage canal wall crack, firewater line break, high-pressure water line break, primary coolant line break)
- Structural failure (PPS room wall failure)
- Missiles (diesel generator set missile, pump motor missile)
- Vehicle damage (forklift accident).

Using predictions based on events most likely to occur, the results of this analysis indicate that the design of the RSS is adequate to accomplish its protective functions for each of the postulated single events. FMEA and PRA results are discussed in Chapter 7 (Instrumentation and Controls).

---

[a] The FMEA was performed on the proposed design, not on the as-built construction. The as-built design has been reviewed with regard to fire events with the results reported in Thatcher 2000a and Thatcher 2000b.

The Level 1 ATR PRA examined the following events related to instrumentation and control power and determined that they were not initiating events (i.e., events that threaten to lead to core damage):

- Loss of utility dc power, which may cause loss of switchgear control power and the dc emergency coolant pump
- Loss of instrument dc power (assuming ac power is available)
- Loss of instrument ac power (assuming dc power is available).

3.1.3.5 Criterion 24—Separation of Protection and Control Systems. The protection system shall be separated from control systems to the extent that failure of any single control system component or channel, or failure or removal from service of any single protection system component or channel which is common to the control and protection systems leaves intact a system satisfying all reliability, redundancy, and independence requirements of the protection system. Interconnection of the protection and control systems shall be limited so as to assure that safety is not significantly impaired.

3.1.3.5.1 Discussion—The reactor has a completely independent PPS that is separate from the normal operational control system. The current PPS was installed after the original SAR (deBoisblanc and Cohen 1965) was written; it includes special instruments, and special relays. These safety devices are not used for any operational function except for parameter indication. In addition, the PPS power is supplied from a 32 Vdc distribution system that is independent from other instrumentation power supplies. The updated PPS continues to meet the independence criteria established for the original PPS (Buescher 1993, specifically referring within Buescher's EDF to the December 23, 1988 letter from Vargo to Norin, and the Norin et al. report SAIC-88/1952).

The RSS subsystem of the PPS interfaces with the non-safety SATS. Isolation between these two systems is provided so that a failure of SATS does not affect the ability of the RSS to perform its intended safety function.

3.1.3.6 Criterion 25—Protection System Requirements for Reactivity Control Malfunctions. The protection system shall be designed to assure that Plant Protection Criteria for fuel performance are not exceeded for any single malfunction of the reactivity control systems, such as accidental withdrawal (not ejection) of control rods.

3.1.3.6.1 Information Note—Drop-out of control rods is deleted since it does not apply to the ATR.

3.1.3.6.2 Discussion—Because of the design and unique purpose of ATR, there are four reactivity-control systems (Section 3.9.4), each of different reactivity worth and design. However, only the safety rods operate as an immediate shutdown (scram) system; the action from the safety rods takes place in less than one second for pressurized operation. The remaining systems provide a slower reactivity insertion than the safety rods since they are basically designed for reactivity control during operation. However, they provide a further margin of safety and an alternate shut down mechanism.

Because of stringent design, testing, technical and procedural considerations, compliance with the intent of this functional requirement is satisfactory as applied to operation, testing, and maintenance of safety rods. Safety rod-drop tests, startup checks, and preventive maintenance verify operability of safety rod system prior to each startup. Approximately 20 years of operation during which no safety rods considered operational prior to startup have been found to be stuck when the operating reactor was shut down by a scram demonstrates the reliable nature of the safety rod drive system and supports satisfactory reliability, operation, testing, and maintenance for safe reactor operations.

Because of the low operating temperature (140-170°F), the multiple reactivity control systems, and the Chapter 4 (Reactor) requirement to operate with a sufficient number of operable safety rods to provide shutdown reactivity with one stuck rod (GDC 28), there is no expected fuel damage given any single failure within one of the reactivity control systems.

3.1.3.7 Criterion 26—Reactivity Control System Redundancy and Capability. Two independent reactivity control systems, of different design principles, shall be provided. One of the systems shall use control rods, preferably including a positive means for inserting the rods, and shall be capable of reliably controlling reactivity changes to assure that (under conditions of normal operation, including anticipated operational occurrences, and with appropriate margin for fuel burnup and malfunctions such as stuck rods) Plant Protection Criteria for fuel performance are not exceeded. The second reactivity control system shall be capable of reliably controlling the rate of reactivity changes resulting from planned, normal power changes (including xenon, fuel burnup) to assure Plant Protection Criteria for fuel performance are not exceeded. One of the systems, which controls reactivity, shall be capable of holding the reactor core subcritical.

3.1.3.7.1 Information Note—ATR has four reactivity control systems (safety rods, outer shim cylinders, regulating rods, and neck shims) that collectively are applicable to meeting GDC 26.

3.1.3.7.2 Discussion—Because of the design and unique purpose of ATR, there are four reactivity control systems (Section 3.9.4), each of different reactivity worth and design. However, of the four, only the safety rods operate as an immediate shutdown (scram) system.

The outer shim control cylinders (OSCCs) are used primarily to shift neutron flux (i.e., to adjust power in the individual loop positions) and secondarily, to compensate for fuel burnup. The OSCCs are the separate, redundant backup for the Safety Rod System. The neck shim rods are used primarily to compensate for fuel burnup and secondarily, to shift the neutron flux. The regulating rod servo control system provides a means for automatic power level control. The regulating rod, OSCC, and the neck shims are also used for power reversals and slow setbacks. Power reversal and slow setbacks can reduce reactor power without a complete shutdown.

Because of the low operating temperature (140-170°F), the multiple reactivity control systems, and the Chapter 4 (Reactor) requirement to operate with a sufficient number of operable safety rods to provide shutdown reactivity with one stuck rod (GDC 28), there is no expected fuel damage given any single failure within one of the reactivity control systems.

3.1.3.8 Criterion 27—Combined Reactivity Control Systems Capability. The reactivity control systems shall be designed to have a combined capability of reliably controlling reactivity changes to assure that under postulated accident conditions and with appropriate margins for stuck rods the capability to cool the core is maintained.

3.1.3.8.1 Information Note—The phrase, "in conjunction with poison addition by an emergency core cooling system," has been deleted from GDC 27 because the reactivity control systems are intended to meet this criterion without resorting to poison addition by the emergency core cooling system.

3.1.3.8.2 Discussion—See discussion for Criterion 25, Section 3.1.3.6.2. Because of the low operating temperature (140-170°F), the multiple reactivity control systems, and the Chapter 4 (Reactor) requirement to operate with a sufficient number of operable safety rods to provide shutdown reactivity with one stuck rod (GDC 28), there is no expected fuel damage given any single failure within one of the reactivity control systems.

The shim control system is used to compensate for the reactivity effects of the fuel and water temperature changes, fuel depletion, experiments, and fission-product buildup during reactor operation. The safety rods are used for fast shutdown of the reactor during abnormal operating conditions and for safely maintaining the reactor in a subcritical state. Preoperational analysis to determine the excess reactivity for each cycle, coupled with administrative controls on the permissible excess reactivity, ensures that the reactor cannot become critical from the withdrawal of the safety rods alone.

Core Safety Assurance calculations performed prior to each cycle of operation ensure that the reactor will be operated with sufficient safety rods to provide a reactivity worth of at least 5.8$ or 6.4$, dependent on the number of operating primary coolant pumps and assuming that the most reactive rod remains fully withdrawn, typically resulting in 5 or 6 safety rods being operable. This Chapter 4 (Reactor) requirement and assumption of the analyses described in Chapter 15 (Accident Analyses) does not ensure that the reactor will remain subcritical following shutdown under postulated accident conditions. However, an evaluation of the seismic shutdown reactivity basis (Atkinson 1997) considers the positive reactivity effects following reactor scram of fuel and moderator cooldown, regulating rod withdrawal, and xenon decay, coupled with seismically-induced draining of the loop inpile tubes. The evaluation concludes that complete insertion of three safety rods would be expected to maintain subcriticality, and that partial insertion of the three rods would be expected to marginally maintain subcriticality. Thus, operation with at least four operable safety rods provides adequate assurance of a successful shutdown.

3.1.3.9 Criterion 28—Reactivity Limits. The reactivity control systems shall be designed with appropriate limits on the potential amount and rate of reactivity increase to assure that the effects of postulated reactivity accidents can neither (1) result in damage to the primary coolant pressure boundary greater than limited local yielding nor (2) sufficiently disturb the core, its support structures, or other reactor vessel internals to impair significantly the capability to cool the core. These postulated reactivity accidents shall include consideration of rod ejection (unless prevented by positive means), changes in primary coolant temperature and pressure, and cold water addition.

3.1.3.9.1 Information Note—Concerning postulated reactivity accidents in GDC 28, two of the larger potential reactivity insertions result from (1) an experiment loop upset that voids the loop and (2) the postulated startup accident. These accidents are intended to be addressed under Criteria 70 and 25, respectively. The term "steamline rupture" (as a postulated reactivity accident) in GDC 28 has been deleted as not applicable to ATR, which does not have a steam-generator/turbine system.

3.1.3.9.2 Discussion—The ATR has a strong negative reactivity coefficient for temperature increases or coolant voiding in the fuel elements, which tends to naturally correct for power cooling mismatches. The reactivity coefficient for fuel-temperature increase is only weakly negative. The fuel temperature coefficient results from a decrease in distance between fuel plates caused by the expansion of the fuel with temperature. However, the temperature and voiding reactivity coefficients in the flux traps and the reflector are positive. Potential sources of positive reactivity or power increases are shim drum or shim rod movements, regulating rod movement, rapid cooldown of the primary coolant, seating of a perched fuel element, or experiment loop voiding.

The PPS includes two subsystems designed to trip the reactor during reactivity transients. The neutron level subsystem is a two-out-of-three system with a high power trip setpoint of ≤1.15 times full power during pressurized operation. The wide range neutron level subsystem is also a two-out-of-three system with a high power trip setpoint of ≤1.15 times full power during pressurized operation. The wide range system does not offer continuous period protection. Instead, it monitors reactor period by timing power increase over discrete intervals. Eleven scram points are provided over the five-decade range protected by the system.

A simultaneous withdrawal of all control elements (except the two regulating rods) was analyzed in Chapter 15 (Accident Analyses) as the maximum credible control rod ramp accident. The analyses indicate that the wide range neutron level system will shut down the reactor before fuel damage occurs.

The worst case fuel misloading accident has been identified as a perched fuel element transient. During refueling, a perched fuel element is defined as a fuel element left above its seated position. A reactivity transient would occur if the perched fuel element were subsequently to fall into its seat after the reactor is critical. Strict administrative procedures have been instituted to ensure that a significant perch of a fuel element does not occur.

The administrative procedures contain a series of checks and measures that constitute sufficient independent verification that each fuel element is seated or within one in. or less of being fully seated. The safety analyses discussed in Chapter 15 (Accident Analyses) demonstrate that the reactivity control system mitigates credible perched fuel accidents within the acceptable fuel element design limits.

No mechanism for a control rod drop accident (that inserts positive reactivity) has been identified. Thus, analysis of a control rod drop accident has not been performed.

The safety analysis discussed in Chapter 15 (Accident Analyses) analyzed credible reactivity accidents. In all cases analyzed, the postulated reactivity accidents did not challenge the integrity of the PCS pressure boundary.

3.1.3.10 Criterion 29—Protection Against Anticipated Operational Occurrences. "The protection and reactivity control systems shall be designed to assure an extremely high probability of accomplishing their safety functions in the event of anticipated operational occurrences."

3.1.3.10.1 Discussion—The reactor has a completely independent PPS separate from the normal operational control system. The PPS function is mitigative. These safety devices are not used for any operational function other than buffered outputs for system diagnostics and parameter indication. In addition, the PPS power is supplied from a 32 Vdc distribution system that is independent from other instrumentation power supplies. The PPS continues to meet the independence criteria established for the original PPS (Buescher 1993, specifically referring within Buescher's EDF to the December 23, 1988 letter from Vargo to Norin, and the Norin et al. report SAIC-88/1952).

The RSS subsystem of the PPS interfaces with the non-safety SATS. Isolation between these two systems is provided so that a failure of SATS does not affect the ability of the RSS to perform its intended safety function (Durney 1988).

As described in the original SAR (deBoisblanc and Cohen 1965), the control system has historically been divided into two parts: (a) nuclear instrumentation and (b) process instrumentation. The current design maintains this philosophy. The control system provides graded corrective actions to reduce the frequency of protective actions by the PPS. The PPS is capable of mitigating any credible control system malfunction.

Because of its unique purpose and design, ATR operations are cyclical in nature, requiring many startups and shutdowns. Safety rod-drop tests, startup checks, and preventive maintenance verify operability of safety rod system prior to each startup. Over 20 years of operation during which no safety rods considered operational prior to startup have been found to be stuck when the operating reactor was shut down by a scram, demonstrate the reliable nature of the safety rod drive system and supports satisfactory reliability, operation, testing, and maintenance for safe reactor operations. See discussion for Criterion 25, Section 3.1.3.6.2.

Because of the low operating temperature (140-170°F), the multiple reactivity control systems and the Chapter 4 (Reactor) requirement to operate with a sufficient number of operable safety rods to provide shutdown reactivity with one stuck rod (GDC 28), there is no expected fuel damage given any single failure within one of the reactivity control systems.

3.1.4 Fluid Systems

3.1.4.1 Criterion 30—Quality of Primary Coolant Pressure Boundary. Components which are part of the primary coolant pressure boundary shall be designed, fabricated, erected, and tested to the highest quality standards practical. Means shall be provided for detecting and, to the extent practical, identifying the location of the source of primary coolant leakage.

3.1.4.1.1 Discussion—The primary coolant pressure boundary was designed, fabricated, erected, and tested meeting the codes, standards, and requirements applicable at the time. As modifications to the primary coolant pressure boundary were implemented, the codes, standards, and requirements current at the time of implementation were met. Prior to operation, all piping of the PCS was pressure tested at 150% of design pressure. Also before operation, the safety relief valve seats were tested at 95% of nominal set pressure with air and were "bubble tight" per the methods of API Standard 527 (EG&G Idaho 1987, 1988a).

System leakage tests at nominal operating pressure are conducted before startup following each operating cycle per the requirements of ASME Section XI (ASME 1989b). Pressure boundary leakage is detected by a walkdown inspection of the pressurized primary system prior to reactor operation. During reactor operation, instrumentation is available for monitoring PCS leakage and the gland-seal and degassing-system makeups. A system pressure test is conducted at least once each ten-year period.

3.1.4.2 Criterion 31—Fracture Prevention of Primary Coolant Pressure Boundary. "The primary coolant pressure boundary shall be designed with sufficient margin to assure that when stressed under operating, maintenance, testing, and postulated accident conditions (1) the boundary behaves in a nonbrittle manner and (2) the probability of rapidly propagating fracture is minimized. The design shall reflect consideration of service temperatures and other conditions of the boundary material under operating, maintenance, testing, and postulated accident conditions and the uncertainties in determining (1) material properties, (2) the effects of irradiation on material properties, (3) residual, steady state, and transient stresses, and (4) size of the flaws."

3.1.4.2.1 Discussion—An evaluation of irradiation embrittlement of the reactor vessel has been completed. Analysis of the vessel shows that neutron embrittlement is not currently a concern and will not be significant for operation through the year 2014 (Durney et al. 1987).

The PCS, was designed, fabricated, erected, and tested to pertinent codes and standards current at the time of construction. The PCS was subsequently analyzed ASME Section III, Class 2, 1977 Edition (Class I for Seismic) and found to meet the intent of Section III. The PCS surge tank and surge tank supports meet the intent of Section VIII of the ASME Boiler and Pressure Vessel Code (ASME 1989b) edition (Snow 1991a, 1993, 1994a). PCS construction materials were chosen that are ductile and resistant to erosion, corrosion, intergranular stress corrosion cracking, and embrittlement. Over-pressure protection is provided by two sets of two safety relief valves.

3.1.4.3 Criterion 32—Inspection of Primary Coolant Pressure Boundary. "Components which are part of the primary coolant pressure boundary shall be designed to permit (1) periodic inspection and testing of important areas and features to assess their structural and leak-tight integrity, and (2) an appropriate material surveillance program for the reactor pressure vessel."

3.1.4.3.1 Information Note—Periodic inspection and testing is performed in accordance with the *ATR Inservice Inspection (ISI) Plan* (based on the ASME 1989b Edition, ASME Boiler and Pressure Vessel Code, Section XI).

3.1.4.3.2 Discussion—Piping of the PCS was pressure tested at 150% of design pressure. In accordance with the ISI Plan (INEEL 2002), the piping is pressure tested every 10 years. An ISI plan was originally developed for the systems and components within the PCS pressure boundary using the ASME Boiler and Pressure Vessel Code, Section XI, 1974 Edition as a guide. The ISI Plan has been updated to the 1989 Edition of the Code. The ATR, however, was designed and constructed before requirements for ISI were implemented so that some limitations in accessibility are encountered during the inspection and testing of the PCS components and systems. Vessel material surveillance specimens were not included with the original installation of the reactor vessel.

The PCS leak rate is calculated prior to reactor operation in the pressurized mode, and instrumentation is available to monitor PCS leakage during reactor operation in the pressurized mode, or reactor shutdown mode. During pressurized operation, gland-seal makeup and degassing-system makeup can be monitored. A walkdown of the PCS (pressure boundary fault leakage) is performed prior to reactor operation after having been in reactor shutdown with the PCS at atmospheric pressure.

3.1.4.4 Criterion 33—Primary Coolant Makeup. "A system to supply primary coolant makeup for protection against small breaks in the primary coolant pressure boundary shall be provided. The system safety function shall be to assure that Plant Protection Criteria for fuel performance are not exceeded as a result of primary coolant loss due to leakage from the primary coolant pressure boundary and rupture of small piping or other small components which are part of the boundary. The system shall be designed to assure that for on-site electric power system operation (assuming off-site power is not available), and for off-site electric power system operation (assuming on-site power not available) the system safety function can be accomplished using the piping, pumps, and valves used to maintain coolant inventory during normal reactor operation."

3.1.4.4.1 Discussion—Reactor primary coolant makeup is provided by one of two systems, the low pressure demineralized water (LDW) system for normal PCS makeup and the EFIS for off-normal PCS makeup.

The normal PCS makeup is achieved by using the pressurizing pumps, which are supplied by the LDW. The pressurizing pumps can be powered either from a commercial or diesel bus. LDW can also be supplied to the PCS through the low head flush system, but must be manually valved in. The normal supply LDW pumps (demineralized water transfer pumps) are on the commercial power bus with diesel back-up power.

The EFIS provides emergency reactor core cooling and flooding of the reactor vessel in the event of a major break in the PCS piping. It also provides makeup for the long-term complete loss of flow accident (CLOFA) if other means are not available. This ESF is designed to activate at very low pressure or at a low water level in the reactor vessel. The EFIS is supplied by the overhead raw water storage tank or by any one of three safety related firewater pumps: one pump is an electric motor-driven by commercial-diesel power; the other two pumps are diesel-driven.

3.1.4.5 Criterion 34—Residual Heat Removal. A system to remove residual heat shall be provided. The system safety function shall be to transfer fission product decay heat and other residual heat from the reactor core at a rate such that Plant Protection Criteria for fuel performance and design conditions of the primary coolant pressure boundary are not exceeded.

Suitable redundancy in components and features, and suitable interconnections, leak detection, isolation, and confinement capabilities shall be provided to assure that for on-site electric power system operation (assuming off-site power is not available), and for off-site electric power system operation (assuming on-site power is not available), the system safety function can be accomplished, assuming a single failure.

3.1.4.5.1 Discussion—The ATR has multiple means for performing decay heat removal (DHR) as shown in Table 3.1-3. The first two decay heat removal methods involve closed-loop heat transfer paths from the PCS to the atmosphere via the cooling tower (i.e., the normal heat sink). As noted in the Level 1 PRA (Eide, Khericha, and Thatcher 1991), no losses of normal heat sink have occurred in 18 years of operation. From this operating history, an expected frequency of loss of normal heat sink is 0.013/yr.

Heat-transfer paths involved in the next three DHR methods (3, 4, and 5 in Table 3.1-3) provide makeup to the PCS and remove heat by draining water from the PCS (i.e., into the reactor building which acts as the heat sink). DHR method 3 was used to mitigate the loss of heat sink and loss of flow event in Chapter 15 (Accident Analysis). Using this method, ATR Plant Protection Criteria described in Chapter 15 (Accident Analysis) were met. The final decay heat removal method involves passive heat transfer from the PCS to the reactor building. Passive heat transfer is a short-term method. Long term DHR is accomplished by methods 3, 4, and 5 in Table 3.1-3.

Primary coolant inventory makeup normally is performed by the primary degassing and pressurizing system. Emergency makeup can be provided by Methods 3, 4, and 5 of the open-loop DHR methods shown in Table 3.1-3.

Table 3.1-3 shows that redundant and diverse systems are available for accomplishing the DHR function, as well as the primary coolant inventory makeup. The DHR functions can be accomplished by means that are not dependent on the commercial electric power (i.e., passive DHR, or firewater injection for DHR and primary coolant makeup).

3.1.4.6 Criterion 35—Emergency Core Cooling. A system to provide abundant emergency core cooling shall be provided. The system-safety function shall be to transfer heat from the reactor core following any credible loss of primary coolant at a rate such that (1) fuel and clad damage that could interfere with continued effective core cooling is prevented and (2) clad metal-water reaction is limited to negligible amounts.

Suitable redundancy in components and features, and suitable interconnections, leak detection, isolation, and confinement capabilities shall be provided to assure that for on-site electric power system operation (assuming off-site power is not available), and for off-site electric power system operation (assuming on-site power is not available), the system safety function can be accomplished, assuming a single failure.

3.1.4.6.1 Information Note—As in GDC 16, the word "containment" is replaced by "confinement." For justification, see information note for Criterion 16.

3.1.4.6.2 Discussion—The EFIS provides emergency reactor core cooling and flooding of the reactor vessel in the event of a major break in the PCS piping or in an event that results in loss of primary coolant. This ESF is designed to activate at a predetermined low pressure, or when the water level falls to a predetermined height above the top of the core. The ATR firewater system consists of the raw-water storage tanks, diesel-driven and electric driven firewater pumps, buried distribution piping, and associated valves and controls necessary to supply water to the EFIS in the ATR reactor building. The bottom head and upper vessel EFIS provide emergency core cooling by injecting firewater into the reactor vessel.

Two 4,700 gpm emergency coolant pumps (one a standby) operate in the closed primary loop. Their capacity is based on flow requirements to prevent exceeding Plant Protection Criteria for fuel performance during low-power flux runs and reactor flow requirements after loss of electrical power to all primary coolant pumps.

To ensure the required flow after primary coolant pump coastdown without reliance on emergency pump startup, one emergency coolant pump operates continuously during reactor operations. On loss of primary coolant pressure, the check valve on the emergency coolant pump discharge opens, enabling the emergency coolant pump flow to circulate through in the primary coolant loop.

The standby emergency coolant pump is available in case of a loss of flow event in the operating emergency coolant pump. One emergency coolant pump is adequate for removal of reactor heat during low-power flux mapping runs. Both pumps typically are operated during the low-power runs so that loss of a single electrical system or pump will not result in a complete loss of flow. A scram is initiated on low flow.

3.1.4.7 Criterion 36—Inspection of Emergency Core Cooling System. The emergency core cooling system shall be designed to permit appropriate periodic inspection of important components to assure the integrity and capability of the system.

3.1.4.7.1 Information Note—Examples of the term "important components" in GDC 36, which refer to power reactors, do not all apply to ATR and have been deleted.

3.1.4.7.2 Discussion—Prior to the initial reactor startup, flow tests were performed for the Bottom Head EFIS using raw water from the EFIS. Since then, firewater has not been injected into the reactor from the EFIS.

The instrumentation and control components of the EFIS are, to the extent practical, located in areas that are accessible during reactor operations that permit periodic inspections. EFIS equipment and instruments scheduled for periodic inspection include level control valves, pressure indicators, flow indicators, and solenoid valves (INEEL 2002).

The emergency pumps and associated systems are periodically inspected as specified in the inservice inspection plan (ISI) (INEEL 2002). ATR, however, was designed and constructed prior to implementing an ISI program. As a result, some areas of the PCS are inaccessible. Chapter 14 (Initial Test Program, Inservice Surveillance, and Maintenance) describes ATR's ISI program.

3.1.4.8 Criterion 37—Testing of Emergency Core Cooling System. The emergency core cooling system shall be designed to permit appropriate periodic pressure and functional testing to assure (1) the structural and leak-tight integrity of its components, (2) the operability and performance of the active components of the system, and (3) the operability of the system as a whole and, under conditions as close to design as practical, the performance of the full operational sequence that brings the system into operation.

3.1.4.8.1 Information Note—The details concerning the term "full operational sequence that brings the system into operation" in GDC 37 have been deleted. The specific systems listed in GDC 37 apply to power reactors and do not all apply to the ATR.

3.1.4.8.2 Discussion—The EFIS valving and controls are capable of being tested through the control range without injecting firewater into the vessel. The flow instrumentation is capable of inplace testing and calibration (see discussion under GDC 36).

The emergency firewater pumps, emergency coolant pumps, and selected valves for each set of pumps are periodically tested as part of the ISI Program (INEEL 2002). Chapter 14 (Initial Test Program, Inservice Surveillance and Maintenance) describes ATR's ISI program.

3.1.4.9 Criterion 38—Confinement Heat Removal. "A system to remove heat from the reactor containment shall be provided. The system safety function shall be to reduce rapidly, consistent with the functioning of other associated systems, the containment pressure and temperature following any loss-of-coolant accident and maintain them at acceptable low levels.

"Suitable redundancy in components and features, and suitable interconnections, leak detection, isolation, and containment capabilities shall be provided to assure that for onsite electric power system operation (assuming offsite power is not available) and for offsite electric power system operation (assuming onsite power is not available) the system safety function can be accomplished, assuming a single failure."

3.1.4.9.1 Basis—The objective of the containment heat removal system in GDC 38, 39, and 40 is to reduce rapidly and maintain the containment pressure and temperature at acceptable levels, following a loss-of-coolant accident. Since the ATR is a moderate pressure, low temperature facility, a confinement heat removal system is not needed. Criteria 38, 39, and 40 are not applicable.

3.1.4.10 Criterion 39—Inspection of Confinement Heat Removal. "The containment heat removal system shall be designed to permit appropriate periodic inspection of important components, such as the torus, sumps, spray nozzles, and piping to assure the integrity and capability of the system."

3.1.4.10.1 Discussion—This criterion is not applicable to the ATR (see Section 3.1.4.9.1).

3.1.4.11 Criterion 40—Testing of Confinement Heat Removal System. "The containment heat removal system shall be designed to permit appropriate periodic pressure and functional testing to assure (1) the structural and leak-tight integrity of its components, (2) the operability and performance of the active components of the system, and (3) the operability of the system as a whole and under conditions as close to the design as practical, the performance of the full operational sequence that brings the system into operation, including operation of applicable portions of the protection system, the transfer between normal and emergency power sources, and the operation of the associated cooling water system."

3.1.4.11.1 Discussion—This criterion is not applicable to the ATR (see Section 3.1.4.9.1).

3.1.4.12 Criterion 41—Confinement Atmosphere Cleanup. Systems to control fission products, hydrogen, oxygen, and other substances which may be released into the reactor confinement shall be provided as necessary to reduce, consistent with the functioning of other associated systems, the concentration and quantity of fission products released to the environment following postulated accidents, and to control the concentration of hydrogen or oxygen and other substances in the confinement atmosphere following postulated accidents to assure that confinement integrity is maintained.

Each system shall have suitable redundancy in components and features and suitable interconnections, leak detection, isolation, and confinement capabilities to assure that for on-site electric power system operation (assuming off-site power is not available) and for off-site electric power system operation (assuming on-site power is not available), its safety function can be accomplished, assuming a single failure.

3.1.4.12.1 Information Note—Here, as in GDC 16, the word "containment" is replaced with "confinement." For justification, see the information note for Criterion 16.

3.1.4.12.2 Discussion—The confinement system does not use filters for atmospheric cleanup of airborne radioactive contamination. A nonsafety-related spray system, arranged to wash down the walls and air inside the reactor area, is provided to reduce the concentration of fission products in the air contained in the confinement area should a severe nuclear accident occur. However, the evaluation of off-normal sequences including the severe accidents does not assume a reduction in fission products as a result of the spray system. Therefore, Criteria 41, 42, and 43 are not applicable.

3.1.4.13 Criterion 42—Inspection of Confinement Atmosphere Cleanup System. "The confinement atmosphere cleanup system shall be designed to permit appropriate periodic inspection of important components, such as filter frames, ducts, and piping to assure the integrity and capability of the system."

3.1.4.13.1 Discussion—This criterion is not applicable to the ATR (see Section 3.1.4.12.2).

3.1.4.14 Criterion 43—Testing of Confinement Atmosphere Cleanup System. The confinement atmosphere cleanup system shall be designed to permit appropriate periodic functional testing to assure (1) the structural and leak-tight integrity of its components, (2) the operability and performance of the active components of the system such as fans, filters, dampers, pumps, and valves, and (3) the operability of the system as a whole and, under conditions as close to design as practical, the performance of the full operational sequence that brings the system into operation.

3.1.4.14.1 Information Note—The details concerning the term "full operational sequence that brings the system into operation," in GDC 43 have been deleted. The specific systems listed in GDC 43 apply to power reactors and do not all apply to the ATR.

3.1.4.14.2 Discussion—This criterion is not applicable to the ATR (see Section 3.1.4.12.2).

3.1.4.15 Criterion 44—Cooling Water. A system or systems to transfer heat from SSC important to safety, to an ultimate heat sink, shall be provided. The system safety function shall be to transfer the combined heat load of these SSC under normal operating and accident conditions.

Suitable redundancy in components and features, and suitable interconnections, leak detection, and isolation capabilities shall be provided to assure that for on-site electric power system operation (assuming off-site power is not available) and for off-site electric power system operation (assuming on-site power is not available) the system safety function can be accomplished assuming a single failure.

3.1.4.15.1 Information Note—Passive means of cooling SSC important to safety also contribute to meeting the intent of this GDC.

3.1.4.15.2 Discussion—The PCS is described in detail in Chapter 5 (Primary Coolant System).

3.1.4.16 Criterion 45—Inspection of Cooling Water System. The cooling water system shall be designed to permit adequate periodic inspection of important components, such as heat exchangers and piping, to assure the integrity and capability of each system.

3.1.4.16.1 Discussion—An ISI plan has been developed for the PCS using the ASME Code, Section XI as a guide (ASME 1989b). System leakage tests at nominal operating pressure are conducted before startup following refueling outages. A system pressure test is conducted once each ten-year period.

3.1.4.17 Criterion 46—Testing of Cooling Water System. The cooling water system shall be designed to permit appropriate periodic pressure and functional testing to assure (1) the structural and leaktight integrity of its components, (2) the operability and performance of the active components of the system, and (3) the operability of the system as a whole and, under conditions as close to design as practical, the performance of the full operational sequence that brings the system into operation.

3.1.4.17.1 Information Note—The details concerning the term "full operational sequence that brings the system into operation" in GDC 46 have been deleted. The specific systems listed in GDC 46 apply to power reactors and do not all apply to the ATR.

3.1.4.17.2 Discussion—An ISI plan has been developed for the PCS using the ASME Code, Section XI (ASME 1989b) as a guide. System leakage tests at nominal operating pressure are conducted before startup following refueling outages. A system pressure test is conducted once each ten-year period.

3.1.5 Reactor Confinement

3.1.5.1 Criterion 50—Confinement Design Basis. The reactor confinement structure, including access openings and penetrations, shall be designed to limit leakage to the environment to be consistent with ATR Plant Protection Criteria for radioactive releases.

3.1.5.1.1 Basis—This GDC has been significantly altered because the ATR has neither a commercial-type containment nor a containment heat removal system. Instead the ATR is provided with a confinement that acts as a barrier to limit the release of fission products resulting from an accident. A containment and containment heat removal system are not necessary because of the ATR's low energy content and its remote location.

3.1.5.1.2 Discussion—Unlike commercial nuclear plants, the ATR does not have containment purge valves to control the containment pressure, or isolation valves to isolate the containment in case of a severe accident. Instead, the ATR uses a ventilation system, including exhaust and supply fan systems, exhaust stack, and closure dampers to control confinement atmospheric conditions during normal operation (deBoisblanc, Cohen, and Walker 1966). In addition, the ATR has a confinement that can withstand a pressure differential of 7.5 in. of water (Close 1988a).

In case of high radiation in the confinement, the RMSS will realign the ventilation system and seal the confinement (deBoisblanc, Cohen, and Walker 1966; Atkinson 1988). A number of possible failure modes of the ventilation system's critical components were assessed with results showing that the failure modes could not defeat the confinement system (deBoisblanc, Cohen, and Walker 1966).

In addition to the ventilation system, the ATR has a nonsafety grade water spray feature that could be used to reduce airborne radioactivity under accident conditions (Atkinson 1988). Finally, ATR's missile shield plug placed into the transfer plate for inpile experiments is used to shield the confinement roof against any missile projectiles ejected from the inpile tube.

3.1.5.2 Criterion 51—Fracture Prevention of Confinement Pressure Boundary. "The reactor containment boundary shall be designed with sufficient margin to assure that under operating, maintenance, testing, and postulated accident conditions (1) its ferritic materials behave in a nonbrittle manner and (2) the probability of rapidly propagating fracture is minimized. The design shall reflect consideration for service temperatures and other conditions of the containment boundary material during operation, maintenance, testing, and postulated accident conditions, and uncertainties in determining (1) material properties, (2) residual, steady state, and transient stresses, and (3) size of flaws."

3.1.5.2.1 Basis—This GDC is not applicable to the ATR confinement structure, because the confinement is not a high pressure boundary built to ASME standards or other code. Prevention of confinement overpressure is implicit in Criterion 16, which states "that the confinement design conditions important to safety are not exceeded for as long as postulated accident conditions require."

3.1.5.3 Criterion 52—Capability for Confinement Leakage Rate Testing. The reactor confinement and other equipment which may be subjected to confinement test conditions shall be designed so that periodic integrated leakage-rate testing can be conducted.

3.1.5.3.1 Information Note—The word "confinement" has been substituted for "containment," and the final phrase in GDC 52 "at containment design pressure" has been deleted. ATR has a confinement which can withstand a small pressure differential (measured in inches of water). The ATR conducts confinement leakage tests measuring the air exchange rate.

3.1.5.3.2 Discussion—The ATR is designed to permit periodic confinement leakage tests and operability tests on the ventilation system components. A conservative limit of 100% of the total volume of confinement (when EFIS is actuated) is used for an analysis upper limit (Lucas 2000). A study has shown that consequences could still not reach the 10 CFR 100 thyroid limits of 300 rem at the low population zone boundary even under the postulated hypothetical severe accident (Close 1988b). The confinement leak rate testing is described in Chapter 6 (Engineered Safety Features).

3.1.5.4 Criterion 53—Provisions for Confinement Testing and Inspection. The reactor confinement shall be designed to permit (1) appropriate periodic inspection of all important areas, such as penetrations, and (2) an appropriate surveillance program.

3.1.5.4.1 Basis—Item (c) of GDC 53 has been deleted. It calls for periodic testing of individual penetrations at containment design pressures. The ATR does not have provisions for such testing. Instead, all confinement penetrations are verified by surveillance to be properly sealed prior to any reactor startup after the PCS boundary has been opened. The major penetrations are monitored continuously on the reactor data acquisition system (RDAS) during reactor operation and outage periods. The approach is consistent for a confinement structure because there are no credible accident sequences that challenge the design.

3.1.5.4.2 Discussion—The confinement portion of the reactor building is designed to act as a final barrier to delay release of airborne radioactive contamination resulting from an accidental release of radioactivity from the reactor or experiments. All fixed penetrations of the confinement area are sealed, and ventilation penetrations are equipped with gasketed dampers. Should high radiation be detected in the building exhaust, the confinement will be closed by dampers and by shutoff of the ventilation supply and exhaust fans.

Personnel periodically conduct confinement leakage tests and operability tests on the ventilation system components. The building seal-actuating control system (RMS-1) is tested periodically. The channels (detector to comparator, inclusive) are periodically checked for operability and setpoint. The position of the dampers, open or closed, is displayed on the RDAS. This provides information after activation of the system as to the position of the dampers.

3.1.5.5 Criterion 54—Fluid Systems Penetrating Confinement. Piping and other fluid systems penetrating confinement shall be provided with appropriate capabilities, which reflect the importance to safety of isolating these fluid systems, while giving due consideration to the overall function of the confinement and the type of penetration. Such systems shall be designed so that the established confinement leak-rate is not exceeded.

3.1.5.5.1 Basis—GDC 54 has been extensively modified. In particular, reference to specific capabilities (leak detection, isolation, containment, redundancy, reliability and performance) has been deleted from the first sentence. Also the capabilities specified in the second sentence (testing operability of isolation valves and determining valve leakage) have been deleted. ATR piping systems do not have the specific, detailed isolation valve requirements delineated in GDC 54-56. Criterion 54 is intended to replace Criteria 55 and 56.

3.1.5.5.2 Discussion—Fluid systems that penetrate the confinement boundary include:

- Firewater
- Potable water
- Secondary cooling water
- Plant air
- Warm waste water

- Primary coolant recycle system (PCRS)[a]
- Heating and ventilating (H&V) supply and exhaust
- Raw water
- Demineralized water
- Utility cooling water
- Instrument air
- Hot waste water
- Steam (disconnected)
- Cold waste water
- High pressure air.

All of the above systems, except plant air, instrument air, high pressure air, warm waste, hot waste, primary coolant recycle system[a], the H&V system, and supply and exhaust ducts, are closed systems that do not connect directly to the confinement atmosphere. The Radiation Monitoring and Seal System (RMSS), discussed in Criterion 50, isolates the H&V duct penetrations. Plant air and instrument air are part of the utility compressed air system; the compressed air is normally significantly above the confinement air pressure. Although the plant air and instrument air are not isolated by the RMSS, the utility compressed air penetrations will not provide pathways from the confinement to the environment. The same is true for the high-pressure air system which operates at pressures even higher than plant and instrument air.

3.1.5.6 Criterion 55—Reactor Coolant Pressure Boundary Penetrating Confinement. "Each line that is part of the reactor coolant pressure boundary and that penetrates primary reactor containment shall be provided with containment isolation valves [as shown in the following list], unless it can be demonstrated that the containment isolation provisions for a specific class of lines, such as instrument lines, are acceptable on some other defined basis:

A. One locked closed isolation valve inside and one locked closed isolation valve outside containment; or

B. One automatic isolation valve inside and one locked closed isolation valve outside containment; or

C. One locked closed isolation valve inside and one automatic isolation valve outside containment. A simple check valve may not be used as the automatic isolation valve outside containment; or

D. One automatic isolation valve inside and one automatic isolation valve outside containment. A simple check valve may not be used as the automatic isolation valve outside containment.

---

[a] The primary coolant recycle system (PCRS) is located in TRA-689 and tied to TRA-670 by pipe. TRA-689 is not in use at this time. The piping between TRA-689 and TRA-670 is isolated by both MOV-32-1 and MOV-1-909. Since the piping connections to TRA-689 are downstream of either a <3-in. orifice or valve, any break is bounded by the analysis in Chapter 15.6.

"Isolation valves outside containment shall be located as close to containment as practical and upon loss of actuating power, automatic isolation valves shall be designed to take the position that provides greater safety.

"Other appropriate requirements to minimize the probability or consequences of an accidental rupture of these lines or of lines connected to them shall be provided as necessary to assure adequate safety. Determination of the appropriateness of these requirements, such as higher quality in design, fabrication, and testing, additional provisions for inservice inspection, protection against more severe natural phenomena, and additional isolation valves and containment, shall include consideration of the population density, use characteristics, and physical characteristics of the site environs."

3.1.5.6.1 Discussion—GDC 55 is replaced by GDC 54 (see Section 3.1.5.5.1).

3.1.5.7 Criterion 56—Primary Confinement Isolation. "Each line that connects directly to the confinement atmosphere and penetrates primary reactor confinement shall be provided with confinement isolation valves as follows, unless it can be demonstrated that the confinement isolation provisions for a specific class of lines, such as instrument lines, are acceptable on some other basis:

- One locked closed isolation valve inside and one locked closed isolation valve outside confinement; or
- One automatic isolation valve inside and one locked closed isolation valve outside confinement; or
- One locked closed isolation valve inside and one automatic isolation valve outside confinement. A simple check valve may not be used as the automatic isolation valve outside confinement; or
- One automatic isolation valve inside and one automatic isolation valve outside confinement. A simple check valve may not be used as the automatic isolation valve outside confinement.

"Isolation valves outside confinement shall be located as close to confinement as practical and upon loss of actuating power, automatic isolation valves shall be designed to take the position that provides greater safety."

3.1.5.7.1 Information Note—As in GDC 16, the word "containment" is replaced by "confinement." For justification, see information note for GDC 16.

3.1.5.7.2 Discussion—GDC 56 is replaced by GDC 54 (see Section 3.1.5.5.1).

3.1.5.8 Criterion 57—Closed System Isolation Valves. Each line that penetrates the confinement and is neither part of the reactor coolant pressure boundary nor connected directly to the confinement atmosphere and which has the potential to carry radioactive material out of the confinement because of reactor coolant pressure boundary leakage or has the potential to provide a direct path out of the confinement due to a reasonably probable component failure shall be capable of being sufficiently and successfully isolated to successfully mitigate or control the radioactive material release outside of confinement.

3.1.5.8.1 Basis—GDC 57 has been modified for ATR systems and operation by simplifying the criterion to be performance based rather than to specify specifically how the criterion is to be satisfied. The confinement and fluid systems subject to this criterion are low pressure systems and can be easily isolated. Isolation using manual valves is not precluded when the potential radiation releasing event allows sufficient access and time for successful manual isolation.

3.1.5.8.2 Discussion—This criterion applies to the following fluid systems:

- Firewater
- Secondary coolant water
- Low pressure demineralized water
- Utility cooling water
- Warm waste water
- Hot waste water
- Primary coolant recycle system[a]

Each of these systems is capable of being sufficiently and successfully isolated if a radiation release into the system greater than allowable for normal operations were to occur.

3.1.6 Fuel and Radioactivity Control

3.1.6.1 Criterion 60—Control of Releases of Radioactive Materials to the Environment. "The [ATR Facility] design shall include means to control suitably the release of radioactive materials in gaseous and liquid effluents and to handle radioactive solid wastes produced during normal reactor operation, including anticipated operational occurrences. Sufficient holdup capacity shall be provided for retention of gaseous and liquid effluents containing radioactive materials, particularly where unfavorable site environmental conditions can be expected to impose unusual operational limitations upon the release of such effluents to the environment."

3.1.6.1.1 Discussion—Gaseous wastes are collected by the ventilation system, which is monitored by both a continuous stack gas monitor and by safety-related radiation monitors that actuate confinement isolation.

Liquid radioactive wastes are controlled by piping systems that collect liquid wastes from various sources in the ATR. Liquids are monitored, sampled, treated, and/or stored for proper disposal based on activity content and chemistry. Radioactive waste management is described in Chapter 11 (Radioactive and Hazardous Material Waste Management).

---

[a] The primary coolant recycle system (PCRS) is located in TRA-689 and tied to TRA-670 by pipe. TRA-689 is not in use at this time. The piping between TRA-689 and TRA-670 is isolated by both MOV-32-1 and MOV-1-909. Since the piping connections to TRA-689 are downstream of either a <3-in. orifice or valve, any break is bounded by the analysis in Chapter 15.6.

Radioactive solid wastes are manually collected in controlled accumulation areas. Handling of radioactive solid wastes is controlled by procedures that govern how wastes are accumulated, by packaging and labeling requirements, and by requirements for transportation to an approved treatment, storage, or disposal facility. Radioactive solid waste management is described in Chapter 11 (Radioactive and Hazardous Material Waste Management).

3.1.6.2 Criterion 61—Fuel Storage and Handling and Radioactivity Control. The fuel storage and handling, radioactive waste, and other systems which may contain radioactivity shall be designed to assure adequate safety under normal and postulated accident conditions. These systems shall be designed (1) with a capability to permit appropriate periodic inspection and testing of components important to safety, (2) with suitable shielding for radiation protection, (3) with appropriate, confinement, and filtering systems, (4) with a residual heat removal capability having reliability and testability that reflects the importance to safety of decay heat and other residual heat removal, and (5) to prevent significant reduction in fuel storage coolant inventory under accident conditions.

3.1.6.2.1 Discussion—Fuel storage and handling, irradiated fuel and experiment storage and handling, and radioactive waste management systems are designed to ensure adequate safety under normal operating conditions and postulated accident conditions.

New fuel for the ATR is stored in the Nuclear Materials Inspection and Storage (NMIS) Facility which is the subject of a specific safety analysis report. New fuel is transported from the NMIS to the ATR in the same shipping container used to transfer the element from the off-site vendors.

Irradiated fuel and experiments are temporarily stored in the canal for either reloading into the core or for later shipment to other facilities for examination or disposal. Irradiated fuel and experiments are stored and transported in devices that ensure noncritical configurations. Radiation shielding is provided by the concrete canal walls and floor, and by the water cover of irradiated material stored in the canal. The canal and its safety evaluation are discussed in Chapter 9 (Auxiliary Systems). Chapter 9 describes the equipment and systems associated with the storage canal and the shielding provided by the canal design. Administrative procedures ensure that irradiated fuel and experiments are sufficiently cool and that their internal heat generation rates are sufficiently low that adequate cooling is achieved by simple immersion in the storage canal. To ensure adequate safety, administrative restrictions are placed on cask lifts in the canal area and on placement of the irradiated fuel. In addition, the canal is equipped with an alarm for low canal water level, emergency canal firewater makeup, and bulkheads that can dam sections of the canal. Chapter 15 (Accident Analyses) discusses the safety analysis of postulated canal accidents and their consequences.

There are no confinement and filtering systems associated with the canal area. However, as with the confinement, air pressure is normally maintained slightly less than the atmospheric air pressure, ensuring that leakage is normally into the building. The canal area is monitored by continuous air monitors (CAMs). The CAMs provide local and remote warnings of radiation release within the canal area. ATR ventilation systems are described in Chapter 9 (Auxiliary Systems).

Radioactive solid waste storage and handling for Criterion 60, *Control of Release of Radioactive Material to the Environment*, are discussed in Section 3.1.6.1.1.

3.1.6.3 Criterion 62—Prevention of Criticality in Fuel Storage and Handling. "Criticality in the fuel storage and handling system shall be prevented by physical systems or processes, preferably by use of geometrically safe configurations."

3.1.6.3.1 Discussion—Irradiated fuel and experiments are temporarily stored in the storage canal either for reloading into the core or for later shipment to other facilities for examination or disposal. The canal contains fuel storage grids whose compartments are lined with cadmium. Without taking credit for the cadmium, the physical configuration and the spacing of storage grids 5, 6, 9 through 23, 29, 35, and 36 ensure adequate criticality margin for fuel elements. Fissile material control is governed by criticality safety program requirements. The fuel storage racks are designed to protect the fuel elements while storing them in a non-critical safe array. Holman (1988) found that neither fully loaded racks nor racks loaded on one side only would tip over during the postulated SSE and that, consequently, the fuel elements would remain safely, non-critical, contained in the fuel storage racks.

3.1.6.4 Criterion 63—Monitoring Fuel and Waste Storage. "Appropriate systems shall be provided in fuel storage and radioactive waste systems and associated handling areas (1) to detect conditions that may result in loss of residual heat removal capability and excessive radiation levels and (2) to initiate appropriate safety actions."

3.1.6.4.1 Discussion—If the storage canal develops a leak, the fuel can be isolated using the canal bulkheads from the leak or moved to other areas of the canal that can be isolated from the leaking area with bulkheads. A canal low-level alarm will promptly notify operators that the canal is leaking, thus allowing ample time for operators to take corrective actions and/or move the fuel. The emergency firewater canal makeup will initiate automatically on a canal low level condition to keep the fuel cooled. The discussion for Criterion 61 further discusses the canal design; see Section 3.1.6.2.1.

3.1.6.5 Criterion 64—Monitoring Radioactivity Releases. Means shall be provided for monitoring the reactor confinement atmosphere, effluent discharge paths, and the plant environs for radioactivity that may be released from normal operations, including anticipated operational occurrences, and from postulated accidents.

3.1.6.5.1 Information Note—As in GDC 16, the word "containment" has been replaced with "confinement." For justification, see information note with Criterion 16. In GDC 64, the phrase "spaces containing components for recirculation of loss-of-coolant accident fluids" has been deleted because the ATR design does not require recirculation to maintain coolant inventory.

3.1.6.5.2 Discussion—The reactor confinement and plant atmosphere are constantly sampled for airborne reactivity. The continuous air monitors (CAMs) provide local and remote warnings of radiation releases within the plant. The CAMs interface with the RMSS. Potential airborne contamination is swept by air flow from clean areas to potentially contaminated areas and then to the exhaust stack. Stack effluent is monitored. Upon abnormal radiation detection in the stack effluent, the RMSS will isolate the confinement and sound the alarm.

Monitored and controlled effluent discharge paths for Criterion 60, *Control of Release of Radioactive Material to the Environment*, are discussed in Section 3.1.6.1.1.

3.1.7 New Criteria for ATR

3.1.7.1 Criterion 70—Experiment Facilities. Experiment facilities, installed in the reflector tank both within and outside the reactor core shall be designed so their fault consequence limits are consistent with the ATR Plant Protection Criteria. Experiment facilities and their associated out-of-reactor SSC important to safety shall meet applicable overall requirements (GDC 1-5).

3.1.7.1.1 Basis—Criterion 70 addresses the experiment facilities which represent the reason for ATR's existence and which are not addressed in the GDC for nuclear power units. The criterion establishes that the design basis for these facilities is consistent with the design basis for the reactor. Two important aspects of that consistency are the: (1) consequences of various types of failures, and (2) applicable overall GDC requirements, such as quality and fire protection. In this manner, Criterion 70 is intended to assure that the experiment facilities are at least as safe as the ATR Facility itself. The specific application of Criterion 70 and overall GDC requirements is detailed in Chapter 10 (Experiment and Irradiation Facilities).

3.1.7.1.2 Discussion—A structured approach to evaluating each cycle of operation, including experiment/reactor interactions, is used at ATR. This evaluation includes compliance with safety limitations established during the safety evaluation process. The established operation limits are verified for accuracy by several levels of review. The analysis required for each evaluation is described in controlled procedures and performed using validated analytical tools.

A large range of accidents involving experimental loop voiding failures has been analyzed. The most serious effect of experimental loop failures is the positive reactivity insertion. The worst-case experimental accident has been identified, analyzed, and is discussed in Chapter 15 (Accident Analyses).

3.1.7.2 Criterion 71—Emergency Response Systems Design. Adequate monitoring equipment and warning devices to support the emergency response of the ATR and TRA shall be provided to meet applicable overall requirements (GDC 1-5).

3.1.7.2.1 Basis—Since the control room is not designed to be habitable during all accident conditions, the safety of the operating crews is dependent upon the Emergency Response Systems. Therefore, a criterion addressing these systems is considered necessary.

3.1.7.2.2 Discussion—The emergency response system comprises the hardware and procedures for acquiring data on emergency conditions and responding to the warnings produced by the equipment. The hardware consists of:

- The two remote area monitoring systems backed up with alternate radiation monitoring instrumentation.
- The stack monitoring system backed up by the RMSS stack exhaust monitoring subsystem.
- The primary wind direction/speed instrumentation, which is located near the TRA-658 guard house, and the INEEL-VIZ; alternate information can be obtained from the Materials Tests Reactor (MTR) wind sock, National Oceanic and Atmospheric Administration (NOAA)-CFA, or Idaho Nuclear Technology and Engineering Center (INTEC).
- The two emergency evacuation alarm systems that provide sirens: alternating (for "evacuation") and steady (for "take cover"); also evacuation direction lights backed up with an alternate TRA voice paging system or security guards equipped with car-mounted sirens.

The procedures are contained in the Emergency Plan Implementing Procedures, the Abnormal Operating Procedures, and the Emergency Procedure Network.

Not all of the provisions of GDC 1 through 5 are applicable to the emergency response system. Applicable requirements for systems hardware are contained in the design documentation (design specifications, engineering drawings, etc.) The Contractor's quality assurance program, as described in Chapter 17 (Quality Assurance), ensures that the applicable requirements are met.

In addition to providing protection to the operating crew, these emergency response features support protection of TRA personnel and the public. Details of emergency response capability are discussed in Chapter 13 (Management, Organization, and Institutional Safety Provisions) in the Emergency Preparedness Program Section.

Table 3.1-1. Comparison of ATR and PWR characteristics.

Reactor operating conditions	ATR	PWR
Power (MW_{th})	250	2,000 - 4,000
Power density (kW/ft^3)	28,300	~1,550
Operating pressure (psig)	355	~2,250
Inlet temperature (°F)	125	~ 550
Outlet temperature (°F)	170	~ 600
Primary coolant flow rate (gpm)	< 48,000	~300,000
Primary coolant weight (lb)	600,000	~450,000
Primary coolant weight/thermal power (lb/MW)	2,400	170
Decay heat (MW)	13 @ 10 s 1.3 @ 1 day	135 @ 10 s 19 @ 1 day
Fuel		
Total Uranium weight (lb)	89	180,000
Enrichment	93% U-235	2-4% U-235
Configuration	48 in. long Al plates attached to sides	Zirc rods containing stacked pellets
Matrix	UAl_x	UO_2
Fuel temperature (°F)	462	2,000 - 3,000
Fission product inventory	< 60 days operation @ 250 MW	10 times ATR

Table 3.1-2. Piping design and safety limit pressures and temperatures at specific locations.

Piping section	Design	Safety limit
Primary pump discharge to first block valve	576 psig	634 psig
First block valve to butterfly valve (BF-A-14)	485 psig	533 psig
BF-A-14 to reactor vessel inlet	390 psig	468 psig
Reactor vessel outlet to pump suction	390 psig	429 psig
Heat exchanger outlet to reactor inlet	150°F	240°F
Reactor outlet to heat exchanger inlet	240°F	240°F

Table 3.1-3. ATR multiple means of decay heat removal.

No.	Core heat removal	Power sources	Removal to heat sink	Power sources	UFSAR Chapter
1	Primary coolant pumps (any 1 of 4)	4160 Vac commercial power	Secondary coolant pumps (any 1 of 4), or Utility cooling water pumps (any 1 of 2)	4160 Vac commercial power 4160 Vac diesel power	Chapter 5
2	Primary emergency flow pumps (any 1 of 2)	480 Vac commercial power or diesel power (one pump from diesel-commercial or 250 Vdc utility dc power (one pump from dc control center	Secondary coolant pumps (any 1 of 4), or Utility cooling water pumps (any 1 of 2), or natural circulation to air and thermal radiation to surroundings from uninsulated vessel and piping (short term)	4160 Vac commercial power 4160 Vac diesel power	Chapter 5
3	Firewater injection (any 1 of 3 pumps)	Gravity flow (initial injection), diesel engine (two pumps), commercial power or diesel power (one pump)	Reactor vessel drain to reactor building	Vessel drain valves can be opened manually	Chapter 6
4	Low pressure demineralized water purge	Commercial power or diesel power	Reactor vessel drain to reactor building	Vessel drain valves can be opened manually	Chapter 9
5	Pressurizing system feed & bleed	Commercial power or diesel power via dual feeds to pressurizing pump motors	Reactor vessel drain to reactor building	Vessel drain valves can be opened manually	Chapter 5
6	Natural circulation in reactor vessel (short term)	None needed	Natural circulation to air and thermal radiation to surroundings from uninsulated vessel	None needed	—

FOIA Exemption 3 UCNI, Exemption 7f (Columns 3 & 5, Rows 1 & 2 -- Electrical bux identifiers)

3.2 Classification of Structures, Components, and Systems

Certain SSC of a nuclear facility are important because they perform safety functions required to avoid or mitigate the consequences of design-basis events, abnormal operational transients, or accidents. This section discusses the classification of SSC according to the importance of the safety function they perform. Appropriate design requirements are imposed upon such SSC to ensure that they perform safety actions properly when required.

The broadest safety category is "important-to-safety." Important-to-safety SSC are the SSC that provide reasonable assurance that the facility can be operated without undue risk to the health and safety of the public. Encompassed in important-to-safety are the broad class of plant features, covered (not necessarily explicitly) in the General Design Criteria, that contribute in an important way to safe operation and protection of the public in all phases and aspects of facility operation (Denton 1981). Important-to-safety SSC are SSC whose function can affect safety either directly or indirectly. This category includes safety-related SSC, and in some instances, balance-of-plant SSC. "Safety-related" is a subset of important-to-safety SSC (House 1992).

Examples of important-to-safety SSC are (a) experiment loop piping, instrumentation, and controls; (b) some non-PPS reactor instrumentation and control systems; (c) PCS instrumentation and control systems; (d) reactor vessel, PCS, canal, and experiments loop shielding; (e) pressurizing pumps (670-M-14 and M-15), PCS pump motors (670-M-6, M-7, M-8, and M-9), secondary coolant system pumps (670-M-1, M-2, M-3, and M-4), utility coolant water pumps (670-M-5 and M-6), and high pressure demineralized water pumps (670-M-35 and M-36); and (f) warm waste storage tanks and associated system piping. The examples of equipment important to safety provided above are not intended to be all inclusive. A detailed listing of all equipment important to safety has not been developed for the ATR. In general, requirements for equipment important to safety, are contained in the design documentation (design specifications, engineering drawings, system design descriptions, etc.). The Contractor's quality assurance program, as described in Chapter 17 (Quality Assurance), ensures that the applicable requirements are met.

A detailed listing of safety-related equipment, a subset of equipment important to safety, has been developed. SSC at the ATR are currently classified into two categories: (a) safety-related and (b) nonsafety-related. The term "safety-related" refers to those SSC that are relied upon during or following design-basis events[a] to ensure (a) the integrity of the primary coolant pressure boundary, (b) the capability to shut down the reactor and maintain it in a safe shutdown condition, and (c) the capability to prevent or mitigate the consequences of accidents that result in potential offsite exposures comparable to the 10 CFR 100 guidelines (House 1992).

"Safety-related" includes significant subcategories of SSC with respect to the ATR facility. Figure 3.2-1 illustrates the overall classification scheme for the ATR safety-related systems. There are two subcategories for safety-related systems: (a) PPS and (b) non-PPS. Components are designated as either PPS or non-PPS. The PPS consists of those active devices, with the associated equipment that initiates their action, whose function in conjunction with passive structures of the plant is necessary to prevent unacceptable release or spread of radioactive materials by preventing plant variables or conditions from reaching their respective safety limits, or mitigating the consequences of exceeding safety limits. The PPS includes the RSS and the ESF. All other safety-related equipment in the ATR is considered to be non-PPS.

---

[a]. Design Basis Events are interpreted to include all operations, transients, and accidents within Conditions 1 through 4.

This UFSAR provides summary descriptions of the PPS and the non-PPS safety-related SSC; defines both the PPS and the non-PPS safety-related SSC boundaries. The master list of the safety-related SSC is presented in Appendix A.

3.2.1 Seismic Classification

Safety-related SSC have been divided into two classes for the purpose of establishing seismic, wind, and flood performance requirements in accordance with Regulatory Guide 1.70 (NRC 1978a). These classes are Seismic Category I, and Non-Seismic Category I. All safety-related SSC, and parts thereof are classified in accordance with the definitions that follow.

3.2.1.1 Definition of Seismic-Design Classifications. Those safety-related SSC whose functions are needed to mitigate the effects of the SSE are designated Seismic Category I in accordance with Regulatory Guide 1.29 (NRC 1978b). Generally, those SSC designated as safety-related are also designated Seismic Category I (Buescher and VanderBeek 1997). The RSS contains a seismic scram, which is designed to shut down plant operations upon detecting low intensity ground motions (Atkinson 1997). The reactor will be shutdown well before a major earthquake can damage the PPS or the reactor. Because of this, many of the safety related systems are not required to remain functional to mitigate the consequences of an accident and are not designated as Seismic Category I. An example of such a system is the log countrate system (LCR). The LCR system is safety-related because it minimizes the potential for an inadvertent criticality during shutdown core changes.

The PPS must have the following characteristics to ensure that it will shut down the reactor well before a major earthquake can damage the PPS or the reactor (Atkinson 1997):

- The PPS should be designed to remain operable in a Modified Mercalli Intensity VIII earthquake.
- It must initiate shutdown upon detecting a ground acceleration > 0.017 g at seismic frequencies of 2.5 to 6 Hz.
- It must insert the safety rods at least 12 in. within 1 second of detecting a ground acceleration > 0.017 g at seismic frequencies of 2.5 to 6 Hz.
- Seismic design for both Seismic Category I and non-Seismic Category I items are discussed in Section 3.7.

3.2.1.2 Seismic Classification of Structures, Systems and Components. Seismic Category I structures include:

- Reactor Building (TRA-670)
- Firewater Pump Houses (TRA-619, -633, -688)
- Firewater Storage Tanks (TRA-719A, -719B, -719C, -718, -781).

Systems containing Seismic Category I components and structural elements are listed in Table 3.2-1. Appendix A identifies the Seismic Category I components and structural elements by the system groupings listed in Table 3.2-1.

3.2.2 System Quality Group Classification

The components making up the reactor coolant pressure boundary were designed and installed prior to the issuance of Reg. Guide 1.26. Reg. Guide 1.26 "describes a quality classification system related to specified national standards that may be used to determine quality standards acceptable to the NRC Staff for satisfying General Design Criteria 1 for other safety-related components containing water, steam, or radioactive material in light-water-cooled nuclear power plants (NRC 1976)." Since the ATR is not under the jurisdiction of the NRC, and, furthermore, since the components were designed and installed prior to the issuance of guidance documentation on quality classification, no formal classification was completed. New systems are assigned a quality group classification consistent with the applicable design codes and standards at the time of design. Existing systems are assigned quality classifications for inservice inspection, inservice testing, repairs, replacements, and modifications as specified in the ATR ISI Plan (INEEL 2002).

Table 3.2-1. ATR systems containing Seismic Category I components and structural elements.

System	Subsystems, components, and structural elements
Reactor Shutdown System (RSS)	Electronic scram circuits and instrumentation
Engineered Safety Features (ESF)	Emergency Firewater Injection System (EFIS) Vessel Vent System (VVS) Radiation Monitoring and Seal System (RMSS) PCS overpressure relief system LOCA Primary Coolant Pump Shutoff System
Safety-Rod System	Safety rods and release mechanism
Primary Coolant System (PCS)	Primary Coolant System components and piping Reactor vessel Primary coolant heat exchangers and pumps (only PCS pressure boundary) Emergency flow system
Reactor core and internals	Fuel elements Reactor internal tanks Outlet-flow pipes
Reactivity-Control System	Outer shim control cylinders (OSCC)
Firewater system (FIS)	Piping, pumps, and water-storage tanks
Fuel storage and handling	Canal structure (bellows, canal walls, cleanup piping drains) Underwater fuel storage grids
Electrical power system	PPS battery-backed power system Utility battery-backed power system Instrument battery-backed power system
Control complex	Reactor control room console and upright panels

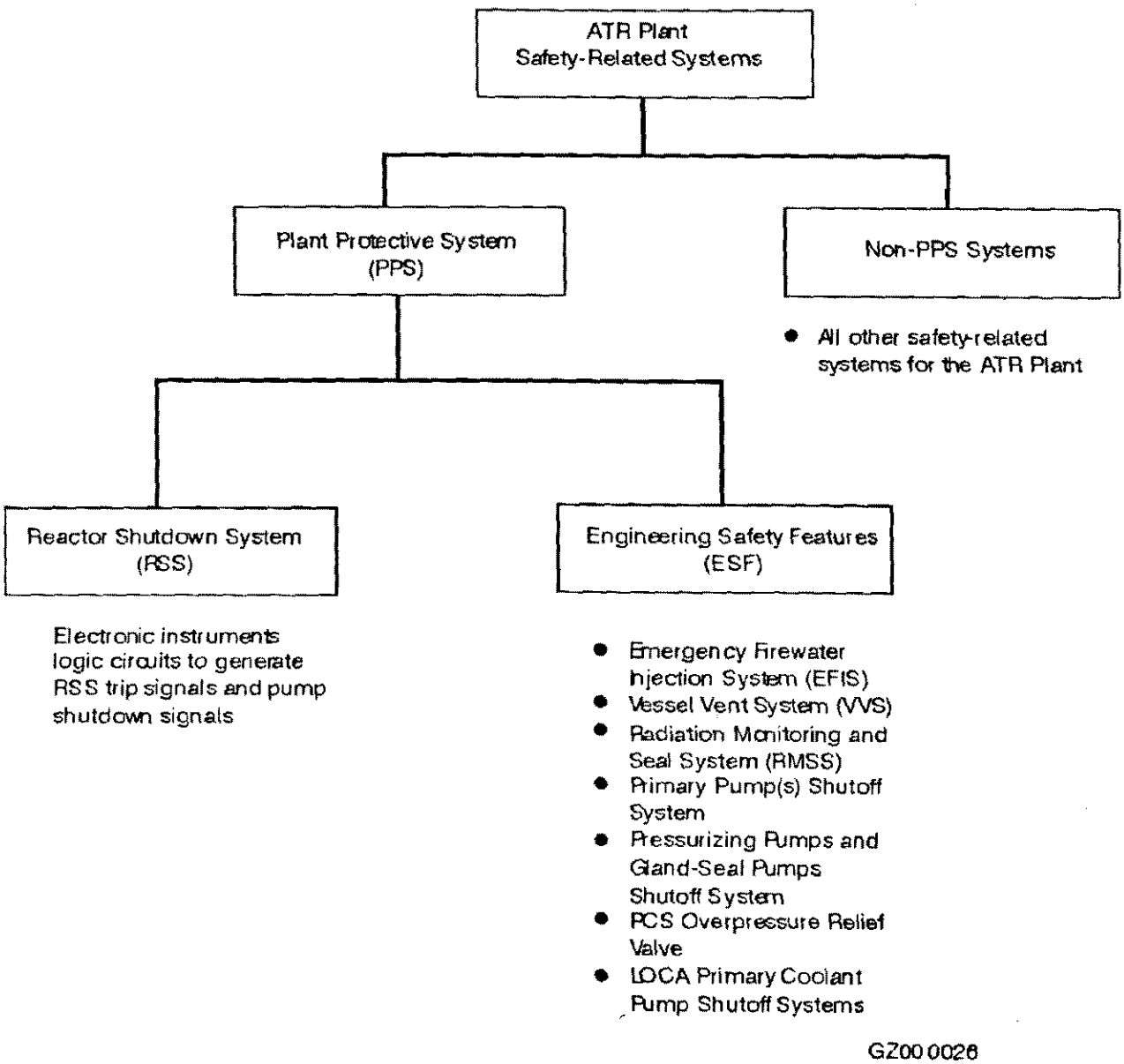

Figure 3.2-1. Methodology of ATR safety-related systems. **(For Information Only)**

3.3 Wind and Tornado Loadings

3.3.1 Wind Loadings

This section discusses the design wind load on Seismic Category I structures. These structures are:

- Reactor Building (TRA-670)
- Firewater Pump Houses (TRA-619, -633, -688)
- Firewater Storage Tanks (TRA-719A, -719B, -719C, -718, -781).

3.3.1.1 Design Wind Velocity. At the time of original design of ATR, it was customary to design the structures to withstand windspeeds with a mean recurrence interval of 50 years, as specified in the American Standards Association ASA-A58.1-1955 (American Society of Mechanical Engineers ASME 1955a). Recent DOE criteria, as given in DOE standard DOE-STD-1020-94 (DOE 1996a), specify design windspeeds of 95 mph for Seismic Category I structures (Performance Category 4).

3.3.1.2 Determination of Applied Forces. Table 3.3-1 tabulates the design pressure to be applied inward or outward on walls and roofs in accordance with ASA-A-58.1 (Ebasco 1964a).

Over the years, the wind-resisting capacities of ATR structures have been evaluated in several reports (Arendts 1989a and 1989b; Gorman 1985 and 1989a). Gorman (1985) shows that the overhead water-storage tank TRA-718 can withstand windspeeds up to 146 mph. Arendts (1989b) and Lippert (1997) shows that the ground-mounted raw-water storage tanks, TRA-719A, -719B, and -719C, can withstand windspeeds in excess of 167 mph, based on the seismic criteria used in the design of the tanks. The roof materials used to construct the firewater pumphouse (TRA-688) have a maximum allowable uniform load pressure limit of 150 pounds per square foot (psf). The wall materials used to construct the firewater pumphouse (TRA-688) have a maximum allowable uniform load pressure limit of 48 psf. The firewater tank (TRA-781) is constructed of 1/4-in. thick, ASTM A36 plate steel (Brower 2001). The allowable pressures for all of these tanks and structures exceed the PC-4 requirement for 95-mph straight wind speed from the DOE standard (DOE 1996a).

Arendts (1989a) shows that the girts and siding of the reactor building would suffer minimal damage at windspeeds in excess of 115 mph. In Eide, Khericha, and Thatcher (1991), the wind capacities of the structures were evaluated as part of the PRA. Table 3.3-2 shows the median capacities (expressed in terms of windspeed in miles per hour), variabilities β_R and β_U, and the High Confidence Low Probability of Failure (HCLPF) windspeed estimated in Eide, Khericha, and Thatcher (1991). The median capacity is defined as the windspeed at which there is a 50% probability of failure. β_R and β_U are variables that represent the randomness and uncertainty in the median estimate of the wind capacity. The HCLPF windspeed is the windspeed at which there is greater than 95% confidence of less than a 5% probability of failure.

Although the ATR was not designed to the criteria of the DOE standard (DOE 1996a), the PRA estimated the fuel damage frequency due to all wind loads to be 1.15×10^{-6} (Atkinson and Thatcher 1994).

The DOE standard (DOE 1996a) specifies a minimum missile criterion for Performance Category 4 structures. The minimum missile criterion is specified to account for objects or debris that could be picked up by straight winds, hurricanes, or weak tornadoes. A 2-in. × 4-in. timber plank weighing 15 lb is the specified missile. Recommended impact speed is 50 mph at a maximum height of 50 ft aboveground. The missile impact test were performed on the roof and wall materials used to construct the firewater pumphouse (TRA-688). The tests were performed using a 2-in. × 4-in. timber plank weighing 15 lb in accordance with the DOE standard (DOE 1996a) at the Hurricane Test Laboratory. The missile never penetrated the roof and wall panel during this testing (Brower 2001). No other structures at TRA have been assessed to withstand this specific missile; however, a 12-ft-long, 4-in. × 12-in. timber plank (139 lb) and a 10-ft-long, 3-in. diameter pipe (76 lb) have been assessed as missiles.

The reactor building and water-storage tanks have been analyzed for impact of wind-borne missiles. Impact of two capable missiles, a 4-in. × 12-in. × 12-ft timber plank and a 3-in. diameter × 10 ft steel pipe, were considered. Missile velocities were considered as a function of windspeeds. Results were presented in terms of limiting windspeeds as shown in Table 3.3-3.

These results were reported in Gorman (1989a). The values for the reactor building are somewhat conservative; the analysis assumes that the aluminum siding on the reactor building offers no resistance to missile impact. Based on these values, the 15-lb, 2-in. × 4-in. timber plank is not expected to penetrate or cause excessive damage to the above structures.

3.3.2 Tornado Loadings

At the time of the ATR's original design, there was no requirement to consider tornado loading. Subsequently, some of the Seismic Category I structures have been evaluated for tornado loadings. The DOE standard (DOE 1996a) states that the Performance Category 4 facilities at INEEL (ATR is included in these) must be designed or evaluated for straight winds with basic windspeed of 95 mph for an annual frequency of exceedance of 10^{-4}, and that the tornado windspeed will be less than the above straight windspeed for annual frequencies larger than 2×10^{-6}. Hence, by current DOE criteria, the ATR does not have to consider tornado loads.

In 1985, the reactor building reactor room and control room (including the adjacent office structure) were evaluated for hazards posed by extreme winds and tornadoes. Findings indicated that the masonry block walls, liner plates, and secondary bracing have low stress levels for all wind speeds considered. The facility will be damaged minimally to moderately by winds with a probability $p = 1 \times 10^{-6}$ per year (i.e., winds with speeds of 115 mph). Winds with probability $p = 1 \times 10^{-7}$ (126-mph straight winds, or 167-mph tornadoes) will cause moderate to severe damage. The main wind-force-resisting frame members were capable of resisting straight-wind speeds up to 154 mph ($p < 10^{-7}$ per year), and tornadoes with speeds up to 176 mph ($p < 1 \times 10^{-7}$ per year).

The study concluded that the reactor building reactor room and control room, including the adjacent office structure, can resist wind speeds greater than established hazard values (Arendts 1989a).

Table 3.3-1. Design wind-pressures requirement.[a]

Height zone (ft)	Buildings (psf)	Tanks and stacks (psf)
Less than 30	30[b]	18
30 to 50	35	21
50 to 75	40	24
75 to 100	45	27
100 to 500	55	33

a. ASA 1955.

b. Thirty psf for the "less than 30 ft" height zone is equivalent to approximately a 90 mph wind, based on the current American Society of Civil Engineers (ASCE) Standard ASCE-7-93, "Minimum Design Loads for Buildings and Other Structures."

Table 3.3-2. Wind capacities of ATR structures.

Structure	Failure mode	Median (mph)	β_R	β_U	HCLPF Windspeed (mph)
Reactor building	Girts	147	0.07	0.14	103
Firewater pumphouse					
TRA-619	Block wall	116	0.07	0.18	77
TRA-633	Exterior wall	120	0.07	0.20	77
Firewater storage tanks					
TRA-718	Diagonal brace	119	0.07	0.25	81
TRA-719A, B, C	Overturning	288	0.18		190

Table 3.3-3. Wind hazard evaluation/probabilities of wind hazards.

Structural components	Acceptable peak wind velocity (mph)	Probability
Building liner plate		
a) Local perforation:	140	3×10^{-7}
b) Overall failure:	> 165	$< 1 \times 10^{-7}$
Masonry block wall		
a) Grout-filled blocks:	> 165	$< 1 \times 10^{-7}$
b) Hollow blocks:	< 95	$\geq 1 \times 10^{-4}$
Building structural columns		
No compressive collapse for:	> 165	$< 1 \times 10^{-7}$
Steel water storage tank		
No perforation for:	> 165	$< 1 \times 10^{-7}$
Girts and siding		
a) Minimal to moderate damage for:	115	1×10^{-6}
b) Moderate to severe damage for:	126 straight wind, 167 tornado	1×10^{-7}
Main wind-resisting frame members		
a) Capable of resisting straight winds up to:	154	$< 1 \times 10^{-7}$
b) Capable of resisting tornado of:	176	$< 1 \times 10^{-7}$

3.4 Water Level (Flood) Design

The plant design for protection of SSC whose failure could prevent safe shutdown of the plant or result in uncontrolled release of significant radioactivity because of flooding meets the relevant requirements of General Design Criterion 2, "Design Bases for Protection Against Natural Phenomena."

3.4.1 Flood Protection

The flooding of the ATR reactor facilities from natural causes has been considered for PMF, for probable maximum precipitation (PMP) runoff from the Site and adjacent areas, and for groundwater as discussed in Chapter 2 (Site Characteristics).

Four PMF scenarios were evaluated by Koslow and Van Haaften (1986) for their effects on ATR as discussed in Chapter 2.

A. Seismic failure of the Mackay Dam concurrent with the 25-year-recurrence-interval flood

B. Hydraulic (piping) failure of the Mackay Dam concurrent with the 100-year-recurrence-interval flood

C. Hydraulic (piping) failure of the Mackay Dam concurrent with the 500-year-recurrence-interval flood

D. Overtopping failure of the Mackay Dam caused by a PMF.

Of these scenarios, only the fourth is expected to produce floodwaters that reach the TRA. The predicted maximum peak water elevation at the center of the flood path for this scenario is 4,924 ft-msl (Koslow and Van Haaften 1986). The peak water elevation would decrease with distance from the center of the path to an elevation no greater than 4,923 ft-msl at the flood path edge (Atkinson 1995). Since the reactor building grade elevation is 4,926.6 ft-msl (4.6 ft above the expected water level), no flooding of the building is predicted. However, some support facilities housing such equipment as the raw-, fire-, and domestic-water system pumps, the LDW pumps, and the diesel-fuel transfer pumps, could be flooded (Eide, Khericha, and Thatcher 1991).

The PRA results indicate a mean frequency for external flooding event sequences between 1.0×10^{-8} and 8.5×10^{-8} per year. The total mean frequency of all sequences is 1.3×10^{-7} per year (Eide, Khericha, and Thatcher 1991).

To date, no study has been undertaken to predict the effects of a local PMP, which would include a runon/runoff study to determine floodwater levels [see Chapter 2 (Site Characteristics)]. However, although no formal evaluations have been performed, forty years of experience have shown that even for rapid thawing of heavy snow over frozen earth (the PMP scenario that occurred in 1961) the water levels would be less than those predicted for the PMF.

Other effects, such as surge or seiche, coincident wind-generated waves, and groundwater hydrostatic effects, are not considered to be applicable for ATR, as discussed in Chapter 2 (Site Characteristics).

3.4.1.1 Flood Protection Measures for Seismic Category I Structures, Systems, and Components. Of the Seismic Category I SSC identified in Appendix A of this chapter, only the firewater system, and diesel-fuel transfer pumps may be subject to the effects of flooding. Since special measures to protect structures housing these pieces of equipment neither exist nor are planned for the immediate future, it is assumed that these components and systems may be inoperative because of flooding. However, based on the PRA results (Eide, Khericha, Thatcher 1991), fuel-damage sequence due to potential PMF-induced flooding has a very low probability and is, therefore, considered to be a lower priority concern than other identified events. Therefore, special measures to upgrade the facilities have not been pursued.

3.4.2 Analytical and Test Procedures

No dynamic water forces associated with the PMF, PMP, or high groundwater levels have been identified in Chapter 2 (Site Characteristics) for the TRA, site of the reactor building and support structures.

3.5 Missile Protection

In accordance with the requirements of GDC 2 and 4, safety-related SSC are to be designed and constructed with adequate missile protection to ensure that they will not fail or cause a failure in the event of a postulated credible missile impact.

3.5.1 Missile Selection and Description

The following sources are considered for the generation of missiles:

- Internally generated missiles
  - Missiles generated by rotating components
  - Missiles generated by pressurized components
- Turbine missiles (Not applicable to ATR)
- Externally generated missiles
  - Missiles generated by natural phenomena
  - Missiles generated by events near the site
  - Aircraft hazards
  - Gravity-generated missiles.

3.5.1.1 Internally Generated Missiles (Outside Confinement). There are two general potential sources of postulated missiles that can be generated as a result of plant operation:

A. Rotating-component failures (e.g., a fan breaking and throwing its blades)

B. Pressurized-component failures (e.g., a valve bursting and scattering its parts).

Potential rotating-component sources of missiles outside the confinement area are the diesel generators. Diesel generators M-42 and M-43 are aligned on a common longitudinal axis in the diesel-generator room located on the first floor of the reactor building at grade level. The M-6 diesel generator is in a separate diesel building located directly north of the reactor building. Potential missiles have been considered in an evaluation of the PPS (INEEL 2000), and were found to be insignificant hazards.

Potential sources of pressurized-equipment missiles are components in pressurized systems. Failures of these components can generate missiles such as valve bonnets, valve stems, hardware retaining bolts, relief-valve parts, and instrument wells. The potential-energy source that serves as the driving force for such missiles can be classified as either stored strain energy or contained fluid energy (jet-propelled and piston-type missiles). Acceleration of a retaining bolt is due to its stored strain energy. A failed valve bonnet or thermowell is accelerated by a "jet" of escaping fluid, whereas the acceleration of a valve stem or similar component is caused by a piston-type action. Potential missiles have been considered in an evaluation of the PPS (INEEL 2000), and were found to be insignificant hazards.

3.5.1.2 Internally Generated Missiles (Inside Confinement). Potential rotating-machinery sources of missiles inside the confinement area are the primary coolant pumps and the emergency coolant pumps. The four primary coolant pumps are aligned parallel to each other in separate pump rooms located on the first basement of the reactor building. The two emergency coolant pumps are aligned parallel but offset longitudinally to each other in another pump room adjacent to the primary coolant pump rooms. The motors for all these pumps are aligned parallel to each other in a common pump-motor room that is adjacent to pump rooms. Potential missiles have been considered in an evaluation of the PPS (INEEL 2000), and were found to be insignificant hazards.

For potential sources of pressurized component missiles see Section 3.5.1.1 above. A missile shield plug placed into the transfer plate for inpile experiments shields the confinement roof against any missile projectiles ejected from the inpile experiment tubes.

3.5.1.3 Turbine Missiles. Turbine missiles are not applicable since the reactor plant does not have any power-generating turbines as in a commercial power plant.

3.5.1.4 Missiles Generated by Natural Phenomena. Basic NRC guidance for the design of commercial nuclear power plants to withstand the effects of tornado wind and tornado-generated missiles is presented in NRC Regulatory Guides 1.76 and 1.117 (NRC 1974a, 1978c) and Standard Review Plans (SRP) 3.3.2 and 3.5.1.4 (NRC 1981b, 1981c).

An assessment of the adequacy of a plant to withstand the impact of tornado missiles would include:

- Determination of the capability of the exposed SSC to withstand potential missiles (including small missiles with penetrating characteristics and larger missiles that result in an overall structural impact),
- Determination of whether any areas of the plant require additional protection.

At the time that ATR was designed and built, there were no requirements to design for possible tornado-generated missiles. Since that time, with the advent of more-recent rules and regulations, the reactor building and steel water-storage tanks were evaluated based on initially considering the missiles shown in Table 3.5-1.

Of the four missiles in Table 3.5-1, only the wood plank and the 3-in. pipe were finally considered as airborne missiles since the design windspeed for this region was predicted to be no greater than 165 mph for a 10^{-7} probability of exceedance event (Coats and Murray 1985).

In 1989, an assessment of the ability of the reactor building TRA 670 and the firewater storage tanks TRA-719A, -719B, and -719C to resist the effects of wind-borne missiles was conducted based on the missiles in Table 3.5-1 (Gorman 1989a; Lippert 1997). As discussed above, only two missiles were finally considered as capable missiles based on the maximum windspeed of 165 mph for a 10^{-7} probability of exceedance event. They were the 4-in. × 12-in. × 12-ft wood plank and the 3-in.-diameter Schedule 40 × 10 ft long steel pipe. Results of the evaluation show the building's 3/16-in. steel liner plates and the walls of the firewater storage tank will not be locally perforated by these missiles for windspeeds up to 140 mph. The hollow block walls will be perforated by the missiles for windspeeds well below 95 mph. The grouted block walls can withstand the missiles' impacts for windspeeds exceeding 165 mph.

Another possible source of missiles generated by natural phenomena would be floating debris as a result of flooding. Based on a worst-case flood caused by failure of the Mackay Dam (Koslow and Van Haaften 1986), the predicted peak water velocity at the center of the flood path near ATR is 2.8 ft/sec. Since ATR is near the edge of the flood path, where the water is very shallow, the water velocity is expected to be close to zero; thus, floating debris should pose no serious threat because of impacting safety-related SSC.

3.5.1.5 Site Proximity Missiles (Except Aircraft). Missiles in this category occur from such sources as nearby explosions and, if found to be a design basis event according to SRP Section 2.2.3 (NRC 1981d), should be included here. In assessing the nature and extent of offsite activities, the PRA (Eide, Khericha, and Thatcher 1991) states that offsite transportation accidents resulting in explosions do not pose a hazard to ATR.

3.5.1.6 Aircraft Hazards. An aircraft-hazard analysis of the ATR plant site was conducted in 1991 as reported in the PRA (Eide, Khericha, and Thatcher 1991). The site-specific data on air traffic along the air corridors in the vicinity of the plant site were obtained by contacting the Idaho Falls Municipal Airport, Site security, and the NOAA at the INEEL Site. The NOAA occasionally conducts the vortex test flights at the INEEL Site for the Federal Aviation Administration (FAA).

The aircraft-impact analysis was based on an examination of commercial, military, general, Site-security helicopter, and vortex test flights travelling within 20 mi of ATR. The contributions to the total damage frequency from the air travel beyond the radius of 20 mi were judged to be insignificant, based on the models and assumptions used in the analysis. Since there are no nearby airports, the contribution of takeoff and landing crashes was also considered to be negligible.

Eide, Khericha, and Thatcher (1991) found that only one commercial airway passes within 20 mi of ATR (the shortest distance from the ATR to the closest edge of an airway is approximately 5 mi). At the time of this study, five flights (passes) per day to and from Idaho Falls use the airway. The total number of flights per year is estimated as described in Table 3.5-2. No military airway passes within a 20 mi radius of the ATR.

General-aviation air traffic is permitted over the Site. However, all general aircraft are requested to avoid flying at an altitude less than 6,400 ft-msl for reasons of national security. The altitude of ATR site is approximately 4,920 ft-msl. It was assumed that all flight plans for general aircraft entailed at least one pass by the site at a perpendicular distance of 0.5 mi. Air traffic as a result of general-aviation aircraft is described in Table 3.5-2.

Helicopter traffic around the ATR was the result of regular reconnaissance missions by the Site-security personnel. The type of helicopter and the flight patterns were not available from the Site-security for security reasons. It was simply and conservatively assumed that a helicopter passed 200 ft directly over the ATR once a week. INEEL Security no longer operates a security helicopter.

In addition to the commercial-and general-aviation air traffic, the analysis of aircraft hazards considered the vortex test flight that is conducted by NOAA on an occasional basis, as listed in Table 3.5-3. A maximum of 239 test flights (passes by the instrumentation tower) were conducted in the fiscal year (FY) 1990. During FY 1991, 120 test flights were conducted. No test flights have been conducted since FY 1991. For analysis purposes, it was assumed that no more than 250 tests would be conducted per year in the future. The altitude of the test flight must be at least 250 ft above the ground, and the flight path brings the plane no closer than 1 mi to the ATR plant-site. The type of aircraft used for the tests varies. For analysis purposes, however, it was assumed that a Boeing-747 would be used.

Based on the probabilistic risk study (Eide, Khericha, and Thatcher 1991), the frequency of aircraft impact at ATR is presented in Table 3.5-4. In all cases, commercial, general, helicopter, and vortex test flights, the frequency of site impact is negligible. The total site-impact frequency of all types of aviation is 1.4×10^{-7}/yr; therefore, the overall risk is considered negligible.

3.5.2 Structures, Systems, and Components to be Protected from Externally Generated Missiles

The reactor building and support facilities were all designed and built before (mid-1960s or earlier) the rules and regulations were imposed regarding protection of SSC from externally generated missiles. Thus, there is no specific protection incorporated into the design of the SSC other than what is inherently there for other design considerations.

3.5.3 Barrier-Design Procedures

No known barriers have been designed and installed to protect against missile-impact forces.

Table 3.5-1. Missiles considered in evaluating the ATR building and steel water-storage tank.[a]

Missile	Physical properties	Weight (lb)
Wood plank	4 in. × 12 in. ×12 ft	139
Steel pipe	3-in., Schedule 40 × 10 ft	76
Utility pole	13.5 in. diameter × 35 ft	1,490
Automobile	20 ft^2 frontal area	4,000

a. Coats and Murray 1985.

Table 3.5-2. Characteristics of airway travel within 20 mi of ATR.[a]

Airway	Type of aircraft	Altitude above Site (ft)[b]	Distance from Site (mi)	Frequency (number/year)
V-269[c]	Commercial	14,080	5.0	2,737[d]
Miscellaneous	General	1,480	5.0	500[e]
ATR-site	Helicopter	200	0.0[f]	52[f]
Vortex test flight	Commercial	250[g]	1.0	250[g]

a. Eide, Khericha, and Thatcher 1991.

b. Site is at approximately 4,920 ft-msl.

c. V-269 is traveled primarily by Horizon Airlines. The two types of aircraft used by Horizon are the DeHavilland Dash 8 and the Fairchild MetroLiner III. Five flights per day use V-269.

d. Assumed 5% linear growth per year over next 20 years.

e. Total of 460 flights per year is estimated by multiplying 365 by the average number of flight plans (mean = 20) filed with the Flight Service Station in Idaho Falls, Idaho during the first 16 days of November, 1989. The Flight Service Station services 9 different airports within a sixty-mile radius of ATR. It was conservatively assumed that all general aviation aircraft passed the ATR-site once at a distance of 5 mi. Final number is rounded off to 500.

f. It was assumed that a helicopter passed directly over ATR once a week.

g. Telecommunication with NOAA personnel.

Note: *Although security helicopter flights have been discontinued, the frequency calculation has not been changed. Including the provision for these flights is conservative.*

Table 3.5-3. Vortex test flight frequency history.[a]

FY	Number of flights per year
1970s	29
1987	164
1990	239
1991	120
1992	0
1993	0
1994	0
1995	0
1996	0
1997	0
1998	0
1999	0
2000 (planned)	0
2001 (planned)	0

a. Table revised July 1, 1999.

Table 3.5-4. Aircraft crash results.

Type of aircraft	Distance from Site (mi)	Flight frequency (per year)	Site-vicinity impact (P_a) probability	Site impact $P(s/P_a)$ probability	Site impact frequency (per year)
Commercial	5.0	2,555	5.1×10^{-9}	9.4×10^{-6}	1.2×10^{-10}
General	5.0	500	4.5×10^{-7}	3.4×10^{-4}	7.6×10^{-8}
Helicopter	0.0	52	1.8×10^{-8}	6.4×10^{-2}	6.0×10^{-8}
Vortex test flight	1.0	250	9.1×10^{-9}	3.9×10^{-3}	8.9×10^{-9}
				Total	1.4×10^{-7}

3.6 Protection Against Dynamic Effects Associated with the Postulated Rupture of Piping

Acceptability of the plant design for protection against postulated piping failures outside confinement is based on GDC 4, as it relates to accommodating the dynamic effects of postulated pipe rupture, including the effects of pipe whipping and discharging fluids (jet-impingement forces), when designing SSC that are important to safety. Postulated piping failures are defined as longitudinal and circumferential breaks in piping for high-energy fluid systems and as through-wall leakage cracks in piping for moderate-energy fluid systems. Failures are postulated according to the provisions of Branch Technical Position (BTP) Management Evaluation Branch (MEB) 3-1, attached to SRP Section 3.6.2 (NRC 1981e).

3.6.1 Plant Design for Protection Against Postulated Piping Failures in Fluid Systems Outside Confinement

Systems and components of concern are those classified as essential for shutting down the reactor and mitigating the consequences of a postulated piping failure, without offsite power. For ATR, they are (a) the FIS, (b) the utility cooling water system (UCW), and (c) the LDW system.

These systems, by definition, are moderate-energy fluid systems per Appendix A of Branch Technical Position ASB 3-1 (NRC 1981f). Moderate-energy systems are those that, during normal plant conditions, are either in operation or maintained pressurized (above atmospheric pressure) under conditions in which both of the following conditions are met:

- Maximum operating temperature is 200°F or less.
- Maximum operating pressure is 275 psig or less.

Piping systems outside confinement are all low-temperature, low-pressure systems (i.e., less than 200°F and 275 psig). As such, they are classified in Appendix A of SRP 3.6.2 (NRC 1981e) as moderate-energy fluid systems for which through-wall leakage cracks are the postulated piping-failure mode. Further, according to the provisions of item B.1 of BTP MEB 3-1, Appendix A (NRC 1981e), protection from pipe whip need not be provided if the piping is considered to be a moderate-energy (or lower) fluid system, as the ATR systems are. Thus, pipe whip and resulting impact on other SSCs outside of confinement is not a concern. Additionally these systems are, for the most part, isolated from systems and components important to safety. Hence, jet-impingement forces are not considered to be important.

3.6.2 Determination of Rupture Locations and Dynamic Effects Associated with the Postulated Rupture of Piping

GDC 4 requires that SSC important to safety be designed to accommodate the effects of postulated accidents, including appropriate protection against the dynamic and environmental effects of postulated pipe ruptures. In particular, the purpose of this section is to provide (a) information concerning break-and crack-location criteria and (b) methods of analysis for evaluating the dynamic effects associated with postulated breaks and cracks in piping for high- and moderate-energy fluid systems, both inside and outside of confinement.

It is recognized that pipe rupture is a rare event that may occur under unanticipated conditions, such as those that might be caused by errors in design, construction, and operation, or by unanticipated loads and corrosive environments. Although piping failures are rare, observations of actual failures have indicated that when they do occur, they generally occur at high-stress and fatigue locations, such as at the terminal ends of a piping system, at its connection to the nozzles of a component. Thus, based on rules given in BTP MEB 3-1, it is intended to use the available piping design (analysis) information by postulating pipe ruptures at locations having relatively higher potential for failure, such that an adequate and practical level of protection may be achieved.

To date, ATR has not instituted a formalized approach to identify likely pipe break locations and the consequences of such breaks (pipe whip, blowdown forces, and jet impingement) for the PCS. However, ATR has evaluated the effects of the design-basis LOCA on fuel damage. Results of the evaluation are discussed in Chapter 15 (Accident Analyses). An evaluation of experiment loop piping in the vicinity of the PCS piping has been performed as described in Chapter 10 (Experiment and Irradiation Facilities). Additionally the PRA (Eide, Khericha, and Thatcher 1991) considered the potential for and consequences of flooding on important components such as the PPS. The results of these evaluations indicate that there is a limited potential for direct damage to the important systems as a result of pipe failures. These results indicate that a formal effort to evaluate the dynamic effects of piping failures is not warranted.

Wadkins (1988) concludes that the primary system stainless steel piping would fail with small leaks rather than catastrophic blowouts. EG&G Idaho performed pipe tests to failure and correlated the size of the failure with the energy level of the system. Wadkins (1988) shows that for annealed Type 304 stainless steel piping, the lower the system pressure, the smaller the size of the failure. The conclusion is that a low-pressure, low-temperature system such as the ATR will experience a ductile rupture and comparatively small leak rate rather than a complete rupture and high leak rate. Consequently, pipe whip or any similar sudden destructive failures are considered extremely low-probability accidents. In addition, except for the sensors themselves (pressure taps, Resistance Temperature Detectors (RTDs), etc.) and portions of the associated impulse lines and cabling, the PPS is isolated from both the PCS and the loop piping. Failures in the sensors and associated impulse lines and cabling due to pipe ruptures are expected to cause the monitored signals to be outside of the specified ranges, conservatively resulting in a trip of the affected PPS channels.

3.7 Seismic Design

Selected SSC are classified as Seismic Category I. As described in Section 3.2, classification is based on their role in ensuring safe shutdown of the reactor in a seismic event. Seismic Category I SSC are listed in Appendix A.

Seismic Category I SSC must be capable of withstanding the effects of seismic motions such that required safety functions are performed. SSC must be designed to withstand a level of seismic motion consistent with their role in mitigating the effects of the event. Some SSC (e.g., reactor coolant pressure boundary) must be capable of performing intended safety functions for seismic events up to and including the SSE. For other less critical Seismic Category I SSC, failure of the SSC to perform its intended safety function at levels of seismic motion less than that associated with the SSE may be acceptable. Risk-based analyses are typically performed to evaluate the potential impact of failure of an SSC at levels of seismic motion less than those of the SSE.

The ATR was designed and built in the early 1960s. Because of its vintage, the seismic design provisions have undergone several changes over the operating life of the facility. The seismic provisions contained in the 1961 UBC (Ebasco 1964a) were used in the original design. Subsequently, a facility-specific set of criteria for seismic design and analysis was developed for ATR (Gorman 1972) and applied to some SSC. An again revised set of criteria was developed later (Gorman 1989b) and applied to some SSC. This later criteria represents the most recent development in seismic criteria for use at the ATR, and is specified by the DOE-ID Architectural Engineering Standards (DOE-ID 1996). As such, this latest set of criteria is applied to the design of new SSC requiring seismic qualification.

The DOE-ID AE Standards (DOE-ID 2002) have been revised to incorporate new seismic design requirements of DOE Standards DOE-STD-1020 (DOE 2002a) and DOE-STD-1021 (DOE 2002b). The TRA site specific Performance Categories PC 1 and PC 2 seismic design criteria use the International Building Code (IBC 2000) spectral accelerations. The TRA site specific PC 3 and PC 4 horizontal and vertical seismic design criteria for rock Design Basis Earthquake/Safe Shutdown Earthquake (DBE/SSE) is available in the DOE-ID Standard (DOE-ID 2002). The TRA site specific PC 3 and PC 4 horizontal and vertical seismic design criteria for soil DBE is under development, and will be incorporated into the AE Standards when completed.

As new SSC have been installed, they have typically been shown to meet the seismic design criteria applicable at the time of installation. Some, but not all, original SSC have been reanalyzed as new criteria were introduced. The most notable reanalysis effort was performed in the mid-1970's, immediately following development of the first facility-specific seismic design criteria (Gorman 1972). Seismic analyses for selected SSC (considered at the time to be the most critical) were updated as part of the Seismic Analysis Program Plan (Mousseau 1973). Some modifications were performed as a result of these analyses. Similarly, other analyses performed since original construction have resulted in various additional modifications to reduce seismic fragility.

The result of the periodic changes in seismic design criteria over the operating life of the ATR, and the selective upgrades of SSC to these changed criteria, is that not all Seismic Category I SSC are qualified for the SSE as currently defined. Some have not been qualified, some were qualified to the UBC during original construction, some have been qualified or requalified to criteria in effect after original construction (but no longer in effect), and some are fully qualified to the criteria applicable today.

An OBE is not defined for the ATR. The OBE, typically taken as one-half of the SSE, is defined for commercial nuclear power plants as the seismic event for which seismically-qualified SSC are analyzed to withstand without sustaining damage. An important part of the analysis of the OBE is consideration of fatigue cycling. An OBE is not applicable to the ATR since the seismic subsystem of the PPS is designed to scram the reactor at the onset of a seismic event, ensuring safety rod insertion before notable seismic motion occurs. The system is designed to shut down the reactor at accelerations exceeding 0.017g at seismic frequencies of 2.5 to 6 Hz (Atkinson 1997). There is not a risk of fatigue failure of SSC that could impede shutdown at these low levels of motion.

Since SSC are not analyzed for an OBE, there is not a level of seismic motion above 0.017 g for which the plant is qualified to remain fully operational. Therefore, prior to reactor startup following a seismic event that shuts down the reactor (or would have shut down the reactor had it been operating) a thorough inspection and evaluation of damage to plant SSC must be performed.

3.7.1 Seismic Design Parameters

3.7.1.1 Design Response Spectra. The original structure design was governed by the provisions contained in the 1961 UBC (Ebasco 1964a). Building structures, tanks, and the stack were designed to UBC Zone 2 requirements, in general, as follows (Ebasco 1964a):

- For buildings: maximum horizontal force equal to 0.05 times total dead load (including equipment) uniformly distributed over the height of the building
- For tanks on ground: horizontal force equal to 0.05 times dead load plus tank contents
- For stacks: horizontal force equal to 0.05 times dead load
- For interior and exterior walls: horizontal force equal to 0.10 times dead load
- For tanks or vessels inside of building: horizontal force equal to 0.10 times dead load plus contents.

The SSE was first introduced into the ATR design criteria by Gorman (1972). The SSE established by Gorman (1972) was based on a review of site characteristics that project the magnitude and intensity of possible nearby earthquakes (Maulde 1969). The major conclusions contained in Maulde (1969) and summarized in Gorman (1972) regarding the seismic environment at the ATR are:

- The largest earthquake that may be expected to occur near the ATR is no larger than Richter magnitude 7.
- The nearest active fault is the Arco Scarp, with an assumed epicenter approximately 16 miles from ATR. Therefore, for a Richter magnitude 7 earthquake at the Arco fault, a maximum horizontal acceleration of 0.24 g may be expected.
- The faulting near the ATR is dip-slip (near-vertical) faulting, in contrast to strike-slip (horizontal) faulting, which characterizes most California fault planes.
- The foundations of the major ATR plant facilities either rest on or are pinned into the bedrock, which is on the average about 43 ft below grade.

Seismic-design evaluation criteria, the second set of criteria, were prescribed for TRA's Seismic Category I equipment by Gorman (1972). These criteria specified the use of a time-history or step-by-step method of seismic analysis in evaluating Seismic Category I equipment, "where simplified methods are not appropriate." To provide the necessary time history, Gorman (1972) prescribed an ensemble of scaled strong-motion earthquake records to be used as representative seismic-input forcing functions at the TRA basement. The ensemble of time histories collectively produce a Housner-type spectrum. The Housner-type spectrum that Gorman (1972) proposed for design work (Figure 3.7-1) is based on the average, normalized spectra from the two horizontal components of each of four earthquake records. The motion given by Figure 3.7-1, increased by a factor of 1.5 for soil amplification, is defined at the free-field surface (Gorman, Guenzler, and Moore 1976).

The SSE spectrum is obtained from the Housner spectrum shown in Figure 3.7-1 by applying a scale factor of 1.93 times 1.5 to account for soil amplification. This factor accounts for the local geologic and seismic characteristics appropriate for ATR design. Key parameters proposed with the SSE spectrum are a peak ground acceleration of 0.24 g, damping of 5% of critical, and a representative spectrum intensity of 29 in. The spectrum intensity is defined as the area under the pseudo-velocity spectrum between the periods of 0.1 and 2.5 sec.

A third set of criteria was proposed in Gorman (1989b). This report recommended keying a response spectrum from U.S. NRC Regulatory Guide 1.60 to a peak ground acceleration of 0.24 g for design. The resulting spectrum is considered to be the current design response spectrum for use at the ATR. Criteria recommended for use in conjunction with this response spectrum are as follows:

- SSE is based on a Richter magnitude 7.3 earthquake occurring on the Howe Fault.
- The maximum expected peak horizontal bedrock acceleration is based on a lower cutoff value of 0.24 g; the peak vertical component is equal to 2/3 of the horizontal.
- Regulatory Guide 1.60 design response spectra for horizontal motion should be used. Two-thirds of the horizontal curves should be used for vertical motion. These should be applied at the base mat (bedrock) of the ATR structure.
- Regulatory Guide 1.61 damping factors supplemented, where appropriate, with recommendations of ASME Code Case N-411-1 and the Welding Research Council (1984) should be used for analysis.
- In general, soil-structure interaction effects and instructure support point amplification should be considered negligible at and below grade. However, where components are supported by walls or floors with predicted fundamental frequencies less than 33 Hz, determination of input design spectra should be evaluated on a case by case basis.
- Analyses should assume that three mutually orthogonal components of excitation occur simultaneously.
- The preferred method of analysis is to use the response-spectrum technique. Alternatively, use the time-history technique or, where it can be shown to be conservative, the equivalent-static-analysis technique.

Figure 3.7-2 presents the SSE horizontal design response spectrum, keyed to a peak ground acceleration of 0.24 g. Figure 3.7-3 presents the SSE vertical design response spectrum. These design spectra are presented in Tables 3.7-1 and 3.7-2 in numerical format for various damping values.

3.7.1.2 Design Time History. Design time histories were not used in the original building design and analysis. Time histories are not specified for use with the current SSE as defined by the response spectra listed in Tables 3.7-1 and 3.7-2.

3.7.1.3 Critical Damping Values. Gorman (1989b) established that Regulatory Guide 1.61 damping factors supplemented, where appropriate, with recommendations of ASME Code Case N-411-1 and the Welding Research Council (1984) should be used for analysis. Table 3.7-3 presents the modal damping values to be used for all modes considered in elastic spectral or time-history dynamic analyses [Nuclear Regulatory Commission (NRC) 1973a previously U.S. Atomic Energy Commission (AEC)]. The modal damping values given in Table 3.7-3 are expressed as a percentage of critical damping. Figure 3.7-4 presents the alternative damping values to be used with response-spectra analyses of piping.

3.7.1.4 Supporting Media for Seismic Category I Structures. The ATR site is located on the dry flood plain of the Big Lost River. The flood plain deposits consist of coarse sand and gravel with small, well rounded cobbles. Clay and silt are present in minor amounts. These highly permeable deposits range in thickness from a few feet to more than 60 ft, and are underlain by vesicular basalt. Between the basalt and the sand-and-gravel layers are beds of fine sand and silt where depressions occur in the basalt layer. These silt layers have a moderate clay content. The condition of the basalt varies from very dense and massive to very vesicular. Chapter 2 (Site Characteristics) presents more information on the basic geology of the ATR site.

Figure 3.7-5 and Figure 3.7-6 shows a generalized geologic section through the ATR site. The soil section under ATR is characterized by a sandy silt or silty clay layer overlying bedrock under the gravels. The bedrock is generally 40 to 50 ft below the surface, but may, locally, be as shallow as 32 ft or as deep as 70 ft (Cluff 1971). Boring and laboratory soil tests reveal an average of 40 ft of sand and gravel, followed by 2 to 5 ft of clay over a level formation of dense lava rock, which extends hundreds of ft below (Gorman, Guenzler, and Moore 1976).

A soil-structure interaction analysis performed on the Engineering Test Reactor (ETR) facility in 1976 (Gorman, Guenzler, and Moore 1976) used strain-dependent soil shear moduli and damping values based on recommendations for the INTEC, because of similarity with site properties to the ATR. Soil moduli 50% greater were also considered for the analysis because they compare well with recommended values for gravelly soils. Figure 3.7-7 shows how soil moduli vary with depth for the two soil conditions considered by Gorman, Guenzler, and Moore (1976). Figure 3.7-8 shows the recommended (Gorman, Guenzler, and Moore 1976) variations of shear moduli and damping ratios versus shear strain. In a CLASSI (Wong and Luco 1980) soil-structure interaction analysis that was performed to estimate instructure response, Eide, Khericha, and Thatcher (1989) assumed that the shear-wave velocity is 700 ft/sec in the upper 40 ft of the soil, and 3,500 ft/sec in the underlying competent rock.

3.7.2 Seismic System Analysis

3.7.2.1 Seismic-Analysis Methods. The Seismic Category I structures, include the reactor building (TRA-670), the firewater pump houses (TRA-619, -633), and the firewater storage tanks (TRA-719A, -719B, -719C, -718), were originally designed using equivalent-static-analysis procedures in accordance with the 1961 UBC (ICBO 1961). Ebasco (1964a) states that an equivalent static load of 0.05 times the building's dead weight (including equipment) be distributed uniformly over the building's height for seismic design. For tanks inside a building, a similar methodology was used; however, the coefficient of 0.05 was increased to 0.10.

Several analyses to more stringent criteria have been performed on the Seismic Category I structures since the original analysis as indicated in Blandford (1991). Gorman (1989b) specifies the use of either response-spectrum, time-history, or equivalent-static-analysis procedures as acceptable methods for dynamic analysis. The reactor building was analyzed in 1976 (Davidson 1976) using a response-spectrum technique. A response-spectrum analysis of the ATR storage canal has also been performed (Miller 1980). Both of these analyses used the Housner spectra anchored to 0.24 g (Figure 3.7-1) as the forcing function, and the analyses concluded that the reactor building and canal met design-allowable loading for the SSE.

The remaining Category I structures include the firewater pump houses (TRA-619, -633), and the firewater storage tanks (TRA-719A, -719B, -719C, -718). Fors (1982) concluded that the TRA-719 raw-water tanks "would be lifted and rotated essentially as a rigid body, being resisted only by downward forces" under SSE loads. The TRA-719 tanks were evaluated using the response-spectra loading shown in Figure 3.7-1 and TID-7024 (AEC 1963; Goodell 1985) evaluation methods. The results indicated that for water levels greater than 19 ft, some uplift and sliding of the tanks may occur but stresses will remain below allowable stresses up to a water level of 27 ft. In order to alleviate breaking off the main water supply line attached at the bottom of the tank, a flexible expansion type joint was installed on each tank to allow for uplift and sliding should they occur. The previously unanchored raw water storage tanks TRA-719A and –719B were removed and replaced with new foundations and new anchored tanks. The new tanks were seismically designed, evaluated, and constructed as PC-4 structures in accordance with DOE-STD-1020 (DOE 1996a) and the AE Standards (DOE-ID 1996) to NRC Regulatory Guide 1.60 seismic design response spectra for the 0.24g SSE for a maximum water height of 28 ft (Bragassa and Lippert 2000). The remaining raw water storage tank TRA-719C was modified to reduce the height of the tank from 40 ft to 30 ft and provide a new conical roof. This modified tank was evaluated as a PC-4 structure to the same seismic response spectra for a maximum water height of 26 ft (Rahl 1994; Lippert 1997). The overhead raw-water storage tank (ATR-718) has been the subject of numerous studies (Gorman 1985, 1986a; Siemer 1982b). Gorman (1986a) performed a response-spectrum analysis of the overhead raw-water storage tank, and concluded that it met design allowables for the SSE presented in Figure 3.7-1.

The TRA firewater tank (TRA-781) and pumphouse (TRA-688) are also Seismic Category I structures. These structures were designed and constructed to meet DOE standard (DOE 1996a) PC-4 seismic design criteria using NRC Regulatory Guide 1.60 design response spectra for the 0.24 g SSE (Brower 2001).

3.7.2.2 Natural Frequencies and Response Loads. Natural frequencies were not computed for Seismic Category I structures in the original analysis; however, several structures have been the subject of more recent dynamic analysis. Davidson (1976) analyzed all abovegrade structural components for the reactor building, and reports the lowest 81 frequencies for the reactor building's superstructure as ranging from 1.6 to 13 Hz. The lowest 30 modes and the areas in which they manifest themselves are listed in Table 3.7-4.

A subsequent analysis completed by Miller in 1980 investigated the response of the canal structure (belowgrade). Miller reports frequencies from 2.0 to 25 hz for the ATR Canal model (Miller 1980). Gorman (1986a) reports fundamental frequencies for the TRA Overhead Water Storage Tank and Tank Tower (TRA-718) of about 0.4 hz in the horizontal direction and 3.1 hz in the vertical. The remaining storage tanks (TRA-719A, B, and C) were evaluated using the peak acceleration from the governing response spectra and TID-7024 criteria; hence, no frequencies were reported in the stress analysis document. No seismic analysis other than the original design have been completed on the Firewater Pump Houses (TRA-619, -633), hence, no frequencies are available for these facilities.

The summary reports listed above present the analytical results in terms of factors of safety for the most critically loaded members in each of the facilities. Table 3.7-5 presents a summary of the results as contained in the stress analysis reports. From this table, it can be seen that, with few exceptions, the stresses at the critical locations are within the allowable limits.

In the Reactor Building several columns and beams were reported to be slightly overstressed. The W10x66 columns supporting the girders in the reactor vessel area were reported to have capacity to demand ratios of 0.84, indicating an approximate overstress of 19%. Recommendations to strengthen these columns by adding a plate to the flange of the columns was made in Davidson (1976). The remaining overstresses reported in Davidson (1976) are within 10% of the allowable stresses. Since conservative assumptions were made in the analysis, no further recommendations for upgrade were proposed in Davidson (1976). The remaining category I facilities show no indication of overstress. A later reevaluation of the W10x66 columns by Gorman in 1980 using plastic design methods of the ASIC manual showed the columns stresses were within allowables. As a result, no modifications were recommended for the columns (Gorman 1980).

The reactor building's substructure and superstructure portions were included in an approximate model used to generate floor response-spectra as part of the probabilistic risk assessment (Eide, Khericha, and Thatcher 1989).

3.7.2.3 Procedure Used for Modeling. Eide, Khericha, and Thatcher (1989) developed an approximate structural model of the reactor building as part of the probabilistic risk assessment[a]. The reactor building's structure was represented by an equivalent-stiffness, lumped-mass model. The substructure, which consisted of the heavy concrete shear walls and slabs at and below grade, was modeled explicitly. The superstructure was modeled as a rigid mass attached to the top floor of the substructure. The substructure portion of the structure was modeled as discrete lumped masses interconnected by vertical beam elements. Lumped masses were located at the mass centroids, elevations of 79 ft (first basement) and 98 ft (first floor). The masses included the weights of the structure, the attached equipment, and the water in the storage canal. Mass properties of the superstructure, including weight of the structure, roofing, and other attached components, were added to the substructure's first-floor mass.

---

[a] The approximate structural model was required for the ATR probabilistic risk assessment (PRA). Floor response spectra were generated from the simplified model and were used in estimating demand on the seismic category I components. Simplified lumped-mass stick models were often used in generating floor response spectra for this purpose. The lumped mass stick models need to be sufficiently detailed to capture the dynamic response characteristics of the superstructure including frequencies, mode shapes, and participation factors. Response quantities of the supporting structure such as story shears, overturning moments, and perhaps wall forces are not required.

The simplified model used for the PRA was developed to approximately match the eigensolution (for the major structural modes) from the more detailed model used in the evaluation of the ATR structure itself (Davidson, 1976). A comparison of the structural response quantities was not performed, as it was not needed for the generation of floor response spectra.

Stiffnesses of the beam elements connecting the lumped masses were represented by equivalent elastic properties that condense the stiffness of the shear walls. The stiffnesses of all major walls continuous between the base mat and the first floor were included. Overall structure stiffnesses were calculated assuming that the floors act as rigid diaphragms. Equivalent elastic properties, including axial areas, shear areas, and torsional and flexural moments of inertia, were used as model input. Beam elements were located, in plan view, at the centers of rigidity. Displacements of the centers of mass and centers of rigidity were rigidly linked.

3.7.2.4 Soil-Structure Interaction. No soil-structure interaction (SSI) analyses were performed as part of the original design for the Seismic Category I structures. The reactor building has had some limited SSI analyses completed on it. Gorman (1974) performed a limited assessment of the supporting media, and concluded that the effects of SSI would be to reduce the instructure horizontal motion from that of the free-field, and that vertical motion would be nearly the same.

The current recommendations for inclusion of SSI effects in the design analysis criteria of SSC are given in Gorman (1989b): "In general, soil-structure interaction effects and instructure support-point amplification should be considered negligible at and below grade. However, where components are supported by walls or floors with predicted fundamental frequencies less than 33 Hz, determination of input design spectra should be evaluated on a case-by-case basis."

A median-centered response analysis was performed by Eide, Khericha, and Thatcher (1989) to obtain realistic floor spectra. As part of this work, a soil-structure interaction analysis was performed. The SSI response analysis was performed using the substructure technique. The CLASSI family of computer programs, an implementation of the substructure approach, was the basis for the SSI and structural-response calculation.

The free-field input motion for the SSI analysis was specified at the top of the bedrock outcropping. The control motion consisted of acceleration time histories. For the ATR site, Eide, Khericha, and Thatcher (1989) defined the seismic input for the SSI analysis as the median NUREG/CR-0098 (Newmark and Hall 1978) ground-response spectra for rock sites. Three synthetic acceleration time histories were generated from previous U.S earthquakes record for use as the free-field input motions for the SSI analyses. Response spectra generated from the resulting synthetic time histories enveloped the median NUREG/CR-0098 response spectra for rock sites.

The ATR is anchored directly to the bedrock. For other structures at TRA, Eide, Khericha, and Thatcher (1991) noted that essentially no amplification of the bedrock motion by the soil overburden is expected. Therefore, SSI is judged to have negligible influence on the seismic fuel damage frequencies.

A site-response analysis (Eide, Khericha, and Thatcher 1989) was performed to obtain ground motion time-histories at the free surface for the SSI analysis. The soil profile used assumed a shear-wave velocity of 700 ft/sec for a 60-ft layer of soil, and a shear-wave velocity of 3,500 ft/sec in the underlying bedrock. One-dimensional wave-propagation analysis using SHAKE (Schnabel, Lysmer, and Bolton 1972) was used for site-response calculations[a].

---

[a]. The computer code SHAKE has been verified to be in accordance with the EQE Quality Assurance Manual, dated November 15, 1991, Revision 2. The EQE Quality Assurance program was prepared to establish quality assurance policy and practice for engineering services offered to EQE clients. The program is intended to show compliance with the following criteria: (EQE 1991)

- ANSI/ASME NQA-1, "Quality Assurance Program Requirements for Nuclear Power Plants." (ASME 1989a)

3.7.2.5 Development of Floor-Response Spectra. Instructure-response spectra were generated for the reactor building as part of the probabilistic risk assessment (Eide, Khericha, and Thatcher 1989).

3.7.2.6 Three Components of Earthquake Motion. The original design, performed in accordance with the 1961 UBC, assumed one direction of earthquake motion at a time. Gorman (1989b) establishes that for analysis purposes, three mutually orthogonal components of excitation should be assumed to occur simultaneously. The horizontal-direction components are defined as a 0.24 g, rock, Regulatory Guide 1.60 motion. The vertical-direction component is defined as being 2/3 of the horizontal motion. Many analyses completed to date are based on response resulting from one horizontal component (worst) and one vertical component. Recent analysis has been based on three orthogonal components of motion (Miller 1980).

3.7.2.7 Combination of Modal Response. The original design bases did not include modal analyses of Seismic Category I structures. Analysis subsequent to Gorman (1972) combined modal responses by a square-root of the sum of the squares method. Closely spaced modes were not treated any differently.

3.7.2.8 Interaction of Non-Category I Structures with Seismic Category I Structures. No analysis has been performed to assess the effect of seismic motion of non-Category I structures on the performance of Seismic Category I structures. However, seismic walkdowns of the plant have been completed as part of the PRA (Eide, Khericha, and Thatcher 1989) to assess the vulnerability of important systems. These walkdowns consider the potential for related failures. Based on these results, the fuel damage frequency from seismic events has been shown acceptable. Additionally, identified vulnerabilities that are relatively easily removed have resulted in modifications. Based on these results, there is limited need for a formal analysis of interaction between structures.

3.7.2.9 Effects of Parameter Variations on Floor-Response Spectra. No response spectra have been developed for use in equipment design or qualification; thus, the effects of parameter variations on floor-response spectra have not been quantified. Response spectra developed in support of the PRA (Eide, Khericha, and Thatcher 1989) were based on best estimates of the soil and structure properties. The effects of parameter variation in soil and structure properties were not accounted for explicitly.

3.7.2.10 Use of Constant Vertical Static Factors. Constant vertical static factors are not used in the analysis of Seismic Category I structures.

3.7.2.11 Method Used to Account for Torsional Effects. No additional corrections are used in the analysis of Seismic Category I structures to account for the effects of torsion. In general, analyses that have been completed subsequent to the original plant design have been three dimensional. These three-dimensional models have explicitly modeled any plan irregularities so that torsional effects would be accounted for.

3.7.2.12 Comparison of Responses. Subsequent to the original plant design, response-spectrum approaches have been used in the analysis of Seismic Category I structures. No time histories have been developed for use in upgrade design, or additional analysis to the SSE.

3.7.2.13 Methods for Seismic Analysis of Dams. The ATR is located on the Big Lost River basin. Streamflow in the basin is affected by storage and release of irrigation water (a) in the Mackay Reservoir (capacity 44,370 acre-ft), 30 mi upstream from Arco and 4 mi northwest of Mackay and (b) by the irrigation of about 57,500 acres of land by diversion from the river (Bennett 1990). The INEEL flood-control diversion system, located upstream from the ATR, diverts flow from the main river through the INEEL diversion channel into spreading areas to prevent flooding at downstream facilities. The maximum diversion capacity of the diversion channels is about 9,300 ft^3/sec (Bennett 1986).

Mackay Dam is located in a region of historical seismicity, as evidenced by the 1983 Borah Peak earthquake. The performance of the dam during this earthquake demonstrated the stability of the embankment during moderate ground motion. However, Mackay Dam was built without seismic-design criteria, and it is unclear how seismically secure the structure really is. Because of the historical seismicity in the area and the lack of seismic-design criteria for the structure, a seismically-induced failure has been analyzed (Koslow and Van Haaften 1986).

The postulated seismic failure of Mackay Dam was assumed to occur during an inflow to the reservoir equal to the 25-yr recurrence interval flood (peak flow 4,030 cfs). Because a seismic event would disrupt a significant part of the dam's structure, the breech was assumed to be trapezoidal, extending to the bottom of the structure at 5,997 ft-msl, and developing over a 1-hr period (Koslow and Van Haaften 1986).

Koslow and Van Haaften (1986) concluded that floodwaters resulting from this scenario would not reach the TRA facilities area (where ATR is located) because of the area's elevation above the nearby flood plain.

3.7.2.14 Determination of Seismic Category I Structure Overturning Moments. The reactor building consists of a substructure made of heavily reinforced concrete, and a superstructure of steel-frame construction with exterior walls made primarily of insulated aluminum sandwich panels. The building's substructure is supported by subsurface rock. Approximately 2/3 of the substructure bears directly on bedrock. The remainder of the substructure is supported by concrete piers to bedrock (Gorman 1974). The average depth of the substructure is about 42 ft, and the average superstructure height is about 38 ft. Overturning of the reactor building is not expected because of the geometry of the structure. Davidson (1976) investigated member stresses due to the SSE.

The remaining Seismic Category I structures include the firewater pump houses (TRA-619, -633, -688) and the firewater storage tanks (TRA-719A, -719B, -719C, -718, -781). Section 3.7.2.1 summarizes the seismic evaluations of these structures, including overturning moments.

3.7.2.15 Analysis Procedure for Damping. Damping values specified in Table 3.7-3 were used in dynamic analysis. Equivalent modal damping values for coupled soil-structure systems were not used, since soil-structure interaction analyses were minimal.

3.7.3 Seismic Subsystem Analysis[a]

Seismic Category I systems and components (see Section 3.2.1) were originally designed to seismic loads specified in the 1961 Uniform Building Code (ICBO 1961). Subsequent to the original design, safety standards have been developed that follow more stringent criteria than the Uniform Building Code. Recognizing this situation, the Seismic Analysis Program Plan was initiated in early 1973 to assess the safety significance of differences between the as-built condition of vital systems and components and the more recent safety standards (Mousseau 1973).

In general, the seismic-loading criteria for systems and components parallels that for structures. No instructure-response spectra or amplified structural responses have been estimated for the evaluation of equipment. Because amplification of ground motion resulting from the structural response of the reactor building is not expected (Gorman 1974), systems and components, which have been analyzed subsequent to the original design, have been analyzed to ground-response spectra. Section 3.7.1.1 describes the evolution of the SSE as it is now defined.

3.7.3.1 Seismic-Analysis Methods. Gorman (1989b) contains recent criteria for the seismic analysis of SSC. Methods applicable for subsystems are equivalent to those used in the analysis of structures. For systems that have been qualified by analysis, the response-spectrum technique is normally used.

3.7.3.2 Determination of Number of Earthquake Cycles. Fatigue requirements for seismic loads were not investigated. The components making up the Reactor Coolant Pressure Boundary were all designed prior to ASME nuclear codes (See UFSAR, section 5.2). The codes in force at the time of design included ASA B31.1-1955 for piping, ASME Unfired Pressure Vessel Code, 1962 for Vessels and Heat Exchangers, and Standards of the Hydraulic Institute, Centrifugal Pumps Section, 10th Edition, 1959 for Pumps. These codes did not specifically address fatigue limits for earthquake loads. In addition, the seismic design and evaluation basis for the ATR subsequent to the original design has specified as the ground motion event from a 0.24 g earthquake. This event has been postulated to be the "Safe Shutdown Earthquake" for the plant. The current seismic fatigue requirements in ASME are specified only for the OBE. Since an OBE was never specified for the ATR, no fatigue requirements are invoked.

3.7.3.3 Procedure Used for Modeling. Procedures used in modeling follow the recommended interim earthquake criteria contained in Gorman (1989b). Analysis was completed as part of the Seismic Analysis Program Plan (Mousseau 1973). Guidance contained in Standard RDT F9-2T (AEC 1974) was also followed for subsystems analysis (Davidson and Thinnes 1974; Davidson 1975, 1976).

3.7.3.4 Basis for Selection of Frequencies. It was not necessary to separate fundamental frequencies of components and subsystems from the forcing frequencies of the supporting structure because coupled structure-system analyses were not performed.

---

[a]. For further information concerning mechanical and electrical systems and components see Section 3.9 and 3.10.

3.7.3.5 Use of Equivalent-Static-Load Method of Analysis. Gorman (1989b) allows the use of the equivalent-static-load method of analysis, "where appropriate." Where this method was used, the procedure contained in RDT F9-2T (AEC 1974) was followed:

- Where response spectra were available for the support point, the equivalent static force for the supported system or component was taken as

$$F = 1.5 W_e A_s \tag{3.7-1}$$

where

F = equivalent static force to be applied at the center of mass of the system or component

W_e = mass of system or component including liquid contents

A_s = peak acceleration from support point response spectrum for the appropriate system or component damping value.

- Where response spectra were not available for the support point, the equivalent static force for the system or component was taken as

$$F = 8.0\ W_e A_g$$

where A_g is the peak acceleration from the ground response spectrum for the appropriate system or component damping value.

3.7.3.6 Three Components of Earthquake Motion. The same procedure as described in Section 3.7.2.6 was used for subsystem analysis.

3.7.3.7 Combination of Modal Responses. The same procedure as described in Section 3.7.2.7 was used for subsystem analysis.

3.7.3.8 Analytical Procedures for Piping. The ATR primary system piping was originally designed to the American Standards Association (ASA) B31.1 Pipe Code. Other equipment was designed to the ASME Section VIII requirements. Neither of these codes provides specific load categorization to be used for earthquakes. Subsequent to the original design, additional analysis of piping systems have followed Section III of the ASME Boiler & Pressure Vessel Code for faulted conditions as guideline criteria for determining the adequacy of the piping and components. Additional guidance concerning seismic loads and dynamic analysis contained in RDT-F9-2T (AEC 1974) was followed.

Seismic Category I piping includes the PCS and branch piping included in the PCS boundary. The boundary is limited by the "maximum leak diameter." The maximum leak diameter for the PCS is 3 in. (Davidson and Thinnes 1974). This means that leaks up to a diameter of 3 in. can be tolerated during safe shutdown of the plant. Therefore, lines larger than 3 in. in diameter, and which were not restricted by an orifice of 3 in. or less, were part of the analysis conducted by Davidson and Thinnes (1974).

The PCS surge tank and surge tank supports meet the intent of Section VIII of the ASME Boiler and Pressure Vessel Code, ASME 1989c edition (Snow 1991a, 1993, 1994a).

PCS piping was analyzed using the response-spectrum method to the SSE defined in Figure 3.7-1 (Davidson 1979). No additional instructure amplification was applied to the support points of the piping. Each model used in the analysis was subjected to two seismic load cases. Each load case contained one horizontal and one vertical component of motion. Thus, the three earthquake input directions were considered in the analysis; however, for each model only 1 horizontal plus 1 vertical direction input was placed on the model in any run. Stress results were based on the larger of two horizontal components plus vertical. Relative displacements between anchor points were neglected. Modal contributions were combined via square-root-sum-of-squares method, with all modes to at least 16 Hz accounted for in the analysis. On smaller systems, all modes to 30 Hz were considered in accordance with RDT-F9-2T (AEC 1974).

The PCS contains non-standard components consisting of field-fabricated tees, y-lateral connections, eccentric reducers, pipe stub-ins, and short-radius elbows. These components cannot be analyzed with the simplified code methods used in the Davidson (1979) analysis. These components were analyzed subsequent to the Davidson (1979) analysis using the response-spectrum method, but using the later-defined SSE (Gorman 1989b) as depicted in Figure 3.7-2 and Figure 3.7-3 (Harris 1989; Harris and Burr 1989; Miller 1988, 1989a, 1989b, and 1989c). Loadings were applied in three orthogonal directions simultaneously, and acceptance was based on a combination of elastic and elastic-plastic techniques.

The firewater redundant line (Miller and Yuan 1986), the firewater piping (Snow and Hendrickson 1996, Snow 2001), the above-ground TRA firewater piping (Siemer 1982a), and the VVS piping (Harris 1988) were later analyzed, again using the response-spectrum method to the SSE. The analyses were performed using the NUPIPE-II Code (See Table 3.9-2), a proprietary structural-analysis code for the static and dynamic responses of linear systems. The response spectra for the Firewater Redundant Line analysis are shown in Table 3.7-6. The response spectra used to obtain SSE loadings were based upon a 1% damping value and were applied in all three directions simultaneously. The response spectra for the Firewater Piping System are shown in Table 3.7-7. The U.S. Atomic Energy Commission Regulatory Guide 1.60 (NRC 1973b) was followed for the damping. Response spectra were applied in the two horizontal directions and the vertical direction simultaneously with the results being combined by the 10% rule for closely spaced modes per NRC requirements. A maximum bedrock acceleration of 0.24 g was used. The response spectra for the VVS analysis are shown in Table 3.7-6. The response spectra used to obtain SSE loadings were based upon a 2% damping value and were applied in all three directions simultaneously.

The Firewater Redundant Line piping meets the design criteria established by the pertinent subsections of Section III of the 1980 ASME Boiler and Pressure Vessel Code (Miller and Yuan 1986; ASME 1980b). The recommended piping support modifications are completed. The Firewater Piping System meets the design requirements of the ANSI/ASME B31.1 Code (Snow and Hendrickson 1996, Snow 2001; ASME 1980a). The portion of the firewater piping that lies within the radiographic boundary also meets the design requirements of the pertinent subsections of Section III of the 1990 ASME Boiler and Pressure Vessel Code (Snow and Hendrickson 1996, Snow 2001; ASME 1990). All supports for that portion of the Firewater Piping System within the radiographic boundary meet the Class 1 support requirements of Section III of the ASME Boiler and Pressure Vessel Code (Snow and Hendrickson 1996, ASME 1990). The TRA utility area piping contained within pumphouses TRA-619 and TRA-633, and the above ground piping attached to water tanks TRA-719A, TRA-719B, and TRA-719C also meets the design requirements of the pertinent subsections of Section III of the 1980 ASME Boiler and Pressure Vessel Code (Siemer 1982a, ASME 1980b). All piping supports in TRA-619 and TRA-633 have been replaced as recommended and meet the ASME Code Rules for Level D service (Siemer 1982a, ASME 1980b). The firewater piping associated with TRA firewater tank (TRA-781) and pumphouse (TRA-688)

meets the design requirements of the 1986 ASME Boiler and Pressure Vessel Code (Brower 2001; ASME 1986). VVS meets the design criteria of the pertinent subsections of Section III of the 1986 ASME Boiler and Pressure Vessel Code (Harris 1988; ASME 1986).

3.7.3.9 Multiply Supported Equipment Components with Distinct Inputs. Anchor points for Seismic Category I piping in the reactor building were assumed to respond rigidly with the ground. They were assumed to do so because all anchor points are at nearly the same elevation and because the reactor building is very stiff, not allowing large relative displacements (Davidson and Thinnes 1974). No multiple-point inputs were used.

3.7.3.10 Use of Constant Vertical Static Factors. Constant vertical static factors are not used in the analysis of Seismic Category I subsystems.

3.7.3.11 Torsional Effects of Eccentric Masses. Torsional effects of eccentric masses on subsystems are generally accounted for through the use of three-dimensional models, which explicitly model eccentricities between the centers of mass and centers of rigidity of subsystems. This guidance is contained in RDT-F9-2T (AEC 1974).

3.7.3.12 Buried Seismic Category I Piping Systems and Tunnels. The firewater system consists of the raw-water storage tanks, electric and diesel-driven firewater pumps, buried distribution piping, and associated valves and controls necessary to supply water to the EFIS in the reactor building. The firewater system's buried piping has undergone numerous studies intended to show compliance with ASME Code Rules for Level D service (Miller 1978; Siemer 1981; Yuan 1983; Gorman 1986b; Call 1986; Miller and Yuan 1986; Brower 2001).

The firewater system has been analyzed to the 0.24 g Housner ground spectrum (Figure 3.7-1) for the horizontal directions, and 2/3 of the horizontal for the vertical (Miller 1978). Subsequent to Miller's (1978) analysis, modifications were completed to reduce the stress in the buried firewater piping to acceptable levels. The upgrades to the firewater system were completed to ensure flexibility in the firewater piping in the vicinity of attachments to buildings and tanks (Gorman 1986b).

3.7.3.13 Interaction of Other Piping with Seismic Category I Piping. The primary coolant pressure boundary is almost entirely isolated from high-energy system piping. For the most part, there is only moderate-energy and low-temperature piping in the vicinity of the pressure boundary. Therefore, there is limited need for piping interaction analyses. The exception is loop piping in the subpile room and in the corridors that surround the reactor vessel (e.g., the safety rod drive corridor). An evaluation of the potential for failure of loop piping in these areas and the potential effects on the primary coolant pressure boundary is discussed in Chapter 10 (Experiment and Irradiation Facilities). The evaluation concludes that primary coolant pressure boundary failures will not result from failures of loop piping.

3.7.3.14 Analysis Procedure for Damping. Damping values specified in Table 3.7-3 were used in dynamic analysis. In coupled system models, the lowest value of damping was used for all modes of response.

3.7.4 Seismic Instrumentation

3.7.4.1 Comparison with Regulatory Guide 1.12. Regulatory Guide 1.12 (NRC 1974b) establishes criteria acceptable to the regulatory staff for satisfying the seismic instrumentation requirements in Paragraph VI (9a)(3) of Appendix A to 10 CFR 100 (CFR 1977) for assuring the safety of nuclear power plants. The purpose of the strong motion instrumentation is to allow comparison of in-structure response, and component response to measured seismic motion. Regulatory Guide 1.12 recommends placing one triaxial peak accelerograph at one location of each of the following:

- A selected location on the reactor equipment
- A selected location on the reactor piping
- The most pertinent location on one of the following outside of the containment structure:
  - Seismic Category I equipment
  - Seismic Category I piping

In addition to the three strong-motion accelerographs, Regulatory Guide 1.12 recommends placing triaxial response-spectra recorders (a) at the containment foundation, (b) on the supports for piping or reactor equipment, (c) at the foundation of an independent Seismic Category I structure where the response is different from that of the reactor containment structure, and (d) at either a Seismic Category I equipment support or appropriate floor location, or a Seismic Category I piping support or appropriate floor location (NRC 1974b).

The instrumentation at the reactor building falls short of meeting the recommendations of Regulatory Guide 1.12 (NRC 1974b); however, the reactor building is considerably less complex than that of a typical pressurized-water reactor, and the instructure response is expected to be less amplified than that of a commercial power reactor. Furthermore, the design basis for SSC for the ATR was established prior to the issuance of Regulatory Guide 1.12. Subsequent analysis have used ground spectra to define the expected instructure response.

3.7.4.2 Location and Description of Instrumentation. One strong-motion accelerograph is mounted in the reactor building basement (TRA-670). An additional strong-motion accelerograph is mounted in the basement of the ETR reactor building (TRA-642). Both instruments are Kinemetrics SMA-1 model triaxial time history accelerographs (Jackson et al. 1991a).

These instruments were located as part of a strong-motion accelerograph network begun at the INEEL in 1973. In conjunction with the strong-motion accelerographs (SMA), a seismic monitoring network is maintained by the Contractor. These instruments form the basis for the INEEL Seismic Network. The INEEL started its network in December 1971 for the purpose of monitoring earthquake activity on and around the eastern Snake River Plain in the vicinity of the INEEL. The INEEL collects earthquake data to develop a historical seismic-data base. The INEEL began its SMA network for the purpose of recording strong ground motions from local moderate or major earthquakes. The INEEL collects SMA data to determine the amount of ground motion and response of the facilities to ground motion during a large earthquake. In addition, the earthquake data are used to assess seismic hazards and develop seismic-design criteria for the INEEL.

3.7.4.3 Control Room Operator Notification. Seismic switches are located in the rod access corridor of the reactor building as part of the PPS. The switches are set to trip the reactor at peak ground accelerations of 0.01 g. Control room personnel would have indication of the cause of a scram thereby recognizing the occurrence of a seismic event. This indication from the PPS is reliable since a failure in the PPS instrumentation is a low probability. Combining the probability of instrument failure with a low probability seismic event results in a negligible probability that the operator would not have indication of the event. The information from the SMA is available after an event to support evaluation and restart of the reactor. The strong-motion accelerograph is maintained by the INEEL (Jackson et al. 1991a,b). After a seismic shutdown, a review of SSC would be required to show readiness for post-earthquake operation.

3.7.4.4 Comparison of Measured and Predicted Responses. No instructure response spectra were developed for SSE design of Seismic Category I SSC. Predicted response is, therefore, not available on a component basis. No procedures are in place to direct the comparison between measured response at the base mat of the reactor building and design-basis spectra. Analyses of other structures at TRA indicated little effect due to soil-structure interactions. Therefore, the analysis of the ATR systems does not include an amplification. Since there is little effect expected, there are no preparations to evaluate the differences.

Table 3.7-1. Horizontal design spectra for safe shutdown earthquake.[a]

		Accelerations (g) for listed percentages of critical damping				
Frequency (Hz)	Period (s)	0.5%	2%	5%	7%	10%
0.10	10.000	0.0282	0.0221	0.0181	0.0166	0.0150
0.20	5.000	0.1130	0.0883	0.0724	0.0664	0.0600
0.25	4.000	0.1766	0.1379	0.1131	0.1037	0.0938
0.30	3.333	0.2083	0.1616	0.1314	0.1200	0.1078
0.33	3.000	0.2292	0.1771	0.1433	0.1305	0.1169
0.40	2.500	0.2705	0.2075	0.1665	0.1510	0.1344
0.50	2.000	0.3313	0.2519	0.2000	0.1805	0.1595
0.60	1.667	0.3909	0.2951	0.2323	0.2088	0.1834
0.70	1.429	0.4496	0.3375	0.2637	0.2361	0.2064
0.80	1.250	0.5075	0.3790	0.2943	0.2627	0.2286
0.90	1.111	0.5648	0.4198	0.3243	0.2886	0.2502
1.00	1.000	0.6215	0.4601	0.3536	0.3140	0.2712
1.20	0.833	0.7334	0.5390	0.4108	0.3632	0.3119
1.40	0.714	0.8436	0.6163	0.4663	0.4108	0.3510
1.60	0.625	0.9523	0.6921	0.5205	0.4570	0.3888
1.72	0.580	1.0191	0.7386	0.5534	0.4851	0.4117
1.80	0.556	1.0598	0.7667	0.5734	0.5021	0.4255
2.00	0.500	1.1661	0.8402	0.6253	0.5462	0.4612
2.20	0.455	1.2715	0.9128	0.6762	0.5894	0.4962
2.40	0.417	1.3760	0.9845	0.7264	0.6319	0.5304
2.60	0.385	1.4201	1.0143	0.7470	0.6492	0.5442

Table 3.7-1. (continued).

		Accelerations (g) for listed percentages of critical damping				
Frequency (Hz)	Period (s)	0.5%	2%	5%	7%	10%
2.80	0.357	1.4052	1.0036	0.7392	0.6424	0.5384
3.00	0.333	1.3915	0.9938	0.7320	0.6362	0.5332
3.20	0.313	1.3788	0.9847	0.7254	0.6304	0.5283
3.40	0.294	1.3670	0.9762	0.7191	0.6251	0.5238
3.60	0.278	1.3559	0.9683	0.7133	0.6200	0.5195
3.80	0.263	1.3455	0.9608	0.7079	0.6153	0.5155
4.00	0.250	1.3358	0.9538	0.7028	0.6109	0.5118
4.20	0.238	1.3265	0.9472	0.6979	0.6067	0.5082
4.60	0.217	1.3095	0.9350	0.6890	0.5990	0.5017
4.80	0.208	1.3016	0.9293	0.6848	0.5954	0.4987
5.00	0.200	1.2941	0.9239	0.6809	0.5919	0.4958
6.00	0.167	1.2610	0.9002	0.6635	0.5769	0.4831
6.67	0.150	1.2423	0.8868	0.6536	0.5684	0.4759
7.00	0.143	1.2337	0.8806	0.6491	0.5645	0.4726
8.00	0.125	1.2105	0.8640	0.6370	0.5539	0.4637
9.00	0.111	1.1904	0.8496	0.6264	0.5448	0.4560
10.00	0.100	1.0454	0.7668	0.5795	0.5098	0.4329
12.00	0.083	0.8350	0.6422	0.5065	0.4544	0.3956
14.00	0.071	0.6906	0.5528	0.4520	0.4123	0.3666
16.00	0.063	0.5858	0.4854	0.4096	0.3790	0.3432
18.00	0.056	0.5066	0.4329	0.3755	0.3518	0.3238
20.00	0.050	0.4449	0.3907	0.3474	0.3292	0.3074
22.00	0.045	0.3956	0.3561	0.3238	0.3100	0.2932
24.00	0.042	0.3554	0.3272	0.3036	0.2934	0.2809
26.00	0.038	0.3220	0.3027	0.2862	0.2790	0.2700
28.00	0.036	0.2939	0.2816	0.2710	0.2662	0.2603
30.00	0.033	0.2699	0.2633	0.2575	0.2549	0.2516
32.00	0.031	0.2493	0.2473	0.2455	0.2447	0.2437
34.00	0.029	0.2400	0.2400	0.2400	0.2400	0.2400
36.00	0.028	0.2400	0.2400	0.2400	0.2400	0.2400
38.00	0.026	0.2400	0.2400	0.2400	0.2400	0.2400
40.00	0.025	0.2400	0.2400	0.2400	0.2400	0.2400
50.00	0.020	0.2400	0.2400	0.2400	0.2400	0.2400
100.00	0.010	0.2400	0.2400	0.2400	0.2400	0.2400

a. Gorman 1989b.

Table 3.7-2. Vertical design spectra for safe shutdown earthquake.[a]

		Accelerations (g) for listed percentages of critical damping				
Frequency (Hz)	Period (s)	0.5%	2%	5%	7%	10%
0.10	10.00	0.0188	0.0147	0.0121	0.0111	0.0100
0.20	5.00	0.0753	0.0588	0.0483	0.0443	0.0400
0.25	4.00	0.1177	0.0920	0.0754	0.0692	0.0625
0.30	3.33	0.1389	0.1077	0.0876	0.0800	0.0719
0.33	3.00	0.1528	0.1181	0.0955	0.0870	0.0779
0.40	2.50	0.1803	0.1383	0.1110	0.1007	0.0896
0.50	2.00	0.2208	0.1679	0.1333	0.1203	0.1063
0.60	1.67	0.2606	0.1968	0.1549	0.1392	0.1223
0.70	1.43	0.2997	0.2250	0.1758	0.1574	0.1376
0.80	1.25	0.3384	0.2526	0.1962	0.1751	0.1524
0.90	1.11	0.3765	0.2799	0.2162	0.1924	0.1668
1.00	1.00	0.4143	0.3067	0.2357	0.2093	0.1808
1.20	0.83	0.4889	0.3594	0.2739	0.2421	0.2079
1.40	0.71	0.5624	0.4109	0.3109	0.2739	0.2340
1.60	0.63	0.6349	0.4614	0.3470	0.3047	0.2592
1.72	0.58	0.6794	0.4924	0.3690	0.3234	0.2744
1.80	0.56	0.7065	0.5111	0.3823	0.3347	0.2836
2.00	0.50	0.7774	0.5601	0.4168	0.3641	0.3075
2.20	0.45	0.8477	0.6085	0.4508	0.3929	0.3308
2.40	0.42	0.9174	0.6563	0.4843	0.4212	0.3536
2.60	0.38	0.9467	0.6762	0.4980	0.4328	0.3628
2.80	0.36	0.9368	0.6691	0.4928	0.4283	0.3590
3.00	0.33	0.9277	0.6625	0.4880	0.4241	0.3555
3.20	0.31	0.9192	0.6565	0.4836	0.4203	0.3522
3.40	0.29	0.9113	0.6508	0.4794	0.4167	0.3492
3.60	0.28	0.9039	0.6455	0.4756	0.4134	0.3463
3.80	0.26	0.8970	0.6406	0.4719	0.4102	0.3437
4.00	0.25	0.8905	0.6359	0.4685	0.4073	0.3412
4.20	0.24	0.8844	0.6315	0.4653	0.4045	0.3388
4.40	0.23	0.8785	0.6273	0.4622	0.4018	0.3366
4.60	0.22	0.8730	0.6233	0.4593	0.3993	0.3345
4.80	0.21	0.8677	0.6196	0.4565	0.3969	0.3325
5.00	0.20	0.8627	0.6160	0.4539	0.3946	0.3305

Table 3.7-2. (continued).

		Accelerations (g) for listed percentages of critical damping				
Frequency (Hz)	Period (s)	0.5%	2%	5%	7%	10%
6.00	0.17	0.8407	0.6001	0.4423	0.3846	0.3221
6.67	0.15	0.8282	0.5912	0.4358	0.3789	0.3173
7.00	0.14	0.8224	0.5871	0.4328	0.3763	0.3151
8.00	0.13	0.8070	0.5760	0.4246	0.3693	0.3091
9.00	0.11	0.7936	0.5664	0.4176	0.3632	0.3040
10.00	0.10	0.6970	0.5112	0.3863	0.3398	0.2886
12.00	0.08	0.5567	0.4281	0.3377	0.3029	0.2637
14.00	0.07	0.4604	0.3685	0.3014	0.2748	0.2444
16.00	0.06	0.3905	0.3236	0.2731	0.2526	0.2288
18.00	0.06	0.3377	0.2886	0.2503	0.2345	0.2159
20.00	0.05	0.2966	0.2605	0.2316	0.2195	0.2049
22.00	0.05	0.2637	0.2374	0.2159	0.2067	0.1955
24.00	0.04	0.2369	0.2181	0.2024	0.1956	0.1873
26.00	0.04	0.2147	0.2018	0.1908	0.1860	0.1800
28.00	0.04	0.1959	0.1877	0.1806	0.1775	0.1735
30.00	0.03	0.1800	0.1756	0.1717	0.1699	0.1677
32.00	0.03	0.1662	0.1649	0.1637	0.1631	0.1625
34.00	0.03	0.1600	0.1600	0.1600	0.1600	0.1600
36.00	0.03	0.1600	0.1600	0.1600	0.1600	0.1600
38.00	0.03	0.1600	0.1600	0.1600	0.1600	0.1600
40.00	0.03	0.1600	0.1600	0.1600	0.1600	0.1600
50.00	0.02	0.1600	0.1600	0.1600	0.1600	0.1600
100.00	0.01	0.1600	0.1600	0.1600	0.1600	0.1600

a. Gorman 1989b

Table 3.7-3. Damping values to be used in dynamic analysis.

Structure or component	Safe shutdown earthquake
Equipment and large-diameter piping systems,[a] pipe diameter greater than 12 in.	3
Small-diameter piping systems, diameter equal to or less than 12 in.	2
Welded steel structures	4
Bolted steel structures	7
Prestressed concrete structures	5
Reinforced concrete structures	7

a. Includes both material and structural damping. If the piping system consists of only one or two spans with little structural damping, use values for small-diameter piping.

Table 3.7-4. ATR superstructure modes of vibration.[a]

Mode number	Frequency (Hz)	Comments
1 - 4	1.6 - 3.0	Roof girder
5 - 11	3.2 - 4.0	Building components (cranes, etc.)
12	4.0	Roof girder
13	4.4	Canal-area roof beams
14	4.4	Building components
15	4.4	Most of ATR building and canal- area roof beams
16 - 18	4.5 - 4.8	Canal-area roof beams
19	4.8	Building components
20	4.8	Canal-area roof beams and reactor-area roof girders
21	4.9	Building components
22	5.0	Canal-area roof beams
23	5.0	Building components
24	5.1	Canal-area roof beams
25	5.1	Building components
26 - 28	5.2 - 5.4	Roof girders
29	5.5	Building components
30	5.6	Most of building

a. Davidson 1976

Table 3.7-5. Summary of Stress Result for Seismic Analysis of Category I Structures (Davidson, 1976; Miller, 1980; Fors, 1982; Gorman, 1986a)

Location	Reported Stress(D)	Allowable Stress (C)	Factor of Safety (C/D)
ATR Reactor Building			
Bracing at Node 67	—	—	2.27
Column-Critical Facility	—	—	1.32
Beam-Critical Facility	—	—	0.93
Beam-Critical Facility	—	—	1.09
Column-Node 49	—	—	1.19
Beam-Node 49	—	—	1.72
Column-Nodes 125, 144, 177, 186	—	—	> 1[a]
Column-Lines 7-C	—	—	2.08
Column-Nodes 45, 53	—	—	1.01
Roof Beam - Nodes 45, 53	—	—	0.95
Column - Node 229	—	—	1.03
Reactor Area Liner	—	—	8.33
Confinement Boundary	—	—	2.08
Confinement Boundary	—	—	1.06
ATR Storage Canal			
Worst Loaded Member: Bending (M_{xx}) Bending (M_{yy}) Shear Tension	 11.12 k-ft/ft 19.49 k-ft/ft 21.4 psi 47.9 psi	 92.4 k-ft/ft 59.0 k-ft/ft 93.1 psi 493 psi	 8.31 3.03 4.35 10.29
MTR Storage Tanks (TRA-719A, 719B, 719C)[b]			
Plates (TRA-719A, -719B)	7.6 ksi	17.0 ksi	> 1
Plates (TRA-719C)	12.6 ksi	20 ksi	> 1
Overhead Water Storage Tank (TRA-718)			
Leg (Beam No. 2)	—	—	1.1
Horizontal Bracing (Truss No. 53 & 55)	—	—	1.13
Diagonal Bracing (Truss No. 33 & 39)	—	—	1.08
Anchor Bolts (Leg Base)	—	—	4.55
Anchor Bolt Leg Bracket	—	—	1.56
Bearing on Concrete Base	—	—	4.00
Foundation Uplift	—	—	1.02 to 1.87
Soil Bearing	—	—	2.56

a. ASIC Plastic design

b. Water level ≤ 28 ft for TRA-719A and -719B, and ≤ 26 ft for TRA-719C.

Table 3.7-6. ATR response spectra for SSE (Redundant Firewater System and Vessel Vent System).

Accelerations for El Centro and ATR			
Period (s)	El Centro horizontal (ft/s^2)	ATR horizontal[a] (g)	ATR vertical[b] (g)
0.0	10.63	0.240	0.160
0.01	10.67	0.241	0.161
0.02	10.85	0.245	0.163
0.05	12.0	0.271	0.181
0.08	13.5	0.305	0.203
0.10	15.12	0.342	0.228
0.13	18.3	0.413	0.276
0.2	23.0	0.519	0.346
0.3	24.5	0.553	0.369
0.4	23.5	0.531	0.354
0.8	16.0	0.361	0.241
1.0	12.5	0.282	0.188
1.4	9.0	0.203	0.136
2.0	6.8	0.154	0.102
3.0	5.0	0.113	0.075
50.0	5.0	0.113	0.075

a. ATR acceleration = El Centro acceleration $\times \frac{0.24^{\circ}}{0.33 \times 32.2}$

b. Vertical ATR acceleration = 2/3 horizontal ATR acceleration.

Table 3.7-7. ATR Response Spectra for SSE (ATR Firewater System Piping).

Frequency (Hz)	X-Direction acceleration (g)	Y-Direction Acceleration (g)	Z-Direction Acceleration (g)
0.001	0.110	0.073	0.110
0.200	0.110	0.073	0.110
2.500	0.751	0.501	0.751
10.00	0.545	0.363	0.545
13.33	0.480	0.320	0.480
16.67	0.432	0.288	0.432
20.00	0.380	0.253	0.380
33.00	0.240	0.160	0.240

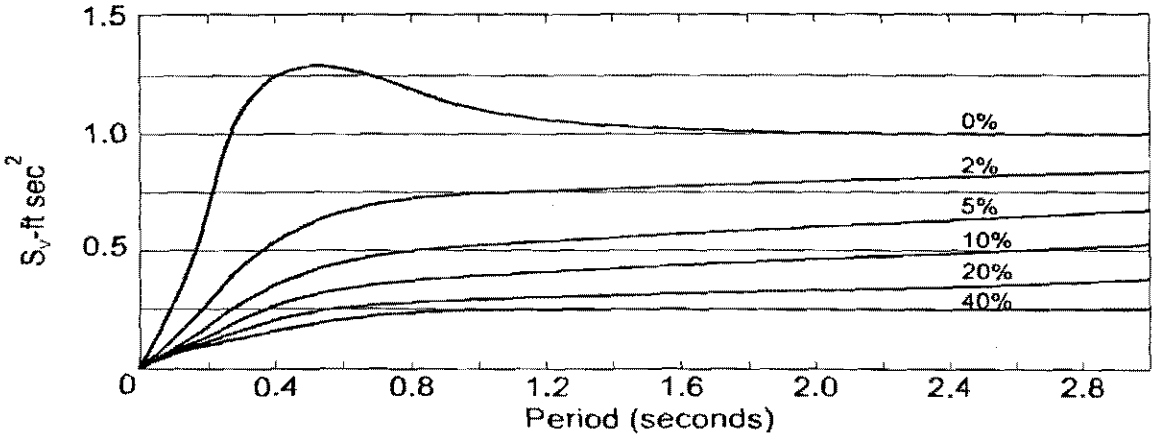

(a) Average velocity spectrum curves

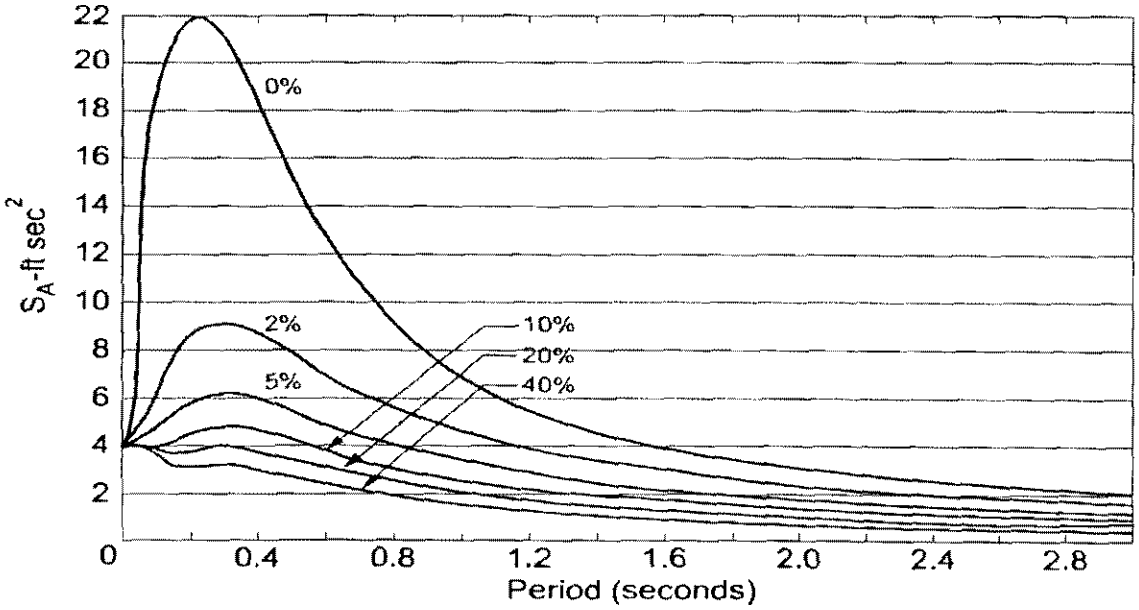

(a) Average acceleration spectrum curves

Scale factors (related to spectrum intensity ratios)

1940 El Centro	2.7
1934 El Centro	1.9
1949 Olympia	1.9
1952 Taft	1.6

To obtain the TRA design spectrum, apply a 1.93 scale multiplier to all of the above acceleration spectrum ordinates.

03-GA50703-01

Figure 3.7-1. Safe Shutdown Earthquake design spectra from Gorman (1972). **(For Information Only)**

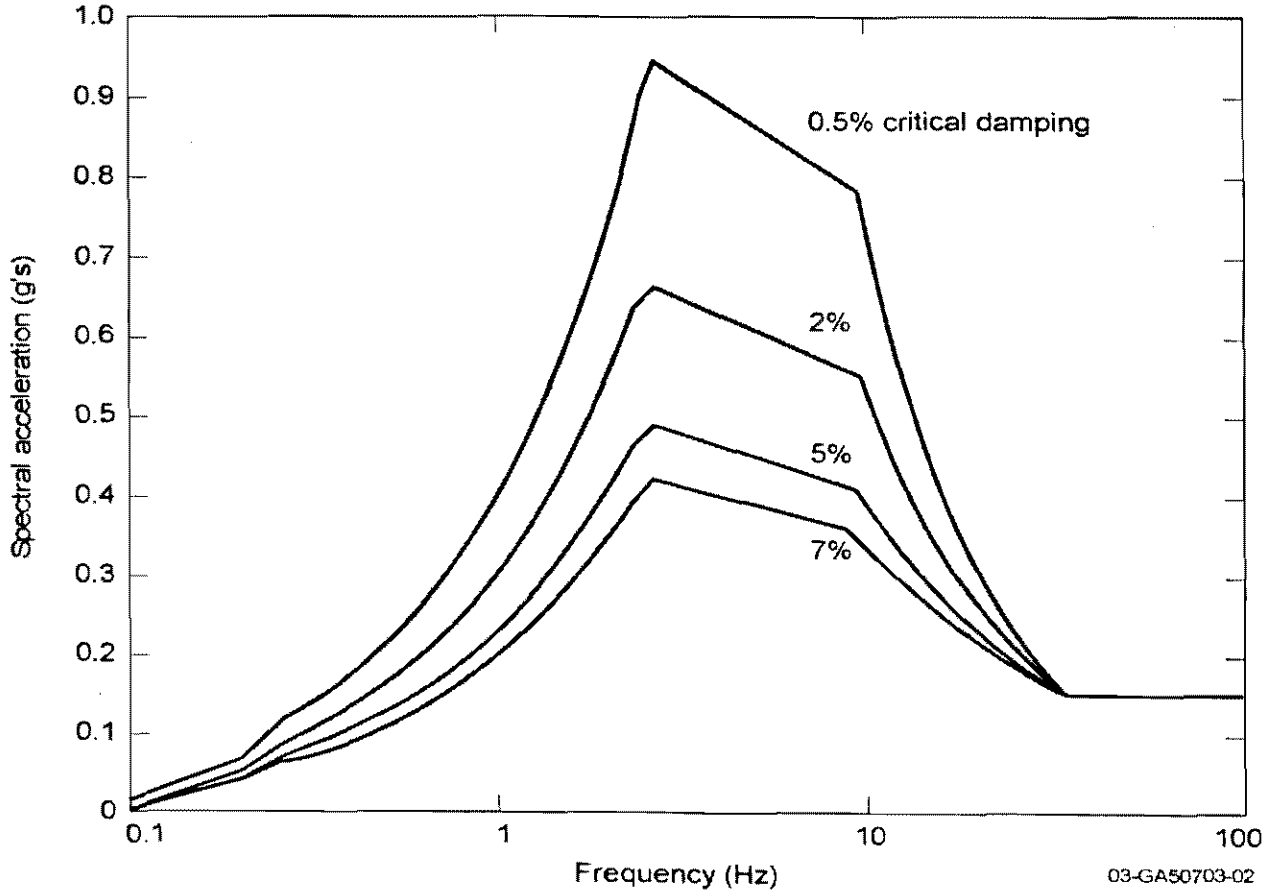

Figure 3.7-2. Safe Shutdown Earthquake horizontal design response spectra (Gorman 1989b).
(For Information Only)

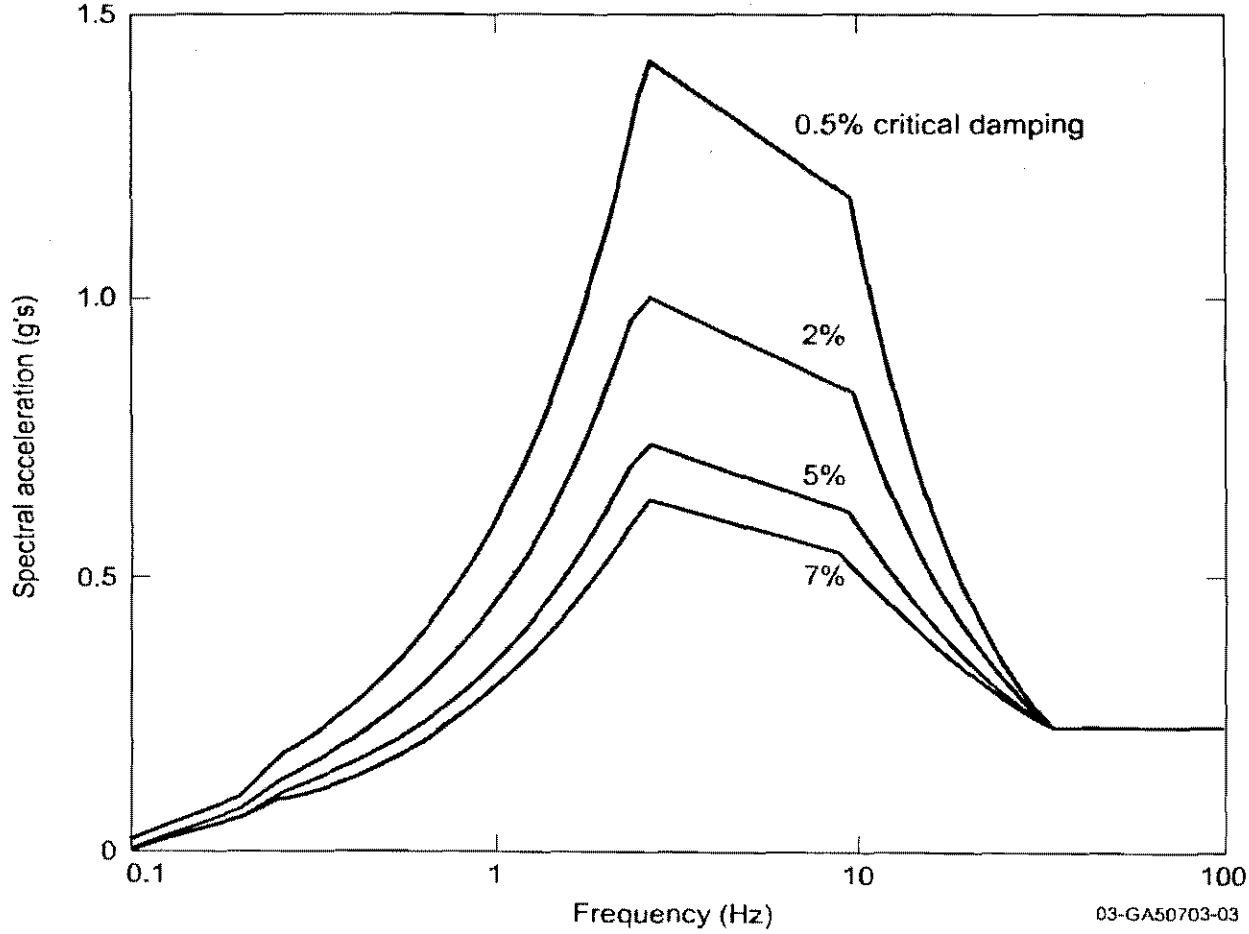

Figure 3.7-3. Safe Shutdown Earthquake vertical design response spectra (Gorman 1989b).
(For Information Only)

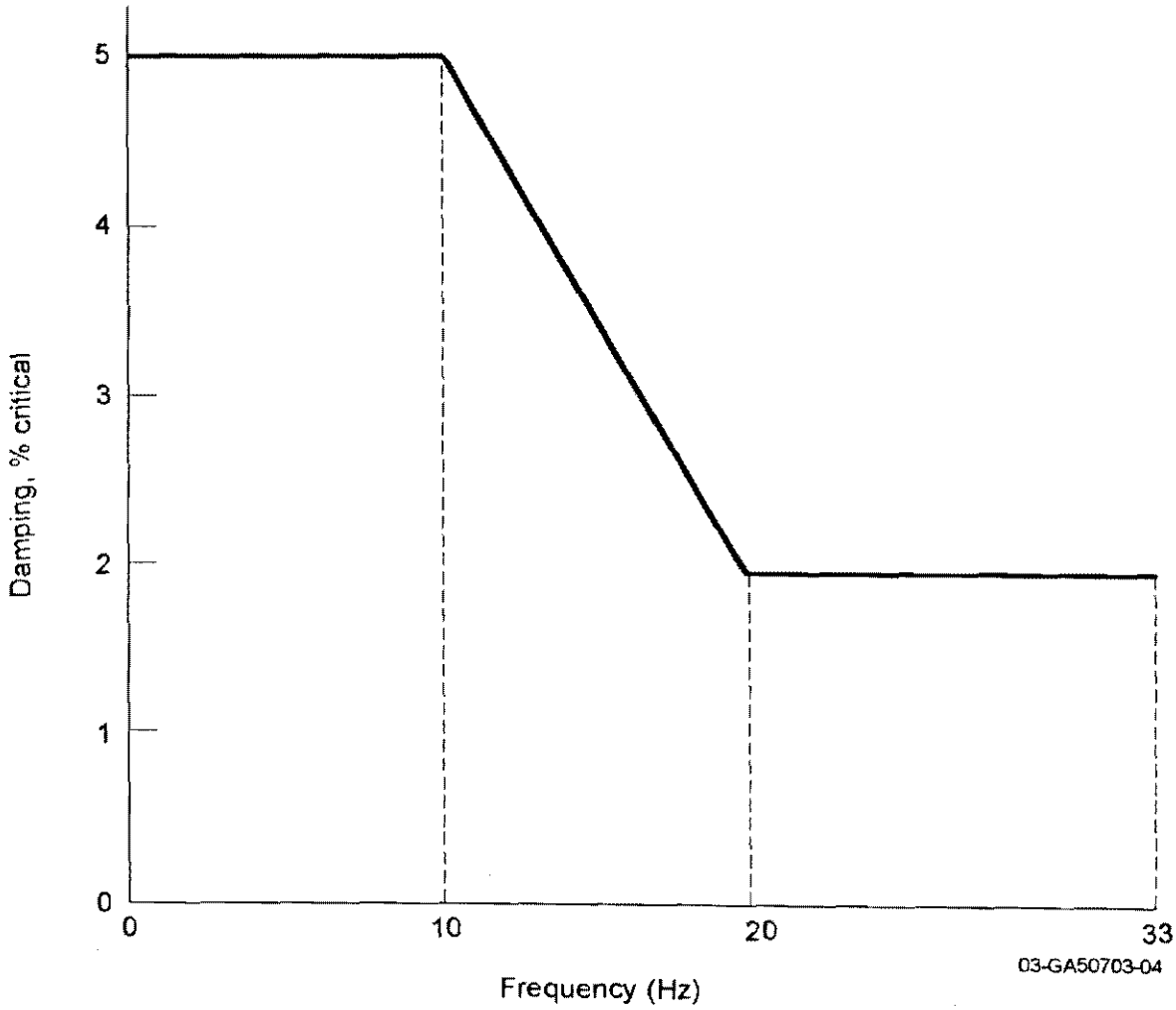

Figure 3.7-4. Alternate damping values for response spectra analysis of Class 1, 2, and 3 piping (ASME Code Case N-411-1). **(For Information Only)**

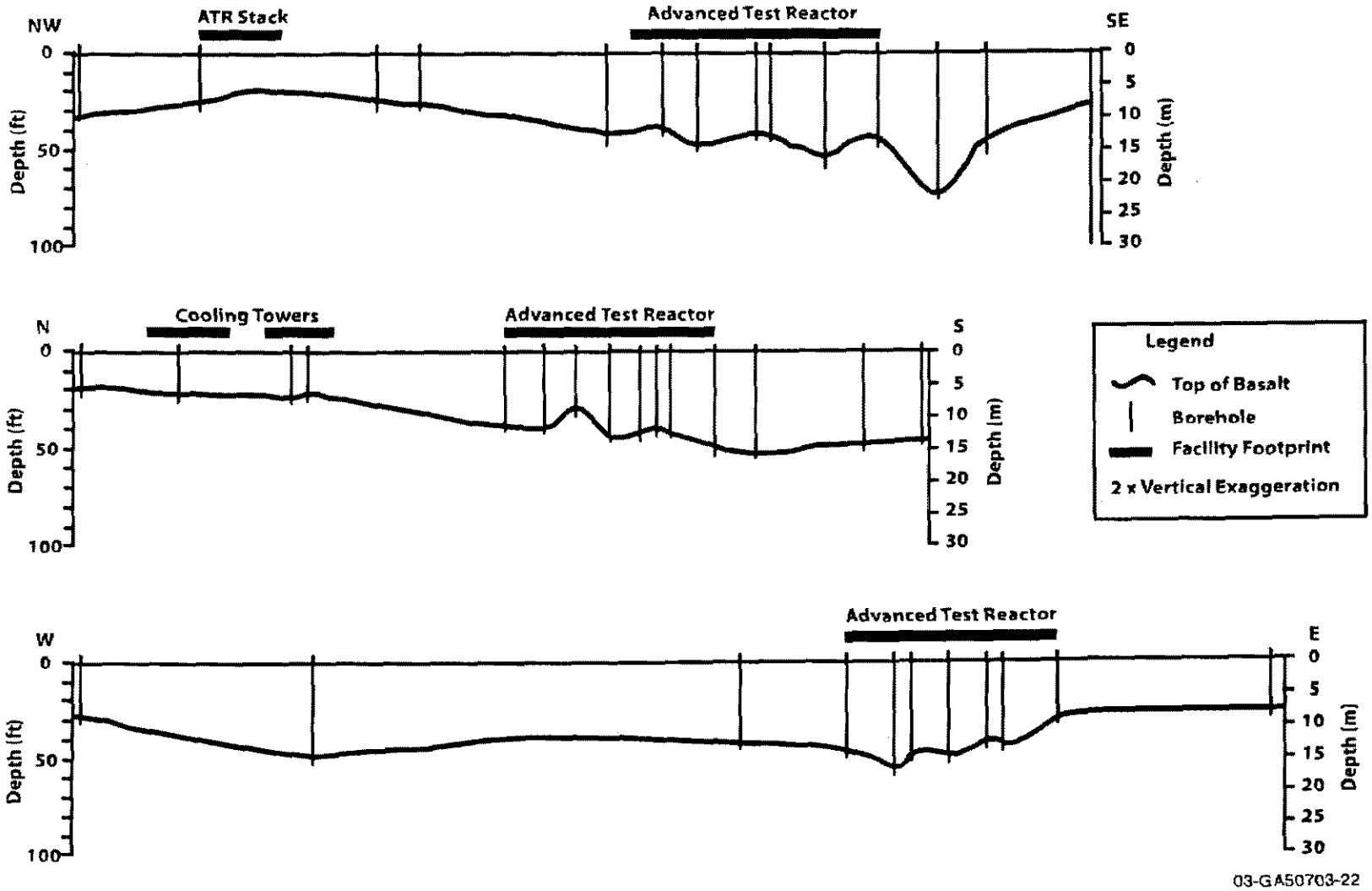

Figure 3.7-5. Cross sections through the Advanced Test Reactor area. (DWG ATR-1075-MTR-104-2) Depths to bedrock are prior to construction. See Figure 3.7-6 for locations of cross sections. **(For Information Only)**

FOIA Exemption 3 UCNI, Exemption 7f (Page 3-92 – map with coordinates)

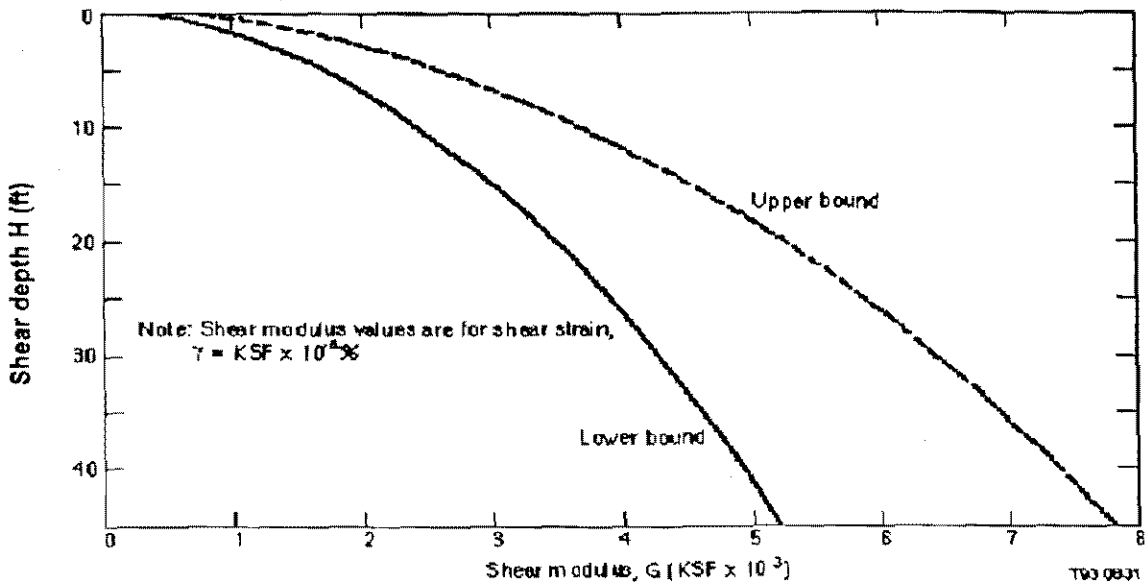

Figure 3.7-7. Shear moduli versus depth at ETR (Gorman, Guenzler, and Moore 1976). **(For Information Only)**

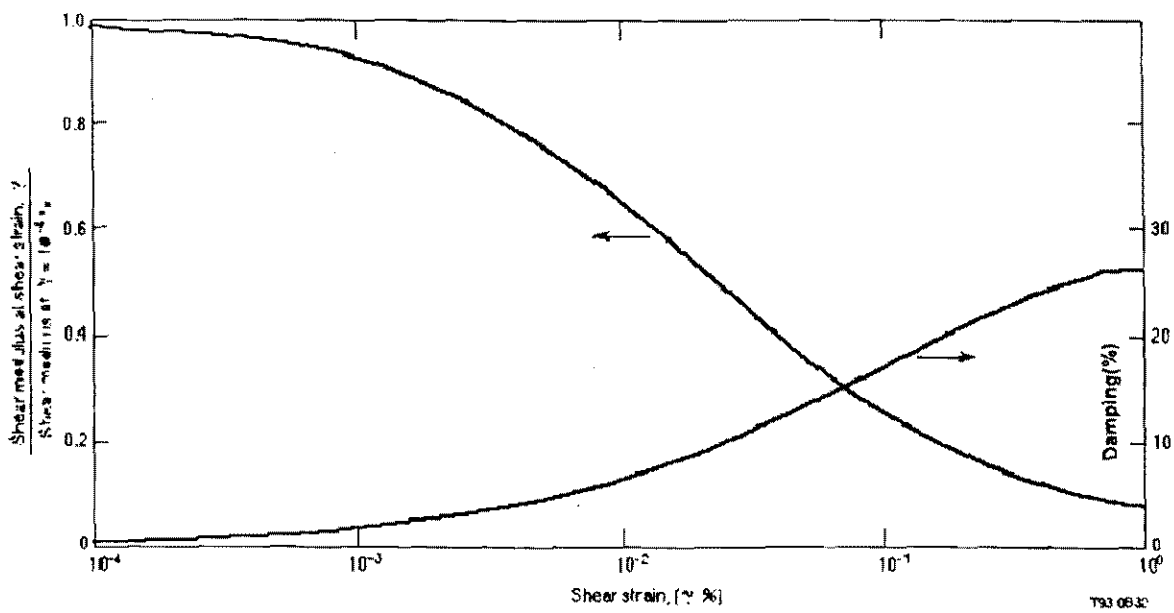

Figure 3.7-8. Shear moduli and damping ratios versus shear strain for sand and gravel (Gorman, Guenzler, and Moore 1976). **(For Information Only)**

3.8 Design of Seismic Category I Structures

3.8.1 Reactor Building

This section provides the following information on the ATR building:

- Physical description
- Applicable design codes, standards, and specifications
- Loading criteria, including loads and load combinations
- Design and analysis procedures
- Structural-acceptance criteria
- Materials, quality-control programs, and special construction techniques
- Testing and inservice-inspection programs.

3.8.1.1 General Description. The reactor building is a complex of enclosed areas approximately 200 × 200 ft, extending a maximum of 60 ft above grade and 60 ft below grade. The average depth of the substructure is about 42 ft, and the average superstructure height is about 38 ft. Building elevations and pertinent cross sections are shown in Figures 3.8-1 through 3.8-6.

The first floor, shown in Figure 3.8-7, is located at grade and is divided into the following areas: reactor area, truck airlock, storage-canal area, utility area (including diesel-generator pit), general storage and laydown area, critical-facility area, control rooms, and offices. The first and second mezzanine floors, shown in Figure 3.8-8, are devoted to rooms for offices and for heating-and-ventilating equipment. The first and second basements, shown in Figures 3.8-9 and 3.8-10, are used for experiment cubicles and equipment, electrical equipment, heat exchangers, demineralizer equipment, heating-and-ventilating equipment, and other associated items.

3.8.1.1.1 Confinement—The building is divided into two basic types of design, confinement and non-confinement. The confinement volumes have been selected to include all areas where an accidental contaminated release from the reactor or loop experiments can occur, or where sealed penetrations from such an area to an otherwise "clean" area would be difficult to maintain during normal operation. The confinement volume includes the following: reactor area, including freight and passenger elevators; reactor-control room; instrument-repair room; data-readout room; Office Number 110; truck airlock; first basement; and second basement. These areas are illustrated in Figures 3.8-3 through 3.8-11. Details of the confinement penetrations and wall sections are shown on Figures 3.8-12 and 3.8-13.

3.8.1.1.2 Reactor Area—The reactor area is located in the south central portion of the building, and measures approximately 88 ft (N-S) × 100 ft (E-W), as shown in Figures 3.8-3, 3.8-4, and 3.8-7. The area is bounded on the east by offices, on the west by the critical facility-area, and on the north by the storage-canal area. The storage canal area is isolated from the reactor area by a steel wall with four doors: a truck door, two personnel doors, and a door over the canal.

The door over the canal is a vertical-lift door made of solid steel plate. To make a confinement seal, the door has an inflated gasket around its sides and top, and extends two ft below the canal's surface water level. Therefore, the working canal water forms a seal between the door and the bulkhead in the working canal south of the door. Two overhead steel doors are located in the south wall to accommodate trucks. A truck airlock extends south from the west truck door on the reactor area's south wall. The airlock measures 82 ft (N-S) by 25 ft (E-W) by 22 ft high. A sliding truck door is located in the south wall of the airlock.

The reactor is located about 66 ft from the south wall. The working canal is located north of and adjacent to the reactor vessel, and connects directly to the storage canal. The nozzle access trench, reached by stairway from the reactor room, is concentrically arranged around the reactor. The trench's outer walls extend 3 ft above the floor and join the working canal's parapet walls on the north side of the reactor. The reactor area is served by a 40-ton-capacity overhead crane furnished with a 10-ton-capacity auxiliary hoist. A 2-ton-capacity bridge crane at a higher level with limited east-west coverage is also provided.

3.8.1.1.3 Storage-Canal Area—The storage-canal area, shown in Figures 3.8-5 through 3.8-7, is located north of the reactor area. It measures approximately 44 ft (N-S) × 200 ft (E-W), and extends 48 ft from floor to roof. A mezzanine level at the east end of the storage-canal area supports heating-and-ventilating equipment. The canal length is approximately 156 ft (E-W). A truck aisle is provided north of the canal with roll-up steel doors in the east and west building walls. The storage-canal area is isolated from the reactor area by a steel wall that has a truck door, a door over the canal, and two personnel doors (Section 3.8.1.1.2). The area is served by a 30-ton-capacity bridge crane furnished with a 5-ton-capacity auxiliary hoist. There is also a 2-ton-capacity jib crane located next to the canal door between the canal area and the reactor area for material transfers.

3.8.1.1.4 Utility Area—The utility area (Figures 3.8-5 through 3.8-7), is located in the northeast corner of the building, and is approximately 68 ft wide (N-S) × 105 ft long (E-W). Two 1,500-kW diesel generators are located on the north side in a 6-ft deep pit that is 25 ft (N-S) × 88 ft (E-W). Heating-and-ventilating equipment is located in the southeast corner, and the process-control room and other offices are located in the southwest corner. The battery banks for the PPS backup power are south and southwest of the 6-ft deep diesel generator pit. The battery banks are enclosed by reinforced concrete block walls (cubicles). Fire walls separate the utility area from the storage-canal area to the south and the storage and laydown area to the west. The exterior wall along the east side of the area is also a fire wall for protection from the main transformers, externally located east of this area. A 7.5-ton-capacity bridge crane is provided over the diesel generators for servicing and maintenance. Truck access to the area is provided by a roll-up steel door in the north wall.

3.8.1.1.5 General Storage and Laydown Area—The storage and laydown area shown in Figures 3.8-3, 3.8-6, and 3.8-7, located west of the utility area, is approximately 68 ft (N-S) × 95 ft (E-W). Space for general storage and a tool room is provided. Concrete floor hatches are located over the heat exchangers and the primary coolant pumps, and a 12-ton monorail is located over the pump hatches. Removable roof hatches permit removal of heat exchangers by a yard crane. Truck access to the area is by means of a roll-up steel door in the north wall. Fire walls separate the storage area from the storage-canal area to the south and from the utility area to the east.

3.8.1.1.6 Critical-Facility Area—The critical-facility area, shown in Figures 3.8-4, 3.8-6, and 3.8-7, is located south of the storage-canal area and west of the reactor area. It measures approximately 50 ft (E-W) × 66 ft (N-S). The ATR Critical Facility (ATRC) is located in an extension of the storage canal. Heating-and-ventilating equipment is located on the mezzanine level south of the ATRC. Each mezzanine is provided with an exterior exit and an enclosed stairway to the first floor. The floor area around the critical facility is adequate for storing casks and other equipment. Truck access is by means of a roll-up door in the west wall. Steel firewalls and doors separate the critical-facility area from the storage-canal and reactor areas. The critical-facility canal may be isolated from the storage canal by a vertical-lift door and an isolation bulkhead. The ATRC is the subject of a separate analysis report.

3.8.1.1.7 Offices—The office area, Figures 3.8-4 through 3.8-8, located east of the reactor area, is approximately 50 ft (E-W) × 88 ft (N-S), and is two stories high. The reactor-control room, instrument-repair and data-readout rooms, and Room 101 are all located on the first floor, north of the entry passage. The control room is adjacent to the reactor area, and windows are provided for viewing the reactor space. The operations laboratory, men's locker and shower room, and health physics staff offices are located south of the main entry. A stairway off the entry hall leads to the mezzanine office area.

Additional office space, Figures 3.8-6 and 3.8-7, is located in the southwest corner of the building and is approximately 26 ft (E-W) × 31 ft (N-S). The room is shielded against background radiation by two-ft-thick concrete walls, floor, and ceiling.

3.8.1.1.8 First Basement—The first basement, Figures 3.8-3 through 3.8-6 and 3.8-9, 19 ft below the first floor, is divided into three main areas. The northeast corner contains electrical switchgear, the battery room, and associated electrical equipment. The northwest corner contains the heat exchangers, which stand in a pit 50 ft below the first floor; primary coolant pumps and motors; and hatches over the demineralizer vaults. A 10-ton capacity monorail is provided over the primary coolant pump motors, and a 6-ton-capacity monorail is provided over the demineralizer hatches. The balance of the first basement floor, south of the canal walls, contains the reactor, the service area for the outer shim rod drive, safety-rod-drive service area, experiment cubicles, experiment-sample rooms, experiment instrument and control panels, sources room, and rod-repair room.

3.8.1.1.9 Second Basement—The second basement, Figures 3.8-3 through 3.8-6 and 3.8-10, 38 ft below the first floor, is divided into three main areas. The northeast area contains the high-pressure demineralized-water equipment room. The northwest area contains the primary heat exchangers. Directly connected with this area is the pipe tunnel, which runs south to the piping space and then to the pipe corridor located on the east and west sides of the subpile room. The subpile room is located directly below the reactor. The balance of the second basement contains five experiment cubicles, experiment sample rooms, experiment-control panels, auxiliary experiment equipment, the main exhaust fan room, and the demineralizer-tank vaults. Sub-basement levels include the liquid-waste pump-motor room, which is south of the reactor, 46 ft below the first floor; the hot- and warm-waste tank vaults, which are 59 ft below the first floor and directly under the waste-pump motor room; the neck shim rod drive room, which is 58 ft below the first floor and directly under the subpile room; and the piping space, which surrounds the neck shim rod drive room and is 58 ft below the first floor. Hatches are provided in the second basement and waste pump room floors for access to the hot- and warm- waste tanks.

3.8.1.1.10 Building Construction—The building substructure is of heavily reinforced concrete construction, either resting directly on and keyed into the subsurface basalt, or supported by concrete piers that extend into the basalt level. While all load-carrying frames are of reinforced concrete, many partition walls and some shielding walls are of masonry (concrete block) construction. Where required, masonry walls below grade are reinforced to resist seismic loads. In general, the building above grade is of steel frame construction with exterior walls of insulated aluminum sandwich panels supported by steel girt and a reinforced masonry base wall that is 3 ft 4 in. high around the building perimeter. Confinement areas of the superstructure are of seal-welded steel plate, reinforced masonry, or concrete construction. It is bounded on the north, south, and top by a 3/16 in. steel plate; the west wall is 8 in. concrete block. The lower 25 ft of the east wall is 6 in. concrete block; the upper portion is steel plate. Special provisions have been made to maintain the integrity of the confinement perimeter's penetrations and doors.

3.8.1.2 Applicable Codes, Standards, and Specifications. The reactor building's design, including the canals, conforms to the requirements of the following codes, standards, and specifications:

- ICBO 1961, Uniform Building Code, Volume I.
- AISC (American Institute of Steel Construction) 1952, "Specifications for the Design, Fabrication, and Erection of Structural Steel for Buildings," American Standard Specification ASA-A57.1.
- AISC, 1960, "Supplementary Provision Governing use of ASTM A-36 Steel," Adopted June 16.
- AISC 1969, "Code of Standard Practice for Steel Buildings and Bridges," revised March 15.
- AISC, 1960, Research Council on Riveted and Bolted Structural Joints of the Engineering Foundation, Structural Joints using ASTM A-325 Bolts, March 1960.
- American Welding Society (AWS), Standard Specification for Welded Highway and Railway, Bridges, Standard D2.0-56.
- American Society of Mechanical Engineers (ASME), "Qualification Standards for Welding procedures, Welders and Welding Operations," Boiler Construction Code, Section IX - 1959.
- American Concrete Institute (ACI), "Building Code Requirements for Reinforced Concrete," ACI-318-1957.
- National Bureau of Standards (NBS), "American Standard Building Code Requirements for Masonry," ASA-41.1-1953.
- American Standards Association (ASA), "American Standard Building Code Requirements for Minimum Design Loads in Buildings and Other Structures," ASA-A58.1-1955.
- Idaho Operations Office reports (IDO) Engineering Standards, revised May 1960.
- IDO, Safety and Fire Protection Criteria Manual, Publication 12008 August 1959.

The specifications for materials used in the ATR building are given in Ebasco (1961, 1962, 1964b, 1965).

3.8.1.3 Loads and Load Combinations. ATR confinement was originally designed to UBC seismic provisions. Subsequently, confinement design has been checked against two load combinations (Davidson 1976), which are defined as:

Load combination A = $D + L$

Load combination B = $D + L + E'$

where

D = dead loads or their related internal moments and forces, including any permanent-equipment loads

L = live loads or their related internal moments, including any movable-equipment loads and other loads that vary with intensity and occurrence

E' = Loads generated by the safe shutdown earthquake (SSE).

In addition, the confinement was designed to withstand both internal and external pressure varying (with the height above ground level) from 30 psf to 40 psf (Ebasco 1964a); calculations using the actual construction details of the wall, roofs, doors, and windows in the confinement area show that they can withstand even higher pressures, as shown in Table 3.8-1 (Burr 1987).

3.8.1.4 Design and Analysis Procedures. The confinement was originally designed using the UBC static-equivalent analysis method. In 1972, ATR adopted new criteria for seismic design and analysis; an SSE was defined with a peak horizontal ground acceleration of 0.24 g. The reactor building was analyzed using dynamic analysis for this SSE as described in Davidson (1976) and Gorman (1972).

3.8.1.4.1 Reevaluation for Safe Shutdown Earthquake—The reactor building, including the confinement and canal, was designed originally using the equivalent static method in the UBC. As part of the Seismic Analysis Program Plan (Mousseau 1973), the reactor building was analyzed to determine its integrity for SSE loading (Davidson 1976; Miller 1980).

A finite-element model of the reactor building was developed and analyzed for the SSE applied at the grade elevation. The internal-member loads and node displacements resulting from seismic loading were determined. The analytical model was constructed using SAP IV finite-element computer program. This program was used to determine nodal displacements and internal-member loads for both seismic and static loads. The mass or weight of the system was lumped at the node points.

This analysis assumed that one horizontal component of excitation occurred simultaneously with the vertical component. Thus, two analyses were performed in two mutually perpendicular horizontal directions, and the one producing the highest loads was used to evaluate the design's adequacy. For load combination A (live load plus dead weight), some of the more highly stressed elements are listed in Table 3.8-2. The W 10 × 66 columns supporting W 30 × 116 girders G-1 (Column Line A and E) were found to be overstressed. However, further evaluation (Gorman 1980) showed that the actual moments are much less than the full plastic moment, and that the column capacity exceeds the imposed tensile and compressive loads. Gorman (1980) used AISC plastic rather than elastic design requirements which showed that the columns are adequate without a need for modification. All other member loads for static loading are within allowable limits.

The dynamic-load cases considered the lowest 81 frequencies of the building, which ranged from 1.6 Hz to 13 Hz. The significant modes in which most of the building is in motion are at 4.4 Hz and 5.6 Hz. Seismic deflections of the building itself did not exceed 1 in. The largest seismic deflections, which occurred on the reactor area, were smaller than 1.3 in. Thus, seismic deflections are not considered to be a problem for the reactor building.

Because of the possible adverse consequences of the reactor-area crane jumping off its rails and dropping to the floor, special emphasis was placed on detailed analysis of this subsystem. It was determined that although the crane could slide along the rail even if the brakes were locked, the end stops were adequate to stop the crane. Further, it was determined that the crane could not jump off its rails because vertical seismic accelerations did not exceed 1 g. A reevaluation of the crane rail, using the minimum yield strength value of 58 ksi (which is higher than the originally-assumed 36 ksi), concluded that the rail is adequate as is (Gorman 1980).

The steel plate and concrete block bounding the above-grade portion of the confinement were analyzed for structural adequacy and permeability concerns. The stress intensity in each steel liner plate was compared to yield stress. Table 3.8-2 shows that the steel plate stress was well below this limit. For the concrete block, both working-stress design (WSD) and ultimate-strength design (USD) criteria were used. All the concrete block walls on the confinement boundary passed the WSD criteria except the 8 in. wall on Column Line 7, which was overstressed in shear by a factor of 2.5. However, this wall passed the USD criteria by a factor of 0.94.

Passing the WSD criteria is certainly adequate to preclude cracking of these walls. However, the design philosophy of USD is to prevent collapse of the structure; therefore, some cracking could occur.

Miller (1980, 1992) analyzed the canal for seismic (SSE) and static loading, and found that the canal has sufficient structural capacity to safely withstand the imposed loading. A review of the canal crane construction indicates that the trolley will stay in place during the SSE and will not fall into the canal (Guenzler 1992). Consequently, severe damage to the canal will not result from the SSE seismic event.

3.8.1.4.2 Seismic Evaluation of the ATR Building in the ATR Probabilistic Risk Assessment—A seismic PRA was conducted by Eide, Khericha, and Thatcher 1991. The following subsections summarize the results of that study.

3.8.1.4.2.1 ATR Structure—In the seismic PRA of ATR conducted by Eide, Khericha, Thatcher (1991), the structural fragility of reactor building was evaluated for the following structural elements of the reactor building:

- Substructure shear walls
- Columns supporting the storage canal
- Superstructure steel frames over the reactor area.

The substructure's seismic-load-resisting system consists of heavy, reinforced-concrete shear walls and floor slabs. Reinforced-concrete columns support the storage canal. The seismic capacity of the substructure is judged to be relatively high, as was confirmed by simplified bounding calculations that were done to estimate available capacities and applied loads for the shear walls and storage-canal support columns.

The superstructure has previously been analyzed for the design basis seismic event (Davidson 1976; Gorman 1980). These analyses determined that the most highly stressed structural elements are the W10 columns that support the roof over the reactor area. With the roof girders, these columns form moment frames that resist roof inertial loads in the N-S direction. They are subjected to significant bending stress at their connections to the roof girders. However, the analysis shows that the columns meet the acceptance criteria for plastic design for the seismic load condition per SRP 3.8.4.

The fragility for superstructure column failure was based on the limited detailed information contained in the available seismic-analysis reports. Conservatisms extracted from the existing seismic analyses included the following:

- Median material strengths
- Full plastic frame capacity (plastic hinges at the top and bottom of columns on both Column Lines A and E)
- Load redistribution to stronger frames
- Inelastic energy-absorption capability.

Median and HCLPF (high confidence of low probability of failure) capacities of 1.6 g and 0.38 g respectively were estimated for superstructure column failure. The median capacity represents the peak ground acceleration at which there is a 50% probability of failure. The HCLPF acceleration represents the peak ground acceleration at which there is high confidence (95%) of a low probability of failure (5%). A relatively large uncertainty was assigned to the fragility because of the lack of detailed information from the existing seismic analyses. Steel-framed structures have exhibited good performance in past earthquakes, with very few instances of actual collapse. The calculated fragility is considered to be consistent with past earthquake experience data.

3.8.1.4.2.2 Reactor-Building Masonry Walls—There are several masonry walls located within the reactor building whose failure may affect functionality of vital equipment components. Seismic evaluations of the following walls were performed:

- Process-control-room north wall (first floor)
- Reactor-control-room north wall (first floor)
- PPS backup-power battery room cubicle walls in the diesel- generator area (first floor)
- West wall of the switchgear-room staircase (first basement)
- Switchgear-area battery-room walls (first basement)
- Brick wall at the degassing tank and pressurizing pumps (second basement).

With the exception of the last item, all of these walls are constructed of concrete masonry units (concrete block). They are typically reinforced in the vertical direction by four Number 3 reinforcement bars spaced at 4 ft. These bars are attached to the slabs or beams above and below. Alternate horizontal courses contain extra-heavy Durowal joint reinforcement.

Reinforced-masonry walls are capable of ductile behavior when subjected to horizontal seismic loads associated with their own inertia. The masonry walls listed above were judged to have relatively high seismic capacities because of their strength, ductility, and low seismic input. Conservative seismic capacities were estimated using simplified bounding analyses, which included the following features:

- Conservative boundary conditions
- Conservative out-of-plane inertial loads based on the peak spectral acceleration within the estimated frequency range
- Spectral accelerations conservatively increased to account for 84%, rather than median, ground motion input
- Ultimate out-of-plane moment capacities based on current UBC design criteria
- Yield line capacities
- Conservative estimate of nonlinear response deamplification.

The masonry wall in the former process-control room was estimated to have a HCLPF capacity of at least 0.4 g. Its seismic capacity is greater than that of the control panel itself. HCLPF capacities of the other masonry walls were estimated to be 0.5 g or greater.

The masonry wall at the degassing tank and pressurizing pumps is constructed of brick. The wall is mortared into the 5 ft 6 in. thick concrete slab above and the 1 ft 6 in. concrete slab below. This wall was judged able to develop arching action to resist out-of-plane inertial loads. Conservatively assuming that the wall is constructed of multiple widths that are independent, a HCLPF capacity greater than 0.5 g was estimated.

3.8.1.5 Structural Acceptance Criteria. In the reevaluation of the reactor building reported in Davidson (1976), the following structural acceptance criteria are used:

- Determination of adequacy of the main structural steel frame is based on limiting the stresses for service load combination A (Table 3.8-3) to basic AISC allowables (AISC 1969) and factored load combination B to 1.6 times basic AISC allowables when elastic analysis methods are used (International Conference of Building Officials (ICBO) 1973).
- For the masonry walls, the 1973 UBC Code (ICBO 1973) is used as the acceptance criteria. This code uses methods and allowable values analogous to the WSD method for concrete structures (ACI 1963). Because this criterion is somewhat conservative when applied to the seismic-load combination B, the allowable values are modified to reflect the use of the USD method consistent with the NRC Standard Review Plan requirements for concrete (NRC 1981g).
- Table 3.8-3 shows the allowable stresses for different load combinations and materials.

3.8.1.6 Materials, Quality Control, and Special Construction Techniques. Materials used in the construction of the reactor building are listed in Table 3.8-4. The building was constructed using the Uniform Building Code Standards (ICBO 1961) and specifications were written by Ebasco, AE firm responsible for design. The specifications included the quality requirements and any special construction techniques. The specifications incorporated applicable codes and standards available at the time of construction.

3.8.1.7 Testing and Inservice-Inspection Requirements. Except for the confinement leak-rate tests, there are no specific procedures for testing and inservice inspection of these structures. Since this testing addresses the significant portion of the building and the test results will be sensitive to physical deterioration, no other procedures are established.

3.8.2 Internal Structures

The reactor building substructure is a heavily reinforced concrete shear-wall-type structure. Sections of the reactor building shown in Figures 3.8-3 through 3.8-6 show the heavy concrete walls, which are used primarily for shielding. The shielding provides biological protection and prevents excessive structural heating caused by radioactive absorption. Separate shielding descriptions are provided in deBoisblanc and Cohen (1965) for the internal shielding, the nozzle trench, the top-head shield, the primary biological shield, the coolant-loop shielding, the subpile and access rooms, the canal, the experimental-loop cubicles, and the demineralizer vaults.

The ATR does not contain an analogous internal structure that is separate from confinement, as is common in commercial nuclear power plants. The structural-design criteria and governing acceptance criteria for the below-grade section of the facility follow the same methods as contained in Section 3.8.1.

3.8.3 Other Seismic Category I Structures

The other Seismic Category I structures at ATR are:

- Firewater pump houses (TRA-619, TRA-633, TRA-688)
- Raw-water storage tanks (TRA-719A, -719B, -719C, -718, -781)
- Demineralized-water storage tanks (TRA-708A, -754).

3.8.3.1 Description of the Structures. Building TRA-619 was constructed in the early 1950s. Various modifications have been installed since its original construction. It typically consists of structural steel framing with masonry exterior walls. The presence of reinforcement in the masonry walls could not be confirmed by the walkdown or review of available drawings. The walls were therefore assumed to be unreinforced. The tops of the walls were also assumed to be attached to the steel framing. TRA-633 is constructed of structural steel-framing, enclosed by steel siding and roof deck. Lateral-load resistance is typically provided by diagonal-rod braces or moment frames. The diesel day tank within TRA-633 is enclosed by masonry walls on all four sides with a sheet metal cover. Details on the wall construction were not available.

The overhead raw-water storage tank (TRA-718) is an elevated tank with a 150,000-gal capacity. It was constructed in the 1950s, and was originally designed for a horizontal static acceleration of 0.05 g. The tank itself is a vertical cylinder with a hemispherical head at the bottom and a conical roof. It has a diameter of 26 ft and a height of approximately 31 ft. The tank is supported by four 30-in.-diameter columns that are approximately 160 ft high. The columns are anchored to individual concrete footings. These columns are laterally braced by diagonal rods and horizontal struts. A central sleeve encloses the tank supply and drain lines.

The ground level raw-water (TRA-719A, -719B, -719C) and demineralized-water (TRA-708A, -754) storage tanks are all flat-bottomed vertical tanks that are supported at grade on concrete foundations or asphalt.

Based on available drawings, important parameters for raw-water storage tanks TRA-719A and -719B are as follows:

Material – A36 carbon steel

Shell height – 35 ft 7 in.

Shell diameter – 48 ft

Shell thickness – 3/4 in. to 1/4 in.

Bottom-plate thickness – 1/4 in.

Based on available drawings, important parameters for the modified raw-water storage tank TRA-719C are as follows:

Material – A285 Grade C carbon steel

Shell height – 30 ft

Shell diameter – 48 ft

Shell thickness – 7/16 in. to 1/4 in.

Bottom-plate thickness – 1/4 in.

Based on available drawings, important parameters for demineralized-water storage tank TRA-708A and –754 are as follows:

Material – 300 series stainless steel

Shell height – 28 ft

Shell diameter – 25 ft

Shell thickness – 1/4 in.

Bottom-plate thickness – 1/4 in.

The million-gallon firewater tank (TRA-781) is an insulated, flat-bottomed vertical steel tank that is anchored at grade on a concrete foundation.

Material – A36 carbon steel

Shell height – 37 ft 7 in.

Shell diameter – 75 ft

Shell thickness – 1/2 in. to 1/4 in.

Bottom-plate thickness – 1/4 in.

The attached firewater pumhouse (TRA-668) is constructed of structural steel-framing, enclosed by steel walls and roof.

3.8.3.2 Applicable Codes, Standards and Specifications. See Section 3.8.1.2.

3.8.3.3 Loads and Load Combinations. The older structures were evaluated using the load combinations present in the UBC 1961 Edition (ICBO 1961). The TRA firewater tank (TRA-781) and pumphouse (TRA-688) were designed and constructed using the PC-4 load combinations present in the DOE standard (Brower 2001; DOE 1996a).

3.8.3.4 ***Procedures for Design and Analysis.*** Two types of seismic evaluations of the older structures have been conducted in recent years. The first type determined whether seismic capacities of the overhead tanks (TRA-718) and ground raw-water tanks (TRA-719A, -719B, -719C) were adequate to withstand the SSE. The overhead tanks were evaluated by Gorman (1986a), and the ground raw-water tanks by Goodell (1985). The second type of evaluation was part of the seismic-risk analysis conducted by Eide, Khericha, and Thatcher (1991) under the PRA program. This evaluation made use of the seismic walkdown of the structures in developing the seismic fragilities of the structures under different critical failure modes.

The TRA firewater tank (TRA-781) and pumphouse (TRA-688) were designed and constructed using the PC-4 load combinations present in the DOE standard (Brower 2001; DOE 1996a).

3.8.3.4.1 Deterministic Evaluation for Tanks for Safe Shutdown Earthquake—In Goodell (1985), the raw-water storage tanks have been evaluated using the American Water Works Association (AWWA) Standard (AWWA 1979). It was found that no uplift of the tanks would occur with the water level maintained at 19 ft. Note that 19 ft represents the minimum water level that would be needed to provide the specified standby capacity of 500,000 gal, assuming that two tanks would always be online. Some uplift would occur with a water level of 27 ft. Shell stresses would be within AWWA limits. Some local damage to the shell would occur in the region where the inlet piping is attached. As the report recommended, flexible piping junction to protect the shell and piping was installed. The previously unanchored raw water storage tanks TRA-719A and –719B were removed and replaced with new foundations and new anchored tanks. The new tanks were seismically designed, evaluated, and constructed to survive the 0.24g SSE PC-4 seismic design requirements in the DOE standard for a maximum water height of 28 ft (Bragassa and Lippert 2000; DOE 1996a). The remaining raw water storage tank TRA-719C was modified to reduce the height of the tank from 40 ft to 30 ft and provide a new conical roof. This modified tank was evaluated to survive the 0.24g SSE PC-4 seismic design requirements for a maximum water height of 26 ft (Rahl 1994; Lippert 1997). The report by Gorman (1986a) documents the results of a structural evaluation of how the support tower for the overhead water-storage tank performs when subjected to a SSE. The results indicate that the tower will survive the SSE.

The TRA firewater tank (TRA-781) and pumphouse (TRA-688) were designed and constructed to survive the 0.24 g SSE PC-4 seismic design requirements in the DOE standard (Brower 2001; DOE 1996a).

3.8.3.4.2 Seismic Evaluation of Buildings and Tanks in the Probabilistic Risk Assessment—In the seismic PRA conducted by Eide, Khericha, and Thatcher (1991), these Seismic Category I structures were evaluated for their seismic fragilities. The following summarizes the results of the PRA.

Reactor-building walls made of unreinforced masonry have performed relatively poorly in past earthquakes. Median and HCLPF capacities for block wall collapse in TRA-619 of 0.35 g and 0.15 g were estimated based on earthquake-experience data and engineering judgement. Because of their low masses, these buildings (TRA-619 and TRA-633) are judged to have very high seismic capacities.

Because the enclosure is of newer construction, the block walls around the diesel day tank within TRA-633 were assumed to have horizontal joint reinforcement at every other course. They were also assumed to have no vertical reinforcement. A median capacity of approximately 0.8 g was estimated for the masonry wall enclosure. The complete fragility was not developed because seismic capacity of the day tank itself is much lower.

3.8.3.4.3 Water Storage Tanks—Fragilities were developed for the following water storage tanks:

- Overhead raw-water storage tank TRA-718
- Raw-water storage tanks TRA-719A, TRA-719B, and TRA-719C.

Data on performance of elevated tanks during earthquakes were reviewed to support the fragility evaluation. Readily available data from earthquakes ranging from the 1933 Long Beach earthquake to the 1987 Whittier earthquake were collected. Elevated tanks have suffered damage and even collapse in past earthquakes. Of a total of 36 elevated tanks identified, nine were undamaged, 20 suffered some type of damage, and 7 collapsed. The most frequent forms of damage were stretched anchor bolts; stretched, buckled, or broken diagonal braces; and other foundation damage. Diagonal-rod damage typically occurred at the upper, rather than lower, tiers.

Detailed tank-experience data from the 1952 Kern County earthquake are reported in Steinbrugge and Moran (1955). The authors distinguish between the performance on wind-braced and earthquake-braced tanks. Of the ten wind-braced tanks, five collapsed or had broken diagonal-rod braces. Of the 12 earthquake-braced tanks closer to the epicenter, only one collapsed. Even though the overhead raw-water storage tank was designed for only a 0.05 g seismic acceleration, this requirement should have provided the tank with greater seismic capacity than the wind-braced tanks, which are apparently prone to failure.

Fragility evaluation of the overhead raw-water storage tank was based upon the seismic analysis and capacity evaluation reported in Gorman (1986a). The tank capacity was found to be controlled by failure of the diagonal-rod braces at the upper tiers. As noted in the review of earthquake-experience data, damage to the rod braces of the upper tiers is one of the more common seismic effects to elevated tanks. The median and HCLPF capacities were determined to be 0.68 g and 0.20 g, respectively. The variabilities are significantly affected by randomness and uncertainty in the spectral shape.

The raw-water storage tanks are all vertical tanks that are supported at grade on concrete foundations or asphalt. These tanks are all unanchored. Unanchored tanks have suffered damage, such as shell buckling, and even failure with a total loss of fluid contents in past earthquakes. The following tank parameters were assumed[a] based on typical values for tanks of this size:

- Material: carbon steel
- Shell thickness: 1/4 in.
- Bottom-plate thickness: 1/4 in.

Manos (1986) has developed an empirical expression to estimate a conservative seismic capacity for shell buckling of unanchored tanks. This expression appears to correlate well with performance of unanchored tanks in actual earthquakes. Manos' expression was used to estimate the HCLPF capacity against shell buckling for the raw-water and demineralized-water storage tanks. These capacities were adjusted (a) to express the seismic capacity in terms of the peak ground acceleration (PGA) at bedrock for consistency with the seismic hazard curves, and (b) to account for potential local amplification of ground-motion effects within the tanks' estimated frequency range. The HCLPF capacity was estimated to have a median factor of safety of about 2.3, based on engineering judgement, review of limited data from shake-table tests of unanchored tanks, and review of anchored-tank fragilities. The following values were estimated raw-water storage tanks TRA-719A, -719B, and -719C:

- Median PGA capacity (at bedrock)- 0.32 g
- HCLPF capacity - 0.14 g.

All of the information provided in this section and in the PRA is applicable to the unanchored and unmodified Raw-water storage tanks (TRA-719A, -719B, and –719C). The new replacement tanks TRA-719A and –719B, and the modified tank TRA-719C have not been incorporated into the PRA.

The TRA firewater tank (TRA-781) and pumphouse (TRA-688) have not been evaluated for fragility and have not been incorporated into the PRA.

3.8.3.5 Structural Acceptance Criteria. These criteria have been described in the seismic evaluation conducted on the unmodified tanks by Goodell (1985) and Gorman (1986a). The new replacement tanks TRA-719A and –719B were evaluated by Bragassa and Lippert (2000), and the modified tank TRA-719C was evaluated by Rahl (1994) and Lippert (1997). The raw-water tanks were evaluated to the American Water Works Association (AWWA) requirements, whereas the overhead storage tank was evaluated to the requirements of AISC (1980) and the NRC Standard Review Plan (1981g). The Standard Review Plan allows the members to be stressed up to 1.6 times the normal allowables for dead and live loads; that is, up to about 96% of yield strength.

The TRA firewater tank (TRA-781) and pumphouse (TRA-688) were designed and constructed to survive the 0.24g SSE PC-4 seismic design requirements in the DOE standard (Brower 2001; DOE 1996a).

---

[a]. Average shell thickness is 5/16 in. Bottom-plate thickness is 1/4 in.

3.8.3.6 Materials, Quality Control and Special Construction Techniques. Materials used in the tanks are found in Table 3.8-5. The original construction information relative to quality control and special construction techniques is not available. However, the tanks have been evaluated as noted in Section 3.8.3.5; the evaluations provide assurance of operability even though original data are no longer available. All of the new tanks TRA-719A, -719B, and –781 have material certifications and quality control records available.

3.8.3.7 Testing and Inservice Inspection Requirements. No specific procedures exist for testing and inservice inspection of these structures. Failure of these structures would not result in immediate danger to the operating plant since they are designed to mitigate consequences of off normal sequences. The plant can be placed in a stable configuration if there is a deterioration of the structures which results in inoperability of a required function. Therefore, there is limited need for formal inspections, and observations by operators performing routine work is utilized for control.

3.8.4 Foundations of Seismic Category I Structures

The foundation for the reactor building is constructed of heavily reinforced concrete. The foundation is keyed into the underlying basalt over approximately 2/3 of the basement plan area. The remaining foundation area is supported on concrete piers, which are founded on the underlying bedrock.

The structural-design criteria and governing-acceptance criteria for the foundation of the ATR structure follow the same methods as given in Section 3.8.1.

Table 3.8-1. Analysis results of internal pressure of confinement structures.

Structure	Internal pressure withstood
Roof	9.0 in. water
Walls	
Concrete block	9.0 in. water (includes a safety factor of 1.5)
Steel-lined	12.2 in. water
Windows	20.5 in. water
Doors	12.5 in. water

Table 3.8-2. Calculated stress ratios in ATR building elements.[a]

					Stress Ratios[b]		
Location[c]	Element Type	Element Number	Material	Section	Static	E-W Seismic + Static	N-S Seismic + Static
Bracing at Node 67	Truss	61	Steel	L 4 × 4 × 1/4	0.16	0.17	0.44
Column—Critical facility	Beam	48	Steel	W 10 × 45	1.00	0.76	0.71
Beam—Critical facility	Beam	495	Steel	W 18 × 45	0.84	1.07	0.83
Beam—Critical facility	Beam	250	Steel	B 10 × 15	0.72	0.92	0.87
Column—Node 49	Beam	93	Steel	W 10 × 54 & W 8 × 31	0.96	0.82	0.84
Beam—Node 49	Beam	389	Steel	W 33 × 141	0.72	0.57	0.58
Column—Nodes 135, 144, 177, 186	Beam	16, 20, 111, 116	Steel	W 10 × 66	1.20	0.57	0.58
Column—Lines 7-C	Beam	66	Steel	W 21 × 68	0.62	0.48	0.46
Column Nodes 45, 53	Beam	96,154	Steel	W 10 × 54	0.96	0.70	0.99
Roof-beam Nodes 45, 53	Beam	394,395	Steel	W 24 × 68	0.85	0.60	1.05
Column Node 229	Beam	126	Steel	W 10 × 77	0.60	0.47	0.97
Reactor area liner	Plate	Max	Steel	3/16 in. thick	0.07	0.12	0.08
Confinement boundary	Plate	Max	Masonry	6 in. thick	0.56	0.41	0.48
Confinement boundary	Plate	Max	Masonry	8 in. thick	0.69	0.94	0.68

a. Davidson 1976.

b. Stress ratio equals actual stress divided by allowable stress. Values greater than 1.0 indicate an over-stressed condition. The allowable stress values are larger for the seismic load combination.

c. See Figures 2, 3, 4, and 5 of Davidson (1976).

Table 3.8-3. Allowable stresses for steel and masonry in load combinations A and B.[a]

Load combination	Material	Stress type	Allowable stress
A (D + L)	Steel	Normal	24 ksi
		Shear	14.5 psi
	Masonry	Normal	445 psi
		Shear	40 psi
B (D + L + E')	Steel	Normal	38.4 ksi
		Shear	23.2 ksi
	Masonry	Normal	1,150 psi
		Shear	74 psi

a. Loads are defined in Section 3.8.1.3.

Table 3.8-4. Materials used in the construction of the ATR reactor building.

Material	Standard procedure	Allowable stress
Structural steel	ASTM A36	Yield stress 36 ksi
Secondary steel	ASTM A7	Yield stress 33 ksi
Concrete masonry units	Reinforced hollow units	Compression strength 1,350 psi

Table 3.8-5. Materials used in the raw-water storage tanks.

Item	Material designation	Yield strength (ksi)	Ultimate strength (ksi)
Raw-water storage (TRA-719A, B)	A36	36	58
Raw-water storage (TRA-719C)	A285 Grade C steel	30	55
Overhead-tank diagonal rods (TRA-718)	A7	33	60
Horizontal struts	A7	33	60
Anchor bolts	A7	33	60
Vertical legs	A283 Grade C	30	55
Firewater Tank (TRA-781)	A36	36	58
Anchor bolts	A36	36	58

CHAPTER 3 - DESIGN OF STRUCTURES COMPONENTS, EQUIPMENT, AND SYSTEMS - UPGRADED FINAL SAFETY ANALYSIS REPORT FOR THE ADVANCED TEST REACTOR	**Identifier:** SAR-153 **Revision:** 10 **Page:** 3-110 of 3-200 **Effective Date:** 08/10/04

CHAPTER 3 - DESIGN OF STRUCTURES COMPONENTS, EQUIPMENT, AND SYSTEMS - UPGRADED FINAL SAFETY ANALYSIS REPORT FOR THE ADVANCED TEST REACTOR	**Identifier:** SAR-153 **Revision:** 10 **Page:** 3-111 of 3-200 **Effective Date:** 08/10/04

CHAPTER 3 - DESIGN OF STRUCTURES COMPONENTS, EQUIPMENT, AND SYSTEMS - UPGRADED FINAL SAFETY ANALYSIS REPORT FOR THE ADVANCED TEST REACTOR	**Identifier:** SAR-153 **Revision:** 10 **Page:** 3-112 of 3-200 **Effective Date:** 08/10/04

CHAPTER 3 - DESIGN OF STRUCTURES COMPONENTS, EQUIPMENT, AND SYSTEMS - UPGRADED FINAL SAFETY ANALYSIS REPORT FOR THE ADVANCED TEST REACTOR	**Identifier:** SAR-153 **Revision:** 10 **Page:** 3-113 of 3-200 **Effective Date:** 08/10/04

CHAPTER 3 - DESIGN OF STRUCTURES COMPONENTS, EQUIPMENT, AND SYSTEMS - UPGRADED FINAL SAFETY ANALYSIS REPORT FOR THE ADVANCED TEST REACTOR	**Identifier:** SAR-153 **Revision:** 10 **Page:** 3-114 of 3-200 **Effective Date:** 08/10/04

FOIA Exemption 3 UCNI, Exemption 7f (Pages 3-110 - 3-122 -- Reactor building elevations, confinement areas, floor plans, penetration details, wall sections, miscellaneous plans, DWG Nos. 120103, 120104, 120309, 120111, 120311, 120312)

3.9 Mechanical Systems and Components

3.9.1 Special Topics for Mechanical Components

The reactor vessel and PCS components were designed and constructed to meet the requirements of the ASME Unfired Pressure Vessel Code and the requirements of the code cases and interpretations applicable to pressure vessels for nuclear service at the time of construction (deBoisblanc and Cohen 1965). The completed reactor vessel was approved under the provisions for nuclear vessels as stated in ASME Code Case 1270N-3 and has an ASME Code stamp. The reactor vessel was inspected in accordance with the 1962 edition of the ASME Boiler and Pressure Vessel Codes. The 1962 edition ASME reference documents used are as follows:

- Section II - Material Specifications
- Section VIII - Unfired Pressure Vessels
- Section IX - Welding Qualifications.

Interpretations of ASME Code including Cases 1270N-3, 1270N-5, 1271N, 1272N-5, 1273N-7, 1274N-6, and 1275N, were also used in the original design and approval of the reactor vessel, its attachments, and its penetrations (deBoisblanc and Cohen 1965).

3.9.1.1 Design Transients. All PCS pressure piping was designed in accordance with ASA B31.1, 1955 and Nuclear Code Cases N-1, N-7, N-9 and N-10 (deBoisblanc and Cohen 1967). All piping materials are austenitic stainless steel. Buried and embedded piping is either seamless per ASTM A376-60T, or welded per ASTM A358-60T, as stated in ASA B31.1-1955 *Code for Pressure Piping Case N-7.*

As discussed in deBoisblanc and Cohen (1965), the ATR was designed to accommodate rapid thermal cycling caused by fast start-up and shutdown emergencies. Based on stress calculations, analyses obtained from deBoisblanc and Cohen (1965) show the fatigue limits corresponding to the temperature transients presented in Table 3.9-1. In addition, an analysis (Miller 1987) of the ATR drop tube and cylindrical course weldment has been performed for pressure and thermal loading. The assembly was analyzed for structural adequacy according to criteria of the ASME Code Section III Subsection NB for Class 1 components. This included a comparison of calculated stresses with specified limits for pressure and thermal loading. It also included a fatigue evaluation for all pressure/temperature cycles expected during operation of the ATR.

Table 3.9-2 provides a general guideline of allowable stress limits for the various loading combinations which is consistent with the ASME Boiler and Pressure Vessel code. Table 3.9-3 provides an overall assessment of the reactor vessel for the various loading conditions, load combinations, ASME stress limits, and allowable fatigue cycles as determined by Miller (1987) and Davidson (1978).

Results from the analysis indicate that stresses are within limits specified by the ASME code for Design, Level A and Level B Conditions. In addition, the results showed that the assembly can sustain all 10^7 cycles of pressure loading and thermal gradients that could occur as a result of operation. The number of cycles experienced in a year is conservatively not more than 50 (Durney et al. 1987). It is apparent from this evaluation that the fatigue limit for the vessel is not a concern since it would require 2×10^5 years to accommodate 10^7 cycles. Thus, the evaluation shows that the drop tube assembly meets ASME Code Section III Subsection NB criteria for pressure and temperature loads for the life of the ATR.

The stresses calculated for the drop tube assembly are representative of the worst pressure and thermal stresses expected anywhere in the reactor vessel (Miller 1987). Results from the stress and fatigue evaluations of this assembly indicate that safety margins were ample. Thus, it is concluded that all portions of the vessel meet ASME Section III Subsection NB criteria for pressure and temperature loads for any projected service life of the plant (Durney et al. 1987).

Compliance with codes and code cases for components in the PCS, has been assured through subsequent analysis, as discussed in Chapter 5 (Primary Coolant System). The remaining components of the PCS, include the PCS piping, heat exchangers, surge tank, degassing tank, coolant pumps, pressurizing pumps, and safety relief valves. Chapter 5 (Primary Coolant System) discusses the transient analysis for each of these components.

In addition to operating-temperature transients, Gorman (1972) considered an SSE with peak ground acceleration of 0.24 g as a design transient for mechanical components in the seismic-upgrade program.

3.9.1.2 Computer Programs Used in Analysis. Table 3.9-4 lists the computer programs that the seismic-upgrade program used to do dead-load, thermal, and seismic (dynamic and static) analyses of Seismic Category I systems. Quality-assurance procedures are in place that ensure the validity of program results. The quality-assurance procedures for computer-program documentation and verification are contained in the Contractor's *Engineering and Research*, software management.

3.9.1.3 Experimental Stress Analysis. Before startup of the ATR in 1967, a brittle coating was placed on the PCS pump cases to verify the original axisymmetric finite-element analysis performed on the pump cases for weight, pressure, and thermal conditions. In addition, strain gauges were placed on the PCS piping to verify the stress results from the original Ebasco design calculations.

3.9.1.4 Consideration for the Evaluation of the Faulted Condition. The Faulted Condition defined event under ASME Level D was the SSE combined with internal pressure, temperature, core pressure drop, and dead weight. The SSE used in the analysis of most of the PCS and selected major Seismic Category I components is defined in Gorman (1972) and displayed in Figure 3.7-1. Finite-element methods using the response-spectrum approach were the primary analytical tools used to evaluate SSC for the faulted condition. Section 3.7.3 describes this method in more detail. Components of the PCS were analyzed to the faulted condition. These components include the PCS piping, heat exchangers, surge tank, reactor vessel, and the reactor vessel internals. PCS branch piping analyzed to the faulted condition included the firewater redundant line (piping both internal and external to the ATR, the firewater piping system inside the ATR, and the VVS). All analysis methods used are based on linear elastic solutions.

The PCS contains non-standard components consisting of field-fabricated tees, y-lateral connections, eccentric reducers, pipe stub-ins, and short-radius elbows. These components cannot be analyzed with the simplified code methods used in the Davidson (1979) analysis. Non-standard PCS components were analyzed using the response-spectrum method, but using the later-defined SSE (Gorman 1989b) as depicted in Figure 3.7-2 and Figure 3.7-3 (Harris 1989; Harris and Burr 1989; Miller 1988, 1989a, 1989b, and 1989c). Loadings were applied in three orthogonal directions simultaneously, and acceptance was based on a combination of elastic and elastic-plastic solutions.

3.9.2 Dynamic Testing and Analysis

3.9.2.1 Piping Vibration, Thermal Expansion, and Dynamic Effects. The ASA B31.1 code does not require a fatigue analysis. A design analysis of the PCS piping was updated in 1974 (Davidson and Thinnes 1974), and in 1979 (Davidson 1979), superseding the stress analysis from the original safety analysis (deBoisblanc and Cohen 1965). These analyses identified non-standard piping components that could not be satisfactorily analyzed by the simplified analysis procedures of the ASME code. The non-standard components were successfully analyzed using elastic or elastic-plastic detailed analysis methods (House 1995). All PCS piping was analyzed and found to be acceptable by the 1977 ASME Section III, Division 1, code requirements (ASME 1977). This analysis included both SSE loads as specified by Gorman (1989b) and design-temperature transients.

3.9.2.2 Seismic Qualification Testing of Safety-Related Mechanical Equipment. For Seismic Category I mechanical equipment items, the seismic-testing procedures and criteria employed for qualification are identical to those for electrical equipment, and are described in Section 3.10. For those components qualified, response-spectrum methods using the SSE definition proposed by Gorman (1972) were used. Not all of the Seismic Category I SSC identified in Section 3.2.1 are seismically qualified. The latest listing, in table form, which identifies Category I SCC's and seismic qualification criteria used for each is contained in the Engineering Design File (EDF) by Blandford (1991).

3.9.2.3 Dynamic-Response Analysis of Reactor Internals Under Operational Flow Transients and Steady-State Conditions. Operations at the ATR have continued since 1969. Dynamic systems analysis and preoperational tests were conducted before startup in 1969. The age of the plant and the operating history provide evidence of the acceptability of the reactor internals design for normal operating conditions.

3.9.2.4 Preoperational Flow-Induced-Vibration Testing of Reactor Internals. deBoisblanc and Cohen (1967) note the preoperational test program detected various design and construction problems. During flow testing, significant vibrations of: (a) the PCS piping, (b) certain components within the reactor vessel, and (c) the primary heat exchanger tubes were detected. Initial hydrostatic testing resulted in bulged pipe fittings in the PCS piping system. These results prompted a complete reexamination of the PCS that uncovered additional concerns over weld flaws and the integrity of pump casings and valve bodies. Numerous corrective actions, including redesign, reanalysis, support modification, repair, replacement, and retest, were taken to ensure that the as-built PCS is a high-integrity system that can operate safely.

3.9.2.5 Dynamic System Analysis of the Reactor Internals Under Faulted Condition. Davidson (1978) conducted a response-spectrum finite-element analysis of the reactor vessel, internals, inpile tubes, and vessel supports. The reactor vessel was analyzed using the response-spectrum method for determining structural response to the earthquake loads specified by Gorman (1972). The resulting structure loads were combined in accordance with the ASME Boiler and Pressure Vessel Code, Section III requirements (ASME 1977).

Seismic-load cases, which include horizontal and vertical components, were applied in the directions corresponding to the principal axes of the model. Each seismic-load case excited the vertical component and one principal horizontal component. The horizontal component was taken from Gorman (1972). The vertical component was taken to be two-thirds of the horizontal component. Two percent damping was used in the analysis. The load combinations used in the analysis are shown in Table 3.9-5.

The methodology of the ASME Boiler and Pressure Vessel Code, Section III, NB-3221 was used to determine adequacy of the reactor vessel in the absence of seismic loading (load combination A, Table 3.9-5). Allowable stresses for load combination B (which includes seismic loading) were modified in accordance with ASME, Appendix F (ASME 1977). The internal piping was analyzed in accordance with Subsection NB-3652 and Appendix F (ASME 1977) for load combinations A and B, respectively. The allowable stress intensities for portions of the reactor vessels are shown in Table 3.9-6.

The reactor-vessel shell was modeled in three dimensions because the locations of spacer bolts are not symmetric about the circumference. The internals were modeled using beam elements and lumped masses. The internals section of the model was connected to the shell portion at the center node of the bottom head (Davidson 1978). The reactor vessel was analyzed for two support conditions because the status of spacer bolts used to radially align the vessel plate liner around the reactor vessel could not be determined. Support Condition I considered the spacer bolts touching the vessel wall. Support Condition II did not include the spacer bolts. Tables 3.9-7 and 3.9-8 summarize the stress results at various reactor vessel locations for Support Conditions I and II, respectively. Based upon these results, Davidson (1978) concluded:

> . . .the reactor vessel and internals were found to be adequate for Safe Shutdown loading. The Primary Coolant System Boundary will not be breached. The displacements of the internals are small enough that operation of the control mechanisms is assured. There is a possibility that some of the bolts which fasten the reactor vessel to the concrete foundation will exceed allowable load capacity. However, it has been demonstrated that the reactor vessel total movement is limited to 1/8 in. at this location, and this displacement will not have serious consequences. Therefore, the reactor vessel is considered adequate for Safe Shutdown Earthquake loading with no required modifications.

3.9.2.6 Correlations between Analytical Results and Vibration Tests of Reactor Internals. System operational testing of the reactor began in December 1965 with the primary system full of water. Step-flow rate tests (to approach full reactor operational flow) revealed the vibration of several components within the reactor vessel as well as excessive vibration of the primary piping. Further review, including site walkdowns, additional operations tests, and analytical evaluations, resulted in modifications to (a) safety-rod positions, (b) two dummy flux-trap fillers, (c) the center loop position, (d) latch pins in the inner pressure-tube locator, (e) aluminum filler plates and aluminum-hafnium stop plates, and (f) packing glands around the experiment loops below the reactor head (Manoli 1968).

Manoli summarizes both the vibration tests performed on reactor internals and the basis for these modifications. Manoli also discusses the correlation between vibration-test results and predictions from analytical models, concluding that based upon combined analytical and test results, modifications to reactor internals "are substantially satisfactory to prevent self-induced vibrations and to keep the parallel-flow excitation within tolerable limits."

3.9.3 ASME Code Class 1, 2, and 3 Components, Component Supports, and Core Support Structures

3.9.3.1 Loading Combination, Design Transients, and Stress Limits. ATR components were specified before 1970, and are in compliance with the AEC regulations and codes in effect at that time. Full-power operation was first achieved in September of 1969. A summary of the design basis for the PCS (Class 1 equivalent) is presented here. Further design-basis information on the ASME Code Class 1, 2, and 3 equivalent components can be found in Chapters 5 (Primary Coolant System), 6 (Engineered Safety Features), and 9 (Auxiliary Systems).

The completed reactor vessel was designed and approved under the provision for nuclear vessels as stated in the 1962 Edition of the ASME Code, Section VIII and Code Case 1270N-3. Code Cases 1270N-5, 1271N, 1272N-5, 1273N-7, 1274N-6 and 1275N were also used. The reactor vessel has an ASME Code stamp. The reactor vessel, heads, nozzles, and attachments are designed for 390 psig pressure at a temperature of 240°F. Nominal operating conditions are 372 psig measured at the PPS vessel inlet pressure tap and 125°F at the vessel inlet. Nominal operating reactor outlet fluid temperature is 170°F. Table 3.9-9 provides an overall assessment of the piping and supports for the various loading conditions, load combinations, ASME stress limits, and allowable fatigue cycles as determined by Davidson (1979), Davidson and Thinnes (1974), Durney et al. (1987), Harris (1989), Harris and Burr (1989), Miller (1988, 1989a, 1989b, and 1989c), and Thinnes (1989).

The primary heat exchangers were designed and constructed in accordance with the ASME Unfired Pressure Vessel Code, Section VIII, 1959 Edition, latest addenda and General Requirements for Nuclear Vessels, Special Ruling Case 1270N-5.

The PCS pumps were designed and constructed in accordance with the Centrifugal Pumps Section of the Standards of the Hydraulic Institute, 10th Edition. All pump casings were hydrostatically tested at 585 psig. All preoperational tests of pumps were in accordance with ASME Power Test Code for Centrifugal Pumps, PTC 8.1, 1954 Edition.

The PCS piping was designed to the requirements of ASA B31.1 Code for Pressure Piping, 1955 Edition (ASME 1955b), and the associated nuclear cases N-1, N-7, N-9, and N-10. All piping materials are Type 304 stainless steel except in inaccessible areas (generally adjacent to the reactor vessel), where Type 304L is used. Most of the pipe used in construction is longitudinally welded pipe (per ASTM A-358-60T), but some seamless pipe, especially buried or embedded pipe (per ASTM A-376-60T) may also exist. Type 304L piping meets the chemical requirements of ASTM A-312-61T. Dimensions for nominal-wall pipe are in accordance with ASA B36.19-1957.

The PCS surge tank was designed for 390 psig pressure and 240°F temperature. It was constructed in accordance with the ASME Unfired Pressure Vessel Code, Section VIII, 1959 Edition, latest addenda and General Requirements for Nuclear Vessels, Special Ruling Case 1270N-5. The surge tank was hydrostatically tested at 585 psig per the ASME Unfired Pressure Vessel Code, Section VIII requirements, and all welds were fully radiographed in accordance with Section VIII and Code Case 1270N-5 requirements.

The degassing tank was designed for 50 psig pressure and 170°F temperature, and was constructed in accordance with the ASME Unfired Pressure Vessel Code, Section VIII, 1959 Edition, latest addenda, and General Requirements for Nuclear Vessels, Special Ruling Case 1270N-2. The degassing tank was hydrostatically tested at 75 psig and vacuum tested at 3 psia. All welds were fully radiographed in accordance with Section VIII and Code Case 1270N-2 requirements.

3.9.3.2 Pump and Valve Operability Assurance. Systems and components important to the safe and efficient operation of the ATR, including safety-related systems and components, are periodically inspected or tested. The inspections and testing are conducted in accordance with the *ATR Inservice Inspection (ISI) Plan* (INEEL 2002). Inservice testing of pumps and valves to ensure operability is conducted as part of the ATR ISI plan, and is discussed in Chapter 14 (Initial Test Program, Inservice Surveillance and Maintenance).

Table 3.9-10 lists the ATR safety-related active pumps and valves. These were all installed prior to issuance of the Institute of Electrical and Electronic Engineers (IEEE) Standards and as such functional operability was not considered as presently required and has not been specifically addressed to date. However, the as-installed components and supports have been structurally analyzed and shown to remain within the elastic limits which indicates the deformations are not excessive or permanent. These components are functionally tested routinely as an integral part of the ISI program (INEEL 2002). Further, successful operation of the plant since start up in the late 1960's provides a measure of assurance of their functional operability.

3.9.3.3 Design and Installation Details for Mounting of Pressure-Relief Devices. Two pressure-relief valves are mounted on the reactor vessel's 8-in. overflow line to protect the reactor from overpressurization. Each valve is designed to discharge 350 gpm at 379 psig. In addition to the relief valves on the reactor vessel overflow lines, safety relief valves are mounted at each of the primary pressurizing pumps. These pump-mounted relief valves are set at 380 psig to relieve 345 gpm. These valves protect the primary pressurizing pumps from overpressurization. No safety relief valves are required for the emergency coolant pumps because they are not capable of developing a discharge pressure greater than the PCS design pressure (deBoisblanc and Cohen 1965).

3.9.3.4 Components and Component Supports. Component supports were originally designed in accordance with the 1961 Uniform Building Code (ICBO 1961). Subsequent to the original design, safety standards were developed to follow more stringent criteria than the UBC. Recognizing this situation, the Seismic Analysis Program Plan was initiated in early 1973 to assess the safety significance of differences between the as-built condition of vital systems and components and the more recent safety standards (Mousseau 1973).

The majority of the active components were installed prior to the issuance of IEEE Standards for the qualification of active electrical and mechanical equipment. The component supports were installed using 1961 UBC criteria. The PCS components were designed according to various codes including the 1962 Edition of the ASME Code, Section VIII and Code Case 1270N-3; The ASME Unfired Pressure Vessel Code, Section VIII, 1959 Edition; the Centrifugal Pumps Section of the Standards of the Hydraulic Institute, 10th Edition, and ASA B31.1 Code for Pressure Piping, 1955 Edition.

In the late 1970's, the NRC expressed concern that nuclear equipment seismically qualified to standards preceding IEEE-344-1874 may not provide sufficient assurance of seismic adequacy. This concern was verified through field inspection of older nuclear power plants where equipment lacked adequate anchorage. This NRC concern resulted in NUREG-1030, Unresolved Safety Issue (USI) A-46, "Seismic Qualification of Equipment in Operating Nuclear Power Plants, (August 1985)."

On the basis of research by the national laboratories, the NRC concluded that use of experience data could provide a reasonable alternative for resolution of USI A-46. The NRC also endorsed the methodology developed by Seismic Qualification Users Group (SQUG), Electric Power Research Institute (EPRI), and the Senior Seismic Review and Advisory Panel (SSRAP). In 1987, NRC Generic Letter (GL) 87-02 required utilities to respond to USI A-46 and encouraged participation in generic resolution by using the SQUG approach defined in SQUG's Generic Implementation Procedure (GIP). The NRC has recently accepted the SQUG GIP as a means to resolve USI A-46.

Similar to the USI A-46, the majority of active mechanical and electrical components in place at the ATR were installed prior to the issuance of IEEE-344-1974. Risk-significant components were evaluated using an experience based approach, walked down by a team of SQUG trained Seismic Capability Engineers, and analyzed in support of a PRA of the ATR in 1989 (Eide, Khericha, and Thatcher 1989). The assessment covered most Seismic Category I mechanical systems, equipment items, instrumentation, and electrical equipment. One key result of the assessment was the determination of HCLPF accelerations. The HCLPF acceleration is an indicator of the equipment seismic capacity. The HCLPF acceleration is defined as the level of acceleration at which there is high confidence (i.e., 95%) of a low probability of failure (i.e., < 5%). Although the use of HCLPF accelerations, or fragility analysis, is not used to qualify equipment items, a HCLPF acceleration that exceeds the SSE peak ground acceleration indicates seismic ruggedness.

Table 3.9-11 summarizes the fragility parameters developed for mechanical equipment. The table identifies the equipment by location and component identifier along with the equipment characteristics and failure mode. Also present are the associated median peak ground acceleration capacity (A_m, 50% probability), and the HCLPF acceleration capacity for each component. Components that were effectively screened out from detailed fragility evaluation are denoted in the Table 3.9-11 by > 2.0 in the "A_m" or by > 0.5 in the HCLPF Capacity column. The majority of these components were screened out based on walkdown observations, median response factors, and historical performance of equipment and structures during earthquakes (Eide, Khericha, and Thatcher 1991).

Table 3.9-11 is based on the PRA (Eide, Khericha, and Thatcher 1991); since the time that the PRA was issued, seismic modifications to some of the listed equipment and structures have been completed or are in progress. With the completion of the seismic modifications, the median peak ground acceleration capacity for the affected equipment and structures is judged to be greater than 2.0 g. Table 3.9-11 does not incorporate the effect of these seismic upgrades, although the completed modifications are listed in the footnotes to Table 3.9-11.

3.9.4 Reactivity-Control Systems (Control Element Drive Systems)

Four independent mechanical drive systems provide reactivity control (ANSI 1988, Category 2) for the ATR. The systems are (a) safety rod, (b) outer shim control cylinder (OSCC), (c) neck shim rod control, and (d) regulating-rod control.

The functions of the four systems are as follows:

- The safety-rod system is safety-related; it rapidly terminates the fission process and keeps the reactor subcritical as required.
- The OSCC system primarily shifts neutron flux; that is, it adjusts power at the individual loop irradiation facilities (Figure 3.9-1). Secondarily, it compensates for fuel burnup. It also provides safety-related backup to the safety-rod system for shutting down the reactor.
- The neck shim rod control system is nonsafety-related, and primarily compensates for fuel burnup.
- The regulating rod control system is nonsafety-related, and provides the means for automatic power-level control.

Both the reactivity-control elements (assemblies) and the control-element drive mechanisms for the safety rods and OSCCs are covered in this section. The neck shim and regulating rod control systems are discussed briefly in Section 3.9.4.1.3. Figure 3.9-1 shows the locations of the various reactivity control elements within the reactor core. The locations of the corresponding control-element drive mechanisms outside the reactor pressure vessel are shown in Figure 3.9-2. The control-element drive mechanism is considered to extend to the coupling interface with the reactivity control elements in the reactor vessel.

The design (both mechanical and functional) of the safety-rod and OSCC systems is evaluated here, and materials aspects are addressed in Chapter 4 (Reactor). Descriptive information for the reactivity-control systems is found entirely under the various subheadings in 3.9.4.1.

Any internal guides and supports within the reactor vessel associated with the reactivity-control systems are considered reactor internals. Their mechanical design is addressed in Section 3.9.5, and their materials aspects in Chapter 4 (Reactor).

The vessel-penetration assemblies for the reactivity-control system are treated as part of the primary coolant pressure boundary, and are described in Chapter 5 (Primary Coolant System).

System descriptions are discussed in Section 3.9.4.1; the safety classification, design criteria, and specifications are discussed in Section 3.9.4.2; the design loads, stress limits, and allowable deformation in Section 3.9.4.3; the testing programs in Section 3.9.4.4; and the functions of ancillary systems in Chapter 4 (Reactor).

3.9.4.1 Reactivity-Control Systems Descriptive Information. The subsections under this heading describe the principal safety-related independent reactivity-control systems of the ATR. Presented for each system are (a) performance criteria, (b) drawings, (c) component descriptions and characteristics, and (d) method of operation summary. The descriptions and drawings for each safety-related system synopsize its design.

3.9.4.1.1 Safety-Rod System—This section contains a detailed description of the safety-rod system's subsystems, major assemblies, and components. The major subsystems for each safety rod are its assembly and its control drive.

To accomplish the function of the safety-rod system, up to six safety rods can be provided. Each safety rod is a vertically moving tubular assembly that surrounds the experiment's inpile tube (IPT) or a "dummy" IPT or an irradiation facility within two inner and four outer flux-trap baffles (Figure 3.9-1).

The poison sections of the safety rods are always driven above the core and held there before the reactor is taken to power. The driving force is provided by horizontally mounted motors located outside the reactor vessel below the core elevation (Figure 3.9-2). Upon receiving a scram signal from the RSS,[a] the rods are disengaged from the motors and driven into the reactor by a combination of gravity, downward coolant flow, and spring action. Performance characteristics of the safety-rod system are listed in Table 3.9-12.

3.9.4.1.1.1 Safety-Rod Assembly—The safety-rod assembly (Figure 3.9-3) is composed of the (a) guide tube, (b) drive connection assembly, (c) hafnium absorber plates, (d) flux-trap fillers, (e) flux-wire assemblies, (f) rack tubes, and (g) the latch assembly, which secures the hafnium plates to the guide tube.

Cooling is provided by primary coolant flowing downward through the annuli formed by the flux-trap baffle, guide tube, and the IPT (Figure 3.9-1). Below the core, the coolant passes through orifice holes in the rack-tube and safety-rod sleeves, into the flux-trap plenum, and finally into the flow-distribution tank.[b]

3.9.4.1.1.2 Safety-Rod Control Drive—The major assemblies of the safety-rod control drive (Figure 3.9-4) are (a) the actuator drive assembly, (b) the horizontal drive shaft, and (c) the drive package.

The actuator drive assembly (Figure 3.9-5) consists of the inner and outer snubber tubes and the rack assembly. The rack tube is connected to the bottom of the safety-rod assembly's guide tube by a threaded swivel joint. The rack tube has rack teeth machined along its length on one side and is threaded at both ends.

The horizontal drive-shaft assembly (Figure 3.9-5) consists of (a) the flange tube, (b) shafts, (c) bearing housing, (d) bearings, (e) pinion drive, (f) flexible coupling, (g) inflatable seal, and (h) the rotary seal package. The horizontal drive shaft transmits power from the drive package assembly gearmotor to raise the safety-rod assembly and rack tube to the full-out position.

---

[a]. Refer to Chapter 7 (Instrumentation and Controls) for a description of the RSS.

[b]. Refer to Section 3.9.5.1.1 for a description of the flow-distribution tank.

The drive-package assembly (Figure 3.9-5), which is located outside of the reactor vessel (Figure 3.9-4) and mounted on the outboard flange tube, consists of (a) the gearmotor, (b) gears, (c) electromagnetic clutch, (d) scram-spring assembly, and (e) position-indicating and-control equipment.

The gearmotor (Figure 3.9-5) provides rotational drive to the horizontal drive shaft and pinion gear via the electromagnetic clutch. The gearmotor is powered from the 208/120 V diesel-commercial distribution panel through a stepdown transformer from the 480 V, diesel-commercial, motor-control center (670-E-15).

The electromagnetic clutch is mounted on the clutch shaft and is keyed to the clutch gear, which in turn engages the drive gear installed on the gearmotor's drive shaft. When the electromagnet is energized, the discs and armature are held together so that the gearmotor is coupled to the horizontal drive shaft. The rod clutch coil of the RSS powers the magnet holding current of the electromagnetic clutch.

A ball nut and helical shaft and scram-spring assembly (Figure 3.9-5) is coupled directly to the horizontal drive shaft to provide an energy supply for scram assistance. The spring has an initial static load. The spring is compressed by the drive shaft and ball nut the last 12 in. of withdrawal. The resulting torque is always in the direction of rod insertion.

Upon receipt of a scram signal, power is interrupted to the electromagnetic clutch coil, causing the clutch plates to separate and uncoupling the horizontal drive shaft from the drive motor. The safety-rod assembly is accelerated downward by the combined hydraulic, scram-spring, and gravitational forces acting on the mechanism. The potential energy of the scram spring, released at the moment the electromagnetic clutch is de-energized, is sufficient to overcome the inertial and frictional forces in the horizontal drive shaft assembly. The rods accelerate in the first 12 in. of fall into the core. The remaining 24 in. of fall are slowed by the fluid action in the snubber tubes, thus preventing mechanical damage at the bottom of the drop.

On the flange tubes not containing the horizontal drive shaft components, an interchangeable nozzle closure flange assembly is provided.[a]

3.9.4.1.2 Outer Shim Control Cylinder System—This section contains a description of the OSCC system subsystems, assemblies and components. The major subsystems of the OSCC system are the OSCC and the OSCC drive.

To accomplish the function of the OSCC system, 16 beryllium OSCCs are rotated in 7-1/2-in. holes in the beryllium reflector[b] surrounding the core (Figure 3.9-1). The cylinders have plates of hafnium on 120 degrees of their outer surfaces (Figure 3.9-6). Power is increased by rotating the hafnium away from the core. The reactivity effect is uniform along the vertical dimension of the core, and vertical power distortion does not occur. Table 3.9-13 lists the performance characteristics of the OSCC System.

3.9.4.1.2.1 OSCC—Each OSCC consists of a beryllium cylinder faced with hafnium plates, a stop collar attached to the cylinder bottom, and a column connector attached to the cylinder top (Figure 3.9-6). The beryllium cylinder is 46-2/3 in. long and 7-1/4 in. in diameter.

---

[a]. Refer to Chapter 5 (Primary Coolant System) for a description of the penetration assemblies for the flanged tubes for the horizontal drive shaft assemblies.

[b]. Refer to Chapter 4 (Reactor) for a description of the beryllium reflector.

Six hafnium plates (Figure 3.9-6) 7.667 in. long and 0.250 in. thick are mounted flush with the surface of the cylinder through 120 degrees of arc. The six plates make an active section 46 in. long.

3.9.4.1.2.2 OSCC Drive Subsystem—The major assemblies of the OSCC drive subsystem are (a) the worm-gear box, (b) the gear-box support beam, (c) the connecting shaft, (d) the coupling shaft, (e) the drive shaft and housing, (f) the outer gear box, and (g) the position-indication and-control equipment.

The 16 cylinders are driven by eight OSCC drive subsystems (Figure 3.9-7). The drive systems are mounted in four pairs, located at 90-degree intervals from each other around the reactor. The two cylinders operated by a single motor rotate in the same direction. Each drive system is approximately 20 ft below the reactor head at elevation 83 ft 9 in. The drive is transmitted through the horizontal drive shaft, to the worm-gear box assembly above each cylinder pair.[a] A pair of OSCCs is rotated by the motor and outer gear box.

The OSCC drive subsystem is normally powered from the 208/120 V diesel-commercial distribution panel through a stepdown transformer from the 480 V, diesel-commercial, motor-control center (670-E-15). On loss of diesel-commercial power, the OSCC drive subsystem can be powered through either instrument UPS power panel 670-E-117 or utility UPS power panel 670-E-115 through the manual transfer switch 670-E-457 and the UPS power panel 670-E-456.[b]

3.9.4.1.3 Control System for Neck Shim and Regulating Rod—The neck shim and regulating rods are arranged in four groups of six along the center line of each neck of the neck shim rod housing (Figure 3.9-1). The first, second, third, fifth, and sixth rods in each neck (numbering radially outward from the center) are used for shim control. The fourth position contains a rod that can be used either for shim or regulating (power-level) control. The absorber sections of the neck shim and regulating rods are composed of a fluted hafnium rod 7/16 in. diameter and 48 in. long. The neck shim rod system penetrates the reactor vessel through a pressure housing assembly.[c] Each group of neck shim rods is driven by five shim cable drive systems (Figure 3.9-8).

The regulating rod is rigidly attached at its lower end to a solid drive rod extending down through the pressure envelope below the reactor bottom head. The drive rod penetrates the pressure envelope through a labyrinth-type seal. The regulating rods can be driven by shim or servo drives. Normally, two regulating rods are driven by each type of drive.

3.9.4.2 Applicable Design Specifications. Bases for temperature, stress on structural members, and material compatibility are imposed on the design of the reactivity-control components. The safety-rod drive mechanisms are designed and built using the following codes (Ebasco 1963):

- ASME Boiler and Pressure Vessel Code, Section VIII, 1962 Edition
- ASME Boiler and Pressure Vessel Code, Section II, 1962 Edition
- ASME Boiler and Pressure Vessel Code, Section XI, 1962 Edition

---

[a]. The OSCC controls are described in Chapter 7 (Instrumentation and Control). The OSCC system also interfaces with the reactor interlock system (see Chapter 7), which ensures that the OSCC are completely seated before reactor start up.

[b]. Refer to Chapter 8 (Electric Power) for details of the electric power system.

[c]. Refer to Chapter 5 (Primary Coolant System) for a description of the pressure housing assembly.

- ASME Code for Pressure Piping ASA B31.1
- Interpretations of ASME Codes, including Cases 127ON-5, 127IN, 1272N-5, 1273N-7, 1274N-6, and 1275N
- Electrical Standards of the American Standards Association
- Engineering Standards, Idaho Operations Office
- Reports Supplement to IDO Engineering Standards.

The performance characteristics of the safety-rod system are listed in Table 3.9-12.

The OSCCs are designed and built using the following codes (Ebasco 1963):

- ASTM Part 1, Ferrous Metals Specifications, 1961 Edition
- ASTM part 2, Non-Ferrous Metals Specifications, Electron Tube Materials and Semiconductors, 1961 Edition
- ASTM Part 3, Metals Test Methods (except Chemical Analysis), 1961 Edition.

The performance characteristics of the OSCCs are listed in Table 3.9-13.

3.9.4.3 Design Loads, Stress Limits, and Allowable Deformation. The program to specify design loads, stress limits, and allowable deformation or misalignment of the control-element drive systems consisted of a combination of analyses, as documented in the ATR Design Manual (Ebasco 1964a), and prototype testing, as discussed in Section 3.9.4.4. The following sections discuss specific design considerations for critical components in the safety-rod and OSCC-drive systems.

3.9.4.3.1 Safety-Rod System—The safety-rod drive mechanism has been designed to prevent seizing, galling, corrosion, and wear. Nine design considerations for critical components are presented below.

3.9.4.3.1.1 Rack and Pinion—Design considerations for the rack and pinion are strength and resistance to wear, corrosion, and shock. The rack and pinion use a high contact ratio for greater load-carrying capacity. The calculated nominal contact ratio of 2.3 distributes the load between 2 to 3 pairs of teeth when pitch lines coincide. Based on a maximum backlash of 0.019 in. caused by cumulative tolerances and clearances in the vertical driveline, the contact during one rotational cycle is:

- Two-pair contact: 68% of the cycle
- One-pair contact: 32% of the cycle.

In addition to the stresses in the teeth caused by nominal loading, the design considered impact loading and induced vibration. Prototype-test results and calculations that include stress-concentration factors show that the rack and pinion teeth designs met the design considerations.

3.9.4.3.1.2 Outer Snubber Tube—The critical factors determining design of the outer snubber tube are antigalling properties, wear, and corrosion. Because sliding contact between the outer snubber tube and the rack tube guide bushings is required, the contact materials must be compatible to minimize galling. The snubber-tube material selected was 17-4PH stainless steel precipitation hardened (H1100). The guide bushings, which use Stellite Number 3 as mating surface with the snubber tube, have succeeded in minimizing galling.

3.9.4.3.1.3 Rack-Tube Guide Bushings—Prototype testing required changing the bushing material from 17-4PH stainless steel to Stellite Number 3 because of excessive galling. The guide-bushing design provides diametral clearances within the outer snubber tube of 0.013 in. maximum and 0.010 in. minimum. These clearances provide adequate buffing action and prevent excessive crud buildup. A flow of filtered water has also been provided to minimize crud accumulation in the lower guide bushing area.

3.9.4.3.1.4 Horizontal Shaft Ball Bearings—Calculated maximum dynamic compressive stress for the preloaded Stellite Number 3 pinion bearings is 306,000 psi, compared to a design value of 412,000 psi. Ball separators have been designed for maximum water flow through the bearings. Seal water is used to flush the bearings continuously to prevent crud accumulation.

3.9.4.3.1.5 Scram Spring—The scram spring has been designed to limit stresses to 72,000 psi. The design has minimized the possibility of spring buckling to prevent undue lateral loads on the sliding members. A multiple fracture of the spring coils has been calculated to increase the scram time 40 to 70 msec, but would not prevent a scram.

The safety rod spring has been subjected to 100% liquid-penetrant or magnetic-particle inspection.

3.9.4.3.1.6 Ball Nut and Screw Assembly—A static load of 2,000 lb (maximum) is normally applied by the scram spring to the translating ball nut. This force acts to rotate the screw in the direction of rod insertion when the clutch is deenergized. The design of this assembly considered shock resistance and useful life, and is adequate for the loads.

3.9.4.3.1.7 Electric Clutch—The design of the electric clutch considered the holding requirements and the magnetic and mechanical forces affecting the release and breakaway time. Several modifications were made to improve the clutch characteristics. The modifications included improving the magnetic flux shape by adding a RC circuit, slotting the clutch coil housing and plates, and optimizing the air gap. Modifications to reduce mechanical drag during breakaway include improving clutch-disc's finish, shape, and spring action.

3.9.4.3.1.8 Rotary Seal—The rotary face seal is relatively maintenance free and is inherently free of shaft binding characteristics. The measured amount of wear on the seal face was 0.0024 in. after extensive life testing.

3.9.4.3.1.9 Misalignment of Components—The design of the safety rod and drive assemblies considered interference between the experiment pressure tube assembly, the safety rod, and flux-trap baffle (guide tube). Excessive misalignment of the reactor nozzles as a result of improper fabrication and thermal conditions was also considered.

The vertical assembly incorporates a swivel joint, which permits the maximum misalignment dictated by the clearance between the safety rod proper and the inside diameter of the flux trap baffle (0.060 in.).

The horizontal driveline contains a flexible coupling which has an angular misalignment capability of +0° -15' at the design torque rating. This angular misalignment allows a maximum misalignment of 0.5 in. between the center of the nozzle's outer flange and the true axis of the horizontal nozzle.

3.9.4.3.2 Outer Shim Control Cylinder System—As a safety feature, the system is designed so that water flow through the cylinder provides a torque for rotation in the direction of decreasing reactivity. Bearings have been analyzed for loading during a high-flow event. Although bearing races may be slightly marked by such an event, acceptable rotation capability would be expected as described in Chapter 15 (Accident Analyses).

Design considerations to minimize possible mechanism malfunctions and ensure desired performance include:

- Positive indexing of splined connections using the missing-tooth method
- Total enclosure of springs
- Moisture and overload protection for all electrical components
- Drive-motor high-temperature capability (356°F)
- Captivation of threaded connectors using Class A locking cups.

3.9.4.4 Performance-Assurance Program

3.9.4.4.1 Safety-Rod System—A prototype safety-rod drive mechanism was subjected to three series of tests to determine whether the drive performance was satisfactory. The series consisted of:

- Operational testing. The purpose of these tests was to ensure that operating design conditions were achieved. Various modifications were made during the tests to meet performance objectives.
- Life testing. These tests demonstrated reliability under simulated reactor operating conditions.
- Miscellaneous tests, including
  - Misalignment tests
  - Crud tests
  - Inflatable-seal tests
  - Relay-panel tests
  - Scram tests without filler plates
  - Service-tool tests.

Operating conditions during the tests simulated ATR's hydraulic and temperature conditions. The coolant's pH and oxygen content were not controlled during all tests.

The prototype safety-rod drive mechanism performed satisfactorily during extensive testing in an environment similar to ATR conditions. Scram time was not significantly affected by crud conditions that simulated both probable and accidental concentrations expected in the ATR. Misalignment tests showed that the mechanism performs satisfactorily under conditions more severe than those expected from maximum-tolerance stackup. Wear and corrosion of the prototype components were satisfactory.

The production mechanisms were subjected to vendor testing before site shipment. The safety-rod drive mechanisms, following reactor installation, were tested under both operation and open-head hydraulic conditions before loading fuel in the reactor.

Before reactor startup, following each shutdown in which the vessel has been opened, the safety rods are tested to ensure that release and travel times are within the prescribed limits of Table 3.9-12.

3.9.4.4.2 Outer Shim Control Cylinder System—A prototype OSCC drive mechanism was subjected to extensive testing under conditions simulating the ATR environment. The tests included:

- Life-cycle test
- Environment tests
- Misalignment tests
- Position-accuracy tests.

The OSCC drive mechanism has performed satisfactorily under extensive testing in an environment simulating ATR conditions. Misalignment tests have shown the mechanism capable of satisfactory performance under conditions more severe than expected in the reactor. All production components were inspected and found to be free of corrosion and wear.

Based on design considerations, performance testing, and malfunction analysis, the OSCC drive will meet reactivity control requirements reliably.

3.9.5 Reactor Internals

This section describes those subsystems and components within the reactor vessel that are termed "reactor internals."

The reactor internals are a part of the "reactor core and internals" (ANSI 1988), and include the core support structure and all internals between that structure and the reactor-vessel wall. The reactor core is described in Chapter 4 (Reactor). The details of the reactor vessel are given in Chapter 5 (Primary Coolant System). The reactor internals are described in Section 3.9.5.1; design loading conditions of the reactor internals are discussed in Section 3.9.5.2; the design bases for reactor internals are described in Section 3.9.5.3.

3.9.5.1 Design Arrangements. The subsystems developed for the reactor internals described in this section are (a) the core support and flow distribution, (b) core internal guides, (c) outer reflector, (d) spent-fuel storage racks, and (e) the reactor-internals protective cover. These subsystem terms were developed specifically to identify components of similar function for purposes of this UFSAR. Items indicated in Figures 3.9-9 and 3.9-10 are described in this section. The drawings presented in this section synopsize subsystem design.

3.9.5.1.1 Core-Support and Flow-Distribution Subsystem—The function of the core-support and flow-distribution subsystem is to support and maintain geometry of the reactor-core assembly and to route primary coolant flow to ensure core cooling. The major assemblies of the core-support and flow-distribution system are (a) the internal-tank assembly, (b) the thermal shield and inlet-flow baffle assembly, and (c) the outlet-flow pipe assembly.

The basic reactor-coolant flow path, shown in Figure 3.9-11, is through two 23-in.-ID inlet nozzles located in the hemispherical portion of the bottom head and upward through the two annuli defined by the vessel shell wall, the thermal shield, and the cylindrical inlet-flow baffle. About 5% of the total inlet flow passes upward between the inlet-flow baffle and the core reflector tank to provide cooling around the outer capsule-irradiation tanks and the spent-fuel storage racks. The thermal shield and the inlet-flow baffle end about 3 ft above the core, where the inlet water becomes part of the water reservoir (about 13,800 gal) above the core. This reservoir feeds the coolant flow down through the core and reflector assembly into a lower plenum (the flow-distribution tank), which is divided into quadrants by baffles. Four outlet-piping assemblies transport the split coolant flow from the quadrants to individual 15-in.-ID outlet nozzles located in the vessel wall about 4 ft above the core.

The internal-tank assembly (Figure 3.9-12) is a right-circular cylinder made up of four separate tanks: (a) the core-support tank, (b) the flow-distribution tank, (c) the reflector-support tank, and (d) the core reflector tank. This 14.5-ft-high assembly is bolted together and to the bottom-head closure plate; it supports or contains all tank internals.[a]

Primary coolant flow is routed from the four quadrants of the flow-distribution tank to the reactor-outlet flanges by four outlet-flow pipe assemblies (Figure 3.9-13). These assemblies consist of 16-in.-OD stainless steel pipes flanged at both ends, and are attached to the flow-distribution-tank outflow holes and the reactor-vessel outlet nozzle.[b] Each assembly contains a sliding joint in the vertical run to provide flexibility and to allow for thermal and hydraulic motion between elbows. These sliding joints are sealed with stainless-steel piston rings.

Each outlet nozzle in the reactor-vessel wall contains a siphon breaker (see Figure 3.9-11). This siphon breaker is a 1-in.-diameter pipe that extends 4 in. above the reactor top flange, where it mates to a similar pipe in the reactor top head. These four siphon breakers allow a small amount of primary coolant to bypass the reactor core, as described in Chapter 4 (Reactor). They prevent siphoning of the reactor core if a pipe should break outside the reactor vessel.

3.9.5.1.2 Core Internal Guides—The core internal guides support and guide the reactor-core system. Included are the neck shim rod housing and the flux-trap baffles.

---

[a]. Refer to Chapter 5 (Reactor Coolant System) for a description of the bottom-head assembly.

[b]. Refer to Chapter 5 (Reactor Coolant System) for a description of the reactor vessel.

The neck shim rod housing (Figure 3.9-14) is a cruciform-shaped aluminum extrusion with four radial extensions. It is located in the center of the reactor core (Figure 3.9-10), and is positioned and supported by the 8-in. mounting tube welded to the bottom plate of the flow-distribution tanks. The housing provides support and attachment points for the inner flux-trap baffles and the center flux-trap baffle. It also provides locator ties for experiment-loop pressure tubes. The housing assembly contains 24 longitudinal holes for 20 neck shim rods and four regulating rods.[a] Each "wing" has six holes: five for cable-driven neck shims, and one for the regulating rods. Regulating rods can be installed in the fourth positions. When not used as a regulating rod, the fourth-position neck shim rod is used in the same fashion as the cable-driven neck shim rods. It also contains 16 A-faculty irradiation holes (Figure 3.9-10).

Nine flux traps for irradiation are provided in the ATR (Figure 3.9-10). The outer boundary of these spaces is defined by flux-trap baffles extending through the core area.

The center flux-trap baffle (Figure 3.9-15) fills the space in the center of the neck shim rod housing and encloses an irradiation facility located in the center position of the core. It directs coolant flow round irradiation facilities. Sixteen vertical holes are drilled in the baffle wall for experiments, flux-trap fillers, and the two center N-16 assemblies (Figure 3.9-10).[b] Fourteen of these holes extend 6 in. below the active core, at which point each has a window in the baffle wall to allow the cooling flow through the wall and into the annulus between the baffle and the neck shim housing. The two holes for the N-16 tubes are drilled through the upper section of the baffle to windows in the baffle wall where the upper and lower sections are joined. These windows allow space for the N-16 assembly flow dividers, and also allow the flow through the baffle to rejoin the main coolant stream in the flow-distribution tank.

The four inner and four outer flux-trap baffles are located in a square pattern around the core's center line (Figure 3.9-10). The inner and outer flux-trap baffles serve primarily to support and position the fuel-element assemblies in the ATR core.[c] Each inner baffle has six T-slots machined into the upper section for lateral fuel support and six T-slots in the upper end of the lower section to support the weight of the fuel element. The outer baffles have slots for only four elements. The outer baffles latch to the OSCC gear-box support beams with a twist-lock cam.

Inside each of the eight baffles is a loop inpile tube or an irradiation facility. Between the IPT and the baffle, in six of the eight possible positions, are the reactor safety rods (Figure 3.9-1). In the positions where a rod is not installed, filler pieces maintain the proper metal-water ratio. The baffle serves as a flow container for primary coolant flow around the components inside the baffle.

3.9.5.1.3 Outer-Reflector Subsystem—The outer-reflector subsystem provides special environments for experimental facilities outside of the reactor core. The capsule-irradiation tank assemblies (Figure 3.9-16) locate and contain the outer reflector blocks (Figure 3.9-10). The north tank is a 2 × 5 array with corner positions toward the core reflector tank. Flow through all 12 positions is collected in a plenum below the tank and routed to the flow-distribution tank through a 5-in. pipe. The south irradiation tank is a 4 × 5 array with two corner positions. Flow from the 12 inner positions is routed to the flow-distribution tank. The outermost 10 positions are cooled by natural convection only, so there is a slight upward flow.

---

[a]. Refer to Section 3.9.4.1 for a description of the neck shim and regulating rods.

[b]. Refer to Chapter 9 (Auxiliary Systems) for the N-16 System.

[c]. Refer to Chapter 4 (Reactor) for the fuel elements.

3.9.5.1.4 Storage Racks—The two storage racks are located between the core reflector tank and the inlet-flow baffle along the east-west center line of the reactor (Figure 3.9-10). Each rack assembly consists of a frame, three four-element baskets, and a single one-element basket.

Each basket is attached to the frame by two spring-loaded locking lugs. Each position in the four-element basket is equipped with an aluminum-clad cadmium poison liner that is not removable from the basket.

The one-element baskets have been modified by replacing the aluminum-clad cadmium liners with an aluminum liner. Temporary storage of two fuel elements in the reactor tank during shutdown is allowed in the one-element baskets. The only cooling for stored fuel elements is by natural convection circulation within the box. The T-bars under each basket are slotted to allow free mixing under the baskets to aid circulation. In case of loss of primary coolant, the stored fuel remains water-covered since the frame box has no drains. Overflow weirs on the core reflector tank allow emergency firewater to flow into the fuel-storage racks.

3.9.5.1.5 Reactor-Internals Protective Cover—The protective cover extends from the outer edge of the core reflector tank to within 1/4 in. of the reactor-vessel wall. This cover keeps small items, inadvertently dropped into the reactor vessel, from falling to the bottom head. The cover consists of a stainless-steel expanded-metal screen between the inlet-flow baffle and the vessel wall at elevation 85 ft (just below the outlet nozzles), and a segmented aluminum cover plate between the baffle and the core reflector tank at approximately elevation 82 ft (just below the OSCC drive line nozzles). The metal screen is bolted to the top of the thermal shield and extends over the inside edge of the inlet-flow baffle. The transition pieces around the drop tube are covered by stainless-steel plates perforated with 1/2-in.-diameter holes.

3.9.5.2 Loading Conditions. The loading conditions that provide the basis for the design of the reactor internals are (Ebasco 1964a):

- Weight of fuel and reactor internals
- Differential-pressure and coolant-flow forces
- Temperature gradients
- Seismic forces.

The loading analyses for the reactor internals are based on the ASME Boiler and Pressure Vessel Code, Section VIII, 1962 Edition (Ebasco 1963).

3.9.5.3 Design Bases. Service loading combinations for the core internals have been calculated (Ebasco 1964a; Hanson 1976). Loading for the reactor internal tanks and flux-trap baffles is summarized in Table 3.9-14.

The design bases for the reactor vessel internals are as follows (deBoisblanc and Cohen 1965):

A. The reactor internals, in conjunction with the fuel assemblies, direct primary coolant through the core to achieve acceptable flow so that heat-transfer performance requirements are met for all modes of operation.

B. In addition to the gamma shielding provided by the primary coolant, the inlet-flow baffle and thermal-shield assembly limit gamma heating in the concrete walls surrounding the vessel shell.

C. Provisions are made for installing incore instrumentation and capsule experiment facilities in support of the ATR mission.

D. The core internals are designed to withstand mechanical loads arising from earthquake and pipe rupture, and to meet the requirements of Item 5 below.

E. The reactor has mechanical provisions that are sufficient to support the core and internals adequately and to ensure that the core is intact, with acceptable heat-transfer geometry following Condition 1 and 2 events.

3.9.6 Inservice Testing and Pumps and Valves

An ISI plan (INEEL 2002) has been developed for the PCS. The ISI for pumps and valves is covered under this plan. Refer to Chapter 14 (Initial Test Program, Inservice Surveillance and Maintenance) for more information.

Table 3.9-1. Transients used in the design and fatigue analysis of the ATR vessel.

Allowable cycles (Number)	Temperature range of transient (°F)	Duration of transient (sec)
2,000	120 to 170	45
2,000	170 to 120	3

Table 3.9-2. General guidelines on ASME allowable stress limits for specified service loading combinations.

Plant Event	System Operating Conditions	Service Loading Combination	Service Stress Limit
Normal Operation	Normal	Sustained Loads	A
Plant/System Operating Transients (SOT)[a]	Upset	Sustained Loads + SOT	B
Safe Shutdown Earthquake (SSE)	Faulted	Sustained Loads + SSE	D

a. Transients for ASME components are given in Tables 3.9-3 and 3.9-9.

Table 3.9-3. Load cases considered in ASME Section 3 analysis of ATR reactor vessel.

	Pressure Load		Temperature Gradient						
Load Case	Level	Magnitude (psi)	Level	Reactor Temp. (°F)	Canal Temp. (°F)	ASME Service Condition	Type of Event	Number of Cycles/yr	Allowable No. of Cycles
1	Design	390	NA	NA[a]	NA	Design	NA	NA	NA
2	Operating	375	Normal	125	65	Level A	Normal operating	18	NA
3	Design + 10%	429	Normal	125	65	Level B	High pressure	31[b]	[b]
4	Operating	375	Upset	213	65	Level B	High temperature	17[b]	[b]
5	Operating	375	Faulted	125	65	Level D	SSE	NA	NA

a. Not Applicable

b. Combined Number of cycles/yr=48; Combined allowable number of cycles $\geq 10^7$

Table 3.9-4. Computer programs used in analysis.

Program name	Developer	Description	Application
I-DEAS	Structural Dynamics Research Corporation (SDRC)	PC-based general-purpose finite- element code for linear static and eigensolver. Includes solid and wire-frame modeling packages, a finite-element solver, and a post-processing package.	Remote processing unit (RPU) cabinet, EDF TRA-ATR-680; operator console, EDF TRA-ATR-625; transmitter cabinets, EDF TRA-ATR-608; RPU cabinet, EDF TRA-ATR-606.
PATRAN	PDA Engineering	Pre-Processor used in creating SAP, SAPIV, and ABAQUS models.	
SAPIV	U.C. Berkeley (Klaus-Jurgen Bathe, Edward Wilson, Fred Peterson)	General-purpose finite-element code for linear static and dynamic analysis.	Seismic Category I Piping, relief-valve piping, reactor vessel and internals
SUPERSAP	Algor	PC-based general-purpose finite element code for linear static and dynamic analysis. Contains good pre- and post-processing routines.	Heating and ventilation modifications
ABAQUS	Hibbitt, Karlsson, & Sorensen, Inc.	General-purpose finite-element code for linear and nonlinear static and dynamic analysis, buckling analysis, and large-deformation analysis.	Nonstandard piping components such as branched tees, PCS surge tank, PG-T-91-037.
NUPIPE-II	Quadrex Corporation	Linear elastic analysis of three- dimensional piping systems subjected to static and dynamic loads. NUPIPE-II evaluates piping system stresses to ASME Code Section III and B31 criteria.	Firewater piping, PG-T-90-016, Rev. 1, PCS weight and thermal analysis.

Table 3.9-5. Load combinations used in the reactor vessel faulted analysis.[a]

Load combination and individual contributions	Magnitudes of individual contributions
A (static loads from design conditions)	
Internal pressure	390 psi
Temperature	240°F
Core pressure drop	100 psi
B (Static loads from operating conditions, plus seismic loads)	
Internal pressure	355 psi
Temperature	125°F
Core pressure drop	100 psi
SSE	0.24 g

a. Davidson 1978.

Table 3.9-6. Allowable stress intensities for various portions of the reactor vessel.[a]

Load combination	Location	Material	Allowable stress intensity (ksi)
A	Components (RV shell)	304 SS (SA-182)	30.0
	Piping	304 SS (SA-376)	30.0
	Component supports	Carbon steel (SA-212, Gr B)	34.2
B	Components (RV shell)	304 SS (SA-182)	48.0
	Piping	304 SS (SA-376)	60.0
	Component supports	Carbon steel (SA-212, Gr B)	44.6

a. From stress analysis of faulted condition (Davidson 1978).

Table 3.9-7. Reactor vessel faulted condition: Summary of results for support-condition I.[a]

Effects (stresses, deflections, etc.) produced at given locations by imposed load combination	Effects of specified individual sources of loading				Total effects for load combinations A and B			
					Combination A		Combination B	
	XY Seismic loading	ZY Seismic loading	Dead weight plus core pressure drop	Operating internal pressure	Calculated	Allowable	Calculated	Allowable
Maximum deflections (in.)	< 0.01	< 0.01	< 0.10	0.11	< 0.20	—	< 0.20	—
Reactor vessel shell								
Max. stress intensity (ksi)	< 2.0	< 2.0	< 2.0	20.6	22.6	30.0	24.6	48.0
Max. stress intensity due to spacer bolt loads (ksi)	10.3[b]	5.2[b]	2.6[b]	20.6[b]	23.2	30.0	33.2	48.0
Spacer bolts max. load (kips)	24	12	6	48[b]	54	24	78	32
Internal piping								
Max. stress intensity (ksi)	< 1.0	< 1.0	4.5	3.1	7.6	30.0	8.6	60.0
Core support assembly								
Max. relative deflections (in.)	< 0.01	< 0.01	.03	0	.03	—	.04	—
Maximum shear (kips)	10.0	< 10.0	1.0	0	1.0	—	11.0	—
Maximum moment (in.-kips)	390	464	45	0	45	—	509	—
Maximum bolt load (kips)	1.3	1.6	0.2	0	0.2	15.0	1.8	20.0
Support skirt								
Max. stress intensity (ksi)	< 2.0	< 2.0	2.0	4.8	6.8	34.2	8.8	44.6
Max. radial bolt load (kips)	18.1[c]	18.5[c]	25	44.0	69	22.8	76	32
Avg. radial bolt load (kips)	15.0[c]	15.0[c]	25	1.0	24	22.8	42	32

a. Davidson 1978.

b. These values were derived from a small model constructed specifically for determining the maximum reactor vessel shell stress near the spacer bolts for pressure loading.

c. These values taken from runs with no spacer bolts because the support skirt radial bolts were not modeled in these runs. These loads are conservatively high for this case due to the extra lateral support provided by the spacer bolts.

Table 3.9-8. Reactor vessel faulted condition: Summary of results for support-condition.[a]

Effects (stresses, deflections, etc.) produced at given locations by imposed load combination	Effects of specified individual sources of loading				Total effects for load combinations A and B			
	XY Seismic loading	ZY Seismic loading	Dead weight plus core pressure drop	Operating internal pressure	Combination A		Combination B	
					Calculated	Allowable	Calculated	Allowable
Maximum deflections (in.)	0.12	0.12	< 0.1	< 0.1	< 0.30	—	< 0.30	—
Reactor vessel shell								
Max. stress intensity (ksi)	< 2.0	< 2.0	3.0	13.6	16.6	30.0	18.6	48.0
Internal piping								
Max. stress intensity (ksi)	1.3	1.5	3.6	0.9	4.5	30.0	6.0	60.0
Core support assembly								
Max. relative deflections (in.)	0.05	0.05	0	0	0	—	0.05	—
Maximum shear (kips)	16.3	14.4	0.1	0	0.1	—	16.4	—
Maximum moment (in.-kips)	575	677	12	0	12	—	689	—
Maximum bolt load (kips)	1.9	2.3	0	0	0	15.0	2.3	20.0
Support skirt								
Max. stress intensity (ksi)	4.9	4.9	1.3	3.1	4.4	34.2	9.3	44.6
Max. radial bolt load (kips)	18.1	18.5	25.0	3.0	28.0	22.8	46.5	32.0
Avg. radial bolt load (kips)	15.0	15.0	25.0	1.0	24.0	22.8	41.0	32.0

a. Davidson 1978.

Table 3.9-9. Load cases considered in ASME Section III analysis of ATR piping and supports.

	Pressure Load		Temperature				
Load Case	Level	Magnitude (psi)	Magnitude (°F)	ASME Service Condition	Type of Event	Number of Cycles/yr	Allowable No. of Cycles
1	Design	390, 435, 475, 485, 634	70	Design	NA[a]	NA	NA
2	Operating	≤ 390	≤ 167	Level A	Normal Operating	18	$> 10^7$
3	Upset	390	240	Level B	Worst Limiting Case of Levels A, B, C, & D	50[b]	$> 10^7$[c]
3	Faulted	390	240	Level D	SSE	NA	NA

a. Not Applicable

b. Design Transients are specified in Fershtut and Holman 1989.

c. One Non-standard Type of Component is limited to 9000 cycles where a 36 in. line has a 20 and a 24 in. line stubbed into it in close proximity to each other.

Table 3.9-10. ATR safety related active pumps and valves.

Vessel Vent System	
Valve	Description
	PCS vessel vent valve
	PCS vessel vent valve
Emergency Firewater Injection System	
Valve	Description
	Lower firewater injection control valve
	Lower firewater injection control valve
	Lower firewater injection check valve
	Lower firewater injection check valve
	Lower firewater injection check valve
	Lower firewater injection check valve
	Upper firewater injection control valve
	Upper firewater injection control valve
	Upper firewater injection check valve
	Upper firewater injection check valve
PCS Relief Valves	
Valves	Description
	PCS relief valve
	PCS relief valve
Primary Coolant System	
Valve	Description
	Primary emergency coolant pump
	Primary emergency coolant pump
	Primary pump discharge check valve
	Primary pump discharge check valve
	Primary pump discharge check valve
	Primary pump discharge check valve
	Emergency pump discharge check valve
	Emergency pump discharge check valve
	Check valve, bypass demineralizer to PCS
	Check valve, pressurizing pumps to PCS return header

FOIA Exemption 3 UCNI, Exemption 7f, table columns giving pump and valve numbers and locations

FOIA Exemption 3 UCNI, Exemption 7f, table columns giving pump and valve numbers and locations

Table 3.9-11. Ground-acceleration capacities of ATR structures and equipment.[a]

Equipment item	Location	Equipment characteristics	Median Acceleration capacity, A_m (g)	HCLPF acceleration capacity (g)	Failure mode	Comments
1. Diesel Generator		Flexible (23 Hz)	0.51	0.26	Base isolator	
2. DG[b] M-6 Air Intake Damper		Rigid (> 30 Hz)	> 2.0	—	Anchorage	
3. Valves betw. Tank ATR-776 Day Tank		Flexible piping	> 2.0[c]	—		Based on experience data.
4. Valves up/downstream of Air Tank		Flexible piping	> 2.0[c]	—		Based on experience data.
5. Radiator Fan for DG M-6		Flexible (20-30 Hz)	> 2.0[c]	—	Anchorage	
6. Injector Fuel Oil Cooler Fan		Flexible (16-20 Hz)	0.90	0.35	Anchorage	
7. Day Tank FO			0.21	0.10	Overturning	Pump anchor bolt nuts were observed missing during the walkdown. See note a
8. DG M-6 Attached Cooling Pump		Flexible (23 Hz)	0.51	0.26	Base Isolator	Fragility is based on DG Pump M-6.
9. DG M-6 Day Tank		Flexible (4-5 Hz)	0.52	0.22	Base Anchorage	
10. Fuel Oil Transfer Tank		Flexible	0.18	0.09	Saddle Support	Fragility is based on 619-10 Day Tank as information was not available.
11. Diesel Gen Starting Air Tank		Rigid (> 30 Hz)	> 2.0[c]	—	Base Anchorage	
12. DG M-6 Engine Driven FO Pump		Flexible (23 Hz)	0.51	0.26	Base Isolator	Fragility is based on DG Pump M-6.
13. BHFIS[b] Line upstream of CK's		Flexible piping	> 2.0[c]	—	Supports	Fragility is based on a piping sample review and experience data.

FOIA Exemption 3 UCNI, Exemption 7f, table columns giving equipment items and locations

Table 3.9-11. (continued).

Equipment item	Location	Equipment characteristics	Median Acceleration capacity, A_m (g)	HCLPF acceleration capacity (g)	Failure mode	Comments
14. BHFIS Line downstream of CK's		Flexible piping	> 2.0[c]	—	Supports	Fragility is based on a piping sample review and experience data.
15. UVFIS[b] Line upstream of CK's		Flexible piping	> 2.0[c]	—	Supports	Fragility is based on a piping sample review and experience data.
16. UVFIS Line downstream of CK's		Flexible piping	> 2.0[c]	—	Supports	Fragility is based on a piping sample review and experience data.
17. Line bet Raw Water Tank and		Flexible piping	> 2.0[c]	—	Supports	Fragility is based on a piping sample review and experience data.
18. Line outlet of FIS[b] pumps		Flexible piping	> 2.0[c]	—	Supports	Fragility is based on a piping sample review and experience data.
19. Overhead Stor			0.68	0.20	Rod bracing	
20. Ground Level Tanks		Flexible (2-5 Hz)	0.32	0.14	Shell buckling	See note a. (PRA evaluation of the unmodified tanks)
21. Diesel FW[b] Pump		Rigid (> 30Hz)	> 2.0[c]	—	Anchorage	
22. FW Pump		Rigid (> 30Hz)	> 2.0[c]	—	Anchorage	
23. Diesel FW Pump		Rigid (> 30Hz)	> 2.0[c]	—	Anchorage	
24. Diesel FW Pump		Flexible	0.18	0.09	Support saddle	See note d.
25. Diesel FW Pump		Flexible	0.18	0.09	Support Saddle	Fragility is based on tank 619-10 day tank as no information was available to perform a component specific evaluation. See note d.

FOIA Exemption 3 UCNI, Exemption 7f, table columns giving locations

Table 3.9-11. (continued).

Equipment item	Location	Equipment characteristics	Median Acceleration capacity, A_m (g)	HCLPF acceleration capacity (g)	Failure mode	Comments
26. LDW[b] pumps discharge Lines		Flexible Piping	> 2.0[c]	—	Supports	Fragility is based on a piping sample review and experience data.
27. LDW[b] pump		Rigid (30Hz)	> 2.0[c]	—	Anchorage	
28. LDW[b] pump		Rigid (>30Hz)	> 2.0[c]		Anchorage	
29. LDW[b] Tanks		Flexible (5-10 Hz)	0.62	0.27	Shell buckling	
30. Pressure Control Valve		Flexible Piping	> 2.0[c]	—		Based on Experience Data.
31. Air Dump V			> 2.0[c]	—		Based on Experience Data.
32. Air Compre			> 2.0[c]	—	Anchorage	
33. Air Compressor		Rigid (> 30 Hz)	> 2.0[c]	—	Anchorage	
34. Surge Tank (		Flexible (6-7 Hz)	0.18	0.06	Supports Legs	See note d.
35. Primary Degassing Tank		Flexible (6-7 Hz)	0.92	0.35	Support Legs in bending.	
36. Primary Piping (cold legs)		Flexible Piping	> 2.0[c]	—	Supports	Fragility is based on a piping sample review and experience data.
37. Primary Ht Exchg. (hot legs)		Flexible Piping	> 2.0[c]	—	Supports	Fragility is based on a piping sample review and experience data.
38. Pressurizing Pump		Rigid (> 30 Hz)	> 2.0[c]	—	Anchorage	
39. Pressurizing Pump (		Rigid (> 30 Hz)	> 2.0[c]	—	Anchorage	
40. Emergency Pump		Rigid (> 30 Hz)	> 2.0[c]	—	Anchorage	
41. Emergency Pump		Rigid (> 30 Hz)	> 2.0[c]	—	Anchorage	
42. Vessel vent and drain line		Flexible Piping	> 2.0[c]	—	Supports	Fragility is based on a piping sample review and experience data.

FOIA Exemption 3 UCNI, Exemption 7f, table columns giving equipment items and locations

Table 3.9-11. (continued).

Equipment item	Equipment characteristics	Median Acceleration capacity, A_m (g)	HCLPF acceleration capacity (g)	Failure mode	Comments
43. SV[b] for VVS[b]	Flexible Piping	> 2.0[c]	—		Based on Experience Data.
44. SV for VVS	Flexible Piping	> 2.0[c]	—		Based on Experience Data.
45. VVS N2 Tanks for	Flexible (2-4 Hz)	0.4	0.2	Sliding	Bottles are restrained by chains. Fragility is based on experience data. See note c.
46. VVS N2 Tanks for	Flexible (2-4 Hz)	0.4	0.2	Sliding	Bottles are restrained by chains. Fragility is based on experience data. See note c.
47. FW[b] Sprinl Room alon		0.84	0.29	Bending 1" Branch Line	
48. FW Sprinkler Line in SG Room between cable trays	Flexible (8 Hz)	1.09	0.40	Bending 2" Branch Tee	
49. Diesel Generators	Flexible (2-4 Hz)	0.39	0.17	Overstress	Fragility is based on previous analysis and experience data.
50. Diesel Generators Jacket Water Cooling Lines	Flexible (2-4 Hz)	0.39	0.17	Overstress	Fragility is based on previous analysis and experience data.
51. FW[b] Sprinkler Deluge Valve	Flexible Piping	> 2.0[c]			Based on structural capacity, failure modes & experience data.
52. Direct Damage (Large) LOCA[b] Process Piping	Flexible Piping	> 2.0[c]	—	Supports	Fragility is based on a piping sample review and experience data.
53. Storage Canal Rupture		1.5	0.51		
54. LDW[b] Bldg. 608	Flexible	0.35	0.4		
55. Steam Plant Bldg. 609	Flexible	0.35	0.4		
56. Raw Water Bldg. 619	Flexible	0.35	0.4		

FOIA Exemption 3 UCNI, Exemption 7f - table columns giving equipment items and locations

Table 3.9-11. (continued).

Equipment item	Location	Equipment characteristics	Median Acceleration capacity, A_m (g)	HCLPF acceleration capacity (g)	Failure mode	Comments
57. Firewater Bldg. 633		Flexible	—	> 0.5[c]		
58. Reactor Bldg. 670 – near surge tank		Flexible	—	> 0.5[c]		
59. Reactor Bldg 670 - Reactor Control Room		Flexible (16-20 Hz)	> 2.0[c]	—		Base Anchorage
60. Reactor Bldg. 670 -Process Control Room		Flexible (16-20 Hz)	> 0.9	0.29		Base Anchorage
61. Reactor Bldg. 670 - Pressurizing Pumps and Degassing Tank		Flexible	—	> 0.5[c]		
62. Reactor Bldg. 670				> 0.5[c]		Equipment fragility is reported under Item 20.
63. Reactor Bldg. Superstructure		Flexible	1.6	0.38		
64. Reactor Vessel			1.49	0.60		Based on past PRAs

FOIA Exemption 3 UCNI, Exemption 7f - table columns giving equipment items and loctions

a. Eide et al. 1991.

b. Bottom Head Firewater Injection System (BHFIS); Diesel/Commercial (D/C); Diesel Generator (DG); High Confidence Low Probability of Failure (HCLPF); Firewater (FW); Firewater Injection System (FIS); Fuel Oil (FO); Low-pressure Deminerizated water (LDW); Loss of Coolant Accident (LOCA); Solenoid valve (SV); Switchgear (SG); Upper Vessel Firewater Injection System (UVFIS); Vessel Vent System (VVS).

c. Median capacity judged greater than 2.0 g for this component based on a walkdown review and median response factors.

Table 3.9-12. Performance characteristics of the safety-rod system.[a]

System characteristic	Data
Stroke	36 in.
Bite (normal poison position with rods cocked)	3 in. inserted
Withdrawal rate	9.0 in./min
Scram release time	22 msec (pressurized mode) 29 msec (depressurized mode)
Scram time (including release time), first 12 in. of travel:	
Three-primary-pump operation Two-primary-pump operation	150 msec 170 msec
Scram time (open head operation), first 12 in. of travel:	300 msec
Life expectancy	10 yr
Number of operable rods	Up to 6
Location	Flux-trap baffles surrounding the inpile tubes, dummy inpile tubes, or irradiation facilities
Poison section	Four 80-degree hafnium sector inserts 1/4 in. × 36 in.
Drive type	Rack and pinion with quick-release electromagnetic clutch
Drive motor	
Type	Double-worm reduction
Capacity	1/4 hp
Shaft speed	1725/850 rpm
Torque output	280 to 300 ft-lb

a. deBoisblanc and Cohen 1965.

Table 3.9-13. Performance characteristics of the OSCC system.[a]

System characteristic	Data
Location	Beryllium reflector
Length of hafnium poison insert	46 in.
Configuration	Beryllium cylinders with120-degree poison inserts
Poison inserts	0.250-in.-thick hafnium
Control cylinder speed	0.055 rpm (20.0 degree/min)
Control cylinder travel	160 degree (0 degree full-in and 160 degree full-out)
Drive type	Right-angle worm and wheel
Drive motor	
Type	Instant reversing, 3-phase induction
Number of revolutions	20.33 (max)
Shaft speed	2.2 rpm
Torque clutch	40 ft-lb (max)
Seal	Rotary face type
Number of operable OSCC	16 (4 per quadrant)
Number of drives	8 (2 per quadrant)

a. deBoisblanc and Cohen 1965.

Table 3.9-14. Summary of loading parameters for reactor internals.[a]

Component	Loading parameters	Total stress (psi)
Flux-trap baffles	Material: 6061-T6 aluminum tubing Allowable stress at 200°F: 9,500 psi	Mechanical and thermal Core ΔP=100: 5,550 Core ΔP=140: 5,890
Core reflector tank	Material: 6061-T652 aluminum Minimum yield strength: 33,000 psi	Hoop stress Core ΔP=140: 24,334 psi[b]
Reflector support tank	Material: SG 70A-T71 (A356-T71) aluminum casting Minimum yield strength: 18,000 psi Allowable stress at 200°F: 6,200 psi	Hydraulic and mechanical Core ΔP=140: 4,175
Flow distribution tank	Material: Type 304L stainless steel Design stress intensity at 200°F: 16,600 psi Allowable alternating stress intensity for 7,000 cycles: 65,000 psi	Membrane and bending Core ΔP=100: 35,660 Core ΔP=140: 49,930
Core support tank	Material: Type 304L stainless steel Design stress intensity at 200°F: 16,600 psi Yield strength: 21,300 psi	Mechanical and thermal Core ΔP=140: 3,400 psi

a. Hanson 1976.
b. Burr 1977.

CHAPTER 3 - DESIGN OF STRUCTURES COMPONENTS, EQUIPMENT, AND SYSTEMS - UPGRADED FINAL SAFETY ANALYSIS REPORT FOR THE ADVANCED TEST REACTOR	**Identifier:** SAR-153 **Revision:** 10 **Page:** 3-157 of 3-200 **Effective Date:** 08/10/04

CHAPTER 3 - DESIGN OF STRUCTURES COMPONENTS, EQUIPMENT, AND SYSTEMS - UPGRADED FINAL SAFETY ANALYSIS REPORT FOR THE ADVANCED TEST REACTOR	**Identifier:** SAR-153 **Revision:** 10 **Page:** 3-158 of 3-200 **Effective Date:** 08/10/04

CHAPTER 3 - DESIGN OF STRUCTURES COMPONENTS, EQUIPMENT, AND SYSTEMS - UPGRADED FINAL SAFETY ANALYSIS REPORT FOR THE ADVANCED TEST REACTOR	**Identifier:** SAR-153 **Revision:** 10 **Page:** 3-159 of 3-200 **Effective Date:** 08/10/04

CHAPTER 3 - DESIGN OF STRUCTURES COMPONENTS, EQUIPMENT, AND SYSTEMS - UPGRADED FINAL SAFETY ANALYSIS REPORT FOR THE ADVANCED TEST REACTOR	**Identifier:** SAR-153 **Revision:** 10 **Page:** 3-160 of 3-200 **Effective Date:** 08/10/04

CHAPTER 3 - DESIGN OF STRUCTURES COMPONENTS, EQUIPMENT, AND SYSTEMS - UPGRADED FINAL SAFETY ANALYSIS REPORT FOR THE ADVANCED TEST REACTOR	**Identifier:** SAR-153 **Revision:** 10 **Page:** 3-161 of 3-200 **Effective Date:** 08/10/04

FOIA Exemption 3 UCNI, Exemption 7f (Page 3-157 – 3-168 – detailed reactor drawings)

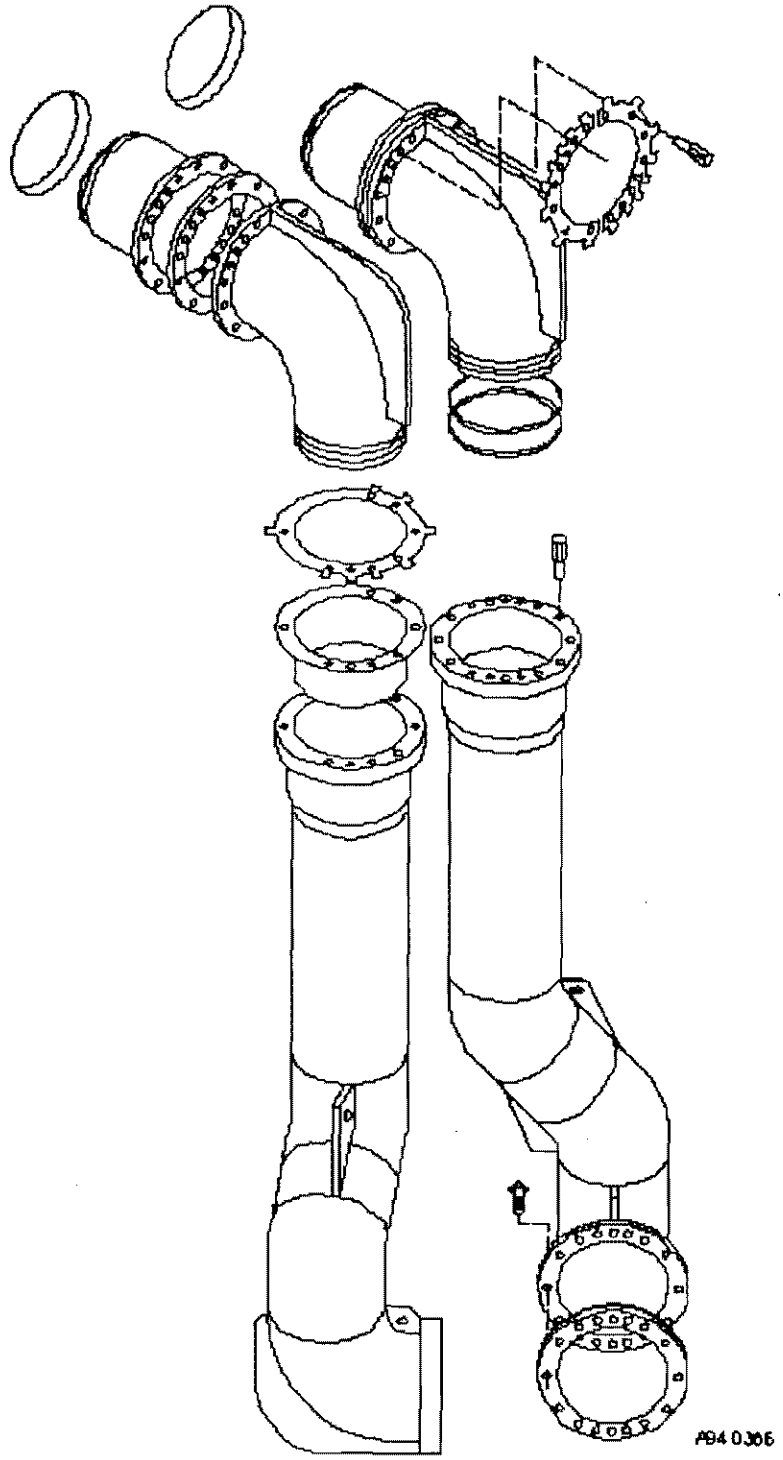

Figure 3.9-13. Outlet-flow pipes. **(For Information Only)**

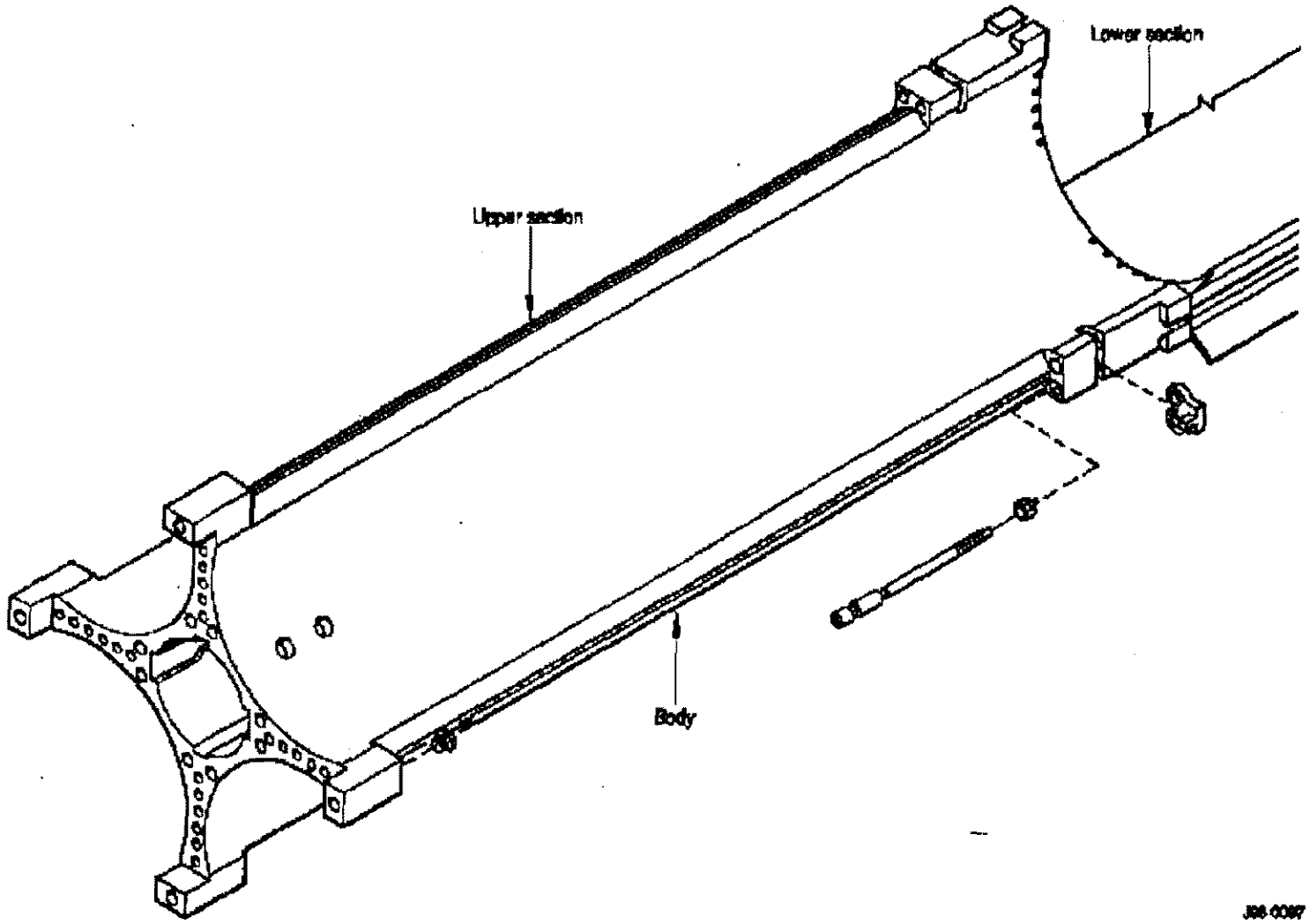

Figure 3.9-14. Neck shim rod housing assembly (EG&G Idaho 1983). **(For Information Only)**

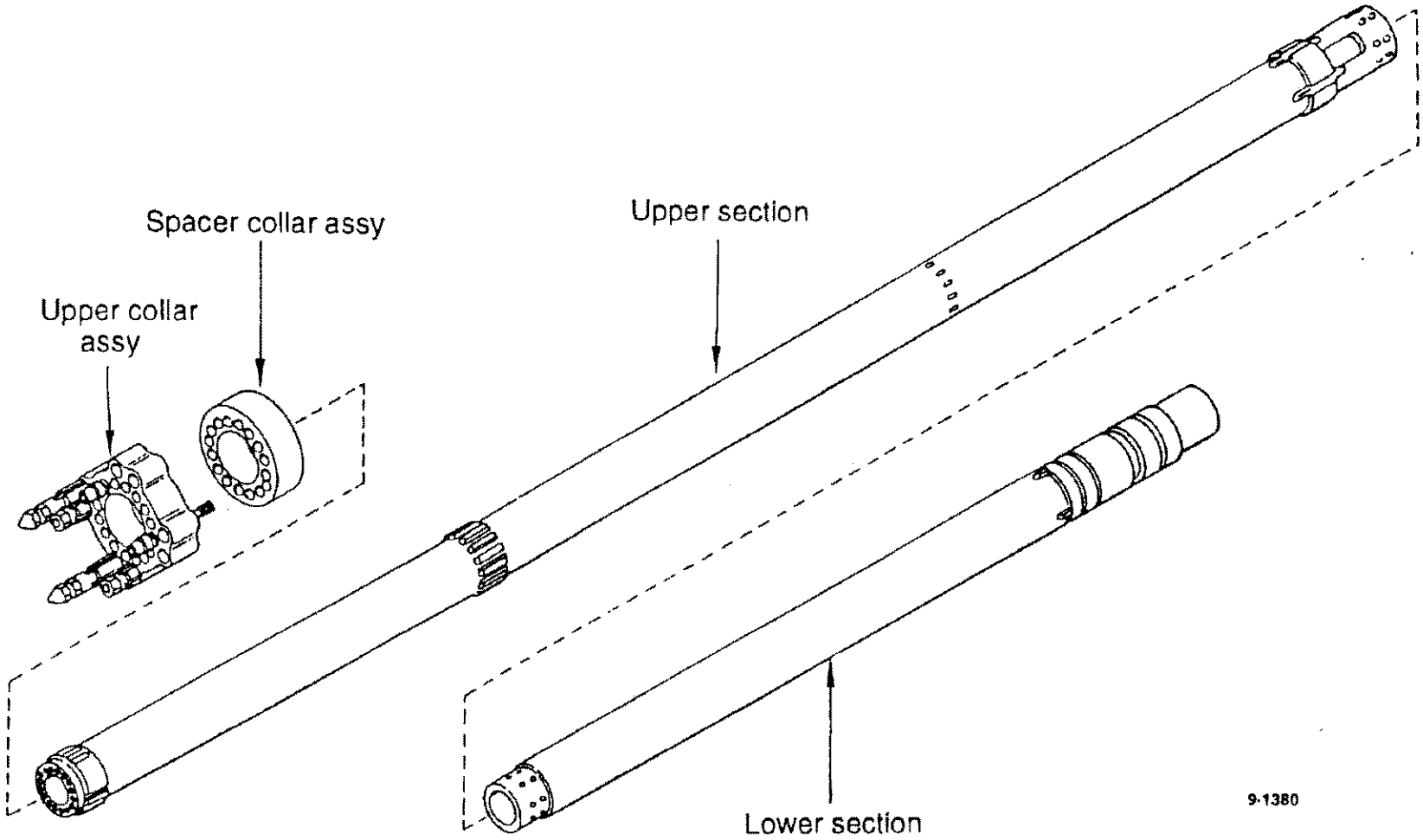

Figure 3.9-15. Center flux trap baffle and N-16 assembly (EG&G Idaho 1983). **(For Information Only)**

FOIA Exemption 3 UCNI, Exemption 7f (Page 3-172 – detailed reactor drawing)

3.10 Seismic Qualification of Seismic Category I Instrumentation and Electrical Equipment

The ATR was designed with nuclear-, process-, and radiation-monitoring instrumentation to permit safe reactor operation under normal and abnormal conditions. Automatic control of reactor power is provided, and automatic corrective and safety actions prevent hazardous conditions from developing. Several independent electrical systems are provided for the ATR to ensure that power sources are available under any credible condition.

Seismic Category I instrumentation and electrical equipment are found in the following safety-related systems:

- Reactor Shutdown System (RSS)
- Engineered Safety Features (ESF)
- Safety Rod System
- Reactivity Control System
- Primary Coolant System
- Electrical power system
- Control complex.

The Seismic Category I components and structural elements whose supports have been seismically qualified are listed by system grouping according to Gorman (1988) as follows:

- PCS piping and related components, including heat-exchanger and surge-tank supports
- Standard and 1A & 1D inpile tube systems and components
- Reactor vessel
- Emergency Firewater Injection System
- Battery racks and equipment anchorage
- Electrical power system
- Control complex.

The location of Seismic Category I instrumentation and electrical equipment may be identified through the use of these two lists. Appendix A is the list of Seismic Category I components and structural elements.

3.10.1 Seismic Qualification Criteria

The ATR was designed in the early 1960s and completed in 1967. The original PCS underwent some major modifications and upgrades after preoperational tests. The ATR began operating in 1969. The original seismic-design criterion used for the ATR was the 1961 Uniform Building Code (UBC) Seismic Zone 2 (ICBO 1961). The code included seismic provisions for buildings, but had no seismic requirements for equipment. As a result, the original seismic Category I instrumentation and electrical equipment were designed and installed without explicit seismic-qualification criteria.

In 1968 and 1969, industry standards were developed that stated that design bases for PPS electrical equipment must include credible single events such as earthquakes. These standards included IEEE (1969a), AEC (1969), and IEEE (1969b). In 1971, site-specific seismic-hazard studies were performed from which a SSE was defined. These standards and studies have provided the basis for seismic-design upgrades in 1971 and for the seismic-design upgrade program plan in 1973. The latter program was established to evaluate all critical SSC required for safe shutdown and maintenance should an SSE affect ATR.

Recent specifications (EG&G Idaho 1992) have invoked IEEE-344 as the governing criteria for seismic qualification (IEEE 1975). IEEE-344 was originally published in 1971. Revisions were issued in 1975 and 1987 (IEEE 1987). The extent of the application of IEEE-344 as the governing criteria for seismic qualification of active electrical and mechanical equipment at the ATR is uncertain. For example, the seismic qualification of the PPS was removed from the original construction specifications (Burr 1992). However, documentation is available to support qualification of the Rosemount transmitters and the PPS Cabinets that enclose the transmitters, which are included as part of the PPS (Burr 1992; Richins 1992).

3.10.2 Methods and Procedures for Qualifying Electrical Equipment and Instrumentation

AEC (1974) allows the use of both analytical and test methods for use in qualifying electrical equipment and instrumentation. AEC (1974) specifies that the minimum requirements of IEEE Standard 344 be used when testing procedures are followed. In addition, analytical methods acceptable for use as qualification documents are provided.

In 1973, a seismic-design upgrade program plan (Gorman 1973) was established to evaluate all critical SSC required for safe shutdown during the SSE. The evaluation was performed using the SSE specified in Gorman (1972). These criteria were discussed in Section 3.7.1. Evaluation of equipment in this program was conducted either by the seismic-analysis methods described in Section 3.7.3, or by test procedures described in IEEE Standard 344 (IEEE 1975).

3.10.3 Methods and Procedures of Analysis or Testing of Supports of Electrical Equipment and Instrumentation

In general, the methods and procedures used in qualifying Seismic Category I equipment supports are documented in Gorman (1972). The original plant was designed to the UBC (ICBO 1961). Supports were analyzed for the additional lateral loads as prescribed by UBC (ICBO 1961). Since the original design, the seismic design requirements for the ATR have undergone several revisions. Section 3.7.1 documents these revisions. For component supports, which were part of the seismic design upgrade plan (Gorman 1973), response spectra analyses have been conducted following the procedures outlined in Section 3.7.3. Systems whose supports have been seismically qualified to date are listed in Section 3.10.

3.10.4 Operating License Review

3.10.4.1 Operational Readiness Reviews. Operational readiness reviews and periodic safety reviews are conducted in accordance with company procedures. Safety reviews are performed upon completion of modifications made to facilities and equipment having safety significance, design upgrade, or system change. Chapter 13 (Management, Organization, and Institutional Safety Provisions) describes the review process.

3.10.4.2 Seismic-Qualification Results. The seismic-design upgrade program of SSC required for safe shutdown began in 1973. It included the evaluation of miscellaneous equipment such as battery racks and anchorage of equipment. Gorman (1988) reports that appropriate modifications were identified, where needed, to bring equipment items within acceptable limits. As of 1988, such modifications were completed.

Burr (1992) reports results for the PPS cabinets and transmitters. Cabinets evaluated by static equivalent seismic analysis indicate low cabinet stresses, but bolt stresses exceed AISC allowables. Review of the Rosemount Transmitter Qualification Report indicated that the transmitters and attachment brackets were properly qualified in accordance with IEEE-344 (Burr 1992).

In 1989, a PRA was performed (Eide, Khericha, and Thatcher 1989). This assessment included walkdowns and evaluation of Seismic Category I instrumentation and electrical equipment. One key result of this assessment was the determination of HCLPF accelerations for equipment items. The HCLPF acceleration is an indicator of the equipment seismic capacity, and is defined as the level of acceleration at which there is high confidence (e.g., 95%) of a low probability (e.g., < 5%) of failure. Although the use of HCLPF accelerations or fragility analyses are not used to qualify equipment items, an HCLPF acceleration that exceeds the design-basis peak ground acceleration indicates seismic ruggedness.

Table 3.10-1 summarizes the fragility parameters developed for ATR equipment. The table identifies the equipment by location and component identifier along with the equipment characteristics and failure mode. Also present are the associated median peak ground acceleration capacity (A_m, 50% probability) and the HCLPF acceleration capacity for each component. Components that were effectively screened out from detailed fragility evaluation are denoted in the table by > 2.0 in the A_m column or by > 0.5 in the HCLPF Capacity column. The majority of these components were screened out based on walkdown observations, median response factors, and historical performance of equipment and structures during earthquakes.

Anchorage of the electrical equipment reviewed during the PRA was inconsistent (Eide, Khericha, and Thatcher 1989). The majority of the motor-control centers (MCCs), switchgear, transformers, and panels observed during the walkdown were marginally anchored or unanchored. Consequently, numerous fragility estimates were based on component sliding or overturning. Significant variability arises because of the nonlinear behavior for this type of failure mode. For example, a sliding failure can affect equipment function by severing cabling that connects to the bus connections at the base of the cabinet. Earthquake-experience data have shown that moving even fractions of an inch can sever a cable. The low fragility estimates presented in Table 3.10-1 reflect the high uncertainty for this type of failure mode.

Table 3.10-1 is based on the PRA (Eide, Khericha, and Thatcher 1991); since the time that the PRA was issued, seismic modifications to some of the listed equipment have been completed or are in progress. The completed modifications are listed in the footnotes to Table 3.10-1. With completion of the seismic modifications, the median peak ground acceleration capacity for the affected equipment is judged to be greater than 2.0 g. To avoid inconsistency between the UFSAR and its reference documentation, Table 3.10-1 will not be revised until the PRA is revised since the table is based directly on the information in the PRA. The seismic equipment upgrades assumed in the PRA analysis that are not completed or in progress are entered the Reactor Program's (RP) internal tracking system. The upgrades are assigned a priority and will be addressed accordingly.

Table 3.10-1. Ground-acceleration capacities of ATR electrical equipment and instrumentation.[a]

	Equipment item	Location	Component identifier	Equipment characteristics	Median capacity A_m (g)	HCLPF[b] capacity (g)	Failure mode	Comments
1.	Utility UPS[b] Power Panel			Flexible (3- Hz)	1.01	0.30	Rack bolting	Supported on same rack as Item 670-E-117. See note d.
2.	Utility UPS Power Panel			Flexible (10-16 Hz)	> 2.0[c]	—	Base anchorage	
3.	Utility UPS Power Panel			Flexible (10-16 Hz)	> 2.0[c]	—	Base anchorage	
4.	Utility U Power P			3-4 Hz)	1.01	0.30	Rack bolting	Supported on same rack as Item 670-E-115. See note d.
5.	Utility DC Battery Bank			Flexible (15-20 Hz)	> 2.0[c]	—	Base anchorage	
6.	Utility DC Battery Bank			Flexible (15-20 Hz)	> 2.0[c]	—	Base anchorage	
7.	32Vdc PPS[b] Battery Bank			Flexible (10-16 Hz)	0.49	0.17	Functional	Battery cells are lead/ antimony. Fragility is based on generic test data.
8.	32Vdc PPS Battery Bank			Flexible (10-16 Hz)	0.49	0.17	Functional	Battery cells are lead/ antimony. Fragility is based on generic test data.
9.	Battery Charger			Flexible (4-8 Hz)	0.15	0.05	Overturning	Charger is unanchored and attached to unanchored Panel E-103. See note d.
10.	250V Utility dc			Flexible (4-8 Hz)	0.15	0.05	Overturning	DC bus is attached to unanchored Panel E-103. See note d.

FOIA Exemption 3 UCNI, Exemption 7f -- table columns giving equipment and locations

Table 3.10-1. (continued).

	Equipment item	Location	Component identifier	Equipment characteristics	Median capacity A_m (g)	HCLPF[b] capacity (g)	Failure mode	Comments
11.	250V dc S.G.[b] Control Panel			Flexible (4-8 Hz)	0.15	0.05	Overturning	DC bus is attached to unanchored Panel E-103. See note d.
12.	250V Utility dc			Flexible (4-8 Hz)	0.15	0.05		DC bus is attached to Panel E-23, which is attached to unanchored Panel E-103. See note d.
13.	32 D				> 2.0[c]	—		
14.	32V dc Distribution			Flexible (> 20 Hz)	> 2.0[c]	—		
15.	120/208V ac Bus			Flexible (> 20 Hz)	> 2.0[c]	—		
16.	ATR-608 C/D[b] 480V ac Bus			Flexible (4-8 Hz)	0.15	0.08	Overturning	MCC[b] is unanchored.
17.	ATR-674 C/D 480V ac Bus			Flexible (4-8 Hz)	0.23	0.10	Overturning	Cabinet is marginally anchored.
18.	ATR-674 C/D 120/208V Bus			Flexible (2.5-4 Hz)	0.42	0.19	Rocking	Deflection of bldg. siding controls failure.
19.	ATR-674 Transformer			Flexible (4-8 Hz)	0.42	0.15	Anchorage	Transformer is marginally anchored.
20.	ATR-670 C/D 480V ac Bus			Flexible (4-8 Hz)	> 2.0[c]	—	Anchorage	

FOIA Exemption 3 UCNI, Exemption 7f -- table columns giving equipment items, locations and component identifiers

Table 3.10-1. (continued).

	Equipment item	Location	Component identifier	Equipment characteristics	Median capacity A_m (g)	HCLPF[b] capacity (g)	Failure mode	Comments
21.	ATR-670 Diesel 4.1kV ac Bus			Flexible (10-26 Hz)	0.26	0.08	Sliding	S. G. sections are marginally anchored.
22.	ATR-670 Diesel 480V ac Bus			Flexible (10-16 Hz)	0.26	0.08	Sliding	Bus sections are marginally anchored. See note d.
23.	ATR-6 2.4kV ac Bus				0.26	0.08	Sliding	Bus sections are marginally anchored.
24.	ATR-609 Diesel 480V ac Bus			Flexible (4-8 Hz)	0.15	0.08	Overturning	MCC is unanchored.
25.	ATR-609 C/D 480V ac Bus			Flexible (4-8 Hz)	0.15	0.08	Overturning	MCC is unanchored.
26.	ATR-619 Diesel 2.4kV ac Bus			Flexible (10-16 Hz)	0.26	0.08	Sliding	Bus sections are marginally anchored.
27.	Diesel Generator Cntrl Panel			Flexible (10-16 Hz)	> 2.0[c]	—	Anchorage	
28.	FW Pump Starting Batteries			Rigid (> 30 Hz)	0.23	0.13	Sliding	Batteries and racks are unanchored. See note d.
29.	FW Pump Starting Batteries			Rigid (> 30 Hz)	0.23	0.13	Sliding	Batteries and racks are unanchored. See note d.

FOIA Exemption 3 UCNI, Exemption 7f -- table columns giving equipment items, locations and component identifiers

Table 3.10-1. (continued).

	Equipment item	Location	Component identifier	Equipment characteristics	Median capacity A_m (g)	HCLPF[b] capacity (g)	Failure mode	Comments
30.	FW Pump			Flexible (10-16 Hz)	1.48	0.51	Base anchorage	
31.	FW Pump			Flexible (10-16 Hz)	1.19	0.50	Anchor bolt bending	
32.	[redacted]			[redacted]Hz)	1.48	0.51	Base anchorage	
33.	Instrument air line			Flexible Piping	> 2.0[c]	—	Supports	Fragility is based on a piping sample review and experience data.
34.	Emergency Pump Panel			Flexible (4-8 Hz)	0.15	0.05	Overturning	Anchorage problems with panels associated with 670-M-11 electrical power (670-E-28, 670-E-26, 670-E-105, 670-E-103). See note d.

FOIA Exemption 3 UCNI, Exemption 7f -- table columns giving equipment items, locations and component identifiers

a. Eide, Khericha, and Thatcher 1991.

b. C/D - commercial/diesel

HCLPF - high confidence low probability of failure

MCC - motor control center

PPS - Plant Protective System

S.G. - switch gear

UPS - uninterruptible power supply

c. Median capacity judged greater than 2.0 g for this component based on a walkdown review and median response factors.

d. The recommended seismic upgrades have been completed per the facility modification procedures. The median acceleration capacity is judged to be greater than 2.0 g.

3.11 Environmental Design of Mechanical and Electrical Equipment

The ATR was designed, constructed, and placed in operation before specific equipment-qualification guidance was available. As part of the ongoing process to adopt current criteria and requirements at ATR, an equipment-qualification program was formulated based on rigorous criteria and requirements currently applied to commercial nuclear power plants. Documented equipment-qualification requirements for DOE reactors are in DOE Order 5480.4, which defines both mandatory requirements and non-mandatory (but appropriate) standard practices (DOE 1993). These practices are based on commercial nuclear power reactor standards and are described in lower-tiered, acceptable-practice documents such as NRC Regulatory Guides, Standard Review Plans (SRPs), and ASME and IEEE standards.

At the top of the hierarchy of the NRC's equipment qualification requirements is 10 CFR 50, Appendix A (CFR 1999), General Design Criteria. Criterion 4 of this Appendix requires that certain systems and components be designed to operate under environmental conditions which could exist during postulated accidents. For electrical equipment, Criterion 4 is implemented by 10 CFR 50.49 (CFR 2001). The application of 10 CFR 50.49 to the ATR Control Room is discussed in Section 3.1.2.10. This regulation is expanded and clarified in NUREG-0588 (NRC 1981h) and Regulatory Guide 1.89 (NRC 1984). SRP 3.11 (NRC 1987) extends these guidelines to active mechanical equipment. The methodology in the ATR Equipment Qualification Report (Slaughterbeck et al. 1992) was adopted from Appendix E of Regulatory Guide 1.89 (NRC 1984).

3.11.1 Equipment Identification and Environmental Conditions

A list of ATR equipment subject to qualification has been prepared following the commercial nuclear power practice of selecting safety-related equipment inside confinement for the equipment-qualification process (Slaughterbeck et al. 1992). This work is the first step in an engineering qualification process that generates and maintains evidence that the required safety-related equipment can meet or exceed performance requirements on demand while being subjected to normal environments, anticipated operational transient environments, and accident environments. After determining which equipment is subject to qualification, an assessment of performance requirements, service conditions, qualification requirements and design requirements is performed to define the specification for equipment qualification.

This assessment encompasses

- The determination of all equipment subject to qualification and the functional requirements of this equipment
- A preliminary determination of accident service conditions including environmental extremes for specific equipment.

Environmental parameters considered include pressure, temperature, humidity, radiation dose, and submergence.

Safety-related electrical and mechanical equipment that is required to survive and function under environmental conditions resulting from either a LOCA or a CLOFA inside confinement must be environmentally qualified. Equipment failure is allowed after safety functions have been performed. For ATR, equipment selected for further qualifications must meet all three of the following criteria:

- The equipment is safety-related. Safety-related equipment is identified in Appendix A.
- The equipment is located inside, or forms part of, the confinement boundary. Equipment outside of the boundary is not considered to be exposed to accident environments. (Equipment locations were determined from System Design Descriptions, engineering drawings, discussions with plant personnel, and a plant tour.)
- The equipment is classified as electrical or active mechanical. All electrical equipment and active mechanical components are considered to be susceptible to failure in accident environments. Excluded under this criterion are passive normal reactor internals, pipes, vessels, supports, and building structures. All pumps and valves are considered to be active components for this screening process.

The resultant equipment subset comprises all safety-related electrical and active mechanical equipment inside the confinement boundary; this equipment is subject to further screening to determine whether the equipment must be environmentally qualified.

For each item of equipment subject to the above three criteria, data sheets are prepared that include the item's equipment number, description, manufacturer, location, pertinent references, and information on environmental conditions. All equipment is classified into one of four categories based on the designation and guidance of Regulatory Guide 1.89, Appendix E (NRC 1984). Table 3.11-1 summarizes the equipment qualification screening methodology of Regulatory Guide 1.89 (NRC 1984). Because the RSS[a] is designed with triple redundancy (i.e., components performing similar functions located in physically separate areas), reactor scram was assumed to have been completed before the RSS or safety-rod components experience accident environments. The remaining equipment items were screened to include Categories 3.a and 3.b. Category 3.a consists of equipment that is exposed to an accident environment and must function to mitigate the accident. Category 3.b consists of equipment that is exposed to an accident environment in which it need not function, but must not fail in a manner detrimental to plant safety (Slaughterbeck et al. 1992).

To determine the environmental envelope for Category 3.a and 3.b equipment, locations were correlated with calculated environmental conditions based on existing accident simulations performed with the MELCOR computer program (Summers et al. 1991; Kelly 1988). Environmental conditions for equipment qualification range from those experienced during normal and abnormal plant operation to those experienced in accident scenarios as defined in assessments of CLOFAs and LOCAs. The environmental conditions reported on the equipment-qualification data sheets are bounding (worst-case) conditions calculated to occur for either the CLOFA or the LOCA, whichever is the more severe for each environmental parameter. These conditions are representative of those determined from the PRA (Atkinson and Thatcher 1994), the original SAR (deBoisblanc and Cohen 1965), and supporting documentation.

---

[a]. The RSS comprises instrument subsystems and logic that cause the release of safety rods. For the purpose of the UFSAR descriptions, the Safety-Rod System is consider a separate system; see Chapter 7 (Instrumentation and Controls) for further discussion.

The master list of safety-related equipment and structures is in Appendix A to this chapter. Certain safety-related SSC are relied upon during or following design-basis events to ensure (a) the integrity of the reactor coolant pressure boundary, (b) the capability to shut down the reactor and maintain it in a safe shutdown condition, and (c) the capability to prevent or mitigate the consequences of accidents that result in potential offsite exposures comparable to the 10 CFR 100 (CFR 1977) guidelines. The term "safety-related" is a broad designation that includes PPS SSCs and non-PPS SSCs. The PPS includes the RSS, and ESF. Appendix A is organized by SSC categories as follows:

- PPS
  - ESF
    - Emergency Firewater Injection System
    - PCS overpressure relief system
    - Radiation Monitoring and Seal System
    - Vessel Vent System
    - LOCA Primary Coolant Pump Shutoff System
  - RSS
- Non-PPS safety-related SSC
  - Safety-rod system
  - Buildings and miscellaneous structures and components
  - Control complex
  - Electrical power system
  - Firewater system
  - Fuel storage and handling
  - Low-pressure demineralized water system.
  - Primary coolant system
  - Reactivity control system
  - Reactor core and internals.

3.11.2 Qualification Tests and Analyses

The PPS within the confinement structure was environmentally qualified to AEC Reactor Development and Technology (RDT) standards at the time of installation. Further review of environmental qualification was performed as part of the ATR Equipment Qualification Program (Slaughterbeck et al. 1992).

The safety-related systems or equipment required after reactor shutdown for design-basis events are (a) VVS, (b) EFIS, (c) emergency coolant pump (30 minutes), (d) confinement, (e) firewater canal makeup to the canal irradiated fuel element storage area, (f) canal bulkheads (Chapman 1995), and (g) LOCA Primary Coolant Pump Shutoff System (until fuel element cooling time is met or until less than two primary cooling pumps are operating). Of these systems, only the EFIS and confinement could experience abnormal conditions (that is, conditions other than those experienced during routine operation). The other safety-related systems and equipment required after a design basis event shutdown would experience environment conditions that are enveloped by their design requirements.

In the event of a LOCA, the EFIS electronics could flood. Except for the vessel liquid-level transmitters, the flooding would occur at approximately the same elevation as the top of the core. The most probable occurrence would be a loss of power to the EFIS, in which case the valves would fail open and the EFIS would continue to flood the reactor building. The least probable occurrence is a false signal to the EFIS actuators that would cause the EFIS valves to close. The core damage frequency, however, of such an occurrence is less than 1.0×10^{-7}/yr.

Also in the event of LOCA that causes flooding, the exhaust air dampers could be submerged. The water pressure could open these dampers; however, the water would form a seal that would block an air flow path out of the confinement.

3.11.3 Loss of Ventilation

The control room is located inside the confinement. The air-treatment unit HVA-2 system supplies the reactor control room. If the stack-monitoring system indicates high radioactivity, the ventilation system to the control room is shut down automatically by closing the HVA-2 butterfly dampers on the control room's air-supply and -return ducts, thereby stopping the HVA-2 fan. Habitability of the control room is maintained during normal operation, and also while operating during incidents that do not breach the fuel cladding or produce levels of airborne activity high enough to require evacuation. If an evacuation were required, reactor scram would be initiated and the control room evacuated. Long-term occupancy of the control room is not necessary to ensure a safe shutdown. The ATR was not designed to require operators to remain in the control room in the event of an emergency. Therefore, the requirement to ensure adequate protection for control-room operators and safe plant operation or shutdown is not applicable to ATR.

3.11.4 Estimated Chemical and Radiation Environment

An evaluation by analyses of irradiation embrittlement of the reactor vessel has been completed. The analyses include calculations in accordance with the procedures called out in Regulatory Guide 1.99 (NRC 1988). However, results from commercial reactor experience do not apply a priori to ATR since the data pertain to low-alloy carbon steels, while the reactor vessel is of Type 304 stainless steel. A program to irradiate samples of the vessel's base-metal, weld-metal, and heat-affected-zone metal materials has been initiated. The specimens can be tested at various fluences to quantify the degree of conservatism in the analyses. It is intended that the irradiation program compensate for the lack of archive and surveillance samples. The program is substantially in agreement with the principles and intent of ASTM 185-82.

The ATR is not subject to the acute vessel embrittlement that occurred at the High-Flux Isotope Reactor (HFIR). An analysis was performed for operating the vessel through the year 2014 (Durney et al. 1987). The analysis shows that neutron embrittlement is not currently a concern and will not be significant over that period.

The ATR Aging and Evaluation and Life Extension Program did not indicate a vulnerability of the reactor vessel supports to radiation embrittlement. The vessel supports are under compression, and are far removed from the beltline region of the vessel. The neutron fluence is well below the damage threshold.

Table 3.11-1. NRC Regulatory Guide 1.89 requirements for equipment qualification.

Regulatory Guide 1.89 Category	Criteria	Qualification requirement	Information required on data sheet
3.a	Equipment that will experience the environmental conditions of accidents through which it must function to mitigate such accidents.	Equipment must be qualified to demonstrate operability in the accident environment for the time required for accident mitigation with safety margin to failure.	- Functional requirement - Environmental envelope - Time safety function is required
3.b	Equipment that will experience the environmental conditions of accidents through which it need not function for mitigation of such accidents but through which it must not fail in a manner detrimental to plant safety or accident mitigation.	Equipment must be qualified to demonstrate the capability to withstand any accident environment for the time during which it must not fail with margin to failure.	- Functional requirement - Environmental envelope - Time safety function is required - Technical basis justifying placement in this category
3.c	Equipment that will experience the environmental conditions of accidents through which it need not function for mitigation of such accidents and whose failure (in any mode) is deemed not detrimental to plant safety or accident mitigation.	Equipment need not be qualified for any accident environment.	- Technical basis justifying placement in this category
3.d	Equipment that has performed its safety function prior to the exposure to an accident environment and whose failure (in any mode) is deemed not detrimental to plant safety and will not mislead the operator.	Equipment need not be qualified for any accident environment.	- Functional requirement - Technical basis justifying placement in this category

3.12 Effects of Volcanism upon Structures

Chapter 2 (Site Characteristics) discusses the potential effects of future volcanism on INEEL and ATR. The most significant volcanic hazard to INEEL and ATR is that basaltic lava flows from nearby volcanic-rift zones could inundate or cause burning of facilities. Basaltic eruptions are characterized primarily by the quiet extrusion of lava that may travel miles. Basaltic flows are controlled by topography and will travel downslope. The ATR site is located downslope from the Axial Volcanic Zone (AVZ) and the Arco volcanic-rift zone, which has exhibited multiple volcanic flows per episode and a 3,000-year mean interval between flows (Kuntz 1978; Kuntz et al. 1980).

The shortest recurrence intervals between episodes of multiple flow of basaltic volcanism is estimated to be 8,000 to 15,000 years. Available data of INEEL basalt lava flows suggest minimum (most conservative) volcanic-recurrence intervals of 10^{-4} to 10^{-5}/yr for the AVZ, and the Arco and Lava Ridge-Hells Half Acre volcanic-rift zones. Therefore, the probabilistic risk of basalt-lava inundation or intrusion-related ground disturbance is estimated to be $< 10^{-5}$/yr for ATR and other sites on the southern INEEL, which represent a small area of the potentially affected region contiguous to the rift zones. The significant impact from other volcanic phenomena, such as growth of new rhyolite domes on the Eastern Snake River Plain (ESRP) or tephra (ash) falls thicker than 3.1 in. from non-ESRP vents, has an estimated probability of $< 10^{-5}$/yr because of the combined effects of great distance, infrequency, low volume, and topographic or atmospheric barriers to the dispersal of tephra on the INEEL.

A significant related hazard is disruption of facilities resulting from ground deformation accompanying magma intrusion along volcanic-rift zones: opening of fissures, normal faulting, and broad-region tilting and uplift within several kilometers of vents. Other, less significant basaltic hazards include volcanic-gas emission and disruption of groundwater.

Design-basis criteria for volcanic activity have not been established for the INEEL. Further, since no mechanism exists to prevent lava from reaching the ATR, it must be assumed that lava could conceivably reach the buildings. However, without a refined analysis, the probability of (or extent of) building damage cannot be stated. With respect to safety at INEEL, a microseismic network covering the region has been in place and augmented since 1971 (Jackson et al. 1993). With this network, any renewed volcanic activity (sensed as microseismic vibration activity) on or near INEEL can be detected and its location ascertained months to years before any impending danger to INEEL facilities. Hence, ATR will have more than sufficient time to shut down and, depending on time estimated for any possible encroachment, remove all the fuel and ship it to a safe location. Within this context, the estimated total annual frequency of ATR fuel damage due to lava inundation was 8.4×10^{-8} (Hackett and Khericha 1993).

3.13 References

ACI, 1963, *Building Code Requirements for Reinforced Concrete*, American Concrete Institute, Ann Arbor, MI.

AEC, 1963, *Nuclear Reactors and Earthquakes*, TID-7024, Prepared by Lockheed Aircraft Corporation and Holmes and Narver, Inc., U. S. Atomic Energy Commission, Washington, D.C., August 1963.

AEC, 1969, *Supplementary Criteria and Requirements for RDT Reactor Plant Protection Systems*, Standard RDT C.16-1T, Division of Reactor Development and Technology, U.S. Atomic Energy Commission, Washington, D.C., December 1969. (Inactivated)

AEC, 1974, *Seismic Requirements for Design of Nuclear Power Plants and Test Facilities*, Standard RDT-F9-2T, U.S. Atomic Energy Commission, January 1974. (Historical)

AISC, 1969, *Specification for the Design, Fabrication, and Erection of Steel Buildings*, American Institute of Steel Construction, New York, NY.

AISC, 1980, *Manual of Steel Construction*, 8th Edition, American Institute of Steel Construction, New York, NY.

Anderson, E. C., Sr., 1994, Letter to W. W. Gay III, ECA-27-94, *Seismic Upgrades*, EG&G Idaho, Inc., June 17, 1994.

ANSI, 1988, *Nuclear Safety Criteria for the Design of Stationary Pressurized Water Reactor Plants*, ANSI/ANS-51.1-1983 (reaffirmed 1988), American National Standards Institute, American Nuclear Society, La Grange Park, IL.

Arendts, J. G., 1989a, *Analysis of ATR Reactor Building for Extreme Wind Loads*, EDF TRA-ATR-338, EG&G Idaho, Inc., August 24, 1989.

Arendts, J. G., 1989b, *Evaluation of TRA Water Storage Tanks for Wind Loading*, EDF TRA-ATR-340, EG&G Idaho, Inc., August 28, 1989.

ASME, 1955a, *American Standard Building Code Requirements for Minimum Design Loads in Buildings and Other Structures*, ASA-A58.1-1955, American Standards Association, American Society of Mechanical Engineers, New York, NY.

ASME, 1955b, *Code for Pressure Piping*, ASA B31.1-1955 American Society of Mechanical Engineers, New York, NY.

ASME, 1977, *Nuclear Power Plant Components, ASME Boiler and Pressure Vessel Code*, Section III, 1977 Edition, American Society of Mechanical Engineers, New York, NY.

ASME, 1980a, *Power Piping*, ANSI/ASME B31.1, American Society of Mechanical Engineers, 1980 edition.

ASME, 1980b, *Nuclear Power Plant Components, ASME Boiler and Pressure Vessel Code*, Section III, Division I, Subsections NB and NC, 1980 Edition, Winter 1980 Addenda.

ASME, 1986, *Nuclear Power Plant Components, ASME Boiler and Pressure Vessel Code*, Section III, Division I, Subsections NB, ND, and NF, 1986 Edition, Winter 1986 Addenda.

ASME, 1989a, *Quality Assurance Program Requirements for Nuclear Facilities*, NQA-1American Society of Mechanical Engineers, New York, N.Y., September 15, 1989. (historical)

ASME, 1989b, *Rules for Inservice Inspection of Nuclear Power Plant Components, ASME Boiler and Pressure Vessel Code*, Section XI, American Society of Mechanical Engineers, New York, NY.

ASME, 1989c, *Pressure Vessels, ASME Boiler and Pressure Vessel Code*, Section VIII, American Society of Mechanical Engineers, New York, New York, 1989.

ASME, 1990, *Nuclear Power Plant Components, Class 1 Components, ASME Boiler and Pressure Vessel Code*, Section III, Division I, Subsections NB and NF, 1990 Edition.

ASME, 1997, *Quality Assurance Program Requirements for Nuclear Facilities*, NQA-1, American Society of Mechanical Engineers, December 31, 1997.

Atkinson, S. A., 1976, *ATR Containment Failure Potential During an ATR Accident*, TR-808, Aerojet Nuclear Co., March 25, 1976.

Atkinson, S. A., 1988, *ATR Safety Basis Summary*, PG-T-88-011, EG&G Idaho, Inc., September, 1988.

Atkinson, S. A., 1995, *ATR Consequences Assessment for a Hypothetical Mackay Dam Failure*, EDF TRA-ATR-964, LMITCO, April 17, 1995.

Atkinson, S. A., 1997, *ATR Seismic Shutdown Basis*, EDF TRA-ATR-1189, LMITCO, June 3, 1997.

Atkinson, S. A. and T. A. Thatcher, 1994, *Level 1, 2, and 3 Advanced Test Reactor Probabilistic Risk Assessment Summary Report*, EGG-PRP-11232, EG&G Idaho, Inc., May 1994.

AWWA, 1979, *AWWA Standard for Welded Steel Tanks for Water Storage*, ANSI/AWWA D100-79 (AWS D5.2-79), American Water Works Association, Denver, CO, November 1979.

Bennett, C. M., 1986, *Capacity of the Diversion Channel Below the Flood- Control Dam on the Big Lost River at the Idaho National Engineering Laboratory, Idaho*, United States Geological Survey Water-Resources Investigations Report 86-4204, DOE/ID-22071, U.S. Department of Energy, Idaho Operations Office, Idaho Falls, ID, October 1986.

Bennett, C. M., 1990, *Streamflow Losses and Ground-water Level Changes along the Big Lost River at the Idaho National Engineering Laboratory, Idaho*, United States Geological Survey Water-Resources Investigations Report 90-4067, DOE/ID-22091, U.S. Department of Energy, Idaho Operations Office, Idaho Falls, ID, April 1990.

Blandford, R. K., 1991, *Preliminary ATR Seismic Category 1 Listing and Component Seismic Qualification Status*, EDF TRA-ATR-535, July 26, 1991.

Bragassa, P. W., and R. F. Lippert, 2000, "TRA-719A and 719B Raw Water Storage Tank Upgrade – Structural/Seismic Analysis Verfication," EDF TRA-ATR-1577/EDF-0721, April 27, 2000.

Brower, J. O., 2001, FY 95 Fire and Life Safety Improvements Project Phase IV – New Firewater Tank and Pumphouse, *Seismic and Natural Phenomena Qualification for TRA-781 and TRA-688*, EDF TRA-ATR-1756, October 24, 2001.

Buescher, B. J., 1993, *Strategic Evaluation Program Safety Issues Review*, EDF TRA-ATR-826, EG&G Idaho, Inc., November 18, 1993.

Buescher, B. J., and R. VanderBeek, 1997, *ATR Systems Required to Remain Functional after a Safe Shutdown Earthquake*, EDF TRA-ATR-1174, LMITCO, January 28, 1997.

Burr, T. K., 1977, Letter to H. J. Reilly, *Loads and Stresses in ATR Gear Box Support Beam and Core Reflector Tank*, TKB-20-77, EG&G Idaho, Inc., November 3, 1977.

Burr, T. K., 1987, Letter to D. R. Mousseau, *ATR Confinement Area Design*, TKB-19-87, EG&G Idaho, Inc., September 9, 1987.

Burr, T. K., 1992, Letter to R. S. Anderson, *Seismic Qualification of ATR-PPS Cabinets*, TKB-13-92, EG&G Idaho, Inc., July 13, 1992.

Call, V. B., 1986, *Analysis of the ATR Firewater Piping System due to Modifications of the ATR Building Penetration*, EPM-A-86-037, EG&G Idaho, Inc., November 1986.

CFR, 1977, *Seismic and Geologic Siting Criteria for Nuclear Power Plants*, 10 CFR 100, Appendix A, *Code of Federal Regulations*, Office of Federal Register, January 10, 1977.

CFR, 1999, *General Design Criteria for Nuclear Power Plants*, 10 CFR 50, Appendix A, *Code of Federal Regulations*, Office of Federal Register, December 23, 1999.

CFR, 2001, *Environmental Qualification of Electric Equipment Important to Safety for Nuclear Power Plants*, 10 CFR 50.49, *Code of Federal Regulations*, Office of Federal Register, December 14, 2001.

CFR, 2002a, *Quality Assurance Requirements*, 10 CFR 830, Subpart A, *Code of Federal Regulations*, Office of Federal Register, February 4, 2002.

CFR, 2002b, Safety Basis Requirements, 10 CFR 830, Subpart B, *Code of Federal Regulations*, Office of the Federal Register, February 4, 2002.

Chapman, J. C., 1995, *Equipment Qualification—Safety-Related Equipment Required after Reactor Shutdown for Design Basis Events*, EDF TRA-ATR-1020, LMITCO, Idaho Falls, Idaho, April 10, 1995.

Close, J. A., 1988a, *ATR Hypothetical Accident Description*, PG-T-88-021, EG&G Idaho, Inc., September 1988.

Close, J. A., 1988b, *ATR Hydrogen Behavior and Confinement Performance*, PG-T-88-020, EG&G Idaho, Inc., September 1988.

Cluff, L. S., 1971, *Preliminary Seismic Risk Evaluation for the National Reactor Testing Station, Idaho*, Woodward-Lundgren & Associates, Project G-12389, for Idaho Nuclear Corporation, Construction Engineering Division, June 30, 1971.

Coats, D. W. and R. C. Murray, 1985, *Natural Phenomena Hazards Modeling Project: Extreme Wind/Tornado Hazard Models for Department of Energy Sites*, UCRL-53526, Revision 1, Lawrence Livermore National Laboratory, Livermore, CA, August 1985.

Companywide Manual, *Engineering and Research*.

Companywide Manual, *Quality and Requirements Management*.

Croucher, D. W., 1989, Letter to R. V. Furstenau, *Advanced Test Reactor General Design Criteria*, DWC-94-89, EG&G Idaho, Inc., September 29, 1989.

Davidson, R. F., 1975, *ATR Standard Loop Cubicle Seismic Analysis*, TR-656, Aerojet Nuclear Company, June 1975.

Davidson, R. F., 1976, *ATR Building Seismic Analysis*, RE-E-76-081, EG&G Idaho, Inc., December 1976.

Davidson, R. F., 1978, *ATR Reactor Vessel Seismic Analysis*, RE-A-78-038, EG&G Idaho, Inc., March 2, 1978.

Davidson, R. F., 1979, *ATR Primary Coolant System Piping Design Analysis*, RE-A-79-011, EG&G Idaho, Inc., January 22, 1979.

Davidson, R. F. and G. L. Thinnes, 1974, *ATR Primary Coolant System Seismic Analysis*, TR-570, Aerojet Nuclear Company, December 26, 1974.

deBoisblanc, D. R. and S. Cohen, 1965, *Safety Analysis Report Advanced Test Reactor*, IDO-17021, Phillips Petroleum Company, April 1965.

deBoisblanc, D. R., S. Cohen, and V. A. Walker, 1966, *Second Supplement Safety Analysis Report, Advanced Test Reactor*, PTR-781, Phillips Petroleum Company, April 1966.

deBoisblanc, D. R., and S. Cohen, 1967, *ATR Primary Coolant System Rework Digest for Safety Evaluation*, CI-1045, Idaho Nuclear Corporation, National Reactor Testing Station, June 1967.

Denton, H. R., 1981, Letter to Distribution, *Standard Definitions for Commonly-Used Safety Classification Terms*, Office of Nuclear Reactor Regulation, November 1981.

DOE, 1986, *Safety of Department Of Energy-Owned Nuclear Reactors*, Order 5480.6, U.S. Department of Energy, Washington, D.C., September 23, 1986. (Order cancelled)

DOE, 1993, *Environmental Protection, Safety, and Health Protection Standards*, Order 5480.4, Change 4, U.S. Department of Energy, Washington, D.C., January 7, 1993.

DOE, 1994, *Nuclear Safety Analysis Reports*, Order 5480.23 Change 1, U.S. Department of Energy, Washington D.C., March 10, 1994. (historical)

DOE, 1996a, *Natural Phenomena Hazards Design and Evaluation Criteria for Department of Energy Facilities*, DOE-STD-1020-94, Change 1, U.S. Department of Energy, Washington, D.C., January 1996. (historical)

DOE, 1996b, *Advanced Test Reactor Safety Evaluation Report*, U.S. Department of Energy, February 1996.

DOE, 2001a, *Nuclear Reactor Safety Design Criteria*, Order 5480.30 Change 1, U.S. Department of Energy, Washington, D.C., March 14, 2001. (historical)

DOE, 2001b, *Quality Assurance*, Order 414.1A, U.S. Department of Energy, Washington, D.C., Change 1, July 12, 2001.

DOE, 2002a, *Natural Phenomena Hazards Design and Evaluation Criteria for Department of Energy* Facilities, DOE STD-1020-2002, U.S. Department of Energy, Washington, D.C., January 2002.

DOE, 2002b, *Natural Phenomena Hazards Performance Categorization Criteria for Structures, Systems, and Components*, DOE STD-1021-93, Change 1, U.S. Department of Energy, Washington, D.C., April 2002.

DOE-ID, 1996, *DOE-ID Architectural Engineering Standards*, Revision 19, U.S. Department of Energy, Idaho Operation Office, Idaho Falls, Idaho, September 1996. (historical)

DOE-ID, 2002, *DOE-ID Architectural Engineering Standards*, Revision 29, U.S. Department of Energy, Idaho Operations Office, Idaho Falls, Idaho, September 2002.

Durney, J. L., 1988, *ATR Shutdown Assurance*, PG-T-88-012, EG&G Idaho, Inc., July 1, 1988.

Durney, J. L., et al., 1987, *ATR Vessel Lifetime and Primary Coolant System IGCSS Assessment*, PG-T-87-009, EG&G Idaho, Inc., December 1987.

Ebasco, 1961, *ATR Specification for Steel Reinforcement and Steel Insert Material*, Specification S-6, Ebasco Services, Inc., New York, NY, June 22, 1961.

Ebasco, 1962, *ATR Specification for Structural Steel*, Specification S-10, Revision 4, Ebasco Services, Inc., New York, NY, September 24, 1962.

Ebasco, 1963, *ATR Specification for the Core Support Assembly*, Specification M-102, Revision 1, Ebasco Services, Inc., New York, NY, March 14, 1963.

Ebasco, 1964a, *Design Manual for the Advanced Test Reactor*, Volume 20, Ebasco Services, Inc., New York, NY, in conjunction with Babcock & Wilcox Company, Lynchburg, VA.

Ebasco, 1964b, *ATR Specification for Masonry*, Specification A-3, Revision 3, Ebasco Services, Inc., New York, NY, June 18, 1964.

EG&G Idaho, 1983, *ATR Reactor Configuration Management and Indentured Parts List - Mechanical*, October 28, 1983.

EG&G Idaho, 1986, *ATR Stack Exhaust Radiation Monitoring Subsystem of the Containment Isolation System, System Design Description for the ATR Plant Protection System (PPS)*, SDD 7.7.4, February 14, 1986.

EG&G Idaho, 1987, *ATR Primary Coolant System ASME Section III Class I, Relief Valves SF-A-71 and SF-A-72*, Specification ES-50972, Revision C, EG&G Idaho, Inc., December 21, 1987.

EG&G Idaho, 1988a, *ATR Primary Pressurizing Pump ASME Section III Class 2 Relief Valves SF-A-75 and SF-A-76*, Specification ES-50974, Revision A, EG&G Idaho, Inc., June 6, 1988.

EG&G Idaho, 1988b, *ATR Vessel Vent System, System Design Description for the ATR Reactor Vessel System*, SDD 7.1.6, September 30, 1988.

EG&G Idaho, 1992, *ATR Nuclear Qualified Class 1E Pressure Transmitters*, Specification ES-51463, EG&G Idaho, Inc., April 2, 1992.

Eide, S. A., S. T. Khericha, and T. A. Thatcher, 1989, *Advanced Test Reactor Probabilistic Risk Assessment, Appendix O - Seismic Risk Analysis*, EGG-PRP-8823, EG&G Idaho, Inc., December 1989.

Eide, S. A., S. T. Khericha, and T. A. Thatcher, 1991, *Advanced Test Reactor Probabilistic Risk Assessment*, EGG-PRP-8823, Rev. 1, , EG&G Idaho, Inc., September 1991.

EQE, 1991, *EQE Quality Assurance Manual*, Revision 2, November 1991.

Fershtut, S. and G. Holman, 1989, *ATR Primary Coolant System Design Specification for Modifications*, PR-T-78-003, Rev. 6, EG&G Idaho, Inc., May 1989.

Fors, R. M., 1982, *Stress Analysis of the MTR 719 Raw Water Tanks*, PR-T-82-019, EG&G Idaho, Inc., August 1982.

Goodell, R. A., 1985, Letter to R. L. Rolfe, GO-9-85, *AWWA Evaluation of ATR Raw Water Storage Tanks for Seismic Load Conditions*, EG&G Idaho, Inc., November 6, 1985.

Gorman, V. W., 1972, *TRA Seismic Analysis Method & Design Evaluation Input*, A-196/TR-336, Aerojet Nuclear Co., November 15, 1972.

Gorman, V. W., 1973, *Proposal and Estimate for Seismic Analysis of Advanced Test Reactor*, TR-403, Aerojet Nuclear Co., June 14, 1973.

Gorman, V. W., 1974, Letter to D. R. Mousseau, VWG-9-74, *Soil-Structure Interaction at ATR*, Aerojet Nuclear Co., November 11, 1974.

Gorman, V. W., 1980, Letter to F. E. Cerven, VWG-3-80, *Reevaluation of W10x66 Column and Crane Rail in ATR Building*, EG&G Idaho, Inc., July 24, 1980.

Gorman, V. W., 1985, *TRA Overhead Water Storage Tank Support Tower Tornado Analysis*, PG-T-85-004, EG&G Idaho, Inc., February 1985.

Gorman, V. W., 1986a, *Seismic Analysis of TRA Overhead Water Storage Tank Support Tower*, PG-T-86-010, EG&G Idaho, Inc., September 1986.

Gorman, V. W., 1986b, Letter to R. L. Rolfe, VWG-03-86, *TRA Firewater Seismic Upgrade*, EG&G Idaho, Inc., August 28, 1986.

Gorman, V. W., 1988, *ATR Seismic Safety Basis*, PG-T-88-026, EG&G Idaho, Inc., July 1988.

Gorman, V. W., 1989a, *Analysis of ATR Reactor Building and Water Storage Tank for Wind-Borne Missile Impact*, EDF TRA-ATR-337, EG&G Idaho, Inc., August 24, 1989.

Gorman, V. W., 1989b, *Recommended Interim Safe Shutdown Earthquake Criteria for ATR*, PG-T-89-012, EG&G Idaho, Inc., May 1989.

Gorman, V. W, R. C. Guenzler, and C. A. Moore, 1976, *Soil-Structure Interaction Study of ETR Facility*, RE-E-76-059, EG&G Idaho, Inc., November 4, 1976.

Guenzler, R. C., 1992, Letter to E. C. Anderson, Sr., *ATR Canal Crane Under Seismic Loads*, RCG-17-92, EG&G Idaho, Inc., April 24, 1992.

Hackett, W. R. and S. T. Khericha, 1993, *Probabilistic Volcanic-Risk Assessment for the Test Reactor Area*, EDF TRA-ATR-804, EG&G Idaho, Inc., September 30, 1993. (Also contained in Appendix U in Update to the ATR Probabilistic Risk Assessment Level 1, 2, and 3, EGG-PRP-11229, May 1994.)

Hanson, G. H., 1976, *ATR Core Structural Components: Stresses Resulting from High-Flow Accidents*, TR-710, Aerojet Nuclear Co., January 8, 1976.

Harris, B. L., 1988, *Design Report for the ATR Vessel Vent System*, PG-T-88-006, Rev. 1, EG&G Idaho, Inc., March 28, 1988.

Harris, B. L., 1989, *Stress Analysis of the ATR Primary Coolant System Stub-In Branch Connections*, PG-T-89-013, EG&G Idaho, Inc., May 1989.

Harris, B. L., and T. K. Burr, 1989, *Detailed Stress Analysis of the ATR PCS Non-Standard Eccentric Reducers*, PG-T-89-017, EG&G Idaho, Inc., May 1989.

Holman, G. W., 1988, Letter to D. R. Mousseau, *Review of the ATR Canal Fuel Storage Racks*, GWH-04-88, February 2, 1988.

House, R. K., 1992, *Bases for Designation of Safety-Related Equipment in the ATR*, PG-T-92-114, EG&G Idaho, Inc., July 1992.

House, W. E., 1995, *Stress Analysis Summary of the ATR Reactor Coolant System*, EDF TRA-ATR-873, EG&G Idaho, Inc., February 9, 1995.

IBC, 2000, International Building Code.

ICBO, 1961, *Uniform Building Code Standards*, International Conference of Building Officials, 1961 Edition, Whittier, CA.

ICBO, 1973, *Uniform Building Code Standards*, International Conference of Building Officials, 1973 Edition, Whittier, CA.

IEEE, 1969a, *Proposed IEEE Criteria for Nuclear Power Plant Protection Systems*, IEEE 279, Institute of Electrical and Electronics Engineers, New York, NY.

IEEE, 1969b, *Proposed IEEE Criteria for Class 1E Electrical Systems for Nuclear Power Generating Stations, Committee Report on Work in Progress by the IEEE Nuclear Science Group, K Technical Committee of Standards*, Institute of Electrical and Electronic Engineers, New York, NY, June 1969.

IEEE, 1975, *IEEE Recommended Practice for Seismic Qualification of Class 1E Equipment for Nuclear Power Generating Stations*, IEEE 344-1975, Institute of Electrical and Electronics Engineers, New York, NY.

IEEE, 1987, *IEEE Recommended Practices for Seismic Qualification of Class 1E Equipment for Nuclear Power Generating Stations*, IEEE 344-1987, Institute of Electrical and Electronics Engineers, New York, NY.

INEEL 2000, *ATR Reactor Shutdown System, System Design Description for the ATR Plant Protection System (PPS)*, SDD-7.7.2, October 5, 2000.

INEEL, 2002, "ATR Inservice Inspection Plan Third Inspection Interval June 1994 to May 2004 (PLN-859)," Rev. 4, October 15, 2002.

INEEL 2003, *ATR Emergency Firewater Injection System, System Design Description for the ATR Plant Protection System (PPS)*, SDD-7.7.1, Rev. 3, December 8, 2003.

Jackson, S. M., et al., 1991a, *INEL Seismograph Stations Annual Report January 1 - December 31, 1990*, EGG-G-001, EG&G Idaho, Inc., September 1991.

Jackson, et al., 1991b, *Strong Ground Motion Data Recorded at the Idaho National Engineering Laboratory During the 1983 Borah Peak, Idaho Earthquake*, EGG-BG-9249, EG&G Idaho, Inc., June 1991.

Jackson, S. M., et al., 1993, *Contemporary Seismicity in the Eastern Snake River Plain, Idaho, Based on Microearthquake Monitoring, Bulletin of the Seismological Society of America, 83*, No. 3, June 1993, pp. 680-695.

Kelly, J. E., 1988, *Advances in MELCOR Modeling and Analysis, Transactions of the Sixteenth Water Reactor Safety Information Meeting*, NUREG/CP-0096, October 1988.

Koslow, K. N. and D. H. Van Haaften, 1986, *Flood Routing Analysis for a Failure of Mackay Dam*, EGG-EP-7184, EG&G Idaho, Inc., June 1986.

Kuntz, M. A., 1978, *Geology of the Arco-Big Southern Butte Area, Eastern Snake River Plain, and Potential Volcanic Hazards to the Radioactive Waste Management Complex and Other Waste Storage and Reactor Facilities at the Idaho National Engineering Laboratory, Idaho*, U.S. Geological Survey Open-File Report 78-691.

Kuntz, M. A., et al., 1980, *An Evaluation of Potential Volcanic Hazards at the Radioactive Waste Management Complex, Idaho National Engineering Laboratory, Idaho*, U.S. Geological Survey Open-File Report 80-388.

Lippert, R. F., 1997, "TRA Raw Water Storage System Upgrade, Evaluation of Modified Raw Water Storage Tanks to Current Seismic and Wind Criteria," EFF TRA-ATR-1227, March 5, 1997.

Lucas, D. S., 2000, *ATR Confinement Building Leak Rate Calculations*, EDF TRA-ATR-1543, Rev. 1, July 11, 2000.

Manoli, R. E., 1968, *Advanced Test Reactor Internals Vibration Summary*, BAW-1322, Babcock and Wilcox Company, Prepared for EBASCO Services, Inc., Submitted to AEC, May 1968.

Manos, G. C., 1986, *Earthquake Tank-Wall Stability of Unanchored Tanks*, *Journal of Structural Engineering*, American Society of Civil Engineers, Vol. 112, No. 8, August 1986, pp. 1863-1880.

Maulde, H. E., 1969, *Geologic Investigation of Faulting Near the National Reactor Testing Station. U.S. Geological Survey draft report.*

Miller, C. L. and C. Y. Yuan, 1986, *Design Report for the ATR Fire Water Redundant Line*, PR-T-83-001, Rev. 1, EG&G Idaho, Inc., August 28, 1986.

Miller, G. K., 1978, *Seismic Analysis of the ATR Firewater Piping*, RE-A-78-207, EG&G Idaho, Inc., September 1978.

Miller, G. K., 1980, *Seismic Analysis of the ATR Storage Canal*, PR-T-80-048, EG&G Idaho, Inc., August 1980.

Miller, G. K., 1987, *A Structural Analysis of the ATR Drop Tube and Cylindrical Course Weldment*, PG-T-87-007, EG&G Idaho, Inc., August 1987.

Miller, G. K., 1988, *Detailed Stress Analysis of the ATR PCS 36x14-in. Elbow-Branch Connection*, PG-T-88-038, EG&G Idaho, Inc., December 1988.

Miller, G. K., 1989a, *Stress Analysis of the ATR PCS 36x6-in. and 16x10-in. Elbow-Branch Connection*, PG-T-89-002, EG&G Idaho, Inc., May 1989.

Miller, G. K., 1989b, *Detailed Stress Analysis of the ATR PCS 30-in. Pipe Cap with 10-in. Stub-In Pipe and Evaluation of 30x20-in. Concentric Reducers*. PG-T-89-005, EG&G Idaho, Inc., May 1989.

Miller, G. K., 1989c, *Detailed Stress Analysis of the 36-in. Short-Radius Elbows in the Primary Coolant System*, PG-T-89-006, EG&G Idaho, Inc., May 1989.

Miller, G. K., 1992, Letter to J. L. Durney, *Seismic Evaluation of ATR Storage Canal*, GKM-4-92, EG&G Idaho, Inc., April 17, 1992.

Mousseau, D. R., 1973, Letter to L.F. Burdge, *ATR Seismic Analysis Program Plan*, Mou-27-73, EG&G Idaho, Inc., June 14, 1973.

Newmark, N. M. and W. J. Hall, 1978, *Development of Criteria for Seismic Review of Selected Nuclear Power Plants*, NUREG/CR-0098, NRC, May 1978.

NRC, 1973a, *Damping Values for Seismic Design of Nuclear Power Plants*, Nuclear Regulatory Guide 1.61, U.S. Atomic Energy Commission, October 1973.

NRC, 1973b, *Design Response Spectra for Seismic Design of Nuclear Power Plants*, Regulatory Guide 1.60, Revision 1, U.S. Nuclear Regulatory Commission, Washington, D.C., December 1973.

NRC, 1974a, *Design Basis Tornado for Nuclear Power Plants*, Regulatory Guide 1.76, U.S. Nuclear Regulatory Commission, Washington, D.C., April 1974.

NRC, 1974b, *Instrumentation for Earthquakes*, Nuclear Regulatory Guide 1.12, Rev. 1, U.S. Atomic Energy Commission, April 1974.

NRC, 1976, *Quality Group Classifications and Standards for Water-, Steam-, and Radioactive-Waste-Containing Components of Nuclear Power Plants*, Regulatory Guide 1.26, Rev. 3, U.S. Nuclear Regulatory Commission, Washington, D.C., February 1976.

NRC, 1978a, *Standard Format and Content of Safety Analysis Reports for Nuclear Power Plants*, Regulatory Guide 1.70, Rev. 3, U.S. Nuclear Regulatory Commission, Washington, D.C., November 1978.

NRC, 1978b, *Seismic Design Classification*, Regulatory Guide 1.29, U.S. Nuclear Regulatory Commission, Washington, D.C., September 1978.

NRC, 1978c, *Tornado Design Classification*, Regulatory Guide 1.117, U.S. Nuclear Regulatory Commission, Washington, D.C., April 1978.

NRC, 1981a, *Guidelines for Control Room Design Reviews*, NUREG-0700, U.S. Nuclear Regulatory Commission, Washington, D.C., September 1981.

NRC, 1981b, *Tornado Loadings*, SRP Section 3.3.2, Rev. 2, NUREG-0800, U.S. Nuclear Regulatory Commission, Washington, D.C., July 1981.

NRC, 1981c, *Missiles Generated by Natural Phenomena*, SRP Section 3.5.1.4, Rev. 2, NUREG-0800, U.S. Nuclear Regulatory Commission, Washington, D.C., July 1981.

NRC, 1981d, *Evaluation of Potential Accidents*, SRP Section 2.2.3, Rev. 2, NUREG-0800, U.S. Nuclear Regulatory Commission, Washington, D.C., July 1981.

NRC, 1981e, *Determination of Rupture Locations and Dynamic Effects Associated with the Postulated Rupture of Piping*, SRP Section 3.6.2, Rev. 1, NUREG-0800, U.S. Nuclear Regulatory Commission, Washington, D.C., July 1981.

NRC, 1981f, *Plant Design for Protection Against Postulated Piping Failures in Fluid Systems Outside Containment*, SRP Section 3.6.1, Rev. 1, NUREG-0800, U.S. Nuclear Regulatory Commission, Washington, D.C., July 1981.

NRC, 1981g, *Standard Review Plan for Other Seismic Category I Structures* (Section 3.8.4), Rev. 1, NUREG-0800, U.S. Nuclear Regulatory Commission, Washington D.C., July 1981.

NRC, 1981h, *NRC Interim Staff Position on Environmental Qualifications of Safety-Related Electrical Equipment*, NUREG-0588, Revision 1, U.S. Nuclear Regulatory Commission, Washington, D.C., July 1981.

NRC, 1982, *Supplement 1 - Requirements for Emergency Response Capability*, (Generic Letter No. 82-33), NUREG-0737, U.S. Nuclear Regulatory Commission, Washington D.C., December 17, 1982.

NRC, 1984, *Environmental Qualification of Certain Electric Equipment Important to Safety for Nuclear Power Plants*, Regulatory Guide 1.89, Rev. 1, U.S. Nuclear Regulatory Commission, Washington, D.C., June 1984.

NRC, 1987, *Environmental Qualification of Mechanical and Electrical Equipment*, Section 3.11, Revision 2, SRP for the Review of Safety Analysis Reports for Nuclear Power Plants, LWR Edition, NUREG-0800, U.S. Nuclear Regulatory Commission, Washington, D.C., June 1987.

NRC, 1988, *Radiation Embrittlement of Reactor Vessel Materials*, Regulatory Guide 1.99, Rev. 2, U.S. Nuclear Regulatory Commission, Washington, D.C., May 1988.

Rahl, T. E., 1994, letter to S. W. Shepherd, "AWWA/ASCE 4-86 Evaluation of ATR Raw Water Storage Tanks for Seismic Load Conditions," TER-13-94, August 25, 1994.

Richins, W. D., 1992, *Seismic Evaluation of ATR-PPS Cabinets and Equipment; Instrument Cabinet No's 151A, 151B, 151C, 152A, 152B, 152C*, EDF TRA-ATR-726, EG&G Idaho, Inc., October 5, 1992.

Schnabel, P. B., J. Lysmer, and H. Bolton, 1972, *SHAKE: A Computer Program for Earthquake Response Analysis of Horizontally Layered Sites*, Report EERC 72-12, Earthquake Engineering Research Center, University of California, Berkeley, CA, December 1972.

Siemer, J. M., 1981, Letter to R. L. Rolfe, JMS-04-81, *Seismic Analysis of ATR and MTR Buried Piping*, EG&G Idaho, Inc., May 28, 1981.

Siemer, J. M., 1982a, *Stress Analysis of Above-Ground Water TRA Firewater Piping*, PR-T-82-016, EG&G Idaho, Inc., July 1982.

Siemer, J. M., 1982b, *Stress Analysis of TRA Overhead Water Storage Tank Support Tower*, PR-T-82-020, EG&G Idaho, Inc., August 1982.

Slaughterbeck, D. C., et al., 1992, *ATR Equipment Qualification: Selection of Safety-Related Equipment and the Determination of Environmental Conditions*, PG-T-92-118, EG&G Idaho, Inc., September 1992.

Snow, S. D., 1991a, *ASME Section VIII Stress Analysis ATR Primary Surge Tank With Seismic Supports*, PG-T-91-037, EG&G Idaho, Inc., October 1991.

Snow, S. D., 1991b, *Seismic Analysis of Remote Processing Unit Cabinet for ATR*, EDF TRA-ATR-606, EG&G Idaho, Inc., December 6, 1991.

Snow, S. D., 1992a, *Seismic Analysis of the ATR Operator Console*, EDF TRA-ATR-625, EG&G Idaho, Inc., January 30, 1992.

Snow, S. D., 1992b, *Seismic Analysis of Process Control System Remote Processing Unit Cabinet for ATR*, EDF TRA-ATR-680, EG&G Idaho, Inc., June 11, 1992.

Snow, S. D., 1993, *ATR PCS Surge Tank Support Analysis*, EDF TRA-ATR-764, EG&G Idaho, Inc., March 15, 1993.

Snow, S. D., 1994a, *ATR PCS Surge Tank Seismic Supports, Anchor Evaluations*, EDF TRA-ATR-1003, EG&G Idaho, Inc., August 19, 1994.

Snow, S. D., 1994b, *Seismic Analysis of Transmitter Cabinets for ATR*, EDF TRA-ATR-608, Rev. 2, EG&G Idaho, Inc., May 10, 1994.

Snow, S.D., 2001, *Design Report for the ATR Firewater Redundant Line and the ATR Vessel Vent and Relief Systems*, EDF TRA-ATR-1208 Rev. 1, June 28, 2001.

Snow, S. D., and M. B. Hendrickson, 1996, *Analysis of the Complete ATR Firewater Piping System*, PG-T-90-016, Rev. 2, LMITCO, August 1996.

Steinbrugge, K. V. and D. F. Moran, 1955, *Earthquake Damage to Elevated Water Tanks, Earthquakes in Kern County California During 1952*, Division of Mines Bulletin 171, State of California, San Francisco, November 1955.

Summers, R. M., et al., 1991, *MELCOR 1.8.0: A Computer Code for Nuclear Reactor Severe Accident Source Term and Risk Assessment Analyses*, NUREG/CR-5531, SAND90-0364, Sandia National Laboratories, Albuquerque, NM, January 1991.

Thatcher, T.A., 2000a, *Evaluation of ATR Safety-Related & Risk Significant Equipment Location Dependent Vulnerability*, EDF-TRA-ATR-1564, September 2000.

Thatcher, T.A., 2000b, *Comparison of Postulated Fire Events in the ATR Building*, EDF TRA-ATR-1610 November 16, 2000.

Thinnes, G. L., 1989, *Structural Analysis of the ATR PCS 24x18 in. Y-Lateral Piping Component*, PG-T-89-014, May 1989.

Wadkins, R. P., 1988, *ATR Loss of Coolant Accidents*, PG-T-88-017, EG&G Idaho, Inc., July 1, 1988.

Welding Research Council, 1984, *Technical Position on Piping Installation Tolerances and Technical Position on Damping Values for Insulated Pipe - Summary Report*, WRC Bulletin 316 (Supplement to WRC Bulletin 300), New York, NY, July 1984.

Wong, H. L., and J. E. Luco, 1980, *Soil Structure Interaction: a Linear Continuum Mechanics Approach (CLASSI)*, Report CE, Dept. of Civil Engineering, University of Southern California, Los Angeles, CA.

Yuan, C. Y., 1983, Letter to K. H. Latham, CYY-04-83, *Review of Design Reports for ATR Fire Water Line Valves*, EG&G Idaho, Inc., July 29, 1983.

CHAPTER 3 APPENDIX A

MASTER LIST OF SAFETY-RELATED EQUIPMENT

FOIA Exemption 3 UCNI, Exemption 7f -- Appendix A, pp. 3A-1 through 3A-74 -- redacted in entirety -- master list of safety-related equipment

CHAPTER 4

REACTOR

INTENTIONALLY BLANK

CONTENTS

ACRONYMS/ABBREVIATIONS 4-10

4. REACTOR 4-12

4.1 Summary Description 4-13

4.2 Fuel Element and Reflector Design 4-15

4.2.1 Design Bases 4-15
4.2.2 Description and Design Drawings 4-22
4.2.3 Design Evaluation 4-25
4.2.4 Testing and Inspection 4-42

4.3 Nuclear Design 4-66

4.3.1 Design Bases 4-66
4.3.2 Description 4-69
4.3.3 Analytical Methods 4-94

4.4 Thermal and Hydraulic Design 4-143

4.4.1 Design Bases 4-143
4.4.2 Description of Thermal and Hydraulic Design of the Reactor Core 4-144
4.4.3 Description of the Thermal and Hydraulic Design of the Reactor Coolant System 4-152
4.4.4 Evaluation 4-153
4.4.5 Testing and Verification 4-161
4.4.6 Instrumentation Requirements 4-162

4.5 Reactor Materials 4-177

4.5.1 Control Element Drive System Structural Materials 4-177
4.5.2 Reactor Internal Materials 4-178

4.6 Functional Design of Reactivity Control Systems 4-182

4.6.1 Information for Control Element Drive Systems 4-182
4.6.2 Evaluations of the Reactivity Control Systems 4-182
4.6.3 Testing and Verification 4-183

4.7 References 4-184

FIGURES

4.2-1. Typical Advanced Test Reactor core cross-sectional diagram 4-50

4.2-1a. Advanced Test Reactor core cross-sectional diagram with ICE facility installed 4-51

4.2-1b. Representative ATR core plan view 4-52

4.2-2. Advanced Test Reactor core cutaway 4-53

4.2-3. Fuel element/core cutaway 4-54

4.2-4. Advanced Test Reactor fuel element 4-55

4.2-5. Fuel element assembly 4-56

4.2-6. Reflector block assembly, bottom view 4-56

4.2-7. Reflector block assembly, top view 4-57

4.2-8. Advanced Test Reactor beryllium reflector block ligaments 4-58

4.2-9. Reflector support tank assembly 4-59

4.2-10. Core reflector tank assembly 4-60

4.2-11. Lower alignment cup (typical) 4-61

4.2-12. Typical capsule facilities arrangement 4-62

4.2-13. Phase diagram of the uranium-aluminum system 4-63

4.2-14. Swelling of uranium aluminide fuel plates as a function of fission density 4-64

4.2-15. Blister temperatures of uranium aluminide fuel plates as a function of fission density 4-65

4.3-1. Consumption and buildup of U and Pu isotopes 4-112

4.3-2. Reactivity change due to boron in the fuel 4-113

4.3-3. Azimuthal power distribution in Fuel Element 9, 0 days exposure, 50/50 lobe power split, Plates 1-3 4-114

4.3-4. Azimuthal power distribution in Fuel Element 9, 0 days exposure, 50/50 lobe power split, Plates 5, 8, 11 4-114

4.3-5. Azimuthal power distribution in Fuel Element 9, 0 days exposure, 50/50 lobe power split, Plates 15-16 4-115

4.3-6. Azimuthal power distribution in Fuel Element 9, 0 days exposure, 50/50 lobe power split, Plates 17-19 4-115

4.3-7. Azimuthal power distribution in Fuel Element 9, 38 days exposure, 50/50 lobe power split, Plates 1-3 4-116

4.3-8. Azimuthal power distribution in Fuel Element 9, 38 days exposure, 50/50 lobe power split, Plates 5, 8, 11 4-116

4.3-9. Azimuthal power distribution in Fuel Element 9, 38 days exposure, 50/50 lobe power split, Plates 15-16 4-117

4.3-10. Azimuthal power distribution in Fuel Element 9, 38 days exposure, 50/50 lobe power split, Plates 17-19 4-117

4.3-11. Azimuthal power distribution in Fuel Element 23, 0 days exposure, 60/40 lobe power split, Plates 1-3 4-118

4.3-12. Azimuthal power distribution in Fuel Element 23, 0 days exposure, 60/40 lobe power split, Plates 5, 8, 11 4-118

4.3-13. Azimuthal power distribution in Fuel Element 23, 0 days exposure, 60/40 lobe power split, Plates 15-16 4-119

4.3-14. Azimuthal power distribution in Fuel Element 23, 0 days exposure, 60/40 lobe power split, Plates 17-19 4-119

4.3-15. Azimuthal power distribution in Fuel Element 23, 31 days exposure, 60/40 lobe power split, Plates 1-3 4-120

4.3-16. Azimuthal power distribution in Fuel Element 23, 31 days exposure, 60/40 lobe power split, Plates 5, 8, 11 4-120

4.3-17. Azimuthal power distribution in Fuel Element 23, 31 days exposure, 60/40 lobe power split, Plates 15-16 4-121

4.3-18. Azimuthal power distribution in Fuel Element 23, 31 days exposure, 60/40 lobe power split, Plates 17-19 4-121

4.3-19. Azimuthal power distribution in Fuel Element 18, 1 day exposure, Env 70 MW lobe power split, Plates 1-3 4-122

4.3-20. Azimuthal power distribution in Fuel Element 18, 1 day exposure, Env 70 MW lobe power split, Plates 5, 8, 11 4-122

4.3-21. Azimuthal power distribution in Fuel Element 18, 1 day exposure, Env 70 MW lobe power split, Plates 15-16 4-123

4.3-22. Azimuthal power distribution in Fuel Element 18, 1 day exposure, Env 70 MW lobe power split, Plates 17-19 4-123

4.3-23. Azimuthal power distribution in Fuel Element 18, 17 days exposure, Env 70 MW lobe power split, Plates 1-3 4-124

4.3-24. Azimuthal power distribution in Fuel Element 18, 17 days exposure, Env 70 MW lobe power split, Plates 5, 8, 11 4-124

4.3-25. Azimuthal power distribution in Fuel Element 18, 17 days exposure, Env 70 MW lobe power split, Plates 15-16 4-125

4.3-26. Azimuthal power distribution in Fuel Element 18, 17 days exposure, Env 70 MW lobe power split, Plates 17-19 4-125

4.3-27. Lobe and fuel element power comparisons at Day 0 for the 50/50 lobe power split 4-126

4.3-28. Lobe and fuel element power comparisons at Day 38 for the 50/50 lobe power split 4-127

4.3-29. Lobe and fuel element power comparisons at Day 0 for the 60/40 lobe power split 4-128

4.3-30. Lobe and fuel element power comparisons at Day 31 for the 60/40 lobe power split 4-129

4.3-31. Lobe and fuel element power comparisons at Day 0 for the enveloping 70 MW lobe power 4-130

4.3-32. Lobe and fuel element power comparisons at Day 17 for the enveloping 70 MW lobe power 4-131

4.3-33. Power factors in peak power Fuel Element Numbers 20 (beginning of cycle [BOC]) and 40 [end of cycle (EOC)] for the balanced 50/50 case 4-132

4.3-34. Power factors in peak power Fuel Element Number 23 for beginning of cycle (BOC) and end of cycle (EOC) for the nominal 60/40 case 4-133

4.3-35. Power factors in peak power Fuel Element Numbers 17 (end of cycle [EOC]) and 18 (beginning of cycle [BOC]) and for the enveloping 70 MW case 4-134

4.3-36. Plate 17 fuel temperature in Element Number 18 (100% power) 4-135

4.3-37. Nuclear instrumentation thimble positions 4-136

4.3-38. Cross sectional diagram of the Advanced Test Reactor core showing the N-16 monitor locations 4-1

4.3-39. N-16 center and outer sample tube assembly diagram 4

4.3-40. Relative worth of regulating rods versus rod position .....

4.3-41. Safety rod worth versus rod position .....

4.3-42. OSCC integral worth versus degrees withdrawn 4-141

4.3-43. Beryllium poison chains 4-142

4.4-1. Normalized mass flux and enthalpy rise distributions with three-pump operation for beginning of cycle enveloping 70 MW lobe power split 4-173

4.4-2. Normalized mass flux and enthalpy rise distributions with two-pump operation for beginning of cycle 60/40 MW lobe power split 4-174

4.4-3. Thermal conductivity of UAl_x + Al fuel 4-175

4.4-4. Thermal conductivity of 6061-0 aluminum cladding 4-175

4.4-5. Cross section of Advanced Test Reactor SINDA fuel plate model 4-176

4.5-1. ATR Reactor internal core support structure 4-181

TABLES

4.2-1. Advanced Test Reactor zone-loaded fuel element 7F: U-235 and B-10 nominal loadings 4-44

4.2-2. Fuel element materials, dimensions, and loadings 4-45

4.2-3. Fuel Element Historical Impurity Content 4-47

4.2-4. Boron Equivalents for Impurities in Uranium Aluminide Powder 4-48

4.2-5. Fuel elements confirmed by soak testing to be fission product leakers 4-49

4.3-1. Reactor core description 4-96

4.3-2. Fuel element loadings 4-98

4.3-3. Nominal nuclear parameters 4-98

4.3-4. Point-to-average power density for 50/50 lobe power split case 4-99

4.3-5. Point-to-average power density for 60/40 lobe power split case 4-99

4.3-6. Point-to-average power density for the enveloping 70 MW lobe power split case 4-99

4.3-7. Summary of shim positions for the 50/50 lobe power split PDQ analysis 4-100

4.3-8. Summary of shim positions for the 60/40 lobe power split PDQ analysis 4-100

4.3-9. Summary of shim positions for the enveloping 70 MW lobe power split PDQ analysis 4-101

4.3-10. PDQ result for scram recovery and restart study 4-101

4.3-11. Reactivity coefficient values 4-102

4.3-12. Reactivity worth of voiding experiment loops 4-103

4.3-13. Reactivity control element worth summary 4-104

4.3-14. Neck shim rod reactivity worth 4-105

4.3-15. Summary of safety rod reactivity measurement results 4-106

4.3-16. Minimum shutdown worth for the safety rods 4-107

4.3-17. Maximum reactivity insertion rates of control elements 4-108

4.3-18. Typical control element positions during a core cycle 4-109

4.3-19. Summary of fast flux data (E > 1 MeV) 4-110

4.3-20. Summary of thermal flux data 4-111

4.4-1. Thermal and hydraulic comparison table 4-164

4.4-2. Design DNB and flow instability margins 4-166

4.4-3. Reactor vessel flow distribution 4-166

4.4-4. SINDA-SAMPLE statistical uncertainties 4-167

4.4-5. Peak nominal and statistical fuel plate centerline temperatures 4-168

4.4-6. Reactor coolant system component thermal and hydraulic data 4-169

4.5-1. Materials in safety rod drive mechanisms 4-179

4.5-2. Materials in outer shim control cylinder drive mechanisms 4-179

4.5-3. Materials in neck shim rod drive mechanisms 4-180

4.5-4. Materials in reactor internal components 4-180

INTENTIONALLY BLANK

ACRONYMS/ABBREVIATIONS

ANS	American Nuclear Society
ANSI	American National Standards Institute
ASM	American Society of Metals
ASME	American Society of Mechanical Engineers
ASTM	American Society for Testing and Materials
ATR	Advanced Test Reactor
ATRC	Advanced Test Reactor Critical Facility
AWS	American Welding Society
BOC	beginning-of-cycle
CIC	core internals changeout
CHF	critical heat flux
CSAP	core safety assurance package
DNB	departure from nucleate boiling
DOE	U.S. Department of Energy
EDF	engineering design file
EFIS	emergency firewater injection system
EFPD	effective full-power day
EOC	end-of-cycle
ETR	Engineering Test Reactor
GDC	general design criteria
HFIR	High-Flux Isotope Reactor
ICE	Irradiation Capsule Experiment
INEEL	Idaho National Engineering and Environmental Laboratory
IGSCC	intergranular stress corrosion cracking
IPT	inpile tube
ITV	Irradiation Test Vehicle
LIPT	large inpile tube
LGWd	lobe-gigawatt-days
LPMS	loose parts monitoring system
MICE	Multiple Irradiation Capsule Experiment
MTR	Materials Test Reactor
MTU	metric tons uranium
MW	megawatt
MWd	megawatt day
MW/L	megawatt/liter

N_F	The reactor operating steady power level (pressurized operation, up to and including 250 MW). The power level N_F represents may change, not only for each reactor operating cycle but also during an operating cycle. During a scheduled startup, N_F is the projected/anticipated full operating power level. Actual experiment requirements or operational considerations may necessitate small deviations from the projected value. The neutron level and wide range neutron subsystems are adjusted such that upon reaching N_F the indication is equal to or greater than 100%.
N_L	For power operation and low power operation, a power level which corresponds to 1% N_F. For depressurized operation, the maximum allowed reactor power level (500 kW).
NPSH	net positive suction head
NRC	U.S. Nuclear Regulatory Commission
ONB	onset of nucleate boiling
OSCC	outer shim control cylinder
ORNL	Oak Ridge National Laboratory
PCP	primary coolant pump
PCS	primary coolant system
PPS	plant protective system
PWR	pressurized water reactor
RDAS	reactor data acquisition system
SAR	Safety Analysis Report
UFSAR	Upgraded Final Safety Analysis Report

4. REACTOR

The ATR is designed as an experiment irradiation facility and therefore provides for the insertion of numerous experiments into the core. Facilities supporting experiments are subject to change because experiment programs conducted at ATR are constantly being updated to meet specific needs. The discussion of the experiment facilities in this chapter is limited to their impact on the nuclear design characteristics of the reactor. Detailed descriptions of experiment facilities are provided in Chapter 10 (Experiment and Irradiation Facilities). A detailed safety analysis of each experiment is documented separately in an experiment safety analysis as described in Chapter 10.

The reactor core and internals, consisting of those systems, structures, and components located within the reactor vessel, is more heterogeneous than a commercial pressurized water reactor (PWR); the core is designed to provide a neutron flux peak in a number of the experiment facilities. While a commercial PWR has a single mechanical system for reactivity control (incore control components integral to the fuel elements) and alternate non-mechanical systems, the ATR has four mechanical systems with different functions, configurations, and motions. Instead of a single fluid (light water) acting not only as coolant but also as both moderator and reflector, the ATR has a beryllium reflector. Other differences, with less impact on system definition are as follows:

- ATR fuel plates are aluminum-uranium clad with aluminum rather than uranium oxide pellets clad by zircaloy.
- ATR has a low-temperature, low-pressure coolant with a more complex flow path.

These physical differences result in some deviations from the definition of the reactor and core internals used by the American National Standards Institute (ANSI) and American Nuclear Society (ANS) to describe commercial PWRs (ANSI 1988). The reactor core and internals or "reactor" as described in this Upgraded Final Safety Analysis Report (UFSAR) includes the fuel elements, reflector, reactivity control elements, reactor internals, and experiment/irradiation facilities. There are four reactivity control systems; the safety rod system, the outer shim control cylinder (OSCC) system, the neck shim rod system, and the regulating rod system. The reactivity control systems include the reactivity control elements, the drive mechanisms, and the associated control instrumentation. The reactor internals consist of the core support and flow distribution subsystem, the core internal guides, the outer reflector subsystem, the in-vessel fuel storage racks, and the reactor-internals protective cover. The reactor core is the general region in the reactor vessel, within the core reflector tank, containing the fuel elements, reactivity control elements, experiment facilities, and reflector.

This chapter discusses the mechanical design bases, description, and design evaluations for the fuel elements, reflector, and reactivity control element poison material; the nuclear and thermal-hydraulic design bases for the reactor; the reactor materials; and the functional design of the reactivity control systems. The experiment and irradiation facilities are discussed in Chapter 10 (Experiment and Irradiation Facilities). The reactivity control elements are not integral to the fuel elements as are the control components in a commercial PWR, therefore, the mechanical design of the reactivity control systems including the drive mechanisms is discussed in Chapter 3 (Design of Structures, Components, Equipment, and Systems) along with mechanical design of the reactor internals. Control system instrumentation is discussed in Chapter 7 (Instrumentation and Controls). The burnable poison is integral to the fuel elements and is discussed in this chapter.

4.1 Summary Description

The ATR, located at the Idaho National Engineering and Environmental Laboratory (INEEL) is a 250 MW (thermal) high flux test reactor designed to study the effects of radiation on samples of reactor structural materials, fuels, and poisons. The reactor is a general irradiation test reactor and may also be used for the production of radioactive materials. Construction began in November 1961 and completed in late 1965. Fuel loading commenced in 1967 and core testing completed in 1969. Full power operation began in August 1969 and the first experiment operating cycle began in December 1969.

The core contains forty fuel elements arranged in a serpentine or "clover-leaf" pattern to form nine flux trap regions. Each fuel element forms a 45 degree sector of a right circular cylinder and consists of nineteen fuel plates with coolant channels on both sides of each plate. The fuel plates are 49.5 in. long with an active fuel length of 48 in. loaded with highly enriched uranium matrix (UAl_x) in an aluminum sandwich plate cladding. Boron is included in certain plates as a burnable poison to minimize radial power peaking and extend the cycle life of the fuel elements.

The ATR has four separate systems for reactivity control each with different functions, configurations, and motions. The individual reactivity control systems are the safety rod system, the OSCC system, the neck shim rod system, and the regulating rod system. All four systems depend upon the mechanical movement of various solid hafnium pieces. The safety rods consist of aluminum tubes containing hafnium inserts typically positioned in six of the nine flux trap regions. During power operation the safety rods are withdrawn to where the leading edge of the hafnium inserts is just below the top of the active fuel. There are 16 OSCC. These are beryllium cylinders with 120 degree hafnium inserts arranged to operate in pairs around the core periphery. The OSCC are positioned by rotation to establish the lobe[a] power split and compensate for fuel burnup. There are a total of 24 rods in the neck shim rod and regulating rod systems, six situated in a row within each of the four arms of the neck shim housing. These rods typically begin a cycle fully inserted and are fully withdrawn as needed during the cycle to compensate for fuel burnup and lobe power balancing. Two of the neck shim rods (one active; one in a standby mode) serve as the regulating rods via the regulating rod servo system to maintain reactor power at a preset value.

The reactor internals include the core support structure and all internals between that structure and the reactor vessel wall. Major subsystems include the core support and flow distribution subsystem and the outer reflector subsystem. The reactor vessel is pressurized with a core inlet pressure (top of the fuel elements) of about 360 psig and a core outlet pressure of about 260 psig for three primary coolant pump (PCP) operation at the nominal primary coolant system (PCS) operating pressure of 371.9 psig at the plant protective system (PPS) vessel inlet pressure tap. The same PCS and core inlet pressure are maintained for two-PCP operation resulting in a core outlet pressure of 283 psig. The nominal maximum core inlet and outlet coolant temperatures are 125°F and 170°F, respectively. A part of the primary coolant flow is directed through the fuel elements and the remainder through the reactor internals. The PCS flow rate with three PCPs is nominally 50,000 gpm resulting in a flow rate of 27,950 gpm through the fuel elements with a nominal channel coolant velocity of 46.9 ft per second; with two PCPs operating,

---

[a] The core contains 40 fuel elements arranged in a clover-leaf pattern around nine flux traps. The flux traps are in a 3 × 3 square array. The eight fuel elements surrounding each corner flux trap and the eight elements surrounding the center flux trap are referred to as lobes. The lobes are labeled NW, NE, C, SW, and SE (northwest, northeast, center, southwest, and southeast) as representative of their position in the core. The reactivity control elements can shift the azimuthal power distribution to/from non-uniform power distributions, or power imbalances. The lobe powers are specified as high-center-low when there is symmetry and as NW-NE-C-SW-SE, if symmetry does not exist.

the PCS flow rate is nominally 43,500 gpm resulting in a flow rate of 24,320 gpm through the fuel elements with a nominal coolant velocity of 40.9 ft per second. The experiment loop facilities have inpile tubes (IPT) in the core flux trap regions and operate with independent thermal-hydraulic systems. Cooling in the non-loop irradiation facilities is maintained by transfer of heat to the primary coolant.

This chapter describes the mechanical design of the fuel elements and reflector and the nuclear and thermal-hydraulic design of the reactor. The design bases for the mechanical aspects of the fuel elements, reflector, and neutron poison material components are given in Section 4.2.1. The mechanical aspects of the fuel elements and beryllium reflector are described in Sections 4.2.2, the design evaluation in Section 4.2.3, and testing and inspection program in Section 4.2.4.

The bases for the nuclear design is given in Section 4.3.1 and discussions of the nuclear operation, core reactivity and control parameters, and monitoring methods are given in Section 4.3.2. Computational methods for analysis of the nuclear system are described in Section 4.3.3.

The thermal and hydraulic design of the reactor to ensure that adequate heat removal is available to meet performance and safety criteria for both normal and emergency conditions is described in Section 4.4. The design bases are discussed in Section 4.4.1 and a description of the thermal and hydraulic design in Section 4.4.2. Evaluation of the thermal performance is given in Section 4.4.4 through Section 4.4.6.

Specifications for internal reactor materials and fabrication methods relevant to safety considerations are described in Section 4.5 and a functional description of the reactivity control systems is provided in Section 4.6.

4.2 Fuel Element and Reflector Design

This section covers important mechanical aspects of the fuel element and reflector design. It also provides an evaluation of the mechanical, materials, and irradiation performance of the fuel elements, the reflector, and the reactivity control element poison material. The mechanical design of the reactivity control elements and their associated drive mechanisms is described in Chapter 3 (Design of Components, Equipment, and Systems). The pressurized water loop IPTs and other irradiation facilities are addressed in Chapter 10 (Experiment and Irradiation Facilities). The plant conditions for design are divided into four categories according to their expected frequency of occurrence and subsequent risk to the public:

- Condition 1—Normal Operation
- Condition 2—Anticipated Faults
- Condition 3—Unlikely Faults
- Condition 4—Extremely Unlikely Faults.

Postulated events in each of these categories are described in Chapter 15 (Accident Analyses).

The reactor is designed so that its components meet the following performance and safety criteria:

- The mechanical design of the reactor core components and their physical arrangement, together with corrective actions of the reactor control, and reactor protective systems (when applicable) ensure that the ATR plant protection criteria of Chapter 15 (Accident Analyses) are met.
- The fuel elements are designed to withstand various loads induced during handling and reactor operation.
- The reactor core and reflector are designed to accommodate movement of OSCC, neck shim rods, regulating rods, and safety rods in order to provide the required reactivity control for power operations and outage conditions.
- The reactor vessel and internals, reactivity in conjunction with the fuel elements, control components, and reflector blocks, direct reactor coolant through the core. The flow distribution is such that the heat transfer performance requirements can be met for all modes of reactor operation.

4.2.1 Design Bases

The fuel element design bases are shown to satisfy the general performance and safety criteria presented in Section 4.2. The detailed fuel element design establishes such parameters as fuel plate dimensions, fuel meat dimensions, fuel composition and density, coolant channel width, and initial oxide film thickness. The design considers effects such as maximum fission density, fission product swelling, and other properties that vary with burnup. The integrity of the fuel elements is ensured by designing to prevent excessive fuel temperatures, excessive fission gas buildup leading to blistering, and excessive fuel and cladding stresses and strains. This is achieved by a fuel element design which satisfies the design bases described in the following sections during Condition 1 over the fuel element lifetime. For some Condition 2 events, transient fuel temperatures may exceed allowable design temperatures. If one of these events were to occur, breach of the cladding is not expected to occur. However, evaluation and inspection of the fuel elements may be required before continued use.

Because of the integrated design of the fuel elements (i.e., cladding metallurgically bonded to fuel; fuel plates roll swaged into side plates), the entire fuel element is considered in stress evaluations. Fuel element integrity is ensured by setting limits on various operating parameters and, for all fuel elements manufactured prior to fuel element serial number XA567R, integrity was demonstrated by hydraulically testing each fuel element prior to reactor use (Fillmore 1995). Beginning with fuel element serial number XA567R, new fuel element integrity is demonstrated by excellent past performance and analysis of extremely low expected failure rates (Atkinson 1997). Beginning with fuel element serial number XA094T fuel element integrity is ensured by setting limits on various operating parameters and ensuring the fuel manufacturing process meets the requirements contained in the fuel element manufacturing specifications (Vinnola 1996; Richins and Miller 1995). The change in fuel element integrity verification was supported by Hamilton (1996a, 1996b) and approved by the Department of Energy (DOE) in May 1996 (Ziemianski 1996). Use of non-hydraulically tested fuel elements began with fuel element serial number XA571R in operating Cycle 109B in May of 1996.

The design bases for the reactivity control poison material and reflector components are described in Sections 4.2.1.6 and 4.2.1.7, respectively.

4.2.1.1 Cladding

4.2.1.1.1 Material Properties—The fuel plate cladding may be aluminum alloy 6061-O unclad or clad on one side with aluminum alloy 1100. The fuel plate frames are fabricated from the same material, unclad or clad on both sides with alloy 1100. The thickness of alloy 1100 on the cladding and frames should not exceed 5.5% of the total thickness of the composite fuel plate.

A high aluminum content alloy was selected as the cladding material because of its low absorption cross section (an important advantage when the goal is a high neutron flux) and its compatibility with the fuel. Further, aluminum alloys are light and can be easily formed, machined, or cast, while maintaining sufficient strength to withstand the reactor environment. They also have high thermal conductivity for efficient heat transfer and exhibit excellent fission product retention. The fully annealed 6061 condition was chosen to prevent possible over-aging effects during irradiation. These advantages outweigh negative features such as a low melting temperature and relatively low strength. Susceptibility to corrosion in a water system presents some disadvantage, but it is controlled with proper chemistry.

Historically, the impurity limits for the cladding have been taken from ASTM Specification B 209 (ASTM 1996a). Additional historical impurity limits are listed in Table 4.2-3. These limits are given in the fuel element specification. Deviations to these limits require additional evaluation following the Quality Assurance Program described in Chapter 17. Polkinghorne and Lacy (1991) provide information on the thermophysical and mechanical properties of the cladding. The effect of irradiation on mechanical properties is discussed in Section 4.2.3.1.

4.2.1.1.2 Chemical Properties—Aluminum alloy 6061-O, when exposed to water, produces an adherent oxidation product that separates the fuel plate from the cooling water. Because the corrosion product has a very low thermal conductivity, it presents a significant barrier to the removal of heat. As the operating cycle proceeds, the thickness of the corrosion layer increases, thereby increasing fuel plate temperatures and thermal stresses, and decreasing structural strength. The film thickness on the fuel plates is not to exceed 1.0 mil (0.025 mm). This is a maximum expected film thickness based on past film thickness measurements (Ambrosek 1993) and is the minimum thickness assumed in Chapter 15 (Accident Analyses).

All fuel elements manufactured prior to XA567R were hydraulically tested. The hydraulic testing conditions produced a corrosion-product film (i.e., boehmite) that had been proven effective in preventing significant in-reactor buildup of the corrosion product bayerite, which can limit the useful life of the fuel elements (Griebenow, Hanson, and Larrick 1977). In 1994, the aging Hydraulic Test Facility (HTF) could no longer be used to test and prefilm fuel elements. Alternatives to the HTF prefilming were being investigated prior to shutting down the HTF. A method for prefilming in an autoclave was developed and qualified by laboratory testing and production data (Hamilton 1996a, 1996b) and approved by DOE in May 1996 (Ziemianski 1996). Use of fuel elements prefilmed in the autoclave began with fuel element serial number XA571R loaded into operating Cycle 109B in May 1996.

The hydraulic test conditions for prefilming required 4 ±0.5 hours in circulating water at a temperature of 340 +10/-15°F and a pH of 4.6 to 5.5. These conditions were shown to produce a boehmite layer at least 0.1 mil thick. An initial measured oxide thickness greater than 0.06 mils (averaged over the surface using eddy current instrumentation) has been established as the lower limit for acceptable oxide thickness for fuel elements prefilmed in the autoclave. An upper limit to the initial oxide thickness was derived from the ATR-modified Greiss oxide deposition model (Greiss et al. 1964; Griebenow 1971). The model predicts that if the initial oxide film is less than 0.3 mils, the end-of-life oxide layer will not exceed 1.0 mils. All new fuel elements are required to be prefilmed to deposit Boehmite on the fuel element surfaces prior to use in the reactor.

Polkinghorne and Lacy (1991) provide information on the thermophysical properties of the corrosion product film.

4.2.1.2 Fuel

4.2.1.2.1 Material Properties—The fuel cores of the fuel plates consist of UAl_x intermetallic powder dispersed in aluminum. Borated fuel cores also contain small amounts of natural B_4C powder as a burnable poison. Three to 11% voids are fabricated into the fuel matrix to accommodate the increased volume of fission products. Typical UAl_x powder lots contain 8 wt% UAl_2, 78 wt% UAl_3, and 14 wt% UAl_4 (Whitacre 1989). Because UAl_3 is more ductile than UAl_4, the uranium-aluminide powder is required to contain at least 50 wt% UAl_3.

Nominal U-235 and boron (B-10) loadings in each fuel plate of a standard Mark VII fuel element are shown in Table 4.2-1. The required loadings per fuel element (7F prescription) are 1,075 ± 10 grams of U-235 and 0.660 ± 0.025 grams of B-10 at the 95% confidence level. The maximum allowable U-235 concentrations in the fuel cores of each plate are as follows:

Fuel Plates 1, 2, 18, 19	1.000 g/cc
Fuel Plates 3, 4, 16, 17	1.300 g/cc
Fuel Plates 5 through 15	1.600 g/cc.

Historical impurity limits for the fuel core materials are given in Table 4.2-3. The total impurity content of uranium-aluminide powder is limited to an equivalent boron content of 30 parts per million on a weight basis to uranium-aluminide. Table 4.2-4 lists the elements included in the calculation of the equivalent boron content. Deviations to these limits require additional evaluation following the Quality Assurance Program described in Chapter 17.

The UAl_x dispersion fuel system was selected on the basis of its ability to achieve high power densities and burnups (relative to the uranium-aluminum alloy fuel system), its ability to accommodate fission products in deliberate voidage, and its tolerance for fission gas. Additionally, burnable poisons can be readily dispersed in the fuel matrix. Polkinghorne and Lacy (1991) discuss the thermophysical properties of UAl_x dispersion fuel.

4.2.1.2.2 Chemical Properties—Uranium-aluminide fuel is extremely compatible with 6061 aluminum or 1100 aluminum cladding. No adverse chemical interactions occur between the fuel and cladding.

4.2.1.2.3 Burnup Limit—The operating life of the fuel elements is determined by the burnup limit, expressed as total fissions per unit volume of fuel core. The maximum fission density in fuel plate cores is limited to 2.3×10^{21} fiss/cm^3 (a burnup of over 350,000 MWd/MTU for a fuel element with a maximum fission density at the limit). As discussed below, this limit prevents unacceptable swelling and cladding failure from excessive fission densities in the fuel plates.

4.2.1.2.4 Fission Product Swelling—The growth or swelling of the fuel plates at up to 2.4×10^{21} fiss/cm^3 is proportional to the fission density, with the proportionality constant depending on temperature, core porosity, and fuel loading (Beeston et al. 1980). Because of physical constraints in the fuel plates, growth of the fuel core is virtually all in the thickness direction. Adherence to the fuel burnup limit (2.3×10^{21} fiss/cm^3) ensures that unacceptable fuel plate swelling does not occur.

4.2.1.2.5 Blistering—Blistering resulting from excessive fission gas buildup, either within the fuel core or at the core-cladding interface, can lead to fuel plate failure. The fuel temperature limits discussed in Section 4.4.1.2 ensure that fuel temperatures remain below those that have produced blistering during post-irradiation testing of ATR fuel plates and samples. This is believed to be conservative because under irradiation, gaseous atoms in bubbles undergo re-solution from the slowing down process of the fission fragments (Beeston et al. 1980). Therefore, in-reactor blister temperatures should be equal to or greater than those observed in post-irradiation tests.

4.2.1.3 Side Plates, End Fittings, and Combs

4.2.1.3.1 Material Properties—The fuel element side plates and combs are fabricated from aluminum alloy 6061-T6, and thus possess all of the desirable design characteristics of the fuel-plate cladding. The T6 rather than the O condition was chosen because of its greater strength. A roll swaging process is used to attach the fuel plates to the side plates. This allows axial slippage, thereby providing some stress relief during reactor operation. The combs are welded across the top and bottom midspan edges of the fuel plates for added support and spacing.

The fuel element end fittings are cast aluminum alloy 356-T71 or A356-T6. This alloy was chosen for ease of fabrication and compatibility with other components. The end fittings are welded to the side plates and are designed for support and positioning of the fuel elements on the flux trap baffles. The end fittings also increase the lateral stiffness of the fuel elements. The weld filler metal is aluminum alloy ER 4043.

Polkinghorne and Lacy (1991) discuss the material properties of aluminum alloys 6061 and 356. Typical properties of aluminum alloy 4043 are given in the American Society of Metals (ASM) Metals Handbook (1990). The historical material requirements for the side plates, end fittings, and combs are given in ASTM Specifications B 209, B 221, and B 618 (ASTM 1996a, 1996b, 1997). The boron equivalent content of the side plates is limited to 30 ppm. Deviations to these limits require additional evaluation following the Quality Assurance Program described in Chapter 17.

4.2.1.3.2 Strength Requirements—Pull tests are performed on representative samples by the vendor to ensure the mechanical integrity of the fuel plate-to-side plate swage joints. The point of swage joint release is required to be greater than 150 lb per linear inch of joint (26.3 N/mm), applied perpendicular to the axial length of the swage joint. Pull tests are also performed to ensure that the end fitting welds are of adequate strength. A minimum weld joint strength of 1,000 lb (4448 N) per side plate joint is required.

4.2.1.4 Fuel Element Performance. The design basis for fuel element performance related to the safety envelope is summarized as follows. The fuel element dimensions remain within operational tolerances during normal operation and the fuel element capabilities are not reduced below that assumed in the safety analysis. The extent of fuel plate failures remains within the limits assumed in the safety analysis. Fuel plate failure is defined to mean that the fuel plate cladding has been breached allowing the release of fission products. The analytical models, engineering test programs, and historical data reviews used to evaluate fuel element performance are described in Sections 4.2.3.3 and 4.4.4.5.

4.2.1.5 Fuel Element Structural Design

4.2.1.5.1 Stress Limit—Stresses developed in the fuel element during reactor operation result primarily from temperature differences between the fuel plates and the side plates. Differential thermal expansion results in a compressive loading on the fuel plates, which produces a potential for yielding or buckling. The corrosion-product film that forms on the fuel plates causes plate temperatures and thermal stresses to increase with cycle life until decreased power generation (attributed to depleting fuel) overrides the corrosion effect. To ensure that the integrity of the fuel elements is maintained during normal steady-state operation (Condition 1), the thermal stress in the center half-span of the limiting fuel plate, evaluated at temperatures two standard deviations above nominal, is required to remain below the unirradiated yield strength of the plate. The unirradiated condition is specified for conservatism because the effect of irradiation is to increase the strength of the fuel plate (Beeston et al. 1980).

4.2.1.5.2 Vibration and Fatigue—Flow-induced vibration of fuel plates is insignificant over the range of available flows. There are limited cyclical stresses on the fuel element, and the cumulative fatigue cycles are less than the fatigue life of the fuel elements.

4.2.1.5.3 Chemical Compatibility—Chemical compatibility among core components is maintained by the use of high aluminum-content alloys for most of the components in the active core region. Allowable limits on pH, conductivity, and filterable solids in the primary coolant prevent excessive corrosion product buildup on the fuel plates.

4.2.1.5.4 Fuel Element Bowing—Thermal or irradiation-induced bowing of fuel elements does not interfere with their performance or their safe removal from the core.

4.2.1.5.5 Thermal-Hydraulic Design—The thermal-hydraulic design is discussed in Section 4.4.

4.2.1.6 Incore Control Components. Hafnium is the absorber material used in the OSCC, neck shim rods, regulating rods, and safety rods. Detailed descriptions of these components are given in Chapter 3 (Design of Structures, Components, Equipment, and Systems). The design bases for hafnium components are discussed below.

4.2.1.6.1 Material Properties—Hafnium was selected as the absorber material on the basis of its nuclear properties (i.e., high neutron cross section and nondepleting), mechanical properties, corrosion resistance, and prior reactor experience. The material requirements for hafnium components are defined in the material specification for hafnium (EG&G Idaho 1991b). Polkinghorne and Lacy (1991) provides information on the thermophysical properties of hafnium. The effect of irradiation on mechanical properties is discussed in Section 4.2.3.5.

4.2.1.6.2 Fluence Limit—The maximum fast neutron (E > 1 MeV) fluence in hafnium components is limited to 5.0×10^{22} n/cm^2. As discussed by Livingston (1984), the tensile strength of hafnium initially increases with irradiation, then decreases as higher fluence levels are experienced. Increased tensile strength is accompanied by decreased ductility. The fluence limit is based on preserving a sufficient margin in tensile strength over imposed stresses to accommodate the loss of ductility. This ensures that no control component is operated to the point where loss of hafnium could occur because of irradiation damage. Hafnium components are not typically stressed except as the result of non-uniform growth. (The hafnium components are not load-bearing).

4.2.1.7 Reflector

4.2.1.7.1 Material Properties—Beryllium was selected as the reflector material on the basis of its nuclear properties (i.e., high moderating ratio), mechanical properties, corrosion resistance, and prior reactor experience. The material requirements for the reflector are defined in the material specification for beryllium (EG&G Idaho 1991a). Information on the thermophysical and mechanical properties of beryllium are documented in the core materials physical property description (Polkinghorne and Lacy 1991).

The effect of irradiation on mechanical properties is discussed in Section 4.2.3.6.

4.2.1.7.2 Stress Limit—The reflector is exposed to fast neutrons in a nonuniform manner resulting in nonuniform, irradiation-induced growth in the reflector blocks. This growth causes stresses to develop that will eventually cause cracking of the beryllium. Historically, the cracks have been accompanied by small holes through thin ligaments and spalling (Tomberlin 1989). Because this type of aging does not necessarily preclude continued operation, and because the eight reflector blocks do not all crack simultaneously, it is desirable for both economic and programmatic reasons to continue operation even though one or more reflector blocks has started to exhibit signs of aging.

By the time cracking is approached in the B reflector ligaments, the A and E ligaments are expected to exhibit cracking (ligament designations are illustrated in Figure 4.2-8). Relatively tight cracks extending vertically through the axial length of the A and E ligaments are a normal part of reflector aging. With a full-length crack in an A ligament, cracking of a B ligament could result in a large free piece of beryllium which potentially could make contact with a fuel plate. The maximum stress in each B ligament is normally required to be at least two standard deviations less than the failure stress. This criterion and the beryllium surveillance and inspection program (discussed in Section 4.2.1.8.3) ensure that the integrity of the beryllium reflector is maintained consistent with the assumptions of the reflector safety analysis (Durney 1994). Specific evaluation may be used for operation with higher stresses in the B ligaments.

4.2.1.8 Inservice Surveillance. Inspection and testing of irradiated fuel elements, reflector, and reactivity control components on a regular basis allows for early detection of potential problems and ensures that the ATR is operated within prescribed limits. Features of the surveillance program are discussed below.

4.2.1.8.1 Fuel Elements—As soon as practicable following discharge from the reactor, the thickness of the corrosion-product film on selected fuel elements is measured to ensure that the film on recycled elements does not exceed the limit of Section 4.2.1.1. The oxide data are trended and statistically analyzed to provide assurance the limit will not be exceeded. Cooling channel thickness measurements are also made on selected fuel elements to ensure that recycled elements are mechanically sound. The channel thickness measurement data are evaluated for indications of anomalies that indicate unacceptable fuel element performance. Additionally, all recycled fuel elements are visually inspected prior to reinsertion in the reactor.

Cumulative fission densities in the fuel elements are tracked as part of the core physics analysis for each operating cycle (see Section 4.3.1.1). Maximum fission densities are calculated to ensure that the burnup limit of Section 4.2.1.2 is not exceeded.

4.2.1.8.2 Incore Control Components—The safety rods, neck shim and regulating rods, and OSCC are tested periodically to ensure that they operate reliably. Accumulated fast-neutron ($E > 1$ MeV) fluences in the installed hafnium components are updated routinely and replacement dates projected to ensure that the hafnium fluence limit of Section 4.2.1.6 is not exceeded.

4.2.1.8.3 Reflector—The entire length of the reflector adjacent to the fuel is inspected annually until the stress in the highest-stressed ligament is within two standard deviations of cracking or until a crack is detected (whichever occurs first). The frequency and extent of surveillance is then increased (Tomberlin 1989).

As noted in Section 4.2.3.6, reflector lifetime projections are expressed in terms of integrated power (i.e., megawatt-days of reactor operation) in the adjacent corner lobe. Annually, the integrated power of each corner lobe is updated and the end-of-reflector life projected to ensure that the stress criterion of Section 4.2.1.7 is satisfied.

4.2.1.8.4 Online Fuel Failure Monitoring—Abnormal radioactivity levels, resulting from fission product leaks, will be detected by the stack effluent monitoring system and/or routine sampling of the primary coolant. Stack effluents are normally monitored continuously for noble gases, iodine, and particulates. The stack effluent monitoring instrumentation is discussed in Chapter 12 (Radiological Protection). Gross beta and gamma activity levels in the primary coolant are measured routinely during greater than 3 MW operation. The PPS fission break subsystem [discussed in Chapter 7 (Instrumentation and Controls)] initiates a rapid reactor shutdown in the event of a major fission break.

4.2.2 Description and Design Drawings

The subsections under this heading describe the fuel elements and beryllium reflector. For each component, the following information is presented:

- Component descriptions and characteristics
- Drawings
- Specifications.

Performance and design criteria are discussed in Section 4.2.1.

4.2.2.1 Fuel Elements. Uranium-aluminum alloy fuel elements (UAl_x for the fuel core matrix with 6061 Al cladding and side plates) are used to achieve a very compact core providing high thermal flux levels for experiment irradiation.[a] The use of thin plate-type fuel elements with narrow cooling channels maximizes the heat transfer. The reactivity control systems can unbalance the powers in the four corner lobes of the reactor core by as much as 80 to 20 (relative MWs) during steady-state operation. The term relative power is used to designate lobe powers normalized to 250 MW. Therefore, the fuel elements must be designed to successfully operate with high heat flux and a large power tilt. A significant ATR fuel design and testing effort (Beeston and Malik 1977; Beeston et al. 1980; deBoisblanc and Cohen 1965; Ferris and Moyers 1963; Francis 1966; Francis et al. 1967a; Graber et al. 1971; Griebenow, Fillmore, and Moore 1966; Griebenow 1971; Griebenow, Hanson, and Larrick 1977; Poetschat 1967; Walker, Graber, and Gibson 1966) culminated in the current fuel element design. This fuel element design has proved reliable and safe for over 26 years of operation. The fuel tests demonstrated significant safety/design margins for "burnout" (194% power), and buckling (greater than 80% channel blockage and/or more than 150% flow) (Griebenow 1971; Ferris and Moyers 1963).

Forty fuel elements form a complete fuel loading. The 40 fuel elements are arranged in the form of a four-leaf clover within the 4-ft high core. This geometry is illustrated in Figures 4.2-1 and 4.2-3 and is designed to maximize the neutron flux in the flux trap regions. Figure 4.2-1 shows the configuration with pressurized water loop facilities located in five of the flux traps, and non-loop irradiation facilities in the remaining four flux traps. This is the configuration of the reactor following the 1994 Core Internals Changeout and is the reference configuration for Chapter 4 and the UFSAR. In 1997 the capsule irradiation facility in the northeast flux trap was replaced by the Irradiation Capsule Experiment facility. This configuration is shown in Figure 4.2-1a. The core was reconfigured in 1999 with the installation of the Irradiaton Test Vehicle (ITV) and the Multiple Irradiation Capsule Experiment (MICE) facility. This is the current reactor configuration and is shown in Figure 4.2-1b. The fuel elements are classified safety related (House 1992).

---

[a] Refer to Chapter 10 (Experiment and Irradiation Facilities) for a discussion of the experiment facilities.

The cloverleaf arrangement (Figure 4.2-3) of the fuel annulus requires that the fuel element have a radius of curvature (Thomas 1985). Each fuel element, shown in Figures 4.2-4 and 4.2-5, consists of 19 parallel curved fuel plates attached by roll swaging to two side plates to form a 45-degree sector of a right circular cylinder with the inner radius equal to the outer radius of the inner and outer flux trap baffles (Figures 4.2-1 and 4.2-3). The fuel-plate-to-side-plate swage joint design results in relieving the thermal stresses in fuel elements with significant plate-to-plate power differences (power tilt) (Atkinson 1988). In addition to the fuel plates and side plates, the fuel element consists of upper and lower end fittings and T-bar support keys.

The four fuel element types are designated 7F, 7NB, 7NBH, and YA. They are all versions of the zone loaded fuel element design and are identically constructed, varying only in the content of the fuel matrix. Table 4.2-1 shows the nominal U-235 and B-10 loadings for each fuel plate of the 7F fuel element and indicates (in the footnotes) these loadings for fuel elements 7NB, 7NBH, and YA. The U-235 and B-10 loadings are nonuniformly distributed to provide optimum operating characteristics.

In the 7F fuel element, all 19 fuel plates are loaded with 93% enriched uranium in an aluminum matrix to a total of 1075 g U-235. The eight outer plates (1 through 4 and 16 through 19) contain boron as a burnable poison to a total of 660 mg B-10.

To provide additional reactivity in certain locations [e.g., adjacent to the large inpile tube (LIPT), which have more mass and therefore absorb more neutrons than standard IPTs], the 7NB fuel element contains no burnable poison. In every other respect, the 7NB fuel element is identical to the 7F fuel element. There are four variations of 7NBH fuel elements. The 7NBH fuel element is similar to the 7NB fuel element except that it contains one or two borated plates. The locations of the borated plates in the four 7NBH fuel element types are given in Table 4.2-1. The special YA fuel element is also identical to the 7F fuel element except that fuel plate 19 of the YA fuel element is an aluminum alloy plate containing neither uranium fuel nor boron burnable poison. The total U-235 and B-10 content of this fuel element is reduced accordingly. The YA fuel element is required in positions adjacent to A and E ligaments for high power operation with an aged reflector. A modified YA (YA-M) element has been developed for use at reflector end of life conditions (Anderson 1992) and approved by DOE in November 1992 (Burrell 1992). The fuel annulus begins to close as the core internal components and beryllium reflector age. The YA-M fuel elements have the side plate width reduced by 15 mils and the T-bar thickness reduced by 5 mils allowing easier insertion and removal from fuel locations that have exhibited closure due to aging. Fuel element materials, dimensions, and loadings are summarized in Table 4.2-2.

The fuel element side plates are vented by localized slots (Figure 4.2-5) to provide interconnection between all channels, and thereby reduce lateral pressure differentials between the fuel plates preventing hydraulic buckling (Atkinson 1988). These slots also will tend to limit fuel damage caused by coolant channel blockage. Pads are included on the exterior surface of the side plates to ensure adequate coolant channels between elements and to provide a minimum flow path for interconnecting flow through the vents and external channels.

Channels formed by the outer fuel plates (1 and 19) of the fuel elements, the beryllium reflector blocks, the flux trap baffles, and the neck shim housing allow passages for the downward flow of reactor coolant. Coolant also passes through channels between each fuel plate of the element. Successful heat removal requires high coolant channel velocities that can result in severe cross-plate hydraulic loadings if there are differences in cooling channel thickness (Atkinson 1988). The side-plate vents reduce this hydraulic loading.

The fuel element end fittings are T-bars designed to position the elements as they mate with slots in the flux trap baffles (Figures 4.2-4 and 4.2-5). The end fittings are welded to the fuel element side plates and provide minimum restriction to coolant flow through the element. In addition to providing a lifting handle, the top-end fitting includes a curved baffle to direct coolant flow into the fuel channels with a minimum of turbulence. The top-end fitting also acts as a spacer to position the top end of the fuel element relative to the adjacent flux trap baffles in lieu of an upper grid fuel plate. Combs are also provided at each end of the fuel plates to improve the lateral support of the fuel plates.

Fuel element storage facility is provided in the reactor vessel for use during reactor refueling. Two storage racks are located in the annular water space between the core reflector tanks and the inlet flow baffle in diametrically opposed positions, east and west.

When required, during a reactor outage, dummy fuel elements are used in regular fuel element positions in the reactor core. When not in use, the dummy elements are normally stored in the reactor canal in the dummy fuel element grid. A dummy fuel element is made with 19 parallel, curved fuel plates and two side plates. The dummy fuel plates and side plates are swaged together. The dummy elements are normally made of aluminum, and the fuel plates contain no active fuel. Some of the dummy fuel plates, however, do contain depleted uranium.

4.2.2.2 Beryllium Reflector. As previously mentioned, the beryllium reflector aids in generating the high neutron flux environment for experiments inserted into the core. The beryllium reflector is safety related (House 1992). This reflector fills the space between the fuel annulus and the core reflector tank wall (see Figures 4.2-1 and 4.2-2). It consists of eight, 45-degree segments machined from hot-pressed beryllium block, of which four are "right-hand" and four are "left-hand" or mirror images (Figures 4.2-6, 4.2-7, and 4.2-8). When assembled, these eight segments make up a portion of a right circular cylinder, 51-in. high with a 25-1/4-in. radius, that extends from 2 in. above to 1 in. below the 4-ft active core. Reflector segments are numbered in a clockwise manner beginning with No. 1 at the one o'clock position (see Figure 4.2-1).

The beryllium used in the reflector is a high-grade material manufactured per contractor specification (EG&G Idaho 1991a). The specification addresses requirements for the beryllium powder, average grain size, chemical composition, trace impurity limits, physical properties, mechanical properties, quality assurance provisions, and preparation for shipment.

The core reflector tank and reflector support tank[a] provide bottom and outer support, respectively, to the beryllium reflector assemblies (see Figure 4.2-2). The beryllium reflector block segments (see Figures 4.2-6, 4.2-7, and 4.2-11) per segment, which fit into the outer shim control cylinder holes, and by 0.030-in. thick pads machined on the inner wall of the core reflector tank. Each segment also has 0.030-in. thick spacer pads on its flat sides to allow for reactor coolant flow between the segments. The outer corners of each segment contain a pad retainer fitting at the bottom to locate the support pads between the beryllium segment and the lip of the core reflector tank. The lower alignment cups serve secondarily to guide and align the outer shim control cylinders. Alignment sleeves in the webbed upper face of the reflector support tank serve to position the lower alignment cups.

---

[a] Refer to Chapter 3 (Design of Structures, Components, Equipment, and Systems) for a description of the core reflector tank and reflector support tank.

Design changes were made for reflector III to reduce the tensile stresses in the reflector and thereby increase the life of the reflector (Thomas 1985). This design was installed during the 1977 core internals changeout (CIC). The reflector III beryllium segments are identical to reflector II except for 13 horizontal saw cuts extending from the fuel side radially outward to a depth of about 4 in. (Figure 4.2-6) and changes to the cooling-hole pattern (Thomas 1985). The 13 saw cuts serve to relieve growth stresses encountered in the reflector II segment design by providing gaps in the highly irradiated region of the reflector. With the saw cuts 4 in. deep, as compared with a total depth of about 17 in. for the segment, each piece remains a single piece of beryllium. In addition, a reduced number of cooling holes were drilled through each segment. The reflector II segment had 36 cooling holes; the reflector III segment has only four.

The beryllium reflector was further redesigned (Reflector IV) to incorporate four additional 1-1/2-in. B-hole positions (B-9 to B-12) and four additional 1-1/2-in. I-hole positions (I-21 to I-24) (Figure 4.2-1). The positions are located at the faces of the beryllium segments such that one-half holes are machined in each segment for each type of hole. The added B-holes intersect the saw cuts incorporated in the earlier design. Except for these changes, the reflector IV beryllium segments are identical to the reflector III beryllium segments. Reflector IV was installed during the 1986 CIC. Reflector V was installed during the 1994 CIC, and is identical to Reflector IV.

Each reflector segment is cooled on the exterior surfaces of the segments (as previously mentioned) and through four full-length 5/16-in.-diameter holes bored through the block near its inner edge (Figure 4.2-6). The coolant arrangement was selected to avoid thermal gradients, which would create thermal stress problems in the reflector, and to maintain temperatures close to present design values (Thomas 1985).

4.2.3 Design Evaluation

The fuel elements, control components, and reflector are designed to satisfy the performance and safety criteria of Section 4.2, the mechanical design bases of Section 4.2.1, and other interfacing nuclear and thermal-hydraulic design bases specified in Sections 4.3 and 4.4.

The effects of Condition 2, 3, and 4 events on fuel element integrity are discussed in Chapter 15 (Accident Analyses).

4.2.3.1 Cladding. There is considerable reactor operating experience with aluminum as a fuel plate cladding. Aluminum alloys have been used successfully in many research reactors including the Materials Testing Reactor (MTR), the Engineering Test Reactor (ETR), the Oak Ridge Research Reactor, the High Flux Beam Reactor, the High Flux Isotope Reactor (HFIR), and the ATR. As noted in Section 4.2.1.1, aluminum alloy 6061 is an excellent cladding material because of its low neutron absorption cross section and good physical and mechanical properties.

4.2.3.1.1 Chemical Evaluation—The corrosion-product film that forms on water-cooled aluminum fuel plates is chiefly a mixture of alumina hydrates. X-ray diffraction analyses of the film on irradiated ATR fuel plates show the corrosion product to be primarily boehmite (• -AlOOH) and/or bayerite [• -$Al(OH)_3$]. The insulating effect of the film is more of a limitation to the fuel than is corrosion damage. As corrosion proceeds, the formation of a surface layer of corrosion products of low thermal conductivity results in increased cladding temperatures and decreased structural strength. Corrosion of the cladding is controlled by prefilming all fuel elements with boehmite prior to reactor use and by strict primary system chemistry controls.

Extensive ex-reactor corrosion studies performed by Oak Ridge National Laboratory (ORNL) in support of the ATR design (Griess, Savage, and English 1964) showed that the corrosion rate decreases with exposure time and increases with surface temperature. The controlling temperature is at the corrosion product-water interface (i.e., surface temperature). For a coolant pH of 5.0 and heat fluxes between 1×10^6 and 2×10^6 Btu/hr·ft^2 (3×10^6 and 6×10^6 W/m^2), the following empirical equation was found to predict the thickness of the corrosion layer reasonably well:

$$X = 443\theta^{0.778} \exp\left(\frac{-4600}{K}\right) \tag{4.2-1}$$

where

X = corrosion-product thickness (mil)

θ = time (hr)

K = surface temperature (K).

The ORNL tests also showed that the pH of the coolant is an important variable affecting the rate of corrosion-product buildup. The rate of corrosion-product formation was 2.7 times greater when the pH was 5.7 to 7.0 than when the pH was 5.0. On the basis of the ORNL experiments, it was concluded that 6061 aluminum would have adequate corrosion resistance for use as ATR fuel plate cladding provided the pH of the primary coolant was maintained at 5.0 with nitric acid. PCS pH was originally controlled at 5.0 ± 0.2 during power operation. The method of control was changed from nitric acid addition to use of the bypass demineralizer system. After a trial period (Durney 1980), the upper limit was raised to 5.4 giving an allowable range of 4.8 to 5.4 starting with Cycle 49A (Durney 1982). Many years of operating experience have shown that the current limits (4.8 to 5.4 for reactor operation at greater than 3 MW) are sufficient to control corrosion.

One of the start-up tests was an aluminum-cladding corrosion test (Griebenow et al. 1971). A special fuel assembly fabricated for the test contained a double-core instrumented fuel plate. Post test analysis of the temperature-rise data indicated that operating temperatures of ATR fuel plates could be predicted using corrosion-product film thicknesses that are 0.7 of those obtained using Equation 4.2-1. Consequently, a multiplier of 0.7 is applied to Equation 4.2-1 when computing best-estimate film thicknesses for fuel plate temperature and stress evaluations.

As discussed in Section 4.2.1.1, the thickness of the corrosion-product film on fuel plates is not to exceed 1.0 mil (0.025 mm). This is a maximum expected film thickness based on past film thickness measurements (Ambrosek 1993) and is the minimum thickness assumed in Chapter 15 (Accident Analyses). Verification that films do not exceed this limit is provided by surveillance measurements on selected fuel elements at the end of each operating cycle (see Section 4.2.1.8).

The measured fuel plate oxide thickness vs. accumulated exposure data from Cycle 22B through Cycle 100C (1974 to 1994) are summarized in McCracken (1993b). The data follow similar trends over the entire period. Except for a small number of observations around 1 mil, the data show the oxide thickness tends to be self-limiting in the range of 0.4 to 0.6 mil. PCS water chemistry limits on pH and filterable solids are established in part to control oxide growth. PCS pH is controlled at 4.8 to 5.4. The nominal concentration of filterable solids sized between 0.45μ and 20μ and > 20μ is limited to ≤ 0.1 ppm and ≤ 1 ppm, respectively. The filterable solids limits are based on work reported in Griebenow, Hanson and Larrick (1977).

Pitting corrosion of the fuel plates is discussed in Section 4.2.3.3.

4.2.3.1.2 Irradiation Stability—The effect of irradiation on the mechanical properties of 6061 aluminum cladding is an increase in strength and hardness with an accompanying decrease in ductility (Gronbeck 1967; Weir and King 1971). Test results show significant increases in tensile and yield strength with relatively little loss of ductility for fast neutron (E > 1 MeV) fluences exceeding 10^{22} n/cm^2 and test temperatures up to 392°F (473 K).

Two recent studies (Ismail and Mohamed 1989; Ismail 1990) indicated that age-hardenable aluminum alloys such as 6061 aluminum might exhibit irradiation-induced softening at very low neutron doses ($0.87 - 2.5 \times 10^{13}$ n/cm^2). To investigate this effect, further testing was performed at ORNL as part of the Advanced Neutron Source Project. The attempts to reproduce the softening effect at ORNL were not successful (Buescher 1998) and the conclusion reached at ORNL was that γ heating of the test samples in the original low dose neutron study had resulted in temperatures high enough to cause thermally induced softening. More recent testing by Ismail and Birt (1995) run to a slightly higher dose (3.7×10^{13} n/cm^2) produced hardening in the alloy. The test configuration in the more recent study minimized heating during irradiation. From the ORNL work and the more recent result by Ismail, it is concluded that the historical data of Gronbeck and Weir and King on the effect of irradiation on mechanical properties is the relevant data for mechanical properties.

Electron microscopy studies and measurements of the immersion density of irradiated aluminum alloys have suggested that swelling from void formation is strongly related to chemical composition and microstructure (Weir and King 1971). Irradiation to 1×10^{22} n/cm^2 (E > 0.8 MeV) at 140°F (333 K) caused about 7% swelling in nominally 99.9999% aluminum and 1% swelling in solid-solution alloys, but caused no swelling that could be resolved experimentally in the 6000 series aluminum alloys. Density measurements on an irradiated HFIR target holder of 6061 aluminum that had been exposed to a maximum neutron fluence of 5.4×10^{22} n/cm^2 (E > 0.8 MeV), indicated a total density decrease of only 1.06%.

Density and tensile property measurements were also made on specimens cut from a dummy flux trap filler piece (Atkinson et al. 1974). These specimens (6061-T6 aluminum) received exposures of 1.03 to 1.55 × 10^{22} n/cm^2 (E > 1 MeV). The measured volume changes agreed with a correlation derived from the HFIR target basket data given by

$$\frac{\Delta V}{V}\% = 0.039(\varphi t)^{2.1} \tag{4.2-2}$$

where

φt = fast fluence (10^{22} n/cm^2, E > 1 MeV).

The irradiation stability of composite fuel plates (fuel plus cladding) is discussed in Section 4.2.3.2.

4.2.3.1.3 Consequences of Power-to-Coolant Flow Mismatch—This subject is discussed in Chapter 15 (Accident Analyses).

4.2.3.2 Fuel. Past operating experience and experimental tests have shown the UAl_x dispersion fuel system to have greater performance and stability characteristics than the uranium-aluminum alloy system used previously in the MTR and ETR at the INEEL. The anticipated benefits of powder dispersion fuel-high power density, accommodation of fission products in deliberate voidage, structural tolerance of fission gas, and effective dispersion of burnable poison-have been realized. The UAl_x fuel system has performed well in extended service in several high flux test reactors including the Missouri University Research Reactor, the Massachusetts Institute of Technology Reactor-II, the University of Michigan's Ford Nuclear Reactor, the French-German High-Flux Reactor, and the ATR.

4.2.3.2.1 Chemical Interactions—The equilibrium phase diagram for the uranium-aluminum system is shown in Figure 4.2-13 (Van Horn 1967). As indicated in the phase diagram, only UAl_4 forms stable dispersions with Al. Both UAl_2 and UAl_3 react with the Al matrix to form UAl_4. The kinetics of these reactions have been studied by Nazaré, Ondracek, and Thümmler (1975). The first signs of reaction in UAl_3-Al dispersions are visible at about 752°F (673 K). However, at this temperature, the reaction rate is so low that a further increase in temperature is necessary to observe the progress of the reaction. The reaction between UAl_2 and Al proceeds in essentially the same manner as between UAl_3 and Al, the final reaction product again being UAl_4. It is possible that UAl_3 is formed as a short-lived intermediate product.

Reaction rates between UAl_x and Al are enhanced under irradiation (Dienst, Nazaré, and Tümmler 1977). Fuel plate irradiations conducted in the FR-2 at Karlsruhe have shown that even at low irradiation temperatures (158 to 356°F, 343 to 453 K), UAl_2 and UAl_3 react with excess Al to form nonstoichiometric $U_{1-x}Al_4$. However, the reaction does not cause a measurable change in fuel volume. Volume changes in dispersion fuel are determined primarily by the volume requirements of the fission products. Diffusion of the Al matrix into the UAl_x fuel particles is actually desirable from the standpoint of irradiation behavior because as noted below, the crystal lattice of UAl_4 is more effective in retaining fission gas than UAl_3.

If the fuel plate cladding is breached, then the uranium-aluminide fuel particles are susceptible to oxidation. It may be reasonable to assume that aqueous corrosion of UAl_x is similar to that of UO_2 because the oxidation of UAl_x occurs via UO_2 by the following mechanism (Openshaw and Shreir 1964):

$$UAl_x + O_2 \rightarrow UO_2 + xAl \tag{4.2-3}$$

$$3UO_2 + O_2 \rightarrow U_3O_8 \tag{4.2-4}$$

giving the overall reaction

$$3UAl_x + 4O_2 \rightarrow U_3O_8 + 3xAl \tag{4.2-5}$$

The release of fission products from failed fuel plates resulting from aqueous corrosion-erosion of the UAl_x fuel is discussed in Section 4.2.3.3.

4.2.3.2.2 Irradiation Stability—Post-irradiation examination of ATR fuel plates and samples has shown that the uranium-aluminide fuel system does not swell excessively during irradiation (Beeston et al. 1980). As noted in Section 4.2.1.2, swelling of ATR fuel plates occurs primarily in the thickness direction. This can be explained by the plastic flow of the fuel core. The cladding has a higher strength than the fuel core in the length and width directions. As growth occurs, the compressive yield stress of the core is reached while the cladding, loaded in tension, remains well below yield. The cladding produces very little lateral restraint, therefore, the plastic core flows primarily in the thickness direction.

The swelling data from four fuel elements and sixteen samples are shown in Figure 4.2-14 (Beeston et al. 1980). A least-squares linear regression analysis of the data gives

$$\frac{\Delta V}{V}\% = 2.6\% F / 10^{21} \tag{4.2-6}$$

where

F = burnup (fiss/cm^3 of fuel plate core).

Several parameters affect the scatter in the swelling data including irradiation temperature, fuel core porosity, and fuel loading. For high fuel loadings (~1.6 g U-235/cm^3 of fuel core), the swelling corresponds to 0.11 vol%/% burnup. A similar value (0.12 vol%/%) was obtained for sample fuel plates irradiated in the FR-2 at Karlsruhe (Dienst, Nazaré, and Tümmler 1977). At 2.3×10^{21} fiss/cm^3 (i.e., the current burnup limit), Equation 4.2-6 predicts ~6% fuel core swelling, corresponding to a 1.2-mil (0.030 mm) increase in fuel core thickness. This increase is insufficient to threaten the integrity of the cladding or to restrict flow in the adjacent coolant channels.

The uranium aluminide fuel system has shown exceptional tolerance for fission gas, which accounts for the low swelling rate and excellent blister resistance (Beeston et al. 1980).[a] The principal gaseous atoms are krypton, xenon, helium, and hydrogen. Krypton and xenon are fission products while helium and hydrogen are nuclear reaction products primarily from B_4C and impurities. Several studies (Francis 1966 and 1970; Francis and Moen 1966) have addressed the gas retention behavior of the aluminide fuels. The good gas retention has been attributed to the defect structure of UAl_4 (although UAl_3 also retains the gas) and to the porosity.

In 1969, a program for irradiating the pure uranium aluminides was undertaken to study the high temperature stability of these fuel compounds (Francis 1970). Samples of UAl_3 and UAl_4 in the form of 1/2-in. (1.27-cm) diameter pellets were irradiated in the MTR and ETR. Following irradiation, the specimens were heated to progressively higher temperatures and the fission gases collected. It was found that the principal releases of fission gas were associated with the isothermal transformations in the U-Al phase system (see Figure 4.2-13). About 28% of the fission gas was released from UAl_4 when passing through the 1,346°F (1003 K) peritectic where UAl_4 transforms into liquid and UAl_3. For UAl_3, the temperature of gross fission gas release was about 135°F (75 K) below the 2,462°F (1623 K) peritectic. This work confirmed the excellent fission gas retention capability of UAl_3 for test reactor fuel.

The gas-retention properties of UAl_x fuel plates were studied under meltdown conditions in 1966 (Francis and Moen 1966). Sample fuel plates containing ~50 wt% UAl_3 were irradiated in the ETR. The sample fuel plate fabrication procedures and irradiation conditions were designed to duplicate those expected in the ATR. Following irradiation, the samples were heated to progressively higher temperatures and the fission gases collected. The results showed that most of the fission gas was released above the solidus temperature of the 6061 aluminum cladding (1,080°F, 855 K). At 1,112 to 1,238°F (873 to 943 K), ~99% of the Kr and Xe gas atoms were released (Beeston et al. 1980). It was concluded that the liquid aluminum matrix reacted with UAl_4 to release the fission gas at a lower temperature than the 1,346°F (1,003 K) peritectic temperature of pure UAl_4.

4.2.3.3 Fuel Plate Performance

4.2.3.3.1 Dimensional Stability—Visual examinations, plate length measurements, plate thickness measurements, and density measurements have been made to determine the dimensional stability of ATR fuel plates and samples at different burnups (Graber et al. 1971; Griebenow 1971; Beeston and Malik 1977). Visual examinations have revealed no plate warping, buckling, gross swelling or blistering, and no cooling channel deformation or blockage at fission densities up to the current burnup limit (2.3×10^{21} fiss/cm^3). The measurements have shown that essentially no plate lengthening takes place, and any swelling that occurs during irradiation leads to increases in plate thickness rather than plate length (see Section 4.2.3.2). Although the potential for buckling from the swelling process is greater than that from thermal expansion, the measured dimensional changes have been insignificant. Consequently, buckling from axial compressive loads developed from thermal or irradiation growth stresses has not been detected in ATR fuel plates.

[a] Fuel plate blistering is discussed in Section 4.2.3.3.

4.2.3.3.2 Blister Resistance—Past experience in the blister testing of irradiated UAl_x fuel plates has shown that blistering results from the accumulation of gaseous fission products, mainly xenon and krypton, in voids adjacent to fuel particles, and the formation of helium gas from the B_4C particles dispersed in the matrix (Francis 1970). As the irradiated plate is heated during blister testing, the gases accumulate and the internal pressure of the gas inside the voids increases. Expansion occurs when the internal gas pressure exceeds the strength of the material.

As discussed in Sections 4.2.1.2 and 4.4.1.2, blister testing performed on previously irradiated ATR fuel plates and samples is the basis for predicting incipient in-reactor failure of fuel plates from blistering. The results have shown that the gas atoms are retained in the fuel core structure, and do not agglomerate appreciably until a temperature of 836°F (720 K) is reached (Beeston et al. 1980). Figure 4.2-15 shows blister temperatures of UAl_x fuel plates as a function of fission density. The good blister resistance of ATR fuel plates is attributed to the good fission gas retention capability of the uranium aluminides (see Section 4.2.3.2).

All fuel plates are subjected to a blister anneal during their manufacture. After a fuel plate has been hot rolled, it is annealed at 900°F (755K) (nominal) for two hours and cooled in air. An ultrasonic inspection of the entire fuel plate is performed following cold rolling to look for debonds or blisters.[a] The presence of blistering can be cause for rejection of the fuel plate.

4.2.3.3.3 Failure Experience—A limited number of fuel plate failures (i.e., breach of the fuel plate cladding leading to fission product release) have been encountered over the years of operation, and the failure trends in recent years have been favorable. When failures have occurred, only small amounts of fission products have been released. Consequently, operation of the reactor has never been interrupted by a fuel plate failure.

Investigation of fission product leaks from fuel elements between 1969 (reactor start-up) and 1978 have shown that the older, standard-type fuel elements were more leak-prone than the zone-loaded (7F) fuel elements used today (Newton 1979). Over the years, several changes have been made in fuel element design, fabrication, and inspection procedures that have improved the performance and reliability of fuel elements. Some of the more significant changes are listed below (Newton 1979).

- Tapered Compacts. The ends of the pressed UAlx-Al compacts (fuel cores) were tapered to reduce the amount of "dog-boning" that occurs during hot rolling. Dog-boning, the thickening of the plate core near the plate ends, results in clad thinning over the dog-bone areas with attendant increased probability of cladding failure via corrosion or cracking.
- Zone Loading. Zone loading, the use of adjusted U-235 loadings in each plate in a fuel element, is designed to produce a more uniform flux distribution in the reactor core. Consequently, flux peaking and hot spot development are minimized.
- Min-Clad Gauging. An ultrasonic minimum-cladding-thickness detection device is used to detect thin spots in the cladding. Rejection of plates with thin cladding reduces the probability of cladding failure.

---

[a] It should be noted that any blisters that form during this anneal are the result of gas entrapped during the plate rolling process, rather than fission gas agglomeration during irradiation.

From reactor start-up in December 1969 through November 1974, a total of 55 fuel elements exhibited evidence of cladding failures as determined by post-cycle visual examination (Newton 1979). Most of the defects were described as "pimples," which occurred in areas of thin cladding (i.e., dog-bone areas), and were caused by breaches of the cladding, allowing stagnant water to become entrapped next to the fuel core. The cause of the breaches may have been microcracks in the thin cladding. In a radioactive environment, the stagnant water dissociates and becomes corrosive to the exposed fuel. The volume increase associated with fuel oxidation produced the pimples.

Soak test analysis has provided more definitive results on leaking fuel elements than visual inspection (Newton 1979). The technique consists of soaking a fuel element in clean water and then counting a sample of the water for I-131 and I-132 radioactivities. A "confirmed leaker" is defined as one where a high-count test result is obtained from an element in a core that demonstrated a rise in stack gas or primary coolant activity. Between 1969 and 1978, 8 confirmed leakers and 42 suspected leakers were identified by soak testing (Newton 1979). There have been 17 confirmed leakers through July of 1996. Table 4.2-5 summarizes the confirmed fission product leakers through July 1996.

It should be noted that several instances have occurred where sharp increases in stack or primary coolant activity could not be traced to a specific leaking element (Newton 1979). One possible explanation was that the leaks were self-healing, perhaps becoming plugged with oxide, so that soak tests did not detect a significant amount of activity. Commercial reactors have had similar experience. Leakers are sometimes hard to find. The usual reason given for not locating a leaking fuel rod or assembly is that it was a pinhole failure that closed up or healed. Detecting the activity over the background levels is also not always possible.

Five confirmed leaky fuel elements have been destructively examined to determine the nature and cause of the failures (Seiffert and Novick 1979; Seiffert 1979; Vinjamuri 1982). In each case, the leaks were believed to have been caused by pinhole failures, which resulted from pitting corrosion.[a] In the latter investigation (Vinjamuri 1982), it was concluded that the failures probably resulted from corrosive attack of the cladding at an existing defect (pit) at a hot spot. Strict primary system chemistry controls and fuel element fabrication requirements have kept pitting corrosion failures to a minimum.

4.2.3.3.4 Burnup Experience—The burnup limit has been extended in steps to a fission density of 2.3×10^{21} fiss/cm^3 of fuel core. The burnup extensions were made possible as a result of favorable irradiation performance data (Graber et al. 1971; Griebenow 1971; Francis 1974a; Beeston and Malik 1977; Beeston et al. 1980). These data consist of postirradiation measurements, both destructive and nondestructive, made on fuel elements and sample fuel plates.

Two 7F fuel elements were operated to high burnup in 1976 and 1977 to demonstrate the feasibility of extending the burnup limit from 1.8 to 2.3×10^{21} fiss/cm^3. The two elements, XA130K and XA135K, were irradiated to calculated peak fission densities of 2.27×10^{21} and 2.30×10^{21} fiss/cm^3, respectively (Durney 1977). Postirradiation examinations indicated that the elements performed satisfactorily (Beeston and Malik 1977). In addition, no defects were found that would lead to incipient failure upon further irradiation.

[a] Pitting corrosion of aluminum cladding is discussed further by Beeston (1978) and Henslee (1980).

Burnups from 1.97×10^{21} to 2.88×10^{21} fiss/cm^3 were achieved during an irradiation experiment conducted in the ETR (Francis 1974a). Nine sample fuel plates covering the range of 7F fuel compositions were irradiated in sodium bonded capsules instrumented with thermocouples. No fuel blistering occurred during irradiation, and the postirradiation examinations revealed that the fuel had sound microstructure, exhibited no more than the theoretically expected swelling, and had excellent blister resistance.

4.2.3.3.5 Fuel Plate Temperatures—The methods used to evaluate fuel plate temperatures are discussed in Section 4.4.2.11.

4.2.3.3.6 Fuel Plate Burnout and Potential Energy Release—As discussed in Sections 4.4.1.1 and 4.4.2.2, the core is protected from reaching critical heat flux (CHF) during Condition 1 and 2 events. Note that the term CHF may be used in this chapter to denote both critical heat flux and flow instability and CHF may be used interchangeably with departure from nucleate boiling (DNB). In the event that CHF should occur, the cladding temperature will rise because of steam blanketing at the fuel plate surface and the consequent degradation in heat transfer. During this time, there is a potential for chemical reaction between the cladding and the steam. However, the energy release resulting from this reaction would be insignificant compared to the power produced by the fuel.

4.2.3.3.7 Coolant Flow Blockage Effects on Fuel Plates—This subject is discussed in Section 4.4.4.7.

4.2.3.4 Fuel Elements. Each fuel plate in a fuel element is supported by and furnishes support to the side plates. Consequently, the element acts as an integral unit, and the deformation of any plate induces deformations and stresses in all the other plates.

4.2.3.4.1 Thermal Stresses—A variety of loads must be sustained by a fuel element. The primary loads are the result of azimuthal and axial thermal gradients developed in the fuel plates during reactor operation. The restraint of fuel plate expansion by the relatively cool side plates produces compressive stresses in the fuel plates. If the thermal stress significantly exceeds the yield strength of the fuel plate, axial buckling may occur. Because the fuel plates are curved, the temperature variation in the azimuthal direction produces a slight change in the radius of curvature rather than azimuthal buckling. As discussed in Section 4.2.1.1, the effect of corrosion product buildup on the fuel plates is to increase temperatures and thermal stresses and decrease structural strength.

Prior to ATR startup, differential thermal expansion tests were performed to determine if compressive thermal stresses would distort or ripple fuel plates clad with 6061 aluminum (Deville 1963; Francis and Tingey et al. 1967a). Deville (1963) subjected sample fuel plates to compressive thermal stresses greater than or equal to those expected during reactor operation. No significant ripples or ripple patterns formed during the tests. In tests conducted in 1966 (Francis and Tingey et al. 1967a), it was found that fuel plate rippling was not obtained until the yield stress of the unirradiated cladding was exceeded substantially. Compression testing of sample fuel plates clad with 6061-O Al, and containing either U_3O_8-Al (Sumpter 1968) or UAl_x-Al (Hayner 1970) cores, showed that the compressive yield strength of composite fuel plates is significantly greater than that of 6061-O aluminum cladding.

The CAM computer code was historically used in the analysis of fuel plate bending stresses and deflections (Moore 1969). The thermal stresses calculated with the CAM code were compared to the operating requirement that the thermal stress in the center half span of the limiting fuel plate, evaluated at temperatures two standard deviations above nominal, would not exceed the unirradiated yield strength throughout the cycle (Section 4.2.1.5). The yield strength was defined at 0.2% offset, which corresponds to a 0.2% plastic strain.

This requirement originated with the operating experience of ETR fuel elements. In the mid 60's the fabrication process of one type of ETR fuel elements was changed to have the fuel plates pinned in place rather than swaged. Fuel plate rippling or buckling was observed in these elements when run at high power to extended burnups (Griebenow, Hanson, and Larrick 1977). The ATR fuel element is resistant to buckling due to its curved fuel plates (allowing for increased plastic strain levels) and the swaged joints can allow slippage between the fuel plates and the side plates (reducing plate stresses).

An updated evaluation was made of the fuel element for a series of temperature profiles simulating the normal operating temperatures plus two standard deviations (Snow 1997). The updated evaluation looked at strain levels in the fuel plates and addressed the stability of the fuel plates as indicated by the strain histories. The evaluation model used finite element methods to predict the response of a fuel element to temperature and flow loadings using ABACUS software. The material properties defined elastic behavior up to the yield point and then simulated a perfectly plastic response for further straining.

The finite element evaluation (Snow 1997) indicates that the geometry of the fuel element is stable (not prone to buckling or tearing) to thermally induced stresses and strains. The plastic strain data shows that the acceptance criteria of 0.2% plastic strain (set to insure against fuel plate buckling) was very conservative, and an updated strain limit of 0.6% will conservatively protect against buckling of fuel plates. The finite element case run with a peak fuel centerline temperature of 559°F resulted in a maximum plastic strain less than 0.4%. The peak temperature of this case is higher than the maximum (nominal plus two sigma) fuel centerline temperature reported in Section 4.4.2.11 for steady state operation.

4.2.3.4.2 Swage Joint Strength—Experiments have been conducted (Lloyd 1989) to determine the force required to initiate relative axial motion in the swage joints of a fuel element. The principal findings were:

- The general force-displacement curve of the joints can be separated into three regions: a linear elastic region prior to the initiation of slip; a post-slip region, wherein the stiffness falls off (but the force required to induce motion continues to rise); and a stick slip region, where the average force drops off slightly in a mechanism controlled alternately by static (high) and kinetic (low) friction.
- There was a wide range of scatter in the data, with variations in the breakaway force as high as a factor of two for joints with no visible differences.
- The fuel plate 1 joint was consistently and significantly weaker than the other joints.
- Environmental factors such as temperature, immersion in water, direction of pull, and length of specimen showed no statistical effect on the results.

- The average breakaway force for the plate 1 joint was 55 lb per linear inch of joint (9.6 N/mm), compared to 356 lbf/in. (62 N/mm) for all other joints.
- The average maximum force for plate 1 was 188 lbf/in. (33 N/mm), compared to 440 lbf/in. (77 N/mm) for the other plates.

This information is significant because the initiation of slip in the joint, and the subsequent maximum force sustainable, puts an upper limit on the amount of stress that can be built up in fuel plates because of the restraint of thermal growth. Experimental force-displacement data (Lloyd 1989) have been incorporated into a three-dimensional finite element model developed to predict the mechanical behavior of fuel elements under steady state (Snow 1997) and accident conditions (Lacy and Thinnes 1991).

During fuel element production, pull tests are performed on swage joint specimens to ensure that the swaging process provides adequate strength perpendicular to the long axis of the fuel element (see Section 4.2.1.3).

4.2.3.4.3 Creep—The three-dimensional finite element model mentioned above was benchmarked by simulating the operating history of an actual fuel element (Lacy and Thinnes 1991). Creep data for 6061-O aluminum were obtained from isochronous stress-strain curves developed by Martin and Weir (1964). Coolant channel thickness measurements were made following hydraulic testing of the element (prior to insertion in the core) and again after a full cycle of irradiation. Differences between calculated and measured channel thicknesses were found to be within the accuracy of the measurements. Creep was shown to be a beneficial effect because it tended to open the coolant channels and reduce fuel plate stresses.

4.2.3.4.4 Flow-Induced Vibration—Detrimental vibration of fuel plates does not occur during normal operation because of the high degree of structural stability inherent in the curved plate design.

4.2.3.4.5 Bowing—The primary cause of deformation in a fuel element is the presence of temperature differentials. Thermal expansion of the hot fuel plates is restrained by the cooler side plates. Because the fuel plates are curved, the resultant axial expansion force is located radially outside the resultant axial restraint force. Hence, a bending moment is generated that causes the fuel element to bow. Adding to this bending moment, there is generally a temperature variation across the element from inside to outside (plate 1 to plate 19), which causes the outer plates to grow longer than the inner ones. Some bowing was observed to occur during hydraulic proof testing. This is thought to be a pressure-induced column effect, rather than a thermal effect (Lacy and Thinnes 1991).

The extent of thermal bowing, analyzed assuming the fuel element to be a simply supported beam (Griebenow, Fillmore, and Moore 1966), was found to be limited only when portions of the side plate extending beyond plate 19 contacted either the beryllium reflector or the neck shim rod housing, depending on the fuel element position in the core. The bowing causes channels 1 and 20 to have an axially varying flow area, which in turn produces a velocity variation within these channels. Based on thermal-hydraulic calculations performed with the MACABRE II code (Griebenow and Richert 1967), it was concluded that thermal bowing would not be detrimental to operation of the fuel elements. Furthermore, detrimental hydraulic deflections resulting from thermal bowing (or irradiation dimensional changes) have not been observed during ATR operation.

Fuel element removal from, or insertion into, the core is occasionally hampered by binding problems. This can be attributed to bowing (and/or irradiation growth) of the fuel elements, flux trap baffles, neck shim rod housing, or reflector blocks. Specific procedures have been developed to ensure that fuel elements with binding problems can be safely removed from or inserted into the core. A modified YA (YA-M) fuel element has been developed to reduce binding problems near the end of reflector life. The side plate width and the T bar thickness have been reduced in the YA-M fuel elements. Specific loading sequences and YA-M fuel elements may be used when binding is encountered.

4.2.3.4.6 Hydraulic Loads—There are small differences in coolant pressure between adjacent fuel element cooling channels. Coolant flow through the core also generates axial pressure on the leading edges of the fuel plates, and drag forces along the fuel plate faces. Lateral pressure differentials are caused by differences in entrance, exit, and friction losses in adjacent coolant channels of different thickness. The largest possible differential pressure occurs across the innermost plate (plate 1) or the outermost plate (plate 19) because the thickness of channels 1 and 20 can vary considerably due to the accumulation of manufacturing tolerances (or bowing). The vents in the fuel element side plates (see Figure 4.2-5) provide interconnection among all coolant channels and thereby reduce lateral pressure differentials. The location and quantity of side plate vents were optimized in an analytical and experimental program started in 1964 (Walker 1964). In-core hydraulic measurements made by Griebenow (1968) showed that pressures acting across the fuel plates are small and should not adversely affect any fuel element that is properly constructed.

All fuel elements manufactured prior to XA567R were tested in the HTF to demonstrate that they were capable of withstanding hydraulic conditions in the reactor (and to provide a protective boehmite coating). The testing consisted of circulating water at nominally 340°F through each element at 120 to 130% of nominal reactor flow for a minimum of 3 hours. Any changes in coolant channel dimensions beyond specification limits or loosening of fuel plates at swage joints was cause for rejection of the element. No fuel element of the current design and manufacturing process was rejected as result of fuel plates shifting during the HTF testing (Fillmore 1995). The current manufacturing process roll swages fuel plates into the side plates. A technical review of the process was performed that showed that the manufacturing process is of sufficient quality to avoid structural integrity failures and that the hydraulic testing can be replaced by quality control checks made during fabrication and receipt inspection (Richins and Miller 1995). These controls were implemented in the manufacturing process starting with fuel element XA094T (Vinnola 1996).

Fuel element fabrication continued during the development of alternatives to the HTF resulting in an inventory of fuel elements fabricated prior to implementing the recommendations of the manufacturing process review and swaging analysis. An assessment of the risk associated with the use of this inventory of fuel elements was made that concluded that there is no change in the risk accepted in the authorization basis (Atkinson 1997) and that these fuel elements could be used.

A request was made to operate with fuel elements not tested in the HTF (Hamilton 1996a, 1996b) and approval was received in May 1996 (Ziemianski 1996).

4.2.3.4.7 Core Restraint Loads—Each fuel element is bottom-supported by a flange on the lower end of the adjacent flux trap baffle. A slot on the flux trap baffle receives a T-bar key on the fuel element lower end fitting for accurate bottom positioning. The upper end of each fuel element is positioned similarly. Thus, the fuel elements are free-standing and not normally subjected to core restraint loads. However, as noted above, fuel elements sometimes bind because of bowing or irradiation growth of adjacent core structures. Prior to installation of Reflector IV, a fuel annulus spreader tool was used to insert or remove bound elements. When the spreader tool was used to insert an element, loads were imposed on the element when the tool is removed. Evaluation of fuel element stresses and deflections following spreader tool removal showed that stresses in the fuel element and pullout forces between the fuel plates and side plates were below allowable values (Harris 1984). In addition, no appreciable closing of the cooling channels was found to occur from use of the spreader tool.

The inspection of the discharged Reflector III beryllium blocks showed some damage that was attributed to the use of the spreader tool and its use was discontinued in Reflector IV. A fuel element loading sequence was developed for use late in the reflector lifetime when fuel element insertion and discharge difficulties develop. Additionally, the use of small fuel elements proved very successful in alleviating refueling difficulties. Small fuel elements were initially selected from the dimensional inspection data for new fuel elements. The YA-M fuel element was developed specifically to alleviate refueling difficulties. The YA-M fuel elements are manufactured to minimum side plate and T-bar tolerances.

4.2.3.5 Incore Control Components. Hafnium is the absorber material used in the OSCC, neck shim rods, regulating rods, and safety rods. The only hafnium components that have the potential to cause reduced safety margins are the safety rod inserts. The hafnium inserts are in the form of curved plates 1/4 in. (0.64 cm) thick by 3-1/2 in. (8.9 cm) wide by 36 in. (91.4 cm) long (see Figure 3.9.4-6). Because only the bottom 3 in. (7.6 cm) of the hafnium plates extend into the core region during reactor operation, the aluminum support structure is largely unaffected by irradiation. The configuration of all hafnium shims and safety rods makes it extremely improbable that a fracture of hafnium would cause a positive reactivity insertion (Livingston 1984).

4.2.3.5.1 Stress Evaluation—The hafnium inserts on the safety rods are the highest stressed of the hafnium components and are subjected to 13.3×10^3 psi (91.7 MPa) maximum tensile stress from thermal, pressure, and deceleration effects (Livingston 1984). Three-point bending tests were performed on hafnium samples irradiated to a fast neutron ($E > 1$ MeV) fluence of 4.6×10^{22} n/cm^2 to determine the yield and ultimate strength of irradiation-embrittled hafnium (Tupper 1984). Of the four specimens tested, one had small void-type flaws in the fracture surface that caused it to fail at a lower stress than the unflawed specimens. On the basis of the bend tests, the ultimate tensile strength of hafnium at the fluence limit (5.0×10^{22} n/cm^2) was estimated to be 112×10^3 psi (772 MPa) without flaws and 68×10^3 psi (469 MPa) with flaws. Dividing these tensile strengths by the maximum applied stress during safety rod insertion yields safety factors of $112/13.3 > 8$ (without flaws) and $68/13.3 > 5$ (with flaws).

4.2.3.5.2 Thermal Stability—The maximum temperature of the safety rod hafnium was conservatively calculated to be 407°F (481 K) for the thermal stress evaluation discussed above (Burr 1976). This temperature is significantly less than the melting temperatures of either the hafnium inserts (4,040°F, 2,500 K) or the 6061 aluminum support structure (1,079°F, 855 K). Hafnium also has a relatively low coefficient of thermal expansion (Polkinghorne and Lacy 1991). As discussed below, the safety rods are designed to accommodate expansion and contraction of the hafnium inserts without causing restraint stresses.

4.2.3.5.3 Irradiation Stability—The deterioration in mechanical properties of hafnium during irradiation is the result of fast-neutron damage and change in impurity content from thermal neutron capture. The microstructure of hafnium is not greatly affected by irradiation. The principal effect is the appearance of a second phase, apparently resulting from measurable amounts of tantalum resulting from the irradiation (Beeston 1977). Gas release is not a concern because no gas is produced by hafnium during irradiation. The property changes of prime concern are embrittlement (loss of ductility) and dimensional stability.

Test results indicate that hafnium essentially loses all measurable tensile ductility by the time the fluence level reaches 1.5×10^{22} n/cm^2 (Livingston 1984). As noted in Section 4.2.1.6, the current hafnium fluence limit (5.0×10^{22} n/cm^2) is based on maintaining a sufficient margin in tensile strength over imposed stresses to accommodate the loss of ductility. Extensive operating experience has demonstrated that almost total loss of ductility can be accommodated by hafnium components.

Hafnium undergoes a contraction in length and an increase in density during irradiation. Shrinkage measurements were made on two hafnium samples irradiated in the ATR to peak fast fluences of 1.06×10^{22} and 1.37×10^{22} n/cm^2 (Beeston 1977). The measured length changes were $\Delta L/L = -0.135\%$ and -0.270%, respectively. Linear extrapolation of the latter to the fluence limit (5.0×10^{22} n/cm^2) yields a maximum $\Delta L/L = -1.0\%$. Because the mounting mechanisms for hafnium components are designed to accommodate expansion and contraction without causing restraint stresses, 1% shrinkage from irradiation is acceptable.

4.2.3.5.4 Chemical Evaluation—As noted in the ASM Metals Handbook (1987), hafnium shares many properties with zirconium, especially its high corrosion resistance. Hafnium resists attack by many chemicals because of the thin, tenacious layer of oxide that forms naturally on the surface of the metal. Corrosion tests performed prior to ATR startup (Koch, Riskevics, and Ritchie 1963) showed the corrosion rate of hafnium to be negligible. Many years of operating experience have confirmed that no corrosion problems exist for hafnium in the ATR.

4.2.3.6 Reflector

4.2.3.6.1 Stress Evaluation—A full-length finite element model of a reflector block is used to determine reflector stresses and predict reflector service life (Fors 1980; Miller and Rahl 1992). The analysis approach is based on the assumption that irradiation-induced swelling can be treated in essentially the same manner as thermally-induced swelling, i.e., thermal expansion (Winkel 1974). Although this assumption may oversimplify the microscopic response, it has been substantiated by comparison with measured and predicted deformations and failures (Winkel 1974; Miller and Rahl 1992). The thermal analogy permits use of the structural finite element code ABAQUS (Hibbit, Karlsson, and Sorensen 1990), which is capable of analyzing thermal stresses and deformations.

Fast flux contours for a given core configuration are calculated using the PDQ-7 neutron diffusion code (see Section 4.3.3). An intermediate code, FLUXTEM, converts flux values to pseudo-temperatures for input to ABAQUS. From Beeston (1976), the change in length, ΔL/L, of beryllium as a function of fast neutron fluence, ϕt, is

$$\frac{\Delta L}{L} = 1.829 \times 10^{-3} (\phi t)^{1.035} \tag{4.2-7}$$

where

ϕ = fast flux (10^{22} n/cm^2·s, E > 1 MeV)

t = time (s).

The standard deviation in the data used to derive Equation 4.2-7 is $\sigma = 6.6 \times 10^{-4}$. Pseudo-temperatures are calculated as follows:

$$T(x,y) = \frac{1.829 \times 10^{-3}}{\alpha} \left[\sum_{i=1}^{n_1} \phi_i(x,y) t_i + \sum_{j=n_1}^{n_2} \phi_j(x,y)_j \right]^{1.035} \tag{4.2-8}$$

where

ϕ (x,y) = two-dimensional flux distribution at core midplane

α = expansion coefficient

n_1, n_2 = operating cycle numbers.

The first summation accounts for the fluence accumulated in prior operating cycles and the second accounts for the fluence increase during the cycles being evaluated. The times, t, are obtained by dividing the megawatt-days (MWd) of each cycle by the average power (MW) during the cycle (with subsequent conversion to seconds). The neutron flux distribution in the axial (z) direction varies as a cosine function; hence, the three-dimensional pseudo-temperature field is computed as follows:

$$T(x,y,z) = T(x,y) \left[\cos \frac{\pi(z - L/2)}{(L + 2d)} \right]^{1.035} + T_0 \tag{4.2-9}$$

where

L = reflector height (51 in., 129 cm)

d = flux extrapolation distance (1.25 in., 3.18 cm)

T_o = reference temperature (70°F, 294 K).

Once the temperature distribution is known, the ABAQUS code calculates stress levels in the reflector block. Miller and Rahl (1992) describe the criteria used to determine when failure (cracking) of a reflector ligament occurs. The tensile strength of irradiated beryllium is calculated using correlations derived from experimental data (Beeston 1976). The reflector lifetime is defined as the operating time in megawatt-days (or equivalent) when a predicted ligament crack is sufficient to loosen a large piece of beryllium from the rest of the block as noted in Section 4.2.1.7.

Lifetime predictions for the reflector are updated periodically (usually yearly after two or three years of initial irradiation). As discussed in Section 4.2.1.7, cracking in the A ligament normally precedes cracking in the B ligament. Consequently, a crack in the B ligament could potentially cause a large piece of beryllium to separate from the rest of the block (see Figure 4.2-8). Therefore, operation of the reflector is limited to ensure that stresses in the B ligament remain at least two standard deviations less than the cracking stress of the ligament unless a specific evaluation is performed to support operation with higher stresses. The benchmark calculations of Miller and Rahl (1992) demonstrate that the PDQ-ABAQUS method of analysis successfully predicts reflector service life. The PDQ-ABACUS method employs an updated cracking criteria based on the material strengths corresponding to the combined states of membrane and bending stresses in the ligament portions of the reflector. Benchmark calculations on Reflectors III and IV showed that an amplifying factor "k" should be applied to the time used in the analysis. The value of "k" is established from the correlation between the analysis and the actual reflector history.

4.2.3.6.2 Thermal Stability—The two-dimensional steady-state and transient heat conduction code SIMIR/6 (Kraus 1977) was used to calculate temperature distributions in the reflector (Mousseau et al. 1973). Heat generation from gamma ray absorption in the reflector was based on a peak (core midplane) value of 24 W/g (for a 70 MW lobe) at the beryllium face next to the fuel element annulus (Nielsen 1973). The heating decreased exponentially away from the fuel. Convective heat transfer coefficients were applied at all fluid interfaces; all solid interfaces were assumed to be adiabatic. Because SIMIR/6 is a two-dimensional code, heat transfer in the vertical direction was neglected. This is conservative because it results in higher beryllium temperatures than would be calculated by modeling axial heat conduction.

The maximum reflector block temperature was computed to be 266°F (403 K) during operation with three primary coolant pumps (Nielsen 1977) and 278°F (410 K) during operation with two pumps (Fillmore 1980). These temperatures are well below the melting temperature of beryllium (2,348°F, 1,560 K). Analyses have shown that thermal stresses have little effect on the life of the reflector (Mousseau et al. 1973). At the time of crack initiation in the first reflector (Reflector I), irradiation growth was responsible for approximately 95% of the stress producing fracture.

4.2.3.6.3 Irradiation Stability—The reflector is subjected to high total exposures of fast neutrons with large flux gradients. These conditions produce dimensional changes and changes in the mechanical strength of the reflector blocks. The formation of gas in the beryllium lattice is by the $Be^9(n,2n)2He^4$ and $Be^9(n,\alpha)He^6$ reactions (Francis and Moen 1966). The result of the flux gradient is a nonuniform concentration of helium in the reflector. Because reflector growth (swelling) occurs from helium in the beryllium matrix, internal stresses are induced to compensate for the nonuniform dimensional change.

Radiation hardening increases the ultimate fracture strength of beryllium to a point where the material becomes so brittle that fracture toughness drops to near zero (Francis 1970). At this point, very small flaws dominate and the fracture strength decreases. Meanwhile, the residual stress increases because of differential growth resulting from the flux gradient. When the loading stress, including residual stress, exceeds the decreasing fracture strength, the beryllium will spall and crack.

Tests performed on beryllium samples irradiated in the ETR and ATR have extended the strength and growth data for beryllium to a fast fluence (E > 1 MeV) of 3×10^{22} n/cm^2 (Beeston 1976). The swelling threshold temperature was measured by annealing the irradiated specimens at successively higher temperatures for one hour. The results showed that a threshold temperature of 572°F (573 K) is required before measurable swelling occurs, and 797°F (698 K) is required before 1% swelling occurs. Thus, runaway swelling (from rapid agglomeration of helium into bubbles) is highly unlikely in the reflector.

The reactivity effects of reflector irradiation are discussed in Section 4.3.2.4.

The following summarizes irradiation experience with the first four reflectors. The experience from the first three reflectors was taken from Tomberlin (1989). The experience from the fourth reflector was taken from (Durney 1987; Holman 1994; Loret 1994).

- Reflector I: The operating period for the first reflector was from February 1968 (Cycle I) to October 1972 (Cycle 15A). Cracks were discovered in three of the eight reflector blocks in March 1972 after 113,593 megawatt-days of reactor operation with a balanced lobe power distribution. All cracks were in the A ligaments and were determined to have initiated at the top of the reflector. It should be noted that Reflector I did not include horizontal saw cuts, which were incorporated in the reflector design beginning with Reflector III. A thorough technical evaluation after the cracks were discovered proved that the reflector could safely continue operating as long as certain restrictions were met. Reactor operation continued, without incident, for another 27,647 MWd; the reactor was then shut down to replace the reflector. Reflector I therefore operated a total of 141,240 MWd. No malfunctions of the moving reactor internal components were experienced and radiation levels in the process systems remained at their normal levels.

- Reflector II: The operating period for the second reflector was from October 1972 (Cycle 15A) to April 1977 (Cycle 35A-1). Reflector II was similar in composition and geometry to Reflector I, but was subjected to reactor power tilts. The greatest power tilt was produced during Cycle 16E when the southwest lobe operated at 55.0 MW and the northeast lobe at 26.2 MW. Reflector II operated for 153,734 MWd. Some control over cracking in the A ligaments was obtained by scribing certain A ligaments to induce cracking.

- Reflector III: The operating period for the third reflector was from April 1977 (Cycle 35A-1) to February 1986 (Cycle 73A-1). The major difference between Reflector III and previous reflectors was the incorporation of horizontal saw cuts in the beryllium blocks (see Figure 4.2-6) to delay buildup of radiation-induced stresses. Inspection of Reflector III during Shutdown 64A-1 revealed the onset of cracking in three saw cut segments in ligament A of one of the beryllium blocks. Shutdown 64A-1 (March 1984) occurred after Reflector III had operated for 228,438 MWd. Reflector III went on to operate for 305,246 MWd, a significant extension beyond the lifetimes of Reflectors I and II.

- Reflector IV: The operating period for the fourth reflector was from February 1986 (Cycle 73A-1) to February 1994 (Cycle 102B-1). Reflector IV was similar in composition and geometry to Reflector III. Reflector IV incorporated four additional 1-1/2-in. B-hole positions (B-9 to B-12) and four additional 1-1/2-in. I-hole positions (I-21 to I-24). Except for these changes, the Reflector IV beryllium segments are identical to the Reflector III beryllium segments. Reflector IV exhibited minor cracking before it was replaced. Reflector IV operated for 267,254 MWd.

4.2.3.6.4 Chemical Evaluation—Reported corrosion results for beryllium often do not seem consistent or reproducible (ASM Metals Handbook 1987). This is perhaps because of past inconsistencies in the quality of metal studied. Stonehouse and Beaver (1965) noted that in low-temperature (< 210°F, 372 K), high purity water, there is little or no corrosion problem with beryllium. The corrosion rate in good-quality, low-temperature water is typically less than 1 mil/yr (0.025 mm/yr) (Wanklyn and Jones 1962).

Corrosion testing of four grades[a] of beryllium was carried out under simulated ATR conditions of temperature (226°F, 381 K) and water flow (45 ft/s, 13.7 m/s) in the out-of-pile section of the ETR G-12 facility (Francis and Moen 1966). After 138 days of exposure, the samples were only slightly tarnished and the corrosion rates for each specimen were nearly identical (~1 mil/yr, 0.025 mm/yr). After 213 days of exposure, the corrosion rates were all less than 1 mil/yr (Beeston and Moen 1966). The corrosion rate of one of the ATR hot-pressed beryllium samples was only 0.66 mil/yr (0.017 mm/yr). In an earlier corrosion study (Koch, Riskevics, and Ritchie 1963), stressed beryllium specimens were found not to be susceptible to stress corrosion in the ATR environment.

Beryllium reflectors were previously used in the MTR and ETR. Like the ATR, the cooling water for these reactors was demineralized in cation and anion resin beds and maintained slightly acidic with small quantities of nitric acid. Beryllium corrosion was not a problem in the MTR or ETR, nor has it been a problem in the ATR.

4.2.4 Testing and Inspection

4.2.4.1 Quality Assurance Program. An appropriate quality assurance program is maintained at the INEEL's Test Reactor Area. It provides for control over all activities of design, procurement, fabrication, storage, testing, inspection, and transportation of ATR fuel elements, reflector and reactivity control system components. The quality assurance program is discussed further in Chapter 17 (Quality Assurance).

The Contractor's drawings and material specifications identify the tests and inspections to be performed.

4.2.4.2 Quality Control. Quality control of core components is achieved by a detailed test and inspection program. Tests and inspections are usually performed by the component supplier, or the supplier's subcontractors. Final inspection and acceptance (or rejection) of core components is made by the Contractor.

---

[a] Two ATR hot-pressed beryllium samples, one extruded sample, and one vacuum cast sample were tested.

4.2.4.2.1 Reflector—Quality control of beryllium components (i.e., reflector blocks and outer shim control cylinders) is achieved by an analysis and inspection program with the following features:

- Prior to fabrication, the proposed procedures for beryllium manufacture, powder processing, casting, and hot pressing are submitted to the Contractor for approval. Sieve tests are performed to verify compliance with particle size requirements (EG&G Idaho 1991a).
- Analyses are performed to ensure that the chemical composition and nuclear properties of each beryllium pressing comply with material requirements (EG&G Idaho 1991a).
- Tests are performed to ensure that the tensile and physical properties of each beryllium pressing conform to requirements (EG&G Idaho 1991a).
- Each rough-machined component is radiographically inspected for internal defects. After final machining, all pressings or components are liquid-penetrant and visually inspected for surface defects (EG&G Idaho 1991a).
- All pressings or components are marked to ensure positive identification and traceability (EG&G Idaho 1991a).
- The finished components, when received onsite, are inspected by Contractor personnel to verify compliance with the above requirements. Inspections are also performed to ensure that all dimensions are within drawing tolerances.

4.2.4.3 Incore Control Component Testing. The mechanical adequacy of the various reactivity control components (i.e., safety rods, neck shim and regulating rods, and outer shim control cylinders) was confirmed by extensive prototype testing (deBoisblanc and Cohen 1965). The prototype safety rod drive mechanism was subjected to more than 1,500 scram cycles under simulated reactor operating conditions. Additional tests were run to investigate the effects of safety rod misalignment and the introduction of probable and accidental concentrations of crud into the reactor. The safety rod mechanism performed satisfactorily in all tests. Scram time was not significantly affected by crud accumulation, and the misalignment tests showed the mechanism capable of satisfactory performance under conditions more severe than expected from maximum tolerance stackup. Wear and corrosion of the safety rod components were also satisfactory.

Minor modifications have been made to the OSCC and safety rod drive mechanisms since the initial prototype testing. The modifications were supported by prototype testing prior to installation. The reactivity control systems are periodically tested for operability and drive speed.

Each new reactivity control component is functionally tested following installation in the reactor, but prior to criticality, to demonstrate that it operates reliably. Prior to reactor startup for each cycle of operation and following an outage in which the vessel has been opened (e.g., a refueling or experiment changeout outage), the safety rods are tested to demonstrate compliance with rod release and drop time requirements.

4.2.4.4 Inservice Surveillance. Surveillance and testing of irradiated core components is discussed in Section 4.2.1.8.

Table 4.2-1. Advanced Test Reactor zone-loaded fuel element 7F: U-235 and B-10 nominal loadings.[a,b,c,]

Plate number	U-235 (g)	Boron (B-10) (mg)
1	24.3	63
2	29.1	78
3	38.7	44
4	40.4	45
5	52.1	0
6	54.6	0
7	57.0	0
8	59.4	0
9	61.8	0
10	64.2	0
11	66.6	0
12	69.0	0
13	71.4	0
14	73.8	0
15	76.3	0
16	64.0	71
17	65.9	73
18	53.8	143
19	52.6	143
	1075.0	660

a. In the 7NB fuel element, boron values are zero. Nominal U-235 values are identical to 7F fuel element, with a total nominal weight of 1075 g.

b. In the YA fuel element, the U-235 and B-10 values are zero for plate 19.

The total nominal weight of U-235 is 1022.4 g and B-10 is 517 mg.

c. A 7NBH fuel element is identical to the 7NB, except B-10 is contained in one or two fuel plates as follows:

Type I has a borated plate 19.

Type II has a borated plate 18.

Type III has borated plates 16 and 17.

Type IV has borated plates 1 and 2.

Table 4.2-2. Fuel element materials, dimensions, and loadings.

Fuel element characteristic	Data
Total Wt. U-235 – grams	1,075[ba]
Fuel loading, U-235 g/cm^3 core	
Plates 1, 2, 18, 19	1.000[b]
Plates 3, 4, 16, 17	1.300
Plates 5 through 15	1.600
Fuel material	UAl_x
Nominal Ual_x concentration	
Plates 1, 2, 18, 19	45% by weight[b]
Plates 3, 4, 16, 17	52% by weight
Plates 5 through 15	60% by weight
Core matrix material	X8001
Burnable poison material	B_4C[c]
Nominal B_4C[c]	
Plates 1, 2, 18, 19	0.53% by weight[b]
Plates 3, 4, 16, 17	0.19% by weight
Plates 5 through 15	0.0% by weight
Total wt. boron (B-10)[c] – grams	0.660[d]
Boron loading, mg natural B/cm^3 core[c]	
Plates 1, 2, 18, 19	14.2[b]
Plates 3, 4, 16, 17	7.5
Plates 5 through 15	0.0
UAl_x chemical composition	
Uranium	69.0 wt% UAl_x powder
Aluminum	8.0 wt% UAl_2
	78.0 wt% UAl_3
	14 wt% UAl_4
Uranium isotopic composition[e]	
U-235 content	93.0 wt% of total U
U-238 content	6.05 wt% of total U
U-236 content	0.7 max. wt% of total U
U-234 content	1.2 max. wt% of total U
B_4C chemical composition[c]	Minimum
B-10	14 wt%
Boron (total)	76.5 wt%
Carbon	19 wt%
Boron plus carbon	98 wt%

Table 4.2-2. (continued).

Fuel element characteristic	Data
Nominal dimensions	
Fuel element length	66-1/4 in.
Fuel plate length	49.5 in.
Active fuel length	48 in.
Coolant channel thickness	0.078 in. (channels 2 through 19)[f]
Plate 1	Thickness 0.080 in. Fuel 0.020 in. Clad 0.030 in.
Plate 19[b]	Thickness 0.100 in. Fuel 0.020 in. Clad 0.040 in.
Plate 2 through 18	Thickness 0.050 in. Fuel 0.020 in. Clad 0.015 in.
Minimum cladding thickness	
Plates 2 through 18	0.008 in.
Plates 1 and 19	0.018 in.
Plate cladding material	6061-O aluminum
Side plate material	6061-T6 aluminum
End fitting material	356-T71 or A356-T6 aluminum
Comb material	6061-T6 aluminum
Weld filler metal	ER 4043 aluminum

a. Fuel elements 7F, 7NBH and 7NB. 1022.4 g for fuel element YA.

b. Plate 19 contains 0 g/cm3 U-235 and B-10 in fuel element YA.

c. Fuel element 7NB contains no burnable poison, 7NBH contains B-10 in 1 or 2 plates only as described in Table 4.2-1.

d. 517 mg for fuel element YA.

e. Variations for U-235 and U-238 are each +1%.

f. Coolant channels 1 and 20 are formed by the interface between the fuel element and other incore components.

Table 4.2-3. Fuel Element Historical Impurity Content.

Fuel Element Component	Historical Impurity Limits
Fuel Cladding, Fuel Frames	
Impurity Limits	wt% maximum
Cadmium	0.003
Lithium	0.008
Cobalt	0.001
Boron	0.001
Fuel Core Component Materials	
Uranium metal	98.5 wt% uranium minimum
Impurity Limits	ppm maximum (wt basis)
Aluminum	100.0
Beryllium	15.0
Boron	5.0
Cadmium	20.0
Calcium	100.0
Carbon	500.0
Cobalt	10.0
Copper	100.0
Chromium	200.0
Iron + Nickel	400.0
Lithium	10.0
Magnesium	50.0
Manganese	30.0
Molybdenum	150.0
Lead	25.0
Silicon	300.0
Sodium	25.0
Aluminum Powder	98.5% free metallic aluminum
Impurity Limits	wt. % max.
Cadmium	0.003
Lithium	0.008
Boron	0.001
Silicon + Iron	0.250
Zinc	0.100
Copper	0.200
Al_2O_3	0.700
Other impurities	0.05
Boron Carbide Powder	98.5 wt% boron + carbon
Impurity Limits	wt% maximum
Iron	0.5
Aluminum	0.2
Calcium	0.25
Magnesium	0.05

Table 4.2-4. Boron Equivalents for Impurities in Uranium Aluminide Powder.

Impurity	EBC (ppm)
Barium	0.000122
Beryllium	0.000015
Boron	0.999999
Calcium	0.000158
Cadmium	0.325097
Chromium	0.000799
Cobalt	0.009239
Copper	0.000868
Iron	0.000672
Lead	0.000011
Magnesium	0.000040
Manganese	0.003443
Molybdenum	0.000403
Nickel	0.001122
Phosphorous	0.000087
Silicon	0.000066
Silver	0.008236
Tin	0.000072
Tungsten	0.001496
Vanadium	0.001406
Zinc	0.000241
Zirconium	0.000029
Samarium	0.524575
Europium	0.433973
Gadolinium	4.194580
Dysprosium	0.097064

Table 4.2-5. Fuel elements confirmed by soak testing to be fission product leakers.

Serial number	Cycle	Cycle end date	Element type	Vendor[a]	Specification	Fuel core material	Soak test activity (10^3 dis/min/ml)	Reference
A504D	26B-1	8/7/75	Standard	AI	Mark V	UAl_x-Al	4970.0 (I-132)	Newton (1979)
A474D	27A-1	9/23/75	Standard	AI	Mark V	UAl_x-Al	152.0 (I-131)	Newton (1979)
A152D	28A-1	11/21/75	Standard	AI	Mark V	UAl_x-Al	1080.0 (I-132)	Newton (1979)
A277D	32B-1	10/5/76	Standard	AI	Mark V	UAl_x-Al	4.4 (I-131)	Newton (1979)
A137C	33A-1	12/8/76	Standard	S	Mark IV	U_3O_8-Al	602.0 (I-131)	Newton (1979)
A211F	35E-1	12/6/77	Standard	NLC	Mark VI	UAl_x-Al	19.5 (I-131)	Newton (1979)
A197F	37A-1	3/26/78	Standard	NLC	Mark VI	UAl_x-Al	7.0 (I-131)	Newton (1979)
XA029HK	39B-1	9/26/78	7F	GUNFC	Mark VII	UAl_x-Al	20.7 (I-131)	Newton (1979)
XA373N	49A-1	10/26/80	7F	AI	Mark VII	UAl_x-Al	46.4 (I-131)	Rowsell and Simpson (1980)
XA374N	49A-1	10/26/80	7F	AI	Mark VII	UAl_x-Al	215.0 (I-131)	
XA377N	49A-1	10/26/80	7F	AI	Mark VII	UAl_x-Al	391.0 (I-131)	
XA379N	49A-1	10/26/80	7F	AI	Mark VII	UAl_x-Al	380.0 (I-131)	
XA446N	62B-1	12/7/83	7F	AI	Mark VII	UAl_x-Al	398.0 (I-131)	Rowsell (1984)
XA159P	89A-1	4/22/90	7F	AI	Mark VII	UAl_x-Al	34.7 (I-131)	Rowsell et al. (1990)
XA118P	93A-1	5/12/91	7F	AI	Mark VII	UAl_x-Al	9.3 (I-131)	Rowsell et al. (1991)
XA122P	96A-1	2/28/92	7F	AI	Mark VII	UAl_x-Al	5.4 (I-131)	Rowsell et al. (1992)
XA211P	98B-1	11/22/92	7F	AI	Mark VII	UAl_x-Al	25.0 (I-131)	Rogers et al. (1993)

a. AI = Atomics International (a division of Rockwell International)
GUNFC = Gulf United Nuclear Fuel Corporation
NLC = National Lead Corporation
S = Sylcor

CHAPTER 4 – REACTOR **UPGRADED FINAL SAFETY ANALYSIS REPORT FOR THE ADVANCED TEST REACTOR**	**Identifier:** SAR-153 **Revision:** 9 **Page:** 4-50 of 4-196 **Effective Date:** 08/10/04

CHAPTER 4 – REACTOR **UPGRADED FINAL SAFETY ANALYSIS REPORT FOR THE ADVANCED TEST REACTOR**	**Identifier:** SAR-153 **Revision:** 9 **Page:** 4-51 of 4-196 **Effective Date:** 08/10/04

CHAPTER 4 – REACTOR **UPGRADED FINAL SAFETY ANALYSIS REPORT FOR THE ADVANCED TEST REACTOR**	**Identifier:** SAR-153 **Revision:** 9 **Page:** 4-52 of 4-196 **Effective Date:** 08/10/04

CHAPTER 4 – REACTOR **UPGRADED FINAL SAFETY ANALYSIS REPORT FOR THE ADVANCED TEST REACTOR**	**Identifier:** SAR-153 **Revision:** 9 **Page:** 4-53 of 4-196 **Effective Date:** 08/10/04

CHAPTER 4 – REACTOR **UPGRADED FINAL SAFETY ANALYSIS REPORT FOR THE ADVANCED TEST REACTOR**	**Identifier:** SAR-153 **Revision:** 9 **Page:** 4-54 of 4-196 **Effective Date:** 08/10/04

CHAPTER 4 – REACTOR **UPGRADED FINAL SAFETY ANALYSIS REPORT FOR THE ADVANCED TEST REACTOR**	**Identifier:** SAR-153 **Revision:** 9 **Page:** 4-55 of 4-196 **Effective Date:** 08/10/04

FOIA Exemption 3 UCNI, Exemption 7f (Pages 4-50 – 4-62 – detailed reactor drawings)

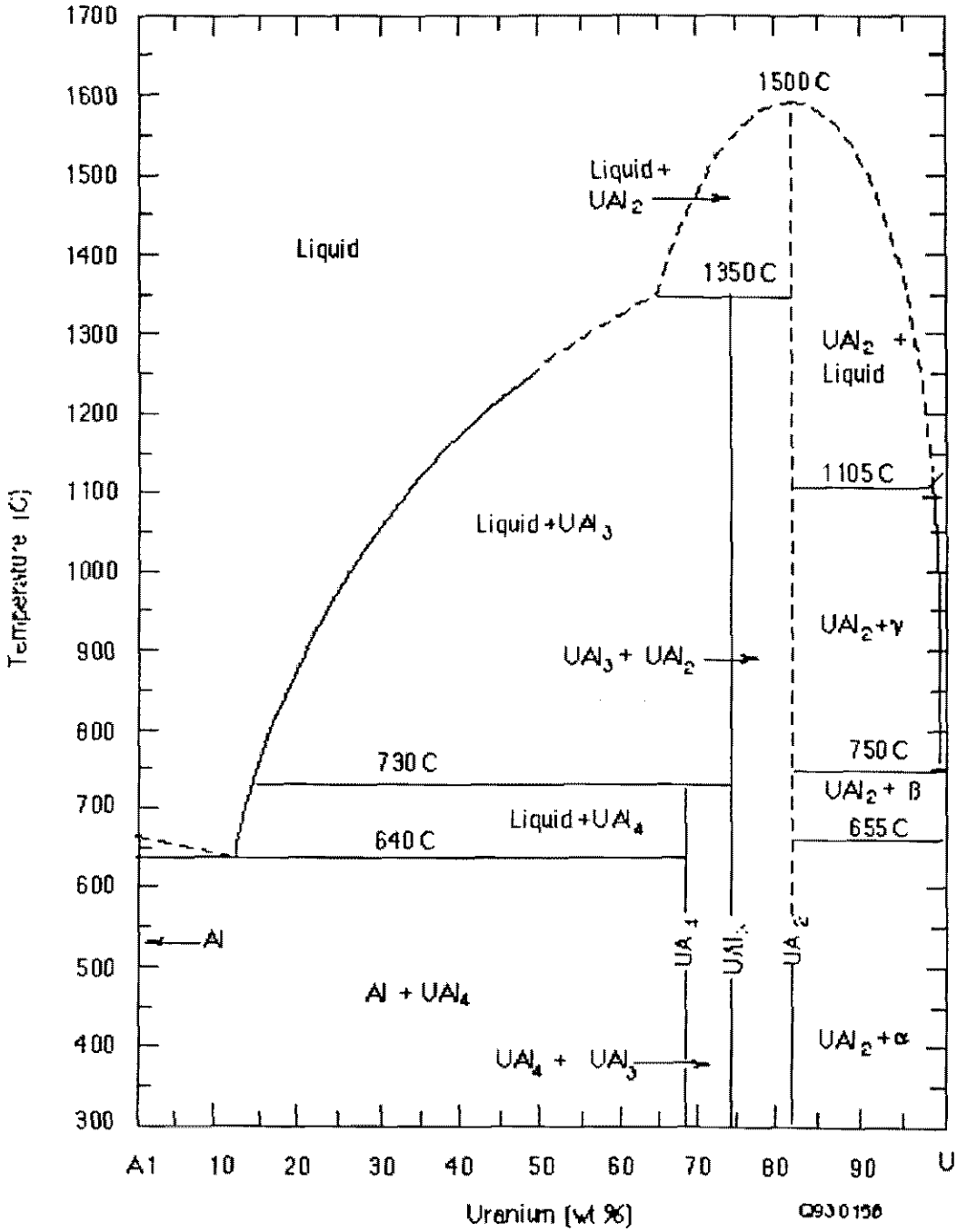

Figure 4.2-13. Phase diagram of the uranium-aluminum system. **(For Information Only)**

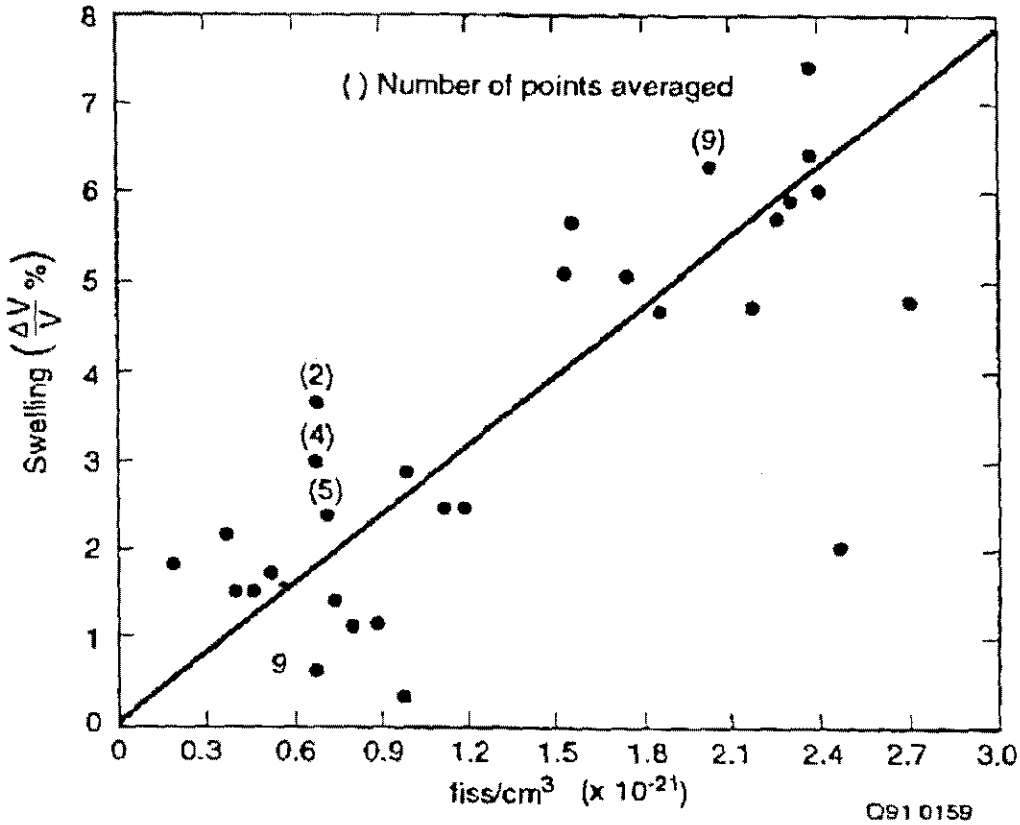

Figure 4.2-14. Swelling of uranium aluminide fuel plates as a function of fission density.
(For Information Only)

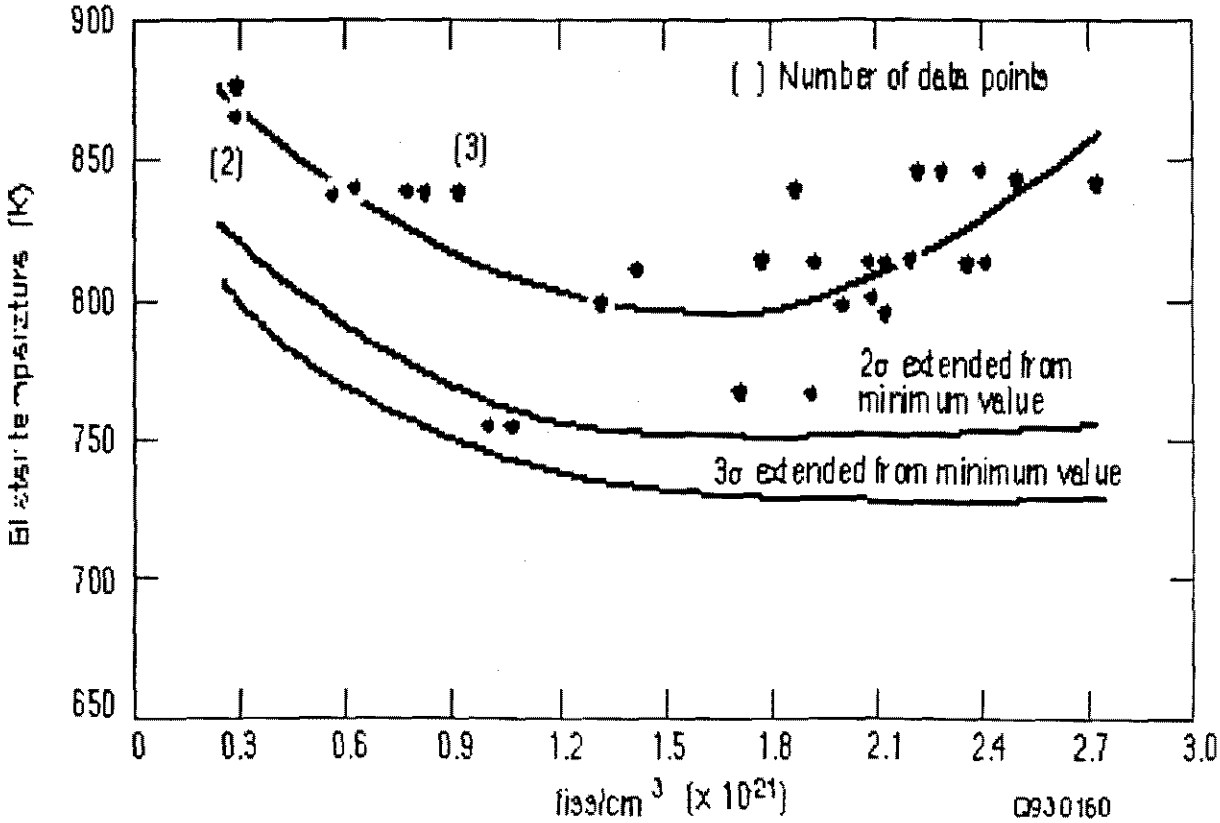

Figure 4.2-15. Blister temperatures of uranium aluminide fuel plates as a function of fission density. **(For Information Only)**

4.3 Nuclear Design

4.3.1 Design Bases

The ATR differs from a commercial PWR in several respects consistent with its purpose as a high neutron flux generator. The steady state overall thermal power is relatively low (100 to 250 MW), but the core is uniquely designed to operate at high power densities (0.96 MW/L average) and in a radially unbalanced condition. The five lobes of the reactor are designed to be operated with a lobe power imbalance ratio of up to four (high lobe power/low lobe power) across the core. As with commercial PWRs, the core loading for a given cycle may contain all fresh fuel elements or a mixture of new and recycled fuel elements. Operating cycles for the core are of short duration, typically running from two to eight weeks between refueling outages. Several independent systems are provided to maintain reactivity control during operations and to maintain the prescribed lobe power split. Multiple experiment facilities are located in and around the core to accommodate various experiment installations.

In this section, the design bases for the nuclear design of the fuel elements and reactivity control systems are described and these design bases are related to the ATR General Design Criteria (GDC) (Chapter 3 (Design of Structures, Components, Equipment, and Systems)). The nuclear design of the reactor core, core power distribution and control of reactivity, ensures that the plant protection criteria of Chapter 15 (Accident Analyses) are met.

4.3.1.1 Fuel Burnup

4.3.1.1.1 Basis—The fuel element design basis is described in Section 4.2. As discussed in Section 4.2.1.2, the maximum fission density in the fuel plates is limited to 2.3×10^{21} fissions/cm^3 to prevent unacceptable irradiation induced swelling.

4.3.1.1.2 Discussion—A combination of new and recycled fuel elements compose the typical core loading at the start of an operating cycle. The cumulative fission densities in the fuel elements are developed as part of the core physics analysis for each cycle. To comply with the requirements on burnup, the maximum fission densities to be reached during the cycle are calculated prior to loading the core and only fuel elements having predicted fission densities less than the limiting value are loaded.

4.3.1.2 Reactivity Feedbacks

4.3.1.2.1 Basis—The fuel and moderator/coolant temperature coefficients of reactivity in the fuel elements are negative for power operating conditions, providing major negative reactivity feedback characteristics. The reactivity feedback is negative during normal operation thus meeting GDC 11. The ATR GDC are presented in Chapter 3 (Design of Structures, Components, Equipment, and Systems).

4.3.1.2.2 Discussion—Temperature effects on reactivity have an important bearing on the operation, and ultimately, on the safety of the system. Doppler broadening of the absorption cross section in the fuel with increasing temperature causes the resonance escape probability to decrease, thereby lowering the effective multiplication factor. Because of the highly enriched uranium in the fuel, the effect of Doppler broadening is small and the fuel temperature coefficient, although negative, is not significant compared to the moderator/coolant coefficient in the fuel region. An increase in the moderator/coolant temperature causes a reactivity change that must be negative to maintain stability and limit the effects of positive transient reactivity insertion events. Moderator temperature coefficients in the fuel regions are negative as required. Void coefficients in the flux traps are positive but their maximum total worth is limited. The reactivity feedback from experiments may or may not be negative depending on the type of the experiments and their location, but the magnitude is small. Additional information is provided in Section 4.3.2.3.

4.3.1.3 Control of Power Distribution

4.3.1.3.1 Basis—Under normal steady state operation, the nuclear design bases are as follows:

- The maximum reactor power will not exceed 250 MW.
- Peak power in the fuel elements will be limited during Condition 1 to values that will maintain the thermal-hydraulic margins (DNB margins) discussed in Section 4.4.1.1 for Condition 1 and 2 events.
- The reactor will not operate in Condition 1 with a power distribution for which any fuel element exceeds the minimum flow instability margins discussed in Section 4.4.1.4 for Condition 1 and 2 events.
- The reactor will not operate with a power distribution that causes the thermal stress limits or blister temperature limits (discussed in Sections 4.2.1.5 or 4.4.1.2) of any fuel elements to be exceeded during Condition 1 operation.

The above basis meets ATR GDC 10.

4.3.1.3.2 Discussion—The lobe power distribution varies from cycle-to-cycle depending on experiment requirements. The operating envelope is determined by the number of primary coolant pumps being operated, the thermal stresses in the fuel, thermal-hydraulic limits, and the degree of aging in the beryllium reflector. The fission power density and related thermal-hydraulic calculations for the operational envelope are performed with proven analytical methods and verified with measurements from the operating reactor. Conservative assumptions are made in developing models for the analysis.

4.3.1.4 Maximum Reactivity Insertion Rate

4.3.1.4.1 Basis—The maximum reactivity insertion rate resulting from postulated failures in the reactivity control systems (i.e., failures resulting in withdrawal of safety rods, neck shim rods, regulating rods or the OSCC) will be limited to rates that result in reactor conditions not exceeding the ATR plant protective criteria, (i.e., controlled by the PPS). This basis meets ATR GDC 25 and ATR GDC 28.

4.3.1.4.2 Discussion—The reactivity insertion rate associated with the failures in the reactivity control systems is determined by the rate of travel or rotation and the worth of the control elements. The worth of the control elements can be affected by the core power division and loading. Control system failures resulting in uncontrolled withdrawal of various combinations of the reactivity control elements are considered in Chapter 15 (Accident Analyses). The insertion rates used in analysis of control system failures are determined in Section 4.3.2.4.

4.3.1.5 Shutdown, Holddown, and Excess Reactivity

4.3.1.5.1 Basis—A minimum safety rod worth is required during reactor operation to provide sufficient shutdown reactivity to bring the reactor into a subcritical state. The maximum excess reactivity is limited to support this basis. The neck shim rods and OSCC provide an auxiliary or backup means of inserting shutdown reactivity.

A minimum holddown reactivity margin is required during outage core changes to provide sufficient reactivity margin from criticality.

This design basis meets ATR GDC 26 and ATR GDC 27.

4.3.1.5.2 Discussion—The shim control systems, including OSCC, neck shim rods, and regulating rods, are used to compensate for the reactivity effects of the fuel and water temperature changes, fuel depletion, experiments, and fission product buildup during reactor operation. The safety rods are designed solely for fast shutdown of the reactor. During startup operation, the core will remain subcritical with all OSCC and neck shim rods (includes regulating rods) fully inserted and all the safety rods fully withdrawn. A sufficient number of safety rods will always be in service to ensure sufficient shutdown reactivity under normal operating conditions with the assumption that the highest worth safety rod remains untripped in its fully withdrawn position. The minimum shutdown reactivity required is 5.8$ for reactor operation with three PCP and 6.4$ for operation with two PCP.

During outage core changes,[a] the effective multiplication of the core (k_{eff}) is maintained less than or equal to 0.95.

4.3.1.6 Stability

4.3.1.6.1 Basis—Spatial power oscillations within the core during power operation are insignificant. The core is stable to power oscillations including those caused by xenon, meeting ATR GDC 12.

---

[a] The manual movement or manipulation of any component within the core reflector tank with two or more fuel elements in the reactor core. The manual movement of components (e.g., safety rods) using their normal drive mechanisms is not considered a core change, however, movement of these components with their drive mechanisms disconnected is considered a core change.

4.3.1.6.2 Discussion—Xenon instability was a concern during the initial design and was extensively studied. The three possible types of xenon instability considered are interlobe, intralobe, and axial. Axial instability, which may be undetectable to the nuclear instruments, was a particular concern and the N^{16} power monitoring system installation included provisions in the center lobe N^{16} tubes to allow detecting anomalies in the axial flux distribution (one center lobe N^{16} tube is full core height and the other center lobe N^{16} tube is half core height). Extensive power variation, neutron noise spectral correlations, and reactor transfer function tests were completed during initial startup. Operating history, analysis, and testing show that the core is stable for power oscillations including xenon oscillations. Reactor power variation is routinely monitored using high speed traces from the nuclear instruments and spectral analyses of the neutron noise. An anomalous power variation would be detected by this monitoring program.

4.3.1.7 Anticipated Transients Without Scram. The effects of anticipated transients with failure to scram are not considered in the Nuclear Design Bases. These events are discussed in Chapter 15 (Accident Analyses).

4.3.1.8 Limits on Experiments

4.3.1.8.1 Basis—The design basis for experiments is such that the consequence limits of any experiment fault shall be consistent with the ATR plant protection criteria.

This design basis meets ATR GDC 70.

4.3.1.8.2 Discussion—Physical, operational, and parametric limits are imposed on any experiment. All the experiments must have adequate safety analysis, independent safety review, management review, and quality assurance for safe operation in the reactor. The experiment safety analysis and review process is described in Chapter 10 (Experiment and Irradiation Facilities). The ATR plant protection criteria are defined in Chapter 15 (Accident Analyses).

4.3.2 Description

4.3.2.1 Nuclear Design Description. The core contains 40 fuel elements in the form of a four-leaf clover. Each fuel element consists of 19 concentrically curved plates attached to two aluminum side plates forming a 45-degree sector of a right circular cylinder. The fuel elements are loaded with highly enriched (93%) uranium in an aluminum matrix and clad with aluminum. The major components of the reactor core having significance to the nuclear design are the neck shim rods, experiment facilities, fuel elements, safety rods, OSCC, and beryllium reflector blocks. Figure 4.2-1 shows a cross-sectional view of the core and the outer reflector irradiation facilities. Experiment facility components located in the flux traps are shown in their configuration following the 1994 CIC. This is the reference configuration for the UFSAR. During 1997 to support the sponsors test program, the northeast flux trap was reconfigured and the Irradiation Capsule Experiment facility installed. The reconfiguration was supported with analyses (Gougar 1998; Schnitzler 1998; Ambrosek 1998) which show the reconfiguration is enveloped by the analyses described in this chapter.

Fresh and/or partially depleted fuel elements are used in an operating cycle core loading to establish the desired core reactivity and the desired lobe and fuel element power distribution. The reactor core normally operates for short durations ranging from two to eight weeks between refueling. The selection of fuel elements is determined by the amount of fissionable material needed to provide the desired core lifetime and lobe power split requirements. The partially depleted fuel elements that are recycled must meet requirements specified in the fuel burnup design basis.

Four different types of fuel elements (i.e., 7F, 7NB, YA, and 7NBH), described in Section 4.3.2.1, are available. All are loaded with uranium that is distributed more heavily in the inner plates and less heavily in the outer plates to reduce radial power peaking. The 7F fuel contains boron as a burnable poison in the fuel matrix of some of the outer plates to further reduce power peaking and to help compensate for reactivity loss due to fuel burnup and fission product buildup in the core. The 7NB fuel element is a non-borated 7F fuel element. The special YA fuel element is the same as the 7F, but does not have fuel or boron in the outermost plate (Plate 19). The YA fuel element is required in positions adjacent to A and E reflector ligaments for high power operation with an aged reflector. The 7NBH fuel element is the same as a 7NB except that the 7NBH contains boron in one or two plates.

The reactor core is loaded to have excess reactivity at the beginning of any cycle to allow for moderator temperature change, the depletion of fuel and burnable poison, experiments in the core, and buildup of fission products including xenon and samarium over the cycle life. The core is loaded to have a nominal 2$ excess reactivity at the end of each operating cycle. The decrease in excess reactivity during an operating cycle is compensated by movable neck shim rods and OSCC. The reactor fuel and moderator temperature coefficients are negative and stay negative during power operation conditions. The buildup of Pu isotopes is not significant in the highly enriched (93%) fuel. Figure 4.3-1 shows a typical buildup of Pu isotopes relative to consumption of U-235 in the center lobe. The burnable poison in the fuel is depleted during operation adding positive reactivity to offset reactivity loss from fuel depletion and fission product buildup. Reactivity change due to boron in the fuel versus core depletion is plotted in Figure 4.3-2.

Summaries of the nominal parameters of the reactor core, including reactivity coefficients, delayed neutron fraction, and control rod worths are presented in Tables 4.3-1 to 4.3-3.

4.3.2.2 Power Distribution. As described in Section 4.3.2.1 and illustrated in Figure 4.2-1, the core contains 40 fuel elements arranged in a four-leaf clover shape entwined around the flux traps that contain the pressurized water loop IPTs or capsule irradiation facilities. Control shims are located both interior and exterior to the core cloverleaf permitting asymmetrical power distributions during operation. The operating power condition is nominally described by specifying the lobe power split where the four corner lobes consist of eight fuel elements surrounding the corner flux traps, and the center lobe consists of eight fuel elements around the center flux trap. The lobes are labeled NW, NE, C, SW, and SE (northwest, northeast, center, southwest, and southeast) as representative of their position in the core. The lobe power split values are often normalized to the total core maximum power rating of 250 MW. The term relative power is used to designate lobe powers normalized to 250 MW as discussed in Section 4.2.2.1.

Because the ATR is designed for neutron irradiation experiments, it operates with variable lobe power distributions and configurations within a safe operating envelope. This section includes three lobe power split variations that demonstrate respectively, balanced, typical or nominal unbalanced, and extreme lobe power splits (Kim and McClure 1993; Judd 1992). These lobe power splits are: a 50-50-50-50-50 (NW-NE-C-SW-SE) MW balanced power split designated as 50/50, a 34-34-43.2-49.1-44.2 MW power split with a total power of 204.5 MW designated as 60/40 (SW relative lobe power of 60 MW, NW and NE relative lobe powers of 40 MW), and a 26.0-26.3-45.7-62-70 MW split with a total power of 230 MW designated as an enveloping 70 MW split. The enveloping 70 MW lobe power split results in the most limiting power distribution expected in the ATR. This distribution has the steepest power gradient and the highest lobe power (70 MW) anticipated in the ATR operation. The total power of 230 MW for the 70 MW split results from the lobe power split with the above constraint, not a limit on the total core power, which is 250 MW.

Due to the nature of ATR operation new experiments are occasionally inserted into the reactor. When new experiments are placed into the reactor, additional analysis is performed to provide assurance that the reactor response with new experiments meets the established safety envelope.

Because of the particular core and fuel element design (see Section 4.3.2.1), power distributions contain axial, radial, and azimuthal components localized by element. Power distributions resulting from analytical calculations by Kim and McClure (1993), were developed for display using the existing operating cycle analysis methods (Smith and Cook 1989) as discussed in Section 4.3.3 and are described in the following sections. Power densities derived from the PDQ analysis reference homogenized regions representing the fuel matrix, cladding, and water mixture. Peak-to-average azimuthal power factors from two-dimensional analyses contain correction factors to convert homogeneous power densities to those based on the fuel matrix volume (Smith and Cook 1989). This correction factor is given by Equation 4.3-1:

$$N_i = [(A * D)/R] * M_i \qquad (4.3\text{-}1)$$

where

N_i = correction factor for the I-th fuel plate

A = correction for nonuniform axial power profile

D = ratio of nominal to calculated lobe power fraction

R = correction factor for non-fueled Plate No. 19

M_i = homogenized cell to fuel matrix correction factor for the I-th fuel plate.

Experimental measurements supporting the calculated values are given and limiting values identified.

These fuel element power distributions were developed with a core model that included a pressurized water loop IPT in each flux trap (LIPTs in the NW and NE flux traps, an advanced high temperature loop IPT in the W flux trap, and standard IPTs in the remaining flux traps). This was the core configuration prior to the 1993 process control upgrade outage. During that outage, three loop facility IPTs (the LIPT in the NW and the standard IPTs in the N and SW flux traps) were removed and replaced with large and standard sized capsule irradiation facilities. Then, during the 1994 CIC outage, the core was configured for capsule irradiation facilities in four of the flux traps and loop facility IPTs in five of the flux traps. The configuration has a large capsule facility in the NE, small capsule irradiation facilities in C, S, and E, an LIPT in NW, the advanced high temperature loop IPT in the W, and standard IPTs in the remaining flux traps (SW, SE, and N). The reconfigurations were supported with analysis (McClure et al. 1993), ATR Critical Facility (ATRC) measurements (McCracken 1993a; McCracken and Loret 1994), and low-power reactor physics testing (McCracken and Yarbrough 1994; McCracken et al. 1994). The results of the analysis, ATRC Measurements and low power testing show that the reactor physics characteristics of the reconfigured core were comparable to those described in this chapter. The ATRC is a low power, full-size nuclear duplicate of the ATR, designed to test prototypical experiments prior to irradiation of the actual experiments in the ATR.

4.3.2.2.1 Radial and Azimuthal Power Distribution—Power distributions are shown with radial effects characterized according to the fuel element plate number (1-19), and azimuthal effects characterized according to relative position across the fuel plates. The power distributions shown are obtained from the 2D analyses because the methods for calculating azimuthal powers are restricted to using the 2D PDQ data with GOPP (Brown 1976). The power distributions over a fuel cycle are illustrated by radial and azimuthal profiles and tabulated values for a sequence of fuel plates and exposure values. The exposure values selected include the beginning-of-cycle (BOC), xenon equilibrium (three full power days), the exposure point where the peak relative power factor occurs, mid-cycle, and the end-of-cycle (EOC). Azimuthal profiles are given for the peak power factor exposure and EOC. The fuel cycle analyses started with all fresh 7F fuel elements in the core (no fission product inventory). The end point of a cycle occurs when criticality cannot be maintained for the reactor at the specified lobe power split. The azimuthal power profiles, in all cases, are representative of the fuel element having the maximum point-to-average power value.

The power distribution in the fuel elements is influenced by the position of the adjacent OSCC and neck shim rods, which affect the radial and azimuthal point-to-average power factors. An asymmetric power shape occurs where the neutron flux in the fuel element is locally depressed by the hafnium in neck shim rods or OSCC when positioned adjacent to the fuel element. This effect is limited to the outer plates in a fuel element and is largest in the plates closest to the OSCC (i.e., Plate Nos. 18 and 19). The azimuthal asymmetry in power decreases with exposure because the OSCC are gradually rotated away from the fuel elements and the neck shims withdrawn to maintain criticality and the lobe power split as the fuel burnup increases.

4.3.2.2.1.1 50/50 Lobe Power Split—The peak point-to-average power density in the core derived from the 50/50 case is located in the NE lobe in Fuel Element No. 9. Total peak point-to-average power densities at the BOC (Day 0), xenon equilibrium (Day 3), middle-of-cycle (Day 17), and EOC (Day 38) are listed in Table 4.3-4.

At the beginning-of-cycle, the peak point-to-average power density is 2.53 at the left edge of the uranium-aluminum fuel matrix in Plate No. 5. Because of the nonuniform axial burnup and flux flattening effects, the peak point-to-average value decreases to 1.66 at the end of the cycle. The point-to-average power density values in Plate No. 5 at the relative azimuthal positions of 10%, 50%, and 90% of the distance from the left edge of the fuel matrix are also given in Table 4.3-4.

The azimuthal power profiles for several of the fuel plates from Element No. 9 at the BOC (0 days exposure) are shown in Figures 4.3-4 through 4.3-7. The asymmetry in the azimuthal power due to the presence of the neck shim rods adjacent to the left side of the fuel element is shown in Figure 4.3-6. Azimuthal power profiles for the fuel plates from Element No. 9 at the EOC (38 days exposure) are shown in Figures 4.3-8 through 4.3-11. The neck shim rods are withdrawn at this exposure level resulting in more nearly symmetric power profiles.

4.3.2.2.1.2 60/40 Lobe Power Split—The peak point-to-average power density in the core from the 60/40 case is located in the SW lobe in Fuel Element No. 23. Total peak point-to-average power densities at the BOC (Day 0), xenon equilibrium (Day 3), middle-of-cycle (Day 17), and at the EOC (Day 31) are listed in Table 4.3-5. At the BOC, the peak point-to-average power density is 2.81 at the left edge of the uranium-aluminum fuel matrix in Plate No. 15. Because of the nonuniform axial burnup and flux flattening effects, the peak point-to-average value decreases to 2.20 at the EOC. The point-to-average power density values in Plate No. 15 at the relative azimuthal positions of 10%, 50%, and 90% of the distance from the left edge of the fuel matrix are also given in Table 4.3-5.

The azimuthal power profiles for several fuel plates from Element No. 23 at the BOC (0 days exposure) are shown in Figures 4.3-12 through 4.3-15. The small amount of azimuthal asymmetry present in the outer fuel plates is due to the presence of an OSCC near the right edge of the assembly. Azimuthal power profiles for the fuel plates from Element No. 23 at the EOC (31 days exposure) are shown in Figures 4.3-16 through 4.3-19. The OSCC have been withdrawn at this exposure level resulting in nearly symmetric power profiles.

4.3.2.2.1.3 Enveloping 70/20 Lobe Power Split—The peak point-to-average power density in the core from the Enveloping 70 MW case is located in the SE lobe in Fuel Element No. 18. Total peak point-to-average power densities at the BOC (Day 0), time when peak value occurred (Day 1), Xenon equilibrium (Day 3), mid-cycle (Day 10), and EOC (Day 17) are listed in Table 4.3-6. The BOC peak point-to-average power density is 3.59 at the left edge of the uranium-aluminum fuel matrix in Plate No. 15 increasing to 3.69 at the 1 day exposure point and decreasing to 3.27 at the EOC. The point-to-average power density values in Plate No. 15 at the relative azimuthal positions of 10%, 50%, and 90% of the distance from the left edge of the fuel matrix are also given in Table 4.3-6.

The azimuthal power profiles for several fuel plates from Element No. 18 at the Day 1 exposure point (peak azimuthal power factor) are shown in Figures 4.3-20 through 4.3-23. The azimuthal profiles in this fuel element near the BOC are nearly symmetric because the OSCC are initially withdrawn from the fuel elements in the lobe to obtain the specified power split. Azimuthal power profiles for the fuel plates from Element No. 18 at the EOC (17 days exposure) are shown in Figures 4.3-24 through 4.3-27.

4.3.2.2.2 Fuel Element Power Distribution—Power generation in the fuel elements is determined in both the 2D and 3D analysis cases by integrating over the plate volume in the fuel elements with the power given in megawatts. The fuel element power values are normalized to a total core average of unity resulting, respectively, in relative XY and XYZ point-to-average element power factors. The XYZ power values are also integrated axially to obtain the average fuel element power factors from the 3D analysis for comparison with the XY values from the 2D analysis. Critical control shim positions at the specified lobe power splits are determined at each exposure step in the 3D analysis cases, and the same shim positions are input into the 2D PDQ model to provide a basis for comparing the power distributions.

4.3.2.2.2.1 50/50 Lobe Power Split—The OSCC and neck shim positions used to achieve the balanced lobe power split in the 3D PDQ depletion runs are summarized in Table 4.3-7. For this case, the OSCC positions start at 56.6 degrees with all neck shim rods inserted except the regulating rods. The OSCC are rotated out and neck shims withdrawn as the cycle progresses to compensate for the reactivity loss as the fuel burnup increases. To maintain the balanced lobe power distribution, the 16 OSCC are all moved when necessary by the same rotational increment.

The lobe and fuel element power values obtained from the 2D and 3D PDQ analyses are shown in Figures 4.3-28 and 4.3-29. Total core power for all exposure steps in the case is 250 MW. The power distribution at the BOC (0 days exposure) is shown in Figure 4.3-27. Fuel elements generating the largest power levels are located in the center lobe where the peak value of 7.22 MW occurs in Element No. 20. The axial peaking factor in the fuel element is 1.43, and the element-averaged x-y peaking factor is 1.16. Power values at the EOC (38 days exposure) are shown in Figure 4.3-28 where the peak value is 6.72 MW in Element No. 40. The axial peaking factor in the fuel element is 1.14, and the element-averaged x-y peaking factor is 1.08. Because the lobe power split is balanced among the lobes, power levels are nearly the same in several fuel elements causing the location of peak values to vary among the fuel elements. (Note that the azimuthal peak point-to-average power density is located in Element No. 9, while the peak integrated element power occurs in Element No. 20.)

4.3.2.2.2.2 60/40 Lobe Power Split—The OSCC and neck shim positions used to achieve the 60/40 lobe power split in the 3D PDQ depletion runs are summarized in Table 4.3-8. For this case, the OSCC are positioned to obtain the lobe power split with all neck shim rods inserted except the regulating rods. The OSCC are rotated out and neck shims withdrawn as the cycle progresses to compensate for the reactivity loss as the fuel burnup increases. The OSCC are positioned to maintain the lobe power split throughout the cycle.

The lobe and fuel element power values obtained from both the 2D and 3D PDQ analyses are shown in Figures 4.3-30 and 4.3-31. The total core power for this case is 204.5 MW limited by the LIPT thermal load capacity in the NW and NE lobes. Power values in the fuel elements at the BOC (0 days exposure) are shown in Figure 4.3-29. Fuel elements with the largest power levels are located in the SW lobe with a peak value of 6.86 MW occurring in Element No. 23. The axial peaking factor in the fuel element is 1.44, and the element- averaged x-y peaking factor is 1.34. Power values at the EOC (31 days exposure) are shown in Figure 4.3-30 where the peak value is 6.64 MW in Element No. 23. The axial peaking factor in the fuel element is 1.24, and the element-averaged x-y peaking factor is 1.33.

4.3.2.2.2.3 Enveloping 70 MW Lobe Power Split—The OSCC and neck shim positions used to achieve the enveloping 70 MW lobe power split in the 2D and 3D PDQ depletion runs are summarized in Table 4.3-9. For this case, the OSCC are positioned to obtain the lobe power split with all neck shim rods inserted except the regulating rods. The OSCC are rotated out and neck shims withdrawn as the cycle progresses to compensate for the reactivity loss as the fuel burnup increases. The OSCC are positioned to maintain the lobe power split throughout the cycle.

The lobe and fuel element powers obtained from both the 2D and 3D PDQ analyses are shown in Figures 4.3-32 and 4.3-33 where the total power is 230 MW. The core power for this case is limited by the SE lobe thermal load capacity. Power values in the fuel elements at the BOC (0 days exposure) are shown in Figure 4.3-31. Fuel elements with the largest power levels are located in the SE lobe where the peak value of 9.43 MW occurs in Element No. 18. The axial peaking factor in the fuel element is 1.45, and the element- averaged x-y peaking factor is 1.64. Power values at the EOC (17 days exposure) are shown in Figure 4.3-32 where the peak value is 9.62 MW in Element No. 17. The axial peaking factor in the fuel element is 1.26, and the element-averaged x-y peaking factor is 1.67.

4.3.2.2.3 Axial Power Distribution—Axial distributions of the relative fuel element power factors from the 3D PDQ analysis cases described above are shown in Figures 4.3-34 through 4.3-36 for BOC and EOC exposures. The peak XYZ point-to-average power factor, in all cases, occurs at low exposure levels (0 to 3 days) where the axial profiles most closely approximate a cosine function. These factors are 1.69 for the 50/50 case, 1.95 for the 60/40 case, and 2.40 (2.37 at 0 days exposure) for the enveloping 70 MW case. The axial distributions become flattened after three days exposure (Xe equilibrium) as the fuel burnup increases, which decreases the point-to-average power factors. The peak power factors from the EOC exposure cases are 1.24, 1.55, and 2.10, respectively, for the above cases.

Peak fuel plate temperatures, analyzed with thermal feedback in the 3D PDQ model, occur at BOC where the power peaking factors are at a maximum. Temperatures in the hot channel from the enveloping 70 MW case are illustrated in Figure 4.3-36 as a function of coolant flow rate. At 100% of rated flow conditions, plate temperatures reach 325°F rising to 342°F for flow rates at 90% of the maximum rate.

4.3.2.2.4 Local Power Peaking—The fuel element design (see Section 4.2) uses fully enriched U-235 in a UAl_x-Al dispersion with deliberate voidage. The dispersion is clad with aluminum. The fuel element fabrication process verifies that fuel non-homogeneity is within the acceptable limits. The UAl_x-Al matrix does not permit uranium densification or formation of non-fueled gaps in the fuel matrix during irradiation. Therefore, local power peaking effects as a result of fuel irradiation will not occur. Local power peaking effects occur near the fuel plate edges in the azimuthal direction, as described above, due to the fuel element side plates and water gaps between elements. Local peaking also occurs axially in the fuel elements because control elements in the core are designed to maximize the neutron flux as well as limit axial flux perturbations. These peaking factors are described in the above sections. Alternative fuel element types, as described in Section 4.3.2.1, are used to minimize possible externally induced power peaking such as may develop from failed reflector ligaments.

Local power peaking in fuel elements may occur from loading errors where a non-borated (type 7NB) element is loaded in place of a 7F type, or in fuel elements near experiment holes or flux traps where the experiment has axially varying compositions. These factors have been investigated with sensitivity studies done with the zero exposure enveloping 70 MW PDQ model. Conservative cases were used in the studies to maximize any flux peaking effects. Peaking factors from loading errors were investigated by replacing all the 7F type fuel elements in the high power lobe with other types. Exchanging 7F type fuel elements with alternate types resulted in a maximum azimuthal point-to-average power density of 3.88 relative to the reference value of 3.57. These values are not absolute maximum values for every possible condition. But conformance to the UFSAR envelope is ensured by limiting the effective plate powers set in Chapter 15 (Safety Analysis).

The effects of axial variations in the experiment were investigated by using a conservative high-low-high axial variation in a neutron absorber composition in the experiment locations. The maximum effect on power peaking factors from varying experiment compositions resulted in an XYZ point-to-average peaking factor of 2.55 relative to the reference value of 2.37.

4.3.2.2.5 Limiting Power Distributions—The enveloping 70 MW lobe power split represents the steady state power distribution having about the largest power gradient obtainable resulting in maximum power densities and peaking factors. The values of these peaking factors for normal operational conditions are described above. The buildup and decay of fission product poisons during scram recovery periods will distort the equilibrium power distributions, which may result in distributions with peaking factors exceeding those from nominal conditions. The low excess reactivity in the core effectively limits recovery to a short period following a scram or requires waiting several hours to allow the Xe-135 to decay. Several time periods, which follow a scram from an equilibrium Xe-135 condition (three days exposure) and are consistent with the above time constraint, have been analyzed for the effect of fission product concentrations on peaking factors. These results are shown in Table 4.3-10 and, in all cases, the peak power densities do not exceed a reference value of 3.63. Thus, the limiting power distributions are encountered at BOC in fresh fuel.

4.3.2.2.6 Experimental Verification of Power Distribution Analysis—The power distribution in the core is monitored during operation with ex-core detectors as described in Section 4.3.2.2.8. The fuel element power distributions described in previous sections are derived with the analytical methods described in Section 4.3.3.1. The analysis methods have been benchmarked (Kim and Judd 1991) against the low-power experimental measurements of the specific power (W/kg) with fission rate monitors performed after the 1986 CIC (Dwight et al., 1986). The measured data are from fission rate monitors that were loaded in the fuel element water channels to map fission rate profiles at core midplane and axially. The mean relative error in the 2D PDQ results at core midplane is +2.6 ± 9.3% where the relative error is defined as (PDQ - measured)/measured. The 3D benchmarking analysis cases included both flux synthesis and explicit solution methods. The mean relative error in the 3D results is -1.6 ± 9.3% for the synthesis methods and -0.3 ± 9.0% for the explicit solution methods.

Errors between fuel element powers calculated with the 2D PDQ and measurement were shown to be less than 5.9 percent for all elements except the tip core positions in the corner lobes. The errors for these positions ranged from 8.1 percent low to 7.8 percent high. Results with the 3D synthesis gave a difference of 6.2 percent for all elements except the tip elements which ranged from 8.3 percent low to 8.5 percent high. An analysis of errors in the measurement technique (Durney 1967) showed that the magnitude of the measurement error, depending upon position, varied from 0.5 to 4.0% with an additional azimuthal positional error in Channel 19 of ± 0.06 in.

4.3.2.2.7 Precycle Testing—The operating cycle length is short and variable (about 2 to 8 weeks) as described in Section 4.3.1, necessitating frequent reloads. Control shim positions at criticality for each cycle after a core change are predicted prior to start-up. Administrative controls require the reactor to be shut down if the absolute difference between the calculated and actual shim positions at criticality exceeds a specified limit.

Nuclear testing is completed after installation of each reflector and after significant core reconfigurations. The test program and results from testing after the installation of Reflector V are in McCracken et al. (1994). This testing included mapping of the core power profile, calibration of the reactivity control elements, isothermal temperature coefficient measurements, and verification of the core physics model for operating cycle analysis.

4.3.2.2.8 Monitoring and Control Instrumentation—The monitoring instrumentation significant to this chapter on the reactor is the nuclear instrumentation, the power monitoring instrumentation, and the control instrumentation for the reactivity control systems. The reactor instrumentation systems provide the information necessary to ensure safe operation during outage core changes and from start-up through full power operation. This instrumentation provides plant protective (scram) functions in the event of accidents, malfunctions, or detector responses outside the range of acceptable values; plant control functions (reactivity control system interlocks and power control functions); and information about the lobe power distribution to ensure that the reactor is operating at the prescribed power levels throughout an operating cycle. Design and system descriptions for all of this instrumentation are contained in Chapter 7 (Instrumentation and Controls).

4.3.2.2.8.1 Nuclear Instrumentation—The nuclear instrumentation includes the log count rate metering system, log-N period system, PPS neutron level subsystem, PPS wide range neutron subsystem, and neutron level Channel 8. These systems provided monitoring and indication of the neutron flux level for outage core changes and from the source range through the full power range, plant protective functions, and reactor control system functions. The nuclear instrumentation detectors are located in the reactor instrument thimbles outside the core reflector tank as illustrated in Figure 4.3-37. Redundancy in the monitoring systems provides enhanced safety through high reliability and multiple defenses against failure.

The neutron flux level in the core during outage core changes and in the source range during reactor start-up is monitored by fission chambers in the log count rate metering system. Two independent channels are provided for this monitoring system, thus enhancing reliability through redundancy. The fission chambers can be positioned via a drive mechanism to maintain the indication on-scale. These systems provide audible, visual, and recorded information on the subcritical neutron flux level. The log count rate metering system is the most sensitive to low neutron levels (10^{-11} N_F to 10^{-5} N_F) present in the source range and during startup and will respond rapidly to small changes in neutron population. Thus, it is a required system with indication available to the operators during core changes and during the initial withdrawal of reactivity control elements during reactor startup.

The neutron flux level and its rate of change in the intermediate reactor start-up range to full power range (instrument range from 10^{-7} N_F to 10 N_F) are monitored by compensated ion chambers in the log-N period system. The log-N period system is also used for primary indication of reactor power level during depressurized reactor operation. Two independent channels are provided for this monitoring system, thus enhancing reliability through redundancy. These systems provide visual and recorded information on the neutron flux level and reactor period. The PPS wide range neutron subsystem also provides indication of neutron flux level from the intermediate range through full power range.

During power operation, the neutron flux level is monitored by the PPS neutron level subsystem, neutron level channel 8, and the PPS wide range neutron subsystem. Each PPS subsystem has three independent data channels. These channels have ion chambers located adjacent to the NE, NW, and SE lobes. Neutron level channel 8 provides a fourth neutron level channel adjacent to the SW lobe. This arrangement provides indication of neutron level in all four corner lobes of the core. The wide range neutron subsystem covers the range from 10^{-6} N_F to 1.5 N_F. The neutron level subsystem covers the range from 1×10^{-4} N_F to 1.5×10^{-2} N_F in the depressurized operating mode, and from 0.005 N_F to 1.5 N_F in the pressurized operating mode. The PPS neutron level and wide range neutron subsystems provide plant protection (scram) on high neutron level. The PPS wide range neutron subsystem also provides the protective function on high rate of change of flux level over its full range (10^{-6} N_F to 1.5 N_F).

4.3.2.2.8.2 Lobe Power Monitoring Instrumentation—Lobe powers are determined from data from the water power calculators and the N-16 power monitoring system. Output from these two systems is reduced by the reactor data acquisition system (RDAS) yielding the lobe powers. The resulting lobe powers are displayed to the reactor operator on the console display system. These systems together make up the lobe power calculating and indicating system.

The N-16 power monitoring system has ten data channels, which are sensitive to the fast neutron flux through the production of N-16 from O-16 in water flowing through incore reentrant tubes. The activated water from the reentrant tubes is routed through a bank of ten separate beta detectors to measure N-16 activity. Signals from the detectors are proportional to the β activity in the activated water and thus to the local fast flux and the power near the ten reentrant tubes. The signal from each detector is sent to the RDAS for processing. The data reduction process involves a least-squares matrix inversion of ten equations (one for each reentrant tube/detector channel) for the five lobe powers. The locations in the ten reentrant tube assemblies are shown in Figure 4.3-38. Each sample tube consists of an inner and outer flow path where the water flows from the bottom of the core through the outer tube, reverses, and flows back down the inner tube, making a double pass through the core. One of the center sample tubes extends only to the core center line while all others extend to just above the active core. A diagram of an N-16 sample tube is shown in Figure 4.3-39.

Two water power calculators monitor the core power derived from the flow rate and temperature rise across the core. The water power calculators determine the total core and quadrant[a] water (thermal) power. At power levels with significant thermal powers, the sum of lobe powers determined from the N-16 power monitoring system is constrained to be essentially equal to the water power.

4.3.2.2.8.3 Control Instrumentation—The control instrumentation of significance to this chapter includes the regulating rod servo control system, the control power reduction system, the position indications for the various reactivity control elements, and the plant control system interlock and permissive circuits. The regulating rod servo control system provides automatic power level control during power operation. The servo control system is designed to automatically regulate reactor power in the power range (i.e., 1 to 100% of full power). Automatic control is achieved with an ion chamber measuring reactor power, and a closed-loop control system that positions a regulating rod to maintain the desired power level. There are two complete, independent control channels: one is typically in standby to minimize downtime due to control system failures. The regulating rod servo control system automatically regulates reactor power over long periods of time. The regulating rod servo control system also allows the operator to take manual control of the two regulating rods.

The control power reduction system consists of monitoring channel and actuating circuits that provide control power reduction and alarms. These functions complement the PPS and enhance the ability of the reactor operator to maintain reactor conditions within desired limits without invoking PPS action. The power reduction actions are 1) a setback which is a lowering of the regulating rod servo control system setpoint at a controlled rate and 2) a reverse which is an insertion of all OSCC and withdrawn neck shim rods at the nominal drive speed. Additionally, all OSCC and withdrawn neck shim rods will automatically insert after a 25-minute time delay after a PPS scram. Signals resulting in setback and reverse actions are discussed in Chapter 7 (Instrumentation and Controls).

The control system includes indication of the position of each of the reactivity control elements (safety rods, OSCC pairs, neck shim rods, and regulating rods). Both position indication and upper and lower limit switches are provided. The position indications are used by the reactor operators for reactor control.

---

[a] A quadrant is a portion of the core consisting of 10 fuel elements cooled by approximately one fourth of the total core flow. Core flow is divided into quadrants by the primary coolant system flow path in the reactor vessel. The quadrants are designated NW, NE, SW, and SE.

The plant control system interlock and permissive circuits interact with the reactivity control element drive mechanisms to restrict positive reactivity insertions to safe and controllable rates. Safety rod, OSCC, and neck shim rod withdrawal is blocked when reactor power < $10^{-5}N_F$ (log-N indication) if both log count rate channels go off-scale or if a log count rate metering system fission chamber is moving. When the log-N indication is less than 10^{-5} N_F, safety rod, neck shim rod and OSCC withdrawal is restricted to intermittent (one out-of-five second timer) and group neck shim rod withdrawal is permitted. When the log-N indication is greater than 10^{-5} N_F, continuous safety rod, neck shim rod and OSCC withdrawal is permitted and group neck shim rod withdrawal is inhibited. When the reactor is above $10^{-5}N_F$ log-N indication, withdrawal is limited to one rod at a time. The greater than $3N_L$ signal is also sent to the RDAS where it is used to initiate constrained or unconstrained lobe power display. If either log-N is above $3N_L$, the lobe power display is constrained to the water power.

4.3.2.3 Reactivity Coefficients. The overall core reactivity coefficient is negative with respect to power increases providing a stable control environment. Reactivity feedback effects in the reactor fuel annulus arise from fuel element moderator density variations with temperature and fuel element thermal expansion. The dominant feedback mechanism is the fuel element moderator feedback which is strongly negative. Fuel element thermal expansion also results in a negative feedback, but the magnitude is small. The reactivity feedback from changes in coolant density in many of the experiment facilities is positive (i.e., positive reactivity inserted for density reductions or temperature increases). The effects of coolant density changes in the experiment loop facility IPTs are of particular interest since these facilities have cooling systems that are separate from the PCS. Off-normal conditions in the loop facilities can result in positive reactivity insertions. The reactivity addition from voiding a loop facility is limited to values for which the probability of exceeding the limits of the established safety envelope is small. The reactivity worth and feedback of the experiments are determined by calculation and/or measurement in ATRC prior to operation of the experiment to ensure compliance with all safety limits and criteria. The required evaluation of experiments is described in Chapter 10 (Experiment and Irradiation Facilities).

Due to the nature of ATR operation new experiments are occasionally inserted into the reactor. When new experiments are placed into the reactor, additional analysis is performed to provide assurance that the reactor response with new experiments meets the established safety envelope.

The preparation of this UFSAR included development of a RELAP5 reactor kinetics model (Judd and Terry 1992). The development of this model included reviews of experimental and analytical work used in the development of earlier reactor kinetics models (ANC 1973) and new analytical work (Judd and Terry 1992). The moderator feedback is dependent on operational variables like lobe power split, OSCC position, fuel element type and depletion. The model development considered these factors and resulted in reactivity coefficients that represented several core configurations. As discussed in Chapter 15 (Accident Analyses), application of the kinetics model in the accident analyses included selecting a conservative set of feedback coefficients for the accident sequence. The same methodology employed in developing the reactivity coefficients for the detailed reactor kinetics model was applied to develop global reactivity coefficients for presentation in this chapter.

The analyses of accident sequences included consideration for positive reactivity insertion from the experiments both as an initiating event and from positive feedback added during reactor power or PCS temperature transients (i.e., reactivity insertion accidents and PCS flow coastdown). The positive reactivity addition during a reactor power transient is called cascading feedback. The experiment facility reactivity insertions and feedback values used in the accident analyses are assumed values that become limits or envelopes for the operation. This approach is taken because these reactivities and feedbacks are complicated functions of various operating conditions. Worst-case conditions do not occur simultaneously in all experiment facilities so an envelope is established and the planned operation is compared to the envelope.

The lobe power split, fuel element and experiment facility loadings are routinely changed as required by the irradiation programs. Because of these varying conditions, reactivity values and coefficients will vary from cycle to cycle. The experiment loading and planned operating conditions for each operating cycle are carefully analyzed prior to start-up to ensure that the parameters are within the prescribed range and that the probability of exceeding established safety envelope limits is small. In addition, a full-scale critical facility (ATRC) is available for measuring the reactivity worth of experiments as necessary.

Temperature reactivity coefficients for the fuel and moderator/coolant are presented for a set of three power distributions used in the development of the reactor kinetics model (Judd and Terry 1992). These power divisions range from a near balanced 60/40 MW split to a limiting 70/30 MW lobe power split where the lobe power is normalized to a total core power of 250 MW. The reactivity coefficients are derived from results obtained from a three-dimensional (3-D) PDQ-7 model utilizing thermal-feedback effects in the fuel element cross sections. The base PDQ-7 model used in this analysis is described in Section 4.3.3. The resulting reactivity coefficients are listed in Table 4.3-11 for conditions representing all new 7F fuel elements at full power xenon equilibrium and with OSCC withdrawn. The configuration of OSCC substantially withdrawn results in minimum reactivity coefficients.

The fuel temperature reactivity coefficients in Table 4.3-11 include increased resonance absorption from Doppler broadening of the cross sections, but Doppler coefficients are not specifically evaluated. The Doppler components of the fuel temperature coefficients are small because the fuel elements contain uranium highly enriched in U-235.

Density coefficients of reactivity are derived for the fuel element volume from differences in PDQ 7 eigen values between a base and a perturbed density case for each of three lobe power split conditions. These values are listed in Table 4.3-11 under the column heading "Eigenvalue". Global reactivity coefficients for both moderator density and fuel temperature are also derived for the same set of cases by applying perturbation theory methods to the perturbed data. These latter values are listed in Table 4.3-11 under the column heading "Perturbation". Perturbations are made in the feedback variables by modifying the appropriate values in the fuel element cross section model. A delayed neutron fraction (β_{eff}) of 0.0072 (ANC 1973) is used to convert reactivity in this section from units of "delta rho" to dollars. This value for β_{eff} is the best-estimate value for BOC conditions. The moderator temperature coefficients are derived from the density coefficients using the rate-of-change of density with temperature evaluated at 160°F (average fuel element coolant temperature) as follows:

$$\alpha_{T_m} = \frac{\Delta R}{\Delta T_m} = \frac{\Delta R}{\Delta \rho_m}\frac{d\rho_m}{dT_m} \tag{4.3-2}$$

where

α_{Tm} = moderator temperature coefficient of reactivity

ρ_m = $\rho_m(T_m)$ moderator density

T_m = moderator temperature

R = reactivity

$\frac{\Delta R}{\Delta \rho_m}$ = density coefficient of reactivity.

Representative reactivity coefficients are obtained by averaging values from the cases listed in Table 4.3-11. These values are -0.00028 \$/°F for the fuel temperature coefficient and -.0067 ± 0.0004 \$/°F for the fuel element moderator temperature coefficient. The error assigned to the moderator coefficient is one standard deviation based on the range of values in Table 4.3-11.

The regional reactivity worth of both fuel temperature and moderator density changes are functions of the lobe power splits with larger worth values generally associated with lobes having the higher power fractions. The range of this variation for the reactivity worth of moderator temperature changes is illustrated in Table 4.3-11 and given in the form of relative weight factors. The weight factor for a variable is defined as the ratio of the reactivity worth for the variable in a given lobe to the total core reactivity worth. As stated above, the weight factors correlated directly with the lobe power fractions where the larger weight factors are generally associated with lobes having the larger power fractions.

Moderator temperature coefficients for a near balanced 60/40 MW lobe power split condition have been derived for both BOC and EOC exposures. These coefficients are evaluated from a two-dimensional (2-D) version of the ATR PDQ-7 model. The resulting coefficients, evaluated at a nominal moderator temperature of 160°F, are -0.0092 \$/°F at the BOC and -0.0069 \$/°F at the EOC. The decrease in magnitude of the moderator temperature coefficient with cycle exposure is consistent with temperature reactivity response described in the initial safety analysis report (SAR) for the ATR (deBoisblanc and Cohen 1965). The dominant effect on the reactivity effect over the life of the cycle is the change in core leakage as the reactivity control elements are withdrawn. Note that the EOC value from the 2D EOC case is similar in magnitude to the 3D value from Table 4.3-11. The 3D value was calculated at full power xenon equilibrium conditions with OSCC substantially withdrawn.

As discussed above, positive reactivity feedback effects may be encountered if coolant density changes occur in the experiment facilities. Of particular concern are potential reactivity insertions during off-normal conditions in the pressurized water loop facilities. Potential for abnormal conditions (e.g., depressurization, loss of flow, and uncontrolled heat up) in these independently controlled facilities can result in a reactivity insertion accident. These accidents have been analyzed in Chapter 15 (Accident Analyses) resulting in limitations on the total IPT voiding reactivity and control of loop parameters that affect the reactivity insertion rate. The magnitude of the void worth in the experiment loops varies by position because of differences in the loop volumes and the effects of unbalanced lobe power splits. To determine the range of reactivity potentially available to the system by voiding any one loop, the reactivity worth of voiding each of the nine experiment loops[a] is given at BOC conditions for the same set of lobe power split cases used for evaluating the reactivity coefficients in Table 4.3-11 (Judd and Terry 1992). The voided reactivity worth for each experiment loop and lobe power split case is listed in Table 4.3-12. Values range from 0.24 to 1.11$ and result from differences in the PDQ-7 eigenvalues for the voided cases relative to the completely flooded case. In general, the voided loop worth from these calculations correlated directly with the loop power fractions except for the NW and NE loops that contain the LIPT. The voided worth for these experiment loops in each case are larger than the corresponding voided worth of the standard SIPT located in the N loop because of their larger volume. Typical experiment compositions were used in these calculations. In general, the IPT void worth will depend upon the particular experiment components, the loop facility operating conditions, and the lobe power split. The IPT void worth is calculated using the specific loading and operating conditions for each loop facility as part of the operating cycle safety evaluation. The IPT void insertion is considered in the operating cycle analyses and operating conditions are established to limit the potential void insertion to the values assumed in the accident analyses. The operating cycle analyses are discussed further in Chapter 10 (Experiments and Irradiation Facilities).

During the 1994 CIC outage, the core was configured with capsule irradiation facilities in four of the flux traps and loop facility IPT in five of the flux traps. The configuration has a large capsule facility in the NE, small capsule irradiation facilities in C, S, and E, an LIPT in NW, the advanced high temperature loop IPT in the W, and standard IPTs in the remaining flux traps (SW, SE, and N). Capsule irradiation facilities are cooled by reactor water rather than independent cooling water systems. There is little potential for these facilities, including those in the flux traps, to initiate local reactor coolant density changes resulting in a reactivity insertion accident (Hendrickson 1994). Therefore, there are no specific analyses of capsule facility initiated reactivity insertion accidents in Chapter 15 (Accident Analyses). Any such events would be addressed in the experiment safety analyses for the capsule facility loading.

During 1997 to support the ongoing test program the northeast flux trap was again reconfigured and the Irradiation Capsule Experiment (ICE) facilities installed. During 1999, the ICE facility was replaced with the Multiple Irradiation Capsule Experiment (MICE) facility. As with the capsule irradiation facilities, there is little potential to initiate reactor coolant density changes which result in a reactivity insertion accident (Hendrickson 1998b). Any such events would be addressed in the experiment safety analysis for the MICE facility.

---

[a] At the time these analyses were completed there were nine pressurized water loop facilities. The NW and NE flux traps had LIPTs, the W flux trap had the advanced high temperature loop IPT, and the remaining six flux traps had standard loop facility IPTs.

During 1999 the center flux trap capsule facility was replaced with the Irradiation Test Vehicle (ITV). This facility allows experiment testing in a gas atmosphere, typically helium and neon. The experiment facility is cooled by reactor water similar to capsule facilities while the actual test temperatures are controlled by adjusting the helium/neon gas mixture. As with the capsule irradiation facilities, there is little potential to initiate reactor coolant density changes that result in a reactivity insertion accident (Ingram 1999). Any such events would be addressed in the experiment safety analysis for the ITV facility.

As stated above, a second concern with the experiment facilities is the potential for adding positive reactivity feedback during a reactor power or PCS temperature transient. The positive reactivity addition during a power transient is called cascading feedback. Cascading occurs when the reactor power transient results in increased heat generation in an experiment resulting in further heat up of the experiment cooling water and additional positive reactivity insertion. Cascading is particularly significant in fueled loop facility experiments. Cascading is considered in Chapter 15 (Accident Analyses) resulting in limitations on the potential positive reactivity feedback from the flux trap experiment facilities.

Potential flux trap reactivity insertions during PCS temperature excursions such as a PCS flow coastdown event were considered in Chapter 15 (Accident Analyses) resulting on the limitations on the positive reactivity insertion from heat up of the PCS water in the flux traps. These limitations are considered in the operating cycle analyses as discussed in Chapter 10 (Experiment and Irradiation Facilities).

4.3.2.4 Control Rod Patterns and Reactivity Worths. The reactivity control elements include the safety rods, OSCC, regulating rods and neck shim rods. Reactivity control element withdrawal sequences are used for reactor startup and approach to power. The safety rods are fully withdrawn (≥ 35 in. and ≤ 36.5 in.) first, then the regulating rods are both fully withdrawn. The safety rod upper limit switches are set such that the bottom of the safety rod hafnium is nominally three in. below the top of the active core thus providing a reactivity bite upon a scram. The regulating rod and neck shim rod upper limits are nominally at the top of the active core. If any neck shim rods are specified for withdrawal for startup, those rods are withdrawn to the upper limits. The neck shim rods are generally left inserted for the initial startup of an operating cycle after a refueling. Neck shims are typically withdrawn prior to OSCC for restart of an operating cycle loading after a mid-cycle outage. When withdrawn, the neck shim rods are fully withdrawn to minimize the perturbation to the axial power profile.

After positioning the other reactivity control elements, the OSCC are withdrawn to establish criticality. The OSCC are driven in pairs using ganged and balanced withdrawal for startup (all OSCC withdrawn simultaneously at nominally the same rotational position). Ganged and balanced withdrawal is maintained until about $N_F/3$ (one-third of full power for the operating cycle). For balanced OSCC withdrawal, all OSCC positions are maintained within ± 5 degrees of the average position of all 8 pairs of OSCC. Count rate monitoring is performed during OSCC withdrawal to monitor subcritical multiplication and to project the OSCC positions at criticality. Control element positions at criticality are calculated for each cycle after a core change. Administrative controls require the reactor to be shut down if the absolute difference between the calculated and actual shim positions at criticality exceeds a specified limit.

Automatic control by the regulating rod servo control system is established at roughly N_L with one regulating rod providing power level control and the second one on standby as a back-up unit. At roughly $N_F/3$, the reactivity control elements are adjusted to establish the lobe power split providing the requested experiment source powers.[a] The power division is established by unbalancing the OSCC and, in some cases, withdrawing neck shim rods. When unbalancing the OSCC, the OSCC in each quadrant are operated as a group and the position of the two OSCC pairs in the group are maintained within ± 5 degrees of the average position of the group. Neck shim rods, when withdrawn, are fully withdrawn. During power operation, the neck shim rods are withdrawn individually. The normal withdrawal sequence in each quadrant is to start with the #6 position in the quadrant and progress inward (lower neck shim rod number) with the #1 neck shim rod the last withdrawn in a quadrant. Neck shim rods are normally withdrawn in the high power quadrant first.

Once low-power experiment verifications are completed, final adjustments are made to the lobe power split and the total core power is increased to the full power determined to provide the requested experiment conditions. OSCC and neck shim rod positions are adjusted to maintain the power division and to maintain the regulating rod within a nominal operating range. At the beginning of the operating cycle, there are adjustments made for core heatup and the buildup of fission products. Once xenon equilibrium is reached, OSCC and neck shim rod movements compensate for fuel depletion. After xenon equilibrium, general neck shim rod withdrawal guidance is to maintain an OSCC excess reactivity for recovering from power reductions and to maintain the OSCC in the range of 80 to 100 degrees rotation to provide consistency in cycle-to-cycle experiment conditions. Once the neck shim rods are withdrawn, fuel burnup is compensated by further OSCC withdrawal. Each operating cycle fuel loading is designed for an end-of-cycle OSCC excess reactivity of 2$ normally resulting in all neck shim rods withdrawn and OSCC positioned in the range of 100 to 150 degrees.

If a power reduction occurs and conditions permit recovery, safety rods are withdrawn and then OSCC are gang withdrawn (all OSCC withdrawn simultaneously) to over-ride xenon poisoning. OSCC withdrawal is typically stopped when each quadrant set of four OSCC reach 150 degrees to provide a reactivity bite for turning power transients and to prevent shadowing effects in the nuclear instrumentation detectors. Xenon over-ride capability is limited to the excess reactivity available in the OSCC. During a power recovery, power is increased to approximately 0.87 N_F (87% of the operating power level prior to the power reduction) to burn xenon poison. Power is maintained at or below 0.87 N_F until xenon is burned as indicated by a comparison of OSCC position before and after the power reduction.

The above practices for positioning the reactivity control elements are factored into the operating cycle calculations for core reactivity, power division, and fuel element power peaking. As discussed previously, the positions of the reactivity control elements can affect the power distributions in the fuel elements. Mispositioning of reactivity control elements is addressed as an off-normal condition in Chapter 15 (Accident Analyses). Certain measurements of the reactivity worth of the control elements may require deviations from the standard positioning requirements. When performed, the reactivity control element positions required to support the measurements are specifically considered and shown to be acceptable in the operating cycle calculations.

---

[a] The term source power is used to define the effective power level that is the source of the neutron flux to an incore component. The flux trap source power is the power generated in the vicinity of a flux trap. For the inner flux traps (i.e., those inside of the fuel annulus), the source power is the local lobe power. For the outer flux traps, the source power is the average of the three adjacent lobe powers. The source power for the #1 and #2 neck shim rods is the center lobe power. The source power for the #3 and #4 neck shim rods is the average of the center and adjacent lobe powers. The source power for the #5 and #6 neck shim rods is the adjacent lobe power.

The worths of the reactivity control elements are periodically measured. The measurements determine the integral worth of the safety rods and neck shim rods and the integral worth vs position of the OSCC and regulating rods. The measurements have shown that the reactivity worth of the reactivity control elements can depend upon several factors. The core position, fuel element loading (i.e., new or irradiated fuel elements), lobe power split, depletion of the reactivity control material, and amount of reflector poisons present are the dominant factors. The loading of the experiment and irradiation facilities also affects the worth. The OSCC are most affected by these factors and the safety rods the least affected. These factors result in cycle-dependent variations in some of the control element reactivities. Measured integral worths of the reactivity control elements are given in Table 4.3-13 for a core loading with all fresh, 7F fuel elements, new hafnium on the control elements, a new reflector, and a balanced (50-50-50 MW) power division. The experiment facilities were loaded with dummy fillers or empty. These are essentially base case conditions established for low-power nuclear testing after each CIC. The subsections below discuss the significant variations from these nominal conditions. The calculated worth of the burnable poison (boron-10) is also given in Table 4.3-13.

4.3.2.4.1 Neck Shim Rod Reactivities—Twenty-four hafnium shim rods are located in the narrow neck regions of the four quadrants with six neck shim rods in each quadrant. Any two of the #4 neck shim rods can be used as regulating rods. With the exception of the operating regulating rod, the neck shim rods are normally positioned either fully inserted or withdrawn.

The nominal neck shim rod worth given in Table 4.3-13 is the sum of the 22 neck shim rod integral worths from measurements after the 1994 CIC (McCracken et al. 1994). Individual neck shim rod worths from those measurements are listed in Table 4.3-14. The uncertainty is ± 0.01$ for any individual rod measurement. The neck shim rod worths are affected by the core position, power division, position of adjacent neck shim rods, and hafnium depletion. Functional relationships were developed by Tappendorf (McClure 1991b) for core power division and adjacent neck shim rod position and for hafnium depletion (McCracken 1994). Effects of the loadings in the adjacent flux trap experiment facilities result in relatively small differences in the worth of neck shim rods in the different quadrants (McCracken et al. 1994). Such differences are determined analytically or in the ATRC as necessary for the major changes in the flux trap experiment and irradiation facility loadings. The effect of hafnium depletion as a function of exposure was determined from differences in neck shim rod reactivities over the lifetime of Reflector IV.

The neck shim rod reactivities are primarily used in operational support calculations (e.g., cycle loading lifetime projections and prediction of shim positions at criticality for restart) and for evaluation of the holddown reactivity margin. Nominal reactivities including the effects of hafnium depletion are used for these applications. The safety analysis considers the neck shim rod reactivities in the analyses of reactivity control element withdrawal and mispositioning accidents. These safety analyses are based on conservative assumptions. The neck shim rod reactivity addition rates used in the analyses of control system faults are derived in Subsection 4.3.2.5.

4.3.2.4.2 Regulating Rod Reactivities—The nominal position of the regulating rods during power operation is for the stand-by rod to be fully withdrawn and the active regulating rod partially inserted. The nominal regulating rod worth (0.26$/rod) given in Table 4.3-13 is from reactivity measurements after the 1994 CIC (McCracken et al. 1994). The uncertainty is ±0.01$ for any individual rod measurement. The regulating rod worths are affected by the core position, power division, and position of adjacent neck shim rods. Functional relationships were developed by Tappendorf for core power division and adjacent neck shim rod position (McClure 1991a). The regulating rod core position is established by the installation of the drive mechanisms (any #4 neck shim rod position can be used) and is typically not changed between CICs. The effect of position is determined by measuring the regulating rod reactivities.

Because of the operating mode, the hafnium burnup in the regulating rods is greatest in the rod tips. Measurements of the integral worth of the regulating rods show their total worth to be independent of the hafnium exposure to at least 30 lobe-gigawatt-days (LGWd). These measurements (McCracken and Yarbrough 1994) made at various exposures ranging from 0 to 29 LGWd result in an average value of 0.24 ± 0.02$, which is within the uncertainty range for the worth of the unirradiated neck shim rods. The shape of the regulating rod worth versus position curve, however, does depend upon exposure because the rods are depleted in an axially nonuniform manner with the lower portion of the rods receiving the greater exposure. This is illustrated by the worth curve in Figure 4.3-40, which shows the fractional withdrawal worth versus position of regulating rods containing new and depleted (29 LGWd) hafnium.

The regulating rod reactivities are primarily used in operational support calculations (e.g., evaluation of movement of driven experiments, cycle loading lifetime projections and prediction of shim positions at criticality for restart) and evaluation of holddown reactivity. Nominal values are used for these applications. The only safety analysis application of the regulating rod reactivities is in the analyses of control element withdrawal accidents. These safety analyses are based on conservative assumptions. The regulating rod reactivity addition rates used in the analyses of control system faults are derived in Subsection 4.3.2.5.

4.3.2.4.3 Safety Rod Reactivities—Safety rods provide the mechanism for fast shutdown of the reactor during abnormal operating conditions. A manual scram of the safety rods is used for normal reactor shutdown (e.g., end of an operating cycle).

The nominal safety rod worth given in Table 4.3-13 is based on the results of measurements over the lifetime of Reflector IV and measurements after the installation of Reflector V. The measurement results, reported in the nuclear test report from the 1994 CIC (McCracken et al. 1994), are listed in Table 4.3-15. The measurement uncertainty is shown for the individual safety rods. The uncertainties on the averages are from statistical combination of the individual rod uncertainties. The measurements show the safety rod reactivities are not significantly affected by core position, fuel element loading, hafnium depletion, experiment facility loading or reflector poisons. The initial rate of reactivity insertion during a scram of the safety rods does depend upon the core power division at the initiation of the scram. The functional relationship for this effect was developed by Tappendorf and modified by Brown (McClure 1991b). The safety rod reactivities in Table 4.3-15 have been adjusted to a flat 50-50-50 MW power division for comparison.

Table 4.3-15 shows that the minimum safety rod worth requirement of 5.8$ or 6.4$ depending on the PCS flow rate (Section 4.3.1.5 is easily met by the nominal worth of the six installed safety rods. These minimum requirements are based on the reactivity insertion rates used in Chapter 15 (Accident Analyses). The effects of the core power division on the initial safety rod reactivity insertion worth are evaluated as part of the operating cycle analysis. This evaluation conservatively considers the uncertainty in the safety rod reactivity and assumes the highest worth safety rod does not insert. Operation with less than six safety rods typically can be supported as demonstrated in Table 4.3-16 which shows the variation in safety rod reactivity as a function of the core power division and decreasing number of safety rods. In each case in Table 4.3-16, the highest worth rods were deleted from the summation of rods worths.

Since the safety rods are withdrawn during reactor operation, safety rod reactivities are not used in operational reactivity calculations. The safety rod reactivities are used in the evaluation of holddown reactivity margin for outage core changes. The safety rod reactivities used for holddown reactivity evaluations are the same conservatively low values used for the scram reactivity evaluation discussed above. The safety analysis considers the safety rod reactivities in the analyses of reactivity control element withdrawal and mispositioning accidents. These safety analyses are based on conservative assumptions (high safety rod reactivities for insertion rate evaluation). The safety rod reactivity addition rates used in the analyses of control system faults are derived in Subsection 4.3.2.5.

The worth of the safety rods can be derived analytically from differences in the PDQ-7 eigenvalues calculated with the 3-D model for cases with the rods inserted relative to the initial rod state. A total of five safety rods are described in the PDQ-7 model resulting in a calculated worth of 13.3$ at the fully inserted position of 39 in., which is within the uncertainty range of the measured worth for five rods. An integral rod worth curve as a function of rod position for the five safety rods is shown in Figure 4.3-41 for a nominal 60/40 MW lobe power split condition. The curve in Figure 4.3-41 has been extended to a rod insertion of 48 in. to show the fully inserted shape. The initial position of the safety rods during operation is 3 in. into the core providing a more immediate response during a scram than available from the fully withdrawn position. Actual rod motions are limited to a maximum travel distance of 36 in. resulting in a maximum insertion position of 39 in. The integral rod worth curve in Figure 4.3-41 is not normalized with respect to a balanced lobe power split because the model does not determine the worth of individual rods.

4.3.2.4.4 Outer Shim Control Cylinder Reactivities—The 16 OSCC provide the primary control for criticality and maintenance of the lobe power split. The OSCC are identical with hafnium plates covering a 120-degree sector on the outer surface of each cylinder. The OSCC are operated in pairs with two pairs per quadrant, adjusting the position of the poison sectors away from or toward the core to maintain criticality and the lobe power split. The nominal OSCC worth given in Table 4.3-13 is the sum of the OSCC pair worths from measurements after the 1994 CIC (McCracken et al. 1994). The uncertainty is ±5% for any OSCC pair reactivity measurement. The OSCC worths are affected by the core loading, lobe power split, and the reflector poisons. Functional relationships for core power division were developed by Tappendorf and modified by Brown (McClure 1991b). The effects of the core loading result from variation of the fuel element loading in the adjacent lobe (e.g., new or depleted, borated or nonborated fuel elements) and from the variation in the loading in the adjacent lobe experiment facilities. Such differences are determined from reactor or ATRC measurements as necessary.

The OSCC reactivities are primarily used in operational support calculations (e.g., cycle loading lifetime projections and prediction of shim positions at criticality for startup and restart) and for evaluation of the holddown reactivity margin. Nominal reactivities are used for these applications. Some of these applications require an integral worth curve (i.e., worth vs. position). The incremental reactivity worth as a function of rotational position is derived from measurements (McCracken et al. 1994). An example of a worth curve is shown in Figure 4.3-42. For this curve, the total integral worth of the OSCC is 12.9$.

4.3.2.4.5 Reactivity Addition Rate—The reactivity insertion rate associated with the failures in the reactivity control systems is determined by the rate of travel or rotation and the worth of the control elements. Control system failures resulting in uncontrolled withdrawal of various combinations of the reactivity control elements are considered in Chapter 15 (Accident Analyses). The insertion rates used in analysis of control system failures are given in Table 4.3-17. The control system design data (number of elements, withdrawal speed and active travel are from Chapter 3 (Design of Structures, Components, Equipment, and Systems). Reactivity data are from the summary of control element reactivity measurements (McCracken et. al. 1994) unless otherwise noted. The reactivities are based on an 80-50-20 lobe power split to maximize the insertion.

The nominal total safety rod worth in Table 4.3-17 is the average flat-power rod worth from Table 4.3-15 for all measurements (2.83$/rod) for a total of 17.0$ for six rods. The nominal total neck shim rod worth is the flat-power total neck shim rod worth from the Cycle 103A measurements reported in Table 4.3-14 (McCracken, et. al., 1994). Individual neck shim rod worths are summed to obtain the total. The nominal worth for the most reactive neck shim rod is the average of the four #6 neck shim rod flat-power worths from Cycle 103A measurements. The nominal flat-power regulating rod worth is from Cycle 103A measurements. The nominal total outer shim cylinder worth is the total flat-power outer shim cylinder worth (four sets) from the Cycle 103A measurements (fresh fuel and reflector provide the highest worth).

The maximum differential worth for the safety rods, neck shim rods, and regulating rods is expressed as a fractional worth per inch of travel ($/in per $). The value is obtained by taking the derivative of the flat-power regulating rod integral worth curve derived from Cycle 103A measurements. Since all of these elements have a uniform cross section and move in the unperturbed axial flux profile, the shape of the integral worth curve is assumed the same. The maximum differential worth for the outer shim cylinders is obtained by taking the derivative of the flat-power integral worth curve for each outer shim cylinder set from the Cycle 103A measurements. The maximum differential worth for each set is summed to obtain the total for all four sets.

The magnitude of a reactivity insertion is a function of the neutron flux level at the location of the reactivity insertion relative to the core average neutron flux level. Functional relationships have been developed for reactivity evaluations. The functional relationships are expressed in terms of relative power. The functional relationships were developed by Tappendorf and modified by Brown (McClure 1991a and 1991b). The analysis of startup accidents has historically been done assuming an 80-50-20 lobe power split. This assumption maximizes the rate of reactivity insertion resulting in a conservative analysis. The 80/20 total worth is determined by adjusting the nominal total worth (flat-power or 50-50-50 lobe power split) by the applicable relative power relationship.

For the 80/20 safety rod reactivity, the nominal safety rod reactivity of 2.83$/rod plus the one standard deviation (0.22$) uncertainty from Table 4.3-15, was adjusted for relative power effects using the rod locations and assuming the 80 MW lobes were on the south side of the core. For the neck shim rods, an enhancement factor of 1.33 was applied to account for the effect of pulling adjacent rods (McClure 1991a). This is the same neck shim rod enhancement factor used in the ATR Design Basis Report (EG&G Idaho 1994). For the regulating rods, the accident analysis has historically (EG&G Idaho 1994) assumed a maximum total regulating rod worth of 0.57$ which is conservative.

The analysis of startup accidents is based on the response of the RELAP reactor kinetics model to the input reactivity insertion as a function of time. The input reactivities are based on the insertion rates for the control element moving at the point of maximum differential reactivity in the 80-50-20 lobe power split. The 80/20 insertion rate for the safety rods, neck shim rods and regulating rods is the 80/20 total worth times the maximum fractional differential worth times the element speed. For the outer shim cylinders, it is the maximum differential worth adjusted by the corner lobe relative power adjustments.

The average single element differential worth, provided for information in Table 4.3-17, is the nominal total worth divided by the number of elements divided by the active length.

4.3.2.4.6 Burnable Poison Reactivity—The 7F fuel elements contain boron (B-10) in the fuel matrix of the outer fuel plates (plates 1-4 and 16-19) to minimize radial power peaking and to provide a burnable poison as partial compensation for fuel burnup. The reactivity worth of the B-10 poison in nonirradiated 7F fuel elements, derived from PDQ-7 calculations with and without B-10 in the fuel plates, results in a reactivity change of -0.078 $\Delta\rho$ or -10.9$ using the best- estimate value of 0.0072 for β_{eff} (ANC 1973).

4.3.2.4.7 Reflector Poison Reactivity—Irradiation of the beryllium reflector results in a complicated series of nuclear transmutations. Irradiation products and some decay daughters have neutron cross-sections that are large enough to result in significant change in core reactivity. The reflector neutron poisoning phenomenon does not have reactor safety significance but is important to core reactivity calculations.

The major reaction chains in beryllium are shown in Figure 4.3-43. The dominant reflector poison isotopes are Li-6 and He-3 (both found in Chain 2 in the figure). For practical purposes, Li-6 is a direct product of neutron absorption in beryllium. Li-6 is a stable isotope and is only lost through neutron absorption. The production and loss rates of Li-6 are proportional to neutron flux. The concentration of Li-6 reaches an equilibrium value after about 100 to 200 EFPD (Equivalent Full Power Days).

He-3 is formed by the decay of H-3 which is a product of neutron capture in Li-6. He-3 builds up during reactor outages due to decay of H-3 and burns out during reactor operation due to loss by neutron absorption. Since the half-life of H-3 is long relative to the lifetime of a reflector, the operating concentrations of the H-3 precursor and, correspondingly, He-3 increase approximately linearly with reflector exposure after the Li-6 parent isotope equilibrates (after about 100 to 200 EFPD). After these few hundred days, both the He-3 buildup rate during outages and its quasi-equilibrium operating concentration increase nearly linearly with total operating time. H-3 decay to -He-3 during outages results in the slow buildup of poison. Since the concentration of H-3 increases with operation, the rate of He-3 poisoning increases over the life of the reflector.

The reactivity changes due to reflector poisons are manifested by changes in the reactivity worth of the OSCC. There are two effects. A general poisoning of the reflector and a poisoning of the beryllium portion of the OSCC making the withdrawal of the hafnium section less effective.

The reflector poisons at full power operating conditions are not significant. Reactivity effects of poisoning were estimated (Burdick 1971). After the first few hundred days of operation the operating poisoning level reaches a value around -0.5$. This value slowly increases during the life of the reflector reaching a value of about -0.6$ at the end of the reflector lifetime. The effect of the shutdown poisoning is small for the typical 7 and 14-day outage durations. The effect is more significant for longer outages particularly those occurring late in the reflector lifetime. Longer outages sometimes occur between CIC outages to support major modifications. The buildup rate for outages is about -0.01$/day at mid-reflector life and about -0.03$/day at the end of reflector life. Reflector poisoning for a three-month outage near the end of reflector lifetime can add several dollars of poisoning. The reflector poisoning effect appears as a decrease in the OSCC worths. The measured total OSCC worth at the end of the 6-month process control upgrade outage near the end of Reflector IV lifetime was 8.3$ compared to the nominal OSCC worth of 12.9$ (McCracken et al. 1994).

The effects of reflector poisons are conservatively neglected in the holddown reactivity evaluation. The effects of the reflector poisons are factored into the estimate of shim positions at criticality. The reflector poison isotope chains are included in the XY core model used for operating cycle analyses (Smith et al. 1990).

4.3.2.5 Control Requirements. There are four reactivity control systems as described in Section 4.1. To summarize, the safety rods are reserved for fast reactor shutdown, the OSCC and neck shim rods are used for maintaining criticality and lobe power distributions during operation and holddown margin during outages. The servo-controlled regulating rods provide fine power adjustment (one regulating rod active and one on stand-by). The safety rods are designed to ensure that the reactor can be safely and rapidly shut down. The OSCC, neck shim rods, and regulating rods are used to establish criticality and for control of the lobe power split and total core power level. This section describes the requirements for the core reactivity control. Compensatory measures as defined in procedures and the Technical Safety Requirements may be taken in the event these requirements are not met.

4.3.2.5.1 Safety Rods—Preoperational analysis to determine the excess reactivity of each cycle ensures that the reactor cannot become critical from the safety rods alone. During reactor startup, the plant control system interlock and permissive controls discussed, in Section 4.3.2.2, that interact with the reactivity control element drive mechanisms to restrict positive reactivity insertions to safe and controllable rates are required. The control element types and the respective maximum reactivity insertion rates expected from withdrawal of the each type are summarized in Table 4.3-17. The reactivity insertion rates are based on the maximum worth but not the effect of the plant control system interlock and permissive controls.

The safety rods are withdrawn to ≥ 35 in. and ≤ 36.5 in. except for specifically analyzed cases. The safety rod position indications, lower limit and seat switches are required. The hafnium sections may be removed from a safety rod assembly and the assembly left in the inserted position provided the minimum shutdown reactivity requirement can be met (Clemons 1979; Fillmore 1979).

Compressed springs aid in the insertion of the safety rods during a scram. Safety rod scrams are actuated in the reactor by uncoupling the horizontal rod drive shaft from the drive motor, thus allowing the rods to fall into the core. The rods are accelerated downward by the spring and gravitational forces under all conditions whether the reactor vessel is depressurized or in full operational status. In addition, operation at normal power levels where the PCPs are in service generates an additional acceleration from hydraulic forces on the safety rods during a scram because the primary coolant flow is in the same direction as the rod motion. Thus, the insertion time of the safety rods will vary with the coolant flowrate because the hydraulic force on the rods varies with the flowrate.

Drop times of the safety rods to the 12-in. insertion distance, including a margin for conservatism, are required to not exceed 150 msec for three PCP operation and 300 msec for low pressure (atmospheric) operations where nominal flow rates of approximately 4500 gal/min are maintained. The core pressure drop and frictional forces on the safety rods are reduced for two PCP operation resulting in a slightly longer drop time for the safety rods. Analysis (Chapter 15 [Accident Analyses]) shows that the scram reactivity worth during 2 PCP operation will equal or exceed that for 3 PCP operation by requiring that the rod drop time to the 12 in. insertion distance not exceed 170 msec including a margin for conservatism. Whenever the reactor vessel is opened, safety rod testing for compliance with the drop time requirements is completed prior to restart of the reactor.

4.3.2.5.2 OSCC, Neck Shim Rods, and Regulating Rods—A unique feature of the core design is the ability to operate the lobes at different, controllable power levels. Control during a cycle makes use of the neck shim rods, regulating rods, and OSCC. The strong coupling among the lobes means that the worth of each control type depends upon the positions of the other types. Over a cycle, the reactivity control element positions are manually adjusted to maintain a constant lobe power split and, hence, to maintain the target neutron flux level for experiments. In order to maintain manual control, the neck shim rod position indications or inner and outer limit indications are required. The position indications for the operating regulating rod and OSCC are required. The OSCC in each quadrant are operated as a group and the position of the two OSCC pairs in the group are maintained within ±5 degrees of the average position of the group except for specifically analyzed cases. The control elements are required to move on demand from the control room console. Operation with stuck OSCC can continue provided the position balance can be maintained. Operation can continue with one stuck neck shim or regulating rod per quadrant (does not include neck shim rods that are stuck and positioned at the inner limit). Since the OSCC and neck shim rods provide auxiliary means of inserting shutdown reactivity, the timed automatic insert capability is required.

A typical control pattern calculated for the nominal 60/40/E lobe power split case is shown in Table 4.3-18 covering a 24-day cycle. The lobe power values at each time in the cycle have been normalized to 250 MW total core power.

4.3.2.6 Criticality of the Reactor During Refueling. Maintaining a sub-critical state during refueling operations requires that the reactor core, fissile material involved in the transfer process, and the storage facilities for such material outside the core all be kept in a criticality-safe condition. This section describes the methods of controlling criticality during transfer of fissile material into and out of the reactor. Maintaining the reactor core in a safe sub-critical condition during refueling operations utilizes administrative controls, adequate shut-down margins in the reactivity control system, and observable signals from the neutron count rate monitoring instrumentation. The nuclear design bases for maintaining the reactor subcritical is presented in Section 4.3.1.5, and a discussion on the control element reactivity is given in Sections 4.3.2.4. Additional discussion of the storage and handling processes for

fissile material is given in Chapter 9 (Auxiliary Systems). Neutron monitoring instrumentation is described in Section 4.3.2.2.8. Administrative procedures require that $k_{eff} \leq 0.95$ and monitoring instrumentation is operational during fissile material transfers into and out of the core. Analysis of the holddown reactivity ensure that adequate shutdown margins are maintained ($k_{eff} \leq 0.95$).

Fissile materials in the reactor and storage facilities include fueled experiment structures and both fresh and irradiated fuel elements for the reactor. Criticality safety evaluations are required for various operations involving fissile materials outside the reactor core. These operations include:

- Storage of fissile material in the "in-process" areas such as the in-vessel fuel storage
- Storage of irradiated fissile material in underwater racks and containers in the canal
- Handling of fissile material during processing or transfer of fissile material either as fuel elements or as fueled experiments.

Criticality of fissile materials outside the reactor core is controlled by the physical design of fuel storage and handling facilities and by administrative control procedures as discussed in Chapter 9 (Auxiliary Systems).

Fuel elements may be temporarily stored in the in-vessel fuel storage racks to facilitate fuel element transfer operations; no fuel is present in these racks during reactor operation.

Criticality analysis of the in-vessel fuel storage racks (Tingey 1965) shows that the k_{eff} is less than 0.90 with the two center positions blocked and the remaining positions containing single elements and will be lower with fewer elements in the racks.

The design criteria and methods described above satisfy the ATR GDC 62 Chapter 3 (Design of Structures, Components, Equipment, and Systems) and criticality safety criteria specified in DOE Order 420.1A (DOE 2002), Facility Safety.

4.3.2.7 Stability. Spatial power oscillations induced by transient spatial xenon concentrations are possible in PWR, particularly ones having large, loosely coupled core volumes, or smaller ones with high power densities such as the ATR. The stability of a reactor to oscillations is characterized by the diminishing or growth of the oscillation amplitude with time. The reactor is stable if the amplitude decreases with time, unstable if the amplitude increases with time. The xenon-induced power oscillations can usually be classified in three modes as follows: an intralobe mode where power periodically shifts radially back and forth in the lobe fuel elements, an interlobe mode where power shifts back and forth among lobes, and an axial mode where power shifts upward and downward in the core.

The three xenon oscillation modes were studied (deBoisblanc and Cohen 1965) resulting in the conclusion that the core is stable for all oscillation modes. The current core size and configuration are the same as for the stability studies and, therefore, the conclusions remain applicable. Interlobe oscillations are completely suppressed by the tight reactivity coupling among the lobes and the reflector controls (OSCC), which are designed to maintain steady interlobe power imbalances. The tight reactivity coupling among lobes is demonstrated by using a single regulating rod for fine reactor power control. A single lobe is stable against intralobe oscillations because of the combination of lobe size and tight reactivity coupling. This study concluded that the threshold core length for axial instability is greater than the 48 in. core height and therefore, the core is stable against axial xenon oscillations.

Xenon oscillations are most likely to occur in the direction of the longest axis in high-power density reactors such as the ATR because this dimension provides the greatest possibility for flux-tilt oscillations. The reactivity control systems do not include specific mechanisms such as part-length control rods for axial flux tilt suppression to avoid local flux perturbations. Hence, it is particularly important to show that the core is stable for axial xenon oscillations. An experimental test in the ATR (Durney et al. 1972) confirmed this stability.

The axial stability test consists of establishing an asymmetric equilibrium flux and xenon distribution with the neck shim rods, changing the rod positions to an axially symmetric configuration while keeping the power level constant, and monitoring the time-dependent flux shape. The axial flux shape is represented analytically as a harmonic power series with particular attention given to the amplitude of the first harmonic. It is assumed in this analysis that if the first harmonic is stable, all harmonics are stable (Randall and St. John 1958). The test results show that the axial flux shape oscillations are highly damped, and the flux shape attains the asymptotic distribution characteristic of a symmetric rod configuration thus demonstrating stability.

Xenon oscillation studies (Ash 1965) indicate that stability is enhanced by having a negative power coefficient of reactivity, which is the case for the ATR. Measurements of the power coefficient in an ATR core for BOC conditions (Durney et al. 1972) resulted in a value of -0.0015 ± 0.0001 \$/MW, demonstrating its negative value. This negative coefficient provides an added assurance that the core is stable for all types of xenon oscillation modes and, likewise, that the immediate response to any power increase is stable because of the negative power feedback coefficient.

Since reactor startup, power variations with small amplitudes and various frequencies have been observed. Reactor power variation is routinely monitored by observing peak-to-peak amplitude of high speed traces from the nuclear instruments and power spectral density analyses of the neutron noise signals from the nuclear instruments. The baseline power variation is 1 to 2% peak-to-peak. A baseline neutron signature is obtained after each CIC. Anomalies in the power variations whether in amplitude or in frequency are investigated and appropriate corrective actions taken.

4.3.2.8 Vessel Irradiation. The vessel measures 12 ft in diameter and is 2 in. thick at the elevation of the reactor core. The service life of stainless steel pressure vessels is defined by the fracture mechanics method of the American Society of Mechanical Engineers (ASME) Boiler and Pressure Vessel Code, Section XI (ASME 1986). This method defines the minimum fracture toughness that must be available in the vessel material to resist brittle fracture in the presence of measured or assumed flaws. The fracture toughness of the material in combination with applied stresses and flaws contained in the material determine the resistance to brittle fracture.

The interaction of high energy ($E > 1$ MeV) neutrons with stainless steel causes an increase in tensile strength and a decrease in ductility. As the ductility decreases, so does the fracture toughness resulting in a higher probability of brittle fracture. This change to the material properties occurs relatively slowly and does not become significant until rather large fluences are accumulated. The interaction of low energy neutrons with stainless steel results in the production of activation products within the steel. This change to the basic structure of the material can reduce its strength leading to premature failure. The fast and thermal neutron fluence limits imposed on the reactor vessel as well as a detailed irradiation surveillance program are discussed in Chapter 5 (Reactor Coolant System).

The materials that serve to attenuate neutrons originating from the fuel elements are the OSCC, beryllium reflector blocks, core reflector tank, transition filler, and water located between core reflector tank and pressure vessel (Dwight 1986). The nearest surface of the vessel wall to the fuel annulus of the core is the inner surface of the drop tube dimple wall at the elevation of the core horizontal midplane. The drop tube dimple located at the north side of the reactor is an indentation in the vessel wall that facilitates the transfer of fuel and experiments between the core and storage canal. Peak neutron fluxes at the inner vessel wall occur at the location of the drop tube dimple.

The peak fast (E > 1 MeV) neutron flux levels at selected locations in the core and vessel are determined by the irradiation of flux monitor wires. The results (Durney et al., 1987) of the fast flux measurements applicable to the vessel fluence are summarized in Table 4.3-19. The measured flux data have been normalized to a nominally full power (250 MW), balanced power division, as shown in the last column. The peak fast flux predicted by curve fitting at the inner surface of the drop tube dimple is 4.29×10^9 neutrons/cm^2/sec. One standard deviation on the value from the fit is 33%. The thermal flux data (Durney et al., 1987) taken from capsule irradiation files and measurements are shown in Table 4.3-20. The thermal flux predicted at the inner surface of the drop tube dimple is 3.74×10^{11} neutrons/cm^2/sec. One standard deviation in the flux value is 64%. This study determined that vessel properties are largely unaffected by the exposure limits. As a result, the margins to failure are considerable resulting in a very low probability that any failure causing loss of coolant will occur.

Fluences were determined from a data base of neutron flux measurements, the actual operating history through Reflector III (reflector changeout), and a projection of the reactor operating powers through the year 2014. A reactor operating mode was assumed which conservatively maximized the fluence to the drop tube thimble. The projected fluence to the vessel from neutrons with energies greater than 1 MeV is 1.2×10^{19} n/cm^2 for base metal and 3.1×10^{18} n/cm^2 for weld material. The projected fluence to the vessel from thermal neutrons is 7.6×10^{20} n/cm^2 for base metal and 2.3×10^{20} n/cm^2 for weld material. The projected fluences cause little change in material properties; the effects can be reevaluated as the vessel exposure approaches these values.

4.3.3 Analytical Methods

4.3.3.1 Spatial Power Distribution Calculations. The principal analysis tool for calculating the two-dimensional (2D) and three-dimensional (3D) power distributions, as well as core reactivity, is the few-group neutron diffusion theory code PDQ-7 (Pfeifer 1971).

Both 2D and 3D PDQ models have been used in the analysis to represent the full core. The 2D PDQ model is an updated version of the ATR Core Safety Assurance Package (CSAP) full core model (Brown et al. 1990). The core is modeled in rectangular (XY) geometry using a 280 × 286 mesh. The planar region description permits a detailed representation of the core cross-sectional configuration. The 3D PDQ model represents the full core in rectangular (XYZ) geometry using the same planar representation as in the 2D model with axial variation in materials across the 51 axial mesh planes. Benchmark analyses, performed to validate the 2D and 3D PDQ models with the cross section database, are described in Section 4.3.2.2.

The azimuthal power distributions across the fuel plates are calculated from the partition power profile generated from the 2D (XY) PDQ analysis, which is input into the GOPP (Brown 1976) program to calculate and plot the azimuthal power distributions of the fuel plates. The fuel plates of interest are Nos. 1, 2, 3, 5, 8, 11, 15, 16, 17, 18, and 19, where Plate 19 has the maximum radius. The 2D partition power file contains point-to-average power densities, i.e., the relative power densities for the average plane, defined by:

$$\text{relative power density} = [\text{power in region/region volume}]/[\text{total reactor power/total fuel volume}] \quad (4.3\text{-}3)$$

The total (XYZ) point-to-average power density for the core midplane is obtained by multiplying the relative power density at the point of interest in the average plane, by the normalization factor calculated from the ROSUB program (Smith and Cook 1989). This normalization factor accounts for uneven axial fuel depletion as well as the power being generated only in the fuel matrix for the PDQ homogenized fuel cell. The normalization factor calculated from ROSUB is based on the nominal lobe power division.

Integrated power values from fueled regions are calculated in both 2D and 3D PDQ analyses. The integration region varies from single homogenized plate volumes to the complete core volume. Axial power distributions in the elements of interest are obtained from the 3D synthesis PDQ analysis. The 3D PDQ analysis uses the flux synthesis method with discontinuous trial functions in which the 2D PDQ model is used to generate trial functions. The 2D (XY) trial functions represent flux shapes expected in the upper reflector, active core with and without safety rods, and the lower reflector regions. The composition overlay in the safety rod, outer shim, and/or the fuel regions is varied in the 2D runs to generate the axially discontinuous trial functions. The average axial assembly power factors in the 3D analyses are integrated over all the plates in a fuel element, and are relative to a total core average of unity (i.e., an XYZ point-to-average element power factor). The azimuthal power calculational method using GOPP is not available for 3D data, so the total point-to-average power densities are calculated using GOPP with 2D PDQ data. Both criticality and target lobe power splits are held constant for the 3D cycle analysis. The end of cycle is defined as when either of these two criteria fails.

4.3.3.2 Cross Section Generation. The four-group microscopic/macroscopic cross section sets for 2D and 3D PDQ analyses are generated using COMBINE (Grimesey et al. 1990) and SCRABL (Judd 1991). COMBINE calculates the spectrum averaged multigroup neutron cross sections using the data base derived from the ENDF/B-V cross section libraries. The energy range treated is from 0.001 eV up to 16.905 MeV, spanned by a total of 166 discrete energy points/groups. The equations solved for the energy-dependent fast and thermal neutron spectra are the B-1 or B-3 approximations to the neutron transport equation. COMBINE has been validated by the applicability of the computed cross sections to benchmark experiments representative of many applications (Nigg 1990).

SCRABL is a cross section generation code that is a combination of SCAMP (Putnam 1964) S_n transport code, and RABBLE (Kier and Robba 1967) resolved resonance code. It solves the one-dimensional multigroup transport equation, allowing up to 99 energy groups. RABBLE permits calculation of resonance effects in one dimension to account for interference effects of resonance sequences of different isotopes. The resonance calculation uses the COMBINE ENDF/B-V cross section library. The code also provides a very generalized cross section coalescing option for both macroscopic and microscopic cross sections.

A four-group cross section database for fuel elements, reflector, and core structural materials is generated (Judd and Terry 1992) for input into PDQ. Cross sections for isotopes and materials in the fuel plates are generated with COMBINE and SCRABL. In the COMBINE unit cell calculation, the fuel meat, cladding, and coolant/moderator are homogenized. Disadvantage factors are calculated for the different fuel plates with the SCAMP code in slab geometry for use with the four-group fuel cross sections. An increase in fuel temperature will increase resonance absorption from Doppler broadening of the cross sections; however, the Doppler effect for the ATR fuel is not significant because the fuel element contains uranium fully enriched in U-235.

The cross sections for the reflector materials and structural materials are generated with COMBINE. Cross sections for experiment loop materials are generated using COMBINE, SCAMP, and PDQ. In the calculation, the four-group absorption rates by region are extracted from SCAMP output and made to match with those obtained from PDQ one-dimensional (1D) radial calculations. Iterative 1D PDQ and SCAMP runs are made to generate the cross section set representing the loop regions. First, the four-group cross sections calculated from SCAMP are input into a 1D PDQ model to compare absorption rates in the loop regions. The PDQ loop material absorption cross sections are then adjusted to match the SCAMP absorption rates. The 1D PDQ and SCAMP runs are repeated until the group-wise PDQ absorption rates in loop regions match the values calculated by SCAMP within the specified tolerance. This converged cross section data set is then input to the 2D PDQ model to represent the loop regions. The hafnium cross sections are generated with COMBINE and SCRABL. An infinite dilution COMBINE calculation for the hafnium isotopes is performed first, and SCRABL performs detailed resonance calculations for the specific hafnium-bearing component.

4.3.3.3 Reactivity Coefficients. Reactivity coefficients are calculated from perturbation theory methods by summing the normalized local perturbation integrals over the core volume. The adjoint fluxes used in the perturbation integrals are calculated with the 3D PDQ model described above using the adjoint option. Forward fluxes are calculated for both perturbed and nominal cases with the flux synthesis method using the thermal feedback model in PDQ with trial functions representative of the respective cases. Moderator density and fuel temperature reactivity coefficients are obtained from the reactivity change associated with each perturbation variable.

Table 4.3-1. Reactor core description.

Number of fuel elements in the core	40
Fuel element	
Type	Parallel curved plates
Number of plates per element	19
Fuel material	UAlx dispersed in Al
Nominal UAlx concentration	45% by weight
Meat thickness (in.)	0.020
Fuel cladding material	6061 O Al
Clad thickness (in.)	
Plate 1	0.030
Plates 2-18	0.015
Plate 19	0.040

Table 4.3-1. (continued).

Coolant gap between plates (in.)	0.078
Core loading (kg U-235)	Variable (30 kg to 43 kg)
Heat transfer area per element (ft^2)	33.8
Equivalent core diameter (in.)	54
Active fuel length (in.)	48
Side plate material	6061 T6 Al
Metal-to-water ratio	0.8
Coolant/moderator	Demineralized water
Reflector	
Material	Beryllium
Height (in.)	51
Reactivity control elements	
Outer shim control cylinders	
Location	Beryllium reflector
Configuration	Beryllium cylinders with 120° poison inserts
Poison inserts	1/4-in.-thick hafnium
Active length (in.)	46
Number of cylinders	16 (4 per quadrant)
Number of drives	8 (2 per quadrant)
Neck shim and regulating rods	
Location	Necks of corner lobes (4)
Poison section	48-in. long, 7/16 in. diameter fluted hafnium hollow rod
Follower section (Shim rods)	48 × 1/4-in. diameter Al rod
Extension rod (Regulating rod)	Inconel X
Number of rods	24 (6 per neck)
Number of drives	22 neck shim rod drives 2 regulating rod drives
Safety rods	
Location	SW, SE, N, W, E, and S flux traps
Poison section	4 80° hafnium sector inserts
Length (in.)	36
Follower section	4 80° Al sector inserts
Number of rods	up to 6

Table 4.3-2. Fuel element loadings.

Type element	7F	7NB	YA	7NBH
Fuel loading, U-235 g/cc				
Plates 1,2,18,19	1.0	1.0	1.0[a]	1.0
Plates 3,4,16,17	1.3	1.3	1.3	1.3
Plates 5 through 15	1.6	1.6	1.6	1.6
Burnable poison material	B_4C	None	B_4C	B_4C
Boron loading, mg nat B/cc				
Plates 1,2,18,19	14.2	0.0	14.2[a]	—[b]
Plates 3,4,16,17	7.5	0.0	7.5	—[c]
Plates 5 through 15	0.0	0.0	0.0	0.0

a. YA does not have fuel or boron in Plate 19.

b. Type I contains 0.143 gms B-10 in Plate 19.
Type II contains 0.143 gms B-10 in Plate 18.
Type IV contains 0.141 gms B-10 in Plates 1 and 2.

c. Type III contains 0.144 gms B-10 in Plates 16 and 17.

Table 4.3-3. Nominal nuclear parameters.

Reactivity coefficients	
Fuel temperature coefficient[a]	-2.8×10^{-4} \$/°F[a]
Moderator temperature coefficient (BOC)[a]	-9.2×10^{-3} \$/°F
Moderator temperature coefficient (EOC)[a]	-6.9×10^{-3} \$/°F
Power coefficient[b]	-1.5×10^{-3} \$/MW
Nominal delayed neutron fraction (β_{eff})	0.0072
Reactivity control elements[c]	
Safety rods (nominal worth 6 rods)	17.0 \$
Stuck safety rod worth (maximum 80 MW relative power)	6 \$
Neck shim rods (22)	5.2 \$
Outer shim control cylinders	
Total worth	12.9 \$
Shutdown worth from 80 degrees	8.2 \$
Burnable poison (BOC)[d]	11 \$

a. These values were determined analytically as described in Section 4.3.2.3.

b. This value was determined experimentally as discussed in Section 4.3.2.7.

c. These values were determined from reactor measurements as discussed in Section 4.3.2.4.

d. This value was determined analytically as discussed in Section 4.3.2.4.

Table 4.3-4. Point-to-average power density for 50/50 lobe power split case[a].

Day	Peak value[b]	10% Value[c]	50% Value	90% Value
0	2.53	2.18	1.80	2.13
3	2.36	2.03	1.69	1.99
17	2.03	1.75	1.54	1.77
38	1.66	1.55	1.38	1.50

a. Fuel element position 9 plate 5.

b. Value at left edge of fuel matrix.

c. Relative position from left edge of the fuel matrix.

Table 4.3-5. Point-to-average power density for 60/40 lobe power split case[a].

Day	Peak value[b]	10% Value[c]	50% Value	90% Value
0	2.81	2.38	1.95	2.16
3	2.65	2.23	1.90	2.19
17	2.52	2.24	1.94	2.16
31	2.20	2.03	1.86	2.06

a. Fuel element position 23 plate 15.

b. Value at left edge of fuel matrix.

c. Relative position from left edge of the fuel matrix.

Table 4.3-6. Point-to-average power density for the enveloping 70 MW lobe power split case.[a]

Day	Peak value[b]	10% Value[c]	50% Value	90% Value
0	3.59	2.88	2.43	2.74
1	3.69	2.93	2.42	2.66
3	3.65	2.93	2.45	2.72
10	3.46	2.90	2.47	2.73
17	3.27	2.84	2.43	2.62

a. Fuel element position 18 plate 15.

b. Value at left edge of fuel matrix.

c. Relative position from left edge of the fuel matrix.

Table 4.3-7. Summary of shim positions for the 50/50 lobe power split PDQ analysis.

Time (days)	Shim positions							
	NW lobe		NE lobe		SW lobe		SE lobe	
	Outer shims (degrees)	Neck shims inserted	Outer shims (degrees)	Neck shims inserted	Outer shims (degrees)	Neck shims inserted	Outer shims (degrees)	Neck shims inserted
0.0	56.6	1 2 3 4 5 6	56.6	1 2 3 4 5 6	56.6	1 2 3 5 6	56.6	1 2 3 5 6
1.0	85.4	1 2 3 4 5	85.4	1 2 3 4 5	85.4	1 2 3 5	85.4	1 2 3 5
3.0	75.0	1 2 3 4	75.0	1 2 3 4	75.0	1 2 3	75.0	1 2 3
10.0	85.4	1 2 3 4	85.4	1 2 3 4	85.4	1 2 3	85.4	1 2 3
17.0	95.2	1 2 3 4	95.2	1 2 3 4	95.2	1 2 3	95.2	1 2 3
24.0	111.7	1 2 3	111.7	1 2 3	111.7	1 2 3	111.7	1 2 3
31.0	124.4	1 2	124.4	1 2	124.4	1 2	124.4	1 2
38.0	134.2		134.2		134.2		134.2	

Table 4.3-8. Summary of shim positions for the 60/40 lobe power split PDQ analysis.

Time (days)	Shim positions							
	NW lobe		NE lobe		SW lobe		SE lobe	
	Outer shims (degrees)	Neck shims inserted	Outer shims (degrees)	Neck shims inserted	Outer shims (degrees)	Neck shims inserted	Outer shims (degrees)	Neck shims inserted
0.0	40.1	1 2 3 4 5 6	46.5	1 2 3 4 5 6	69.7	1 2 3 5 6	56.5	1 2 3 5 6
1.0	56.6	1 2 3	56.6	1 2 3	89.8	1 2 3	75.2	1 2 3
3.0	56.6	1 2 3	56.6	1 2 3	95.2	1 2 3	75.2	1 2 3
10.0	46.5	1 2 3	51.2	1 2	85.4	1 2	69.7	1 2 3
17.0	56.6	1	61.0	1 2	95.2	1 2	79.3	1 2
24.0	56.6	1	79.3	1 2	95.2	1 2	79.3	1 2
31.0	64.7	1	100.1	1 2	116.4	1 2	104.2	1

Table 4.3-9. Summary of shim positions for the enveloping 70 MW lobe power split PDQ analysis.

Time (days)	Shim positions							
	NW lobe		NE lobe		SW lobe		SE lobe	
	Outer shims (degrees)	Neck shims inserted	Outer shims (degrees)	Neck shims inserted	Outer shims (degrees)	Neck shims inserted	Outer shims (degrees)	Neck shims inserted
0.0	0.0	1 2 3 4 5 6	0.0	1 2 3 4 5 6	89.8	1 2 3 5 6	104.2	1 2 3 5 6
1.0	40.1	1 2 3 4 5 6	40.1	1 2 3 4 5 6	111.7	1 2 3 5 6	134.4	1 2 3 5 6
3.0	0.0	1 2 3 4 5	0.0	1 2 3 4 5	104.2	1 2 3 5	119.6	1 2 3 5 6
10.0	13.5	1 2 3 4	10.0	1 2 3 4	104.2	1 2 3	119.6	1 2 3
17.0	34.4	1 2	28.8	1 2	124.4	1 2 3	146.5	1 2 3

Table 4.3-10. PDQ result for scram recovery and restart study.

Reactor scram time	Lobe power (MW)					Eigenvalue	Δρ ($)	Peak point-to-average power density
	NW	NE	C	SW	SE			
0 (reference case)	23.8	24.4	47.5	62.8	71.5	0.983846	0.00	3.63
10 min	24.6	25.2	47.8	62.6	69.8	0.973003	-1.54	3.61
20 min	25.4	25.8	48.2	62.3	68.4	0.963720	-2.87	3.60
40 min	26.9	27.1	48.8	61.6	65.6	0.946805	-5.33	3.43
60 min	28.3	28.3	49.4	60.9	63.2	0.931761	-7.55	3.56
48 hr	27.0	26.9	49.9	61.6	65.5	0.974193	-1.37	3.55
54 hr	26.0	26.0	48.5	62.1	67.3	0.986927	0.43	3.45

Table 4.3-11. Reactivity coefficient values.

Reactivity coefficients					
			Moderator coefficient		
Reactor cycle		Fuel temperature coefficient	Density ($/lb/ft^3)		
ID	Power split	Perturbation ($/°F)	Eigenvalue	Perturbation	Temperature ($/°F)
82A	Nominal 30/70	-2.70 × 10-4	0.329	0.343	-6.45 × 10-3
60/40/E	Nominal 40/60	-2.68 × 10-4	0.343	0.340	-6.55 × 10-3
86C	Limiting 30/70	-2.89 × 10-4	0.362	0.372	-7.04 × 10-3
	Average	-2.76 × 10-4	0.35 ± 0.02	(-6.7 ± .4) × 10-3	

Lobe moderator reactivity weight factors lobe power normalized to 250 MW						
	Nominal 30/70 Core Configuration S SIPT voided		Nominal 40/60 Core Configuration NW LIPT voided		Limiting 30/70 Core Configuration SW SIPT voided	
Lobe	Power (MW)	Weight factor	Power (MW)	Weight factor	Power (MW)	Weight factor
NW	31	0.0655	42	0.2170	30	0.0658
NE	30	0.0740	41	0.1284	30	0.0640
C	55	0.2605	53	0.2517	55	0.2359
SW	66	0.3090	60	0.2335	74	0.4168
SE	68	0.2912	54	0.1694	61	0.2174

Table 4.3-12. Reactivity worth of voiding experiment loops.[c]

Conditions	Eigenvalue	Reactivity	
		Delta-rho[a]	($)
Nominal 30/70 Core Configuration			
All loops flooded	1.072025	0.00000	0.0000
NW loop voided	1.076826	0.00416	0.5776
N loop voided	1.074220	0.00191	0.2647
NE loop voided	1.076805	0.00414	0.5751
W loop voided	1.076524	0.00390	0.5414
C loop voided	1.076981	0.00429	0.5962
E loop voided	1.076474	0.00386	0.5354
SW loop voided	1.079433	0.00640	0.8891
S loop voided	1.080623	0.00742	1.0308
SE loop voided	1.079314	0.00630	0.8749
Nominal 40/60 Core Configuration			
All loops flooded	1.074630	0.00000	0.0000
NW loop voided	1.083960	0.00801	1.1124
N loop voided	1.079015	0.00378	0.5252
NE loop voided	1.083451	0.00758	1.0523
W loop voided	1.080464	0.00502	0.6979
C loop voided	1.079736	0.00440	0.6112
E loop voided	1.079775	0.00443	0.6158
SW loop voided	1.081173	0.00563	0.7822
S loop voided	1.081340	0.00577	0.8020
SE loop voided	1.080156	0.00476	0.6612
Limiting 30/70 Core Configuration			
All loops flooded	1.054867	0.00000	0.0000
NW loop voided	1.059285	0.00395	0.5491
N loop voided	1.056786	0.00172	0.2391
NE loop voided	1.059168	0.00385	0.5347
W loop voided	1.059340	0.00400	0.5559
C loop voided	—[b]	—	—
E loop voided	1.058669	0.00340	0.4729
SW loop voided	1.063063	0.00731	1.0151
S loop voided	1.063042	0.00729	1.0125
SE loop voided	1.061061	0.00553	0.7686

a. $\Delta\rho = \frac{k - k_o}{kk_o}$.

b. Not calculated.

c. The NE, C, E, and S flux traps no longer contain loop facility IPTs.

Table 4.3-13. Reactivity control element worth summary.

Component	Nominal Worth ($)
Neck shim rods[a] (22 rods)	5.2 (0.24$/rod)
Safety rods[a] (6 rods)	17.0 (2.83$/rod)
Outer shim control cylinders[a] (16 cylinders)	
Total (0 to 160°)	12.9 (3.23$/quadrant)
80-degree position (80 to 160°)	4.7 (1.18$/quadrant)
Regulating Rods[a] (2 rods)	0.52 (0.26$/rod)
Burnable poison[b] (max 40 7F fuel elements)	10.9 (0.27$/fuel element)

a. Measured reactivity after the 1994 CIC. All new 7F fuel elements, new reflector, and new hafnium components in core.

b. Calculated value.

Table 4.3-14. Neck shim rod reactivity worth.[a]

Position	Worth ($)
NW-1	0.23
NW-2	0.21
NW-3	0.20
NW-4	0.21
NW-5	0.22
NW-6	0.26
NW-Total	1.33
NE-1	0.23
NE-2	0.21
NE-3	0.20
NE-4	0.20
NE-5	0.22
NE-6	0.25
NE-Total	1.31
SW-1	0.26
SW-2	0.23
SW-3	0.24
SW-4 (reg rod)	(0.26)
SW-5	0.27
SW-6	0.31
SW-Total[b]	1.31
SE-1	0.25
SE-2	0.23
SE-3	0.23
SE-4 (reg rod)	(0.26)
SE-5	0.27
SE-6	0.31
SE-Total[b]	1.29

a. Measured reactivity after the 1994 CIC. All new 7F fuel elements, new reflector, and new hafnium components in core.

b. SW and SE totals do not include the regulating rod worths.

Table 4.3-15. Summary of safety rod reactivity measurement results.

Safety Rod Integral Reactivity [a,b] ($) (adjusted to flat relative powers)							
Cycle	North	West	East	Southwest	South	Southeast	Average
73A	3.067 ± 0.446	2.878 ± 0.316	2.986 ± 0.332	2.700 ± 0.294	3.077 ± 0.388	3.044 ± 0.519	2.959 ± 0.146
77C	2.128 ± 0.400	2.788 ± 0.508	2.612 ± 0.250	2.988 ± 0.465	2.986 ± 0.405	3.127 ± 0.539	2.772 ± 0.363
81B	2.601 ± 0.410	3.409 ± 0.370	2.716 ± 0.328	2.963 ± 0.384	3.359 ± 0.448	3.184 ± 0.373	3.039 ± 0.335
87A	2.058 ± 0.479	—	2.999 ± 0.311	2.891 ± 0.539	3.351 ± 0.415	3.062 ± 0.360	2.872 ± 0.486
90A	2.540 ± 0.312	—	2.505 ± 0.176	2.773 ± 0.290	2.717 ± 0.226	2.742 ± 0.240	2.655 ± 0.124
95A	2.448 ± 0.335	—	2.877 ± 0.354	3.207 ± 0.605	3.025 ± 0.264	2.864 ± 0.430	2.884 ± 0.281
97A	2.474 ± 0.338	—	3.196 ± 0.381	2.413 ± 0.258	2.898 ± 0.192	3.035 ± 0.422	2.803 ± 0.346
101A[c]	2.715 ± 0.256[d]	—	2.598 ± 0.171	2.711 ± 0.242	2.459 ± 0.123	2.550 ± 0.272	2.607 ± 0.109
103A[e]	2.379 ± 0.179	2.836 ± 0.212	2.891 ± 0.192	2.790 ± 0.2.43	3.396 ± 0.251	2.589 ± 0.239	2.814 ± 0.342
Average	2.490 ± 0.302	2.978 ± 0.290	2.820 ± 0.227	2.764 ± 0.287	3.030 ± 0.314	2.911 ± 0.235	2.834 ± 0.218

a. The uncertainty shown for the individual safety rod reactivities is the standard deviation in the extrapolated values from each insertion point.

b. The uncertainty shown for the average safety rod reactivities is the statistical combination of the standard deviations in the individual safety rod reactivities.

c. The N and SW flux traps were reconfigured from small capsule irradiation facilities to SIPT during the Cycle 103A (CIC) outage. The E and S flux traps were reconfigured from SIPT to small capsule irradiation facilities during the Cycle 103A outage. There were no statistically significant changes in the safety rod reactivities due to the reconfigurations.

d. The hafnium plate in the N-2 position was changed.

e. The N and SW flux traps were reconfigured from SIPT to small capsule irradiation facilities during the Cycle 101A (PCU) outage. There were no statistically significant changes in the safety rod reactivities as a result of the reconfigurations.

Table 4.3-16. Minimum shutdown worth for the safety rods.[a]

Number of rods	80/20 lobe power split ($)	50/50 lobe power split ($)
5	15.1	12.0
4	10.0	9.6
3	5.9	7.2

a. Based on the nominal safety rod worth less two standard deviations in the uncertainty in the worth measurement (i.e., 2.39$/rod)

Table 4.3-17. Maximum reactivity insertion rates of control elements.

Control element	Number	Speed	Active length	Nominal total worth ($)	Max. differential worth	80/20 total worth ($)	80/20 insertion rate ($/sec)	Average single element differential worth
Safety rods	6	9 in/min	36 in	17.0	0.037 in^{-1}	25.78	0.14	0.08 $/in
Neck shim rods	22	6 in/min	48 in	5.23	0.037 in^{-1}	6.92	0.026	0.005 $/in
Neck shim rod (most reactive rod)	1 #6 rod	6 in/min	48 in	0.28	0.037 in^{-1}	0.52	0.002	0.005 $/in
Regulating rod	1	6 in/min	48 in	0.26	0.037 in^{-1}	0.57[a]	1.05	0.005 $/in
Outer shim cylinders	16 cylinders 4 per set	20 deg/min	160 deg	12.9	0.135 $/deg	16.6	0.053	0.02 $/deg

a. Maximum worth is assumed to be 0.57$ for the accident analysis. The actual 80/20 enhanced reactivity is 0.41$.

Table 4.3-18. Typical control element positions during a core cycle.

Core position	Cycle time (days)	Neck shim[a] positions	OSCC position relative (deg)	Lobe power (MW)
NW	0	1 1 1 1 1 1	40.1	39.55
	1	1 1 1 1 0 0	56.6	39.43
	3	1 1 1 0 0 0	51.2	39.07
	10	1 1 0 0 0 0	56.6	39.66
	17	1 1 0 0 0 0	64.7	39.91
	24	1 0 0 0 0 0	69.7	40.54
NE	0	1 1 1 1 1 1	46.5	40.31
	1	1 1 1 1 0 0	56.6	38.26
	3	1 1 0 0 0 0	51.2	38.07
	10	1 1 0 0 0 0	56.6	38.64
	17	1 1 0 0 0 0	64.7	38.83
	24	1 0 0 0 0 0	69.7	39.79
SW	0	1 1 1 0 1 1	69.7	60.56
	1	1 1 1 0 0 0	89.8	62.91
	3	1 1 0 0 0 0	89.8	61.36
	10	1 1 0 0 0 0	95.2	61.55
	17	1 1 0 0 0 0	111.7	62.97
	24	1 0 0 0 0 0	134.2	60.73
SE	0	1 1 1 0 1 1	56.6	51.78
	1	1 1 1 0 0 0	75.2	54.40
	3	1 1 0 0 0 0	75.2	53.53
	10	1 1 0 0 0 0	79.3	53.63
	17	1 1 0 0 0 0	89.8	54.35
	24	1 0 0 0 0 0	100.1	54.27

a. Neck Shim Positions 1-6
1 = Fully Inserted
0 = Fully Withdrawn.

Table 4.3-19. Summary of fast flux data (E > 1 MeV).

Location	Distance from vessel center (in.)	Cycle number	Power division (MW)	Normalization factor[a]	Measured fast flux (10^{10} n/cm^2 sec)	Normalized fast flux[b] (10^{10} n/cm^2 sec)
OS-5	30.5	5A	43.2-43.2-43.2-43.2-43.2	1.16	20.4	23.60
OS-10	35.0	5A	43.2-43.2-43.2-43.2-43.2	1.16	6.74	7.80
OS-15	39.5	5A	43.2-43.2-43.2-43.2-43.2	1.16	2.33	2.70
OS-20	44.0	5A	43.2-43.2-43.2-43.2-43.2	1.16	0.710	0.82
Drop tube	54	41D	52.2-21.9-34.0-25.1-22.9	1.35	0.00718	0.00969
I-1	22.5	41D	52.2-21.9-34.0-25.1-22.9	1.35	68.0	227.0
I-6	22.5	42A	52.2-21.9-34.0-25.1-22.9	2.29	135.02	309.0
ON-5	30.5	67B	19.4-20.7-31.1-24.2-38.9	2.49	9.04	22.50
ON-10	35.0	67B	19.4-20.7-31.1-24.2-38.9	2.49	2.93	7.31
OS-5	30.5	67B	19.4-20.7-31.1-24.2-38.9	1.58	19.60	31.10
ON-10	35.0	67B	19.4-20.7-31.1-24.2-38.9	1.58	6.68	10.60
OS-15	39.5	67B	19.4-20.7-31.1-24.2-38.9	1.58	1.99	3.15
OS-20	44.0	67B	19.4-20.7-31.1-24.2-38.9	1.58	0.618	0.979
I-1	22.5	67B	23.0-23.0-28.7-30.9-37.0	2.17	175.0	381.0
ON-5	30.5	76B-1	23.0-23.0-28.7-30.9-37.0	2.17	19.30	41.90
ON-10	35.0	76B-1	23.0-23.0-28.7-30.9-37.0	2.17	6.38	13.80
OS-5	30.5	76B-1	23.0-23.0-28.7-30.9-37.0	1.47	35.10	51.60
OS-10	35.0	76B-1	23.0-23.0-28.7-30.9-37.0	1.47	11.50	16.90
OS-15	39.5	76B-1	23.0-23.0-28.7-30.9-37.0	1.47	3.89	5.72
OS-20	44.0	76B-1	23.0-23.0-28.7-30.9-37.0	1.47	1.16	1.71

a. Correction for unbalanced lobe power.

b. Normalized to 250 MW balanced power.

Table 4.3-20. Summary of thermal flux data.

Location (10^{12} n/cm^2 sec)	Distance from vessel center	Normalized[a] thermal flux (in.)
I-6	22.5	38.9
ON-5	30.5	9.69
ON-5	30.5	8.74
ON-10	35	4.53
OS-5	30.5	5.55
OS-5	30.5	7.86
OS-10	35.0	2.69
OS-10	35.0	2.98
OS-15	39.5	1.26
OS-15	39.5	1.24
OS-20	44.0	0.60
OS-20	44.0	0.56

a. Normalized to 50 MW source power (average of the two adjacent corner lobe powers).

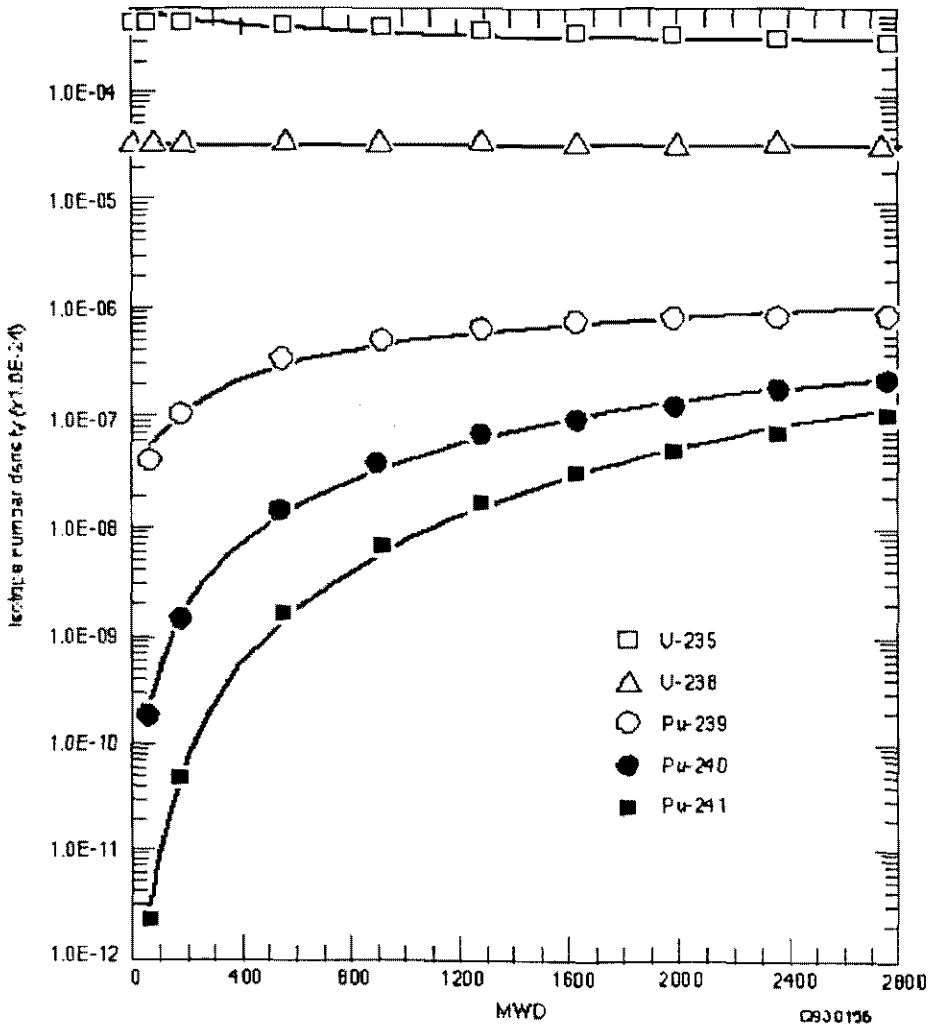

Figure 4.3-1. Consumption and buildup of U and Pu isotopes. **(For Information Only)**

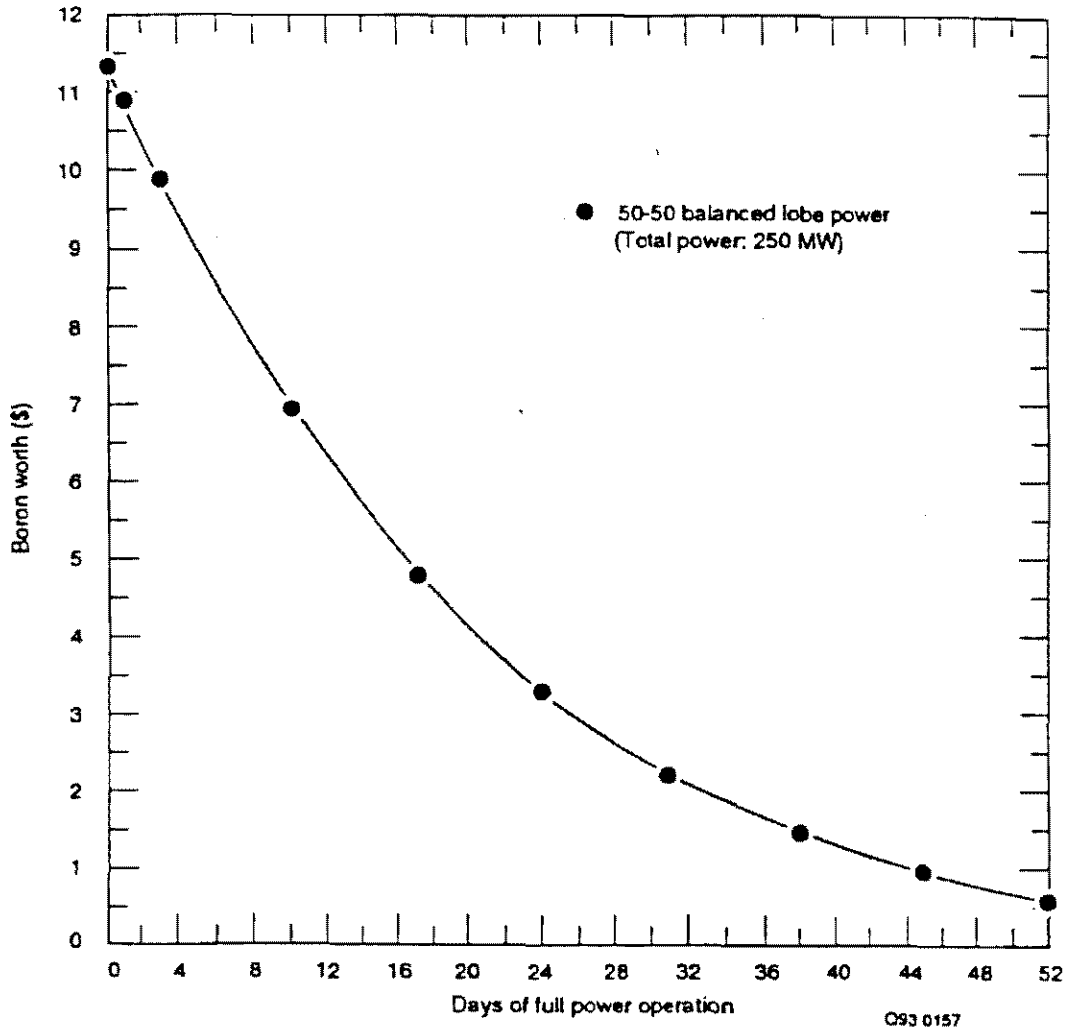

Figure 4.3-2. Reactivity change due to boron in the fuel. **(For Information Only)**

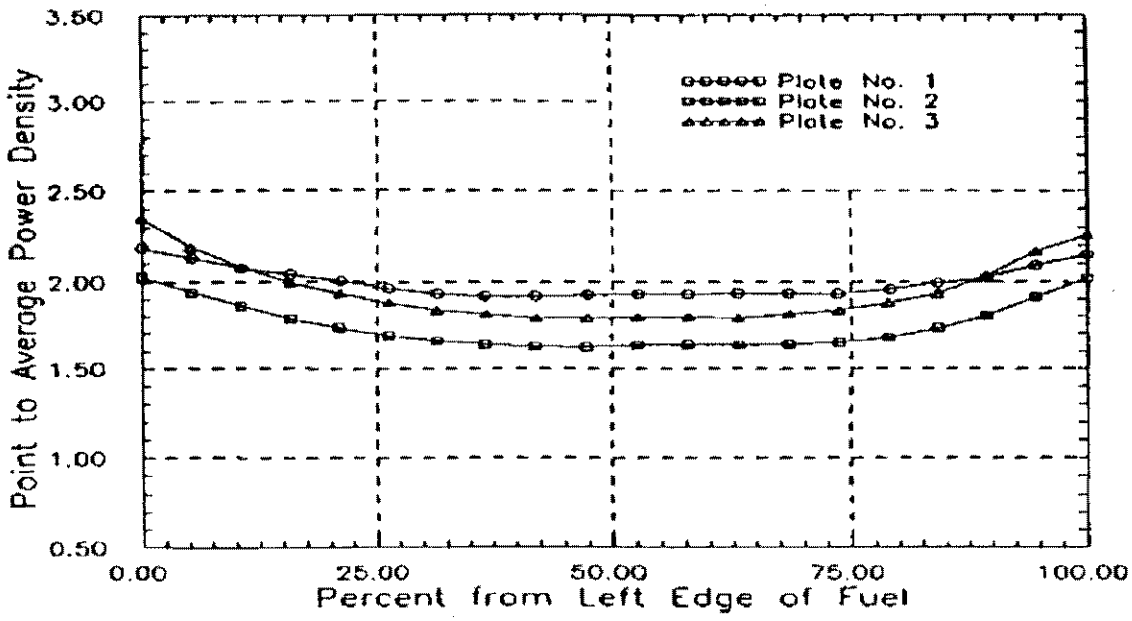

Figure 4.3-3. Azimuthal power distribution in Fuel Element 9, 0 days exposure, 50/50 lobe power split, Plates 1-3. **(For Information Only)**

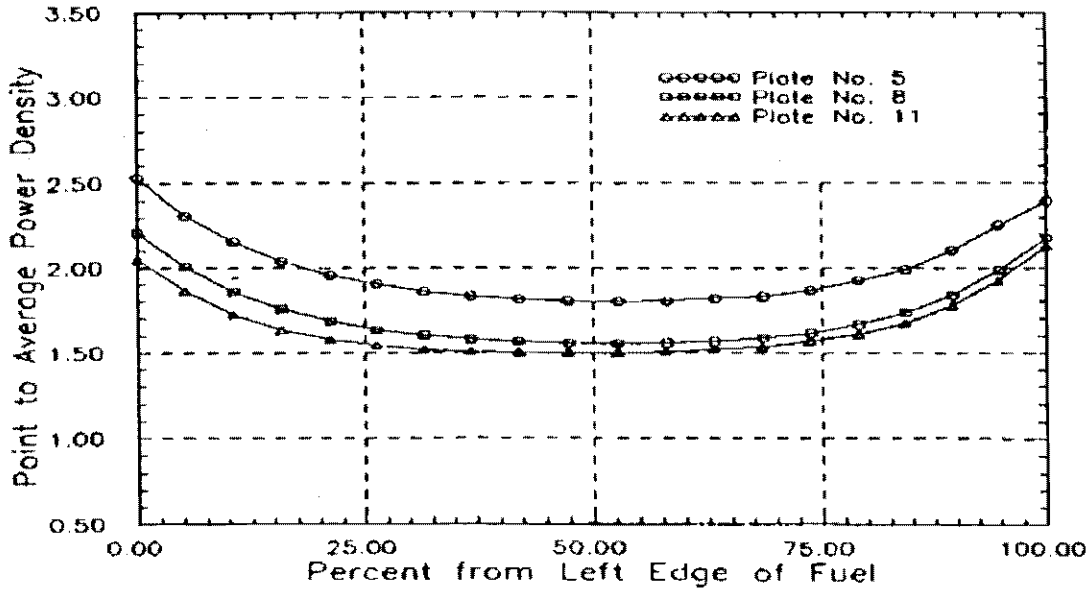

Figure 4.3-4. Azimuthal power distribution in Fuel Element 9, 0 days exposure, 50/50 lobe power split, Plates 5, 8, 11. **(For Information Only)**

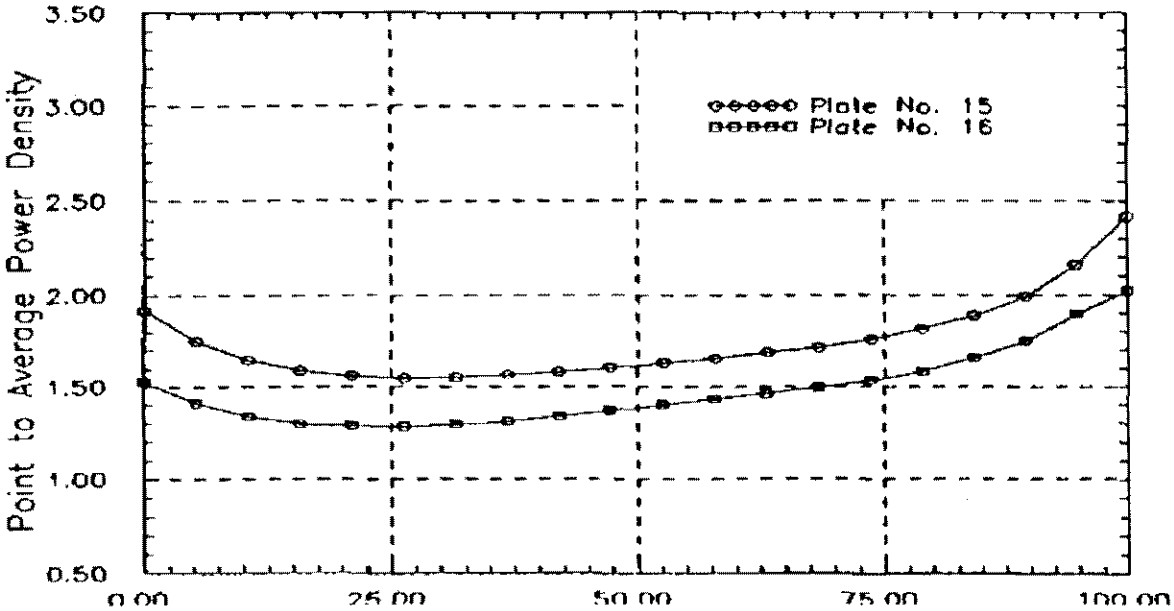

Figure 4.3-5. Azimuthal power distribution in Fuel Element 9, 0 days exposure, 50/50 lobe power split, Plates 15-16. **(For Information Only)**

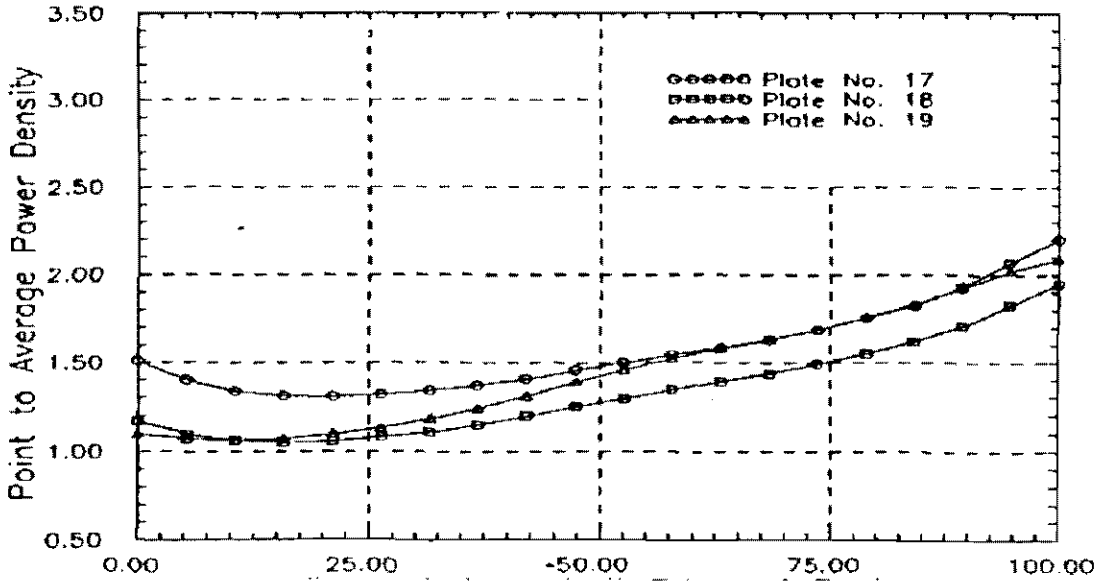

Figure 4.3-6. Azimuthal power distribution in Fuel Element 9, 0 days exposure, 50/50 lobe power split, Plates 17-19. **(For Information Only)**

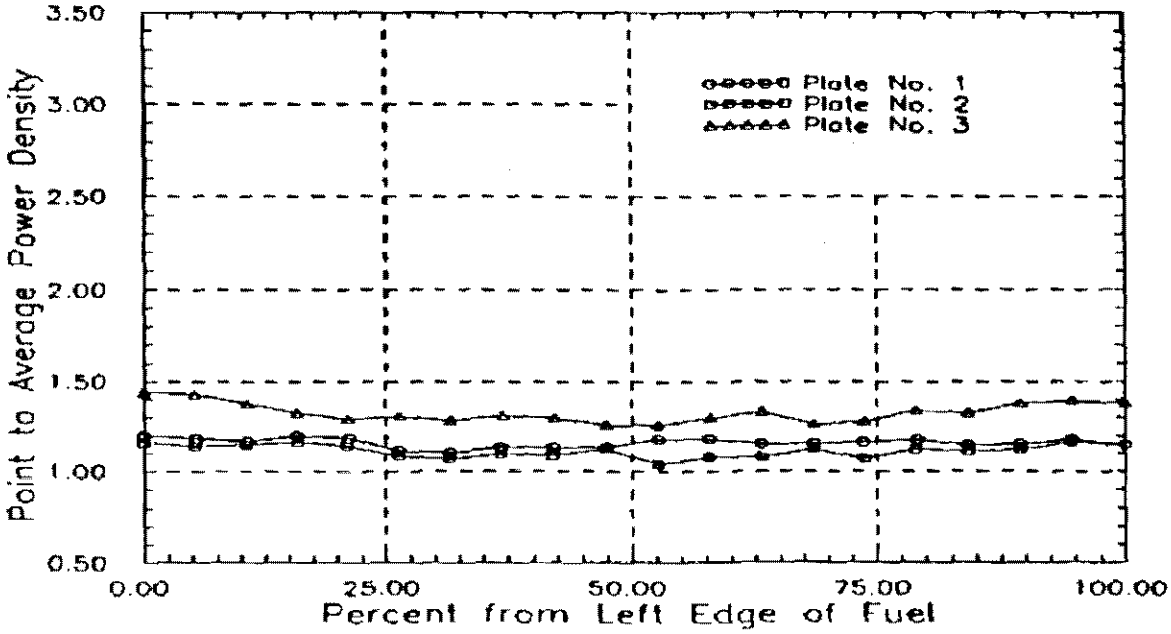

Figure 4.3-7. Azimuthal power distribution in Fuel Element 9, 38 days exposure, 50/50 lobe power split, Plates 1-3. **(For Information Only)**

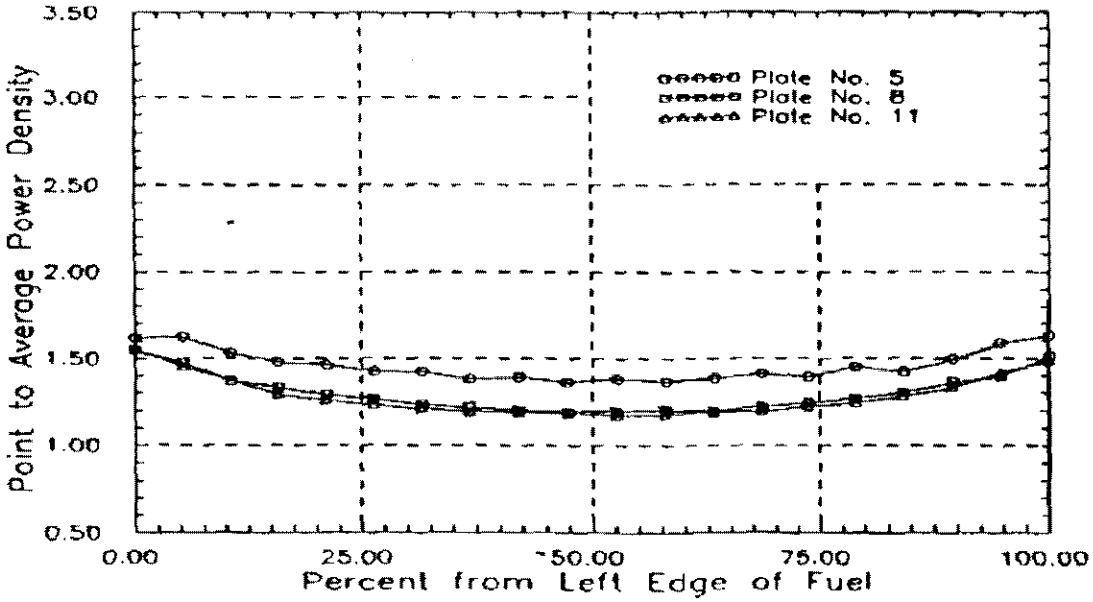

Figure 4.3-8. Azimuthal power distribution in Fuel Element 9, 38 days exposure, 50/50 lobe power split, Plates 5, 8, 11. **(For Information Only)**

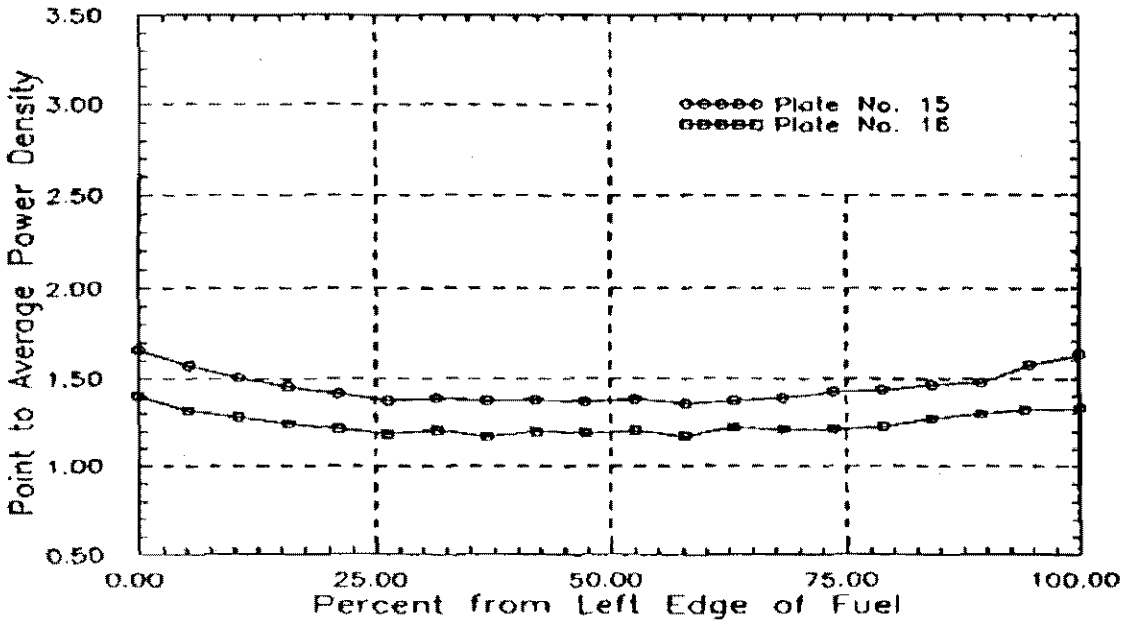

Figure 4.3-9. Azimuthal power distribution in Fuel Element 9, 38 days exposure, 50/50 lobe power split, Plates 15-16. **(For Information Only)**

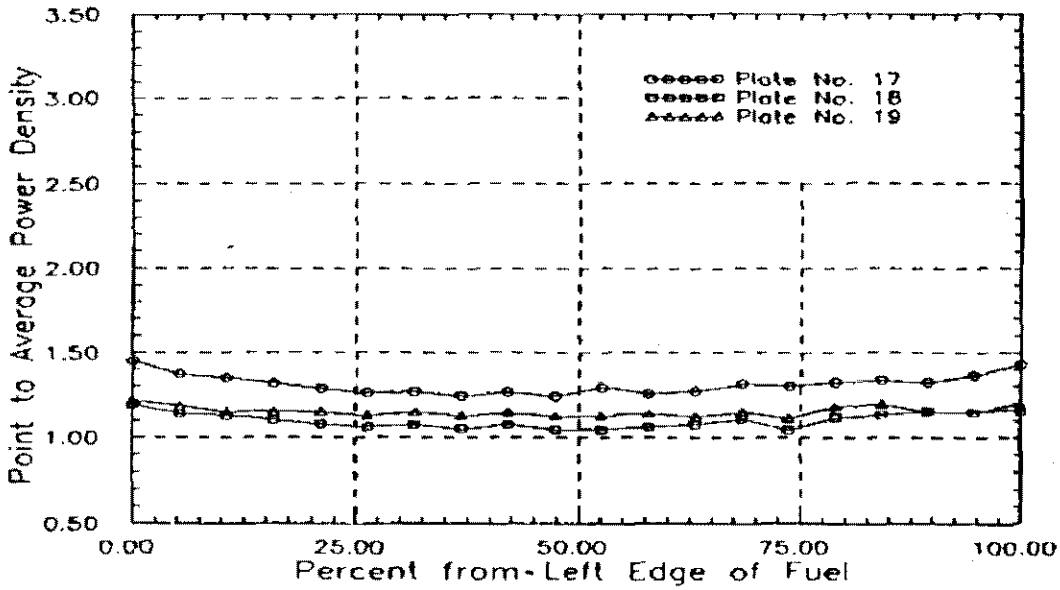

Figure 4.3-10. Azimuthal power distribution in Fuel Element 9, 38 days exposure, 50/50 lobe power split, Plates 17-19. **(For Information Only)**

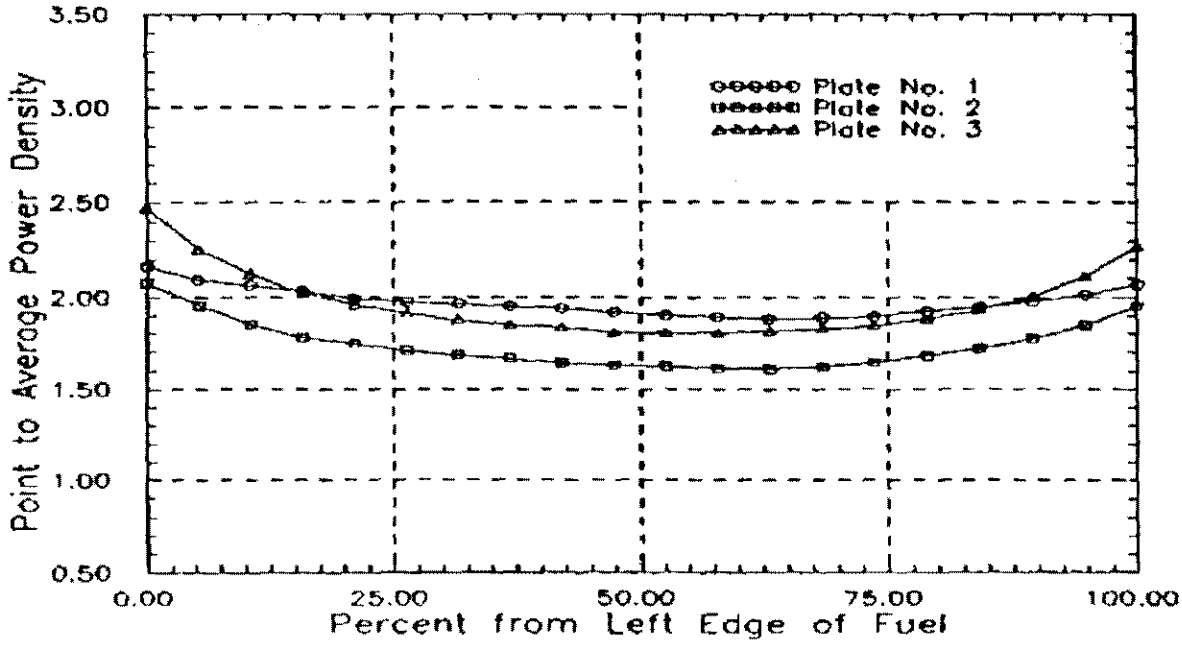

Figure 4.3-11. Azimuthal power distribution in Fuel Element 23, 0 days exposure, 60/40 lobe power split, Plates 1-3. **(For Information Only)**

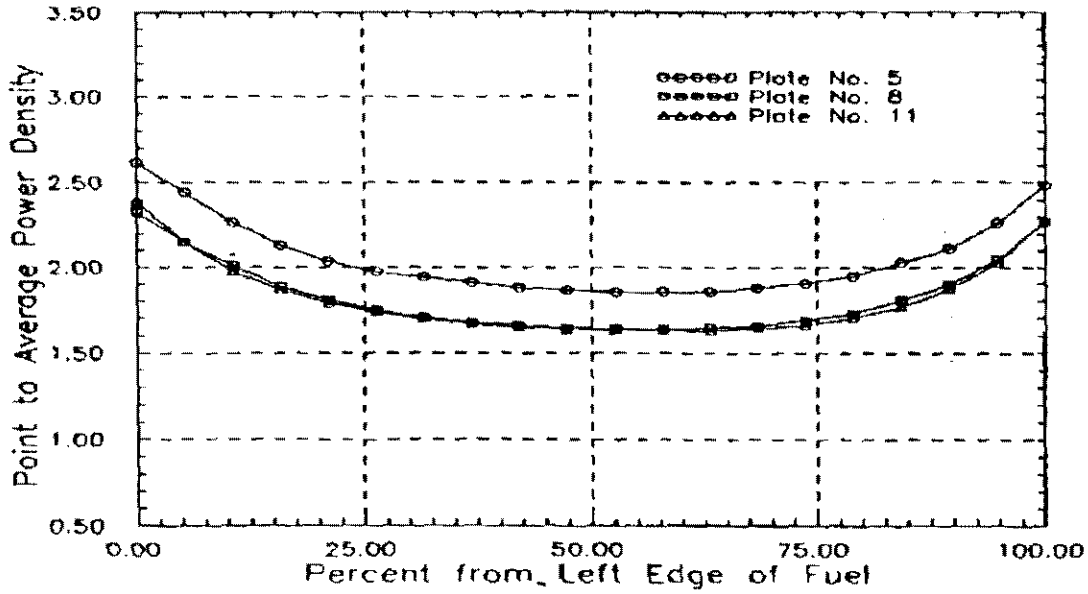

Figure 4.3-12. Azimuthal power distribution in Fuel Element 23, 0 days exposure, 60/40 lobe power split, Plates 5, 8, 11. **(For Information Only)**

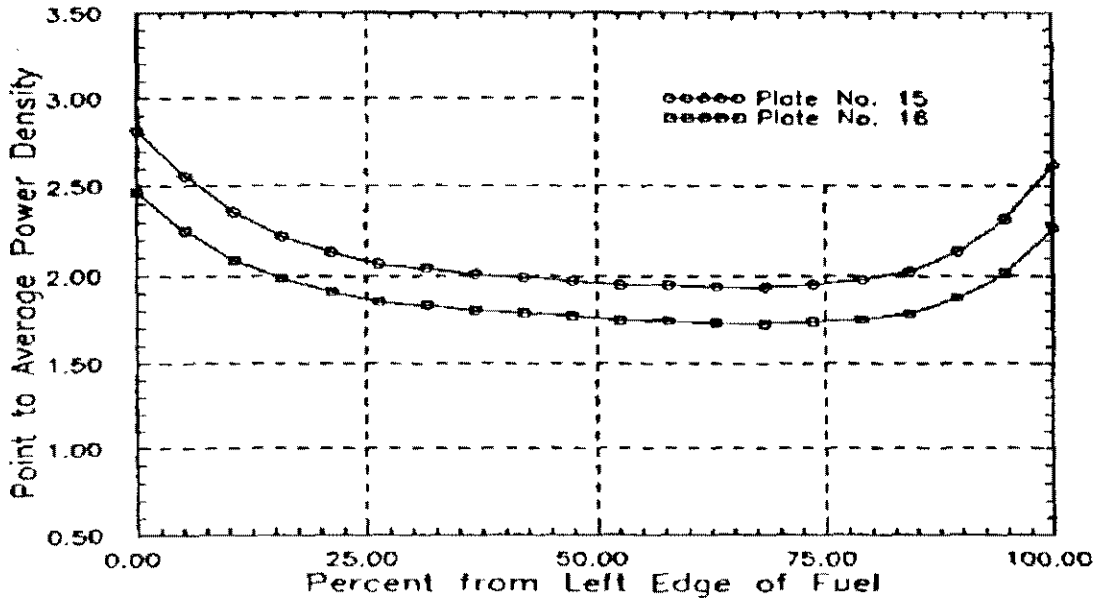

Figure 4.3-13. Azimuthal power distribution in Fuel Element 23, 0 days exposure, 60/40 lobe power split, Plates 15-16. **(For Information Only)**

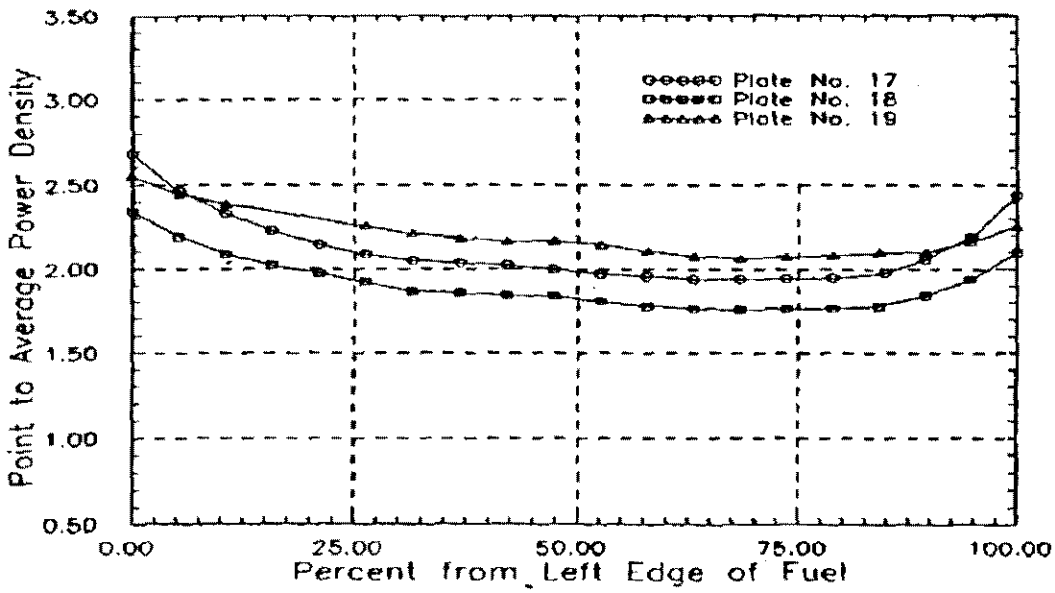

Figure 4.3-14. Azimuthal power distribution in Fuel Element 23, 0 days exposure, 60/40 lobe power split, Plates 17-19. **(For Information Only)**

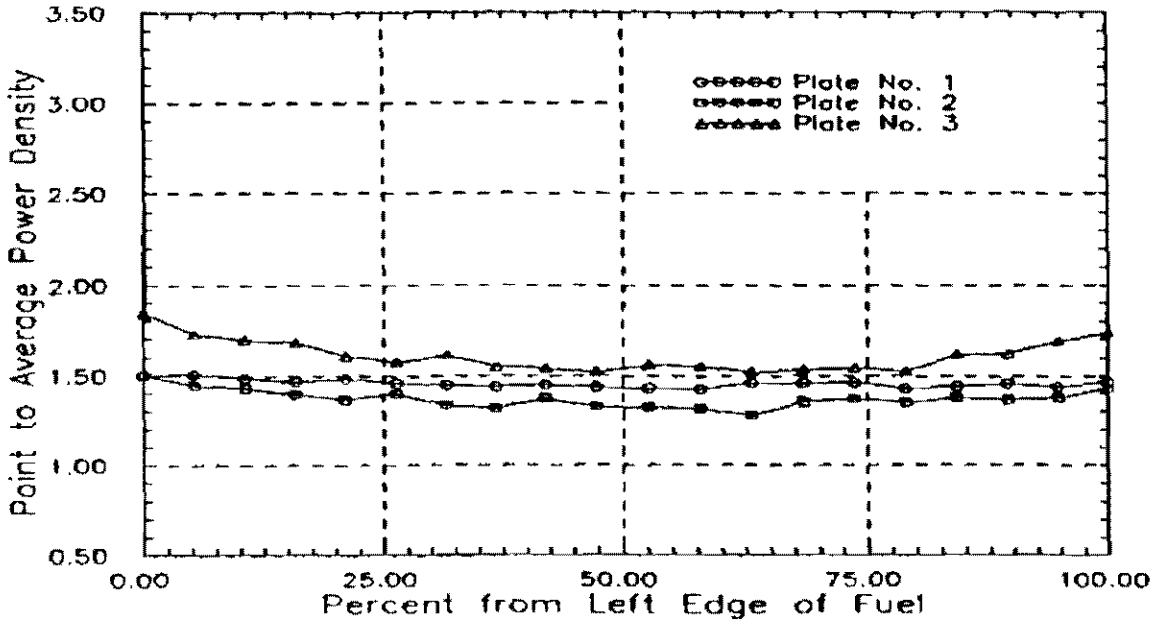

Figure 4.3-15. Azimuthal power distribution in Fuel Element 23, 31 days exposure, 60/40 lobe power split, Plates 1-3. **(For Information Only)**

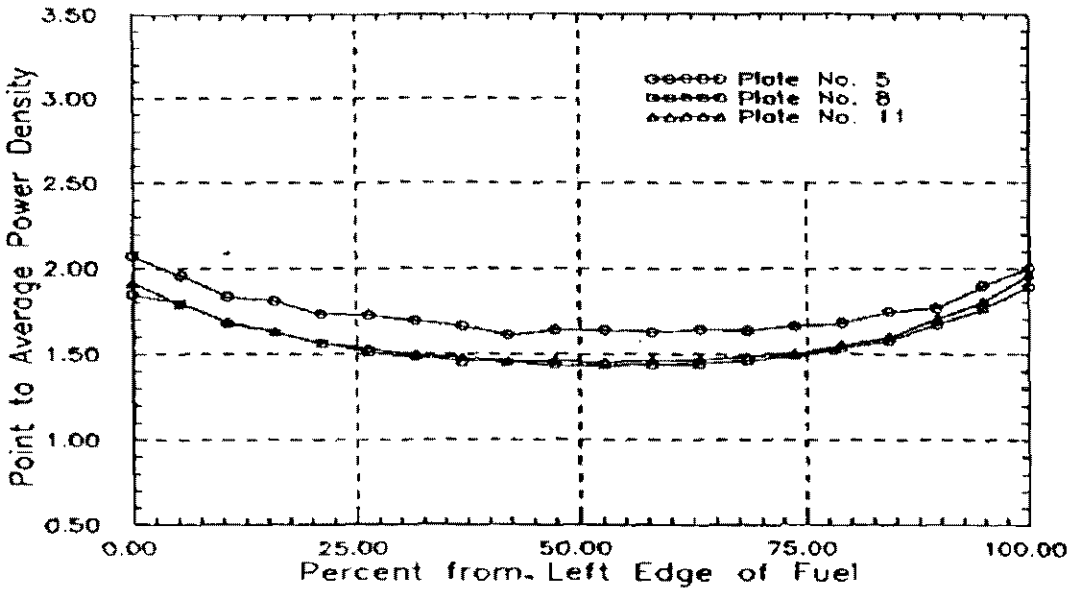

Figure 4.3-16. Azimuthal power distribution in Fuel Element 23, 31 days exposure, 60/40 lobe power split, Plates 5, 8, 11. **(For Information Only)**

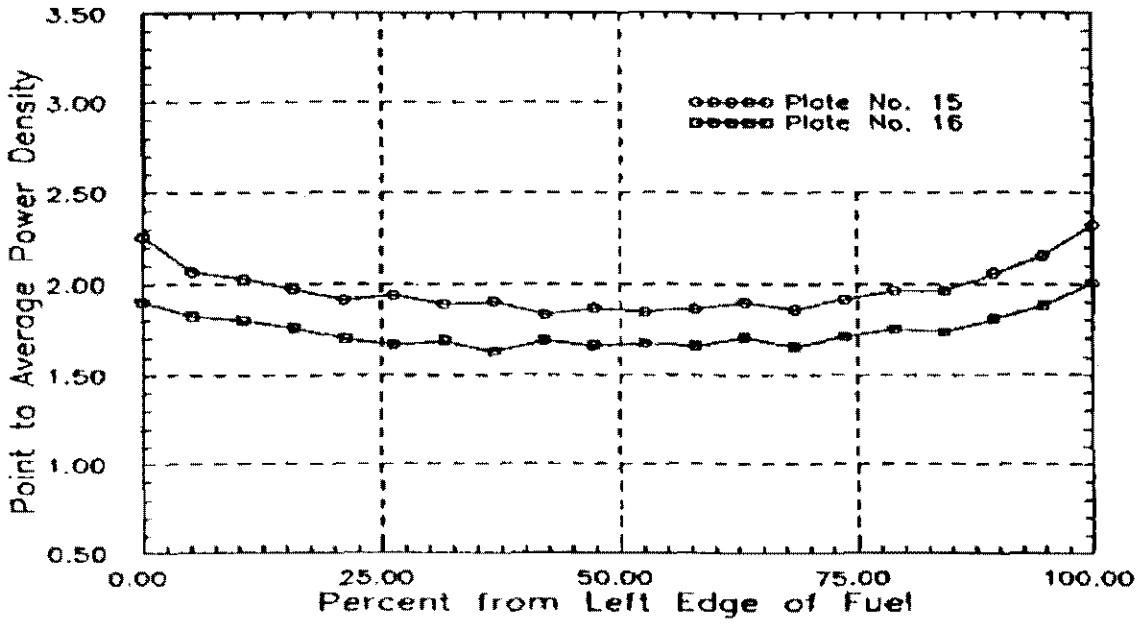

Figure 4.3-17. Azimuthal power distribution in Fuel Element 23, 31 days exposure, 60/40 lobe power split, Plates 15-16. **(For Information Only)**

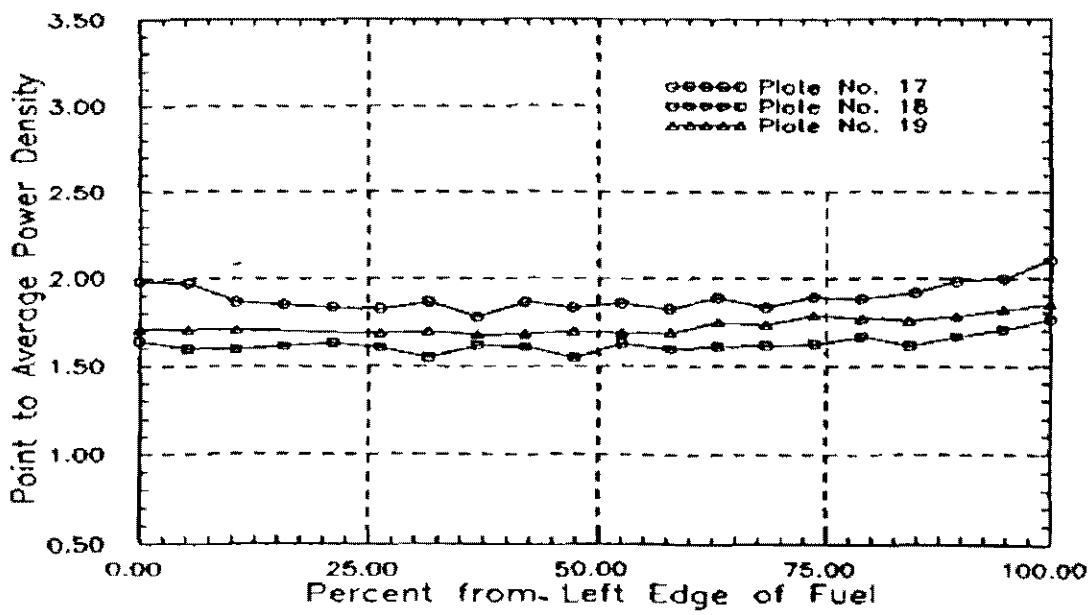

Figure 4.3-18. Azimuthal power distribution in Fuel Element 23, 31 days exposure, 60/40 lobe power split, Plates 17-19. **(For Information Only)**

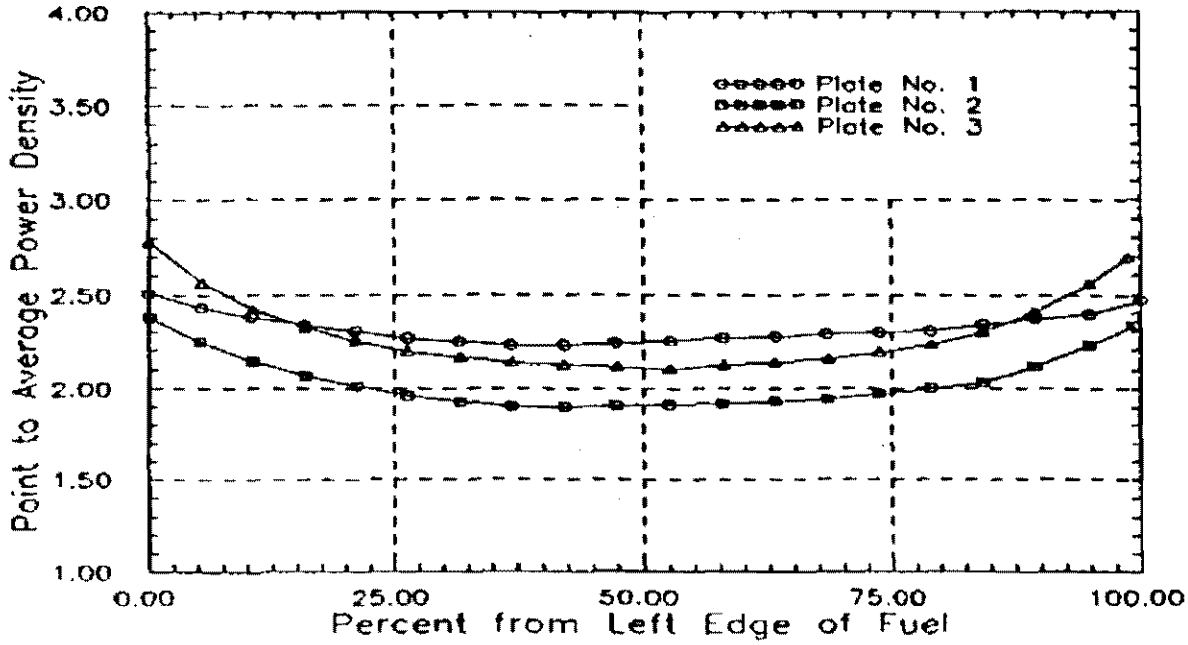

Figure 4.3-19. Azimuthal power distribution in Fuel Element 18, 1 day exposure, Env 70 MW lobe power split, Plates 1-3. **(For Information Only)**

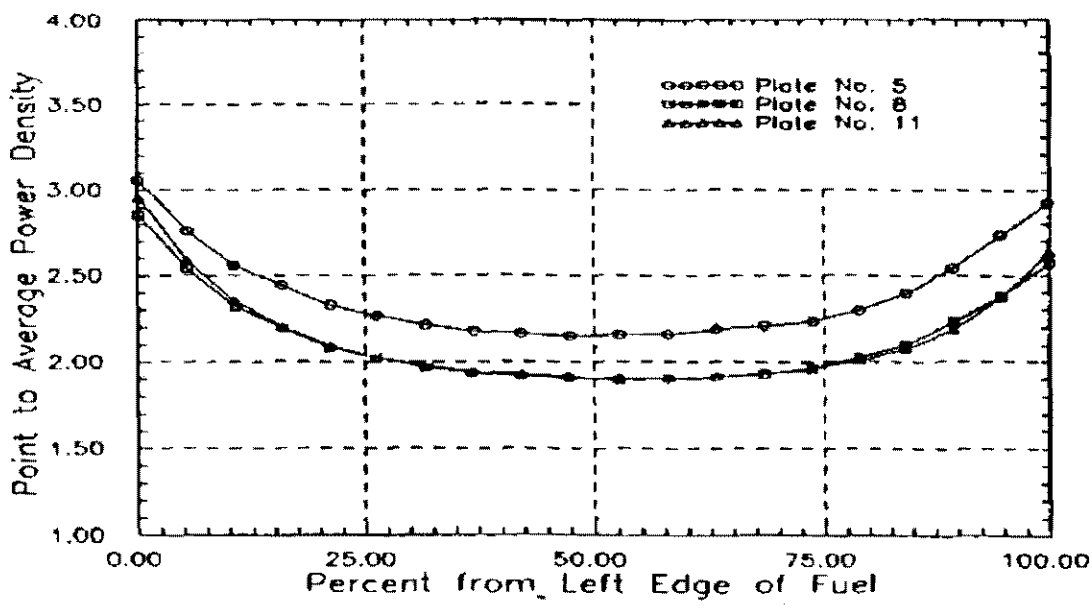

Figure 4.3-20. Azimuthal power distribution in Fuel Element 18, 1 day exposure, Env 70 MW lobe power split, Plates 5, 8, 11. **(For Information Only)**

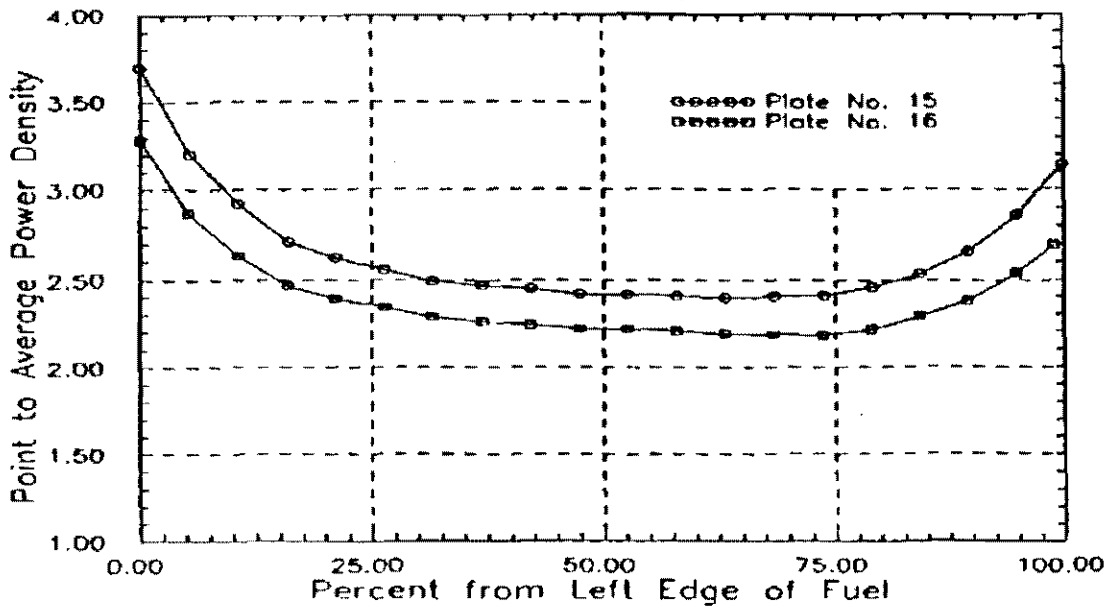

Figure 4.3-21. Azimuthal power distribution in Fuel Element 18, 1 day exposure, Env 70 MW lobe power split, Plates 15-16. **(For Information Only)**

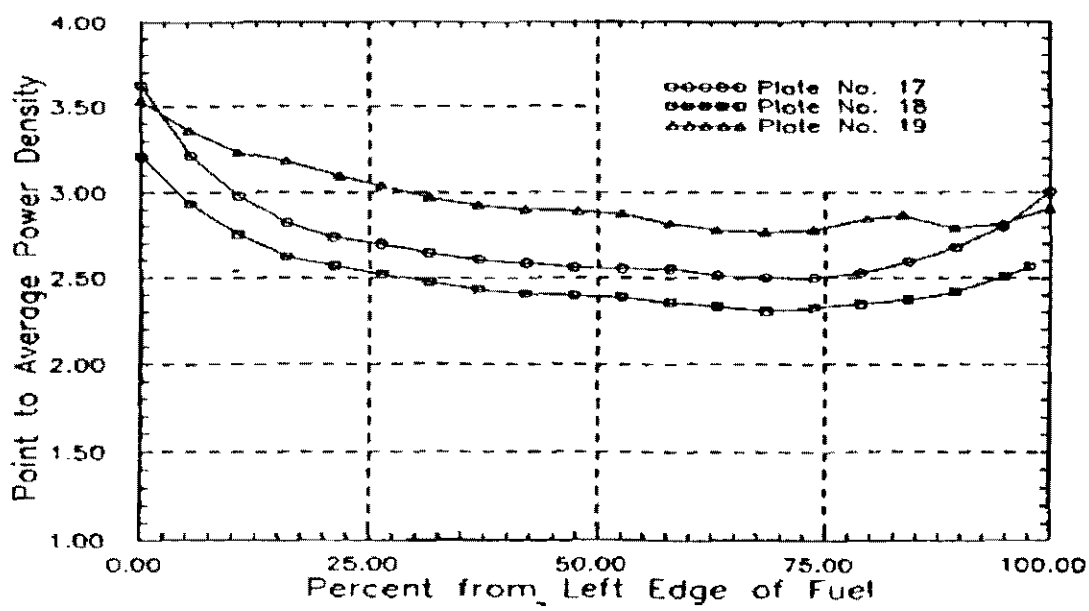

Figure 4.3-22. Azimuthal power distribution in Fuel Element 18, 1 day exposure, Env 70 MW lobe power split, Plates 17-19. **(For Information Only)**

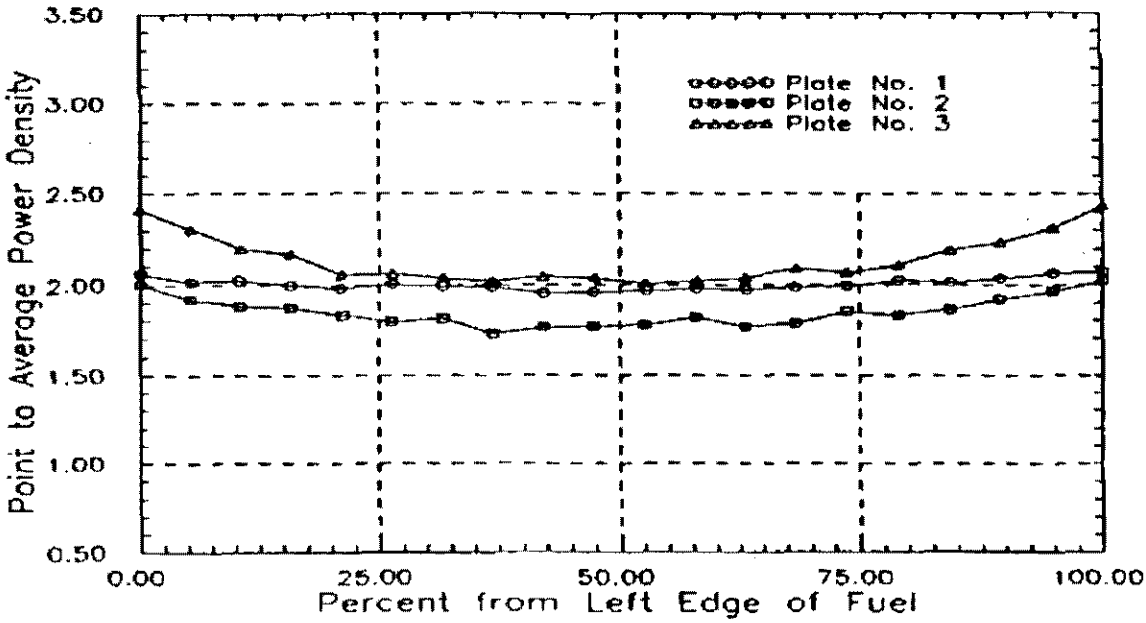

Figure 4.3-23. Azimuthal power distribution in Fuel Element 18, 17 days exposure, Env 70 MW lobe power split, Plates 1-3. **(For Information Only)**

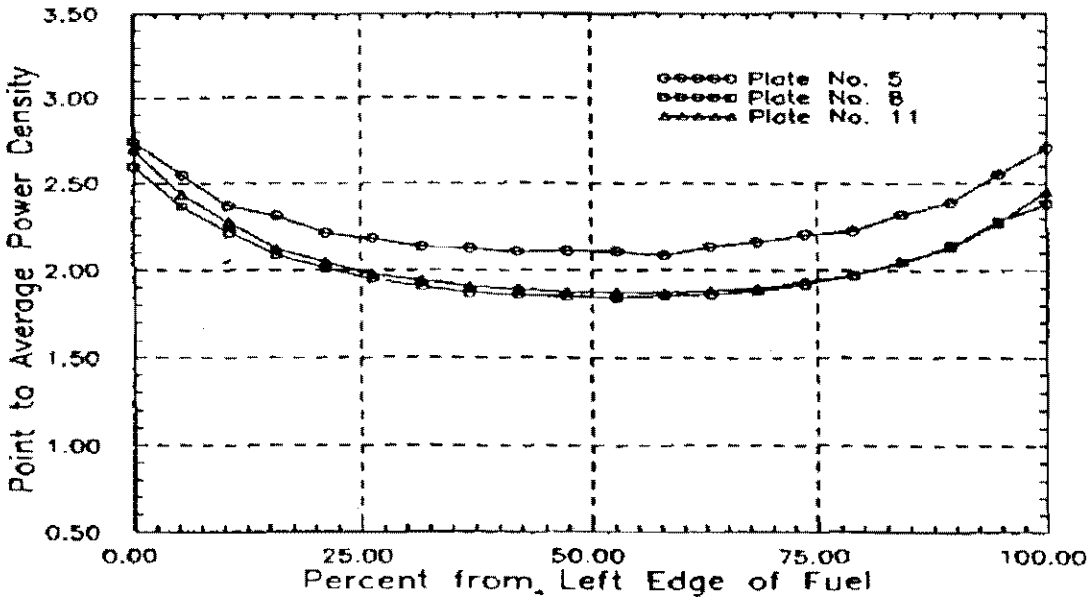

Figure 4.3-24. Azimuthal power distribution in Fuel Element 18, 17 days exposure, Env 70 MW lobe power split, Plates 5, 8, 11. **(For Information Only)**

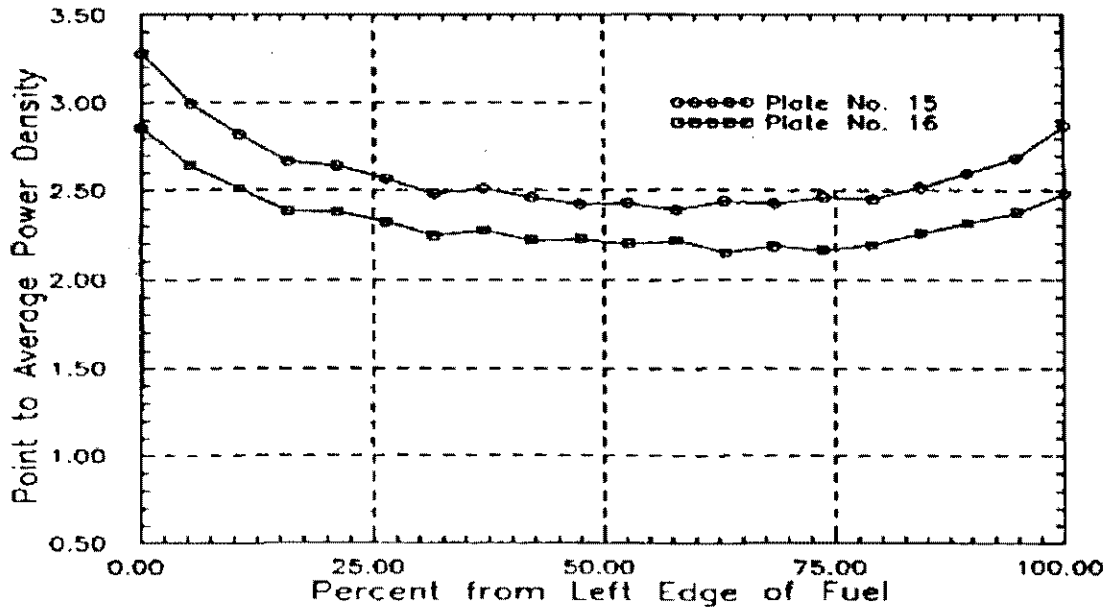

Figure 4.3-25. Azimuthal power distribution in Fuel Element 18, 17 days exposure, Env 70 MW lobe power split, Plates 15-16. **(For Information Only)**

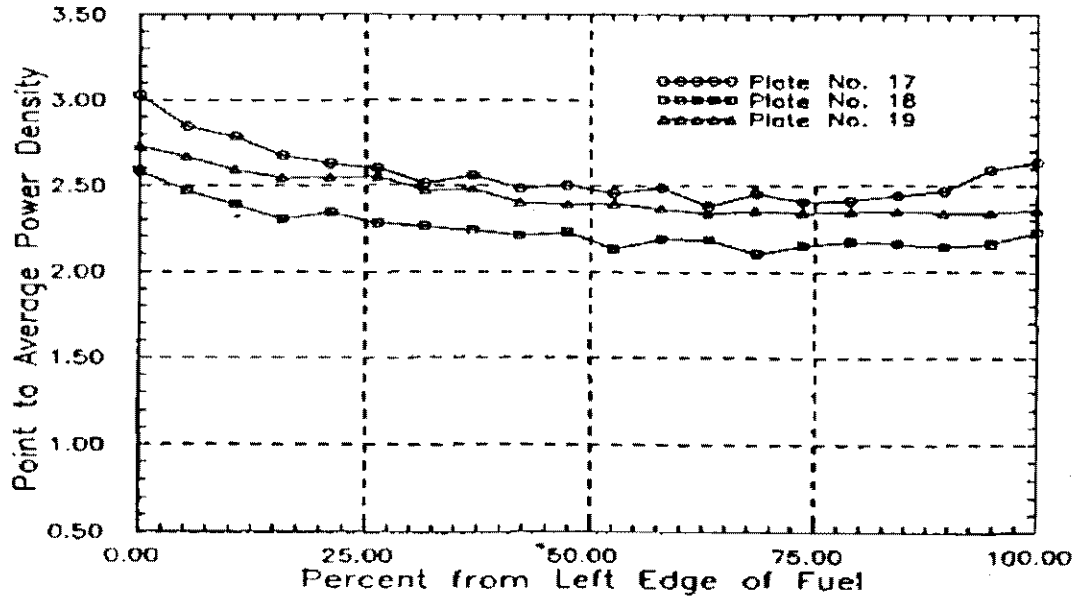

Figure 4.3-26. Azimuthal power distribution in Fuel Element 18, 17 days exposure, Env 70 MW lobe power split, Plates 17-19. **(For Information Only)**

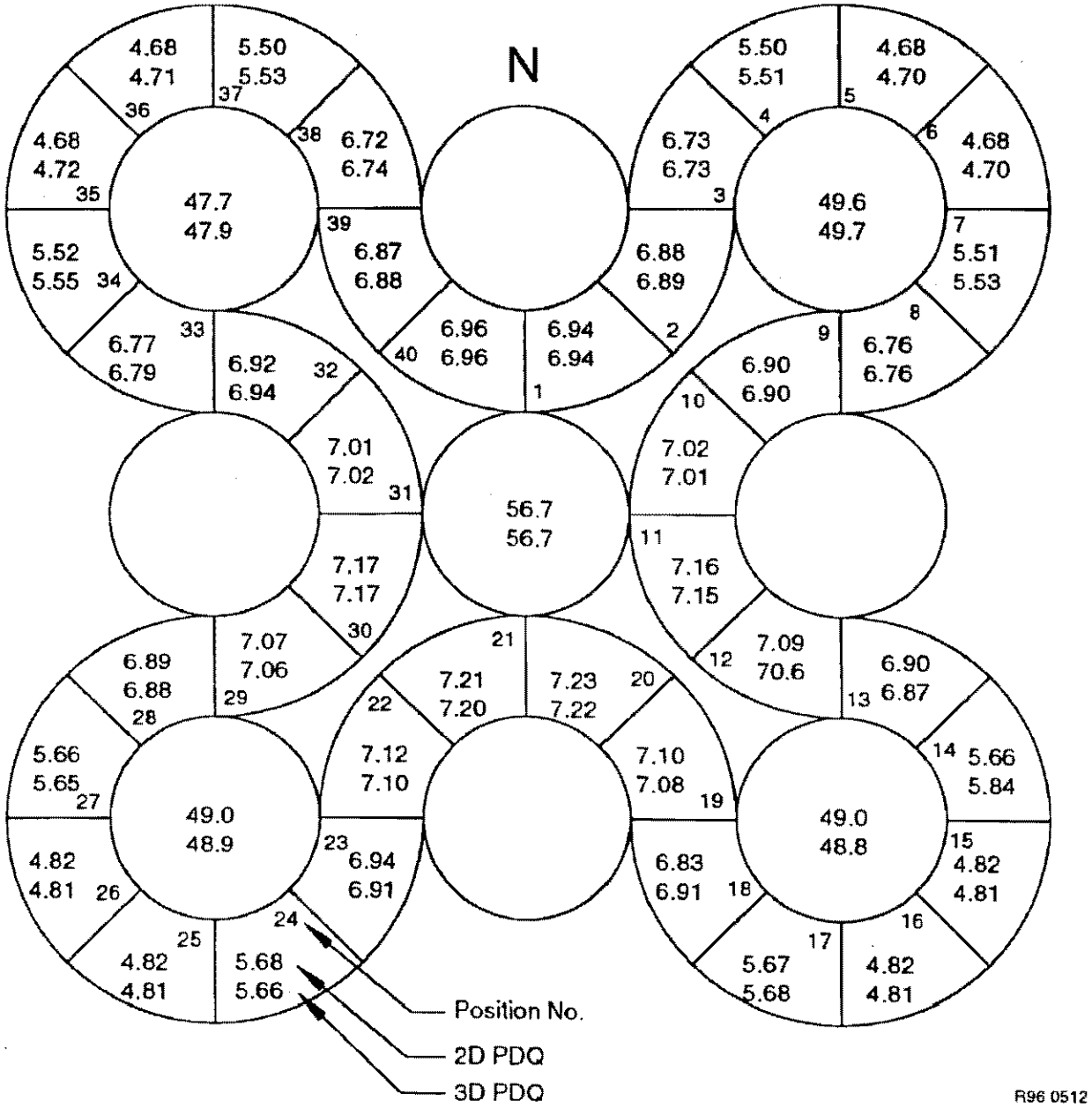

Figure 4.3-27. Lobe and fuel element power comparisons at Day 0 for the 50/50 lobe power split. **(For Information Only)**

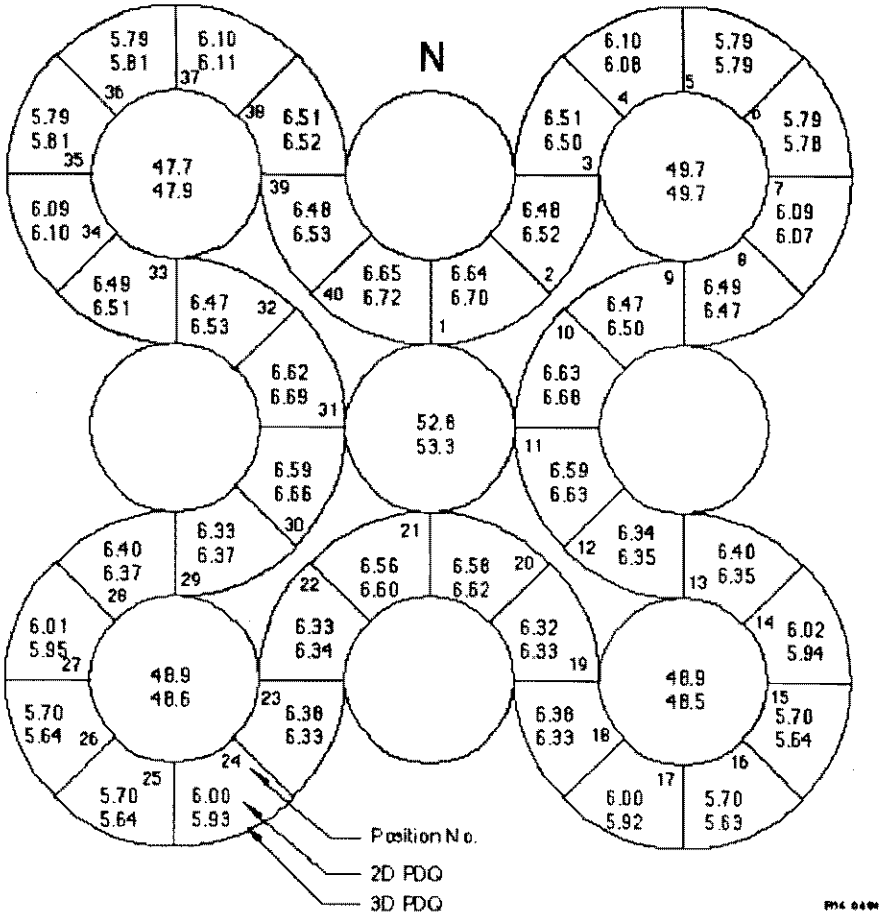

Figure 4.3-28. Lobe and fuel element power comparisons at Day 38 for the 50/50 lobe power split. **(For Information Only)**

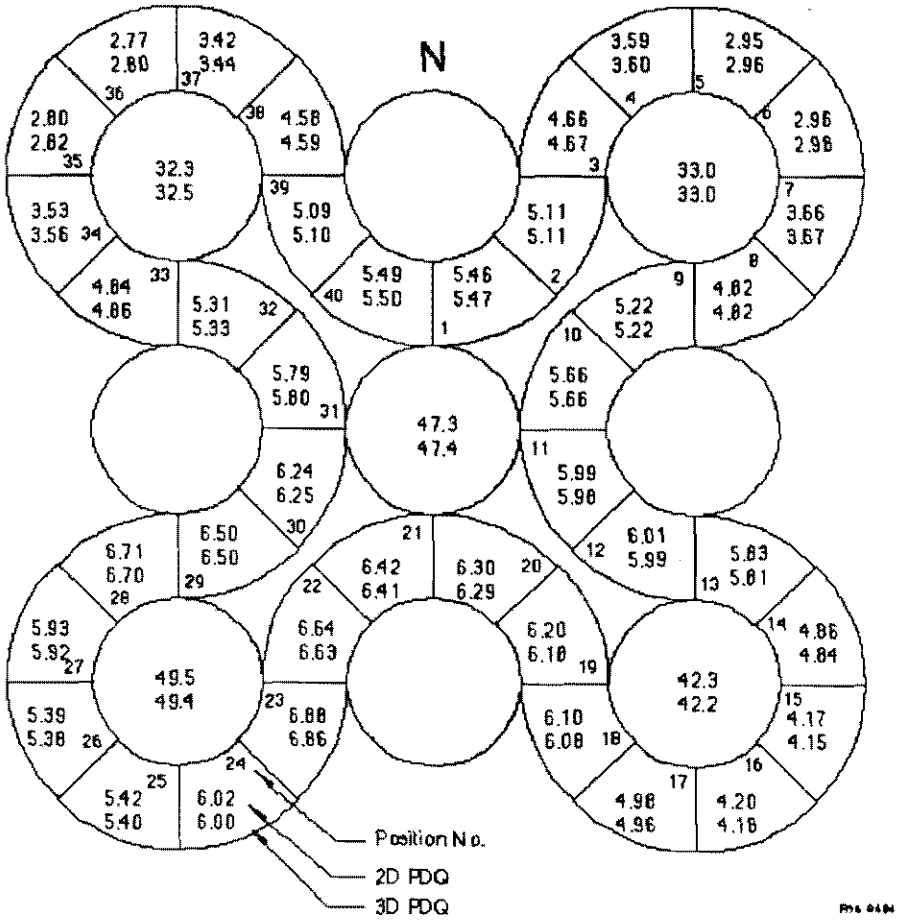

Figure 4.3-29. Lobe and fuel element power comparisons at Day 0 for the 60/40 lobe power split. **(For Information Only)**

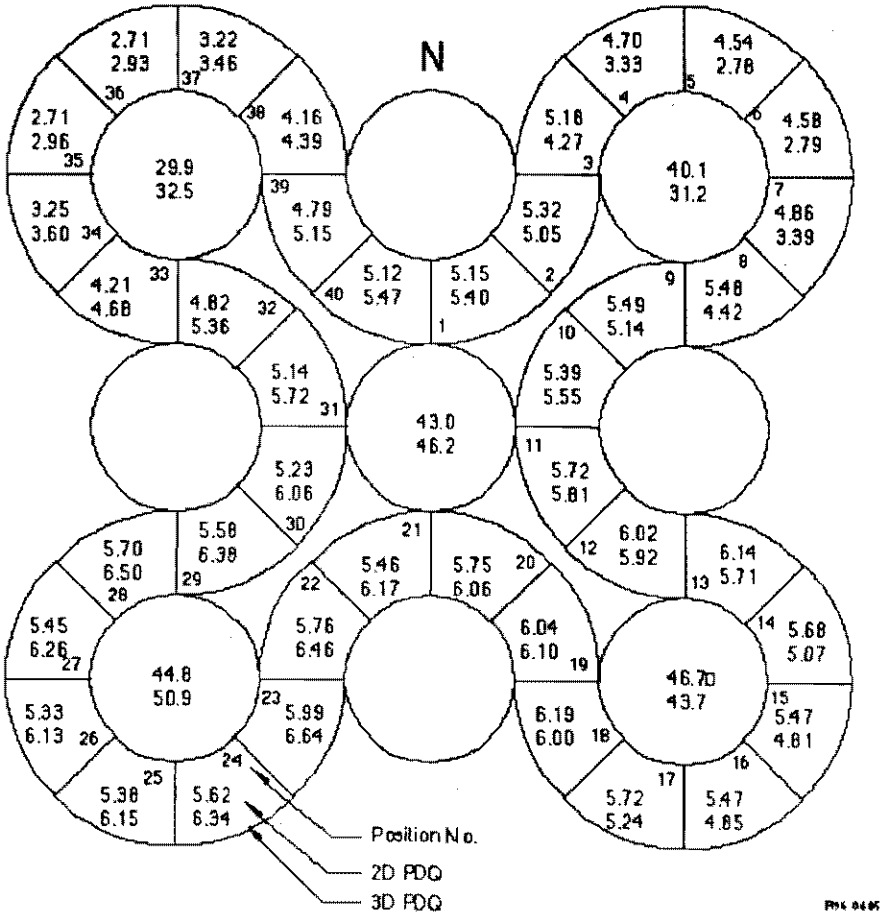

Figure 4.3-30. Lobe and fuel element power comparisons at Day 31 for the 60/40 lobe power split. **(For Information Only)**

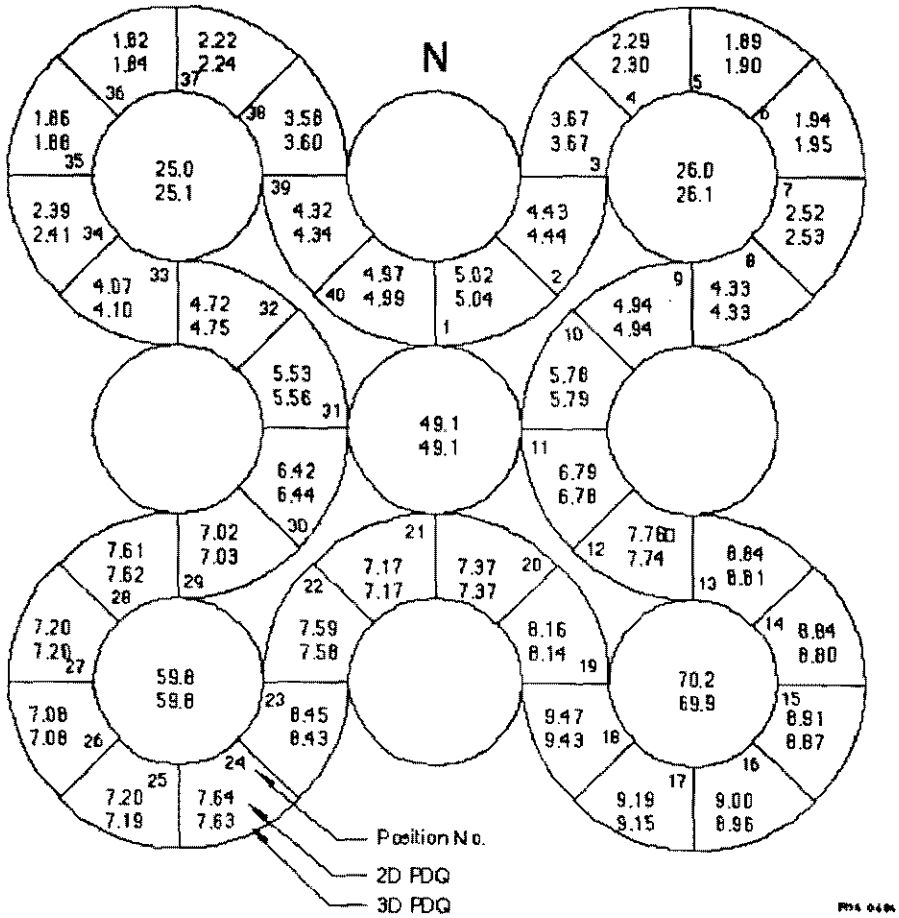

Figure 4.3-31. Lobe and fuel element power comparisons at Day 0 for the enveloping 70 MW lobe power. **(For Information Only)**

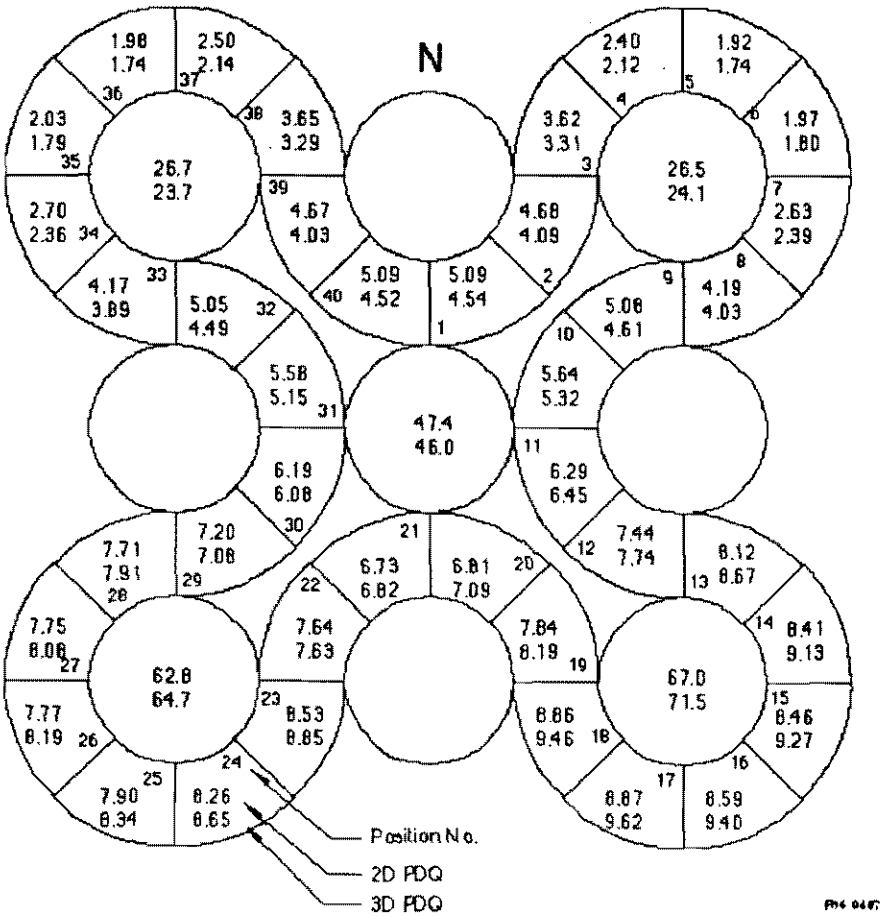

Figure 4.3-32. Lobe and fuel element power comparisons at Day 17 for the enveloping 70 MW lobe power. **(For Information Only)**

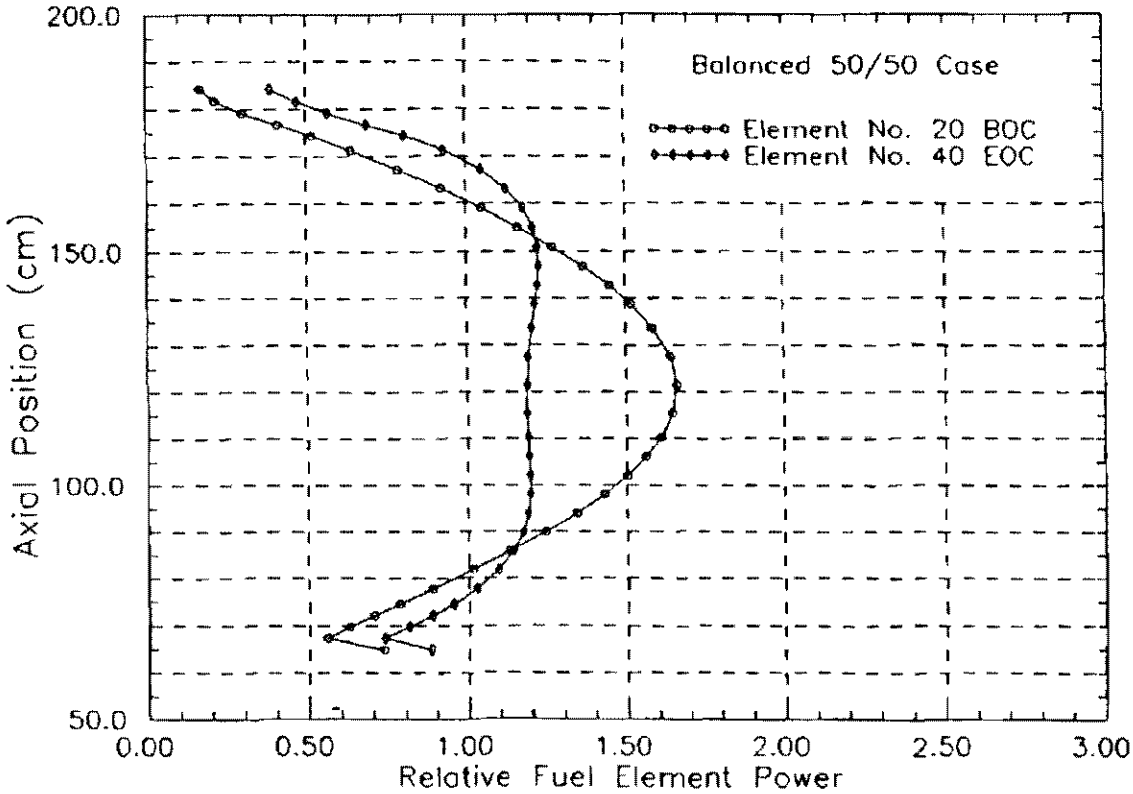

Figure 4.3-33. Power factors in peak power Fuel Element Numbers 20 [beginning of cycle (BOC)] and 40 [end of cycle (EOC)] for the balanced 50/50 case. **(For Information Only)**

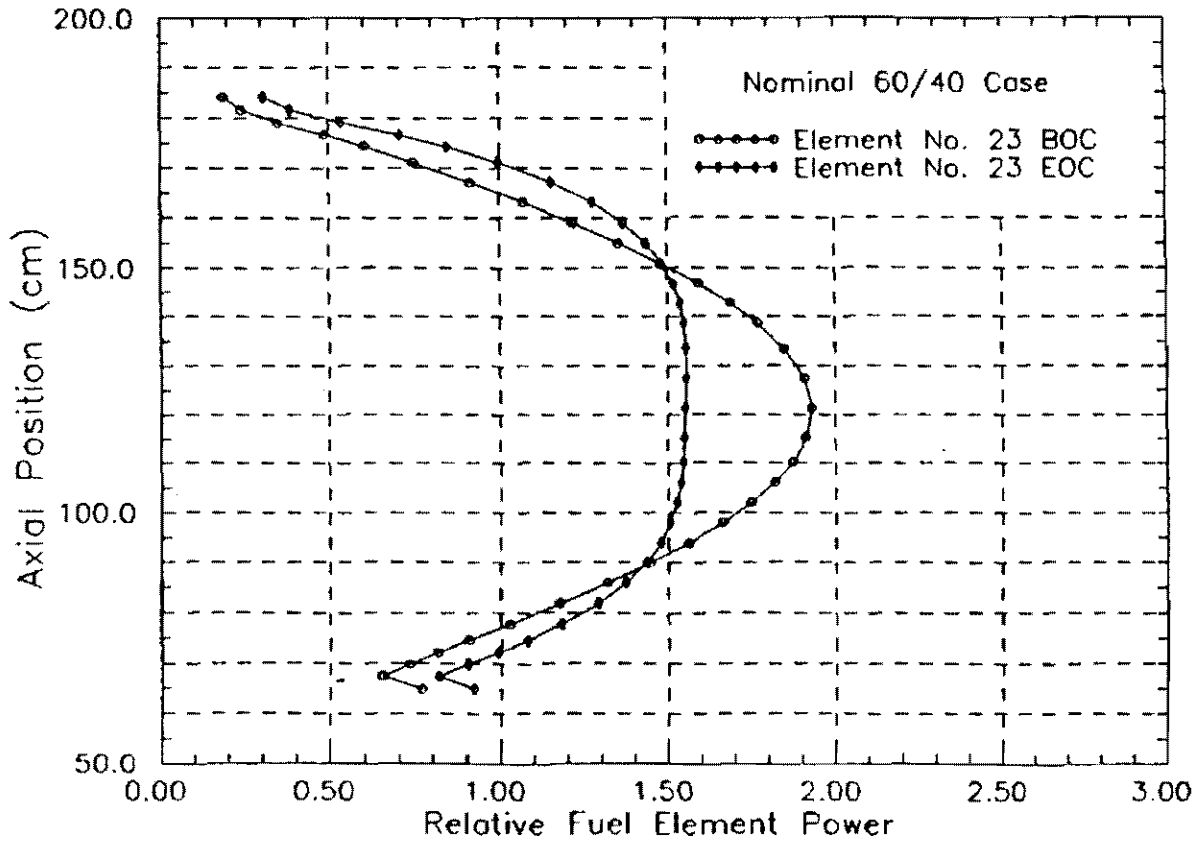

Figure 4.3-34. Power factors in peak power Fuel Element Number 23 for beginning of cycle (BOC) and end of cycle (EOC) for the nominal 60/40 case. **(For Information Only)**

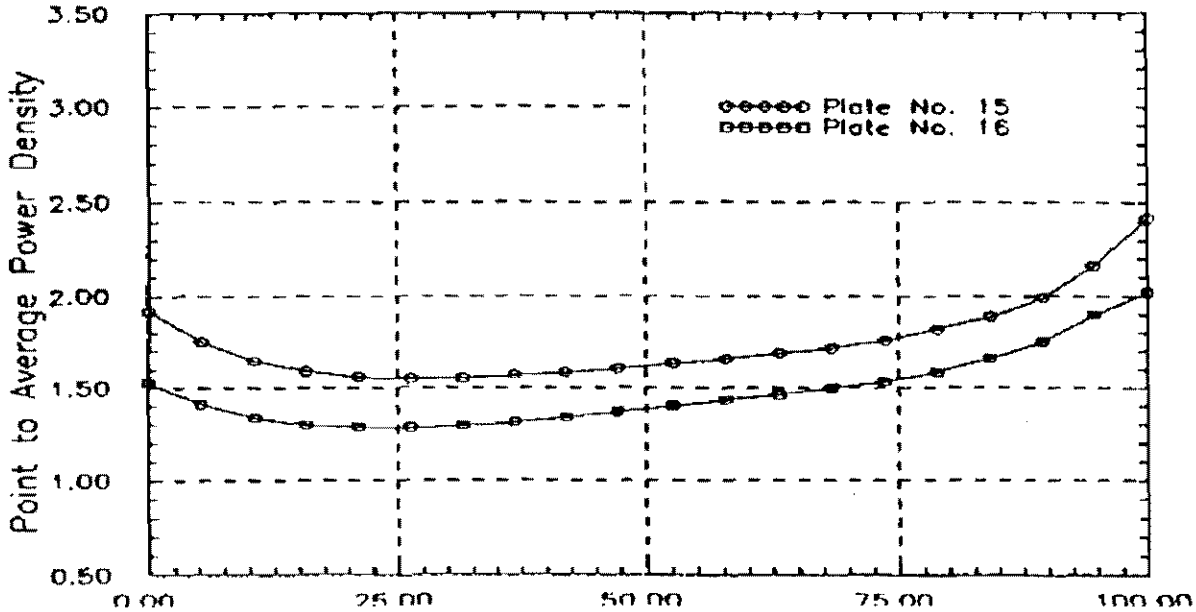

Figure 4.3-35. Power factors in peak power Fuel Element Numbers 17 [end of cycle (EOC)] and 18 [beginning of cycle (BOC)] and for the enveloping 70 MW case. **(For Information Only)**

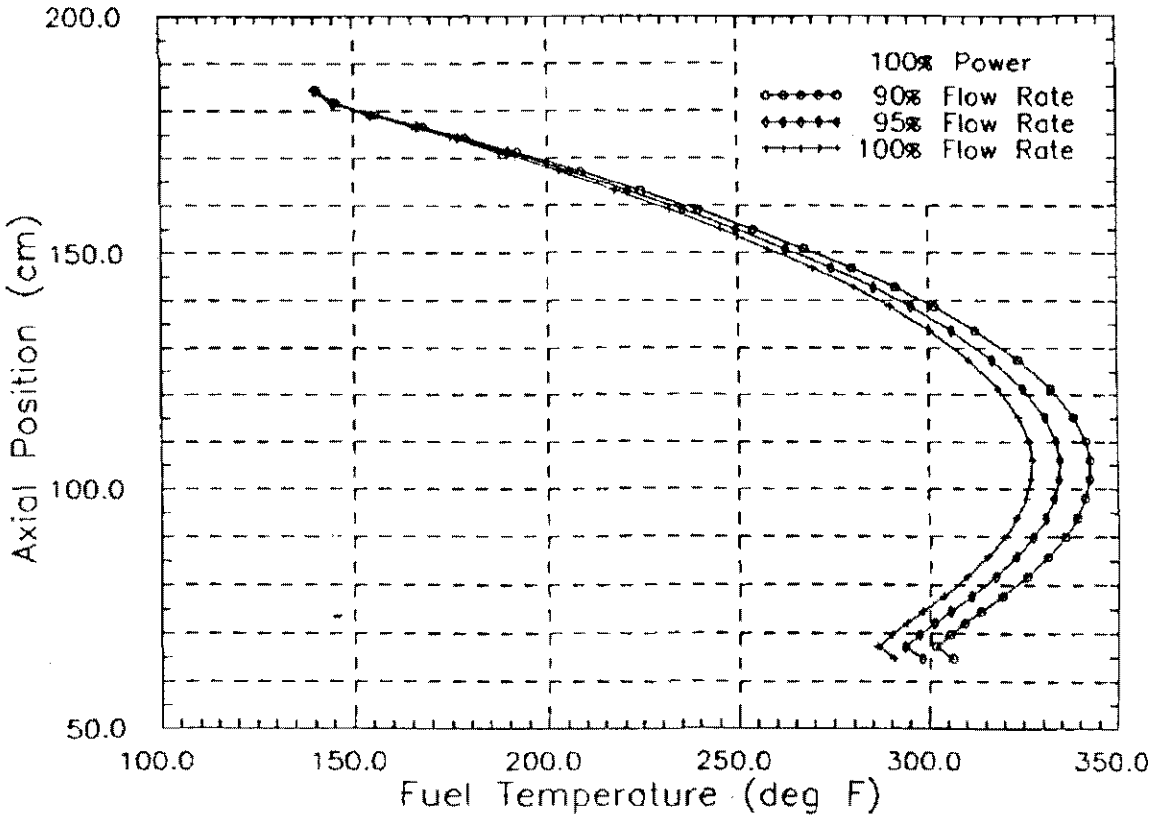

Figure 4.3-36. Plate 17 fuel temperature in Element Number 18 (100% power). **(For Information Only)**

FOIA Exemption 3 UCNI, Exemption 7f (Pages 4-136 – 4-138 – detailed core instrumentation drawings)

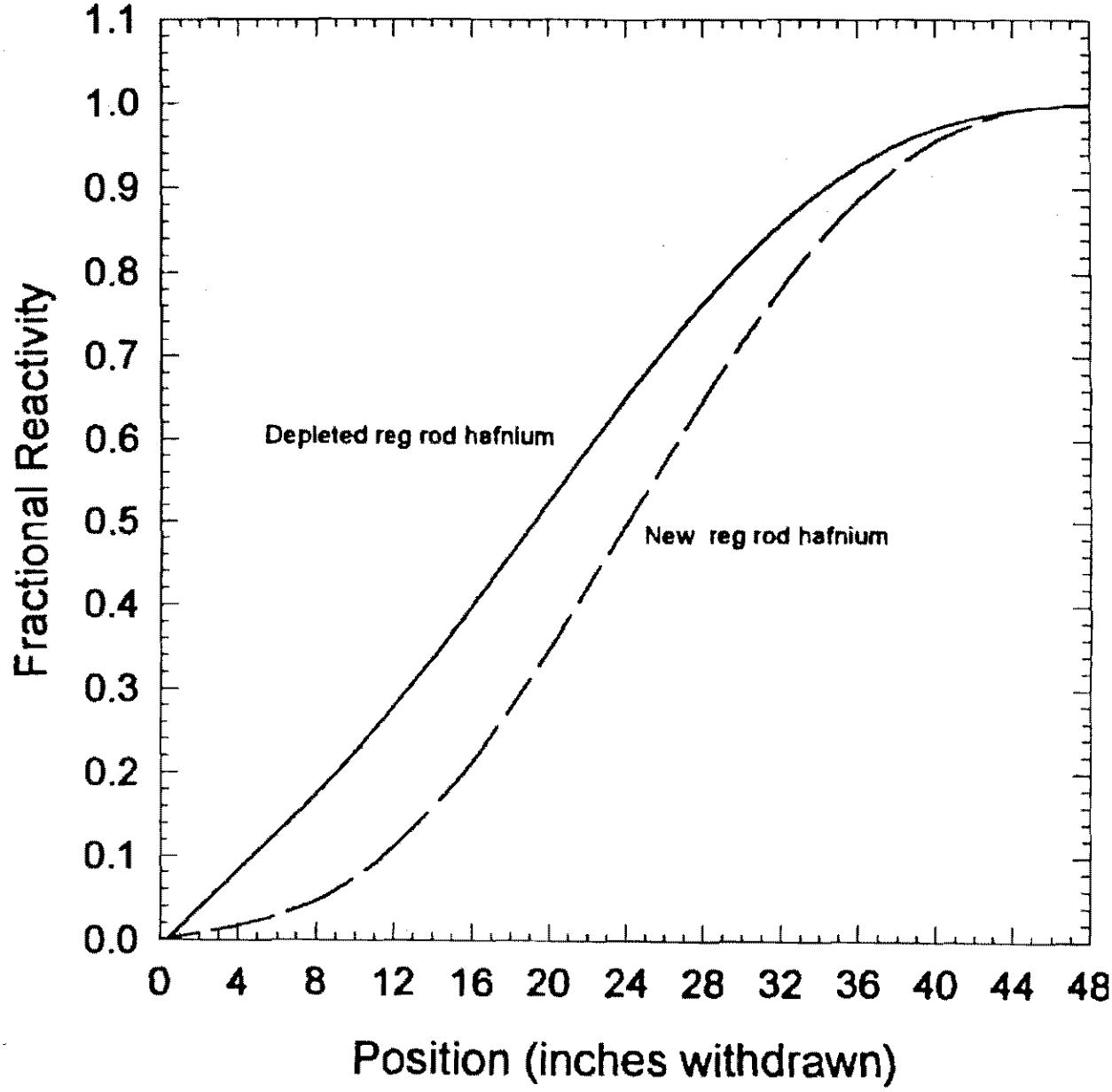

Fractional regulating rod reactivity vs withdrawal position

Figure 4.3-40. Relative worth of regulating rods versus rod position. **(For Information Only)**

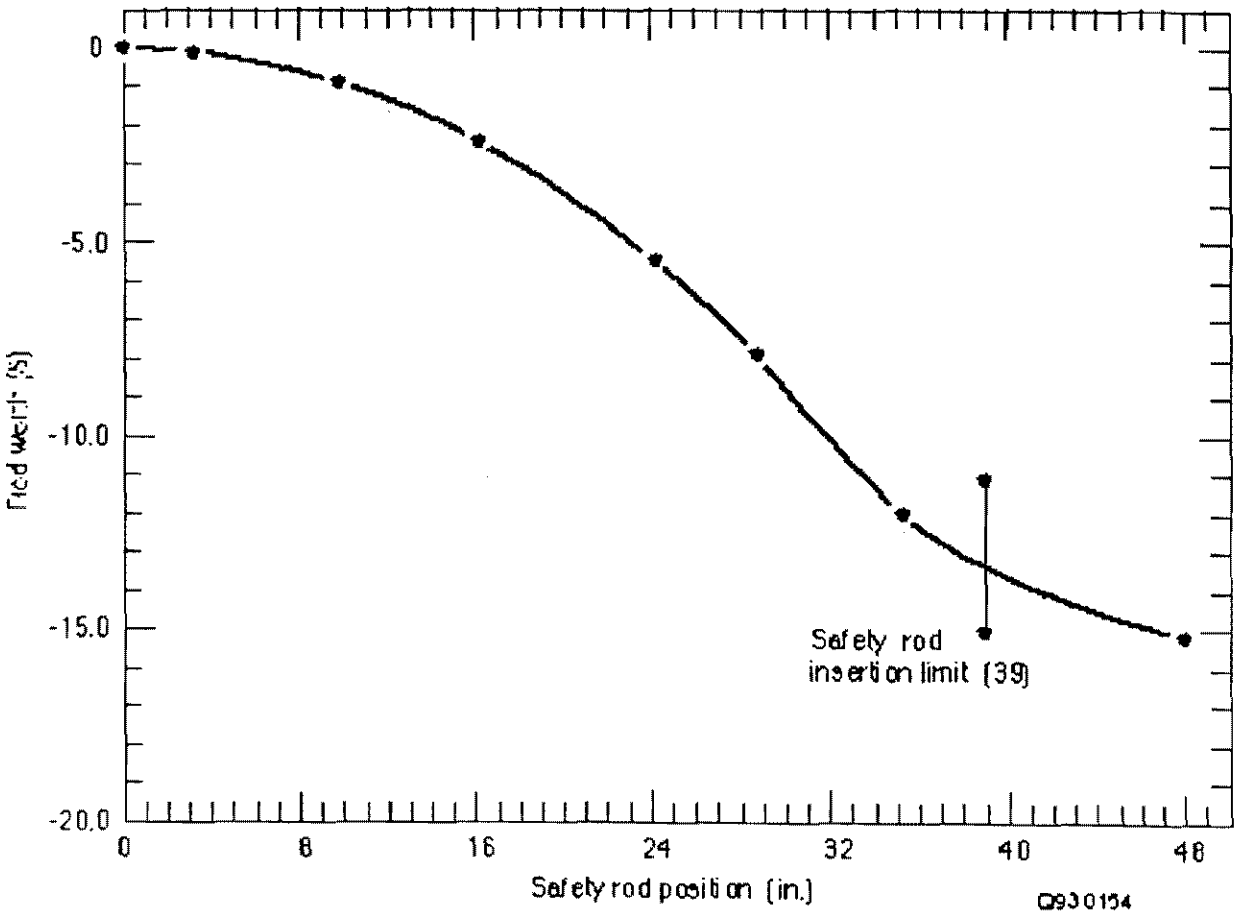

Figure 4.3-41. Safety rod worth versus rod position. **(For Information Only)**

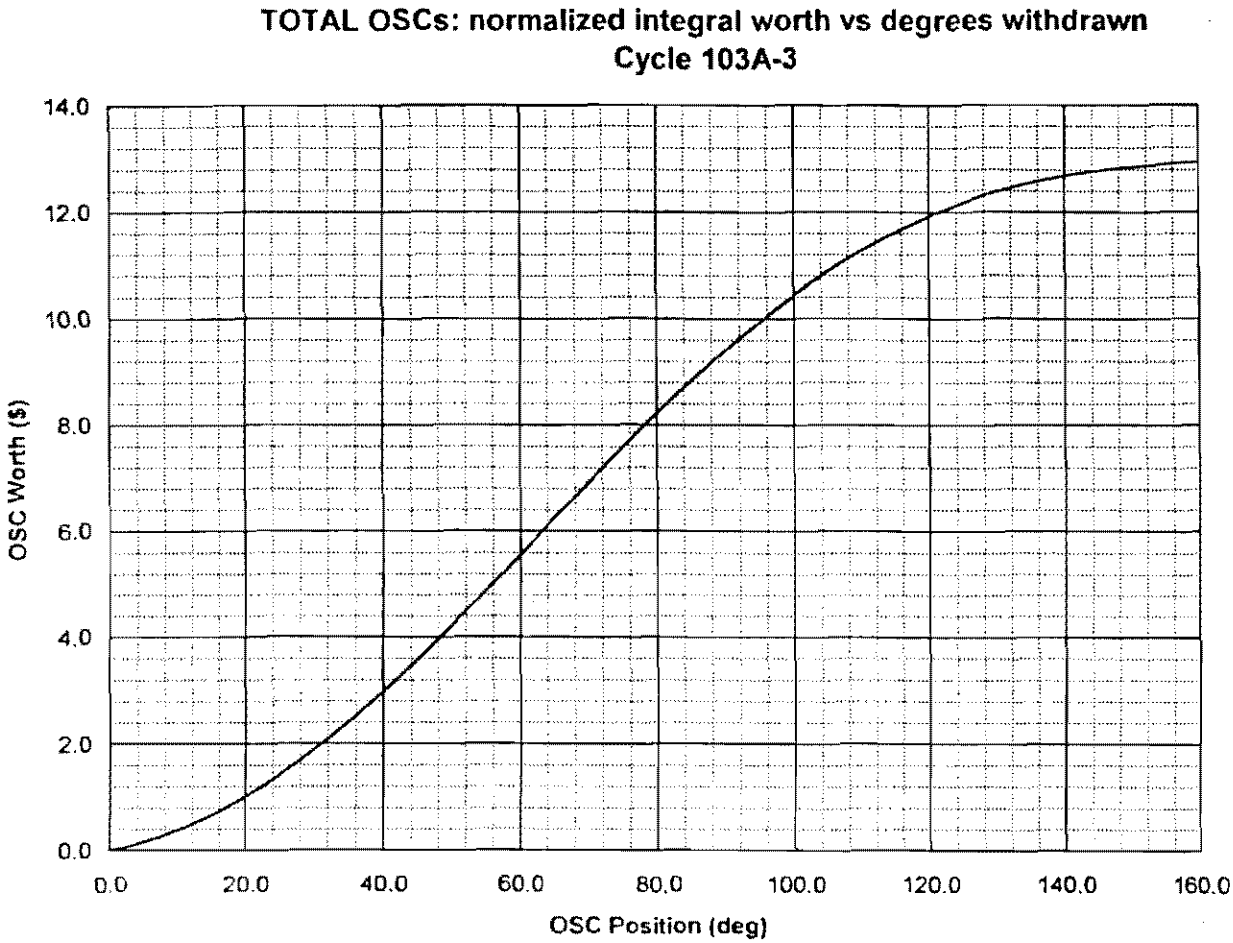

Figure 4.3-42. OSCC integral worth versus degrees withdrawn. **(For Information Only)**

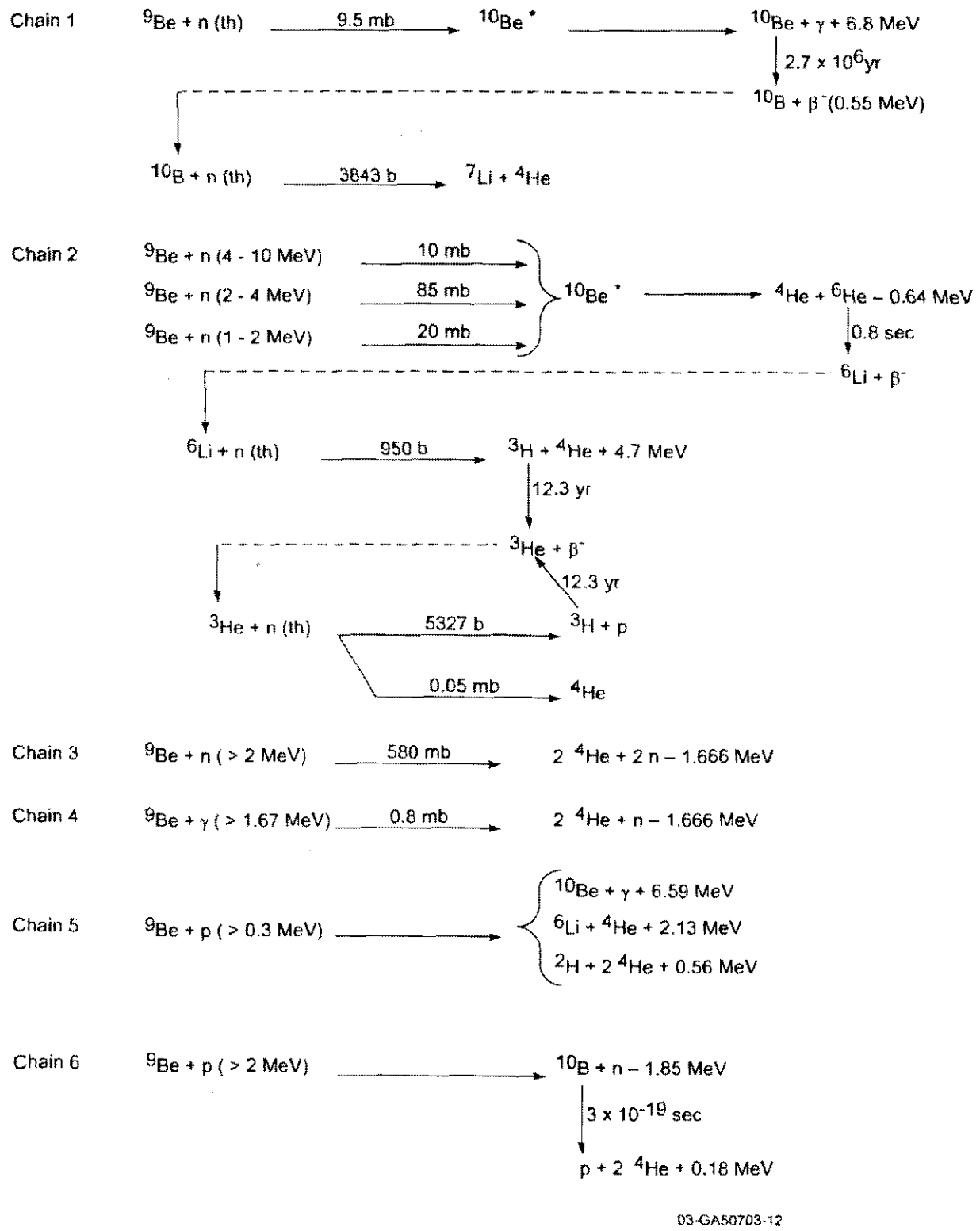

Figure 4.3-43. Beryllium poison chains. **(For Information Only)**

4.4 Thermal and Hydraulic Design

4.4.1 Design Bases

The overall objective of the thermal and hydraulic design of the reactor core is to provide adequate heat transfer, which is compatible with the heat generation distribution in the core such that heat removal by the reactor coolant system or the emergency core cooling system emergency firewater injection system (EFIS) (when applicable) ensures that the ATR plant protection criteria of Chapter 15 (Accident Analyses) are met.

To satisfy these criteria, the following design bases have been established for the thermal and hydraulic design of the reactor core.

4.4.1.1 Departure from Nucleate Boiling Design Basis

4.4.1.1.1 Basis—There will be at least a 3σ margin to DNB during normal operation and anticipated faults. This corresponds to a 99.7% probability that DNB will not occur on the limiting fuel plates during Condition 1 and 2 events.

4.4.1.1.2 Discussion—By preventing DNB, adequate heat transfer is ensured between the fuel plate cladding and the reactor coolant, thereby preventing cladding damage as a result of inadequate cooling. Limits provided by the PPS are such that this design basis will be met for all Condition 1 and 2 events.

4.4.1.2 Fuel Temperature Design Basis

4.4.1.2.1 Basis—During normal reactor operation, the maximum fuel temperature will be at least 2σ less than 700°F (644 K). Additionally, for any fuel element that has been irradiated in low power positions and then placed in a high power position, the maximum fuel temperature will be at least 2σ less than 500°F (533 K) during irradiation beyond a nominal fission density of 1.5×10^{21} fiss/cm^3. A low power position is defined as a core position where the fuel element generates less than 5.4 MW (Fillmore 1976). Fuel temperatures and statistical margins are calculated as described in Sections 4.4.2.11 and 4.4.4.5.

4.4.1.2.2 Discussion—The fuel temperature limits are based on maintaining temperatures below those that produced blistering during post-irradiation testing of sample fuel plates irradiated in the ETR during the INC-16-1/2 experiments (Francis 1971, 1974b). The testing consisted of incrementally increasing plate temperatures in a furnace until blisters appeared (Brugger et al. 1971). It should be noted that the above temperature limits are significantly lower than blister temperatures measured during other post-irradiation tests (see Figure 4.2-15). One difference between INC-16-1 and other irradiation experiments was that the INC-16-1 samples were irradiated at very low temperatures.[a] It was concluded that low irradiation temperatures, low initial fuel volume fractions, and high burnups may result in reduced blister resistance. One plate that was irradiated at low temperature (257°F, 398 K), had a low initial UAl_3 concentration (22 vol%), and achieved a high U-235 burnup (71%), blistered at 500°F (533K). The temperature limit on recycled fuel ensures that fuel elements irradiated in low-power (i.e., low-temperature) positions do not blister when moved to high-power positions.

---

[a] Preliminary investigations also indicated that the oxygen content of the INC-16-1 samples may have been high (Francis 1974b).

Fuel plate blistering is discussed further in Sections 4.2.1.2 and 4.2.3.3.

4.4.1.3 Core Coolant Flow Design Basis

4.4.1.3.1 Basis—The nonrecoverable pressure drop (ΔP) across the core with three primary coolant pumps operating is approximately 100 psid (689 kPa). With two primary coolant pumps operating, the core pressure drop is approximately 77 psid (531 kPa). The total primary system flow rate during three-pump operation is approximately 50,000 gpm (3.15 m^3/s); during two-pump operation, the flow rate is approximately 43,500 gpm (2.74 m^3/s). PPS limits on minimum core ΔP have been established to ensure that the 3σ margin to flow instability (discussed below) is not violated during Condition 1 and 2 events.

4.4.1.3.2 Discussion—Primary system flow is controlled by the butterfly valve to obtain the desired core pressure drop [$\geq$ 100 psid (689 kPa) or $\geq$ 77 psid (531 kPa)]. The core flow distribution is established by fixed reactor vessel hardware with some very small effects from experiment loadings. Approximately 56% of the flow passes through the fuel elements; the remainder passes primarily through the outer shim control cylinders, flux traps, and reflector blocks. A small amount of coolant bypasses the core because of: (a) flow between the reflector and the reflector tank, (b) flow through the siphon breakers, and (c) in-vessel leakage, for example, at core support tank penetrations.

4.4.1.4 Hydrodynamic Stability Design Basis

4.4.1.4.1 Basis—There will be at least a 3σ margin to flow instability during normal operation and anticipated faults. This corresponds to a 99.7% probability that flow instability will not occur during Condition 1 and 2 events.

4.4.1.4.2 Discussion—Under normal conditions, the ATR operates in the single-phase flow regime and is thus always stable to both static and dynamic flow instabilities. Heat transfer experiments (Croft 1964; Waters 1966) and analyses (Atkinson 1975) have shown that flow instability in an ATR coolant channel occurs when the coolant enthalpy reaches saturation at the hot track exit (see Section 4.4.4.6). This can result in a severe reduction in channel flow, leading to burnout of the adjacent fuel plates. Therefore, the ATR flow instability criterion has always been no saturated (bulk) boiling.

4.4.1.5 Other Considerations. The above design bases together with the fuel element structural design bases described in Section 4.2.1 are sufficiently comprehensive that additional limits are not required. The coolant flow velocity and distribution are not inherently limiting. These parameters are incorporated into the thermal and hydraulic models used to ensure that the above design criteria are met.

4.4.2 Description of Thermal and Hydraulic Design of the Reactor Core

4.4.2.1 Summary Comparison. The HFIR at ORNL shares similar design characteristics with the ATR. Both reactors are light-water cooled and moderated, reflected with beryllium, and use fully enriched (93%) aluminum-clad plate fuel. In both the HFIR and ATR, coolant flow is downward through the core in contrast to the upward flow in most commercial reactors. Selected design and operating parameters are compared in Table 4.4-1.

4.4.2.2 Departure from Nucleate Boiling and Flow Instability Margins. The minimum DNB and flow instability margins for steady state operation and anticipated transient conditions are given in Table 4.4-2. The minimum DNB margin in the limiting flow channel occurs downstream of the peak heat flux location (hot spot) because of the increase in downstream enthalpy. The minimum flow instability margin occurs at the limiting flow channel exit. DNB and flow instability margins are calculated using computer codes and models described in Section 4.4.4.5. The RELAP5 computer code is used to determine the transient behavior of the entire core; local conditions in the hot channel and statistical margins to DNB and flow instability are calculated with the ATR-SINDA and SINDA-SAMPLE computer models, respectively.

4.4.2.2.1 Discussion—Both in-reactor (Hanson, Griebenow, and Wells 1975) and ex-reactor (Croft 1964; Waters 1966) heat transfer experiments have demonstrated that the limiting heat transfer mechanism in the fuel element cooling channels is flow instability. Flow instability occurs when the coolant temperature at the hot track exit reaches saturation.[a] The increased resistance to flow resulting from boiling causes coolant to be redistributed to other channels; consequently, the affected cooling channel is starved, and the adjacent fuel plates overheat.

Still, it is necessary to have a correlation to predict DNB [i.e., critical heat flux (CHF)] under stable conditions. Two correlations are used for the ATR. The first, developed by Savannah River Laboratory and Columbia University (Knoebel et al. 1973), is used when the local subcooling (T_{sat} -T_{bulk}) is greater than 45°F (25 K). The correlation has the form:

$$q''_{CHF} = 1.88\times10^5(1.0+0.0515V)(1.0+0.069\Delta T_{sub}) \qquad (4.4\text{-}1)$$

where

q''_{CHF} = critical heat flux (Btu/hr·ft^2)

V = coolant velocity (ft/s)

ΔT_{sub} = local subcooling (°F).

This equation was derived from experimental data obtained with aluminum heaters cooled by light-water. Its use for ATR applications was evaluated by Ambrosek (1975), who concluded

- The Savannah River DNB correlation satisfactorily predicts the burnout heat flux for a wide range of equivalent diameters, coolant velocities, pressures, and subcoolings.
- It conservatively predicts burnout (i.e., low CHF) when compared to the aluminum experimental data of Gambill and Bundy (1964), which were obtained in support of the HFIR program.
- Using the Savannah River DNB correlation for ATR safety evaluations will provide adequate conservatism.

[a] Both Croft's (1964) and Waters' (1966) heat transfer experiments showed that lateral coolant mixing in ATR cooling channels is quite small, and that bulk boiling across the entire channel width is not required to initiate flow instability. The hot track is defined as that portion of the channel over which the maximum enthalpy rise occurs.

When the local subcooling is less than 45°F (25 K), the following correlation is used (Atkinson 1976):

$$q''_{CHF} = 4.08\times10^5(1.0+0.106V)(1.0+0.0028\Delta T_{sub}) \quad (4.4\text{-}2)$$

where the variables are the same as defined above. This correlation was derived from low subcooling DNB data for stainless steel heaters reported by Knoebel et al. (1973) and Ambrosek (1975). The leading constant in Equation 4.4-2 (4.08×10^5) includes a multiplier of 1.2 to account for Knoebel et al.'s finding that the critical heat flux for aluminum heaters was at least 20% higher than that for stainless steel heaters.

4.4.2.2.2 Statistical Uncertainties—As mentioned above, the SINDA-SAMPLE model is used to calculate statistical margins to DNB and flow instability. Uncertainties in statistical parameters (e.g., fuel plate dimensions, heat transfer coefficients, and heat generation rates) are discussed in Section 4.4.2.9.

4.4.2.3 Linear Heat Generation Rate. The power distribution in the core depends on test requirements. The nominal power distribution would be 50 MW in each of the five lobes, but power imbalance allows significant variation. As discussed in Chapter 15 (Accident Analyses), the highest lobe power permitted is 60 MW (although test requirements generally call for less power). Core average and maximum linear heat generation rates for an enveloping 70 MW lobe power split and a 60/40 lobe power split (normalized to 250 MW) are given in Table 4.4-1. The methods for determining maximum heat generation rates are described in Section 4.3.3.1.

4.4.2.4 Void Fraction Distribution. No boiling occurs in the core during normal operation or anticipated faults (Condition 1 and 2 events). Adherence to the flow instability limit (Section 4.4.1.4) ensures that the coolant saturation temperature is not exceeded.

4.4.2.5 Core Coolant Flow Distribution

4.4.2.5.1 Fuel Elements—Normalized coolant mass flux and enthalpy rise distributions at the core exit calculated with the RELAP5 thermal-hydraulic code are shown in Figures 4.4-1 and 4.4-2 (Polkinghorne 1991). The distributions in Figure 4.4-1 are for an enveloping 70 MW lobe power split at BOC (see Figure 4.3-32), while the distributions in Figure 4.4-2 are for a 60/40 lobe power split at BOC (see Figure 4.3-30) normalized to 250 MW. It should be noted that no orificing is employed in the core design.

4.4.2.5.2 Nonfuel Regions—Nominal flow rates through all regions of the reactor core and vessel are given in Table 4.4-3. As discussed in Section 4.4.4.2, the reactor flow distribution changed somewhat when Reflector III was installed in 1977 (i.e., flow through the reflector blocks decreased while flow through the outer shim cylinders increased). These changes are accounted for in Table 4.4-3.

During the 1994 CIC, the core was configured with pressurized water experiment loop IPT in the N, NW, W, SW and SE flux traps and capsule irradiation facilities in the NE, C, E, and S flux traps. The thermal-hydraulic analysis of the core reconfiguration (Pace 1993) indicates a flow rate increase of less than one percent through the four reconfigured flux traps. The flow distribution given in Table 4.4-3 is representative of those expected with the reconfiguration.

During 1997 to support the ongoing test program, the northeast flux trap was again reconfigured and the Irradiation Capsule Experiment (ICE) facility installed. The thermal-hydraulic analysis of the northeast flux trap (Hendrickson 1998a) indicates that the total flux trap flow slightly decreases by 38 gpm with the ICE facility installed. Table 4.4-3 is unaffected by this small change.During 1999, the center capsule irradiation facility was replaced with the Irradiation Test Vehicle (ITV). The hydraulic analysis (Palmer 1998) determined that the flow through the center flux trap dropped by 13 gpm with the ITV installed. During 1999, the ICE facility was replaced with the Multiple Irradiation Capsule Experiment (MICE) facility. The thermal-hydraulic analysis with this facility (Hendrickson 2001) indictes that the flow through the northeast flux trap increased by 54 gpm over the ICE facility flows or was 16 gpm more than the capsule irradiation facility that was originally installed after the CIC. All these changes are small compared to the total flows and Table 4.4-3 was unaffected by these small changes.

Due to nature of ATR operation new experiments are occasionally inserted into the reactor. When new experiments are placed into the reactor, additional analysis is performed to provide assurance that the reactor response with new experiments meets the established safety envelope.

4.4.2.6 Core Pressure Drops and Hydraulic Loads

4.4.2.6.1 Core Pressure Drops—The nonrecoverable pressure drop across the core during reactor operation with either two or three primary coolant pumps is given in Table 4.4-1. As mentioned previously in Section 4.4.1.3, the primary system flow rate is controlled by a butterfly valve to obtain the desired core pressure drop. The valve is positioned before reactor start-up, and may be adjusted during operation to maintain a core ΔP of $\geq$ 100 psid (689 kPa) during three-pump operation, or $\geq$ 77 psid (531 kPa) during two-pump operation.

4.4.2.6.2 Hydraulic Loads—Because coolant flow is downward through the core, the holddown capability of fuel elements is not a consideration during normal operation (i.e., the pressure drop through the core acts to retain the elements in position). The effect of pressures acting across the fuel plates is discussed in Section 4.2.3.4. Hydraulic loads from high core ΔP under accident conditions are discussed in Chapter 15 (Accident Analyses).

4.4.2.7 Correlation and Physical Data

4.4.2.7.1 Heat Transfer—Forced convection heat transfer coefficients in the ATR-SINDA and RELAP5 computer codes are obtained from the Dittus-Boelter correlation (Dittus and Boelter 1930) with the properties evaluated at bulk fluid conditions:

$$h = 0.023 \frac{k}{D} (\mathrm{Re})^{0.8} (\mathrm{Pr})^{0.4} \tag{4.4-3}$$

where

h	=	heat transfer coefficient (Btu/hr·ft^2·°F)
k	=	thermal conductivity (Btu/hr·ft·°F)
D	=	hydraulic diameter (ft)
Re	=	Reynolds number = GD/μ
G	=	mass flux (lbm/hr·ft^2)
γ	=	viscosity (lbm/ft·hr)
Pr	=	Prandtl number = $C_p\mu/k$
C_p	=	specific heat (Btu/lbm·°F).

Ex-reactor heat transfer experiments verified that this correlation was valid for ETR fuel elements (Griebenow 1964). One of the ATR start-up tests (High Power Forced Convection Test) substantiated the use of the Dittus-Boelter correlation for predicting heat transfer coefficients in ATR fuel elements (Griebenow and Hanson 1976).

The onset of nucleate boiling (ONB) in the ATR-SINDA and RELAP5 computer codes occurs when the cladding wall temperature reaches the amount of superheat predicted by the Bergles and Rohsenow correlation (Bergles and Rohsenow 1964):

$$T_{wall|ONB} = T_{sat} + \left(\frac{q''_{ONB}}{15.60 \times 10^{-3} p^{1.156}} \right)^{p^{0.0234}} / 2.30 \tag{4.4-4}$$

where

T_{wall}	=	cladding surface temperature (°F)
T_{sat}	=	coolant saturation temperature (°F)
q''_{ONB}	=	surface heat flux at boiling onset (Btu/hr·ft^2)
P	=	pressure (psia).

Once ONB is predicted, heat transfer coefficients for subcooled nucleate boiling, saturated nucleate boiling, and film boiling are calculated in ATR-SINDA and RELAP5 as described by Wadkins and Ambrosek (1992) and Dimenna et al. (1988), respectively.

4.4.2.7.2 Core Pressure Drop—Nonrecoverable pressure losses occur as a result of viscous drag (friction) and geometry changes (form) in the fluid flow path. Numerous ex-reactor hydraulic measurements by Idaho Nuclear Corporation have shown the following friction factor correlation to be valid for single-phase, turbulent flow in ATR fuel elements (Griebenow 1968):

$$f = 0.0024 + 0.358\left(\frac{1}{\mathrm{Re}}\right)^{0.437} \tag{4.4-5}$$

where

f = Fanning friction coefficient

Re = Reynolds number (defined above).

This friction factor correlation and the entrance and exit form loss coefficients given in Section 4.4.4.2 are included in the ATR-SINDA model.

The Fanning friction factor, f, is computed in RELAP5 using an engineering approximation to the Colebrook correlation (Colebrook 1939). Entrance and exit form loss coefficients, input by the user, are adjusted as necessary to obtain the desired core pressure drop [100 psid (689 kPa) or 77 psid (531 kPa)].

For two-phase flow conditions, "f" is evaluated in ATR-SINDA as described by Merrill (1980). Two-phase friction and form losses are calculated in RELAP5 as described by Dimenna et al. (1988).

4.4.2.8 Thermal Effects of Anticipated Events. Adherence to the thermal-hydraulic limits (Section 4.4.1) ensures that adequate margins are provided during anticipated faults (Condition 1 and 2 events). The anticipated fault analyses in Chapter 15 (Accident Analyses) demonstrate that the core is capable of withstanding the thermal effects of anticipated faults that would bound any operational transients.

4.4.2.9 Uncertainties in Estimates

4.4.2.9.1 Uncertainties in Fuel and Clad Temperatures—The fuel and clad temperatures are a function of oxide, clad, and meat conductances, hydraulic conditions, power generation, and position relative to the nonfueled portion of the fuel plate. Uncertainties in the fuel temperature calculation are essentially of two types: (a) fabrication uncertainties such as variations in the meat and clad dimensions, and fuel density-homogeneity; and (b) model uncertainties such as variations in the conductivities, oxide thickness, and correlations. These uncertainties have been quantified by three methods: (a) comparison of the thermal model to test data, (b) measurement of physical properties, and (c) measurement of the fuel and clad dimensions during fabrication. The uncertainties are then used in all evaluations to predict fuel plate temperatures.

Another uncertainty that influences the fuel and clad temperatures is the uncertainty in determining the local power. Local power is determined by density, enrichment, neutron flux, and reactor power. These uncertainties have also been quantified and are included in temperature evaluations for the fuel plate.

Reactor trip setpoints as specified in Chapter 16 (Derivation of Technical Safety Requirements) include allowance for instrument and measurement uncertainties such as calorimetric error, channel reproducibility, temperature measurement uncertainties, and heat capacity variations.

The methodology used to predict fuel plate temperatures is a statistical combination of all identified variables and their associated uncertainties using a Monte Carlo sampling technique. Nominal values of the variables and their uncertainties are shown in Table 4.4-4.

4.4.2.9.2 Uncertainties in Pressure Drops—Core and vessel pressure drops vary depending upon the use of either three or two primary coolant pumps. The vessel differential pressure subsystem of the PPS has two functions: prevent damage to the reactor internals from excessive high flow rates (large ΔP) and prevent damage to fuel elements from overheating due to low flow rates (small ΔP). The uncertainty in the vessel differential pressure is listed in Table 4.4-4.

The pressure drop across the fuel elements is not measured directly but has been analytically established from fuel element test data (see Section 4.4.4.2). The uncertainty in fuel element ΔP is assumed to be the same as the uncertainty in vessel ΔP.

4.4.2.9.3 Uncertainty in Departure from Nucleate Boiling Correlation—The DNB correlation used for ATR is based upon data obtained at Savannah River for various operating conditions and for aluminum clad. The standard deviation for the data with subcooling $\geq 45°F$ was calculated to be 10%. The correlation was shown to be conservative for subcooling $< 45°F$.

A low subcooling correlation was developed from Savannah River and other experiments with stainless steel heater data at low subcooling. The resultant constant in the correlation was then increased by 20% as supported by aluminum heater data from other tests. A statistical evaluation resulted in a standard deviation of 6.2%.

A standard deviation of 10% was used for both the low and high subcooling data.

4.4.2.9.4 Uncertainties in Departure from Nucleate Boiling Calculations—The margins to DNB are calculated by the computer code SINDA-SAMPLE. The methodology used to predict margins to DNB is similar to that used for fuel plate temperature evaluations (i.e., Monte Carlo sampling).

The energy equations of the ATR-SINDA model are solved at nine axial locations, which represent an axial strip of the ATR-SINDA thermal network illustrated in Figure 4.4-5. These equations are coupled with an equivalent number of lumped parameter conduction equations that represent the plate "hot" stripe. The solution of these equations gives the plate temperatures, and results in bulk heating rates for the energy equations when combined with the surface heat transfer coefficients. The nominal variables of bulk pressures, bulk velocities, and lumped parameter plate heating rates are obtained from the ATR-SINDA model restart tape, while surface heat transfer coefficients are calculated within the SINDA-SAMPLE model.

Parameters are randomly selected within the statistical limits, and a steady-state or transient analysis is completed. This is repeated the specified number of times until the minimum DNB point and margin is determined. The parameters are the same as previously listed in Table 4.4-4.

4.4.2.9.5 Uncertainties in Flow Rates—The ATR is operated with a constant vessel differential pressure (ΔP). The total flow may vary as a result of experiment changes. The stated uncertainty for the vessel ΔP is listed in Table 4.4-4.

Core thermal performance evaluations are performed with the ATR-SINDA computer model. A ΔP across the fuel element is entered, and the code calculates the fluid flow rate, which results from the input ΔP. Extensive tests were performed on the fuel elements in test facilities. Instrumented elements were placed in the reactor during initial start-up testing to characterize the friction factor and to establish coolant flow characteristics in the fuel elements. The pressure drop is set to provide the correct nominal velocity for the coolant channels being modeled under steady state conditions. The analyses are then completed with a deviation of 6.8% at the 90% confidence level for the calculated fluid velocity.

4.4.2.9.6 Uncertainties in Hydraulic Loads—The fuel assemblies were tested at a differential pressure of 150 psid for many years. This represented a reactor flow at least 120 percent of nominal. These tests are no longer performed. The long term experience with the fabrication process provides assurance of acceptable mechanical integrity of the fuel elements. Analyses for starting an additional primary coolant pump, for pump overspeed, and for other transient overflow conditions have shown that the resultant core differential pressures are no greater than 130 psid. Thus, the fuel assemblies are mechanically stable for the increased loads caused by overflow transients.

4.4.2.10 Flux Tilt Considerations. The lobe power distribution varies from cycle to cycle depending upon experimental requirements. A given reactor lobe may operate at powers up to four times greater (or smaller) than other lobes. Technical Safety Requirement limits on peak-to-average fission power ratios [see Chapter 16 (Derivation of Technical Safety Requirements)] ensure that fuel element temperatures during transients do not exceed those analyzed in Chapter 15 (Accident Analyses).

Possible causes of power tilts or peaking beyond the normal operating condition include xenon oscillations, reactor restart after a scram, or mis-loading of fuel elements. The core is stable against xenon oscillations as described in Section 4.3.2.7 and analysis has shown (Section 4.3.2.2.5) that lobe power shifts during recovery from a scram after reaching equilibrium xenon concentrations do not cause power factors to exceed peak reference values. Analysis has shown that local peaking factors from mis-loading events can exceed the peak reference values by approximately 10% (Section 4.3.2.2.4). Unexpected high power peaking due to loading errors is considered a Condition 2 event and has been analyzed in Chapter 15 (Accident Analyses). As fuel burnup increases, the OSCC are gradually rotated away from the fuel elements and the neck shim rods withdrawn to maintain criticality and the lobe power split. Power peaking factors decrease as burnup increases due to the power flattening which occurs. The N-16 power monitoring system (Section 4.3.2.2) will indicate any unanticipated lobe power shifts that occur during reactor operation. Periodic comparisons of the quadrant power determined from the N-16 power monitoring system are made against the quadrant water power system. These checks provide assurance of correct lobe power indications.

4.4.2.11 Fuel Plate Temperatures. The thermal-hydraulic design and operating controls ensures that maximum fuel plate temperatures do not exceed the limits of Section 4.4.1.2. Fuel plate temperatures and statistical margins are evaluated using the ATR-SINDA and SINDA-SAMPLE computer models, respectively, which are described in Section 4.4.4.5. The temperature distribution is primarily a function of the local power density, surface heat transfer coefficient, and thermal conductances of the fuel core, cladding, and corrosion-product film.

Spatial power distributions in the fuel plates are calculated with the PDQ7 and GOPP codes as described in Section 4.3.3. Surface heat transfer coefficients are evaluated using the correlations discussed in Section 4.4.2.7. The thermal conductivity of UAl_x + Al dispersion fuel as a function of temperature and U-235 concentration is shown in Figure 4.4-3. The curves in this figure were derived from thermal diffusivity measurements made on sample fuel plates at Pacific Northwest Laboratory (Bates 1966). The thermal conductivity of 6061 aluminum cladding is shown in Figure 4.4-4 as a function of temperature (Polkinghorne and Lacy 1991). The thermal conductivity of the corrosion-product film that forms on fuel plates was measured during corrosion experiments performed by ORNL in support of the ATR design (Griess et al. 1964). The thermal conductivity of the corrosion layer was found to be independent of temperature and have a value of 1.3 Btu/hr·ft·°F (2.2 W/m·K). The thickness of the corrosion layer is calculated using Equation 4.2-1 with a multiplier of 0.7 (see Section 4.2.3.1).

Uncertainties that affect fuel plate temperatures are discussed in Section 4.4.2.9. Peak nominal and statistical 2σ fuel plate centerline temperatures for steady state operation are given in Table 4.4-5.

4.4.3 Description of the Thermal and Hydraulic Design of the Reactor Coolant System

4.4.3.1 Plant Configuration Data. Plant configuration data for the thermal hydraulic and fluid systems external to the core are provided in Chapters 5 (Reactor Coolant System), 6 (Engineered Safety Features), and 9 (Auxiliary Systems). Implementation of the EFIS is discussed in Chapter 15 (Accident Analyses). Some specific areas of interest are the following:

- Total coolant flow rates for the PCS and each support system are provided in Table 4.4-6. Flow rates employed in the evaluation of the core are presented in Section 4.4.
- Total PCS volume, including surge tank and surge lines, and PCS liquid volume, which involves surge tank water at steady-state power conditions, are given in Table 4.4-6.
- The flow path length through each volume may be calculated from physical data provided in the above referenced tables.
- The height of fluid in each component of the PCS may be determined from the physical data presented in Chapter 5 (Reactor Coolant System). The components of the PCS are water-filled during power operation with the surge tank being approximately 95% water-filled.
- Line length and sizes for the EFIS are calculated to guarantee a total system resistance that will provide, as a minimum, the fluid delivery rates assumed in the safety analyses described in Chapter 15 (Accident Analyses).
- The parameters for components of the PCS are presented in Chapter 5 (Reactor Coolant System).
- The steady-state pressure drops and temperature distributions through the PCS are presented in Table 4.4-6.

4.4.3.2 Operating Restrictions on Pumps. The minimum Net Positive Suction Head (NPSH) and minimum seal injection flow rate must be established before operating the reactor primary coolant pumps. With the minimum labyrinth seal injection flow rate established, the operator must verify that the system pressure satisfies NPSH requirements.

4.4.3.3 Temperature-Power Operating Map. The ATR does not have a detailed relationship between the PCS temperature and power; therefore, no discussion is presented in this section.

4.4.3.4 Thermal and Hydraulic Characteristics Summary Table. The thermal and hydraulic characteristics are given in Table 4.4-6.

4.4.4 Evaluation

4.4.4.1 Critical Heat Flux. The CHF correlations used in the core thermal analysis and their uncertainties are discussed in Sections 4.4.2.2 and 4.4.2.9, respectively.

4.4.4.2 Core Hydraulics. Primary coolant enters the reactor vessel through two 24-in. (61-cm) nozzles near the bottom of the reactor vessel. Approximately 94% of the coolant flows up through two annuli, one formed by the pressure vessel and thermal shield and the other formed by the thermal shield and inlet flow baffle. The remainder (~6%) is diverted into the large space between the inlet flow baffle and core reflector tank. The coolant recombines in a large plenum above the core, reverses direction, and flows down through the fuel elements and other internals. Approximately 56% of the coolant passes through the fuel elements, the remainder passes primarily through the OSCC, flux traps, and reflector blocks (see Table 4.4-3). A flow distribution tank below the core separates the flow into quadrants. The coolant exits the reactor vessel through four 16-in. (41-cm) outlet pipes that extend from the flow distribution tank to the vessel outlet nozzles.

4.4.4.2.1 Fuel Annulus Hydraulic Measurements—In 1967, thirteen dummy fuel elements were instrumented to measure coolant flow rates and axial and lateral pressure gradients in the core (Griebenow 1968). The objectives of the tests were: (1) evaluate local flow rates and the dependence of any observed irregularities on quadrant flow imbalance and intra-quadrant and intra-element flow restrictions, (2) measure lateral pressures acting across the fuel plates and the change in thickness of channels 19 and 20 caused by these pressures, and (3) measure entrance, exit, and frictional losses within the fuel elements. The principal findings were:

- Lateral pressures, acting across the fuel plates, are low and should not adversely affect any fuel element that is properly constructed.
- Coolant flow rates are not a function of fuel element position in the core.
- The average velocities measured in channels 1 through 18 [at design 100 psi (689 kPa) core ΔP] agreed within 2% of predicted values. However, the average velocities in channels 19 and 20 were 5 and 20% low, respectively. Two standard deviations about the measured mean were 17, 9, 6, 6, 7, 6, 9, and 36% for channels 1, 2, 3, 9, 10, 18, 19, and 20, respectively.
- Fuel element entrance and exit losses differed from those anticipated, resulting in approximately a 6 psi (41 kPa) increase in pressure at any point in the fuel element (at design core ΔP).
- A significant pressure loss occurs between the bottom of the fuel elements and the pressure taps in the flow distribution tank.

The low coolant velocities in channel 20 appeared to be a result of either a flow resistance term not accounted for in the design calculations or variations in channel dimensions along the length and width of the fuel elements.[a] The external channels (1 and 20) are larger than the internal channels and therefore have greater nominal coolant velocities than the internal channels. This, coupled with the fact that the external channels are heated from only one side, minimizes the effect of large velocity variations.

On the basis of the measurements, it was concluded that fuel element performance can best be evaluated using:

- Entrance coefficients of 0.2, exit coefficients of 0.7 for channels 2 through 19 and 0.9 for channels 1 and 20, and friction factors given by Equation 4.4-5 in Section 4.4.2.7
- A full flow core pressure drop during three-pump operation of 94 psid (648 kPa), rather than the 100 psid (689 kPa) measured between the inlet plenum and the flow distribution tank
- Coolant velocities in channels 19 and 20 reduced by 5 and 20%, respectively.

These values are used in the ATR-SINDA and MACABRE II thermal-hydraulic models discussed in Section 4.4.4.5.

4.4.4.2.2 Core Internals Hydraulic Measurements—Reactor internals hydraulic tests were also performed in 1967 (Clemons 1992). The tests generally included all reactor internals flow paths, except those in the fuel element annulus. The objectives of the tests were: (1) verify that the hydraulic design requirements of the reactor were met, and (2) obtain basic hydraulic data in sufficient detail to permit analysis of the reactor as a whole. The principal findings were:

- Quadrant-to-quadrant cross-flow in the flow distribution tank occurred more readily than anticipated which would tend to compromise quadrant thermal power measurements. Consequently, orifices were sized, built, and installed in the reactor outlet pipes. Subsequent measurements indicated that all quadrant discharge pressures were balanced within 0.3 psi (2 kPa) at the design 100 psi (689 kPa) core pressure drop. This was considered to be an adequate balance.
- Measured system pressure drops agreed well with design values with the exception of the inlet line loss, which was about 3 psi (21 kPa) below design, and the outlet line loss, which was about 5 psi (34 kPa) above design because of the addition of the quadrant balancing orifices. These variations from design were considered to be acceptable.
- There was no movement of reactor internals greater than the accuracy of the instrumentation, which was ± 0.002 in. (0.05 mm). This amount of movement will not affect fuel element hydraulics and heat transfer.
- Flux trap flows were fairly close to design and more than adequate for cooling.
- The neck shim rod assemblies had essentially design flow in all channels.
- Beryllium reflector coolant flows were somewhat less than design. However, the flows were considered satisfactory because thermal stresses in the reflector blocks would still be well below yield. (As discussed in Section 4.2.3.6, thermal stresses have little effect on reflector service life.) Flow rates in the channels between the reflector blocks and reflector tank were above design.

---

[a] The fuel elements are packed relatively loosely in the fuel annulus to ensure insertion and retrieval. The spaces separating the fuel elements from each other and from adjacent core structures are not precisely defined.

- The cooling requirements of the OSCC were met.
- Thermal shield coolant velocities and flow distributions agreed well with design values.
- Flows in all irradiation holes were generally satisfactory. However, the H-hole poison insert rod and sleeve assembly had to be modified to ensure adequate cooling.

The first reflector (i.e., Reflector I) was installed when the hydraulic measurements discussed above were made. Beginning with Reflector III, which was installed in 1977, horizontal saw cuts were incorporated in the reflector to delay the buildup of radiation-induced stresses (see Section 4.2.3.6). To reduce or eliminate cross-flow through the saw cuts, the OSCC were also redesigned so that their vertical pressure profile matched that of the fuel elements (Mousseau et al. 1973). Other design changes included reducing the number of cooling holes in the reflector blocks and shim cylinders.

Hydraulic analyses of the saw-cut reflector were performed with the FLOW3 code (see Section 4.4.4.5). Where available, hydraulic test data were used to determine flow resistance coefficients. Because of Reflector III design changes, flow during three-pump operation was predicted to increase about 3200 gpm (12 m^3/min) through the outer shim cylinders and decrease about 1200 gpm (4.5 m^3/min) through the reflector blocks (Nielsen 1973). Based on hydraulic measurements and analyses performed during Reflector III start-up tests (Nielsen 1977), it was concluded that there was little or no pressure difference across the saw cuts and that the fuel elements were essentially isolated hydraulically from the shim cylinders. (The Reflector III thermal evaluation is discussed in Section 4.2.3.6.)

Incore hydraulic measurements were also made in 1986 following installation of Reflector IV (Livingston 1986). Reflector IV included four new 1-1/2-in. (3.8-cm) diameter B-holes and four new 1-1/2-in. (3.8-cm) diameter I-holes as irradiation positions for experiments (Thomas 1985). The gear box support beams were also redesigned to improve their strength and provide access to the new irradiation holes. Pressure differentials were found to be similar to values measured in 1977 following installation of Reflector III. Quadrant and total core flow rates with Reflector IV were very close to those with Reflector III. The differences, on the order of 2%, were within the range of measurement accuracy.

4.4.4.2.3 Friction Factor Correlations—The friction factor correlations used in core thermal-hydraulic evaluations are discussed in Section 4.4.2.7.

4.4.4.3 Influence of Power Distribution. The core is designed to operate with asymmetrical power distributions. As discussed in Section 4.3.2.2, the overall peak point-to-average power densities occur near the beginning of an operating cycle typically in fuel plate 19. Because of nonuniform burnup and flux flattening, the peak point-to-average power densities tend to decrease with fuel burnup. However, the power generated by the limiting fuel plate (typically fuel plate 15) tends to increase with burnup due to broadening of the axial power profile (Polkinghorne 1993b). Therefore, maximum fuel plate temperatures and minimum DNB and flow instability margins occur at or near end-of-cycle.

For three-pump operation and an enveloping 70 MW lobe power split (see Section 4.3.2.2), plate 15 in fuel position 18 controls core thermal limits. For two-pump operation and a 60/40 core power split with a 60 MW lobe, plate 15 in fuel position 23 is limiting (Polkinghorne 1993b).

4.4.4.4 Core Thermal Response. The steady state thermal-hydraulic design parameters are summarized in Table 4.4-1. As discussed in Section 4.4.1, the thermal-hydraulic design bases are intended to prevent CHF and fuel damage during Condition 1 and 2 events. The protective systems described in Chapter 7 (Instrumentation and Controls) are designed to meet these bases. The response of the core to Condition 2 transients is given in Chapter 15 (Accident Analyses).

4.4.4.5 Analytical Methods. The computer codes and models used for both steady state and transient thermal-hydraulic evaluations are discussed in this section.

4.4.4.5.1 RELAP5—The RELAP5 code (Allison et al. 1989) predicts the transient behavior of the ATR under postulated accident conditions. RELAP5 simulates the coolant system including the core, reactor vessel, primary pumps, heat exchangers, surge tank, and emergency systems. The RELAP5 code and the ATR input model are discussed further in Chapter 15 (Accident Analyses).

4.4.4.5.2 ATR-SINDA—The ATR-SINDA model (Ambrosek, Liebett, and Merrill 1993; Merrill 1980, 1981) computes three-dimensional temperature distributions in any of the nineteen fuel plates in a fuel element. The hydrodynamic model developed for the RELAP5 pilot code (Ransom and Trapp 1976) was interfaced with the SINDA thermal analyzer (Gaski 1987) to give ATR-SINDA the capability to:

- Simulate heat transfer processes during forced convection, subcooled transition boiling, subcooled and saturated fully developed boiling, and film boiling.
- Account for the energy associated with material phase change.
- Model steady-state and transient hydraulics in the adjacent cooling channels.
- Predict and simulate hydraulic (flow) instability and flow reversal.

The ATR-SINDA model represents one-half of a fuel plate and a portion of the adjoining side plate (see Figure 4.4-5). Because azimuthal neutron flux profiles are generally flat over the center portion of the fuel plate (see Section 4.3.2.2), a half-plate model is adequate to predict thermal behavior. The model is divided into 9 axial levels, each containing 59 diffusion nodes (nodes with heat capacity), 28 arithmetic nodes (nodes without heat capacity), and 15 water boundary nodes. All the diffusion nodes are meshed with a three-dimensional conductor network; arithmetic nodes are linked with diffusion nodes in the direction of predominant heat flow. Water boundary node temperatures are determined by simultaneously solving two-phase mass, momentum, and energy equations, written in homogeneous form.

The heat transfer correlations used in the ATR-SINDA model are discussed in Section 4.4.2.7. Water properties are obtained from the RELAP5 steam tables. Temperature-dependent material properties (Polkinghorne and Lacy 1991) for the fuel, cladding, side plate, and corrosion-product film are built into the model. Azimuthal and axial power distributions are obtained from PDQ7 (see Section 4.3.3.1). For transient calculations, the following time-dependent data are obtained from RELAP5: reactor power, pressure drop across the flow channels, upper plenum pressure, upper plenum enthalpy, and lower plenum enthalpy (used only if flow reverses).

The friction factor correlations and form loss coefficients used in the ATR-SINDA model are discussed in Sections 4.4.2.7 and 4.4.4.2, respectively. The ATR is designed to operate with a constant core pressure drop nominally 100 psid (689 kPa) during three-pump operation and 77 psid (531 kPa) during two-pump operation. Uncertainties in friction factors, cooling channel thicknesses, core pressure drop, and other parameters that affect coolant velocities are accounted for in the SINDA-SAMPLE statistical model (discussed below).

The ability of the ATR-SINDA model to predict the thermal-hydraulic behavior of fuel plates under steady-state and transient conditions has been demonstrated (Polkinghorne 1993a). Computer-generated results were compared to experimental data obtained during start-up tests. The calculations simulated natural convection, forced convection, flow reversal, and flow instability in specially instrumented fuel elements. Calculated results (fuel plate temperatures, coolant temperatures, and coolant velocities) were in good-to-excellent agreement with the test data.

4.4.4.5.3 SINDA-SAMPLE—The SINDA-SAMPLE model (Liebelt 1996) calculates core thermal-hydraulic margins (i.e., standard deviations to DNB, flow instability, and fuel temperature limits). The SAMPLE statistical technique was developed circa 1975 for use in the WASH-1400 Reactor Safety Study (NRC 1975). SAMPLE uses Monte Carlo sampling to determine the statistical properties of a specified function (for example, DNB margin) given the statistical properties of each variable in the function. The code simulates the function a specified number of times (usually 1,200) using a random combination of input variables. The mean and standard deviation of the function are then calculated from the resulting distribution of function values.

SAMPLE has been incorporated as a subroutine in the SINDA thermal analyzer (Gaski 1987). The resulting SINDA-SAMPLE model solves coupled conduction and energy equations at nine axial elevations coinciding with the hot stripe[a] of the ATR-SINDA fuel plate model (Merrill 1980, 1981). The variables used to evaluate thermal margins and their uncertainties are listed in Table 4.4-4. Nominal values for pressures, velocities, and heating rates are obtained from ATR-SINDA. Surface heat transfer coefficients are calculated within SINDA-SAMPLE so that transitions between heat transfer regimes are accounted for in the statistical analysis (the heat transfer correlations are the same as in ATR-SINDA). Both steady state and transient statistical evaluations can be performed with SINDA-SAMPLE.

4.4.4.5.4 MACABRE II—The MACABRE II code (Griebenow and Richert 1967) was developed specifically to predict the thermal-hydraulic behavior of plate-type reactor fuel elements. It has been used to analyze MTR, ETR, and ATR fuel elements. All of the fuel plates and associated cooling channels in either rectangular (MTR and ETR) or wedge-shaped (ATR) fuel elements are simulated. MACABRE II has been used to calculate the oxide film buildup for the steady state SINDA fuel temperature analysis.

The MACABRE II hydraulic model simultaneously solves the continuity equation, energy equation (assuming single-phase incompressible flow), and Dittus-Boelter forced convection heat transfer correlation, with the requirement that pressures in all cooling channels equilibrate at side plate vents. Pressure drops are computed using the friction factor correlation and form loss coefficients given in Sections 4.4.2.7 and 4.4.4.2, respectively. Heat conduction within the fuel plates is assumed to occur only in the radial direction. Time-dependent heat generation rates are obtained from PDQ7 calculations. Corrosion of the aluminum cladding is calculated using Equation 4.2-1 with a multiplier of 0.7 (see Section 4.2.3.1).

---

[a] As shown in Figure 4.4-5, an ATR-SINDA fuel plate is divided into six azimuthal segments or stripes. The hot stripe is adjacent to the hot track, which is the portion of the coolant channel over which the maximum enthalpy rise occurs.

Comparisons to thermal-hydraulic data obtained during start-up tests (Griebenow 1968; Griebenow and Hanson 1976) have verified MACABRE II's ability to calculate fuel temperatures, coolant velocities, and pressure gradients within fuel elements.

4.4.4.5.5 FLOW3—The FLOW3 code (Beus and Anderson 1974) simulates steady state, two-phase flow in three dimensions. It was used for design and analysis of Reflectors III and IV (Nielsen 1973; Ambrosek, Nielson, and Fillmore 1982; Thomas 1985). Flow networks are constructed from nodes, which describe the physical properties of the flow field, and links, which carry flow between nodes. Pressures at boundary nodes and link flow resistances are input by the user. Pressures at internal nodes and link flow rates are calculated by the code. Conservation equations for mass, energy, and momentum form the basis of the FLOW3 network.

The FLOW3 model of the reflector (Nielsen 1985) simulates one reflector block, three fuel elements, and two outer shim control cylinders. Experimental verification of the model is based on comparisons with Reflector III hydraulic test data (see Section 4.4.4.2).

4.4.4.5.6 SIMIR/6—SIMIR/6 (Kraus 1977) is a two-dimensional heat conduction code used to calculate temperature distributions in the reflector and OSCC (Mousseau et al. 1973). Temperature- or time-dependent heat transfer coefficients, fluid boundary temperatures, material properties, and internal heat generation rates are defined in a user subroutine. A finite difference method is used to solve the heat conduction equation in either cylindrical (r,z) or Cartesian (x,y) coordinates. The accuracy of the code has been verified by comparing calculated results to exact analytical solutions to heat conduction problems (Kraus 1977).

4.4.4.6 Flow Instability. The ATR is designed to operate in the single-phase flow regime and is therefore not normally susceptible to flow instabilities. The core inlet subcooling is nominally greater than 300°F (170 K). During 250 MW, two-pump operation, the average fuel element outlet subcooling is greater than 200°F (110 K). As shown in Table 4.4-2, the minimum margin to flow instability during Condition 2 events is greater than three standard deviations (i.e., greater than 99.7% probability that flow instability will not occur in the hot track of the limiting cooling channel).

Ex-reactor heat transfer experiments conducted by Croft (1964) and Waters (1966) demonstrated that flow instability, not boiling burnout, determined heat flux limits in the ATR. The experiments simulated as closely as possible the operating conditions expected in ATR cooling channels. In general, both studies showed that flow instability did not occur until the test channel exit temperature reached saturation. It was also shown that lateral coolant mixing in the test channels was quite small, and that bulk boiling across the entire channel width was not required to initiate the instability. These experiments showed that DNB in ATR-like cooling channels is preceded by flow instability, which causes large reductions in channel flow.

During ATR commissioning, emergency cooling tests (with 5 to 10% of full flow) were conducted under atmospheric and pressurized conditions, using an instrumented fuel element located in the highest power density region of the core (Griebenow and Hanson 1976). Both hot-channel-flow and hot-plate-temperature sensors were integrated into the reactor scram circuitry. The tests were conducted to determine: (1) the limiting stable power levels for emergency flows, (2) the power-limiting flow instability mechanisms, and (3) the rate of recovery from instability. The results of the last test were analyzed by Hanson, Griebenow, and Wells (1975). The test was conducted by incrementally increasing reactor power, with a constant flow rate of about 3,600 gpm (13.6 m^3/min), until the reactor was scrammed (when low hot-channel flow occurred). The core pressure differential was ~1 psi (6.9 kPa), and the operating pressure was 253 psia (1.74 MPa). Reactor scram occurred as the power level was increased from 33 to 34 MW. Measured hot plate and exit water temperatures showed that recovery from the flow instability following reactor scram was fast (< 7 s). The maximum measured temperature increase during the flow transient was less than 30°F (17 K). An analysis of measured fuel plate temperatures indicated that subcooled nucleate boiling was present in the two hottest cooling channels prior to flow instability. The analysis also revealed that flow instability occurred when the hot track exit temperature reached saturation. It was concluded that subcooled nucleate boiling in ATR cooling channels does not result in flow instability. An analytical study by Atkinson (1975) also showed that flow instability will not occur in ATR fuel element cooling channels until the coolant enthalpy in the hot track reaches saturation.

The start-up test discussed above was simulated using the ATR-SINDA model described in Section 4.4.4.5 (Polkinghorne 1993a). The results showed that ATR-SINDA can adequately predict flow instability in the ATR.

4.4.4.7 Effects of Coolant Flow Blockage. Fuel element flow blockage can occur as a result of foreign material entering the reactor by means of equipment failure, corrosion during operation, or items left in the reactor during outages. ATR design requirements, equipment quality, and inspection procedures minimize the possibility of equipment failure and excessive corrosion. Detailed administrative procedures have been developed to minimize the potential for extraneous material to be left in the reactor during outages. These procedures are based on years of successful outage work at the MTR, ETR, and ATR, and also on several errors that have occurred. The following summarizes three flow blockage incidents that led to fuel damage in the MTR and ETR:

- On December 12, 1961, the flow of cooling water through several ETR fuel elements was obstructed by a sight glass left inside the reactor vessel after an unscheduled outage (Keller 1962). The ETR had been operating at a power level of 90 MW (~1/2 full power) for some 45 minutes when the primary system flow rate began to decrease slowly (~100 gpm/min, 0.38 m3/min/min). The flow rate continued to decrease for approximately 35 to 40 minutes until the reactor was scrammed. Prior to reactor scram, a spike occurred on the N-16 monitor of sufficient magnitude to cause an automatic power reduction to about 70 MW. However, the N-16 monitor was thought to be faulty, and the instrument was separated from the power reduction circuitry. The reactor was brought back to 90 MW and operated about five minutes until progressively worsening conditions led to a manual scram. Eighteen fuel plates in six different fuel elements were found to have melted to varying degrees. An estimated 12.4 g of U-235, contained in 134 g of aluminum, was dispersed in the primary coolant system. There was no evidence that metal-water reaction occurred when the fuel plates melted. Release of activity to the environment during, and immediately following the incident was minor; no overexposures or severe health physics problems were encountered.

- On November 13, 1962, a piece of dislodged gasket material from the MTR primary system caused a significant flow restriction in at least two flow channels of an MTR fuel element (Dykes, Ford, and Hoopingarner 1965). Partial melting of one fuel plate resulted in the loss of approximately 10.5 g of metal, containing an estimated 0.7 g of U-235. A fast setback originating with the N-16 monitoring system and a full scram from the fuel element δP (flow) system occurred almost simultaneously. Contamination of the primary coolant system was not severe, nor were any personnel overexposures received.

- On February 20, 1967, after 13.5 hours at full power (175 MW), an ETR fuel element was partially blocked by a short section of adhesive tape (commonly called "Tuck Tape") that had been inadvertently left on a structural member above the core during a scheduled outage (Francis and Tingey et al. 1967b). An automatic power reduction (to near zero power) was initiated by the N-16 monitor; the reactor was manually scrammed about 25 minutes later. Nine fuel plates experienced varying degrees of melting, and approximately 7.4 g of fuel (UAl3) was lost during the accident. Fission product release to the reactor environment was less than expected, indicating significant fission product retention within the fuel. In addition, metal-water reaction did not occur to the extent expected.

As a result of these incidents, more stringent administrative procedures were instituted at the MTR and ETR to account for all materials, tools, and equipment used for work in or around these reactors. From the ETR sight glass incident, it was concluded that fuel damage and radiation release would have been reduced if a full scram, initiated by high primary coolant activity, had been part of the reactor protective circuitry. Although there does not exist a firm quantitative basis for determining at what radiation level a fission break trip should be set in the ATR, the ETR experience indicates that the trip should be less than 200% of the normal primary system radiation level. The full-power fission break trip is 150% of the normal radiation level [see Chapter 7 (Instrumentation and Controls)]. In addition, during reactor start-up, provision is made for an intermediate setting of approximately one-third the full-power setpoint.

The reactor internals protective cover between the inlet flow baffle and reactor vessel wall will keep large pieces of debris from being swept into the core from the primary system. This cover is a stainless-steel expanded metal screen with maximum openings of 9/16 × 1-11/16 in. (1.43 × 4.29 cm). The core geometry (i.e., serpentine fuel annulus and upper end fitting arrangement), is such that blockage of large areas of the core is unlikely. In the event a flow blockage does occur, the fuel element side plate vents will provide secondary flow paths to the blocked channel(s). It should be noted that neither MTR nor ETR fuel elements had vented side plates.

Isothermal flow blockage tests were conducted in the HTF using a fuel element that was instrumented for pressure and flow measurements (Neder 1971). Azimuthal flow blockages of 30, 50, 70, 80, 90, and 100% were simulated for various core pressure drops. One-hundred percent blockage at 120% of nominal flow (144 psid, 993 kPa) did not result in plate collapse, indicating there will be no hydraulic failure propagation as a result of blocking the ends of the cooling channels. Complete blockage also caused insignificant changes in coolant flow below the first set of side plate vents. Hence, with complete blockage of two adjacent channels, melting will be limited to the ~7-in. (18-cm) region above the first set of side plate vents.

Complete blockage of channel 20 in a fuel element by a piece of beryllium is highly improbable but has been evaluated (Ambrosek, Nielsen, and Fillmore 1982). Blockage of channel 20 will compromise the cooling of plate 19 and cause the temperature of the plate to increase significantly. Flow through the side plate vents, beryllium saw cuts, and channel 19 will provide partial cooling. Temperatures and resulting stresses in plate 19 were evaluated using the ATR-MITAS (now ATR-SINDA) and CAM computer models, respectively.[a] It was assumed: (1) channel 20 was completely blocked by a piece of beryllium just below the bottom set of side plate vents [4 in. (10 cm) below the core midplane], (2) the reactor was operating with two primary coolant pumps, (3) the lobe power level was 48 MW, (4) there was a 1-mil (0.025-mm) corrosion-product layer on plate 19, and (5) there was no slippage at the side plate swage joints. The maximum calculated plate temperature was 648°F (615 K) and the statistical 2° temperature was 736°F (664 K). The calculated stress (at the 2° temperature level) over the entire width of plate 19 at the flow blockage elevation was greater than the yield strength. Axially, less than 13 in. (33 cm) of the plate was above yield.

The above results are considered conservative because ETR experience has shown that the swage joints allow axial slippage and thereby relieve thermal stresses. ETR experience has also shown that fuel plate rippling is a progressive phenomenon in that stresses above yield strength do not produce large initial deflections (Tomberlin 1989). Small amplitude deflections relieve the stresses and the fuel plates reach a stable configuration. Thus, complete blockage of channel 20 is not expected to result in fuel plate failure.

Greater than 80% blockage of a cooling channel in an ATR fuel element is an unlikely (Condition 3) fault. On the basis of the accidents that occurred in the MTR and ETR, it is concluded that the PPS fission break subsystem can limit the consequences of such accidents to plate damage, fuel dispersion, and radiation releases equal to, or less than what occurred in the MTR and ETR. These accidents demonstrated that the melting remains localized, does not propagate significantly, and the molten material is readily cooled after reactor scram. The melting will result in release of fission products to the PCS. The volatile products would reach the exhaust system through the degassing tank. The exhaust stream is monitored, and the fans are stopped if elevated radiation levels are detected. Gaseous releases to the outside are therefore limited. Because nongaseous fission products are for the most part retained in the primary system during a flow blockage accident, and because the radiation releases are not excessive (with proper operational controls for system cleanup and effluent release), the consequences are acceptable for a Condition 3 (unlikely) fault.

4.4.5 Testing and Verification

Tests to ensure that the thermal-hydraulic design characteristics of the core have been provided are summarized below. The initial test program is discussed further in Chapter 14 (Initial Test Program, Inservice Surveillance and Maintenance).

4.4.5.1 Preoperational Testing. In-reactor hydraulic measurements were made in 1967, prior to initial criticality, and in 1977 and 1986, following design changes to the reflector (see Section 4.4.4.2). The measurements verified that flow rates in the core region are adequate to meet heat transfer requirements. As discussed in Section 4.2.3.4, for many years all new fuel elements underwent hydraulic testing prior to reactor use to demonstrate capability of withstanding hydraulic conditions in the reactor. Hydraulic testing has been discontinued as discussed in Section 4.2.3.4.

---

[a] The ATR-SINDA and CAM computer models are described in Sections 4.4.4.5 and 4.2.3.4, respectively.

4.4.5.2 Initial Power Operation Testing. During start-up testing, four loadings of fuel elements were used. These were designated Cores 0, I, II, and III. Core 0 was used for zero-power physics studies to establish the relationship between the ATRC and the ATR (Henscheid et al. 1967). The Core 0 tests demonstrated good correspondence between the two reactors.

Core I was used for intermediate power operation where fuel element performance was evaluated under a number of thermal-hydraulic conditions, for example, normal operation, emergency pump operation, and natural convection (Griebenow and Hanson 1976). The Core I tests showed that the heat removal characteristics of the core can be calculated satisfactorily and that the core has good emergency-flow and natural-convection heat removal capabilities.

The last phase of the start-up program was designed to demonstrate the high-power operational capabilities of the reactor. Core II was used for balanced power demonstration tests. The fuel elements in this core were operated for 35 full-power days. Core III was operated for 27 days at 250 MW while maintaining an unbalanced power division (i.e., 60/40 lobe power split). The Core II and III tests demonstrated that the reactor was capable of operating according to design specifications.

4.4.5.3 Component and Fuel Inspections. Tests and inspections are performed on new core components to ensure that they meet thermal-hydraulic design requirements (Section 4.2.4). Testing and Inspection of new fuel elements is discussed in Section 4.2.4. Surveillance and testing of irradiated core components is discussed in Section 4.2.1.8. Routine surveillance and testing ensures that the thermal-hydraulic design characteristics of the core remain within required limits throughout core life.

4.4.6 Instrumentation Requirements

The instrumentation used to monitor and measure reactor vessel thermal-hydraulic parameters important to safety is discussed in this section. Instrumentation for monitoring the neutron flux level is discussed in Section 4.3.2.2.8.

Unless otherwise noted, the instrumentation discussed in this section is part of the PPS. More detailed information on reactor instrumentation is given in Chapter 7 (Instrumentation and Controls).

4.4.6.1 Pressure Instrumentation. Reactor vessel inlet and outlet pressures are monitored from pressure taps located in the 36-in. (91-cm) reactor inlet and outlet lines, respectively. Redundant, low-pressure alarms and reactor trips protect the core against DNB. Redundant, high-pressure alarms and reactor trips, in conjunction with high-inlet-pressure trips of the pressurizing and gland-seal pumps, protect the reactor vessel against excessive pressure.

Total reactor vessel ΔP is monitored from pressure taps located in the 36-in. (91-cm) reactor inlet and outlet lines. Low ΔP alarms and a low ΔP reactor trip protect the core against low coolant flow. High ΔP alarms and a high ΔP reactor trip, in conjunction with the trip of at least one primary coolant pump, protect the core against excessive flow.

Each of the four reactor quadrants is also instrumented to monitor core quadrant ΔP. The pressure taps are located in the 8-in. (20-cm) reactor vessel upper drain pipe and in each quadrant of the flow distribution tank. Although not part of the PPS, the quadrant ΔP instrumentation will alert the operators to potential problems (via high and low ΔP alarms).

4.4.6.2 Temperature Instrumentation. Reactor vessel inlet and outlet temperatures are monitored by temperature detectors located in the 36-in. (91 cm) reactor inlet and outlet lines, respectively. Redundant, high-temperature alarms and reactor trips protect the core against CHF.

Each of the four reactor quadrants is instrumented to monitor quadrant ΔT. The temperature detectors are located in the 24-in. (61-cm) reactor inlet lines and the 18-in. (46-cm) reactor outlet lines. High quadrant ΔT alarms and reactor trips protect the core against CHF.

4.4.6.3 Vessel Level Instrumentation. The reactor vessel water level is monitored by differential-pressure instrumentation located in the upper plenum of the reactor vessel. An alarm and/or reactor trip, in conjunction with actuation of the EFIS, protect the core against becoming uncovered. As discussed in Chapter 7 (Instrumentation and Controls), the EFIS is also actuated by low upper-plenum pressure.

4.4.6.4 Water Power Instrumentation. Two identical water power calculators that are non-PPS are used to determine the thermal power of each core quadrant and the total thermal power of the reactor.[*] The water power calculators transfer information to the RDAS, which is discussed in Chapter 7 (Instrumentation and Controls). The RDAS provides the operators with real-time monitoring of several key reactor parameters, including thermal power.

Both the water power calculators and the N-16 system which also monitors reactor power are discussed in Section 4.3.2.2.

4.4.6.5 Loose Parts Monitoring System. The ATR does not contain instrumentation to detect loose parts in the reactor coolant system. A risk analysis was performed in 1989 to assess the potential improvement in safety if a Loose Parts Monitoring System (LPMS) were installed (Eide 1989). The analysis showed that a LPMS would result in less than a 0.01% reduction in the total core damage frequency. Therefore, installation of a LPMS cannot be justified based on potential risk reduction.

---

[*] The N-16 system, which also monitors reactor power, is discussed in Section 4.3.2.2.8.

Table 4.4-1. Thermal and hydraulic comparison table.

Design parameters[a]	ATR	HFIR[b]
General		
Reactor type	Pressurized light-water cooled and moderated, beryllium reflected, fully enriched (93%) plate fuel	Pressurized light-water cooled and moderated, beryllium reflected, fully enriched (93%) plate fuel
Mission	Materials testing, isotope production	Materials testing, isotope production
Fuel material	UAl_x-Al dispersion	U_3O_8-Al cermet
Cladding material	6061 aluminum	6061 aluminum
Burnable poison	Boron-10	Boron-10
Number of fuel elements	40	2
Total number of fuel plates	760	540
Core volume (ft^3)	9.81	1.80
Typical core loading (lb U-235)	77.2 to 94.8	20.7
Normal fuel element lifetime (days of reactor operation)	45 (effective full power)	21 to 23
Fuel plate dimensions		
Fuel plate thickness (in.)	0.080 (plate 1) 0.050 (plates 2-18) 0.100 (plate 19)	0.050
Cladding thickness (in.)	0.030 (plate 1) 0.015 (plates 2-18) 0.040 (plate 19)	0.010
Fuel matrix thickness (in.)	0.020	0.030
Active fuel height (in.)	48	20
Coolant channel thickness (in.)	0.108 (channel 1) 0.078 (channels 2-19) 0.113 (channel 20)	0.050
Core power		
Steady state thermal power (MW)	Up to 250	85
Average core volumetric power (MW/ft^3)	25.5 (at 250 MW)	47.2
Average core linear power (kW/ft)	82.2 (at 250 MW)	94.4
Peak core linear power (kW/ft)	279 (with enveloping 70 MW lobe)	Not available
	229 (60/40 lobe power split with 60 MW lobe)	
Average core specific power (MW/lb U-235)	2.64 (at 250 MW and 94.8 lb U-235)	4.11

Table 4.4-1. (continued).

Design parameters[a]	ATR	HFIR[b]
Heat transfer		
Active core heat transfer area (ft^2)	1333	428.8
Average core heat flux (Btu/hr≡ft^2)	6.41×10^5 (at 250 MW)	6.60×10^5
Peak core heat flux (Btu/hr≡ft^2)	1.76×10^6 (with enveloping 70 MW lobe, 3 PCP operation)	1.05×10^6
	1.44 × 106 (60/40 power split with 60 MW lobe, 2 PCP operation)	
Coolant flow		
Core flow direction	Vertically downward through fuel	Vertically downward through fuel
Core flow area (ft^2)	1.329	0.580
Primary system flow rate (gpm)	50,000 (3 PCP operation) 43,500 (2 PCP operation)	16,000
Core flow rate (gpm)	27,400 (3 PCP operation) 24,100 (2 PCP operation)	13,000
Average coolant velocity along fuel plates (ft/s)	46.0 (3 PCP operation) 40.4 (2 PCP operation)	53.1
Pressure		
Core inlet pressure (psig)	360	468
Core pressure drop (psid)	100 (3 PCP operation) 77 (2 PCP operation)	110
Coolant temperature		
Core inlet temperature (EF)	125	120
Average temperature rise in vessel (EF)	36 (at 250 MW and 3 PCP operation) 41 (at 250 MW and 2 PCP operation)	37
Fuel plate temperature		
Peak cladding surface temperature (EF)	358 (with enveloping 70 MW lobe, 3 PCP operation) 345 (60/40 power split with 60 MW lobe, 2 PCP operation)	303
Peak fuel meat temperature (EF)	488 (with enveloping 70 MW lobe, 3 PCP operation) 462 (60/40 power split with 60 MW lobe, 2 PCP operation)	325

a. All parameters are nominal.

b. HFIR data obtained from Sims and Swanks (1979) and Burn (1988).

Table 4.4-2. Design DNB and flow instability margins.

Operating condition	Minimum margin to DNB[a]	Minimum margin to flow instability[a]
Steady state with enveloping 70 MW lobe, three-pump operation	5.35σ	5.95σ
Steady state with 60/40 power split and 60 MW lobe, two-pump operation	8.31σ	9.98σ
Anticipated faults[b]	≥ 3σ	≥ 3σ

a. Polkinghorne 1993b

b. Margins are reported in Chapter 15 (Accident Analyses). Refinements to SINDA-SAMPLE for Chapter 15 analyses result in some differences relative to Polkinghorne (1993b).

Table 4.4-3. Reactor vessel flow distribution.

Region	Flow rate[a] (%)
Fuel elements	55.9
Reflector blocks	5.1
Outer shim control cylinders	19.4
Neck shim rod housing	1.2
Flux traps	11.4
Gap between reflector blocks and reflector tank	2.5
Capsule irradiation tanks	2.1
Internal seal leakage	1.1
Siphon breakers	1.3
Total	100.0

a. Based on design calculations of Croft and Green (1963) and Nielsen (1973).

Table 4.4-4. SINDA-SAMPLE statistical uncertainties.

Parameter	Mean Value	90% Confidence Factor
1. Top-of-core pressure	1.02[a]	0.041
2. Core pressure drop	1.0	0.041
3. Core inlet enthalpy	1.0	0.041
4. Reactor power	1.0	0.041
5. Subcooled force convection heat transfer coeff.	1.0	0.10
6. Onset of nucleate boiling temperature	1.0	0.20
7. Transition nucleate boiling heat transfer coeff.	1.0	0.10
8. Coolant velocity	1.0	0.068
9. Local fuel homogeneity Level 1 of ATR-SINDA model		
8.75" node height	1.0	0.12
5.50" node height	1.0	0.15
Levels 2-8 of ATR-SINDA model	1.0	0.08
Level 9 of ATR-SINDA model		
8.75" node height	1.0	0.12
5.50" node height	1.0	0.15
10. Low subcooling CHF	1.0	0.164
11. Fraction of power generated in fuel	1.0	0.033
12. Cladding solidus temperature	855 K	22.3 K
13. Cladding liquidus temperature	923 K	2.8 k
14. Coolant channel thickness	1.0	0.0
15. Aluminum-water ignition temperature	1,444 K	0.0
16. Thermal conductivity of corrosion film	2.25 W/mAK	0.574 W/mAK
17. Corrosion film thickness	2.54×10^{-5} m (or calculated with MACABRE)	5.92×10^{-6} m
18. Aluminum density	2647 kg/m^3	43.5 kg/m^3
19. Plate fueled length	1.219 m	1.905×10^{-2} m
20. Plate half-thickness		
Plate 15	6.35×10^{-4} m	2.54×10^{-5} m
Plate 19	1.27×10^{-3} m	2.54×10^{-5} m
21. UAl_3 mass		
Plate 15	0.1103 kg	2.16×10^{-3} kg
Plate 19	0.0760 kg	1.49×10^{-3} kg
22. UAl_3 density	6322 kg/m^3	353 kg/m^3
23. Aluminum heat of fusion	3.97×10^5 J/kg	6.51×10^3 J/kg
24. UAl_3 specific heat	1.0	0.049
25. Al-6061 specific	1.0	0.049

Table 4.4-4. (continued).

Parameter	Mean Value	90% Confidence Factor
26. Al-6061 specific heat	1.0	0.082
27. Plate fueled width		
Plate 15	8.054×10^{-2} m	1.905×10^{-3} m
Plate 19	8.618×10^{-2} m	1.905×10^{-3} m
28. Liquid-phase film boiling heat transfer coeff.	1.0	0.20
29. Vapor-phase laminar forced convection film boiling heat transfer coeff.	1.0	0.20
30. Vapor-phase natural convection film boiling heat transfer coeff.	1.0	0.20
31. Subcooled natural convection heat transfer coeff.	1.0	0.10
32. Fully developed nucleate boiling heat transfer coeff.	1.0	0.20
33. High subcooling CHF	1.0	0.164
34. Natural convection CHF	1.0	0.271
35. Core outlet enthalpy	1.0	0.041

a. Absolute values of relative variables are calculated within SINDA SAMPLE or obtained from ATR-SINDA.

Table 4.4-5. Peak nominal and statistical fuel plate centerline temperatures.

Peak temperature (°F)[a]		
Operating condition	Nominal	Nominal + 2σ
Steady state with enveloping 70 MW lobe, three-pump operation	488	556
Steady state with 60/40 power split and 60 MW lobe, two-pump operation	462	525

a. Polkinghorne 1993a.

Table 4.4-6. Reactor coolant system component thermal and hydraulic data.

Component	Data
Primary coolant system	
Design flow	54,000 gal/min
Nominal flow (3 PCP Operation)	50,000 gal/min
Maximum flow	53,200 gal/min
Emergency flow	6,000-7,000 gal/min
Core inlet pressure	360 psig
Core pressure drop (3 PCP operation)	100 psid
Reactor vessel pressure drop (3 PCP operation)	115 psid
Reactor inlet temperature	125°F
Reactor outlet temperature (3 PCP operation at 250 MW)	160°F (typical)
Demineralizing flow rate (maximum)	600 gal/min
Conductance	3 to 6 micromhos
Degassing flow rate	300 gal/min normal 600 gal/min maximum
Maximum total dissolved gases at primary pump suction (15% saturation)	180 cc/liter
Nominal pH	4.8 to 5.4
Piping pressure and temperature, design	
Primary pump discharge to first block valve	576 psig at 150°F
First block valve to butterfly valve	485 psig at 150°F
Butterfly valve to primary pump suction	390 psig at 150°F (240°F from reactor outlet to HX inlet)
Volume of system exclusive of the bypass demineralizer	10,865 ft^3
Bypass demineralizer system	
Design pressure	390 psig
Operating pressure	360 psig inlet
Design temperature	240°F
Operating temperature	120°F
Maximum flow	600 gal/min (2 train)
Operating flow	200 gal/min
Influent water conditions	5 ppm
Total dissolved solids	25 micromhos
ConductanceXmaximum	2.5 micromhos
ConductanceXminimum	
Effluent water conditions	1.0 micromhos

Table 4.4-6. (continued).

Component	Data
Gland seal water system	
Primary gland seal system Nominal flow Pump design flow	35 gal/min 150 gal/min at 750 ft water head
Water supply	Low-pressure demineralized water
Design pressure	615 psig
Supply pressure: Station No. 1-25 psi above reactor inlet pressure Station No. 2-25 psi above reactor inlet pressure Station No. 3A, B, and 4—245 psig Station No. 9-25—25 psi above reactor inlet pressure Station No. 11-395 psig	
Warm seal system	
Nominal flow Pump design flow	60 gal/min 150 gal/min at 350 ft head
Water supply	Primary Coolant
Supply pressure: Station No. 5-35 psi above reactor outlet pressure Station No. 6-35 psi above reactor outlet pressure Station No. 10-35 psi above reactor outlet pressure Station No. 12-35 psi above reactor outlet pressure	
Primary heat exchangers	
Quantity	5
Type	Vertical U-tube
Effective surface, net each	18,330 ft^2
Duty	733,600,000 Btu/hr
Tubes	3/4 in.-No. 18 Bwg, Inconel[a]
Shell	Carbon steel
Tube side design pressure and temperature	390 psig-240°F
Shell side design pressure and temperature	125 psig-200°F
Primary coolant side net volume	355 ft^3/exchanger
Primary coolant pumps	
Quantity	4 (one a spare)
Type	Horizontal volute centrifugal
Capacity each	18,000 gal/min
Total dynamic head	400 ft
Suction pressure	215 psig
Motor horsepower	2,000 nominal
Brake horsepower	2,146
Efficiency	85.5%

Table 4.4-6. (continued).

Component	Data
Net water volume per pump	22 ft^3
Speed	1,780 rpm
NPSH required	50 psig
Angular moment of inertia of pump and motor rotating element	2,000 lb-ft^2
Emergency coolant pumps	
Quantity	2
Type	Horizontal volute centrifugal
Capacity each	4,700 gal/min
Total dynamic head	22 ft
Suction pressure, each	215 psig
Suction pressure, emergency	24 ft
Motor horsepower	40
Brake horsepower	33.5
Efficiency	78%
Constant bypass flow	250 gal/min
Speed	710 rpm
Net water volume per pump	6 ft^3
NPSH	20 ft
Surge tank	
Quantity	1
Size	8 ft 0 in. ID - 22-1/2 ft overall
Total volume	1,000 ft^3
Operating water volume	950 ft^3
Material	Type 304 stainless steel clad carbon steel
Design pressure and temperature	390 psig-240°F
Operating pressure	215 psig
Degassing tank	
Quantity	1
Size	5 ft 0 in. OD x 28 ft overall
Material	Type 304 stainless steel
Maximum design pressure	65 psia
Minimum design pressure	3 psia
Number of spray nozzles	7
Normal water storage volume	197 ft^3
Maximum design liquid spray rate	600 gal/min
Design air flow rate	100 scfm
Normal degassing rate	300 gal/min

Table 4.4-6. (continued).

Component	Data
Primary pressurizing pumps	
Quantity	2
Type	Horizontal centrifugal
Capacity each	300 gpm
Total dynamic head	695 ft
Suction pressure	Flooded
NPSHXdesign	8 ft
Motor horsepower	100
Brake horsepower	88.4
Efficiency	58%
Speed	3,565 rpm

a. The M-3 Heat Exchanger has 12 tubes that are made of stainless steel. Six are 304 and six are 304L.

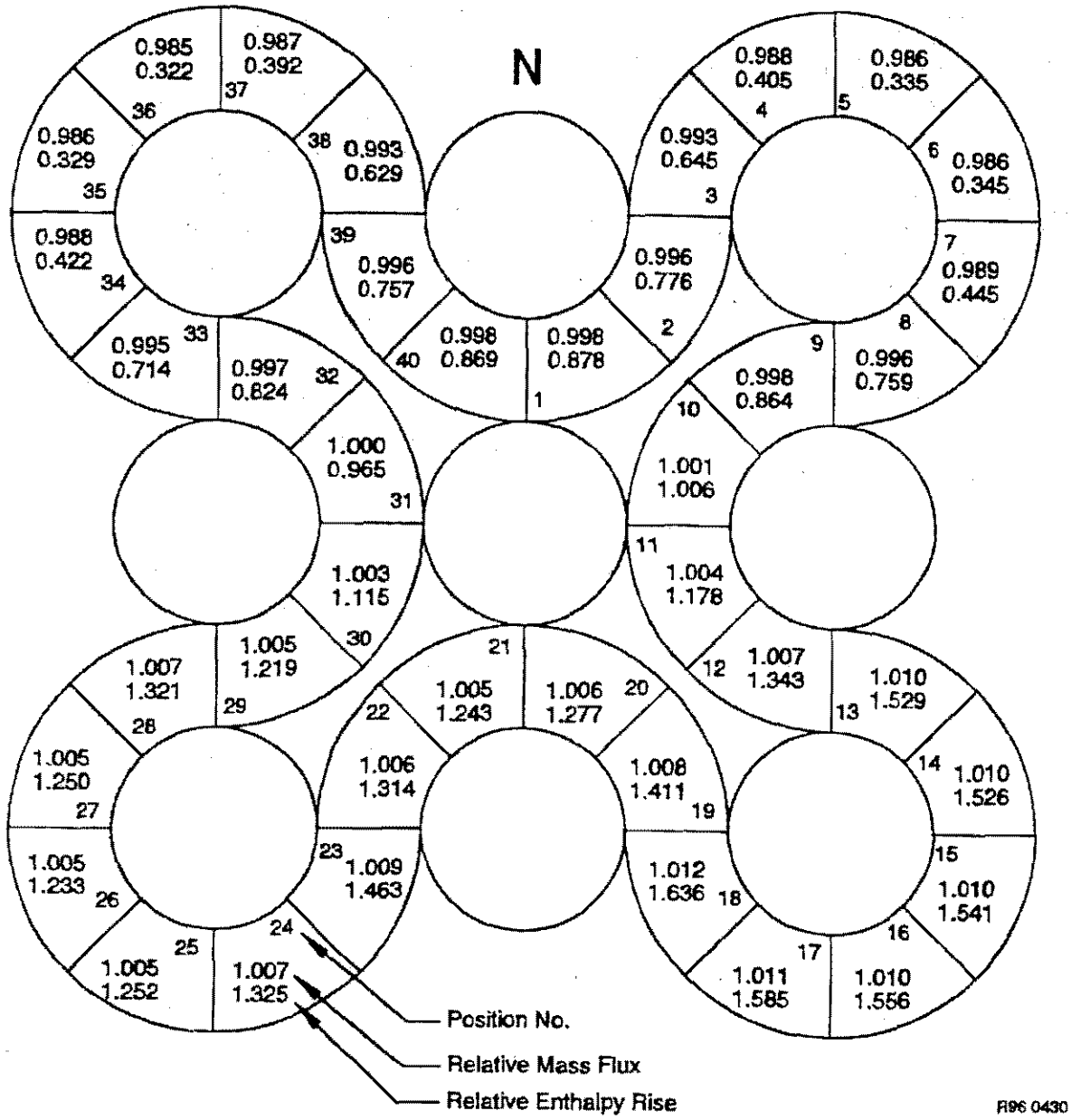

Figure 4.4-1. Normalized mass flux and enthalpy rise distributions with three-pump operation for beginning of cycle enveloping 70 MW lobe power split. **(For Information Only)**

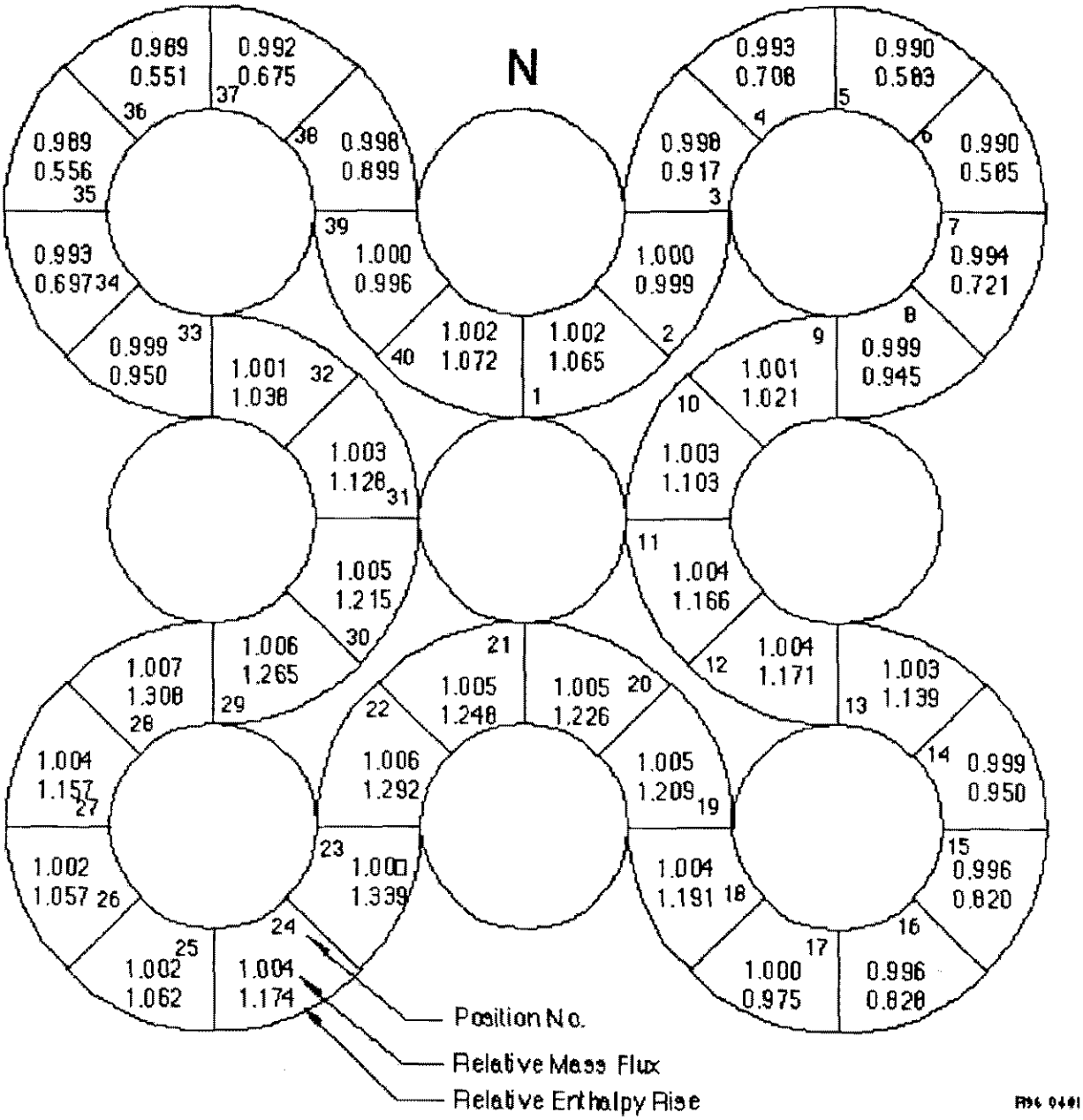

Figure 4.4-2. Normalized mass flux and enthalpy rise distributions with two-pump operation for beginning of cycle 60/40 MW lobe power split. **(For Information Only)**

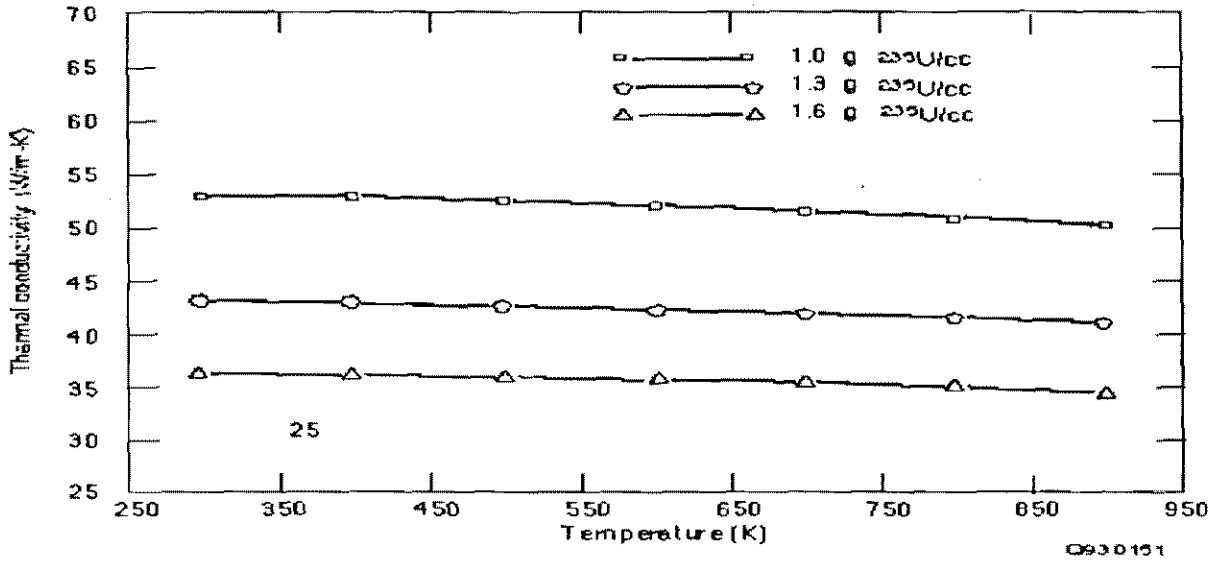

Figure 4.4-3. Thermal conductivity of UAl_x + Al fuel (Polkinghorne and Lacy 1991). **(For Information Only)**

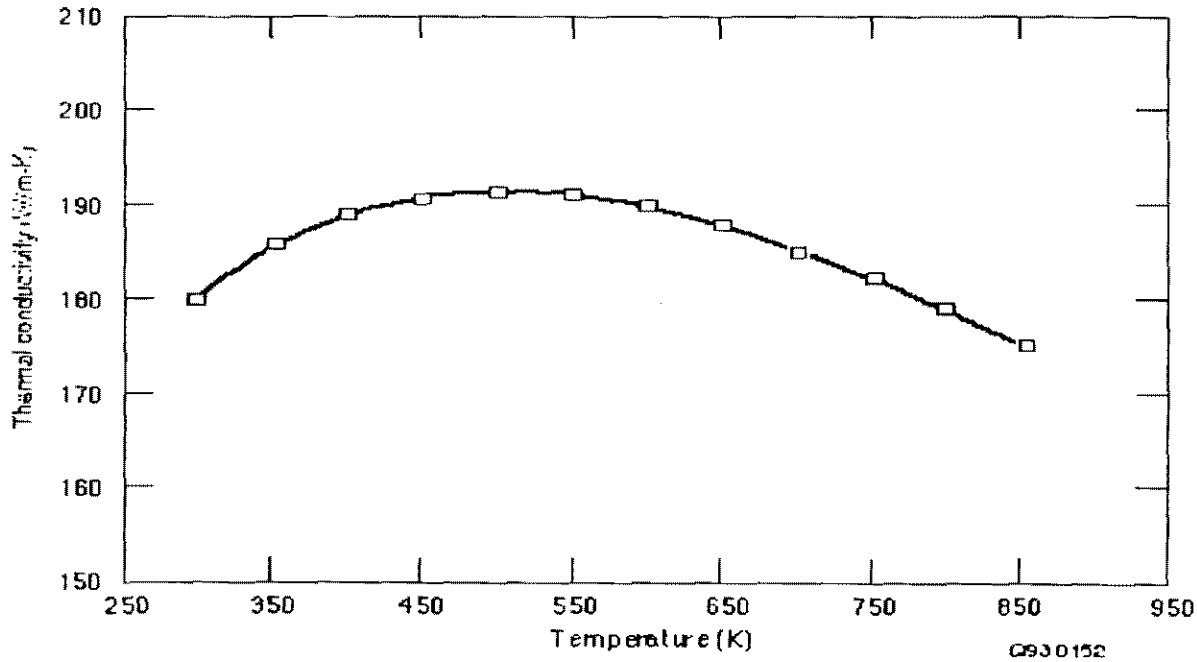

Figure 4.4-4. Thermal conductivity of 6061-0 aluminum cladding (Polkinghorne and Lacy 1991). **(For Information Only)**

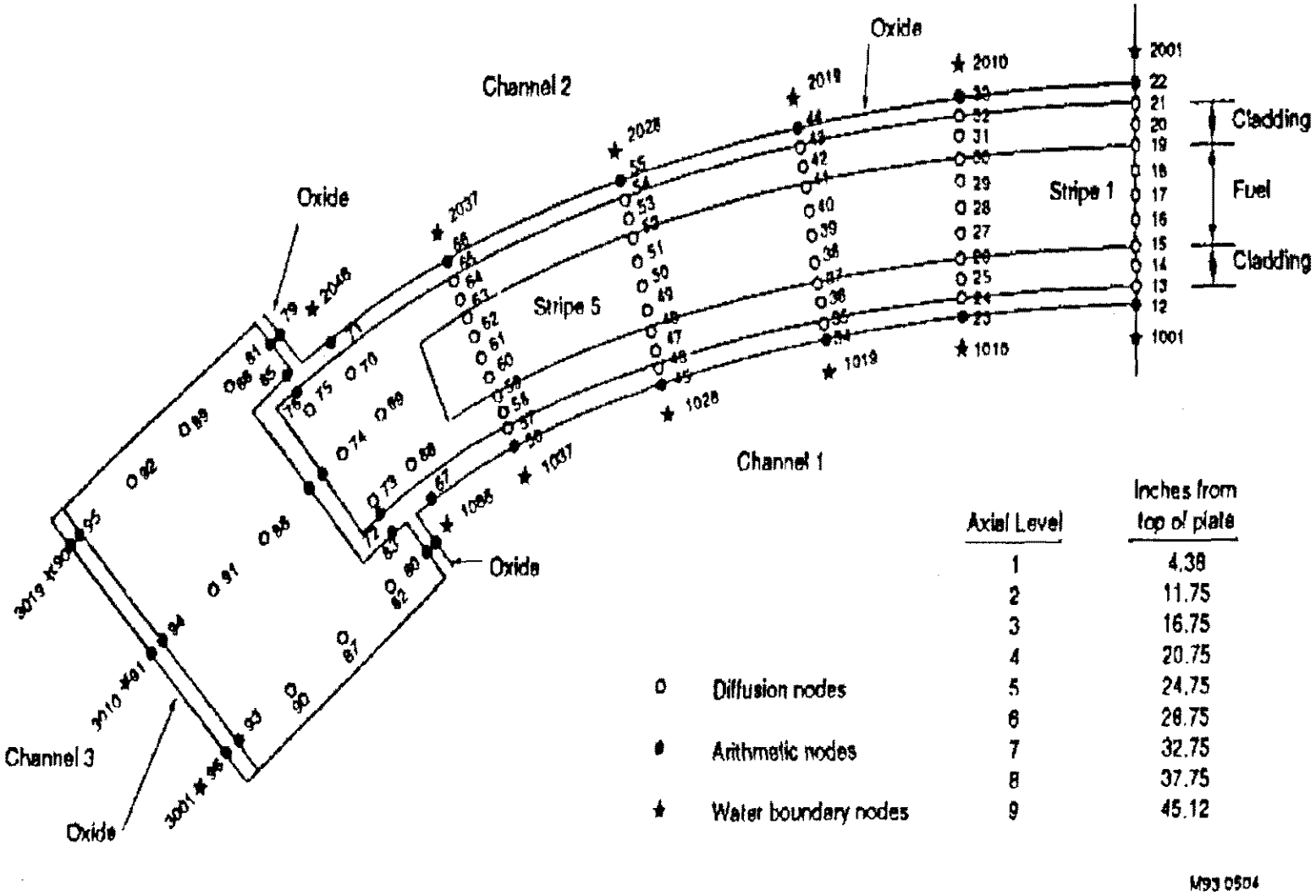

Axial Level	Inches from top of plate
1	4.38
2	11.75
3	16.75
4	20.75
5	24.75
6	28.75
7	32.75
8	37.75
9	45.12

Figure 4.4-5. Cross section of Advanced Test Reactor SINDA fuel plate model. **(For Information Only)**

4.5 Reactor Materials

Materials used in the physical structure of the ATR reactor, fabrication methods for these materials, and structural surveillance programs are required to meet all applicable standards and regulations to ensure quality products that maintain the required adequate safety margins. Structural components relevant to safety include control element drive systems and internal support and flow distribution structures as well as the reactor pressure vessel and PCS associated with the pressure boundaries. Principal materials in the control element drive systems and internal structures are described in this section. Materials in minor parts of components such as pins, nuts, and bolts may differ from the component's principal material. Any specialty materials in these minor components are identified in the composition tables, otherwise the minor components are not specifically listed in the tables. Materials in the PCS and reactor pressure vessel are described in Chapter 5 (Reactor Coolant System).

4.5.1 Control Element Drive System Structural Materials

The reactivity control systems consist of the reactivity control elements and associated drive mechanisms, which provide the means for positioning the control elements. The four independent reactivity control systems consist of the safety rods, the OSCC (rotational motion devices), the neck shim rods, and the regulating rods. The material description of the drive mechanisms includes components extending from the reactor pressure vessel to the coupling interface with the reactivity control (poison) elements. The design of the drive mechanisms is described in Chapter 3 (Design of Structures, Components, Equipment, and Systems) and the nuclear characteristics of the control elements in Section 4.3.2.4.

4.5.1.1 Materials Specifications. All materials in the drive mechanisms exposed to the reactor coolant are made of metals that resist the corrosive action of water. The principle types of metals used for the drive mechanisms include aluminum, austenitic and martensitic stainless steels, and nickel based alloys. Detailed specifications for type 304 stainless steel are given in Chapter 5 (Reactor Coolant System).

Materials used in the safety rod drive mechanisms and housing are listed in Table 4.5-1, in the outer shim cylinders in Table 4.5-2, and in the neck shim and regulating rod drive mechanisms in Table 4.5-3. The standards and regulations for materials and fabrication and/or basis for material selection for the drive mechanisms are contained in Section 3.9.4.

4.5.1.2 Austenitic Stainless Steel Components. The discussions provided in Chapter 5 (Reactor Coolant System) concerning the processes, inspections, and tests on austenitic stainless steel components to ensure freedom from increased susceptibility to intergranular stress corrosion cracking (IGSCC) due to sensitization are applicable to the austenitic stainless steel pressure housing components of the reactivity control system drive mechanisms. Studies of corrosion processes in the reactor materials in contact with the operating environment in the ATR have shown that the possibility of IGSCC (Durney et al. 1987) is kept very low through control of the initiating factors.

4.5.1.3 Other Materials. Structural materials in the reactivity control system drive mechanisms identified in Section 4.5.1.1 that have a yield strength greater than 90,000 psi are 17-4 PH and E4340 type steels and/or Inconel X, and Inconel X-750. These materials are used for machined parts inside the pressure boundary such as gears, drive rods, control rod guide tubes, and control rod housings and do not experience pressure induced stresses. The primary coolant water chemistry is actively controlled as discussed in Chapter 5 (Reactor Coolant System) to minimize the possibility of IGSCC. Thus, the IGSCC probability in these materials is very low.

Stainless steel type E4340 used in the regulating rod drive racks is hardened at 1,500-1,550°F, 1 hour per in. of thickness, then tempered at 950°F for 2 hours. Heat treatment (condition H-1100) for stainless steel type 17-4PH is aging at 1,100°F for 4 hours and air cooling as per specification MIL-H-6875.

4.5.1.4 Cleaning and Cleanliness Control. The reactivity control system drive mechanisms are cleaned prior to packaging and delivery in accordance with ANC-STD-7022, Level B or Level C, or to RTD-STD-F5-1T specifications.

4.5.2 Reactor Internal Materials

Major reactor components internal to the pressure vessel that are not part of the core or reactivity control system drive mechanisms include the core support tank, flow distribution tank, reflector support tank, and core reflector tank as illustrated in Figure 4.5-1. Other components around the core include an inlet flow baffle, capsule irradiation facilities, spent fuel racks, and instrument tubes.

4.5.2.1 Material Specifications. All materials used in the internal reactor components are exposed to the primary coolant and are made of metals resistant to the corrosive action of water. These metals are limited to aluminum, austenitic stainless steel, and nickel based alloys. The principal materials used for the internal reactor components are listed in Table 4.5-4. The nickel based alloy, Inconel X-750, is used in internal parts other than the CRDS only for minor components such as pins and/or bolts.

4.5.2.2 Controls on Welding. The chemical and physical properties of all stainless steel weld deposits conform with the Specification AWS A 5.9, CLASS ER308L. Chemical and physical properties of aluminum weld deposits conform to Specification AWS A 5.10, CLASS ER4043. All welds are inspected with liquid penetrant in accordance with the Contractor's Company Procedure 9.3. Additional information on fabrication processes is given in Chapter 5 (Reactor Coolant System) describing reactor vessel materials.

4.5.2.3 Nondestructive Examination of Tubular Products and Fittings. Methods for nondestructive examination of materials are given in Chapter 5 (Reactor Coolant System) describing reactor vessel materials. Aluminum castings are radiographed in accordance with formal contractor procedures.

4.5.2.4 Fabrication and Processing of Austenitic Stainless Steel Components. The discussion in Section 4.5.1.2 on austenitic stainless steel components is applicable to this section.

4.5.2.5 Contamination Protection and Cleaning of Austenitic Stainless Steel. The discussion in Section 4.5.1.4 on cleanliness is applicable to this section.

Table 4.5-1. Materials in safety rod drive mechanisms.

Component	Material specification
Horizontal Drive Shafts	
Rotary Seal	304 stainless steel, Buna N, Graphitar Grade 67, Stellite[a]
Inflatable Seal	304 stainless steel, Buna N
Bearings	Cobalt Alloy 19&3, 17-4PH stainless steel[b]
Shaft Housing	304L stainless steel
Shaft	304L stainless steel
Pinion	17-4PH stainless steel
Bolts and pins	304 stainless steel
Vertical Actuator	
Rack Tube	17-4PH stainless steel
Bushings	X750 Inconel
Guide Tube	6061 Aluminum alloy
Absorber plates	Hafnium
Retainer	304L stainless steel
Retainer Ring	X750 Inconel
Collar	X750 Inconel
Sleeve	17-4PH stainless steel
Snubber Tubes	17-4PH stainless steel

a. Stellites - cobalt-based alloys.

b. 17-4PH - martensitic stainless steel similar to AISI 630.

Table 4.5-2. Materials in outer shim control cylinder drive mechanisms.

Component	Material specification
Outer Shim Control Cylinder	
Column Connectors	17-4 PH stainless steel
Connecting Bolt	X750 Inconel
Cylinder	Hafnium, Beryllium, 6061 Aluminum alloy
Alignment Cups	347 stainless steel
Coupling Shaft	17-4 PH stainless steel
Gear Box Support Beams	
Housing	6061 Aluminum alloy
Studs	630 stainless steel
Upper Alignment Cups	304 stainless steel
Gears	Stellite

Table 4.5-3. Materials in neck shim rod drive mechanisms.

Component	Material specification
Neck Shim Rods	
Absorber	Hafnium
Follower	6061 Aluminum alloy
Cable Connector	Nitronic 60
Cable	321 stainless steel
Teflon Conduit	304 stainless steel, 25% fiber filled tetraflouroethylene
Regulating Rods	
Absorber	Hafnium
Upper drive rod	6061 Aluminum alloy
Extension	6061 Aluminum alloy
Center and lower drive rod	X750 Inconel
Housing	
Neck shim sleeves	6061 Aluminum alloy, X750 Inconel
Reg rod sleeves	X750 Inconel
Housing	6061 Aluminum alloy
Bolts and pins	Alloy NO7750 Type 2, X750 Inconel

Table 4.5-4. Materials in reactor internal components.

Component	Material specification
Core support tank	304 stainless steel
Flow distribution tank	304 stainless steel
Reflector support tank	Cast aluminum alloy SG 70 A-T71
Core reflector tank	Forged aluminum 6061, T652
Inlet flow baffle and thermal shield	304 stainless steel
Capsule irradiation tank assembly	
Vertical screens	Aluminum plate 6061, T6
Tank	304 stainless steel
Filler pieces	Aluminum 6061, T6
In-vessel fuel storage racks	
Frames	304 stainless steel
Fuel element basket inserts	Aluminum 6061, T6
	Aluminum clad cadmium
Instrument thimbles	304 stainless steel
Internal protective cover	304 stainless steel
	Aluminum 6061, T6
N16 monitor tube assemblies	Aluminum 6061, T6
Experiment loop pressure tube	347 stainless steel

FOIA Exemption 3 UCNI, Exemption 7f (Page 4-181 – internal core support drawing)

4.6 Functional Design of Reactivity Control Systems

4.6.1 Information for Control Element Drive Systems

The reactivity control elements and the associated drive mechanisms are described in Chapter 3 (Design of Structures, Components, Equipment, and Systems). The associated instrumentation is described in Section 4.3.2.2 with more detailed provided in Chapter 7 (Instrumentation and Control). The nuclear characteristics of the reactivity control system are in Section 4.3.2.4. These systems rely entirely upon mechanical means of operation with the exception that the safety rod insertion during scrams is aided by gravity at all times and by hydraulic forces from the primary coolant flow during pressurized operation.

4.6.2 Evaluations of the Reactivity Control Systems

The safety function of the reactivity control systems is to insert the safety rods into the core when a trip signal from the PPS interrupts the electrical power to the electromagnetic clutches connecting the drive motors to the horizontal drive shafts, which keep the rods in position. The instrumentation and controls for the PPS are described in Chapter 7 (Instrumentation and Controls). The safety rods operate independently of one another to ensure that the failure of any one rod to trip would have no effect on the operability of the remaining rods. The shutdown worth of the safety rods described in Section 4.3.2.4 is sufficient to safely scram the reactor assuming the failure of one rod to trip. The OSCC and neck shim rods, while not part of the scram system, may be inserted mechanically to provide additional negative reactivity to the system. During intervals when the reactor is not being operated, it must remain subcritical during core changes and changes in fission product inventories. A holddown reactivity margin is specified to ensure this subcriticality. This holddown reactivity margin is provided by the reactivity control systems.

The safety rod assemblies surround the pressurized water loop facility or chopped dummy IPT in selected flux traps. The experiment loops supporting the IPT operate independently, however, so that even in the highly unlikely event of a failure occurring in one loop, the safety function of the reactivity control systems will not be compromised. The chopped dummy IPT are passive structures so failure in more than one component is highly unlikely. The limiting control system failures are evaluated in Chapter 15 (Accident Analyses). The analysis results demonstrate compliance with the ATR plant protection criteria.

Reliability analyses have been performed on the PPS and are documented in Chapter 7 (Instrumentation and Controls). These analyses show that the reactivity control systems can perform their safety function under both normal and accident conditions. The possibility of common mode failures is kept sufficiently low by employing functional diversity in the system, 2 out of 3 logic in the PPS, maintaining physical separation of redundant components, maintaining test schedules, and applying administrative controls.

4.6.3 Testing and Verification

A failure mode and effects analysis of the Reactor Shutdown System was performed (see Chapter 7 (Instrumentation and Controls)). This analysis indicates that the design will accomplish its protective functions given one failure at any point in the system. A review of the scram frequency and failure rate (Cadwallader 1989) over a twenty-year period shows that no failures to scram upon demand have occurred for the safety rods. Testing of the scram system is done on a frequent basis to verify the safety rod operation. Scram time specifications are listed in Section 4.3.2.5 and the testing and verification to show that the safety rod control system meets the specifications is described in Section 4.2.4.3 (reactivity worth) and in Section 4.3.2.5(release and drop times).

4.7 References

Allison, C. M., et al., 1989, *SCDAP/RELAP5/MOD2 Code Manual, Volumes 1, 2, and 3*, NUREG/CR-5273, EGG-2555, EG&G Idaho, Inc., September 1989.

Ambrosek, R. G., 1975, *The Savannah River Correlation*, ETR Technical Specifications Design Basis, Volume II, Appendix A.6, TR-587, Aerojet Nuclear Co., January 31, 1975.

Ambrosek, R. G., 1993, *ATR Fuel Element Oxide Thickness for UFSAR Analysis*, Engineering Design File (EDF) TRA-ATR-792, EG&G Idaho, Inc., May 7, 1993.

Ambrosek, R. G. 1998, Letter to M. B. Hendrickson, AMB-14-98, *Thermal-Hydraulic Evaluation for Modified ICE-ATR Compliance*, June 11, 1998.

Ambrosek, R. G., H. H. Nielsen, and G. N. Fillmore, 1982, *Safety Analysis for Assumed Reflector III Failure Modes*, PR-T-82-009, EG&G Idaho, Inc., May 1982.

Ambrosek, R. G., K. H., Liebett, and B. J., Merrill, 1993, *User's Manual for ATR-SINDA, Version A, Mod. 0. A SINDA Thermal-Hydraulic Model of an ATR Fuel Plate*, ERA-NRE-93-017, EG&G Idaho, Inc., March 1993.

ANC, 1973, *ATR Operating Envelope Extension*, TR-386, Volume II, Aerojet Nuclear Co., May 1973.

Anderson, E. C., 1992, Letter to R. V. Furstenau, ECA-101-92, *Request for Approval of Facility Change Form (FCF) 7.2.1-3 Modified Non-Fueled (YA) Plate 19 Fuel Elements*, EG&G Idaho, Inc., October 8, 1992.

ANSI, 1988, *Nuclear Safety Criteria for the Design of Stationary Pressurized Water Reactor Plants*, ANSI/ANS-51.1-1983 (reaffirmed 1988), American National Standards Institute/American Nuclear Society, La Grange Park, IL.

Ash, M., 1965, *Nuclear Reactor Kinetics*, McGraw Hill Book Co., 1965.

ASME, 1986, Section XI, Division 1, *ASME Boiler and Pressure Vessel Code*, American Society of Mechanical Engineers, New York, NY, 1986. (historical)

ASTM, 1996a, *Standard Specification for Aluminum and Aluminum-Alloy Sheet and Plate*, American Society for Testing and Materials, West Conshohockon, PA, 1996.

ASTM 1996b, *Standard Specification for Aluminum and Aluminum-Alloy Extruded Bars, Rods, Wire, Profiles, and Tubes*, American Society for Testing and Materials, West Conshohockon, PA, 1996.

ASTM, 1997, *Standard Specification for Aluminum-Alloy Investment Castings*, American Society for Testing and Materials, West Conshohockon, PA, 1997.

Atkinson, S. A., 1975, *A Study of the Onset of Flow Instability in ATR Fuel Channels*, TR-582, Aerojet Nuclear Co., January 21, 1975.

Atkinson, S. A., 1976, *A Forced Convection DNB Correlation for Stainless Steel or Aluminum Heaters for Low Subcooling Based on Savannah River Laboratory Data*, TR-813, Aerojet Nuclear Co., March 25, 1976.

Atkinson, S. A., 1988, *ATR Safety Basis Summary*, PG-T-88-011, EG&G Idaho, Inc., September 1988.

Atkinson, S. A., 1997, *A Study for the Risk of ATR Fuel Element Swage Joint Failure Without Hydraulic Testing*, EDF TRA-ATR-1108, Rev. 1, EG&G Idaho, Inc., February 13, 1997.

Atkinson, S. A., et al., 1974, *ATR Reflector II Lifetime Extension Analysis*, TR-559, Aerojet Nuclear Co., November 27, 1974.

Bates, J. L., 1966, *Thermal Diffusivity of MTR-ETR Type Fuel Plates, Final Report*, BNWL-CC-456, Battelle Northwest Laboratories, January 10, 1966.

Beeston, J. M., 1976, *Properties of Irradiated Beryllium, Statistical Evaluation*, TREE-1063, EG&G Idaho, Inc., October 1976.

Beeston, J. M., 1977, *Hafnium Irradiation Damage*, TREE-1140, EG&G Idaho, Inc., June 1977.

Beeston, J. M., 1978, *ETR Fuel Element Pitting*, RE-M-78-012, EG&G Idaho, Inc., April 1978.

Beeston, J. M., and R. A. Moen, 1966, *Status Report on Advanced Test Reactor Beryllium Surveillance Program*, IN-1043, Idaho Nuclear Corporation, December 1966.

Beeston, J. M., and R. K. Malik, 1977, *Burnup Extension Analysis of Two 7F Fuel Elements*, RE-M-77-011, EG&G Idaho, Inc., November 1977.

Beeston, J. M., et al., 1980, *Development and Irradiation Performance of Uranium Aluminide Fuels in Test Reactors*, Nuclear Technology, 49, June 1980, pp. 136-149.

Bergles, A. E., and W. M. Rohsenow, 1964, *The Determination of Forced-Convection Surface-Boiling Heat Transfer*, Journal of Heat Transfer, 86, 3, August 1964, pp. 365-372.

Beus, S. G., and J. H. Anderson, 1974, *FLOW3 - A Computer Program for Network Analysis of Two Phase Flow in Three Dimensions*, WAPD-TM-1177(L), Bettis Atomic Power Laboratory, Pittsburgh, PA, October 1974.

Brown, A. W., 1976, *GOPP: A General One-Dimensional Plot Program for PDQ*, RE-N-76-041, EG&G Idaho, Inc., December 1976.

Brown, A. W., et al., 1990, *ATR CSA Physics Model Description and Calculation Guide*, NRRT-N-90-011, EG&G Idaho, Inc., April 1990.

Brugger, R. M., et al., 1971, *Nuclear Technology Division Annual Progress Report for Period Ending June 30, 1971*, ANCR-1016, Aerojet Nuclear Co., October 1971, pp. 132-134.

Buescher, B. J., 1998, *Irradiation Testing of 6061 Aluminum*, EDF TRA-ATR-1331, June 30, 1998.

Burdick, E. E., 1971, *Reactor Technology Branch Annual Report for Fiscal Year 1970*, ANCR-1013, Aerojet Nuclear Co., August 1971, pp. 4-7.

Burn, R. R. (ed.), 1988, *Research, Training, Test and Production Reactor Directory, United States of America*, Third Edition, American Nuclear Society, La Grange Park, IL.

Burr, T. K., 1976, Letter to D. R. Mousseau, TKB-4-76, *Hafnium Safety Rod Stresses-Fluence Limit*, Aerojet Nuclear Co., June 29, 1976.

Burrell, N. S., 1992, Letter to E. C. Anderson, RFO-341-92, *Approval of FCF 7.2.1-3 Modified Non-Fueled (YA) Plate 19 Fuel Elements*, U.S. Department of Energy, Idaho Operations Office, November 17, 1992.

Cadwallader, L. C., 1989, *Component Reliability Information for ATR PRA Support*, EDF TRA-ATR-308, EG&G Idaho, Inc., November 14, 1989.

Clemons, R. A., 1979, Letter to J. L. Durney, Clem-7-79, *ATR Stuck Safety Rod Modifications Flow Analysis*, EG&G Idaho, Inc., August 29, 1979.

Clemons, R. A., 1992, *Document Draft Report of ATR S.O.-102, Reactor Internals Hydraulics Test*, EDF TRA-ATR-656, EG&G Idaho, Inc., May 1, 1992.

Colebrook, C. F., 1939, *Turbulent Flow in Pipes, with Particular Reference to the Transition Region Between the Smooth and Rough Pipe Laws*, Journal of the Institution Civil Engineers, 11, 1939, pp. 133-156.

Croft, M. W., 1964, *Advanced Test Reactor Burnout Heat Transfer Tests*, IDO-24465, Phillips Petroleum Co., January 1964.

Croft, M. W., and G. S. Green, 1963, *Design Data, Reactor Flow Distribution*, Design Data Sheet R-80-21, Rev. 7, September 26, 1963.

deBoisblanc, D. R., and S Cohen, 1965, *Safety Analysis Report Advanced Test Reactor*, IDO-17021, Phillips Petroleum Co., April 1965.

Deville, R. E., 1963, *Differential Thermal Expansion Tests on Advanced Test Reactor Fuel Plates*, IDO-24461, Phillips Petroleum Co., October 1963.

Dienst, W., S. Nazaré and F. Thümmler, 1977, *Irradiation Behavior of UAl_x-Al Dispersion Fuels for Thermal High Flux Reactors*, Journal of Nuclear Materials, 64, 1964, pp. 1-13.

Dimenna, R. A., et al., 1988, *RELAP5/MOD2 Models and Correlations*, NUREG/CR-5194, EGG-2531, EG&G Idaho, Inc., August 1988.

Dittus, F. W., and L. M. K. Boelter, 1930, *Heat Transfer in Automobile Radiators of the Tubular Type*, Publications in Engineering, 2, University of California, Berkeley, 1930, pp. 443-461, October 1930.

DOE, 2002, *Facility Safety*, Order 420.1A, U.S. Department of Energy, Washington D.C., May 20, 2002.

Durney, J. L., 1967, *Errors in ATR Fission-Rate Measurements*, *Nuclear Technology Branch Quarterly Report April 1 - June 30, 1967*, IN-1126, Idaho Nuclear Corporation, December 1967.

Durney, J. L., 1977, *ATR Burnup Extension*, PR-T-77-003, EG&G Idaho, Inc., December 20, 1977.

Durney, J. L., 1980, Letter to A. L. Bowman, *ATR Power Limit for Higher pH in the PCS*, JLD-21-80 (Rev. 1), EG&G Idaho, Inc., October 17, 1980.

Durney, J. L., 1982, Letter to D. R. Mousseau, *Effect of pH on ATR Oxides*, JLD-17-82, EG&G Idaho Inc., July 9, 1982.

Durney, J. L., 1987, Letter to D. W. Croucher, *ATR Safety Analysis for Reflector IV*, JLD-27-87, EG&G Idaho Inc., November 3, 1987.

Durney, J. L., 1994, *Evaluation of Reflector Safety Analysis*, EDF TRA-ATR-928, EG&G Idaho Inc., February 7, 1994.

Durney, J. L., J. B. Willis, J. C. Tappendorf, and C. H. Hogg, 1972, *Reactor Physics Results from the ATR Power Demonstration Program*, ANCR-1080, Aerojet Nuclear Company, October 1972.

Durney, J. L., W. G. Reuter, G. K. Miller, and G. A. Reimann, 1987, *ATR Lifetime and Primary Coolant System IGSCC Assessment*, PG-T-87-009, EG&G Idaho, Inc., December 1987.

Dwight, J. E., 1986, Letter to D. R. Mousseau, JEDw-25-86, *Neutron Embrittlement of the ATR Reactor Vessel*, EG&G Idaho, Inc., December 1986.

Dwight, J. E., R. T. McCracken, W. D. Gregory, W. M Yarbrough, 1986, *Results of Physics Tests Following ATR Core Internals Changeout*, PG-T-86-007, EG&G Idaho, Inc., July 1986.

Dykes, J. W., J. D. Ford, and K. R. Hoopingarner, 1965, *A Summary of the 1962 Fuel Element Fission Break in the MTR*, IDO-17064, Phillips Petroleum Co., February 1965.

EG&G Idaho, 1991a, *Material Specification, Beryllium Pressings and Components for Nuclear Reactors and Reactor Systems*, ANC-80005H, June 20, 1991.

EG&G Idaho, 1991b, *Material Specification, Hafnium Wrought Products*, ES-80001, Rev. L, May 10, 1991.

EG&G Idaho, 1994, *ATR PPS and Technical Specifications Design Basis Report*, (SAR-39), Issue 030, EG&G Idaho, Inc., August 2, 1994.

Eide, S. A., 1989, *Advanced Test Reactor Loose Parts Monitoring System Risk Analysis*, EDF TRA-ATR-379, EG&G Idaho, Inc., December 11, 1989.

Ferris, H. D., and J. C. Moyers, 1963, *Advanced Test Reactor Fuel Elements Hydraulic Buckling Tests*, IDO-24463, Phillips Petroleum Co., October 1963.

Fillmore, G. N., 1976, *Low Power Fuel Element Classification*, GNF-6-76, (letter; Fillmore to file), Aerojet Nuclear Co., September 16, 1976.

Fillmore, G. N., 1979, Letter to J. L. Durney, GNF-19-79, *ATR Guide Tube Temperatures for Inserted Safety Rod with Aluminum Fillers*, EG&G Idaho, Inc., August 29, 1979.

Fillmore, G. N., 1980, Letter to J. L. Durney, GNF-1-80, *ATR Reactor Core Component Analyses for Two Pump Operation*, EG&G Idaho, Inc., January 7, 1980.

Fillmore, G. N., 1995, *ATR Fuel Element Hydraulic Testing History*, EDF TRA-ATR-1094, EG&G Idaho, Inc., November 1, 1995.

Fors, R. M., 1980, *Model Development and Analysis Improvements for Determination of ATR Reflector III Lifetime*, RE-A-78-271, Rev. 2, EG&G Idaho, Inc., October 1980.

Francis, W. C. (ed.), 1966, *Annual Progress Report on Reactor Fuels and Materials Development for FY-1965*, IDO-17154, Phillips Petroleum Co., February 1966.

Francis, W. C. (ed.), 1970, *Metallurgy and Materials Science Branch Annual Report, Fiscal Year 1970*, IN-1437, Idaho Nuclear Corporation, November 1970.

Francis, W. C., 1971, Letter to H. R. Hilker, Fra-219-71, *Microcracking Phenomena*, Aerojet Nuclear Co., November 18, 1971.

Francis, W. C., 1974a, Letter to M. L. Griebenow, Fra-34-74, *Extended Burnup*, Aerojet Nuclear Co., March 4, 1974.

Francis, W. C., 1974b, letter to D. R. Mousseau, Fra-113-74, *Transmittal of INC-16-2 Results*, Aerojet Nuclear Co., July 19, 1974.

Francis, W. C., and R. A. Moen (eds.), 1966, *Annual Progress Report on Reactor Fuels and Materials Development for FY 1966*, IDO-17218, Phillips Petroleum Co., November 1966.

Francis, W. C., and F. H. Tingey, et al., 1967a, *Quarterly Report, Status of Test Reactor Fuel Element Activities, Period Ending January 31, 1967*, CI-1035, Idaho Nuclear Corporation, 1967.

Francis, W. C., and F. H. Tingey, et al., 1967b, *Quarterly Report, Status of Test Reactor Fuel Element Activities, Period Ending April 30, 1967*, CI-1052, Idaho Nuclear Corporation, 1967.

Gambill, W. R., and R. D. Bundy, 1964, *Heat-Transfer Studies of Water Flow in Thin Rectangular Channels, Part I-Heat Transfer, Burnout, and Friction for Water in Turbulent Forced Convection*, Nuclear Science and Engineering, January 18, 1964.

Gaski, J. D., 1987, *SINDA 1987/ANSI Computer Code*, Network Analysis Associates, Inc., October 1987.

Gougar, H. D., 1998, *Temperature Coefficient for the Modified ICE Test*, EDF TRA-ATR-1330, May 19, 1998.

Graber, M. J., et al., 1971, *Performance Evaluation of Core II and III Advanced Test Reactor Fuel Elements*, ANCR-1027, Aerojet Nuclear Co., October 1971.

Griebenow, M. L., 1964, *Ex-Reactor Heat Transfer Experiments Simulating ETR Fuel Element Geometry*, PTR-732, Phillips Petroleum Co., December 28, 1964.

Griebenow, M. L., 1968, *Isothermal Hydraulic Measurements in Fuel Elements in ATR Core*, IN-1158, Idaho Nuclear Corporation, September 1968.

Griebenow, M. L., (ed.), 1971, *ATR Extended Burnup Program*, ANCR-1015, Aerojet Nuclear Co., November 1971.

Griebenow, M. L., G. N. Fillmore, and C. A. Moore, 1966, *Engineering Studies Relative to ATR Fuel Element Performance, January through November 1966*, CI-1014, Idaho Nuclear Corporation, December 1966.

Griebenow, M. L., and K. D. Richert, 1967, *MACABRE II*, IN-1107, Idaho Nuclear Corporation, September 1967.

Griebenow, M. L., et al., 1971, *ATR-Startup Fuel-Plate-Cladding Corrosion Test, Preliminary Data and Conclusions*, ATR Core-1 Thermal-Hydraulic Test Results, Contained in TR-727, Section 6 dated September 1976, Aerojet Nuclear Co., February 1971.

Griebenow, M. L., and G. H. Hanson, 1976, *ATR Core-1 Thermal-Hydraulic Test Results*, TR-727, Aerojet Nuclear Co., September 1976.

Griebenow, M. L., G. H. Hanson, and A. P. Larrick, 1977, *TRA Oxide Film Control and Surveillance*, RE-A-77-059, EG&G Idaho, Inc., October 1977.

Griess, J. C., H. C. Savage, and J. L. English, 1964, *Effect of Heat Flux on the Corrosion of Aluminum by Water*, Part IV, Tests Relative to the Advanced Test Reactor and Correlation with Previous Results, ORNL-3541, Oak Ridge National Laboratory, February 1964.

Grimesey, R. A., D. W. Nigg, and R. L. Curtis, 1991, Combine/PC-A Portable ENDF/B Version 5 Neutron Spectrum and Cross-Section Generation Program, EGG-2589, Rev. 1, EG&G Idaho, Inc., February 1991.

Grimesey, R. A., et al. 1990, *COMBINE/PC - A Portable ENDF/B Version 5 Neutron Spectrum and Cross Section Generation Program*, EGG-2589, EG&G Idaho, Inc., April 1990. (historical)

Gronbeck, H. D., 1967, *ETR Radiation Damage Surveillance Programs, Progress Report II*, IN-1036, Idaho Nuclear Corporation, February 1967.

Hamilton, B. H., 1996a, letter to E. J. Ziemianski, *Request for Approval of Advanced Test Reactor (ATR) Technical Specification Change-Hydraulic Test Requirement*, BHH-21-96, Lockheed Martin Idaho Technologies Company, March 7, 1996.

Hamilton, B. H., 1996b, letter to E. J. Ziemianski, *Response to Comments on Advanced Test Reactor (ATR) Technical Specification Change-Hydraulic Test Requirement*, BHH-41-96, Lockheed Martin Idaho Technologies Company, April 25, 1996.

Hanson, G. H., M. L. Griebenow, and R. A. Wells, 1975, *USAEC-INEL Advanced Test Reactor Emergency-Cooling Flow-Instability Experiment*, Transactions of the American Nuclear Society, 21, 1975, pp. 34-436.

Harris, B. L., 1984, *Stress and Deflection Analysis of ATR Mark VII Fuel Element*, PG-T-84-012, EG&G Idaho, Inc., August 1984.

Hayner, G. O., 1970, Letter to M. L. Griebenow, Hayn-38-70, *Best Estimate of the Compressive Yield Strength vs. Temperature of Unirradiated ATR Plate 19*, Idaho Nuclear Corporation, November 17, 1970.

Hendrickson, M. B., 1994, *Loop Reconfiguration Project - Option B*, TRA-SE-94-006, EG&G Idaho, Inc., February 3, 1994.

Hendrickson, M. B., 1998a, *ATR Northeast Flux Trap Flow Rates with ICE Facility Installed*, EDF TRA-ATR-1255, Rev. 1, Lockheed Martin Idaho Technologies Company, July 1, 1998.

Hendrickson, M. B., 1998b, *Installation of the Reconfigured Irradiation Capsule Experiment ICE and Facility*, TRA-SE-98-031, Lockheed Martin Idaho Technologies Company, July 1998.

Hendrickson, M. B., 2001, *ATR Northeast Flux Trap Flow Rates with the MICE Facility Installed*, EDF TRA-ATR-1503, Rev. 2, June 15, 2001.

Henscheid, J. W., et al., 1967, *ATR Startup, Zero-Power Experiments, and Comparison with ATR Critical Facility*, IN-1136, Idaho Nuclear Corporation, December 1967.

Henslee, S. P., 1980, *ATR Fuel Element Pitting*, PR-T-80-030, EG&G Idaho, Inc., April 1980.

Hibbit, Karlsson and Sorensen, Inc., 1990, *ABAQUS User's Manual*, Version 4-8-5, Providence, RI, April 1990.

Holman, G. W., 1994, Letter to E. C. Anderson, GWH-03-94, *Advanced Test Reactor Cycle 103A-1 Beryllium Inspection*, EG&G Idaho, Inc., March 23, 1994.

House, R. K., 1992, *Bases for Designation of Safety-Related Equipment in the ATR*, PG-T-92-114, EG&G Idaho, Inc., July 1992.

Ingram, F., 1999, *Facility Safety Assessment for the Advanced Test Reactor – Irradiation Test Vehicle (ATR-ITV)*, Lockheed Martin Idaho Technologies Company, May 18, 1999.

Ismail Z. H., 1990, *Effect of Low Dose Neutron Irradiation on the Mechanical Properties of an AlMgSi Alloy*, Rad. Effects, 112, 1990, pp. 105-110

Ismail, Z. H., and H. G. Mohamed, 1989, *Effect of Prior History on the Response of Some Commercial Aluminum Alloys to Low Dose Neutron Irradiation*, Scripta METALLURGICA 23, 1989, pp. 2067-2072, September 1989.

Ismail Z. H., and B. Birt, 1995, *Post-Irradiation Mechanical Properties of an AlMgSi Alloy*, J. Nucl. Mater. 218, 1995, pp. 289-292.

Judd, J. L., 1991, *SCRABL-5 An ENDF/B Version 5 Computer Code for Cross Section Collapsing*, EG&G-NE-9904, EG&G Idaho, Inc., September 1991.

Judd, J. L., 1992, *PDQ Reactor Physics Analysis for the ATR FSAR Upgrade*, PG-T-92-003 Addendum 1, EG&G Idaho, Inc., November 1992.

Judd, J. L., and W. K. Terry, 1992, *RELAP5 Kinetics Model Development for the Advanced Test Reactor*, NRRT-N-92-009, Rev. 1, EG&G Idaho, Inc., March 1992.

Keller, F. R., 1962, *Fuel Element Flow Blockage in the Engineering Test Reactor*, IDO-16780, Phillips Petroleum Co., May 10, 1962.

Kier, P. H., and A. A. Robba, 1967, *RABBLE, A Program for Computation of Resonance Absorption in Multiregion Reactor Cells*, ANL-7326, April 1967.

Kim, S. S., and J. L. Judd, 1991, *Two- and Three-Dimensional PDQ Benchmarking Comparisons with the Advanced Test Reactor Cycle 73A-2 Measurement Data*, PG-T-91-017, EG&G Idaho, Inc., June 1991.

Kim, S. S., and J. A. McClure, 1993, *PDQ Reactor Physics Analysis for the ATR-FSAR Upgrade*, PG-T-92-003, Rev. 1, EG&G Idaho, Inc., September 1993.

Knoebel, D. H., et al., 1973, *Forced-Convection Subcooled Critical Heat Flux, D_2O and H_2O Coolant with Aluminum and Stainless Steel Heaters*, DP-1306, February 1973.

Koch, D. W., K. F. Riskevics, and E. E. Ritchie, 1963, *Advanced Test Reactor Investigation of the Corrosion Behavior of Materials of Construction*, IDO-24460, Phillips Petroleum Co., August 1963.

Kraus, H. G., 1977, *SIMIR/6 - A Two Dimensional Steady State and Transient Heat Conduction Code for Use on an IBM 360/75 Computer - A User's Guide*, TREE-1127, EG&G Idaho, Inc., April 1977.

Lacy, J. M., and G. L. Thinnes, 1991, *ATR Fuel Element Structural Behavior for Severe Accident Conditions*, PG-T-91-038, EG&G Idaho, Inc., November 1991.

Liebelt, K. H., 1996, *Users Manual for SINDA-SAMPLE, Version A, Mod. 1, A SINDA Thermal-Hydraulic/Statistical Model of the Hot Stripe in an ATR Fuel Plate*, PG-T-96-006, LMITCO, November 1996.

Livingston, R. A., 1984, *ATR Hafnium Fluence Limits*, EDF TRTSB-ATR-093, Rev. 1, EG&G Idaho, Inc., September 6, 1984.

Livingston, R. A., 1986, Letter to J. A. Hong, Liv-6-86, *ATR Requalification Hydraulic Test PST-5*, EG&G Idaho, Inc., May 17, 1986.

Lloyd, W. R., 1989, *Evaluation of Axial Shear Forces in Swaged Joints of ATR Fuel Elements*, PG-T-89-024, EG&G Idaho, Inc., September 1989.

Loret, L. S., 1994, Letter to E. C. Anderson, LSL-11-94, *ATR Power History Through Cycle 102B-1*, EG&G Idaho, Inc., February 28, 1994.

Martin, W. R., and J. R. Weir, 1964, *Mechanical Properties of X8001 and 6061 Aluminum Alloys and Aluminum-Base Fuel Dispersion at Elevated Temperatures*, ORNL-3557, Oak Ridge National Laboratory, February 1964.

McClure, J. A., 1991a, *Results of Outer and Neck Shim Calibration Studies*, EDF TRA-ATR-542, EG&G Idaho, Inc., September 20, 1991.

McClure, J. A., 1991b, *Tappendorf's Reactivity Formula*, EDF TRA-ATR-543, EG&G Idaho, Inc., July 20, 1991

McClure, J. A., G. G. Gose, and M. A. Moser, 1993, *Reactor Physics Analysis for the ATR Loop Reconfiguration Projects*, PG-T-92-136 Addendum 2, EG&G Idaho, Inc. (Prepared by Computer Simulation & Analysis, Inc.) December 1993.

McCracken, R. T., 1993a, *Results of ATR Critical Facility Core Reconfiguration and Requalification Testing for Post Process Control Upgrade Operation*, PG-T-93-022, EG&G Idaho, Inc., November 1993.

McCracken, R. T., 1993b, *ATR Fuel Element Oxide Data Summary*, EDF TRA-ATR-891, EG&G Idaho, Inc., November 15, 1993.

McCracken, R. T., 1994, Letter to E. C. Anderson, RTMc-4-94, *Review of Hafnium Depletion Data from Reflector IV Control Element Reactivity Measurements*, EG&G Idaho, Inc., May 9, 1994.

McCracken, R. T., and L. S. Loret, 1994, *Results of ATR Critical Facility Core Reconfiguration and Requalification Testing for Post Core Internals Changeout Operations*, PG-T-94-006, EG&G Idaho, Inc., June 1994.

McCracken, R. T., and W. M. Yarbrough, 1994, *Results of Nuclear Requalification Testing following the ATR Process Control Upgrade Outage*, PG-T-94-002, EG&G Idaho Inc., March 1994.

McCracken, R. T., et al., 1994, *Results of Nuclear Requalification Testing following the ATR Reflector V Core Internals Changeout Outage*, INEL-94/089, Lockheed Martin Idaho Technologies Co., December 1994.

Merrill, B. J., 1980, *SINDA ATR Fuel Plate Thermal Hydraulics and SAMPLE Model Descriptions as Used in ATR Technical Specifications Revision Analyses*, PR-T-80-022, EG&G Idaho, Inc., April 1980.

Merrill, B. J., 1981, *Descriptions of the ATR Fuel Plate MITAS Thermal Hydraulics Model and SAMPLE Statistical Model used for Two-Pump Operation Analysis*, RE-A-79-154, EG&G Idaho, Inc., February 1981.

Metals Handbook, 1987, Ninth Edition, Vol. 13, *Corrosion*, ASM International, 1987.

Metals Handbook, 1990, Tenth Edition, Vol. 2, *Properties and Selection: Nonferrous Alloys and Special-Purpose Materials*, ASM International, 1990.

Miller, G. K., and T. E. Rahl, 1992, *Report on Proposed Modifications to the Analysis Procedure for ATR Beryllium Reflectors*, PG-T-92-111, EG&G Idaho, Inc., February 1992.

Moore, C. A., 1969, *Calculations of Pressure-Induced and Thermal Stresses for Advanced Test Reactor Fuel Elements*, IN-1303, Idaho Nuclear Corporation, August 1969.

Mousseau, D. R., et al., 1973, *ATR Reflector III Conceptual Design Report*, TR-395, Aerojet Nuclear Co., February 1973.

Nazaré, S., G. Ondracek, and F. Thümmler, 1975, *Investigations on UAl_x-Al Dispersion Fuels for High-Flux Reactors*, Journal of Nuclear Materials, 56, 1975, pp. 251-259.

Neder, M. J., 1971, Letter to F. L. McMillan, *Irradiation of an ATR Fuel Element with Known Defects*, Ned-29-71, Aerojet Nuclear Co., January 21, 1971.

Newton, D. G., 1979, *ATR Fuel Element Leak Investigation*, PR-T-79-004, EG&G Idaho, Inc., May 1979.

Nielsen, H. H., 1973, *Final Reflector III/Mark II Outer Shim Cylinder Thermal-Hydraulic Design Report*, TR-448, Aerojet Nuclear Co., November 8, 1973.

Nielsen, H. H., 1977, Letter to H. J. Reilly, Ni-10-77, *ATR Reflector III Design Criteria Compliance*, EG&G Idaho, Inc., August 24, 1977.

Nielsen, H. H., 1985, *ATR Beryllium Reflector FLOW3 Model Description*, PG-T-85-012, EG&G Idaho, Inc., September 3, 1985.

NRC, 1975, *Reactor Safety Study, An Assessment of Accident Risks in U.S. Commercial Nuclear Power Plants*, Appendix II, WASH-1400, NUREG-75/014, U.S. Nuclear Regulatory Commission, Washington, D.C., October 1975.

Openshaw, P. R., and L. L. Shreir, 1964, *Oxidation of Uranium-Aluminum Intermetallic Compounds-II, Nature and Surface Topography of Oxide Films*, Corrosion Science, 4, 1964, pp. 335-344.

Pace, N. E., 1993, *ATR Loop Reconfiguration Thermal-Hydraulic Analysis*, PG-T-93-003, EG&G Idaho, Inc., October 1993.

Palmer, A. J., 1998, *ATR-ITV Hydraulic Calculations*, INEEL/INT-98-00334, Lockheed Martin Idaho Technologies Company, April 1998.

Pfeifer, C. J., 1971, *PDQ-7 Reference Manual II*, WAPD-TM-947(L), Bettis Atomic Power Laboratory, Pittsburgh, PA, February 1971.

Poetschat, G. R. 1967, *Physics Studies Relative to the Design of an ATR Radial Zone Loaded Fuel Element*, CI-1053, Idaho Nuclear Corporation, August 1967.

Polkinghorne, S. T., 1991, *Core Coolant Mass Flux and Enthalpy Rise Distributions for Chapter 4 of the ATR UFSAR*, EDF TRA-ATR-598, EG&G Idaho, Inc., October 14, 1991.

Polkinghorne, S. T., 1993a, *Validation of the ATR SINDA Fuel Plate Model*, PG-T-92-133, EG&G Idaho, Inc., January 1993.

Polkinghorne, S. T., 1993b, *ATR-SINDA and SINDA-SAMPLE Calculations for Chapter 4 of the ATR's Updated FSAR*, EDF TRA-ATR-778, EG&G Idaho, Inc., July 13, 1993.

Polkinghorne, S. T., and J. M. Lacy, 1991, *Thermophysical and Mechanical Properties of ATR Core Materials*, PG-T-91-031, EG&G Idaho, Inc., August 1991.

Putnam, G. E., 1964, *TOPIC: A FORTRAN Program for Calculating Transport of Particles in Cylinders*, IDO-16968, Phillips Petroleum Company, April 1964.

Randall, D., and D. S. St. John, 1958, *Xenon Spatial Oscillations*, Nucleonics, 16, 3, March 1958.

Ransom, V. H., and J. A. Trapp, 1976, *RELAP5 Hydrodynamic Model Progress Summary Pilot Code*, PG-R-76-013, EG&G Idaho, Inc., December 29, 1976.

Richins, W. D., and G. K. Miller, 1995, *Analysis of the ATR Fuel Element Swaging Process*, INEL-95/0558, December 1995.

Rogers, J. W., et al., 1993, *Radiation Measurement Laboratory Analyses of ATR Fuel Soak Tests for Cycle 98 B-1 November 1992*, ERA-NRE-93-009, EG&G Idaho, Inc., February 1993.

Rowsell, C. L., 1984, *ATR Fuel Element Soak Test for Cycle 62B-1*, RE-PB-84-012, EG&G Idaho, Inc., February 1984.

Rowsell, C. L., and O. D. Simpson, 1980, *ATR Soak Tests for Cycle 49A-1*, RE-P-80-102, EG&G Idaho, Inc., November 1980.

Rowsell, C. L., et al., 1990, *Radiation Measurements Laboratory/Radiochemistry Analyses of ATR Fuel Soak Tests for Cycle 89A, April - May 1990*, ST-CS-025-90, EG&G Idaho, Inc., June 1990.

Rowsell, C. L., et al., 1991, *Radiation Measurement Laboratory Analyses of ATR Fuel Soak Tests for Cycle 93A-1 May 1991*, ST-PHY-91-034, EG&G Idaho, Inc., July 1991.

Rowsell, C. L., et al., 1992, *Radiation Measurement Laboratory Analyses of ATR Fuel Soak Tests for Cycle 96A-1 January-February 1992*, ST-PHY-92-031, EG&G Idaho, Inc., April 1992.

Schnitzler, B. G., 1998, Letter to M. B. Hendrickson, BGS-08-98, *Irradiation Capsule Experiment Reactivity Worth Estimates*, June 3, 1998.

Seiffert, S. L., 1979, *Destructive Examination of ATR Fuel Element XA029HK which Failed During Operation*, PR-T-79-020, EG&G Idaho, Inc., September 1979.

Seiffert, S. L., and A. H. Novick, 1979, *Destructive Examination of Defective Fuel Plates from ATR Fuel Elements A197F and XA456N*, PR-T-79-016, EG&G Idaho, Inc., August 1979.

Sims, T. M., and J. H. Swanks, 1979, *High Flux Isotope Reactor (HFIR) Experiment Facilities and Capabilities*, Oak Ridge National Laboratory, November 1979.

Smith, A. C., and W. C. Cook, 1989, *ATR CSAP Package on the Cray XMP Version 1 CSCM Reference Number CRN00445*, NRRT-N-89-026, EG&G Idaho, Inc., September 1989.

Smith, A. C., et al., 1990, *Reactivity Effect of Beryllium Reflector Poison in the ATR*, NRRT-N-90-021, EG&G Idaho, Inc., July 1990.

Snow, S. D., 1997, *Partial Structural Evaluation of ATR Fuel Element*, EDF TRA-ATR-1240, LMITCO, July 15, 1997.

Stonehouse, A. J., and W. W. Beaver, 1965, *Beryllium Corrosion, and How To Prevent It*, Materials Protection, 4, pp. 24-28, January 1965.

Sumpter, K. C., 1968, *A Primary Study on the Compressive Properties of Composite Nuclear Fuel Plates*, IN-1179, Idaho Nuclear Corporation, April 1968.

Thomas, R. W., 1985, *Design Report for the Modifications to the ATR Beryllium Reflector (Mark IV) and Associated Core Internals*, PG-T-84-025, EG&G Idaho, Inc., November 1985.

Tingey, F. H., 1965, Letter to J. P. Lyon, Ti-502-65A, *Nuclear Safety Committee Action*, Phillips Petroleum Company, December 20, 1965.

Tomberlin, T. A., 1989, *Advanced Test Reactor (ATR) Reflector Safety Analysis*, PG-T-89-018, EG&G Idaho, Inc., July 1989.

Tupper, M. A., 1984, *Hafnium Irradiation Damage, Continued Surveillance*, PG-T-84-011, EG&G Idaho, Inc., July 1984.

Van Horn, K. R. (ed.), 1967, *Aluminum*, Vol. 1, *Properties, Physical Metallurgy and Phase Diagrams*, American Society for Metals, Metals Park, OH, 1967.

Vinjamuri, K., 1982, *Postirradiation Examination of Advanced Test Reactor Fuel Elements XA377N and XA379N*, EGG-TFBP-5968, EG&G Idaho, Inc., September 1982.

Vinnola, A. J., 1996, Letter to D. N. Alger, *ATR Fuel Specification Advanced Change Notice*, AJV-16-96, Lockheed Martin Idaho Technologies Company, August 9, 1996.

Wadkins, R. P., and R. G. Ambrosek, 1992, *Three-Dimensional Thermal Aspects of Aluminum Fuel Elements*, Nuclear Technology, 97, pp. 344-351, March 1992.

Walker, B. A., M. J. Graber, and G. W. Gibson, 1966, *ATR Fuel Materials Development Irradiation Results — Part II*, IDO-17157, Phillips Petroleum Company, June 1966.

Walker, V. A., 1964, Letter to D. R. deBoisblanc, *ATR Fuel Element Hydraulic Studies Progress Report*, Phillips Petroleum Co., August 7, 1964.

Wanklyn, J. N., and P. J. Jones, 1962, *The Aqueous Corrosion of Reactor Metals*, Journal of Nuclear Materials, 6, 3, 1962, pp. 291-329, March 1962.

Waters, E. D., 1966, *Heat Transfer Experiments for the Advanced Test Reactor*, BNWL-216, Battelle Northwest Laboratories, May 1966.

Weir, J. R., Jr., and R. T. King, 1971, *Irradiation Damage to Aluminum and Aluminum Alloys*, Fuels and Materials Development Program Quarterly Progress Report for Period Ending December 31, 1970, ORNL-TM-3300, Union Carbide Corp., July 1971, pp. 276-294.

Whitacre, R. F., 1989, *The UAl_x Fuel Dispersion System*, EGG-PRP-8783, EG&G Idaho, Inc., November 1989.

Winkel, B. V., 1974, *Stress and Deformation Analysis of Irradiation Induced Swelling*, Pressure Vessels and Piping Conference with Nuclear Engineering and Materials Divisions, Miami Beach, FL, June 24-28, 1974, ASME Publication No. 74-PVP-44.

Ziemianski, E. J., 1996, Letter to B. H. Hamilton, OPE-TRA-96-030, *Approval of ATR Technical Specification Revision-HTF*, U.S. Department of Energy, Idaho Operations Office, May 6, 1996.

CHAPTER 5

PRIMARY COOLANT SYSTEM

INTENTIONALLY BLANK

CONTENTS

ACRONYMS/ABBREVIATION 5-6

5. PRIMARY COOLANT SYSTEM 5-9

5.1 Summary Description 5-9

5.1.1 Schematic Flow Diagram 5-11
5.1.2 Piping and Instrumentation Diagram (P&ID) 5-12
5.1.3 Elevation Drawing 5-13
5.1.4 System Description 5-13

5.2 Integrity of the Primary Coolant Pressure Boundary (PCPB) 5-34

5.2.1 Compliance with Codes and Cases 5-35
5.2.2 Overpressure Protection 5-36
5.2.3 PCPB Materials 5-40
5.2.4 ISI and Testing of the PCPB 5-42
5.2.5 Detection of Leakage Through the PCPB 5-42
5.2.6 System Controls to Preclude Significant PCPB Rupture 5-43

5.3 Reactor Vessel 5-49

5.3.1 Reactor Vessel Materials 5-49
5.3.2 Pressure-Temperature Limits 5-52
5.3.3 Reactor Vessel Integrity 5-53

5.4 Component and Subsystem Design 5-71

5.4.1 Primary Coolant Pumps 5-71
5.4.2 Heat Exchangers 5-72
5.4.3 Primary Coolant Piping 5-73
5.4.4 Main Steam Line Flow Restrictions 5-75
5.4.5 Main Steam Line Isolation System 5-75
5.4.6 Reactor Core Isolation Cooling System 5-75
5.4.7 Decay Heat Removal 5-75
5.4.8 Reactor Water Cleanup System 5-78
5.4.9 Main Steam Line and Feedwater Piping 5-78
5.4.10 Surge Tank, Primary Degassing and Pressurizing Subsystem 5-78
5.4.11 Pressurizer Relief Discharge System 5-82
5.4.12 Valves 5-82
5.4.13 Safety and Relief Valves 5-82
5.4.14 Equipment Supports 5-82

5.5 References 5-90

FIGURES

5.1-1. Simplified diagram of the Advanced Test Reactor Primary Coolant System 5-20

5.1-2. Simplified diagram of the Advanced Test Reactor Degassing and Pressurizing System 5-21

5.1-3. Flow diagram of Primary Coolant System (1 of 8) 5-22

5.1-4. Flow diagram of Primary Coolant System (2 of 8) 5-23

5.1-5. Flow diagram of Primary Coolant System (3 of 8) 5-24

5.1-6. Flow diagram of Primary Coolant System (4 of 8) 5-25

5.1-7. Flow diagram of Primary Coolant System (5 of 8) 5-26

5.1-8. Flow diagram of Primary Coolant System (6 of 8) 5-27

5.1-9. Flow diagram of Primary Coolant System (7 of 8) 5-28

5.1-10. Overall Primary Coolant System flow diagram (8 of 8) 5-29

5.1-11. Advanced Test Reactor Firewater Injection System piping and instrument diagram 5-30

5.1-12. Advanced Test Reactor major equipment and piping sketch showing plant elevations 5-31

5.1-13. Advanced Test Reactor Primary Coolant System main safety relief valves piping isometric layout 5-32

5.1-14. Advanced Test Reactor Primary Coolant System pressurizing pumps safety relief valves isometric layout 5-33

5.2-1. ATR Primary Coolant System Piping Codes 5-48

5.3-1. Reactor vessel 5-62

5.3-2. Reactor vessel assembly 5-63

5.3-3. Top head closure plate 5-64

5.3-4. Bottom head closure plate 5-65

5.3-5. Reactor vessel supports, penetrations, and shielding 5-66

5.3-6. Reactor vessel drop tube assembly 5-67

5.3-7. Safety rod horizontal shaft 5-68

5.3-8. Outer shim control drive 5-69

5.3-9. Instrument thimble positions 5-70

5.4-1. Primary Coolant System pump head curves 5-87

5.4-2. Advanced Test Reactor decay-heat removal options 5-88

5.4-3. Emergency coolant and pressurizing pump performance curves 5-89

TABLES

5.1-1. Radiographic boundary components for Primary Coolant System 5-16

5.1-2. Primary Coolant System design and performance characteristics 5-17

5.1-3. Points of isolation between the Primary Coolant System and other fluids or systems 5-19

5.2-1. Primary Coolant System safety relief valves 5-44

5.2-2. Primary Coolant System overpressure sources 5-45

5.2-3. Primary Coolant System materials of construction 5-46

5.2-4. Material properties of 304 stainless steel 5-47

5.3-1. Reactor vessel design and performance characteristics 5-60

5.3-2. Reactor vessel nozzles and penetrations 5-61

5.4-1. Primary Coolant System component design and performance characteristics 5-83

5.4-2. Advanced Test Reactor multiple means of decay heat removal. 5-86

ACRONYMS/ABBREVIATION

API	American Petroleum Institute
ANSI	American National Standards Institute
AOP	Abnormal Operating Procedure
ASME	American Society of Mechanical Engineers
ASTM	American Society for Testing and Materials
ATR	Advanced Test Reactor
Btu	British thermal unit
BWG	Birmingham wire gauge
BWR	boiling water reactor
CK	check valve
CLOHS	complete loss of heat sink
CFR	Code of Federal Regulations
CSAP	core safety assurance package
DCS	distributed control system
DHR	decay heat removal
DOE	U.S. Department of Energy
EDF	engineering design file
EFIS	emergency firewater injection system
EL	elevation
ESF	engineered safety features
ETR	Engineering Test Reactor
FCF	Facility Change Form
FCV	flow control valve
GB	globe valve
GDC	general design criterion
gpm	gallons per minute
GSW	gland seal water
GT	gate valve
ID	inside diameter
IGSCC	intergranular stress corrosion cracking
ISI	inservice inspection
LCV	level control valve
LDW	low-pressure demineralized water
LOCA	loss of coolant accident
LWR	light water reactor
MeV	million electron volt
MW_t	megawatts thermal

NE	northeast
NPSH	net positive suction head
NRC	U.S. Nuclear Regulatory Commission
NW	northwest
OD	outside diameter
OPP	overpressure protection
OSCC	outer shim control cylinder
PBD	primary bypass demineralizer
PCP	primary coolant pump
PCPB	primary coolant pressure boundary
PCS	primary coolant system
PCV	pressure control valve
P&ID	piping and instrumentation diagram
PPS	plant protective system
PORV	power-operated relief valves
PRA	probabilistic risk assessment
psia	pounds per square inch absolute
psid	pounds per square inch differential
psig	pounds per square inch gauge
PWR	pressurized water reactor
Rad	radial
RDAS	reactor data acquisition system
RSS	reactor shutdown system
SAE	Society of Automotive Engineers
SAIC	Science Applications International Corporation
scfm	standard cubic feet per minute
SE	southeast
SRV	safety relief valve
SSE	safe shutdown earthquake
SW	southwest
Tan	tangential
TDH	total dynamic head
UFSAR	Upgraded Final Safety Analysis Report
UPS	uninterruptible power supply
USQ	unreviewed safety question
VVS	Vessel Vent System

INTENTIONALLY BLANK

5. PRIMARY COOLANT SYSTEM

5.1 Summary Description

The primary coolant system (PCS) is shown in Figures 5.1-1 through 5.1-14 and consists of one main coolant loop. The main loop branches into parallel piping runs at the inlets of major components. The parallel piping runs rejoin the common loop at the outlets of the major components. The PCS consists of the reactor vessel, heat exchangers, primary coolant pumps, emergency coolant pumps, and associated piping and valves. In addition, the PCS includes a surge tank and surge line, a degassing and pressurizing system, pressure relief and safety valves, and instrumentation necessary for operational control and emergency response.

The entire PCS except for chemical cleaning hookups and sample lines is located inside confinement. The primary function of the PCS is to remove the energy generated by the reactor. The energy is transported from the reactor to the heat exchangers, where it is transferred to the secondary coolant system and then dissipated to the atmosphere in the cooling tower.

The Primary Coolant Pressure Boundary (PCPB) provides a geometry for maintaining the heat-removal capability of the PCS for any event, and forms a protective barrier against the release of primary coolant and radioactive material.

The PCS consists of safety-related and nonsafety-related components. Safety-related components are those components relied upon during or following design-basis events to ensure: (a) the integrity of the primary coolant pressure boundary, (b) the capability to shut down the reactor and maintain it in a safe shutdown condition, and (c) the capability to prevent or mitigate the consequences of accidents that result in potential off-site exposures. The safety analysis [see Chapter 15 (Accident Analyses)] has demonstrated any break in the PCPB with an equivalent area of a 3-in.-diameter break or less can be mitigated by plant protective functions such that ATR Plant Protection Criteria are not exceeded. As a result, any PCS component whose failure could result in a break in the PCPB greater than the area of a 3-in. diameter break is classified as safety-related.

The safety-related boundary is physically defined by the primary coolant pressure boundary, restricted flow area through orifice plates and pipe branches, normally closed safety-related isolation valves, and check valves (Atkinson 1995). The isolation valves, the check valves, and the component that results in the restricted flow area are classified as safety-related. The safety-related-nonsafety-related boundary is shown in Figures 5.1-1 through 5.1-10. The welds and major components such as pumps and valves within the safety-related portions of the PCS have been radiographed. As a result, the safety-related—nonsafety-related boundary is often referred to as the radiographic boundary.

To ensure the integrity of the PCPB, safety-related components are subjected to more rigorous testing, inspection, and maintenance than nonsafety-related components.

The PCS is composed of the following safety-related and nonsafety-related components and subsystems (House 1992):

- The reactor vessel, including vessel penetration assemblies that extend the PCPB outside the vessel (Section 5.3)
- Primary coolant pumps (PCPs) (Section 5.4.1)
- The primary side of the heat exchangers (Section 5.4.2)
  - The piping, valves, and fittings that
  - Provide appropriate flow paths between principal components
  - Interface with other systems such as the Vessel Vent System (VVS) and Emergency Firewater Injection System (EFIS)
  - Provide flow control (Sections 5.4.3 and 5.4.12).
- Emergency coolant pumps (Section 5.4.7.4)
- The surge tank and surge line piping (Section 5.4.10.1)
- The degassing (Section 5.4.10.2) and pressurizing subsystems (Section 5.4.10.3)
- PCS overpressure relief piping and valves (Sections 5.2.2 and 5.4.13)
- Equipment supports (Section 5.4.14).

PCS auxiliary systems[a] include the following:

- The Primary Bypass Demineralizer (PBD) subsystem
- The Gland Seal Water (GSW) System
- The Low Pressure Demineralized Water (LDW) subsystem
- The compressed air systems.

Additional supporting subsystems include:

- The N-16 subsystem.[b]
- Instrumentation[c] required for normal operation, for signals to the Plant Protective System (PPS)[d], and for accident monitoring. PCS instrumentation monitors or controls the following parameters and components:
  - Coolant temperature, pressure, flow, conductivity, and pH
  - Water power computation (flow and temperature rise)

---

[a]. Refer to Chapter 9 (Auxiliary Systems) for a description of PCS auxiliary subsystems.

[b]. Refer to Chapter 7 (Instrumentation and Controls) for a description of the N-16 subsystem.

[c]. Refer to Chapter 7 (Instrumentation and Controls) for a description of PCS controls.

[d]. Refer to Chapter 7 (Instrumentation and Controls) for a description of the PPS.

- Emergency coolant flow
- Gland seal water flow
- Primary degassing tank control valves, high- and low-level alarms, tank pressure, air flow rate
- Bypass demineralizer flow control valves, coolant inlet temperature, differential pressure, effluent pH, conductivity, and flow
- Surge tank level control valves and level indication and alarms
- Reactor shielding cooling air and concrete temperatures
- Reactor vessel liquid level
- Bearing temperatures for the primary coolant, emergency coolant, pressurizing, and warm seal booster pumps.

The primary sources of reactor-control information and PPS status are analog indicators, chart recorders, annunciators, and valve position indicators located in the reactor control room. A secondary source of information is the console video display, a computer-generated display of reactor-control and PPS variables and RDAS. The Distributed Control System (DCS) is a computer-based system that monitors and controls primary-system temperatures, pressures, and flows. The DCS has both audible and visual annunciators.

The primary and secondary sources of information are not generally relied upon to mitigate design-basis events. As a consequence, the reactor control room indicators, recorders, annunciators, and console displays are classified as nonsafety-related equipment.

In almost all instances, the design and installation of the primary and auxiliary PCS components and subsystems were completed as part of the original construction. Some subsystems (or parts of subsystems), however, have been added or upgraded since the initial operation of the ATR. All subsystems were designed using standards applicable at the time. Many of the PCS components and subsystems described in this section are original-equipment design, and may not be designed to current regulatory standards. The PCS components and subsystems being addressed are mature and have a considerable operating history that demonstrates reliability consistent with assumptions of the current safety analysis.

Surveillance, inspection, and maintenance programs for these components and subsystems ensure that the PCS can continue to accomplish its intended objective reliably and maintain its integrity under conditions imposed by all foreseeable reactor behavior, under either normal or accident conditions.

5.1.1 Schematic Flow Diagram

Figure 5.1-1 is a simplified schematic flow diagram of the ATR PCS, and Figure 5.1-2 is a simplified schematic of the ATR PCS Degassing and Pressurizing Subsystem. Major radiographic boundaries are shown on Figures 5.1-1, and 5.1-2 for information only. Refer to the P&IDs in Section 5.1.2 for a detailed representation of the radiographic boundaries. The valves and 3-in. orifices that form the radiographic boundary of the PCS piping, taken from Figures 5.1-1 and -2, are listed in Table 5.1-1.

The primary coolant pumps, the heat exchangers, surge tank, and associated piping are located within the radiographic boundary, and are safety-related (House 1992). The safety-related piping for the PCS also includes the EFIS, the VVS, and the PCS Overpressure Relief System. Emergency coolant pumps 670-M-10 and 670-M-11 and connecting piping are also located within the radiographic boundary. The pressurizing and degassing subsystem, and auxiliary subsystems defined in Section 5.1 above are outside the radiographic boundary and are not safety-related. The pump casing is the pressure boundary for the primary and emergency pumps. The tubes, tube sheet, channel, and bottomhead make up the pressure boundary for the primary heat exchangers.

PCS design and performance characteristics, including principal pressures, temperatures, flow rates, and coolant volume under normal steady-state, full-power operating conditions, are provided in Table 5.1-2.

5.1.2 Piping and Instrumentation Diagram (P&ID)

Figures 5.1-3 through 5.1-9 are detailed P&IDs for PCS systems. Figure 5.1-10 is the overall PCS P&ID. Figure 5.1-11 is a P&ID for the EFIS. P&IDs are presented in this section for information only. Current P&IDs are maintained under configuration control at the facility.

All PCS components and subsystems shown on Figures 5.1-3 through -10 are located within the ATR confinement. The heat exchangers of the primary coolant pump's oil system are cooled by the raw-water system[a]; the main PCS heat exchangers are cooled by the secondary coolant system.[b] Except for the PCS heat exchangers, associated piping and isolation valves, the secondary coolant system is located outside the confinement and penetrates the confinement as discussed in Chapter 6 (Engineered Safety Features).

PCS auxiliary subsystems[c] located within the confinement are (a) primary bypass demineralizer and (b) gland seal water. PCS auxiliary subsystems that penetrate the confinement are (a) low pressure demineralized water and (b) compressed air.

Two separate 8-in. firewater lines supplying firewater to the reactor vessel bottom head and upper vessel EFIS[d] penetrate the confinement in two separate locations as discussed in Chapter 6 (Engineered Safety Features) (see Figure 5.1-11).

The points of separation between the PCS and secondary cooling system are the main heat exchangers (M-2 to M-5, and M-85 shown on Figures 5.1-5 and -10). These and other points of isolation between the PCS and other fluids or systems, taken from Figures 5.1-3 through 5.1-10, are listed in Table 5.1-3. Points of isolation between radioactive and nonradioactive sections of the system are listed in Table 5.1-3.

---

[a]. Refer to Chapter 9 (Auxiliary Systems) for a description of the Raw Water System.

[b]. Refer to Chapter 9 (Auxiliary Systems) for a description of the Secondary Coolant System.

[c]. Refer to Chapter 9 (Auxiliary Systems) for a description of PCS auxiliary systems.

[d]. Refer to Chapter 6 (Engineered Safety Features) for a description of the EFIS.

5.1.3 Elevation Drawing

Principal dimensions of PCS components relative to surrounding concrete structures may be taken from the PCS Piping Plan, Ebasco Drawing No. ATR-1075-MTR-670-P-17 (120891). (Portions of the original drawing are illegible; therefore, it is not reproduced in this document.) Figure 5.1-12 is a simplified sketch of PCS equipment and piping, showing principal component elevations. Figure 5.1-13 is a PCS main safety relief valves piping isometric layout, and Figure 5.1-14 is a PCS pressurizing pumps safety relief valves isometric piping layout also showing component elevations.

5.1.4 System Description

The PCS is a forced-flow, closed-loop energy-transport system constructed of ductile material. The coolant is light water at moderate pressure and low temperature (i.e., below saturation temperature at atmospheric pressure). Simplified isometric and line diagrams of the PCS are shown in Figures 5.1-1 and 5.1-12.

In the PCS, coolant at nominally 125°F and 371.9 psig at PPS vessel inlet pressure tap (M-1 shown on Figures 5.1-1 and -10) enters the vessel through two 24-in. pipes that are welded to the two vessel inlet nozzles in the bottom hemispherical head assembly.[a] The coolant flows up through the annuli formed by the cylindrical tanks that support and contain the core, the inlet flow baffle, the thermal shield, and the vessel tank. It then enters an open region above the core, after which it flows down through the core into the flow-distribution tank. There, the flow is divided into quadrants[b] and distributed to four 16-in. outlet lines.

The outlet lines route the coolant up above the top of the core before exiting the reactor vessel through the outlet nozzles. The outlet lines are in the annulus formed by the reflector tank and the inlet flow baffle. The coolant exits the vessel through four 16-in. outlet nozzles.[c]

For reactor thermal power at 250 MW_t, coolant at nominally 167°F and 254 psig leaves the reactor vessel through four 18-in. outlet pipes that are welded to the four outlet nozzles in the reactor vessel shell. Within the vessel, four 1-in. siphon-breaker pipes[d] run from the highest point of each outlet pipe and terminate near the vessel top head. The siphon breakers are designed to prevent siphoning of the primary coolant if an outlet pipe should break outside the reactor vessel.

The four 18-in. outlet pipes combine into two 24-in. lines, which then combine into one 36-in. return header in the shielded pipe space surrounding the rod access room. The coolant flow continues in this header through a shielded pipe tunnel to five parallel shell-and-tube heat exchangers (M-2 to -5, -85 shown on Figures 5.1-1, -5, and -10). Coolant from the heat exchangers is pumped back to the reactor by two or three of the four primary coolant pumps (PCPs) (M-6 to -9 shown on Figures 5.1-1, -4, and -10) that discharge into a header, part of which is 20 in., which connects into a 36-in. supply line.

---

[a]. Refer to Section 5.3.3 for a description of the reactor vessel bottom head assembly.

[b]. A portion of the ATR core consisting of 10 fuel elements cooled by approximately one fourth of the flow is called a quadrant. Quadrant power is measured by one of the quadrant water power channels. The quadrants are designated northwest (NW), northeast (NE), southwest (SW), and southeast (SE).

[c]. Refer to Chapter 4 (Reactor) for details of the reactor vessel internals.

[d]. Refer to Chapter 3 (Design of Structures, Components, Equipment, and Systems) for a description of the siphon breakers.

The non-operating pump(s) is normally isolated by closing block valve(s) in the pump discharge(s). The flow-control butterfly valve is in the 36-in. supply line downstream of the pump discharge header. Downstream of the flow-control valve, the supply line divides into two 24-in. vessel inlet lines. The PCPs can be individually isolated from the system, whereas the primary heat exchangers cannot be isolated on the primary (tube) side.

The emergency coolant pumps are in parallel with the primary coolant pumps taking suction from the 30-in. header that distributes the flow to the primary coolant pumps. The emergency flow pumps discharge into the common 36-in. vessel inlet upstream of flow-control valve. The degassing and pressurizing system take off and return lines are plumbed into the common 36-in. vessel outlet line. The surge line is connected to an outlet line of one of the heat exchangers (M-2).

Safety relief valves, shown in Figures 5.1-13 and 5.1-14, are connected to the vessel lower drain line, and the discharge lines of the pressurizing pumps. The vessel vent system (VVS), shown in Figure 5.1-13, is connected to the vessel upper drain line.

Operation with three of the four PCPs generates a combined design capacity of 54,000 gpm. Operations in the pressurized mode at greater than 3 MW_t power are conducted with at least two PCPs operating to ensure adequate cooling for the fuel cladding.

Primary coolant flow rate is adjusted by a motor-operated butterfly-type flow-control valve (BF-A-14 shown on Figures 5.1-1, -10) to produce a nominal 100 psid pressure drop across the reactor core when in the three-pump operation mode (deBoisblanc and Cohen, 1965). The butterfly valve is positioned before reactor startup by a remote limitorque drive. A mechanical stop on the flow control valve and six 4.29-in. holes in the valve disc prevent full stoppage of the primary coolant flow. The flow control valve is adjusted to maintain the pressure loss across the core.

To obtain a 100 psid pressure differential across the core at 250 MW_t, a nominal flow rate of 50,000 gpm is required, producing a 5,000 gpm excess cooling capacity with three pumps operating. When only two pumps are operated, the pressure drop across the core is nominally 77 psid, with a nominal flow rate of 43,500 gpm. Primary coolant flow is measured by orifice-type flow meters (shown on Figures 5.1-9 and -10) located in each of four reactor outlet pipes.

The primary coolant pumps are interlocked with instrumentation monitoring the pressure drop across the reactor core. Depending on pump configuration, one to two pumps may be automatically shut down during three-pump operation if the reactor core pressure drop maximum limit is reached to prevent damage to reactor internals.

Primary coolant temperature is controlled by controlling the heat removal rate in the heat exchangers. The heat removal rate is controlled by adjusting the secondary coolant flow[a] rate to the heat exchangers or by adjusting cooling tower fans speeds. PCS pressure control is provided by a surge tank and the degassing and pressurizing subsystem[b] (Figure 5.1-2). Primary coolant vessel inlet pressure is regulated by controlling the coolant inventory by balancing pressurizing and degassing flow. A pressure control valve (PCV-1 shown on Figures 5.1-1, -2, and -10) bleeds a varying amount of coolant from the 36-in. PCS return line upstream of the heat exchangers through a 4-in. pipe to the primary degassing tank

[a]. Refer to Chapter 9 (Auxiliary Systems) for a description of the Secondary Cooling System.

[b]. Refer to Section 5.4.10 for further discussion of the degassing and pressurizing subsystem and its role in pressure and reactor inventory control.

(M-13 shown on Figures 5.1-2, -10). The primary coolant entering the degassing tank is sprayed down from the top of the tank through spray nozzles as a stream of air passes through the tank to sweep out excess gasses. Two pressurizing pumps (M-14 and M-15 shown on Figures 5.1-2, -3, and -10), one normally operating and one in standby, obtain suction from the degassing tank and discharge at a nominal flow rate of 225 gpm back into the 36-in. PCS return line to the heat exchangers. The flow rate from the primary pressurizing pumps is preset by flow-control valve FCV-8 (shown on Figures 5.1-1 and -2; FRCV-8 on Figure 5.1-10).

The surge tank (M-12 shown on Figures 5.1-1, -10) damps minor, rapid pressure fluctuations without initiating power reductions from high or low pressure. The surge tank is connected to the heat exchanger outlet piping and is pressurized to maintain primary pump suction pressure. If PCS pressure increases beyond the damping capability of the surge tank, the pressurizing and gland seal pumps are automatically shut off by the PPS[a] to avoid overpressurizing the PCS. However, if the system pressure decreases, such as in a Loss-of-Coolant Accident (LOCA), the pressurizing pumps continue to operate to provide makeup. With the primary coolant pumps operating, the inlet pressure at the core top is established at greater than 360 psig. Rapid and short-duration pressure- and temperature-induced transients are damped by expansion and compression of the cover air (provided by the compressed-air system) in the surge tank. Slower and long-duration pressure variations are damped by controlling the system inventory of coolant. The air-to-water ratio in the surge tank is such that when the pressure in the tank is reduced to atmospheric, the volume of the expanded air will remain contained in the surge tank.

The gland seal system[b], in the process of supplying demineralized water to various PCS seals, adds nominally an additional 60 gpm to the PCS through pump seals and penetration seals.

Primary-coolant pH and purity (which is concerned primarily with radioactivity and dissolved and suspended solids) are maintained by processing primary coolant through an anion-cation bypass demineralizer[c] system before returning to the PCS through a 6-in. pipe. Primary-coolant chemistry is discussed further in Section 5.2.3.2 and Table 5.1-2, Item (f).

Two 4,700-gpm emergency coolant pumps, M-10 and M-11 (normally M-10 operating and M-11 in standby during reactor operation in the pressurized mode) operate in the closed primary coolant loop (Figures 5.1-1, -4, and -10), drawing suction from the primary pump suction header. Their capacity is conservatively based on (a) flow requirements to prevent boiling in the reactor core during operations at atmospheric pressure when the emergency coolant pumps are used to provide coolant flow instead of the primary coolant pumps, and (b) reactor flow requirements after loss of electrical power to, or failure of, all primary coolant pumps. During such loss of all primary coolant pumps, either emergency coolant pump provides adequate decay-heat removal capacity except for accidents as discussed in Chapter 15.3. This decay-heat removal (DHR) function is discussed further in Section 5.4.7.

One emergency coolant pump, M-10, is driven by an ac motor supplied with diesel or commercial power.[d] The other emergency coolant pump, M-11, is driven by a dc motor supplied with utility dc power. One pump is operated continuously during reactor operation to ensure the required flow after primary pump coastdown without reliance on emergency pump start-up. If commercial, diesel, and utility dc power sources are all lost, the dc motor-driven emergency pump M-11 is supplied power directly from a battery bank designed to operate the pump for a minimum of 30 minutes.

---

[a]. Refer to Chapter 7 (Instrumentation and Controls) for a description of the PPS.

[b]. Refer to Chapter 9 (Auxiliary Systems) for a description of the Gland Seal System.

[c]. Refer to Chapter 9 (Auxiliary Systems) for a description of the Primary Bypass Demineralized Water Subsystem.

[d]. Refer to Chapter 8 (Electric Power) for a description of the Diesel and Commercial Power Subsystem.

An 8-in. firewater line[a] is connected to the reactor vessel by four 2-in. connections in the reactor vessel bottom head closure plate (see Figure 5.1-11). An 8-in. firewater line is also connected to the vessel lower drain piping by two 4-in. connections. Should a large loss of primary coolant occur, firewater is automatically admitted to cover the core.

Table 5.1-1. Radiographic boundary components for Primary Coolant System.[a]

Component	Description
GB-23-1, 23-2	Vessel vent valves, Globe valves (GB), normally closed
CK-1-617, -618	Upper vessel Emergency Firewater Injection System (EFIS) check valves, normally closed
SF-A-71, 72	Reactor Vessel safety relief valves (SRV), normally closed
GT-D-70	Gate valve (GT) on lower vessel drain, normally closed
GT-D-39	Gate valve on upper vessel drain, normally closed
CK-1-77, -78, -79, -80	Vessel bottom head EFIS check valves normally closed
FE-37	Flow element (FE) orifice in 6-in. line (1-42) from 36-in. supply line to bypass demineralizer; orifice diameter is 2.5 inches
FE-36	Flow element orifice in 4-in. line (1-34) at the inlet to GT-E-1-85 isolation valve to the degassing tank; orifice diameter is 2.50 inches
Chemical clean connections	4-in. connections from emergency pumps, normally isolated with blind flange
CK-B-90	Check valve (CK), bypass demineralizer return
GT-D-37	Gate valve, bypass demineralizer to drain line, normally closed
GT-D-35	Gate valve, primary system to 10-in. drain, normally closed
GT-D-32,-33	Gate valves, PCS flushing, normally closed
CK-B-89	Check valve in pressurizing line
GT-E-20	Gate valve, demineralized water inlet, normally closed

a. Data from Figures 5.1-1 and –2.

[a]. Refer to Chapter 6 (Engineered Safety Features) for a description of the Emergency Firewater Injection System.

Table 5.1-2. Primary Coolant System design and performance characteristics.[a]

(a) General:

Nominal system characteristics	Data
Design thermal power	250 MW_t
Average core power density	0.96 MW/L
Thermal power	8.53×10^8 Btu/h
Reactor core inlet pressure	360 psig
Reactor core quadrant pressure drop	≥ 100 psid (77 psid for two pumps)
Reactor inlet temperature	≥ 125°F
Reactor outlet temperature	167°F
Total volume of PCS exclusive of bypass demineralizer (including surge tank and surge lines, and PCS liquid volume which involves pressurized water at steady-state power conditions).	10,865 ft^3
Primary coolant weight	600,000 lb
Volume of reactor vessel	3,250 ft^3
Volume of surge tank	1,000 ft^3

(b) Nominal PCS steady state operating pressures and temperatures at 250 MW_t:

	Pressure (psig)		Temperature (°F)	
Piping section	Three pumps	Two pumps	Three pumps	Two pumps
Reactor outlet to heat exchanger inlet	254	272	167	163
Heat exchanger outlet to pump suction	246	253	125	125
Pump discharge to butterfly control valve	400	390	125	125
Butterfly control valve to reactor inlet	374	376	125	125
Relief valve piping-vessel nozzle to pressure relief valves	350	361	≤ 125	≤ 125
Non-running pump inlet	246	253	80	80

(c) Piping design pressures:

Piping section	Design (psig)	Safety limit (psig)
Primary pump discharge to first block valve	576	634
First block valve to butterfly valve (BF-A-14)	485	533
BF-A-14 to reactor vessel inlet	390	468
Reactor vessel outlet to pump section	390	429

(d) Piping design temperatures:

Piping section	Design (°F)	Safety limit (°F)
Heat exchanger outlet to reactor inlet	150	240
Reactor outlet to heat exchanger inlet	240	240

Table 5.1-2. (continued).

(e) PCS flow	Rate (gpm)
Design capacity	54,000
Nominal flow	50,000 (Three pumps) 43,500 (Two pumps)
Maximum flow	53,200
Emergency flow	4,500
Demineralizing flow rate (maximum)	600 280 (nominal)
Degassing flow rate	600 (maximum)
(f) Nominal operating primary coolant chemistry	
Conductivity, reactor power > 3 MW	2-5 μmhos/cm
Conductivity, reactor power < 3 MW	2-8 μmhos/cm
pH, Reactor power > 3 MW	5.0-5.2
pH, Reactor power < 3 MW	4.9-5.8
Filterable solids (0.45-20 μ) before exceeding 3 MW and during operation	< 0.02-0.08 ppm
Filterable solids (>20 μ)	0.025-0.05 ppm
Chloride	< 0.025 ppm
Radioactivity	0.05-0.29 μCi/mL (gross/gamma based on 10 min decay after sampling)
Dissolved aluminum	1.5-4 ppb
Dissolve iron	0.5-2 ppb
Dissolved copper	0.2-1 ppb
(g) ATR PCS Safety design features:	
Core reflector tank and supporting structure	
Highly subcooled	
Moderate pressure	
Stainless steel vessel and coolant system	
Large coolant inventory	
Emergency/backup primary and secondary flow	
High availability/large supply volume EFIS	
Low power and source term	

a. Data from deBoisblanc and Cohen (1965); Pace (1990); Atkinson (1988).

Table 5.1-3. Points of isolation between the Primary Coolant System and other fluids or systems.

System/Fluid	Coordinates P&ID Fig. No. 5.1-10	Type of isolation	Radioactive[a]
Acid connection			No
Bypass demineralizer			Yes
Chemical clean connections			Yes
Degassing tank to Warm Waste			Yes
Primary coolant recycle system[b]			Yes
Demineralized Water			No No
Disposal			Yes
Firewater			No No
Flushing			Yes
Flushing (from gland/warm seal)			Yes
High-Pressure Air			No
Main exhaust plenum			Yes
Overpressure relief			Yes Yes
Process Water Lab			Yes
Reactor Vessel lower drain to Warm Waste			Yes
Reactor Vessel upper drain to Warm Waste			Yes
Secondary Coolant			No
Vessel Venting			Yes
Warm Seal			Yes

a. Yes: system on both sides of the isolation point may contain radioactive fluid during normal operation.
No: the isolation point separates systems that may contain radioactive fluid during normal operation from systems that do not contain radioactive fluid during normal operation.

FOIA Exemption 3 UCNI, Exemption 7f -- coordinates

b. The primary coolant recycle system (PCRS) is located in TRA-689 and tied to TRA-670 by pipe. TRA-689 is not in use at this time. The piping between TRA-689 and TRA-670 is isolated by both MOV-32-1 and MOV-1-909. Since the piping connections to TRA-689 are downstream of either a <3-in. orifice or valve, any break is bounded by the analysis in Chapter 15.6.

CHAPTER 5 – PRIMARY COOLANT SYSTEM - UPGRADED FINAL SAFETY ANALYSIS REPORT FOR THE ADVANCED TEST REACTOR	**Identifier:** SAR-153 **Revision:** 9 **Page:** 5-19 of 5-92 **Effective Date:** 08/10/04

CHAPTER 5 – PRIMARY COOLANT SYSTEM - UPGRADED FINAL SAFETY ANALYSIS REPORT FOR THE ADVANCED TEST REACTOR	**Identifier:** SAR-153 **Revision:** 9 **Page:** 5-20 of 5-92 **Effective Date:** 08/10/04

CHAPTER 5 – PRIMARY COOLANT SYSTEM - UPGRADED FINAL SAFETY ANALYSIS REPORT FOR THE ADVANCED TEST REACTOR	**Identifier:** SAR-153 **Revision:** 9 **Page:** 5-21 of 5-92 **Effective Date:** 08/10/04

CHAPTER 5 – PRIMARY COOLANT SYSTEM - UPGRADED FINAL SAFETY ANALYSIS REPORT FOR THE ADVANCED TEST REACTOR	**Identifier:** SAR-153 **Revision:** 9 **Page:** 5-22 of 5-92 **Effective Date:** 08/10/04

CHAPTER 5 – PRIMARY COOLANT SYSTEM - UPGRADED FINAL SAFETY ANALYSIS REPORT FOR THE ADVANCED TEST REACTOR	**Identifier:** SAR-153 **Revision:** 9 **Page:** 5-23 of 5-92 **Effective Date:** 08/10/04

CHAPTER 5 – PRIMARY COOLANT SYSTEM - UPGRADED FINAL SAFETY ANALYSIS REPORT FOR THE ADVANCED TEST REACTOR	**Identifier:** SAR-153 **Revision:** 9 **Page:** 5-24 of 5-92 **Effective Date:** 08/10/04

FOIA Exemption 3 UCNI, Exemption 7f (Page 5-19 – 5-33 – details of primary coolant system)

5.2 Integrity of the Primary Coolant Pressure Boundary (PCPB)

A very high integrity of the PCPB is maintained such that the estimated probability for a significant PCPB failure sufficient to result in direct core fuel damage is extremely low and beyond design basis. The integrity of the PCPB is controlled and maintained by the following measures.

- Compliance with applicable design codes and code editions for the PCS and the reactor vessel (Section 5.2.1)
- Overpressure protection (Section 5.2.2) including:
  - Overpressure protection analysis
  - ESF functions to shut off pressurizing and gland seal pumps in response to high detected PCS pressure
  - Pressure relief devices.
- Control of PCPB materials, chemistry, and environment to prevent brittle fracture failure modes or overtemperature (Section 5.2.3 and 5.3 for reactor vessel). Critical parameters are controlled by TSRs such as those for pressure, temperature, and primary coolant pH.
- Inservice inspection and testing for the PCS and reactor vessel according to Section XI of the ASME code (Section 5.2.4 and 5.3 for the reactor vessel).
- PCPB leakage detection and leakage controls (Section 5.2.5). PCPB leakage is controlled by TSRs and Abnormal Operating Procedures (AOPs). An important and highly effective element of ATR PCPB leakage detection and control is the capability for and performance of visual inspection of the bare, uninsulated PCPB including the vessel inlet nozzles after PCS pressurization before power operation.
- Control of changes to the safety-related PCPB design configuration and materials by the formal ATR Facility Change Form (FCF)/Engineering Change Form (ECF) processes and the associated Unreviewed Safety Question (USQ) determination process. Any significant change from the PCS design, materials, coolant chemistry control, or inspections, tests, and surveillances described or important to the safety-related PCPB in the ATR UFSAR need to be evaluated and concluded not to significantly increase the estimated probability for a significant PCPB failure.
- Control and prevention of potential causes of a significant PCPB rupture (Section 5.2.6).

The following discusses the measures used to provide and maintain the integrity of the PCPB.

5.2.1 Compliance with Codes and Cases

5.2.1.1 Compliance with 10 CFR 50.55a. The following list identifies PCS components and applicable design codes and code editions.

PCS Component	Applicable Design Code
Piping (Original)	Code for Pressure Piping, American Standards Association ASA B31.1-1955 (American Society of Mechanical Engineers ASME 1955)
Piping (Modification)	ATR Inservice Inspection (ISI) Plan. (INEEL 2002)
Vessel	ASME Unfired Pressure Vessel Code, Section VIII, 1962 (unfired pressure vessels)
	ASME Unfired Pressure Vessel Code, Section II, 1962 (materials)
	ASME Unfired Pressure Vessel Code, Section IX, 1962 (welding qualifications)
Heat exchangers	ASME Unfired Pressure Vessel Code, Section VIII, 1959
Degassing tank	ASME Unfired Pressure Vessel Code, Section VIII, 1959
Surge tank	ASME Unfired Pressure Vessel Code, Section VIII, 1959
Primary coolant pumps	Standards of the Hydraulic Institute, Centrifugal Pumps Section, 10th Ed., 1959
Emergency coolant pumps	Standards of the Hydraulic Institute, Centrifugal Pumps Section, 10th Ed., 1959 for M-11. ASME Section III, Division 1 Subsections NB 2573, 2575, and 2576, 1989 edition or later for M-10.
Pressurizing pumps	Standards of the Hydraulic Institute, Centrifugal Pumps Section, 10th Ed., 1959.
Safety relief valves (SRVs)	ASME Boiler and Pressure Vessel Code, (SF-A-71, -72) Section III, 1983 edition, 1984 addenda.
Pressurizing Pump SRVs	ASME Boiler and Pressure Vessel Code, (SF-A-75, -76) Section III, 1983 edition, 1984 addenda.

The ATR PCS subsequently has been analyzed to ASME Section III, Class 2, 1977 Edition and for seismic analysis, the ASME Section III, Class 1, 1973 edition rules and found to meet the intent of the code rules (Davidson 1979). The phrase "meet the intent" means that the codes were used as analysis tools, but material was not replaced per codes. Figure 5.2-1 shows the applicable PCS piping codes.

5.2.1.2 Applicable Code Cases. As discussed in deBoisblanc and Cohen (1965), the following identifies PCS components and corresponding applicable code cases:

PCS Component	Applicable Code Cases
Piping	N-1, N-7, N-9, N-10
Vessel	1270 N-3, 1270 N-5, 1271 N, 1272 N-5, 1274 N-6, 1275 N
Heat Exchangers	1270 N-5, 1270 N
Surge Tank	1270 N-5, 1270 N
Degassing Tank	1270 N-2

5.2.2 Overpressure Protection

ATR PCS overpressure protection (OPP) is provided by (a) the Plant Protection System (PPS) which trips the pressurizing pumps to keep the pressure at all locations from exceeding 110% of its design pressure, (b) two safety relief valves (SRVs), SF-A-71 and SF-A-72 (shown on Figures 5.1-1, -7, -10, and -13), mounted on the 8-in. vessel lower drain line (shown on Figure 5.1-13), and (c) two SRVs (SF-A-75, SF-A-76 shown on Figures 5.1-2,-10, and -14), one mounted on each pressurizing pump discharge line (M-14 and M-15 shown on Figures 5.1-2, -3, and -10) discharge line to protect the pressurizing pumps for 15% overspeed operation of an isolated pump. SF-A-71 and SF-A-72 discharge to the Warm Waste System; SF-A-75 and SF-A-76 discharge to the degassing tank.

Unlike typical pressurized water reactors (PWRs), the ATR pressure relief system does not include power-operated relief valves (PORVs) and block valves (excluding the vessel vent valves). The present ATR SRVs are conventional spring-operated SRVs designed to meet ASME Boiler and Pressure Vessel Code, Section III, 1983 edition (ASME 1983). They can be locally opened manually.

The PCS OPP analysis (Pace 1990) covers all operating conditions described in Chapter 15 (Accident Analyses) transients, and overpressure sources, except for waterhammer and experiment facility inpile tube rupture, which are too rapid to protect against with SRVs. SRVs provide OPP for the two pressurizing pumps as isolatable components. The design-basis waterhammer and the design-basis inpile-tube rupture events are addressed in Chapter 15 (Accident Analyses), which demonstrates that neither event results in the loss of PCPB integrity.

The PCS OPP analysis (Pace 1990) shows the adequacy of the OPP devices, the maximum allowable SRV set pressure, and the required SRV flowrate. A stress analysis (Burr 1978; House 1995) shows that the ATR PCS piping is within the ASME Code Section III, 1977 Edition (ASME 1977) allowable stresses at 120% of its design pressure (Pace 1990). The primary OPP for upset conditions (Level B) is provided by the PPS.[a] SRVs provide OPP for the emergency conditions (Level C), which assume the PPS is unavailable. The pressure limit for upset conditions is 1.1 times the design pressure, and ≥ 1.2 times the design pressure for emergency conditions. Design pressures for different PCS sections at 1.0, 1.1, and 1.2 times the PCS design pressures for the various piping sections are listed below.

	Design pressure (psig)		
System segment	Times 1.0	Times 1.1	Times 1.2
Primary pumps to isolation valves	576	634	—[b]
Isolation valves to BF-A-14	485	533	—[a]
BF-A-14 to reactor vessel inlet	390	429	468
Reactor vessel	390	429	468
Reactor vessel outlet to primary pumps inlet	390	429	—[a]

Table 5.2-1 lists the SRVs, pressure settings, and certified capacities. Table 5.2-2 lists the sources of overpressure in the ATR. Refer to Table 5.1-2 for PCS design and performance characteristics; Figures 5.1-12, -13, and -14 for relative elevations of PCS piping; and Figures 5.1-13 and -14 for simplified schematics of OPP components.

---

[a]. Refer to Chapter 7 (Instrumentation and Controls) for a description of the PPS.

[b]. Not analyzed

5.2.2.1 Design Bases. Failure to trip pressurizing pumps, loss of PCS heat rejection, and pump overspeed conditions caused by high power supply frequency are significant overpressure sources, providing the design bases for the functional design of the overpressure protection system (Pace 1990).

The enveloping overpressure event (excluding waterhammer events) in the PCS pump outlet pipe sections (pump to isolation valve, and isolation valve to flow control butterfly valve) occurs during pump start-up (Pace 1990). Per operating procedure, only one pump is started at a time, so the PCS has flow when the second and third pumps are started.

Loss of instrument air is the enveloping anticipated fault, causing PCV-1-1 (PCV-1 shown on Figures 5.1-1, -2, and -10) to close, FCV-1-8 (FCV-8 shown on Figures 5.1-1, -2, and -10) to open, and the standby pressurizing pump to start (Pace 1990). This anticipated fault or upset condition requires the PPS to mitigate the transient to prevent exceeding 110% of design pressure. The SRVs are not required for this or any upset condition. The loss of instrument air fault also envelops the unlikely faults or emergency conditions except for the waterhammer transient and start-up of a primary coolant pump against a fully closed isolation valve with an abnormally high pump suction pressure.

The startup of a primary coolant pump against a fully closed isolation valve, with an abnormally high pump suction pressure, is an unlikely event because two off-normal conditions must exist simultaneously; an abnormally high pump suction pressure, and an operator error or control system failure in the startup of the primary coolant pump. The event is analyzed for over-pressure protection in Pace 1990. Analysis of this fault is expanded to include starting the pumps with the butterfly valve BF-A-14 (shown on Figures 5.1-1, -10) fully closed. The pressurizing pump normal speed shutoff head and the PPS pressurizing pump(s) trip keep the maximum PCS pump suction pressure below the upset condition allowable pressure. The PCS SRVs keep the maximum pump suction pressure below the allowable pressure for emergency conditions.

The extremely unlikely faults include occurrences of all the anticipated and unlikely faults concurrent with a PPS failure to trip the pressurizing pumps and/or scram the reactor (Pace 1990). The fault that requires the greatest SRV flowrate is the loss of instrument air with failure to trip the pressurizing pumps; this fault is the enveloping transient for sizing the main SRVs. The second most demanding transient for flowrate is the complete loss of heat sink (CLOHS) without reactor scram. Start-up of the primary coolant pumps with abnormally high suction pressure is the enveloping event for the two pipe sections between the pumps and the butterfly valve BF-A-14.

5.2.2.2 Design Evaluation

5.2.2.2.1 Primary PCS OPP—Overpressure protection (OPP) from the PCS pump head is provided by the pressurizing pump design, the written operating procedures, and the PPS with back up from the SRVs (Pace 1990). The operating procedures limit the pump suction pressure during pump start-up (when the discharge isolation valves are closed) to between 50 and 230 psig.

As required by the ASME Code, 1986 Edition (ASME 1986), overpressure protection is provided for all upset (Level B) conditions by the PPS. The PPS keeps the PCS pressure at all locations from exceeding 110% of its design pressure. Safety relief valves (SF-A-71 and SF-A-72, Figures 5.1-1, -10) set at ≤ 390 psig provide overpressure protection for emergency (Level C) conditions and prevent the PCS pressure at all locations from exceeding 120% of its design pressure (Pace 1990). SRVs SF-A-71 and SF-A-72 are not required for expected conditions, but are required for unexpected conditions where the PPS is assumed to fail. SRVs SF-A-71 and SF-A-72 each have a 350 gpm certified capacity. A minimum of two SRVs are required for redundancy with a combined certified capacity of ≥ 688 gpm (344 gpm for each SRV) (ASME 1986). ATR OPP pressure settings and flow rates therefore meet the ASME Code, Section III, 1986 Edition (ASME 1986) requirements. The opening pressure tolerance required by the code is ± 3% of the set pressure or 11 psi for the safety relief valves.

The enveloping emergency condition is loss of instrument air with failure of the PPS to trip the pressurizing pumps (see note on loss of instrument air in 5.2.2.1). The PCS pump discharge pipe sections can reach high pressures during pump start-up if the isolation valves remain closed. The operating procedures guide the start-up, and the pressurizing pump design and the PPS limit the pressure in these sections of piping to ≤ 110% of their design pressures. The main SRVs ensure these sections of piping do not exceed 120% of their design pressures in the event the PPS fails to trip the pressurizing pumps.

With the ≤ 390 psig SRV set pressure, the maximum PCS pressure would be 453 psig. This pressure is below the allowable 468 psig pressure (120% of design pressure).

Complete loss of heat sink (CLOHS) with failure of the PPS is the next most severe transient and requires a 622 gpm relief flow rate (311 gpm for each SRV). The certified capacity of 350 gpm for each SRV therefore meets this requirement. Primary PCS OPP is therefore adequate for all PCS upset and emergency conditions.

5.2.2.2.2 Pressurizing Pumps OPP—The design pressure (390 psig) is higher than the normal speed shutoff head (382 psig) of the pressurizing pumps. The pressurizing pump SRVs are only needed for 15% overspeed operation of an isolated pump. Each pressurizing-pump discharge has an SRV (SF-A-75 and -76 shown on Figures 5.1-1 and -10) that protect the pumps and discharge piping. The SRVs have a set pressure of ≤ 390 psig and a certified capacity of 345 gpm (required capacity is 325 gpm) at 10% overpressure. Pressurizing pumps OPP is therefore adequate for the 15% overspeed condition. SRVs SF-A-75 and -76 are installed in such a way that water remains in their discharge pipes. A pipe length of 34 ft remains filled with water and provides a 7-ft head of water pressure against the outlets. This configuration has been tested and found acceptable for this application even though it deviates from the ASME Code requirements (Pace 1990).

5.2.2.3 Piping and Instrument Diagrams. Figure 5.1-13 is a simplified schematic of the ATR PCS main SRVs SF-A-71 and SF-A-72. Figure 5.1-14 is a simplified schematic of the ATR PCS pressurizing pumps SRVs SF-A-75 and SF-A-76. The detailed piping layouts may be found in Figures 5.1-7 and -10 for SF-A-71 and SF-A-72, and Figures 5.1-3 and -10 for SF-A-75 and SF-A-76. Figures 5.1-13 and -14 also show the relative elevations of the PCS main and pressurizing pump SRVs respectively.

5.2.2.4 Equipment and Component Description. The PCS SRVs (SF-A-71 and SF-A-72 shown on Figures 5.1-7, -10) and the pressurizing pumps SRVs (SF-A-75 and SF-A-76 shown on Figures 5.1-3, -10) are angle body relief valves equipped with backpressure bellows, an enclosed spring, a full nozzle, and a bolted bonnet. SRVs SF-A-71 and -72 have 3-in. inlet flanges and 4-in. outlet flanges discharging to the warm waste; SRVs SF-A-75 and -76 have 2 1/2-in. inlet flanges and 4-in. outlet flanges discharging to the degassing tank. Design inlet pressure for the SRVs is 390 psig, and design inlet temperature is 240°F. SRV settings are summarized in Table 5.2-1.

The SRVs are designed to operate with a clean lift action free from detrimental simmering, chattering, fluttering, vibration, or other adverse effects, followed by full reliable closure. The SRVs are designed to be capable of operating for 1,000 cycles of opening and closing over a 20-year period (EG&G Idaho 1987, 1988).

The valves are designed to operate in the following environmental conditions:

External Pressure	12.2 psia
External Temperature	60 to 120°F
Relative Humidity	Up to 100%
Radiation Fluence	1.3×10^5 R total integrated dose.

The vessel relief-valve discharge forces and the piping stress analysis considering these forces for the original piping were reported in 1974 (Burr and Magelby 1973). Under normal operating conditions the ATR primary coolant is subcooled, even for atmospheric pressure. Therefore, system depressurization through the relief valves does not expose the relief valves to large temperature variations as in the case of typical PWRs and BWRs.

5.2.2.5 Mounting of Pressure Relief Devices. The relief valves are mounted by raised face flanges per American National Standards Institute ANSI B16.5 (ANSI 1981; EG&G Idaho 1987, 1988). The design piping loads imposed on the inlet and outlet flanges are per the alternate design rules of ASME Section III, Subsection NB-3512.2 (b)(2), 1983 Edition (ASME 1983; EG&G Idaho 1987, 1988).

5.2.2.6 Applicable Codes and Classification. The SRVs were designed, manufactured, tested, certified, and marked in accordance with ASME Code, Section III, 1983 edition with addenda through summer 1984 (ASME 1983; EG&G Idaho 1987, 1988). The PCS SRVs are Code Class 1 and the pressurizing pump SRVs are Code Class 2. Additional conditions are established to ensure that the PCS pressure boundary component construction is consistent with applicable design requirements (EG&G Idaho 1987, 1988).

5.2.2.7 Material Specification. Refer to Table 5.2-3 for applicable materials of construction for the PCS main and pressurizing pump SRVs.

5.2.2.8 Process Instrumentation. Refer to Chapter 7 (Instrumentation and Controls) for a description of the PCS pressure-sensing and control circuitry.

5.2.2.9 System Reliability. The SRVs were designed and constructed according to specification (EG&G Idaho 1987, 1988) for 1000 cycles of opening and closing over a 20-year period. Preventive and corrective maintenance plus inservice testing and inspection ensure the continued operability of the SRVs.

Failures associated with the SRVs are (a) failure of both SRVs to open at their set pressure, and (b) failure of the SRVs to reclose after an overpressure event leading to a small LOCA (0.5 to 3-in. diameter break). The total opening area for both vessel SRVs is equivalent to only one 2.2-in. diameter hole, and therefore the analysis for a 3-in. diameter break envelops both SRVs failing to reclose. This event is discussed in Chapter 15 (Accident Analyses). The failure of the SRVs to open at their set pressure concurrent with the Condition 4 overpressure event is beyond design basis.

5.2.2.10 Testing and Inspection. Before operation, the SRV inlet portion was hydrostatically tested to 1.5 times the nominal set pressure and the outlet portion (secondary pressure zone) to 1.5 times the design outlet pressure in accordance with ASME Section III, Subsection NB-3531.2(f), 1983 Edition (ASME 1983; EG&G Idaho 1987, 1988). Also before operation, the SRV seats were tested at 95% of nominal set pressure with air and were "bubble tight" per the methods of API Standard 527 (EG&G Idaho, 1987, 1988). The flow capacity was verified by test with water per ASME Section III, Subsection NB-7740, 1983 Edition (ASME 1983; EG&G Idaho 1987, 1988). During their service life, the SRVs undergo inservice inspection and testing in accordance with the ATR ISI Plan. (INEEL 2002)

5.2.3 PCPB Materials

5.2.3.1 Material Specifications. Table 5.2-3 lists PCS component materials of construction. Refer to Section 5.3.1 for a discussion of reactor vessel materials. Original PCS material specifications are in accordance with the ASME Boiler and Pressure Vessel Code, Section II, 1962 Edition with addenda and revisions in place at the time of the construction contract (ASME 1962a; deBoisblanc and Cohen 1965).

5.2.3.2 Compatibility with Primary Coolant. ATR PCS materials in contact with the primary coolant are austenitic Type 304 stainless steel with additional requirements for limitations on carbon content (Type 304L) in areas that are inaccessible for maintenance or inspection. Type 304 stainless steel was chosen for its resistance to corrosion. Type 304 stainless meets the requirements of American Society for Testing and Materials ASTM A-312-61T (deBoisblanc and Cohen 1965). Those portions of the heat exchanger in contact with both primary and secondary coolant are primarily Inconel 600, with twelve heat exchanger tubes from Type 304 or 304L stainless steel. Inconel 600 is more resistant to possible chloride stress corrosion from the secondary side.

Table 5.1-2, Item (f) lists nominal operating ranges for the primary coolant chemistry. Limits on pH, conductivity, dissolved minerals, and filterable solids help ensure that excessive oxide deposition on the fuel elements or aluminum corrosion does not occur as a result of primary coolant chemistry. Because high relative coolant conductivity indicates the presence of dissolved salts, conductivity is used as a parameter in controlling contaminants such as chloride (Beatty 1980) and copper. Filterable solids are limited because the presence of filterable solids could also contribute to the deposition of foreign materials on the fuel elements and to corrosion of the PCS (Kimmitt 1976).

The pH of the primary coolant can be maintained at nominally 5.2 by using the bypass demineralizer system; however, some variations can occur when a new resin bed is put into service (Durney 1980, 1982).

The conductivity limits of the primary coolant are based on the pH-to-conductivity relationship of pure dilute acid. Conductivity readings higher than these values indicate the presence of dissolved salts. The normal conductivity range for the reactor at power and temperature, and with a pH of 5.2 to 5.4, is 2-5 μmhos/cm. Otherwise, the normal conductivity range is 2-8 μmhos/cm.

Limits are imposed on gross beta and gamma activity level to prevent excessive radioactivity of the primary coolant. These limits (a) allow maintenance to be performed while staying within acceptable personnel-exposure guidelines and (b) ensure control of radioactive releases to the environment. The normal range of gross radioactivity is 0.05 to 0.29 μCi/mL, and it is controlled to be less than 2.0 μCi/mL.

5.2.3.3 Fabrication and Processing of Ferritic Materials. The Primary heat exchangers and the surge tank are constructed of carbon steel; areas that are in contact with the primary coolant are clad with Type 304 stainless steel, and the heat exchanger tube sheets are clad with Inconel 600. These vessels were designed and constructed in accordance with the ASME Unfired Pressure Vessel Code, Section VIII, 1959 Edition, including latest addenda and revisions in place at the time of the construction contract and Case 1270 N-5 (ASME 1959). The applicable codes and preservice tests conducted on the heat exchangers and surge tank are specified in Sections 5.4.2.2 and 5.4.10.1.3, respectively.

5.2.3.4 Fabrication and Processing of Austenitic Stainless Steels. To minimize the possibility of intergranular corrosion in inaccessible PCS piping and in the reactor vessel, the carbon content of the material contacting the primary coolant was restricted to < 0.060% by weight. No additional provisions or special fabrication and processing techniques are required for preventing corrosion of austenitic stainless steels because of the low temperatures and chloride contents of the ATR PCS primary loop. No intergranular stress corrosion cracking (IGSCC) is expected for the stainless steel reactor vessel (Durney et al. 1987). A review of operational history combined with a review of factors that influence IGSCC and crevice corrosion in oxidizing water systems indicates that any crevice corrosion that may have occurred (or will occur) at ATR is expected to be minimal due to the very low temperatures involved, the water quality, and the time of operation (Durney et al. 1987). Because the possibility of IGSCC-induced cracks is remote, chances of encountering cracks exceeding the allowable sizes is very low, especially in the weld material (Durney et al. 1987).

Corrosion behavior of Type 304 stainless steel was examined under coolant conditions expected during ATR operations. The tests were run for a maximum of 4,000 hours. Corrosion rates were negligible (< 1 mil/yr). Tests included welded specimens, specially prepared strips with prior intergranular attack, and stressed specimens (deBoisblanc and Cohen 1965). Metallographic examinations of control and test specimens did not reveal any propagation of the intergranular attack.

The radiation field to which the piping is subjected is not of sufficient magnitude to change the material mechanical properties.

The ATR PCPB components and the reactor vessel are made of Type 304 stainless steel and Type 308 stainless steel weldments; therefore, the methods used for fabrication and processing are similar. Refer to Section 5.3.1.2 for details on welding, and Section 5.3.1.3 for details on nondestructive examination techniques for the reactor vessel. Also refer to Section 5.4 for details concerning testing of individual PCPB components. Table 5.2-4 shows the material properties of Type 304 stainless steel.

5.2.4 ISI and Testing of the PCPB

An ISI plan (INEEL 2002) is developed, and periodically updated, for the PCS using the ASME Code, Section XI, as a guide. The current Section XI edition being used is 1989, no addenda. The ATR was designed and constructed before Section XI was implemented. Therefore, some limitations in accessibility are encountered during ISI or testing of PCS components. Since not all components are accessible, the ISI plan includes inspections for welds that are similar to ensure typical aging behavior is available. The details of the ISI plan including the limitations are internally reviewed and approved by management. Examination results are submitted to the Contractor's Reactor Programs engineering organizations for review and approval. Where applicable, original radiographs and previous ultrasonic examinations are used as baseline data to evaluate inspection results. Unacceptable indications are resolved by repair, replacement, or analysis.

System leakage tests at nominal operating pressure are conducted before startup of each operating cycle. A system hydrostatic test has been conducted once each ten-year interval at nominal operating pressure.

5.2.5 Detection of Leakage Through the PCPB

The purposes of leakage monitoring are to (a) detect Pressure Boundary Fault Leakage[a] and, thus, incipient failures in that boundary; (b) track abnormalities in overall leakage from the PCS; and (c) respond promptly to major changes in that leakage. Leakage may occur through vent and drain valves, gaskets, or fittings. This includes (a) sample flows routed directly to warm waste, and (b) a small amount of flow past equipment seals to the warm drain collection system. The current method for evaluating leakage is to determine the net instrumented flows into and out of the PCPB to arrive at a Net PCS Leak Rate.

Pressure boundary fault leakage is leakage through a fault in a PCS component body, pipe wall, or vessel wall within the radiographic limit, but not past seals, gaskets, and valve packings. Since the PCS is a relatively low-temperature, low-pressure system, failures are not expected to propagate quickly.

The accuracy of measurement and normal flow oscillations make it difficult to obtain a meaningful system leakage and discharge measurement from instantaneous flow meter readings (Klingler and Faller 1988). By estimating average flow over time, however, a more accurate measurement of leakage is possible. With this accuracy, it is possible to identify day-to-day changes in the net PCS leak rate of less than 5 gpm.

The limits on leakage from the PCS are established by consideration of the material and leakage characteristics of the ATR PCPB as evaluated in support of the accident analysis (Section 15.6.2). The PCS is a low-temperature, highly-subcooled, moderate-pressure system constructed of Type 304 stainless steel. The operating range of the PCS results in relatively little stored energy. The chemistry of the coolant has been carefully controlled thereby limiting the potential for degradation of material properties. The piping and vessel are not exposed to extreme radiation fields, and the materials retain significant ductility. Under these conditions of limited stored energy, little degradation of ductility, and careful chemistry control, there is little potential for rapid crack propagation leading to an abrupt failure, and incipient failures can be detected and corrected.

---

[a]. Pressure boundary fault leakage is leakage through a fault in a PCS component body, pipe wall, or vessel wall within the radiographic limit, but not past seals, gaskets, and valve packings. Since the PCS is a relatively low-temperature, low-pressure system, failures are not expected to propagate quickly.

The reactor is not operated with known leakage through the pressure boundary (the piping within the radiographic limits). A walkdown of the PCS is completed routinely with the PCS at operating pressure before reactor operation following an outage and depressurization. The total unidentified leakage during operation is limited to 50 gpm in accordance with the evaluation for the correspondence of leakage limits with potential PCS crack size and propagation (Atkinson 1994). An increase in unidentified leakage over time of 10 gpm or more would be a cause for concern and initiation of actions to identify the cause of the increased leakage and to evaluate the risk for continued operation (Atkinson 1994). Additionally unidentified leakage is limited to 10 gpm prior to reactor operation. The significant activity to verify the PCS integrity is the walkdown of the piping. Sufficient instrumentation is available to detect an increase in leakage of less than 5 gpm. This same instrumentation will allow trending of the leakage consistent with good operating practice.

5.2.6 System Controls to Preclude Significant PCPB Rupture

The ATR reactor vessel primary coolant piping systems are high-quality all-stainless steel systems that are maintained to ensure that the quality does not degrade such that failure might be expected. The ATR ISI program is based on the requirements of 1989 Edition, no addenda, Section XI of the ASME Boiler and Pressure Vessel Code. High quality chemistry control of the PCS has been practiced since initial system operation to maintain a very clean system operated within tight chemistry control bounds. The chemistry control specifications were established based on many years of operating experience with similar materials testing reactors and extensive experimentation. The primary concern upon which the ATR PCS chemistry control specifications were based was prevention of excessive oxide film buildup on the aluminum clad fuel plates (McCracken 1993). However, these controls have also served to maintain good water quality for the stainless steel PCS. With these controls, no leakage has been detected from heat exchanger tubes or other areas of the PCPB (other than for seals and valve seats) in over 30 years of reactor operation.

All welded joints on PCS pipes larger than 3-in. in diameter, including the first isolation valve on branch piping for auxiliary systems, were radiographed. All the accessible welds are re-inspected periodically according to the ATR ISI plan (INEEL 2002). All branches and interfaces to the PCS radiographic boundary meet one of the following criteria:

- The interface is by a valve or orifice with a flow diameter less than or equal to 3-inches, or
- The interface is by a normally closed block or flow control valve incapable of being inadvertently and remotely opened, or
- In those locations in which the interface is by a single check valve:
  - a loss-of-coolant accident (LOCA) analysis shows that the consequences of the interfacing system rupture and a failed open check valve are within the consequences of the limiting 3-inch LOCA for the UFSAR (Section 15.6.4), or
  - a probabilistic analysis shows that the mean frequency for a rupture in the interfacing system and a failure of the check valve to close is sufficiently low that the mean frequency for a significant PCPB rupture from all sources is not significantly affected.

These criteria have been satisfied for the ATR PCS radiographic boundary interfaces (Table 5.1-1).

The ATR PCS is a relatively low energy system normally operated at less than 390 psia at the reactor inlet with cooling water inlet temperature normally not exceeding 125°F. The design is such that the outlet temperature would be less than 175°F. As a result, there is little stored energy and the system is significantly subcooled at atmospheric pressure. If a break were to occur in the PCS, the coolant would not flash to steam. However, the principle significance of the low stored energy in the PCS is in the manner that the piping might fail. A system such as the ATR PCS is not expected to have catastrophic failures because the hydraulic energy is released very quickly and there is no driving force to result in large scale failures.

Although the ATR PCPB design and operating characteristics minimize the potential for a significant PCPB failure, vigilance and precautionary actions are still necessary to ensure that a catastrophic failure will not occur. Potential causes of catastrophic ATR PCPB failures are:

- Intergranular stress corrosion cracking (IGSCC)
- Piping erosion
- Excessive piping vibration
- Fatigue Failure
- Extreme system overpressure
- Waterhammer
- Radiation embrittlement leading to brittle fracture
- Seismic events that overstress the components.

These potential PCPB failure modes have been evaluated and technical analyses, inspections, and preventative actions are taken to preclude their occurrence. The results of the evaluations for the first seven of these failure modes and actions taken and being taken to preclude these failure modes are summarized by Smith (1997). The ATR PCS has been analyzed for the Safe Shutdown Earthquake (SSE) with acceptable results. Additionally, the ATR seismic shutdown function of the RSS ensures that the reactor is shutdown before a serious seismic event with a potential for causing any significant leakage or loss of coolant from the PCS may occur.

Table 5.2-1. Primary Coolant System safety relief valves.[a]

Valve	Location	Pressure setting (psig)	Certified capacity (gpm)
SF-A-71	Vessel, lower drain	379	350
SF-A-72	Vessel, lower drain	379	350
SF-A-75	Pressurizing pump 670-M-14 Discharge	380	345
SF-A-76	Pressurizing pump 670-M-15 discharge	380	345

a. Data from Pace (1990).

Table 5.2-2. Primary Coolant System overpressure sources.[a]

Source	Total dynamic head (psig)	Design flow rate (gpm)
Primary coolant pumps	162 (operating) 251 (shutoff)	18,000 each
Pressurizing pumps	382 (shutoff)	360 (maximum) 256 (operating)
Loss of heat sink	—	622
Warm seal booster pumps	180 (shutoff)	150 (normal) 270 (maximum)
Gland seal pumps	455 (operating) 470 (shutoff)	55
High-pressure air	300	
Emergency coolant pumps	33	4,700
Overvoltage and/or frequency of diesel-generator power supply to pressurizing and/or gland-seal pumps	Overspeed pump head ratio 1.32	Overspeed capacity ratio 1.15 (~475 gpm maximum)

a. Data from Pace (1990).

Table 5.2-3. Primary Coolant System materials of construction.[a]

Component	Material
Primary Pumps:	
Casing	Austenitic stainless steel
Impellers	Austenitic stainless steel
Casing rings	12% chrome steel
Impeller rings	Austenitic stainless steel
Shaft	SAE 4140 Steel
Shaft sleeves	Austenitic stainless steel
Shaft seals	Mechanical face type
Bearings	Sleeve (babbit)
Emergency and Pressurizing Pumps:	
Casing	Austenitic stainless steel
Impellers	Austenitic stainless steel
Casing Rings	Austenitic stainless steel
Impeller Rings	Austenitic stainless steel
Shaft	17-4 pH stainless steel
Shaft Sleeves	Austenitic stainless steel
Shaft seals	Mechanical face type
Bearings	Roller type
Heat exchangers:	
Tubes	Inconel 600 or 304 stainless steel
Tube type	U-bend
Tube size	3/4 in. OD x 18 BWG
Tube sheets	Inconel clad carbon steel
Tube joints	Welded
Shells	Carbon steel
Tube support plates and baffles	Carbon steel
Channels, channel covers, and primary nozzles	Type 304 stainless steel clad carbon steel
Surge tank:	
Shell and heads	Type 304 stainless steel clad carbon steel
Nozzles	Type 304 stainless steel clad carbon steel
Degassing tank:	
Shell and heads	Type 304 stainless steel
Nozzles and internals	Type 304 stainless steel
PCS piping:	Type 304 stainless steel
PCS valves:	Type 304 stainless steel
Safety relief valves:	
Body and bonnet	ASME SA-182, Grade F316, or ASME SA-351, Grade CF3M or CF8M
Nozzle and disc	Type 316 stainless steel

a. Data from deBoisblanc and Cohen 1965.

Table 5.2-4. Material properties of 304 stainless steel.[a]

(a) Young's modulus

70°F	28.3×10^6 psi
250°F	27.4×10^6 psi

(b) Minimum unirradiated tensile properties at room temperature

ASME Specification	Form	Tensile strength (psi)	Yield strength (psi)	Elongation in 2 inches (%)
SA-240	Plate	75,000	30,000	40
SA-182	Forgings	75,000	30,000	45
SA-336	Forgings	70,000	30,000	0
SA-376	Pipe	70,000	30,000	35
SA-213	Tubing	75,000	30,000	35

(c) Coefficient of thermal expansion,[b]

70 - 250°F	0.0203 in/ft

(d) Allowable stresses (ksi) (SA-358 or SA-376)[c]

	SS 304	SS 304L	Equation number[d]
S_c (70°F)	16.8	15.7	
S_h (25°F)	17.2	15.5	8
S_A	27.8	23.5	10
1.2 S_h	20.6	18.6	9
$S_A + S_h$	45.0	39.0	11

a. Data from Davidson (1979); deBoisblanc and Cohen (1965).

b. $S_A = f(1.25\ S_c + 0.25\ S_h)$, $f = 1.0$.

c. Allowable stresses from ASME Section III, 1977.

d. Equation numbers from Subarticle NC-3650, ASME Section III, 1977.

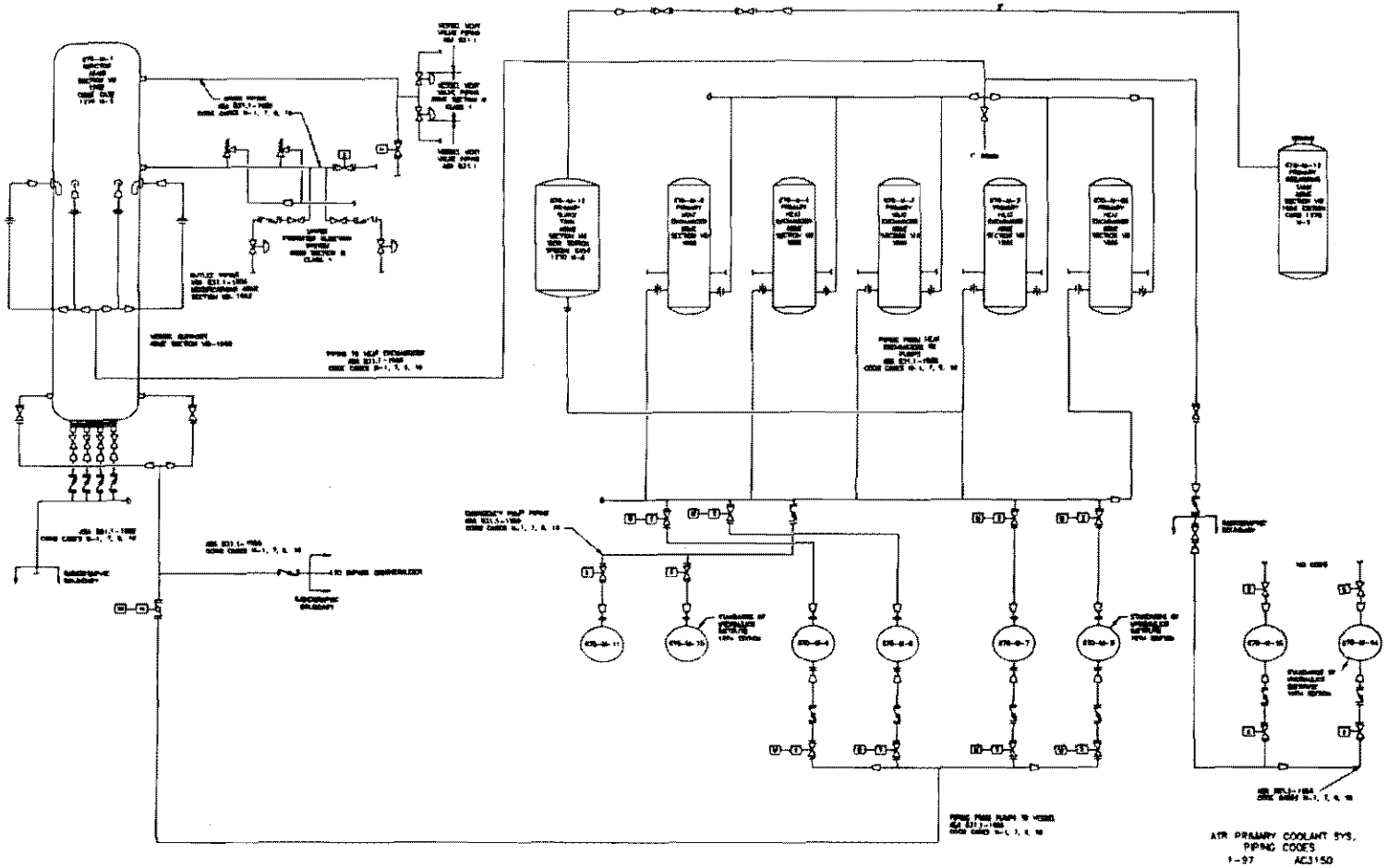

Figure 5.2-1. ATR Primary Coolant System Piping Codes. **(For Information Only)**

5.3 Reactor Vessel

Section 5.3.1 contains pertinent data to demonstrate that the materials, fabrication methods, and inspection techniques used for the reactor vessel conform to all applicable regulations. Section 5.3.2 describes the bases for setting the operational limits on pressure and temperature for normal, upset, and test conditions. Section 5.3.3 contains additional information about reactor-vessel design not covered in other sections.

5.3.1 Reactor Vessel Materials

5.3.1.1 Material Specifications. Original vessel material specifications are in accordance with ASME Boiler and Pressure Vessel Code, Section II, Materials Specifications, 1962 Edition with addenda and revisions in place at the time of the construction contract (ASME 1962a; deBoisblanc and Cohen 1965).

The pressure vessel is constructed of solid Type 304 stainless steel rather than carbon steel clad with stainless. Solid stainless steel was chosen for low probability of brittle fracture after very long exposure to intense radiation and for its resistance to corrosion when in contact with ATR primary coolant (deBoisblanc and Cohen 1965).

5.3.1.2 Special Processes Used for Manufacturing and Fabrication. Fabrication and assembly procedures, including welding, were reviewed by the ATR design contractors before commencing vessel manufacture (deBoisblanc and Cohen 1965). Also included were major tests, inspections, and weld-examination standards. Repair work to the vessel required specific approval. Certified records for all inspections were provided. All mill test reports, chemical analyses, and thermal-treatment histories of vessel components were also provided.

ASME Code-qualified welders performed all vessel welding (deBoisblanc and Cohen 1965). Electrode material provided a deposit containing a maximum carbon content of 0.060 weight percent in accordance with SA-298 Type E 308 ELC-15 (deBoisblanc and Cohen 1965). The completed welds were radiographed in accordance with Paragraph UW-51, Section VIII of the ASME Unfired Pressure Vessel Code (ASME 1962b; deBoisblanc and Cohen 1965) and ASTM designation E-94-52T (deBoisblanc and Cohen 1965). All welded joints on pipes larger than 3 in. in diameter, including the first isolation valve on branch piping, were radiographed.

5.3.1.3 Special Methods for Nondestructive Examination. As discussed in deBoisblanc and Cohen (1965), materials used in the reactor vessel, and the tests performed, were as follows:

- Stainless steel plate and sheet ASME SA-240, Type 304, 0.06 max % carbon
- Ultrasonic inspection for all materials used for pressure containment.
- Stainless steel forgings ASME SA-182, Grade F, Type 304 or ASME SA-336, Class F-8
  - Macro-etch test
  - Ultrasonic inspection for all materials used for pressure containment
  - Carbon content procedure in accordance with ASTM E-30.

- Stainless steel seamless pipe, ASME SA-376, Type 304
  - Carbon content procedure in accordance with ASTM E-30
  - Supplementary Paragraphs S-2 through S-5
  - Ultrasonic and liquid penetrant inspection for all materials used for pressure containment.
- Stainless steel tubing ASME SA-213, Type 304
  - Carbon content in accordance with ASTM E-30
  - Ultrasonic and liquid-penetrant inspection for all materials used for pressure containment.
- Stainless steel welding electrode ASME SA-298 or ASME SA-371
  - Type E-308 ELC except carbon limited to 0.060 weight percent maximum
  - Met requirements of SA-298, Section 7.
- Principal bolting materials and fasteners
  - Met ASME specification for pressure, temperature conditions and locations
  - Ultrasonic inspected
  - 100 percent liquid-penetrant inspected.

As discussed in deBoisblanc and Cohen (1965), the following inspection requirements over and above the ASME Code requirements were imposed on all vessel welds:

Completed weld	Liquid-penetrant inspection on both sides of weld
Adjoining surfaces of the base metal before welding	Liquid-penetrant inspection
After first weld pass	Liquid-penetrant inspection on both sides of weld
After one-half weld thickness	Liquid-penetrant inspection

5.3.1.4 Fracture Toughness. The issue of irradiation effects on the ATR reactor vessel has been defined and evaluated. As plants accumulate more and more service time, neutron irradiation reduces material fracture toughness and initial safety margins.

An evaluation by analyses of irradiation embrittlement of the reactor vessel has been completed (Durney et al. 1987). The analyses include calculations which follow procedures in U.S. Nuclear Regulatory Commission (NRC) Regulatory Guide 1.99 (NRC 1988; Buescher 1993). However, results from commercial reactor experience do not apply directly to the ATR since the data pertain to low-alloy carbon steels while the ATR reactor vessel and its welds are stainless-steel based.

Analysis of the ATR vessel shows that neutron embrittlement is not currently a concern, and will not be significant for operation through the year 2014 (Durney et al. 1987). This analysis of data, applicable to Type 304 stainless steel base metal and for Type 308 stainless steel weld material, was conducted to evaluate the potential for brittle fracture of the ATR vessel at any time up to the year 2014.

Since the ATR began operating in 1968, measurements have been conducted at various locations during various cycles to determine the fast-neutron fluence (E > 1 MeV) to which the vessel is exposed. Because of the desire to evaluate possible irradiation-induced embrittlement, it was necessary to identify the component experiencing the peak fluence; i.e., the one closest to the core. As mentioned in Section 5.3.1.5, the drop tube dimple and associated weld are used for estimating the vessel fluence. In order to calculate the fast fluence, the history of operation was reviewed (Durney et al. 1987). The accumulated fluences through Reflector III, which was removed in 1986, were calculated. For purposes of projecting these fluences into the year 2014, it was assumed conservatively that the reactor operates at 250 MW_t balanced power for 80% of the time. The thermal-neutron fluence was estimated using data taken from capsule irradiation files as well as the history of operation. The fast and thermal fluence for various ATR components are calculated in the Core Safety Assurance Package (CSAP).

The nearest surface of the vessel wall to the reactor fuel annulus is 32.4 in. at the inner surface of the drop tube dimple wall at the elevation of the core horizontal midplane (EL 80 ft). The remaining inner surfaces of the vessel wall at the elevation of the reactor core are at distances ranging from 52.4 in. to 56.5 in. from the nearest fuel elements. A large degree of neutron attenuation is provided by the beryllium reflector blocks, outer shim control cylinders (OSCCs), core reflector tank, and primary coolant water. The nearest weld on the vessel (the weld material behavior is limiting) also occurs on the drop tube dimple, and is located 15 in. above the core horizontal midplane and 49.7 in. from the axial center of the vessel.

The maximum projected thermal neutron fluence at the year 2014 was calculated (95% confidence level) to be 7.62×10^{20} n/cm^2 and 2.27×10^{20} n/cm^2 for the dimple base metal and weld metal, respectively. The effect of transmutation in the material compositions was evaluated, and it was concluded that the thermal-neutron fluence would have negligible effect on structural integrity (Durney et al. 1987). The maximum projected fast-neutron fluence at the year 2014 was calculated (95% confidence level) to be 1.20×10^{19} n/cm^2 and 3.1×10^{18} n/cm^2 (E > 1 MeV) for the dimple base metal and weld metal, respectively (Durney et al. 1987). It was concluded that exposure to the above fast fluences will have a negligible effect on the fracture toughness of either the base metal or the weld metal (Durney et al. 1987). Therefore, this evaluation concluded that changes to the material properties of the ATR vessel are not significant at fluences projected for operation to 2014. The failure mode for the vessel is consistent with the analysis for the unirradiated vessel (Mousseau 1987).

The above lifetime values are operational limits on fast- and thermal-neutron fluence to the reactor vessel established to ensure that an adequate margin is maintained. Additionally, the total fluence to the reactor vessel is evaluated annually.

An independent review (Buescher 1993) concluded: "The ATR is substantially in agreement with the functional requirement, with regard to analysis and supporting tests for embrittlement. Consequence analysis and specific PRA treatment do not appear to be current needs for the ATR."

5.3.1.5 Material Surveillance. The ATR vessel is made of solid Type 304 stainless steel, which has a lower susceptibility to neutron-induced embrittlement than carbon steel. Materials-surveillance specimens were not included with the original installation of the ATR reactor vessel. However, in 1988 a program was initiated to irradiate fracture-toughness and tensile specimens for the vessel. Specimens were fabricated that are representative of the vessel base metal, weld metal, and heat-affected zone. Initial testing on some of these specimens was completed before irradiation to establish the unirradiated properties of the material (Graham et al. 1989). The remaining specimens were then irradiated in the ATR outer grids at an accelerated fluence rate. The specimens have since been removed and tested to determine the irradiated material properties. The data shows (Carlson 2002) that the assumptions about radiation effects on fracture toughness properties made in the aging assessment (Durney et al. 1987) are conservative.

5.3.1.6 Reactor Vessel Fasteners. Section 5.3.1.3 discusses reactor vessel fastener materials and inspection requirements.

Loss of fracture toughness in reactor vessel supports may result in a vulnerability to a transient stress or shock leading to a rapidly propagating fracture and consequent movement of the reactor vessel. However, the ATR Aging Evaluation and Life Extension Program (Dwight 1988a, 1988b) indicates that reactor vessel supports are not vulnerable to radiation embrittlement. The vessel supports are under compression and are far removed from the beltline region of the vessel. The neutron fluence is well below the damage threshold (Buescher 1993).

5.3.2 Pressure-Temperature Limits

5.3.2.1 Limit Curves. Operational limits to maintain the PCS operation within design conditions, are established for (a) PCS pressure at various locations, (b) overall PCS temperature, and (c) PCS pressure during hydrostatic testing (no flow, ambient temperatures).

5.3.2.2 Operating Procedures. As discussed in Section 5.3.2.1, operational limits are established for (a) PCS pressure at various locations, (b) overall PCS temperature, and (c) PCS pressure during hydrostatic testing (no flow, ambient temperatures). Operational procedures[a] are established to ensure that (a) the operational safety limits on temperature and pressure are not exceeded during normal ATR operations (Level A) or any foreseeable upset or emergency conditions (Level B or C), and (b) that the reactor will not be operated with an insufficient number of PCS components or insufficient flow. Refer to Table 5.1-2(b) for nominal PCS steady-state operating pressures and temperatures at 250 MW_t, and Table 5.1-2(c) for PCS piping design pressures, temperatures, and safety limits.

No formal cooldown procedure is needed to protect the primary coolant system or the core as in a commercial reactor. The aluminum-clad metallic-plate fuel elements do not have a pressurized gap, and there is no requirement to maintain the cladding in compression at elevated temperatures as in a commercial plant.

---

[a]. Refer to Chapter 16 (Derivation of Technical Safety Requirements) for a more detailed discussion of operating procedures.

5.3.3 Reactor Vessel Integrity

The reactor vessel (Figure 5.3-1) is a subsystem of the Primary Coolant System (PCS) and, thus, a part of the Primary Coolant Pressure Boundary (PCPB). Its function is to provide an PCPB envelope for the reactor core and internals. As part of the PCPB, the reactor vessel is classified safety-related because the PCPB maintains the heat-removal capability of the PCS and serves as a primary barrier for fission-product release (House 1992).

Section 5.3.3 provides references to other Chapter 5 sections where factors important to reactor vessel integrity have been previously discussed, such as (a) Section 5.2.3, Primary Coolant Pressure Boundary Materials, (b) Section 5.2.3.4, Fabrication and Processing of Austenitic Stainless Steels, (c) Section 5.2.4, Primary Coolant Pressure Boundary ISI and Testing, (d) Section 5.3.1, Reactor Vessel Materials, and (e) Section 5.3.2, Pressure-Temperature Limits. The operational limits, as established for the Technical Safety Requirements, are discussed in Section 5.3.2.2 and in Chapter 16 (Derivation of Technical Safety Requirements). Section 5.3.3.1 provides a description of basic reactor-vessel design. Reactor-vessel codes and bases are discussed in Section 5.2.1.

5.3.3.1 Design. The reactor vessel is a pressurized container constructed entirely of 304 stainless steel, with an ASME design rating of 390 psig at 240°F and an empty weight of about 205,000 lb. The ATR reactor components are housed in a solid stainless steel vessel because stainless steel can be exposed to intense irradiation over long periods of time with only a small probability of brittle fracture (deBoisblanc and Cohen 1965). Table 5.3-1 shows the applicable design and performance characteristics.

The major components of the Reactor Vessel Subsystem (Figures 5.3-1, 2, -3, and -4) are the (a) vessel shell assembly, (b) top head assembly, (c) bottom head assembly, (d) drop tube assembly, (e) various reactor-vessel nozzles and penetrations, (f) miscellaneous reactor-vessel penetration assemblies, and (g) nuclear instrument thimbles. The major reactor-vessel nozzles and penetrations are listed in Table 5.3-2, shown in Figures 5.3-1, -2, -3, and -4, and discussed in the subsection corresponding to the vessel assembly where they are located.

The miscellaneous penetration assemblies provide an PCPB seal for certain nozzles and penetrations, which attach to mechanisms extending outside the reactor vessel. The penetration assemblies are (a) the penetration body assembly for N-16 sample tubes, (b) the inpile tube bottom head seal freeze unit and seal or bottom head closure plug assembly, (c) the pressure housing for the neck shim and regulating rod drives, (d) the flanged tubes for the safety rod horizontal drive shaft assemblies, and (e) the nozzle extension assembly of the OSCC System. Other miscellaneous small nozzles and penetrations (1/8 to 1-1/2 in. ID), above and below the core, provide venting, seal water entry, and flush water line connections.

The shell is closed at the bottom by a welded hemispherical head, and at the top by a flanged and bolted head of a standard elliptical cross section. Both top and bottom heads have the central opening closed by flat circular closure plates seated inside the vessel.

Sufficient vessel volume above the core permits coolant to serve as an upper core shield during reactor operation and outage handling work. The large amount of coolant shielding also minimizes fast-neutron damage to the reactor vessel.

Internal thermal shields[a] reduce gamma heating in the concrete biological shield and vessel wall, and are supported by brackets welded to the vessel inner wall. The vessel is provided with inlet and outlet nozzles for the primary coolant. Elevated exit nozzles provide a continuous envelope that keeps the core covered with coolant.

A drop tube attached to the vessel side is used to transfer fuel, experiments, and small reactor internals from the vessel directly to an adjacent stainless-steel-lined canal system. Additional design features include refueling ports, experiment- and reactor-instrument penetrations and nozzles, and bottom- and top-head penetrations for various functions.

As discussed in deBoisblanc and Cohen (1965), an ASME Code analysis was made during design for the ATR vessel, including top- and bottom-head closure plates, nozzles, and penetrations. A summary of the maximum stresses (combined) for principal locations, together with allowable values, is as follows:

		Design				
Location	Material	Temp (°F)	Pressure (psi)	Thickness (in.)	Allowable Stress (psi)	Combined stress (psi)
Shell	SA 240 Type	240	390	2	15,990	14,744
Shell	SA 240 Type	240	390	5	15,990	6,022
Bottom head	SA 240 Type	240	390	2	15,990	7,724
Top head	SA 182 Type 304 Stainless Steel	240	390	16	23,985 15,990 15,990	10,026 Hub 6,329 Tan 5,807 Rad
Vessel flange	SA 182 Type 304 Stainless Steel	240	390	15.75	23,985 15,990 15,990	8,610 Hub 5,276 Tan 5,638 Rad

The design loads imposed on the reactor vessel and nozzles were included in calculations determining nozzle reinforcement. The bending moments were computed for the safety-rod drive nozzles. Piping reactions for all nozzles were computed, and the resulting loads were used in calculating required nozzle reinforcement.

The results of stress calculations including nozzle reinforcement, weld areas, bolting pipe, and other external reactions show that the ATR vessel design meets all code requirements. All openings in the vessel shell for penetrations and nozzles are reinforced in accordance with the rules of the 1962 edition of Section VIII of the ASME Boiler and Pressure Vessel Code (ASME 1962b; deBoisblanc and Cohen 1965; Burr 1978). As discussed in deBoisblanc and Cohen (1965), the completed vessel is approved under the provisions for nuclear vessels as stated in ASME Code Case 1270 N-3, and has an ASME Code Stamp. Other applicable cases are 1273 N-7, 1270 N-5, 1271 N, 1272 N-5, 1274 N-6, and 1275 N.

[a]. Refer to Chapter 3 (Design of Structures, Components, Equipment, and Systems) for a description of the thermal shields.

In addition, an analysis (Miller 1987) of the ATR drop tube and cylindrical course weldment has been performed for pressure and thermal loading. The assembly was analyzed for structural adequacy according to criteria of the ASME Code Section III Subsection NB for Class 1 components. This included a comparison of calculated stresses with specified limits for pressure and thermal loading. It also included a fatigue evaluation for all pressure/temperature cycles expected during operation of the ATR. Results from the analysis indicate that stresses are within limits specified by the ASME Code for Design, Level A, and Level B conditions. In addition, the results showed that the assembly can sustain 10^7 cycles of pressure loading and thermal gradients that could occur as a result of the operation. The number of cycles experienced for a year is conservatively not more than 50 (Durney et al. 1987). It is apparent from this evaluation that the fatigue limit for the vessel is not a concern since it would require 2×10^5 years to accumulate 10^7 cycles. Thus, the evaluation shows that the drop-tube assembly meets ASME Code Section III Subsection NB criteria for pressure and temperature loads for the life of the ATR.

As discussed in Miller (1987), the stresses calculated for the drop tube assembly are representative of the worst pressure and thermal stresses expected anywhere in the ATR vessel. Results from the stress and fatigue evaluations of this assembly indicate that safety margins were ample. Thus, it is concluded that all portions of the ATR vessel meet ASME Section III Subsection NB criteria for pressure and temperature loads for any projected service life of the plant (Durney et al. 1987).

5.3.3.1.1 Vessel Shell Assembly—The vessel shell assembly (Figure 5.3-2) consists of four cylindrical shell sections and the vessel top flange welded together. The vessel shell wall is 2 in. thick for the bottom and center shell sections. The upper section is 5 in. thick to provide an attachment for the vessel support skirt, instrumentation, and facility nozzles. The vessel support skirt, mounted to the exterior wall of the vessel by welded clamps approximately 10-1/2 ft above the top of the core, extends outward and rests on a sole plate in the structural concrete in the nozzle trench (Figure 5.3-5). The skirt supports the entire weight of the vessel and internals. The vessel shell center section is composed of two cylindrical shell sections welded together and contains an opening for the drop-tube assembly, which is welded to the bottom section of the center shell section.

The vessel upper and lower drain nozzles are welded to piping, which together act to reduce and maintain the reactor water level during outages to simplify maintenance and experiment handling.

The eight safety-rod drive line nozzles provide an attachment point for the flange tube of the horizontal drive shaft.[a] The eight OSCC drive line nozzles are welded to the vessel shell 1 ft above the core and provide an attachment point for the OSCC nozzle extension assembly.[b]

The twelve 5-in.-ID diagonal nozzles for the nuclear instrument thimbles are welded to the reactor vessel 13 ft above the core. The nuclear instrument thimbles[c] are, in turn, welded to the nozzles, and are sealed forming an PCPB seal. The safety rod and OSCC drive line nozzles, and nuclear instrument thimbles are sealed by penetration assemblies. The experiment loop piping penetrations and the instrumented capsule penetrations are normally covered and sealed with a bolted cover and gasket. The coolant outlet nozzle and vessel upper and lower drain nozzles are connected to PCS piping to accomplish their functions during normal operations. The upper and lower lines attached to the nozzles are closed by gate valves located in the nozzle trench area.

---

[a]. Refer to Section 5.3.3.1.5 for a discussion of the flange tube.

[b]. Refer to Section 5.3.3.1.5 for a discussion of the OSCC nozzle extension assembly.

[c]. Refer to Section 5.3.3.1.6 for a discussion of the nuclear instrument thimbles.

5.3.3.1.2 Top Head Assembly—The top head assembly (Figures 5.3-2 and -3) consists of the top head closure plate, the elliptical top head, the bolting flange, and the refueling port covers.

The top head closure plate (Figure 5.3-3 and Item II.2 of Table 5.3-2) is bolted to the top head closure plate flange with 24 closure bolts and is sealed by two O-rings. The top head closure plate is installed from inside the top head. The top head closure plate flange is welded to the top head. The top head is welded to the top head bolting flange. The top head bolting flange is double grooved to contain two O-rings to provide a coolant seal. The top head bolting flange is attached to the reactor vessel top flange with 62 top head closure studs. The studs are installed using a bolt tensioner since the top head is not normally removed during outages. Fuel handling is done through the five refueling ports described below.

The top head closure plate contains nine major penetrations for the inpile tubes or solid metal closure plugs (Table 5.3-2, Figure 5.3-3). Each penetration is sealed with a gland seal, O-rings, and locking rings similar to the bottom head penetration seal, gland seal water connection,[a] and grease fitting.[b] A 1-1/2-in. diameter penetration is positioned directly above each of the four regulating rod positions in the core. These holes are sealed by a stainless steel plug and double O-rings. They are used only when installing a new regulating rod.

The five 20 × 40-in. elliptical refueling access ports and covers (Figure 5.3-2) in the top head are equally spaced around the top closure plate, and are closed with flat-face flanges containing single grooves for O-rings. The groove in the port cover is designed to contain the O-ring when the cover is removed. Two ports are provided with individual aluminum air-purge cover plates and aluminum insets to protect the sealing surfaces during outages. Two port covers typically contain a glass viewing window for observing the reactor internals during operation.

5.3.3.1.3 Bottom Head Assembly—The bottom head assembly (Figures 5.3-2, -4) consists of the bottom hemispherical head, bottom closure plate, membrane, O-ring, and bottom head flange. The circular bottom head closure plate (Figure 5.3-4 and Item III-2 of Table 5.3-2) seats on an offset in the bottom head flange, and is installed from above (i.e., inside the vessel). The closure plate is grooved to contain an O-ring on the flat seating surface. In addition to the O-ring seal, a removable stainless steel weld membrane provides zero leakage between the bottom head and its closure plate. The bottom head flange is welded to the bottom hemispherical head, which in turn is welded to the vessel shell lower section.

The bottom head closure plate nozzles and penetrations (Table 5.3-2, Figure 5.3-4) include nine major penetrations for the in-pile tubes or solid metal closure plugs. The bottom head closure plugs are bolted to the bottom of the snubber tubes. For each position in which an inpile tube is installed, the inpile tube penetration is sealed with a gland seal, O-rings and locking rings, a warm seal water connection[c], and a grease fitting. The plate also contains the four neck shim and regulating rod penetration assembly

---

[a]. Refer to Chapter 9 (Auxiliary Systems) for a description of the Gland Seal Water System.

[b]. Refer to Section 5.3.3.1.5 for description of the in-pile tube penetration assembly.

[c]. Refer to Chapter 9 (Auxiliary Systems) for a description of the Warm Seal System.

nozzles[a], four emergency firewater inlet line nozzles, eight penetrations for the N-16 monitor assemblies, and four flush water line connections.

The center flux trap[b] baffle assembly penetrates the bottom head closure plate through the center penetration, and extends to a point 5-1/2 in. below the plate. The penetration is sealed by two O-rings and a chevron packing seal to prevent primary coolant leakage.

The bottom flange of the core support tank[c] is bolted to the bottom head closure plate.

The bottom head injection subsystem of the Emergency Firewater Injection System (EFIS)[d] is joined to the reactor vessel with welds at four 2-in. pipe stubs in the bottom head closure plate.

5.3.3.1.4 Drop Tube Assembly—Reactor internal components may be transferred underwater to the working canal through the drop tube assembly (Figure 5.3-1, -2, -5, -6). The drop tube connects to a 15-3/4-in. ID penetration in the drop tube assembly about 6 in. above the core. The drop tube assembly is welded to an opening in the vessel shell (Figure 5.3-2).

The penetration is closed during reactor operation by the drop-tube cover. The cover has a double O-ring seal and is held in place by two cam-lock, hold-down lugs.

5.3.3.1.5 Vessel Penetration Assemblies—The major reactor vessel penetration assemblies include (a) the penetration body assembly for N-16 sample tubes, (b) the inpile tube bottom head seal freeze unit and seal or bottom head closure plug assembly, (c) the pressure housing for the regulating rod and neck shim drives, (d) the flanged tubes for the horizontal drive shaft assemblies of the Safety Rod System, and (e) the nozzle extension assembly of the OSCC.

- Penetration Body Assembly (for N-16 Tubes)[e]—The N-16 tube penetration body assemblies use an O-ring seal and gasket to prevent leakage of primary coolant through the eight N-16 penetrations of the bottom head closure plate. If seal maintenance is required, the N-16 assembly must be removed and the sleeve plugged at the bottom head closure plate before the penetration body assembly can be loosened. The N-16 tube assembly is positioned by the penetration body assembly and by a bow in the tube as it passes through the core region. Flow enters the N-16 assembly through the top port in the side of the penetration body assembly and travels up through the outer tube. The flow then returns through the bottom port in the penetration body assembly.

  The center N-16 assembly is part of the center flux trap assembly and thus considered a part of the Reactor Internals.[f]

---

[a]. Refer to Section 5.3.3.1.5 for a description of the neck shim and regulating rod penetration assemblies, and N-16 tube penetration assemblies.

[b]. Refer to Chapter 3 (Design of Structures, Components, Equipment, and Systems) for a description of the center flux trap.

[c]. Refer to Chapter 3 (Design of Structures, Components, Equipment, and Systems) for a description of the Core Support and Flow Distribution System.

[d]. Refer to Chapter 6 (Engineered Safety Features) for a description of the EFIS System.

[e]. Refer to Chapter 9 (Auxiliary Systems) for a description of the N-16 system.

[f]. Refer to Chapter 3 (Design of Structures, Components, Equipment, and Systems) for a description of the center flux trap and N-16 assembly.

- Inpile Tube Bottom Head Seal—The Freeze Units attach to the penetrations for the inpile tubes in the bottom head closure plate. Where inpile tubes are not installed, the inpile tube penetrations are sealed by bolting stainless steel closure plug assemblies to the bottom head closure plate. The closure plug assemblies have four O-ring seals and bolt against the snubber tubes.

  The inner edge of the safety rod[a] inner snubber tube is sealed against the inpile tube with the upper and lower gland caps, packings, and O-rings. The lower gland cap and all packing ring sets are attached by bolts screwed to the upper gland cap. The upper gland cap is bolted to the freeze unit. The freeze unit and seal rings are attached by bolts screwed to the bottom wall of safety rod inner snubber tube forming a coolant seal. The freeze unit allows replacing the packings with inpile tubes installed. A second packing ring set is installed in the freeze unit.

- The Pressure Housing Assembly (for Neck Shim and Regulating Rod Drive Systems)—The pressure housing assembly is made up of an outer pressure housing, and both an upper and lower extension assembly. The assembly extends from the neck shim rod housing[b] vertically downward through the subpile room into the rod access room where the drive units are located, terminating at a point just below the ceiling (Figure 5.3-5).

  The pressure housing assembly serves as a guide path for the shim control drive cables and regulating rod drive rods[c], and extends the primary coolant pressure boundary to a point where the drive rods and drives are accessible for maintenance.

  A closure cap, which is fastened to the pressure housing by a lower ring attached to an upper ring on the pressure housing, serves as a watertight seal for the pressure housing. Tube fittings welded concentrically to the cap provide a means of neck shim drive cable exit.

  The regulating rod drive rod seal assembly is a labyrinth type seal, consisting of a series of bushings and a lantern ring. The seal is held in place by a special nut fitted with an O-ring seal. The seal permits the regulating rod drive rod to extend to the rod access room without breaking the watertight integrity of the pressure housing section. Gland seal water[d] is introduced at the seal assembly to prevent primary coolant from contacting the surfaces.

- Flange Tube Assemblies for the Horizontal Drive Shaft Assemblies of the Safety Rod System—The safety rod horizontal drive shaft penetrates the reactor vessel through a flange tube (Figure 5.3-7) and is supported by ball bearings. The outer wall of the flange tube is welded to the reactor nozzle as shown in Figure 5.3-7. A rotary face seal, serviced by the warm seal water system[e] attached to the flange, provides a seal surface to contain the primary coolant. An inflatable seal permits normal maintenance involving removal of the horizontal drive shaft assembly without draining the reactor vessel.

---

[a]. Refer to Chapter 3 (Design of Structures, Components, Equipment, and Systems) for a description of the Safety Rod System.

[b]. Refer to Chapter 3 (Design of Structures, Components, Equipment, and Systems) for a description of the Neck Shim Rod System.

[c]. Refer to Chapter 3 (Design of Structures, Components, Equipment, and Systems) for a description of the Regulating Rod System.

[d]. Refer to Chapter 9 (Auxiliary Systems) for a description of the Gland Seal Water System.

[e]. Refer to Chapter 9 (Auxiliary Systems) for a description of the Warm Seal Water System.

- OSCC Reactor Nozzle Extension Assembly[a]—The OSCC nozzle extension (Figure 5.3-8) is welded to the reactor vessel OSCC drive line nozzle. It extends the PCPB to the OSCC drive access area, and supports the external portions of the OSCC drive mechanisms. The drive shaft housing assembly is installed in the nozzle extension assembly. The seal between the OSCC drive shaft housing assembly outside diameter and the nozzle extension is provided by three preformed packings in grooves on the outside diameter of the drive shaft housing. The OSCC outer gearbox assembly bolts to the outer end of the nozzle extension assembly.

5.3.3.1.6 Nuclear Instrument Thimbles—The ion and fission chambers for nuclear instrumentation detectors[b] are contained in 5-in.-ID stainless steel instrument thimbles welded at the upper end to the 12 diagonal 5-in. nozzles in the reactor tank wall (see Figure 5.3-1). (See Figure 5.3-9 for a radial location of these thimbles.) Radiation streaming from these air-filled tubes is shielded by a shield plug which is bolted to the thimble flange. This shield plug also defines the air flow path (purge system)[c] out of the instrument thimble.

An adjustable sliding seal closure is installed in the instrument thimbles. The components consist of two flanged tubes designed to slide one inside the other with O-ring seals. One flanged tube fits inside the instrument thimble, suspending the shield plug and seal on the top flange of the thimble. The second flanged tube will slide inside the first flanged tube and will provide for nine individual seals around the instrument leads from the chambers inside the thimble. The sliding closure allows for adjusting the height of the ionization chambers 11.25 in. without breaking the nine seals.

5.3.3.2 Materials of Construction. Refer to Section 5.3.1 and Table 5.3-1 for reactor vessel materials of construction.

5.3.3.3 Fabrication Methods. Refer to Section 5.2.3.4 for reactor vessel fabrication methods.

5.3.3.4 Inspection Requirements. Refer to Section 5.2.4 for reactor vessel inspection requirements.

5.3.3.5 Shipment and Installation. The maturity and considerable operating history of the reactor vessel demonstrates that its as-manufactured integrity was maintained during shipment and installation. Shipping and installation were done in accordance with procedures that would result in avoiding damage to the vessel and preclude application of loads to components.

5.3.3.6 Operating Conditions. Refer to Section 5.3.2.2 for reactor vessel operating conditions.

5.3.3.7 Inservice Inspection. Refer to Section 5.2.4 for reactor vessel ISI.

---

[a]. Refer to Chapter 3 (Design of Structures, Components, Equipment, and Systems) for a discussion of the OSCC System.

[b]. Refer to Chapter 7 (Instrumentation and Controls) for a description of the ATR nuclear instrumentation.

[c]. The thimble purge system is considered a subsystem for the plant air system described in Chapter 9 (Auxiliary Systems).

Table 5.3-1. Reactor vessel design and performance characteristics.[a]

Parameters	Data
Materials	
Vessel	SA-240 304 stainless steel (< 0.06% carbon)
Pressure housing upper extension, and lower extension guide tube	Inconel
Vessel flanges	SA-336, SA-182, 304 stainless steel
Bolts	SA-193, GR.B14 stainless steel
Pipe	SA-376, stainless steel
Tubing	SA-213, stainless steel
Design pressure	390 psig
Design temperature	240°F
Outside diameter	12 ft
Overall height	35 ft
Total volume	3,250 ft^3
Operating pressure (reactor core)	260-360 psig
Operating temperature	125-170°F
Empty weight	205,000 lb

a. Data from deBoisblanc and Cohen (1965).

Table 5.3-2. Reactor vessel nozzles and penetrations.

Nozzle or penetration	Quantity	Nominal size ID (in.)	Plant elevation
I. Reactor- vessel shell			
1. Upper drain nozzle	1	8	96 ft 3 in.
2. Experiment loop piping (L1 through L-4)	4	12	96 ft 3 in.
3. Instrument thimble nozzles (35° from vertical)	12	5	94 ft 9 in.
(T1 through T-12)	9	10	94 ft 7 in.
4. Experiment loop piping penetrations	16	3-1/16	93 ft 6 in.
(L-5 through L-13)	1	8	91 ft 2 in.
5. Instrumented capsule penetrations	4	15-1/4	85 ft 10 in.
(C-1 through C-16)	8	3	82 ft 7 in.
6. Lower drain nozzle	1	16	82 ft 4 in.
7. Coolant outlet nozzles	8	6-3/4	72 ft 5 in.
8. Outer shim control drive line			
9. Drop tube (24° from vertical)			
10. Safety rod drive line nozzles			
II. Reactor vessel top head assembly			
1. Elliptical refueling ports	5	20 x 40	100 ft 5 in.
a. Air purge port	5	9-3/4	100 ft 5 in.
2. Top head closure plate opening	1	38	100 ft 5 in.
a. Loop inpile tube penetrations	9	6-9/16	100 ft 5 in.
b. Regulating rod penetrations	4	1-1/2	100 ft 5 in.
III. Reactor bottom head assembly			
1. Bottom hemispherical head	2	23-1/4	69 ft 5 in.
a. Coolant inlet nozzles			
2. Bottom head closure plate opening	1	52-7/8	66 ft 10 in.
a. Loop in pile tube penetrations	9	5-1/4	66 ft 10 in.
b. Neck shim drive line nozzle	4	2	66 ft 10 in.
c. Flush-water line penetrations	4	1-7/8	66 ft 10 in.
d. N-16 assembly penetrations	8	3/4	66 ft 10 in.
e. Emergency firewater injection inlet	4	2	66 ft 10 in.

CHAPTER 5 – PRIMARY COOLANT SYSTEM - UPGRADED FINAL SAFETY ANALYSIS REPORT FOR THE ADVANCED TEST REACTOR	**Identifier:** SAR-153 **Revision:** 9 **Page:** 5-63 of 5-92 **Effective Date:** 08/10/04

FOIA Exemption 3 UCNI, Exemption 7f (Page 5-62 - 5-63 – detailed reactor vessel drawings)

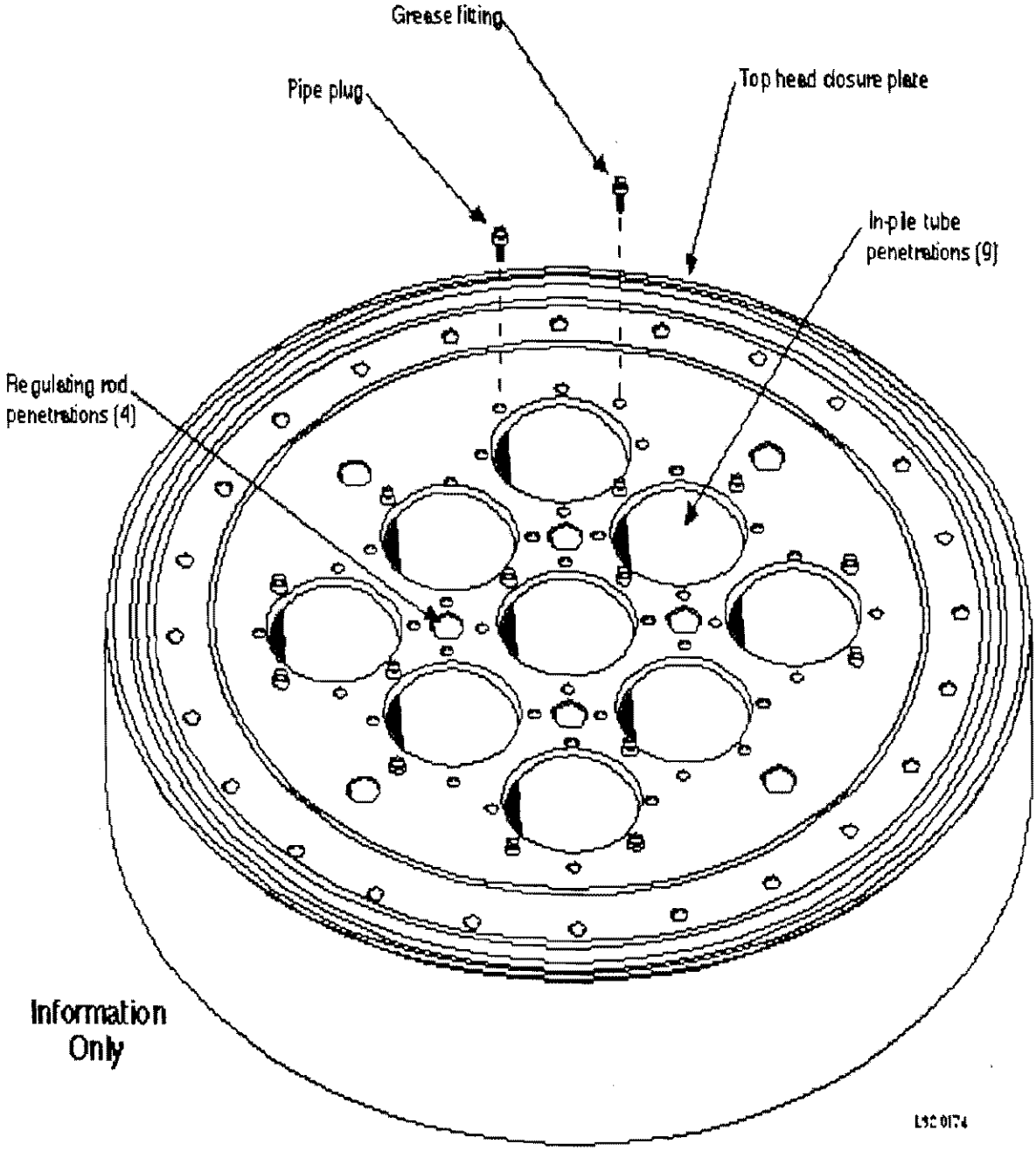

Figure 5.3-3. Top head closure plate. **(For Information Only)**

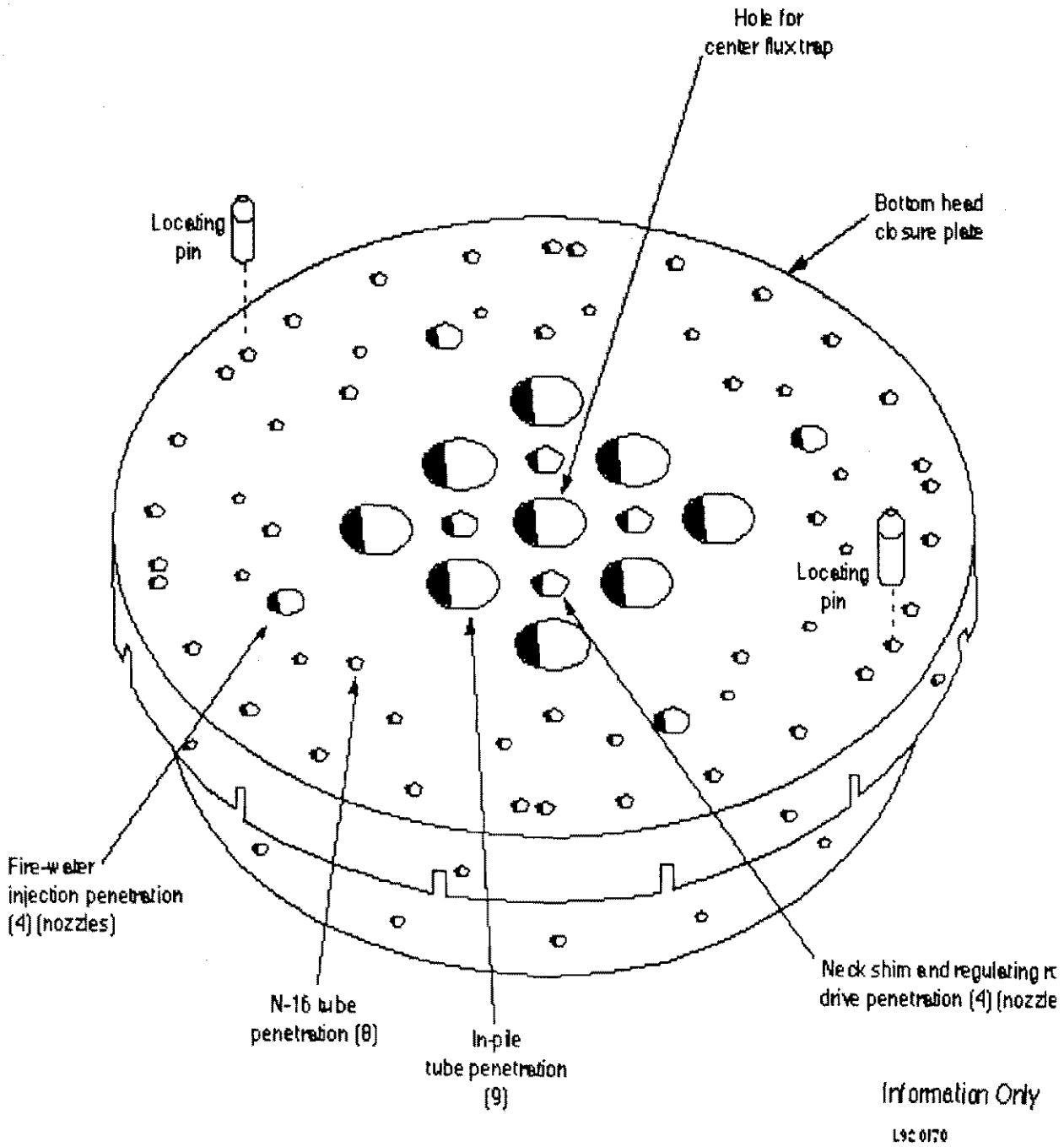

Figure 5.3-4. Bottom head closure plate. **(For Information Only)**

FOIA Exemption 3 UCNI, Exemption 7f (Page 5-66 – detailed reactor drawing)

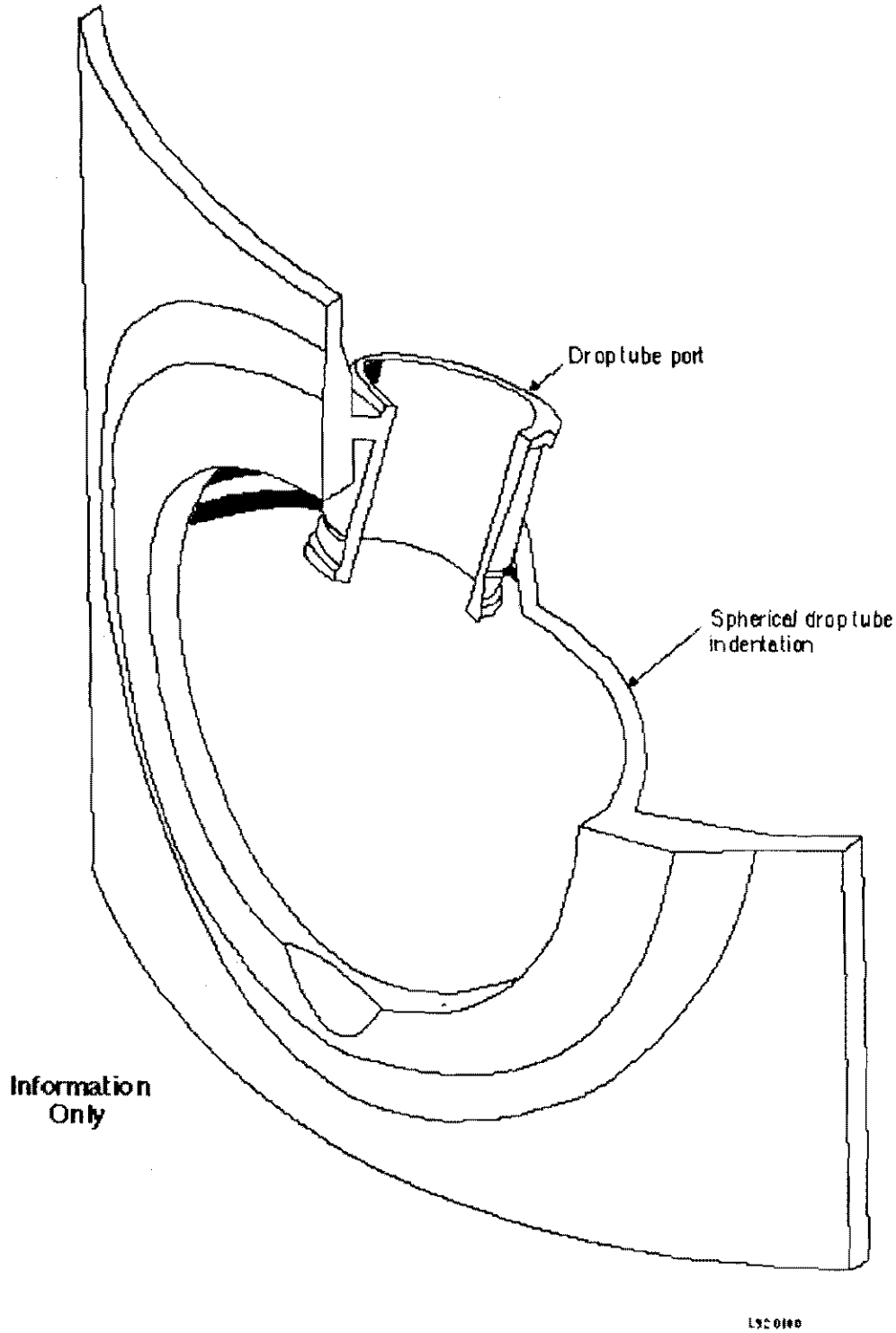

Figure 5.3-6. Reactor vessel drop tube assembly. **(For Information Only)**

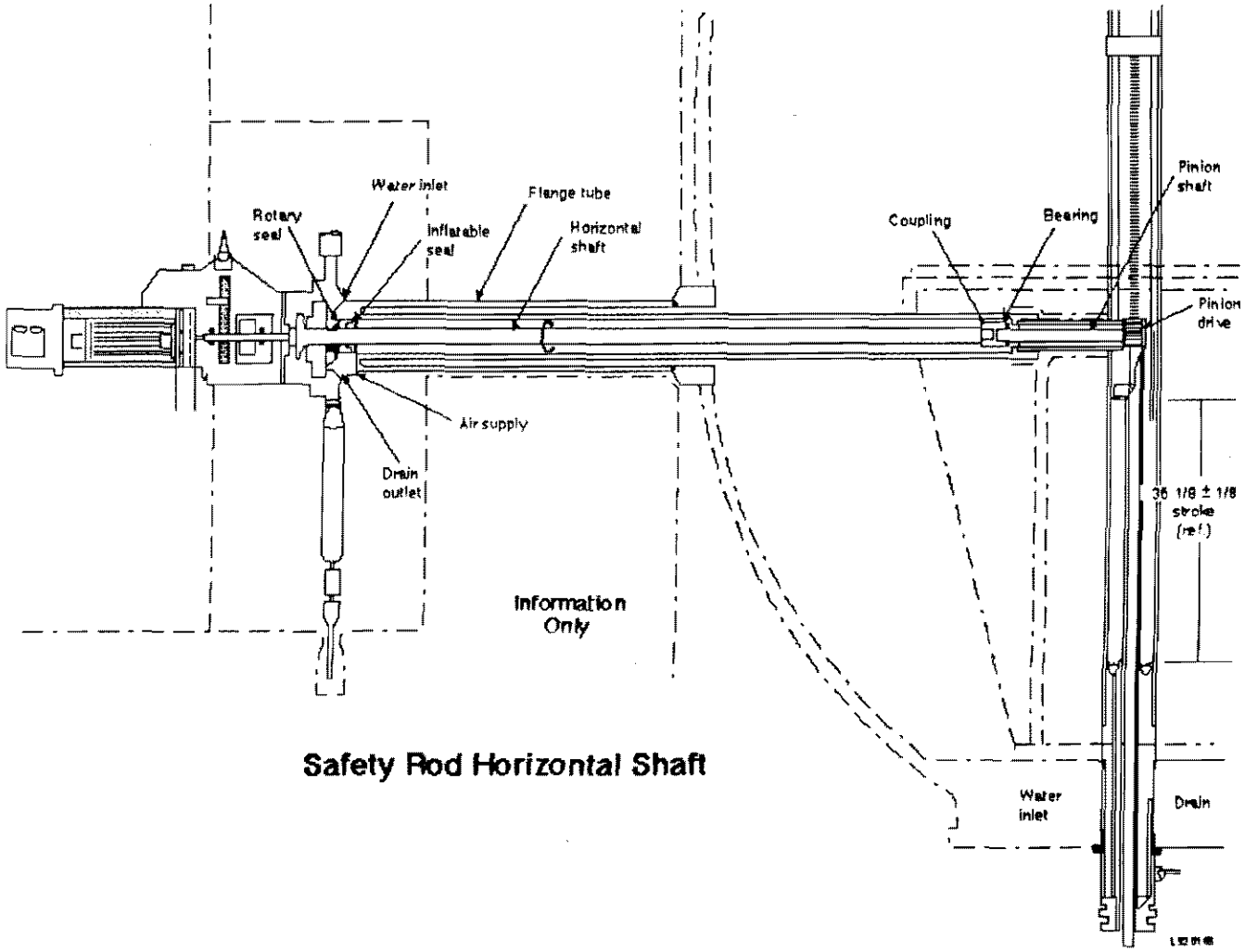

Figure 5.3-7. Safety rod horizontal shaft. **(For Information Only)**

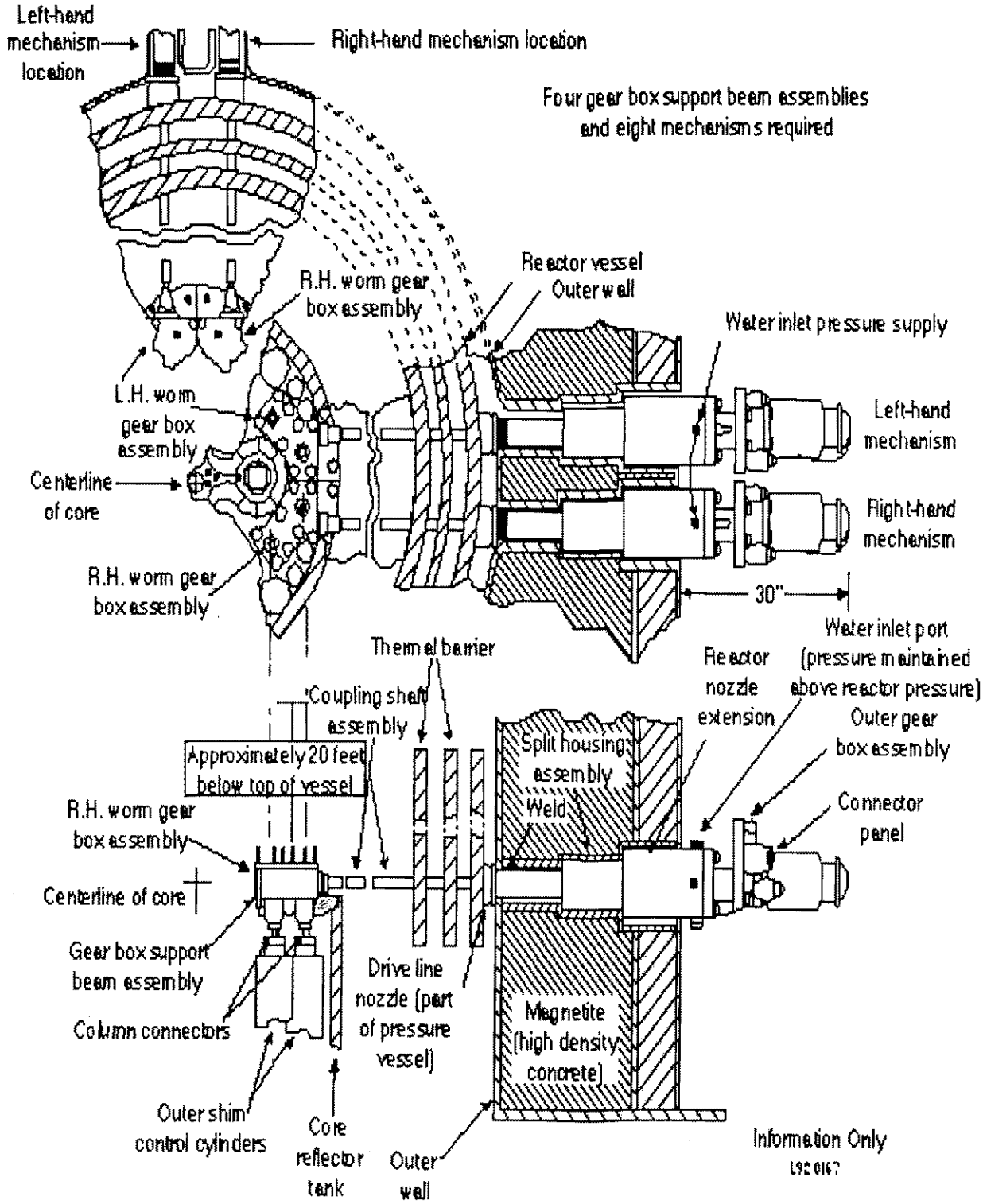

Figure 5.3-8. Outer shim control drive. **(For Information Only)**

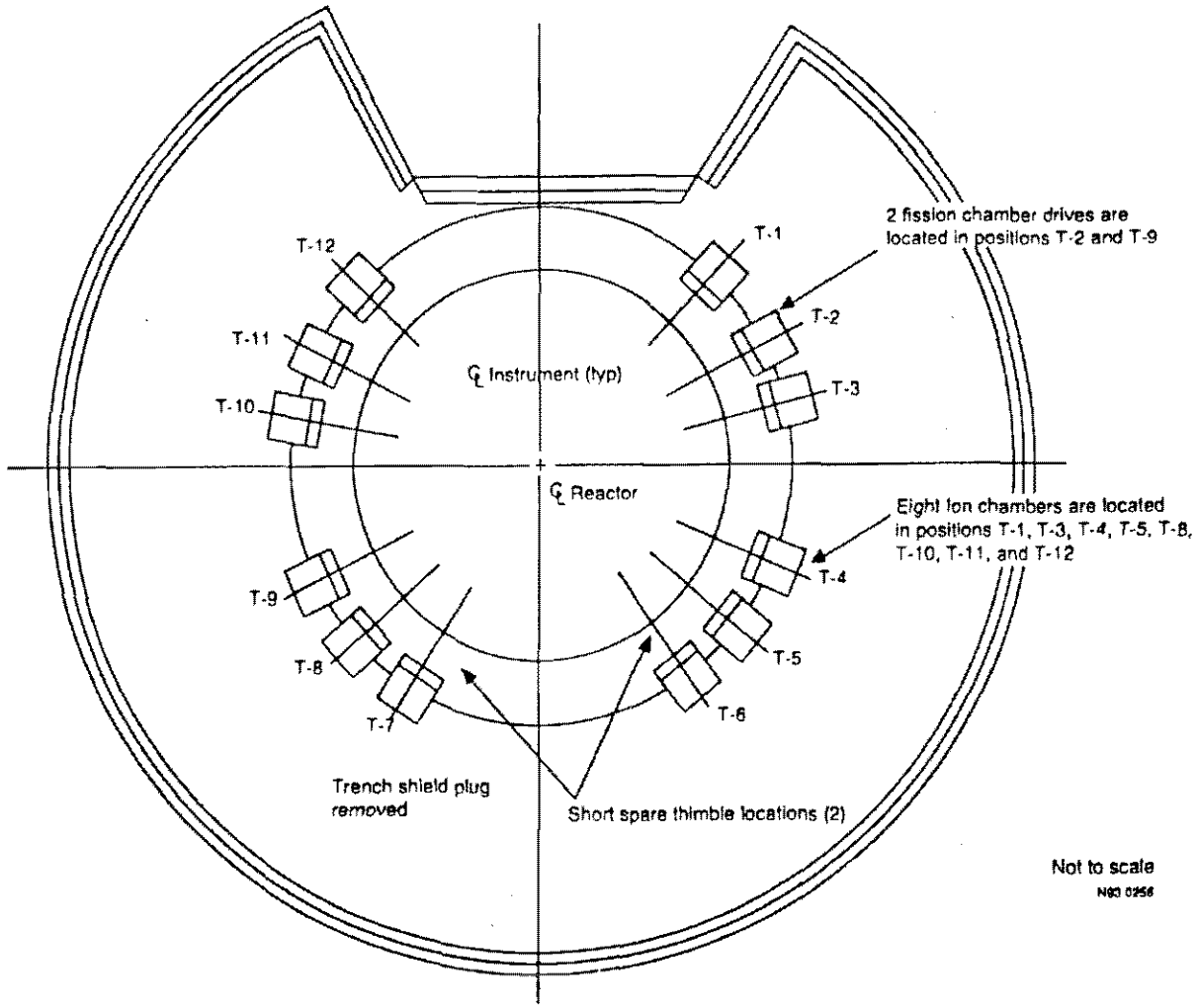

Figure 5.3-9. Instrument thimble positions. **(For Information Only)**

5.4 Component and Subsystem Design

The PCS components described in this section are (a) the PCS primary coolant pumps, (b) the heat exchangers, (c) PCS pipes and valves, (d) the emergency coolant pumps, (e) the surge tank, (f) the degassing tank and pressurizing pumps, and (g) equipment supports. Table 5.4-1 tabulates important design and performance characteristics of the PCS components described in this section.

For future modifications within the PCS radiographic limits, Section XI of the ASME Code as implemented by the ATR ISI Plan (INEEL 2002) shall apply.

Due to the low radioactivity of the fluid in the PCS, there is a negligible effect on the material properties of PCS piping and components.

As previously mentioned in Section 5.2.3.2, radioactivity-level limits allow maintenance to be performed while staying within the acceptable exposure guidelines, and ensure control of radioactive releases to the environment. If necessary, PCS coolant is circulated and cleaned through bypass demineralizer ion-exchange columns before release via the liquid waste effluent discharge system. Refer to Chapter 12 (Radiation Protection) for a summary of calculated dose rates.

Shielding for certain areas has been provided for limited access during particular periods of the overall operation. It is uneconomical to provide shielding in all areas to all unrestricted access (deBoisblanc and Cohen 1965). The non-shielded areas are placed under administrative control with respect to entry procedures and time of access (deBoisblanc and Cohen 1965). Refer to Chapter 12 (Radiation Protection) for a discussion of these areas together with possible radiation sources.

5.4.1 Primary Coolant Pumps

The primary coolant pumps are horizontal, double suction, volute centrifugal-type pumps driven by 2,000 hp electric motors. Each primary coolant pump (M-6, M-7, M-8, M-9 in Figures 5.1-1, -10) was designed for, and will exceed, 18,000 gpm at a total dynamic head (TDH) of 400 ft (171 psi when pumping 130°F primary coolant). The primary pumps start and stop manually with controllers on the Distributed Control System. Pump discharge check valves prevent reverse flow through a standby, or inoperative pump. Following loss and subsequent restoration of power, the pumps require a manual restart.

The four primary coolant pumps, arranged in parallel, are located in the first basement south of the heat exchangers. Each pump is in a shielded cubicle, and is provided with pump casing vent valves and piping drain valves. Refer to Chapter 12 (Radiation Protection) for a discussion of shielding and dose rates in the pump motor area. Hatch covers in the main floor permit servicing individual cubicles.

Primary coolant pumps M-8 and M-9 are powered[a] from the 4160V commercial bus section A (670-E-1), and primary coolant pumps M-6 and M-7 are powered from the 4160V commercial bus section B (670-E-2). Due to the relatively low pressure of the ATR PCS, specific systems to preclude rotor overspeeding of the primary coolant pumps in the event of a design-basis Loss of Coolant Accident (LOCA) do not exist. In addition, rotor overspeeding is not expected because of the unsaturated condition of the primary coolant and the low frequency of operation of the primary pump motors.

---

[a]. Refer to Chapter 8 (Electric Power) for a description of the electrical power systems.

5.4.1.1 Pump Flywheel Integrity. ATR primary coolant pumps do not have flywheels; therefore, this section is not applicable.

5.4.1.2 Design Characteristics. Refer to Table 5.4-1 for the primary coolant pump design characteristics. PCS head curves with one-, two-, three-, and four-pump operation are shown in Figure 5.4-1.

5.4.1.3 Materials of Construction. The materials of construction are given in Table 5.2-3 and discussed in Section 5.2.3.

5.4.1.4 Codes and Tests. As discussed in deBoisblanc and Cohen (1965), the primary coolant pumps were designed and constructed in accordance with the Centrifugal Pumps Section of the Standards of the Hydraulic Institute, 10th edition, and tested and inspected as follows:

- All four pumps were shop tested with cold water at rated speed from the shutoff head to 120% of design capacity. The following data were recorded:
  - Head versus capacity
  - Overall efficiency versus capacity
  - kW input versus capacity
  - Results of seal leakage tests.
- All pump casings were hydrostatically tested at 585 psig.
- All pump tests were in accordance with ASME Power Test Code for Centrifugal Pumps, PTC 8.1, 1954 edition.

The status of programs to protect against passive mechanical failures in components such as standby pumps is addressed in Chapter 3 (Design of Structures, Components, Equipment, and Systems).

5.4.2 Heat Exchangers

The five parallel primary heat exchangers (M-2, -3, -4, -5, -85 in Figures 5.1-1, -10) are vertical, head-down, U-tube type heat exchangers. Flanges are provided at the heat exchanger inlets and outlets. The primary side of each heat exchanger may be isolated with blind flanges for maintenance and/or chemical cleaning. The secondary side of each heat exchanger may be isolated using existing block valves. Heat exchanger primary-side drain and blowdown connections permit individual heat exchanger blowdown and removal of debris, such as broken flux wires.

Access to the tube sheet is by removal of the heat exchanger bottom head or manways in the bottom head. Access platforms permit tube bundle inspection through shell inspection ports.

Refer to Table 5.4-1 for design characteristics of the heat exchanger.

5.4.2.1 Materials of Construction. The materials of construction are given in Table 5.2-3 and discussed in Section 5.2.3.

5.4.2.2 Codes and Tests. The primary heat exchangers are designed and constructed in accordance with the ASME Unfired Pressure Vessel Code, Section VIII, 1959 Edition; and General Requirement for Nuclear Vessels, Special Ruling Case 1270 N-5 (deBoisblanc and Cohen 1965). As discussed in deBoisblanc and Cohen (1965), they were tested and inspected as follows:

- Shell and tube side of each heat exchanger were hydrostatically tested in accordance with Paragraph UG-99 of the ASME Unfired Pressure Vessel Code, 1959.
- All shell and channel pressure welds were fully radiographed in accordance with Paragraph UW-51 and Code Case 1270 N of the ASME Unfired Pressure Vessel Code, 1959.
- All tubes were completely liquid-penetrant tested before bending. After bending, the bent area was liquid-penetrant tested in accordance with the Commercial Dye Penetrant Test Procedure of the Huntington Alloy Products Division of the International Nickel Company, Inc.
- All welded joints, tube-to-tube sheets, were liquid-penetrant tested in accordance with the manufacturer's standard.
- Clad-tube sheet plates and all tubes were examined by ultrasonic test (Immersion Technique) in accordance with the applicable Nondestructive Testing Method described in MIL-STD-271 (deBoisblanc and Cohen 1965).

5.4.3 Primary Coolant Piping

5.4.3.1 General Arrangement. Refer to Figures 5.1-1, -2, and Figures 5.1-3 through -10 for the general arrangement of PCS piping and components. The main PCS piping ranges in size from 6- to 36-in.-nominal diameter.

5.4.3.2 Design Characteristics. The PCS piping was constructed in accordance with rules of the Code for Pressure Piping, ASA B31.1-1955 (deBoisblanc and Cohen 1965). Analyses are on record that the piping satisfied the requirements of that code (Burr 1978).

All welded joints on pipes larger than 3 in. in diameter, including the first isolation valve on branch piping for auxiliary systems, were radiographed. A sampling of accessible welds is inspected periodically. All branches and interfaces of the main PCS connect with a normally closed valve or orifice with a 3-in. or less diameter. As previously described in Section 5.1.1, these interfaces establish the radiographic boundary.

Stainless steel pipe welding was performed by the tungsten inert gas process, or by the combined tungsten inert gas and shielded metal arc process. All welding operators were qualified under the applicable code requirements, and all welds are marked with the welding operators' identification. Socket welds, fillet welds, and hanger attachment welds were not radiographed. All socket, fillet, and groove welds were inspected for surface defects by a liquid penetrant method, and all pressure-retaining welds that could not be radiographed were inspected by the liquid-penetrant method after completion of each half inch of weld thickness. All repair welding of defects was reinspected.

PCS piping is designed to operate with a water chemistry as identified in Table 5.1-2. The radiation field to which the piping is subjected is not of sufficient magnitude to change the material mechanical properties. No provisions need be made for corrosion of austenitic stainless steels.

The PCS was designed, according to construction code ASA B31.1-1955 (ASME 1955), for pressures and temperatures of (a) 390 psig and 240°F (from butterfly valve to pump suction); and (b) 485 psig and 150°F (pump discharge to butterfly valve) (deBoisblanc and Cohen 1965; Hope 1976). Further analysis (Macek 1976; Morton 1983) established that the section from the pump discharge to the first block valve downstream of the pump has a design pressure of 576 psig according to ASME Section III, Class 1 (the most recent evaluation is based on the 1980 version of the code), which is equivalent to the original design code. See Table 5.1-2(c) and (d).

The pressure limits provide an allowance of 10% transient overpressure above design according to the code rules except for the piping section from the butterfly valve to the vessel outlet that has an allowance of 20% transient overpressure (Burr 1978). Periodic hydrostatic testing to demonstrate continued integrity of the PCS is done at 10% above nominal operating pressures.

Additional analysis (Macek 1975) established that the piping between discharge and butterfly valve meets the requirements of ASME, Section III, Subsection NB for emergency temperature conditions of 240°F. The analysis also shows that a safety limit of 468 psig (585 psig when under hydrostatic testing) is acceptable in the ATR vessel and PCS piping downstream of the main butterfly control valve BF-A-14 (Macek 1975).

Nominal PCS steady state operating conditions for two- and three-pump operation are listed in Table 5.1-2(b).

All piping modifications require that nondestructive examinations such as radiography, ultrasonic examination, magnetic particle inspection, liquid penetrant examination, and leak testing are performed and evaluated in accordance with the requirements of the ATR ISI Plan (INEEL 2002).

The only dynamic loads to be considered are those due to earthquake motion. Seismic restraints and snubbers have been incorporated into the PCS design (Davidson and Thinnes 1974). The PCS has been operated since 1967 with no visually observable system vibration.

A design analysis of the ATR PCS piping was completed in 1979 (Davidson 1979), updating the stress analysis from the original safety analysis (deBoisblanc and Cohen 1965). All PCS piping was analyzed except for the reactor vessel drain, relief valve piping, and firewater piping. The calculated stresses were then compared with allowable stresses from ASME Code Section III, 1977, shown in Table 5.2-4. The various hangers and supports were checked for compliance with Subsection NF-3200 and XVII-2000 of the 1977 ASME Code. Overstressed components were identified, and components that did not meet the design criteria were noted. With those exceptions, the report found that the PCS satisfied the 1977 ASME Section III, Division 1, code requirements (ASME 1977).

Among the components of the PCS are nonstandard piping components that do not qualify for the simplified analysis procedures (NB-3650) of the ASME Code, Section III Division 1, Subsection NB. These components have undergone detailed stress analyses for pressure, deadweight, thermal, and seismic loading. They have been successfully evaluated for acceptability for these loads according to the criteria of the code (House 1995).

The nonstandard components include several different configurations:

(a) elbow-branch connections, (b) stub-in branch connections, (c) eccentric reducers, (d) short radius elbows, (e) Y-laterals, and (f) a pipe cap with stub-in pipe. The Y-lateral is constructed of a section of piping that is welded to the PCS piping system at both ends to form a straight run, and a smaller-diameter branch section that intersects the run at a 45-degree angle. The other end of the branch pipe is welded to a short spool piece of piping that, in turn, is welded to a 45-degree elbow.

Refer to Chapter 12 (Radiation Protection) for a discussion of PCS piping shielding and dose rates.

5.4.3.3 Testing Conditions. All piping was hydrostatically tested at 150% of design pressure. In accordance with the ATR ISI Plan (INEEL 2002), the piping is periodically pressure tested.

5.4.3.4 Materials of Construction. The materials of construction are given in Table 5.2-3, and discussed in Section 5.2.3. PCS piping was constructed of materials that provide the least possible amount of contaminants to the PCS. All piping and flange materials for the PCS are 300 series austenitic stainless steel. Type 304L stainless steel piping meets the chemical requirements of ASTM A-312-61T (deBoisblanc and Cohen 1965). Buried and embedded piping is 304L, either seamless per ASTM A376-60T or welded per ASTM A358-60T as stated in ASA B31.1-1955 Code for Pressure Piping Case N-7 (deBoisblanc and Cohen 1965). Dimensions for nominal wall pipe are in accordance with ASA B36.19-1957 (deBoisblanc and Cohen 1965).

5.4.4 Main Steam Line Flow Restrictions

Not applicable in the ATR.

5.4.5 Main Steam Line Isolation System

Not applicable in the ATR.

5.4.6 Reactor Core Isolation Cooling System

Not applicable in the ATR.

5.4.7 Decay Heat Removal

ATR has multiple means for performing the decay heat removal (DHR) function, as shown in Table 5.4-2 and Figure 5.4-2. The first two decay heat removal methods involve closed-loop heat transfer paths from the PCS to the atmosphere via the ATR cooling tower (i.e., the ATR normal heat sink).

The next three DHR methods in Table 5.4-2 involve heat transfer paths in which makeup is provided to the PCS and heat is removed by draining water from the PCS. The final decay heat removal method involves passive heat transfer from the reactor vessel to the building structures. Passive heat transfer is a short-term method. Long-term DHR is accomplished by the methods listed above.

5.4.7.1 Design Bases. Table 5.4-2 lists the UFSAR chapters in which the design basis for the various DHR means are described.

5.4.7.2 System Design. Figure 5.4-2 is a simplified schematic for the various DHR means referenced in Table 5.4-2. The dedicated means for providing DHR, i.e., the emergency coolant pumps, is described in this section under 5.4.7.4. Refer to Chapter 6 (Engineered Safety Features) for a schematic piping and instrumentation diagram (P&ID) of the EFIS, and to Chapter 9 (Auxiliary Systems) for schematics of the Secondary Coolant System, the Low Pressure Demineralized Water System, and the Raw Water and Fire Water Supply Systems.

5.4.7.3 Performance Evaluations.

5.4.7.3.1 General Design Criterion 34: Redundancy—As required by ATR General Design Criterion (GDC) 34[a] for decay heat removal systems, "suitable redundancy in components and features, and suitable interconnections, leak detection, isolation and confinement capabilities shall be provided to ensure that for onsite electric power system operation (assuming offsite power is not available) and for offsite power system operation (assuming onsite power is not available), the system safety function can be accomplished assuming a single failure."

Physical separation of redundant systems is particularly important from the standpoint of reducing the potential for common mode failure caused by external events such as earthquake, flooding, tornados, and fire. Redundancy and related requirements for DHR systems were reviewed (Buescher 1993) as part of a broader evaluation of physical and electrical separation of ATR cooling water systems. As shown in Table 5.4-2, redundant and diverse systems are available for accomplishing the DHR function. These functions can be accomplished by means that do not depend upon the ATR electric power (i.e., passive DHR, or firewater injection for DHR). In addition, physical separation of redundant systems is provided since the firewater storage tanks and pumps are not located in, or in the immediate vicinity of, the ATR reactor building. The review concluded that while the DHR systems are quite different in design from systems performing these functions in commercial nuclear power plants and may not be uniformly designed as safety class systems, the ATR systems substantially meet the same functional requirements. Additionally, the reliability of the emergency flow function was evaluated in Chapter 15 (Accident Analyses).

5.4.7.4 Emergency Coolant Pumps. Two emergency coolant pumps (M-10 and M-11 in Figures 5.1-1, -10), each having a capacity of 4,700 gpm at 22 ft Total Dynamic Head (TDH), provide reactor decay-heat removal capability. The emergency coolant pumps are horizontal, double suction, volute centrifugal type with 40-hp electric motors.

Emergency coolant pump M-10 is ac motor-driven from the 480V diesel-commercial bus 670-E-15. The second pump, M-11, is dc motor-driven from the utility dc power control center, 250 Vdc bus 670-E-23.

The operating emergency coolant pump normally discharges 250 gpm through a recirculation line to the primary pump suction header. On loss of primary coolant pressure, the check valve on the emergency coolant pump discharge (normally closed by primary pump pressure) opens, enabling the emergency coolant pump to circulate approximately 4,500 gpm in the primary coolant loop.

---

[a]. Refer to Chapter 3 (Design of Structures, Components, Equipment, and Systems) for development of ATR General Design Criteria.

When the ac pump M-10 is the operating emergency coolant pump, the dc pump M-11 is placed in standby condition. The dc-driven emergency coolant pump M-11 can be automatically started and reach full speed within seven seconds (deBoisblanc and Cohen 1965). Automatic starting of the M-11 pump backs up the operating ac-driven M-10 pump, should any of the following events (which result in reactor scram) occur (deBoisblanc and Cohen 1965):

- Mechanical or electrical failure of the ac-driven M-10 pump or low M-10 recirculation flow, sensed by means of orifice/transmitter in the recirculation line
- Loss of diesel power or diesel undervoltage sensed by low phase voltage switches
- Loss of commercial power (indirectly by loss of all primary pumps).

Should a scram occur for reasons other than loss of either diesel or commercial power or both, the dc pump is not started because the primary pumps and the ac emergency coolant pump remain in operation (deBoisblanc and Cohen 1965).

When the dc pump M-11 is the operating pump, the ac pump M-10 will start automatically when any of the following occur:

- Low recirculation flow on the operating dc pump M-11.
- All four primary pumps off.
- Undervoltage on the diesel bus.
- Loss of power to pump M-11 due to loss of the 250V dc bus.

If the standby emergency coolant pump does not start in 10 seconds, the PPS scrams the reactor. For operations at atmospheric pressure, the reactor scrams as soon as the operating emergency coolant pump fails.

Operation of emergency coolant pump(s), in addition to the safety limits on core thermal performance parameters, protects the fuel element cladding from adverse effects resulting from low PCS flow. Operation with a minimum of 3,600 gpm flow, as supplied by one emergency coolant pump, is adequate to protect fuel element cladding from overheating for total power levels up to 9 MW_t. The reliability of the emergency flow system is increased by supplying M-11 with battery-backed power. In addition, the overload protection is bypassed when pump M-10 is not running. M-11 is effectively designed to run to destruction in order to supply emergency coolant as long as possible.

During reactor outages, the emergency coolant pumps are needed to ensure that cooling capability is maintained when there is significant decay heat to be removed. This typically occurs following reactor operation at significant power, and is controlled by the time limit for cooling before fuel elements are moved to the canal. During other times, the emergency coolant pumps are not required.

5.4.7.4.1 Design Characteristics—Refer to Table 5.4-1 for the emergency coolant pump design characteristics.

5.4.7.4.2 Materials of Construction—The materials of construction are as given in Table 5.2-3.

5.4.7.4.3 Codes and Tests—The M11 emergency coolant pump was designed and constructed in accordance with the Centrifugal Pumps Section of the Standards of the Hydraulic Institute, 10th edition. The M-10 pump was designed and constructed in accordance with ASME Section III, Division 1 Subsections NB 2573, 2575, and 2576, 1989 edition or later. The pumps were tested and inspected as follows:

- Both pumps were shop tested with cold water at rated speed from shutoff head to 120% of design capacity. The following data were recorded:
  - Head versus capacity
  - Overall efficiency versus capacity
  - kW input versus capacity
  - Results of seal leakage tests
  - Pump vibration amplitude
  - Amplitude, peak to peak
  - Amplitude, maximum displacement from normal.
- Both pumps were shop tested at a capacity of 250 gpm for six hours duration to check performance at the recirculation operating condition.
- Both pump casings were hydrostatically tested at 585 psig.
- The M-11 tests were in accordance with ASME Power Test Code for Centrifugal Pumps, PTC 8.1, 1954 edition. The M-10 tests were in accordance with ASME PTC 8.2, 1989 edition.
- Performance curves for the emergency coolant pumps are shown in Figure 5.4-3.

5.4.8 Reactor Water Cleanup System

Not applicable in the ATR.

5.4.9 Main Steam Line and Feedwater Piping

Not applicable in the ATR.

5.4.10 Surge Tank, Primary Degassing and Pressurizing Subsystem

PCS pressure control is provided by the surge tank and the degassing and pressurizing subsystem. Reactor inlet pressure is controlled by automatic adjustment of the system outflow to the degassing tank, through pressure control valve PCV-1 (Figures 5.1-1, -2), to balance the preset flow from the pressurizing pumps and in-leakage from various seals.

5.4.10.1 Surge Tank. The surge tank (M-12 on Figures 5.1-1, -2) was designed to accommodate primary coolant volume changes during start-up and shutdown pressure transients without initiating power reductions due to high or low pressure. About 50 ft^3 of air at 235 to 245 psig (255 to 265 psig for two-pump operation) is normally contained in the 1,000 ft^3 surge tank, which is connected to the primary loop near the primary heat exchanger outlet in the heat exchanger room.

Compressed air[a] is admitted periodically to the surge tank to restore air inventory lost through absorption in primary coolant or to initially pressurize the tank after draining and refilling. All admission or discharge of air is under manual control. Double control valves and a check valve are used for admitting 285-psig compressed air to the surge tank. Double control valves are also used for air discharge. In addition, a surge tank low-level switch will automatically close the air admission valves. This prevents an excessive air inventory, which could overflow from the surge tank into the primary circulating system if coolant volume is reduced by contraction, leakage, and/or depressurization.

5.4.10.1.1 Design Characteristics—Refer to Table 5.4-1 for surge tank design characteristics.

5.4.10.1.2 Materials of Construction—The materials of construction are given in Table 5.2-3.

5.4.10.1.3 Codes and Tests—The surge tank was designed and constructed in accordance with the ASME Unfired Pressure Vessel Code, Section VIII, 1959, latest addenda (ASME 1959), and General Requirements for Nuclear Vessels, Special Ruling Case 1270 N-5 (deBoisblanc and Cohen 1965).

The surge tank was tested and inspected as follows (deBoisblanc and Cohen 1965):

- The tank was hydrostatically tested in accordance with Paragraph UG-99 of the ASME Unfired Pressure Vessel Code, 1959.
- All welds were fully radiographed in accordance with Paragraph UW-51 and Code Case 1270 N of the ASME Unfired Pressure Vessel Code, 1959.

5.4.10.2 Degassing Tank. The degassing tank (M-13 in Figures 5.1-1, and 5.1-10) removes gases so that bubbles will not form in any part of the primary system (deBoisblanc and Cohen 1965). The degassing tank also serves as a reservoir for the operating pressurizing pump so a fixed volume of water can be forced back into the PCS loop on the suction side of the primary pumps.

The gas concentration in the coolant is maintained in dynamic equilibrium by continuously spraying a preset quantity of primary coolant at reactor exit temperature and pressure into the tank, which is maintained at slightly less than atmospheric pressure.

The primary coolant entering the degassing tank is sprayed down from the top of the tank through spray nozzles. Air from the sweep line, which is open to the atmosphere through check valve VR-A-1-52 (shown on Figure 5.1-3), enters the degassing tank at a level slightly higher than the tank overflow level. This air passes up through the water as it is sprayed from the nozzles, sweeps out the gasses that have been released from the depressurized coolant, and carries them through the separator SP-A-1-51 (shown on Figure 5.1-3), to the blower 670-HVE-18 (shown on Figure 5.1-3), which provides the negative pressure on the degassing tank and discharges the sweep air and gases to the ventilation exhaust plenum.[b]

---

[a]. Refer to Chapter 9 (Auxiliary Systems) for a description of the compressed air system.

[b]. Refer to Chapter 9 (Auxiliary Systems) for a description of the Heating and Ventilation System.

The separator removes any water that has been swept out of the air and diverts this water back to the degassing tank overflow line. A goose-neck in the overflow line prevents spray from the nozzles from running down the overflow line to the warm waste tank. The overflow level is approximately 86%, as read on LRC-1-3 (the degassing tank level).

The gas removal design and capacity is based upon the following calculated gas production rates (deBoisblanc and Cohen 1965):

	cm^3 (STP)/min
Radiolytic decomposition	1,800
H_2 from corrosion	100
Air from the surge tank	4,870
Air in seal and makeup water	3,410
Krypton and xenon (0.5% gas in one fuel plate)	Kr-0.441 × 10-5
	Xe-2.38 × 10-5

With the above gas production rates and available degassing flow rate, the maximum equilibrium gas concentrations in the primary coolant will be as follows (deBoisblanc and Cohen 1965):

H_2 - 1.15 cm^3/L

O_2 - 5.62 cm^3/L

N_2 - 11.7 cm^3/L.

5.4.10.2.1 Design Characteristics—Refer to Table 5.4-1 for degassing tank design characteristics.

5.4.10.2.2 Materials of Construction—The materials of construction are given in Table 5.2-3.

5.4.10.2.3 Codes and Tests—The degassing tank was designed and constructed in accordance with the ASME Unfired Pressure Vessel Code, Section VIII, 1959 Edition, and the General Requirement for Nuclear Vessels, Special Ruling Case 1270 N-2.

As described in deBoisblanc and Cohen (1965), the degassing tank was inspected and tested as follows:

- The tank was inspected and stamped in accordance with the ASME Code for Unfired Pressure Vessels, Section VIII, 1959 Edition, Paragraphs UG-90 through UG-120, UW-46 through UW-52, UCL-50 through UCL-55, and the General Requirements for Nuclear Vessels, Special Ruling Case 1270 N-2 (deBoisblanc and Cohen 1965).
- The completed tank and internals were hydrostatically tested at 1.5 times the maximum design pressure, and vacuum tested at 3 psia.

5.4.10.3 Primary Pressurizing Pumps. Two primary pressurizing pumps (one standby) are horizontal, volute, centrifugal type pumps driven by 100-hp electric motors. Each pump (M-14, M-15 in Figure 5.1-1, -10) was designed for a capacity of 300 gpm at a total dynamic head (TDH) of 695 ft. The two pressurizing pumps, arranged in parallel, are located west of the heat exchangers in the second basement. Each pressurizing pump can be powered from either a diesel or a commercial bus.[a]

5.4.10.3.1 Design Characteristics—Refer to Table 5.4-1 for the pressurizing pump design characteristics.

5.4.10.3.2 Materials of Construction—The materials of construction are as given in Table 5.2-3.

5.4.10.3.3 Codes and Tests—The primary pressurizing pumps were designed and constructed in accordance with the Centrifugal Pumps Section of the Standards of the Hydraulic Institute, 10th edition (deBoisblanc and Cohen 1965).

As described in deBoisblanc and Cohen (1965), the primary pressurizing pumps were tested and inspected as follows:

- Both pumps were shop tested with cold water at rated speed from the shutoff head to 120% of design capacity. The following data were recorded:
  - Head versus capacity
  - Overall efficiency versus capacity
  - kW input versus capacity.
- All pump casings were hydrostatically tested at 585 psig.
- All pump tests were in accordance with ASME Power Test Code for Centrifugal Pumps, PTC 8.1, 1954 edition.
- Pressurizing pump performance curves are shown in Figure 5.4-3.

5.4.10.3.4 Performance Evaluation - General Design Criterion 44: Redundancy—As required by ATR General Design Criterion (GDC) 44[b] for cooling water systems, "suitable redundancy in components and features, and suitable interconnections, leak detection, and isolation capabilities shall be provided to ensure that for onsite electric power system operation (assuming offsite power is not available) and for offsite electric power system operation (assuming onsite power is not available) the system safety function can be accomplished, assuming a single failure."

Fluid systems generally are important to the function of primary coolant inventory control. Physical separation of redundant systems is particularly important from the standpoint of reducing the potential for common-mode failure caused by external events such as earthquake, flooding, tornadoes, and fire.

---

[a]. Refer to Chapter 8 (Electric Power) for a discussion of the Electrical Power System.

[b]. Refer to Chapter 3 (Design of Structures, Components, Equipment, and Systems) for development of ATR General Design Criteria.

Primary coolant inventory control normally is performed in ATR by the primary degassing and pressurizing subsystem (see Figure 5.1-2). Emergency makeup can be provided by any of the open-loop DHR methods in Table 5.4-2 (Items 3, 4, and 5). That table shows that redundant and diverse systems are available for accomplishing the primary coolant inventory control function. The function can be accomplished by means that do not depend on the ATR electric power (i.e., firewater injection for primary coolant inventory control). In addition, physical separation of redundant systems is provided since the firewater storage tanks and pumps are not located inside, or in the immediate vicinity of, the ATR reactor building.

5.4.11 Pressurizer Relief Discharge System

Not applicable for the ATR.

5.4.12 Valves

The PCS valves perform the function(s) of flow and/or pressure control of the primary coolant. The PCS contains 283 valves; of these 61 are 4-in. nominal pipe size or greater.

A mechanical stop on the butterfly valve (BF-A-14 on Figure 5.1-1) is provided to prevent full stoppage of coolant flow and to prevent the primary coolant pumps from operating against a shutoff head. Should the mechanical stop fail, six 4.29-in. holes in the butterfly valve disc will allow adequate coolant flow to prevent exceeding any reactor protection criteria.

5.4.12.1 Materials of Construction. All valves in contact with primary coolant are 300-pound Standard ASA, Type 304 stainless steel, forged, cast, or fabricated per ASTM A182-61T or ASTM A296-60T, Grade CF-81 (deBoisblanc and Cohen 1965).

5.4.12.2 Tests and Codes. All primary system valves were hydrostatically tested at 585 psig, and all valves 4 inches and larger, up to and including the first isolation valve on branch piping for auxiliary systems, were radiographed (deBoisblanc and Cohen 1965).

5.4.13 Safety and Relief Valves

Refer to Section 5.2.2 for a description of the PCS safety relief valves.

5.4.14 Equipment Supports

The piping system and connected equipment are supported, restrained, and guided so as to limit pipe stresses. The PCS piping loads are carried by a combination of adjustable spring hangers, rod hangers (rigid), snubbers, and pedestal supports.

Methods of PCS piping and equipment support are shown on Ebasco drawings (not included in this report) of Primary Coolant System Pipe Hangers and Details (8 sheets), Miscellaneous Systems Pipe Hangers and Details (4 sheets), and various equipment drawings.

PCS structural integrity support and methods of analysis are discussed in Chapter 3 (Design of Structures, Components, Equipment, and Systems).

Table 5.4-1. Primary Coolant System component design and performance characteristics.[a]

Component	Data
Primary Coolant Pumps (M-6, M-7, M-8, M-9)	
Quantity	4 (one or two spares)
Type	Horizontal, double suction, volute centrifugal
Design capacity each	18,000 gpm
Total dynamic head (TDH)	400 ft
Design pressure	485 psi
Suction pressure/temperature each	215 psig/125°F
Motor horsepower	2,190
Brake horsepower	2,000 nominal
Efficiency	85.5%
Net water volume per pump	22 ft^3
Speed	1,750 rpm
Net Positive Suction Head (NPSH) required	50 ft
Angular moment of inertia of pump and motor rotating element	200 $lb\text{-}ft^2$
Emergency Coolant Pumps (M-10, M-11)	
Quantity	2 (one on standby)
Type	Horizontal, double suction, volute centrifugal
Capacity each	4,700 gpm
Total dynamic head	22 ft
Design pressure	485 psi
Suction pressure/temperature	215 psig/125°F
Suction pressure, emergency	200 psig (at start) Atmospheric with flooded suction (30 min after start)
Motor horsepower	40
Motor types	One ac and one dc
Brake horsepower	39
Efficiency	78%
Constant bypass flow	250 gpm
Speed	690 rpm
Net water volume per pump	6 ft^3
NPSH	20 ft
Heat Exchangers	
Quantity	5
Type	Vertical U-tube
Effective surface, net each	18,330 ft^2
Duty	7.336×10^8 Btu/h

Table 5.4-1. (continued).

Component	Data
Tubes	3/4-in. No. 18 BWG, Inconel[b]
Tube side design pressure/temperature	390 psig/240°F
Shell side design pressure/temperature	125 psig/200°F
Primary coolant side net volume	355 ft^3 per exchanger
Total primary coolant flow	2.35×10^7 lb/h
Total heat transfer	9.17×10^8 Btu/h
Temperature in/out	167°F/124°F
Pressure drop	
Tube side	13 psi
Shell side	22 psi
Surge Tank (M-12)	
Quantity	1
Size	8 ft 0 in. ID × 22 ft 6 in. (18 ft tangent to tangent)
Heads	Elliptical
Total volume	1,000 ft^3
Operating water volume	950 ft^3
Design pressure/temperature	390 psig/240°F
Operating pressure	215 psig
Degassing Tank (M-13)	
Quantity	1
Type	Vertical spray
Size	5 ft 0 in. OD × 28 ft
Heads	Elliptical
Maximum design pressure/temperature	65 psia/240°F
Minimum design pressure	3 psia
Number of spray nozzles	7
Normal water storage volume	197 ft^3
Maximum design liquid spray rate	600 gpm
Design air flow rate	100 scfm
Normal degassing rate	300 gpm
Primary Pressurizing Pumps (M-15, M-14)	
Quantity	2 (one on standby)
Type	Horizontal, volute centrifugal
Capacity each	300 gpm (at 256 psig, 598 ft of head)
Total dynamic head	695 ft
Shutoff head	382 psig (895 ft including 25 ft maximum suction head)
Suction pressure/temperature	Flooded/169°F

Table 5.4-1. (continued).

Component	Data
NPSH-design	8 ft
Motor horsepower	100
Brake horsepower	88.4
Efficiency	58%
Speed	3,565 rpm
Primary coolant system relief valves (SF-A-71, SF-A-72)	
Quantity	2
Size	3 in.
Discharge pressure	379 psig (nominal), 390 psig (design)
Discharge flow	Variable to 570 gpm (test), 350 gpm (certified)
Design temperature	240°F
Pressurizing pump relief valves (SF-A-75, SF-A-76)	
Quantity	2
Size	2-1/2 in.
Discharge pressure	379 psig (nominal), 390 psig (design)
Discharge flow	345 gpm (certified)
Design Temperature	240°F

a. The M-3 Heat Exchanger has 12 tubes that are made of stainless steel. Six are 304 and six are 304L.

b. Data from deBoisblanc and Cohen (1965); Pace (1990).

Table 5.4-2. Advanced Test Reactor multiple means of decay heat removal.[a]

No.	Core heat removal	Power sources	Removal to heat sink	Power sources	UFSAR Chapter/ Figure No.
1	Primary coolant pumps (any 1 of 4)[b]	4,160 Vac commercial power (Bus E-1 or E-2)	Secondary coolant pumps (any 1 of 4): or Utility cooling water pumps (any 1 of 2)	4,160 Vac Commercial Power (Bus E-1 and E-2) 4,160 Vac diesel power (Bus E-3)	Chapter 5 Figs 5.1-1, -10 Fig 5.4-2
2	Primary emergency coolant pumps (any 1 of 2)[c]	[redacted]	Secondary coolant pumps (any 1 of 4); or Utility cooling water pumps (any 1 of 2); or natural circulation to air and thermal radiation to surroundings from uninsulated vessel and piping (short term)[f]	[redacted]	Chapter 5 Figs 5.1-1, -10 Fig 5.4-2
[redacted]	injection (any 1 of 3 pumps)[d]	injection), diesel engine (two pumps), commercial power or diesel power (one pump)	Reactor vessel drain to reactor building	Vessel drain or relief valves can be opened manually.[e] Vessel vent valves each on independent nitrogen-backed instrument air, PPS battery-backed power	Chapter 6 Figs 5.1-1, -10, -11 Fig 5.4-2
4	Low pressure demineralized water purge	Commercial power or diesel power	Reactor vessel drain to reactor building	Vessel drain or relief valves can be opened manually.[e] Vessel vent valves (see above)	Chapter 9 Figs 5.1-1, -10 Fig 5.4-2
5	Pressurizing system feed and bleed	Commercial power or diesel power via dual feeds to pressurizing pumps motors	Reactor vessel drain to reactor building	Vessel drain or relief valves can be opened manually[e]	Chapter 5 Figs 5.1-1, -2, -10 Figs 5.4-2
6	Natural circulation in reactor vessel (short term)	None needed	Natural circulation to air and thermal radiation to surroundings from uninsulated vessel	None needed	

FOIA Exemption 3 UCNI, Exemption 7f - pump details

FOIA Exemption 3 UCNI, Exemption 7f - pump details

a. Data from Buescher (1993), Table 4.4.1.

b. Any one pump of the possible four primary coolant pumps.

c. Any one pump of the possible two emergency coolant pumps.

d. Any one pump of the possible three firewater supply pumps.

e. Refer to Chapter 7 (Instrumentation and Controls) for a discussion of the justification of manual versus automatic actions.

f. Natural circulation will successfully remove decay heat for a short term (one or two hours). Other DHR methods will then be used to maintain primary coolant temperature less than design temperature. (Chapter 15.2)

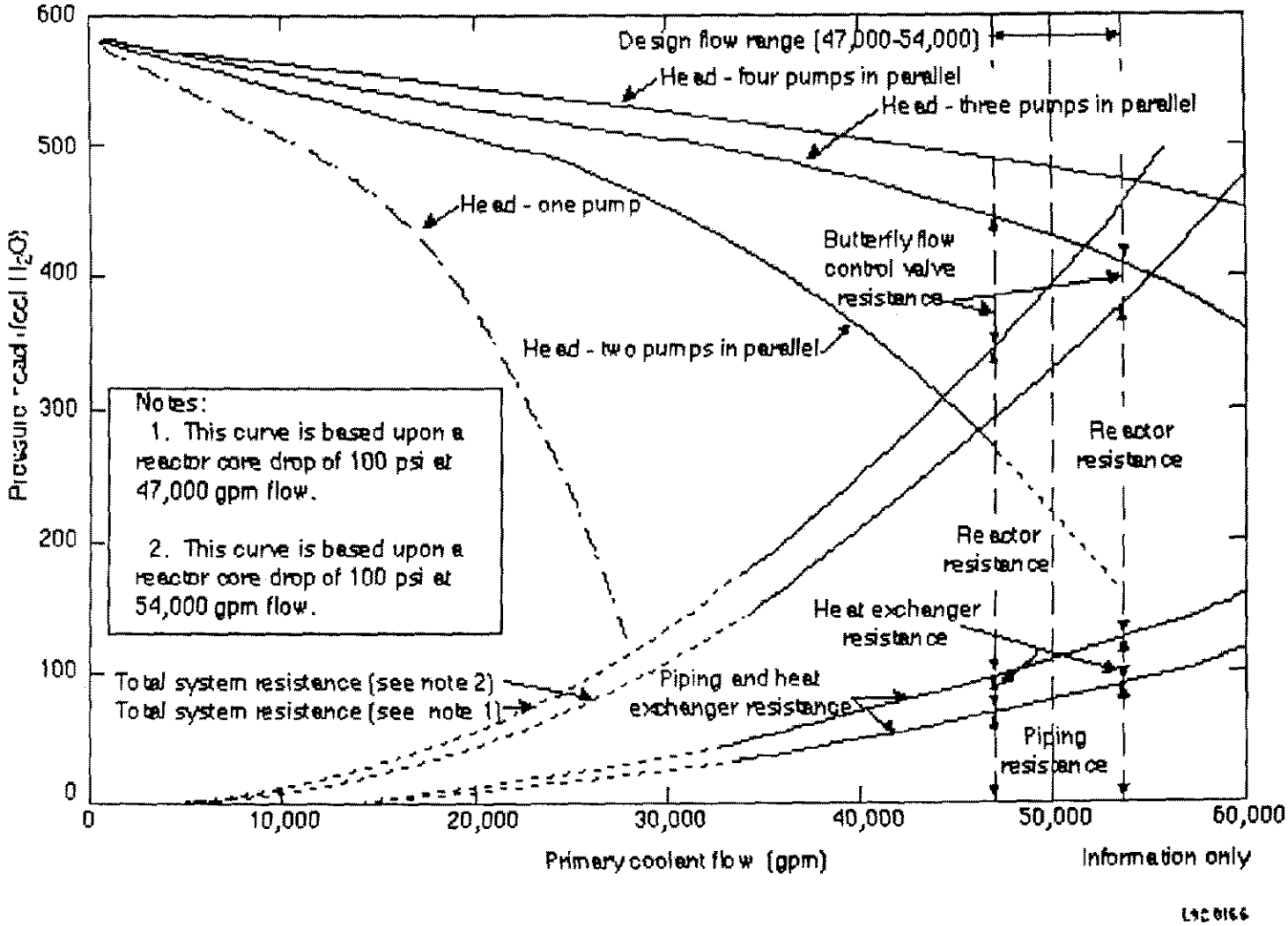

Figure 5.4-1. Primary Coolant System pump head curves. **(For Information Only)**

FOIA Exemption 3 UCNI, Exemption 7f (Page 5-88 – drawing showing decay heat removal options)

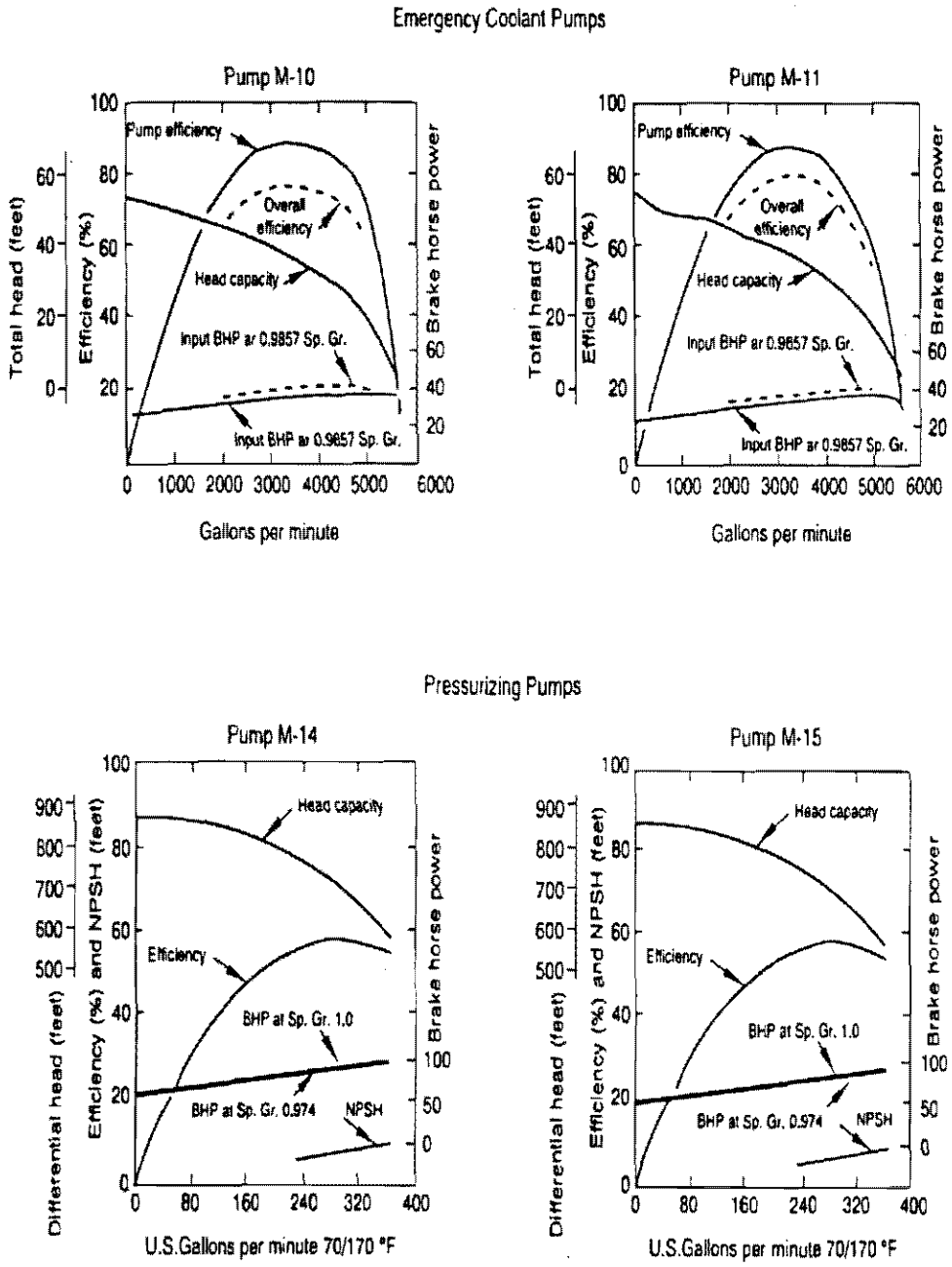

Figure 5.4-3. Emergency coolant and pressurizing pump performance curves. **(For Information Only)**

5.5 References

ANSI, 1981, *Pipe Flanges and Flanged Fittings, Steel Nickel Alloy, and other Special Alloys*, ANSI/ASME B16.5-1981 Edition, American Society of Mechanical Engineers (ASME), New York, NY.

ASME, 1955, *Code for Pressure Piping*, ASA B31.1-1955, American Society of Mechanical Engineers, New York, NY.

ASME, 1959, *Rules for Construction of Unfired Pressure Vessels*, ASME Boiler and Pressure Vessel Code, Section VIII, 1959 Edition, American Society of Mechanical Engineers, New York, NY.

ASME, 1962a, *Materials Specifications*, ASME Boiler and Pressure Vessel Code, Section II, 1962 Edition, American Society of Mechanical Engineers, New York, NY.

ASME, 1962b, *Rules for Construction of Pressure Vessels*, ASME Boiler and Pressure Vessel Code, Section VIII, 1962 Edition, American Society of Mechanical Engineers, New York, NY.

ASME, 1977, *Nuclear Power Plant Components*, ASME Boiler and Pressure Vessel Code, Section III, 1977 Edition, American Society of Mechanical Engineers, New York, NY.

ASME, 1983, *Overpressure Protection*, ASME Boiler and Pressure Vessel Code, Section III, Nuclear Power Plant Components, Subsection NB-3512.2 (b)(2), 1983 Edition, American Society of Mechanical Engineers, New York, NY.

ASME, 1986, *Overpressure Protection*, ASME Boiler and Pressure Vessel Code, Section III, Nuclear Power Plant Components, Article NB-7000, 1986 Edition, American Society of Mechanical Engineers, New York, NY.

Atkinson, S. A., 1988, *ATR Safety Basis Summary*, PG-T-88-011 EG&G Idaho, Inc., Idaho Falls, ID, September 1988.

Atkinson, S. A., 1994, *ATR Primary Coolant System Direct Core Damage Large Rupture Frequency*, EDF TRA-ATR-933, EG&G Idaho, Inc., February 27, 1994.

Atkinson, S. A., 1995, *Bypass Demineralizer Outlet Piping and Pressurizing Pump Outlet Piping Rupture Frequency*, EDF TRA-ATR-1076, September 7, 1995.

Beatty, R. N., 1980, *ATR Primary Coolant System pH Test Run No. 2*, PR-T-80-009, EG&G Idaho, Inc., February 26, 1980.

Buescher, B. J., 1993, *Strategic Evaluation Program Safety Issues Review*, EDF TRA-ATR-826, EG&G Idaho, Inc., November 18, 1993.

Burr, T. K., 1978, *Basis for Pressure Safety Limit for the ATR Vessel and PCS Inlet Piping*, RE-A-78-021, EG&G Idaho, Inc., February 1, 1978.

Burr, T. K. and H. L. Magleby, 1973, *Supplement to A-208 TR-356 Stress Report for ATR Reactor Vessel Drain and Relief Valve Piping*, TR-361, Aerojet Nuclear Co., February 9, 1973.

Carlson, E. R., 2002, *ATR Vessel Specimen Irradiation Program*, EDF TRA-ATR-1823, March 21, 2002.

Davidson, R. F., 1979, *ATR Primary Coolant System Piping Design Analysis*, RE-A-79-011, EG&G Idaho Inc., January 22, 1979.

Davidson, R. F., and G. L. Thinnes, 1974, *ATR Primary Coolant System Seismic Analysis*, TR-570, Aerojet Nuclear Company, December 26, 1974.

deBoisblanc, D. R., and S. Cohen, 1965, *Safety Analysis Report Advanced Test Reactor*, IDO-17021, Phillips Petroleum Co., April 1965.

Durney, J. L., 1980, letter to A. L. Bowman, *ATR Power Limit for Higher pH in the PCS*, JLD-21-80 (Rev. 1), EG&G Idaho, Inc., October 17, 1980.

Durney, J. L., 1982, letter to D. R. Mousseau, *Effect of pH on ATR Oxides*, JLD-17-82, EG&G Idaho, Inc., July 9, 1982.

Durney, J. L., et al., 1987, *ATR Vessel Lifetime and Primary Coolant System IGSCC Assessment*, PG-T-87-009, EG&G Idaho, Inc., December 1987.

Dwight, J. E., 1988a, *ATR Aging Evaluation and Life Extension Program Interim Report-Phase I and Phase II Results*, PG-T-88-008, EG&G Idaho, Inc., April 1988.

Dwight, J. E., 1988b, *ATR Aging Evaluation and Life Extension Program*, PG-T-88-029, EG&G Idaho, Inc., Idaho Falls, ID, July 1988.

EG&G Idaho, 1987, *ATR Primary Coolant System ASME Section III Class 1, Relief Valves SF-A-71 and SF-A-72*, Specification ES-50972, Rev. C, EG&G Idaho, Inc., December 21, 1987.

EG&G Idaho, 1988, *ATR Primary Pressurizing Pump ASME Section III Class 2 Relief Valves SF-A-75 and SF-A-76*, Specification ES-50974, Rev. A, EG&G Idaho Inc., June 6, 1988.

Graham, S. M., W. R. Lloyd, and W. G. Reuter, 1989, *Fracture Toughness and Tensile Test Results for Unirradiated Weldment of Type 304 Stainless Steel*, PG-T-89-001, EG&G Idaho, Inc., Idaho Falls, ID, May 1989.

Hope, R. S., 1976, letter to J.C. Stachew, *Survey of Low Temperature Service Materials in the ATR*, RSH-20-76, Aerojet Nuclear Co., Idaho Falls, ID, August 18, 1976.

House, R. K., 1992, *Bases for Designation of Safety-Related Equipment in the ATR*, PG-T-92-114, EG&G Idaho, Inc., July 1992.

House, W. E., 1995, *Stress Analysis Summary of the ATR Primary Coolant System*, EDF TRA-ATR-873, EG&G Idaho, Inc., February 9,1995.

INEEL, 2002, "ATR Inservice Inspection Plan Third Inspection Interval June 1994 to May 2004 (PLN-859)," Rev. 4, October 15, 2002.

Kimmitt, R. A., 1976, letter to H.J. Reilly, RRK-3-76, *Bases for the ATR Primary Coolant Chemistry Limits*, Aerojet Nuclear Co., Idaho Falls, ID, June 21, 1976.

Klingler, W. B., and J. H. Faller, 1988, *ATR Primary Coolant System Leak-Rate Evaluation*, PG-T-88-003, Rev. 1, EG&G Idaho, Inc., Idaho Falls, ID, January 1988.

Macek, R. W., 1975, letter to S. A. Atkinson, *Consideration of the ATR Primary Coolant System Inlet Piping for Over-Temperatures*, Macek-8-75, Aerojet Nuclear Co., Idaho Falls, ID, November 10, 1975.

Macek, R. W., 1976, *ATR PCS Pump Discharge Piping Evaluation*, TR-824, Aerojet Nuclear Company, Idaho Falls, ID, April 14, 1976.

McCracken, R. T., 1993, *ATR Fuel Element Oxide Data Summary*, EDF TRA-ATR-891, EG&G Idaho, Inc., November 15, 1993.

Miller, G. K., 1987, *A Structural Analysis of the ATR Drop Tube and Cylindrical Course Weldment*, PG-T-87-007, EG&G Idaho, Inc., August 1987.

Morton, D. K., 1983, *Stress Analysis of ATR Primary Coolant Pump Discharge Piping*, EDF TRTSB-ATR-061, EG&G Idaho, Inc., September 19, 1983.

Mousseau, D. R., 1987, letter to F. L. Sims, DOE-ID, *ATR Reactor Vessel Information*, Mou-1-87, EG&G Idaho, Inc., January 12, 1987.

NRC, 1988, *Radiation Embrittlement of Reactor Vessel Materials*, Regulatory Guide 1.99, Rev. 2, U.S. Nuclear Regulatory Commission, Washington, D.C., May 1988.

Pace, N. E., 1990, *ATR Primary Coolant System Overpressure Protection Report*, PG-T-88-005, Rev. 1, EG&G Idaho, Inc., September 1990.

Smith, S. R., 1997, *ATR Primary Coolant System Piping Integrity/TSR Review Comment 15-01-TWS Resolution*, EDF TRA-ATR-1226, Lockheed Martin Idaho Technologies Co., March 13, 1997.

CHAPTER 6

ENGINEERING SAFETY FEATURES

INTENTIONALLY BLANK

CONTENTS

ACRONYMS/ABBREVIATIONS 6-5

6. ENGINEERED SAFETY FEATURES 6-7

6.1 Engineered Safety Feature Materials 6-10

6.1.1 Metallic Materials 6-10
6.1.2 Organic Materials 6-10

6.2 Confinement Systems 6-15

6.2.1 Confinement and RMSS Functional Design Basis 6-15
6.2.2 System Description 6-15
6.2.3 System Performance Evaluation 6-21
6.2.4 Confinement Leakage Testing 6-22

6.3 Emergency Core Cooling System (Emergency Firewater Injection System) 6-29

6.3.1 Design Bases 6-29
6.3.2 System Description 6-30
6.3.3 System Performance Evaluation 6-31
6.3.4 Tests and Inspection 6-32
6.3.5 Instrumentation 6-33

6.4 Habitability Systems 6-35

6.5 Fission Product Removal and Control Systems 6-36

6.5.1 Engineered Safety Feature Filter Systems 6-36
6.5.2 Containment Spray System 6-36
6.5.3 Fission Product Control Systems 6-36

6.6 Vessel Vent System 6-37

6.6.1 Design Bases 6-37
6.6.2 System Description 6-37
6.6.3 System Performance Evaluation 6-40
6.6.4 Testing and Inspection 6-41
6.6.5 Instrumentation 6-41

6.7 Reactor Shutdown System Primary Pump Shutoff System 6-44

6.7.1 Design Bases 6-44
6.7.2 System Description 6-44

6.8 RSS Pressurizing and Gland Seal Pump Shutoff System 6-45

6.8.1 Design Bases 6-45
6.8.2 System Description 6-45

6.9 Vessel Level Alarm System 6-46

6.9.1 Design Bases 6-46
6.9.2 System Description 6-46

6.10 LOCA Primary Coolant Pump Shutoff System 6-47

6.10.1 Design Bases 6-47
6.10.2 System Description 6-47

6.11 References 6-48

FIGURES

6.2-1. Stack exhaust radiation logic diagram 6-25

6.2-2. Radiation Monitoring and Seal System: Part 1 6-26

6.2-3. Radiation Monitoring and Seal System: Part 2 6-27

6.2-4. Radiation Monitoring and Seal System: Dampers 6-28

6.3-1. Emergency Firewater Injection System: Engineered Safety Feature components 6-34

6.6-1. Piping and instrumentation diagram of the Vessel Vent System 6-42

6.6-2. Vessel Vent System 6-43

TABLES

6.1-1. Specifications of principal Engineered Safety Feature pressure-retaining materials 6-11

6.1-2. Specifications of principal Engineered Safety Feature materials exposed to reactor coolant 6-12

6.1-3. Organic protective coatings inside the Advanced Test Reactor confinement 6-13

6.1-4. Other organic materials within the Advanced Test Reactor confinement 6-14

6.2-1. General types of confinement area penetrations 6-23

6.2-2. Radiation Monitoring and Seal System Dampers 6-24

6.3-1. Components of the Emergency Firewater Injection System 6-33

ACRONYMS/ABBREVIATIONS

ANSI	American National Standards Institute
ASA	American Standards Association
ASME	American Society of Mechanical Engineers
ASTM	American Society for Testing and Materials
ATR	Advanced Test Reactor
CFR	Code of Federal Regulations
CIS	Confinement Isolation System
CLOFA	complete loss of flow accident
DBA	Design Basis Accident
dc	direct current
ECCS	Emergency Core Cooling System
EDF	engineering design file
EFIS	emergency firewater injection system
ESF	engineered safety features
FMEA	failure modes and effects analysis
GDC	general design criterion
H&V	heating and ventilating
LCV	level control valve
LOCA	loss of coolant accident
NRC	U.S. Nuclear Regulatory Commission
OD	outside diameter
P&ID	piping and instrumentation diagram
PALM	powered axial locating mechanism
PCRS	primary coolant recycle system
PCS	primary coolant system
PPS	plant protective system
PRA	probabilistic risk assessment
psia	Pounds per square inch absolute
psig	pounds per square inch gauge
PWR	pressurized water reactor
RDAS	reactor data acquisition system
RMS	radiation monitoring system
RMSS	radiation monitoring and seal system
RSS	reactor shutdown system
SAR	Safety Analysis Report

SDD	system design description
SFA	single failure analysis
SR	Safety Rod System
SSE	safe shutdown earthquake
SV	solenoid valve
TRA	Test Reactor Area
UFSAR	Upgraded Final Safety Analysis Report
VVS	Vessel Vent System

6. ENGINEERED SAFETY FEATURES

The Advanced Test Reactor (ATR) Plant Protective System (PPS) consists of those active devices and associated equipment initiating their action, which function with passive structures of the plant to prevent the unacceptable release or spread of radioactive materials by preventing plant variables or conditions from reaching their respective safety limits, or by mitigating the consequences of exceeding safety limits.

The PPS includes the Reactor Shutdown System (RSS) and the Engineered Safety Features (ESF). This chapter provides information about the ESF. The original construction of the ATR included the design and installation of some of the ESF systems. Other ESF systems (or parts of systems) have been added or upgraded since initial operation of the facility. In all cases, the systems were designed using standards applicable at the time to address safety concerns of the facility. The following systems are defined as ESF systems at the ATR.

- The Radiation Monitoring and Seal System (RMSS) provides ATR confinement isolation to limit the release of airborne radioactivity to the environment. The RMSS is composed of three channels of instrumentation that monitor the inlet to the exhaust gas stack and an actuation system that provides a signal to stop fans and shut dampers in the heating and ventilating system based on measurements of radiation levels in the main exhaust stream. This system is discussed in Section 6.2.2.5 and in Chapter 7 (Instrumentation and Controls).

- The Emergency Firewater Injection System (EFIS) provides emergency reactor core cooling and flooding of the reactor vessel in the event of a major break in the Primary Coolant System (PCS) piping or in an event that results in loss of primary coolant. This ESF is designed to activate at a predetermined low pressure, or when the water level falls to a predetermined height above the top of the core. The EFIS is composed of: the upper vessel EFIS subsystem, the bottom head EFIS subsystem, and the EFIS actuation system. The upper vessel and bottom head EFIS piping systems are discussed in Section 6.2.3. The EFIS actuation system is discussed in Chapter 7 (Instrumentation and Controls).

- The Vessel Vent System (VVS) provides the capability to depressurize the ATR vessel. It is needed to mitigate high pressure events such as the long-term complete loss of flow accident (CLOFA). During a CLOFA, the core decay heat produces steam and causes a pressure increase in the vessel in excess of the supply pressure of the EFIS. Venting the vessel under such conditions is required to allow the EFIS coolant to flow into the ATR vessel and keep the core covered. The VVS is manually actuated by an operator rather than automatically actuated. The VVS is discussed in Section 6.6 and Chapter 7 (Instrumentation and Controls).

- The Primary Pump Shutoff System actuation is an ESF function provided by the inputs from the RSS Vessel Differential Pressure Subsystem. The purpose of the Primary Pump Shutoff System actuation is to shut off two primary pumps if a high flow condition occurs in three pump operation. This actuation protects the reactor core components including fuel plates from damage caused by excessive differential pressure across the core. This ESF is discussed in Section 6.7 and Chapter 7 (Instrumentation and Controls).

- The Pressurizing and Gland-Seal-Pump Shutoff System actuation is an ESF function provided by inputs from the RSS Vessel Inlet Pressure Subsystem. The purpose of the Pressurizing and Gland-Seal-Pump Shutoff System is to protect the PCS from exceeding the system design pressure. Upon receiving an overpressure trip signal, the Pressurizing and Gland-Seal-Pump Shutoff System initiates a reactor trip and shuts down the primary pressurizing pumps and the gland-seal pumps. This ESF is discussed in Section 6.8 and Chapter 7 (Instrumentation and Controls).

- The Primary Reliefs or safety relief valves (SRV) protect the PCS from extreme overpressure conditions. It consists of two spring-loaded safety relief valves mounted on the 8-in. reactor vessel lower drain line. This ESF is discussed in Chapter 5 (Primary Coolant System).

- The Vessel Level Alarm System actuation is an ESF function provided by the inputs from the RSS Reactor Vessel Water Level Subsystem or by the reactor vessel water level channels of the EFIS. The purpose of the Vessel Level Alarm System actuation is to alert the operators of low vessel liquid level for potential actuation of the Emergency Firewater Injection System (EFIS). The vessel level alarm is used to alert against low-probability events that result in a loss of PCS inventory during depressurized and outage operations when irradiated fuel elements are in the reactor vessel. This ESF is discussed in Section 6.9.

- The LOCA Primary Coolant Pump (PCP) Shutoff System is an ESF function provided by the inputs from the RSS Vessel Inlet and Outlet Pressure Subsystems. The purpose of the LOCA Primary Coolant Pump Shutoff System is to shutoff all operating primary coolant pumps in the event of a loss-of-coolant-accident (LOCA). Shutoff of the primary coolant pumps needs to occur prior to air being drawn from the surge tank into the primary cooling system (PCS). Air in the PCS could cause a degradation of emergency pump flow. This ESF is discussed in Section 6.10 and Chapter 7 (Instrumentation and Controls).

Materials used in the ESFs are discussed in Section 6.1. Each of the following systems is normally an ESF at power reactors, but is not an ESF at the ATR.

- Containment System (Confinement System)—The ATR has a confinement system rather than a containment system. The confinement is designed to provide resistance to releases of radioactive material at low pressure when the RMSS (an ESF) is activated.

  The confinement has historically at ATR not been classified as an ESF since it was not considered an active device. It is needed along with the RMSS to control the release of fission products following an accident at ATR, and has been classified as safety-related. The confinement is discussed in Section 6.2.

- Habitability System—The control room at ATR is inside the confinement. Unlike commercial power reactors where post-accident control room habitability is required, the design basis events requiring operator action in the control room are (a) high-pressure and high-temperature events which require actuation of the VVS, and (b) events which require manually opening valves outside the control room. The ATR control room can be evacuated after inserting control rods and after performing required operator actions following design basis events. Control room habitability is discussed in Section 6.4.

- Fission Product Removal and Control Systems—The ATR does not use any ventilation filters in the ESF Confinement System. The building spray system, which functions in place of the normal power reactor containment spray system, is not an ESF. Credit is not taken for its use in an accident analysis. Fission product removal and control system including the confinement spray system are discussed in Section 6.5.

6.1 Engineered Safety Feature Materials

This section discusses materials used in ESF components and the material interactions that could potentially impair operation of the ESF.

6.1.1 Metallic Materials

6.1.1.1 Materials Selection and Fabrication. Materials used in the ESF are selected for their compatibility with the PCS.

All pressure-retaining materials in ESF system's components comply with corresponding material specifications permitted by American Society of Mechanical Engineers (ASME) Section III, Division 1, and American Standards Association ASA B31.1 Boiler and Pressure Vessel Codes (ASME 1955, 1980, 1986a). Table 6.1-1 lists principal specifications for pressure-retaining materials used in the ESF.

Table 6.1-2 lists the principal specifications of materials used in ESF components within the confinement that would be exposed to core cooling water in the event of a loss of coolant accident (LOCA). Untreated well water is used for firewater in the EFIS. The ESF components are compatible with the raw untreated water.

All components of the ESF were cleaned before shipment from the vendor. Protective caps were placed on the open ends of pipes or other openings. Components were inspected before installation, and were cleaned if necessary. During construction, open ends of pipes were covered to prevent entrance of foreign material. Grinding wheels or brushes used to prepare joints for welding had not been used on any material other than stainless steel. The ESF components are not insulated, so chloride leaching from nonmetallic insulation does not exist.

6.1.1.2 Composition, Compatibility, and Stability of Emergency Coolant. The following information provides the composition, compatibility, and stability of the EFIS water.

The supply for the EFIS is drawn from the TRA firewater loop [discussed in Chapter 9 (Auxiliary Systems)]. This firewater is untreated raw water, which is compatible with ESF components.

The firewater is stored in a 150,000-gal, carbon steel overhead, raw-water storage tank and three 500,000-gal, carbon steel, ground-level, raw-water storage tanks. The internal surface of each tank has been coated with a corrosion-resistant coating; therefore, the water can be stored for extended periods without significantly corroding the storage vessels.

6.1.2 Organic Materials

Organic materials used inside the ATR confinement in significant amounts are identified in Tables 6.1-3 and 6.1-4. These tables also identify the types, locations, and estimated amounts of material.

The stability of organic materials is of importance since there is the potential for decomposition under accident conditions. The design basis events in Chapter 15 (Accident Analyses) do not result in fuel melting with a large release of radiation to the confinement, and no significant hydrogen formation is expected to occur under Design Basis Accident (DBA) conditions. However, the information has been included for the evaluation of potential hydrogen formation during a severe beyond design basis event.

Paint and coatings are identified in Table 6.1-3. Three different types of paint or coatings have been used. Oil-based enamel was used on the walls inside confinement except those walls inside potentially high-radiation zones or areas expected to require frequent decontamination. Epoxy was used on the walls and floors of the experimental cubicles and around the reactor and primary piping areas; latex was used on wooden objects such as boxes for shoecovers, and anti-contamination clothing.

The amounts of material were determined from a walkdown and visual inspection of accessible areas. The walkdown and visual inspection provided an estimate of the surface areas covered by the various paints and coatings. The thickness of the paint and coating was determined from the number of coats of paint or coatings applied since the reactor went into operation. The volume of material present in the areas of the ATR accessible for the walkdown was calculated from the surface areas and thicknesses. After reviewing the areas not accessible for the walkdown, a corrected total volume was estimated for the various paints or coatings present within confinement.

Table 6.1-4 identifies organic materials other than paint inside the ATR confinement. The estimated volumes were based on inspections made within the ATR confinement area. The total volume and accuracy were determined by the same method as that used in Table 6.1-3.

Table 6.1-1. Specifications of principal Engineered Safety Feature pressure-retaining materials.[a]

Component	Material
Piping/tubing	Seamless per ASTM A376-60T TP304 and TP304L or welded per ASTM A-358-60T TP304 and TP304L. Instrument tubing in accordance with ASTM-A269-60, 1/2-in. OD and smaller 0.035 wall. ASME SA-312 TP304 and Grade TP-304L. 0.375-in. Grade TP304 ASTM A269, 1961
Fittings/flanges	ASTM A358-60T TP304 and TP304L ASTM A376-60T TP304 AND TP304L ASTM A-240-61T ASTM A181-61T Grade II Flareless fittings, 316 Stainless Steel ASTM A182-58T type F304 or F304L ASME SA-403 Grade WP-304L Class I ASME-SA-182 F304.
Bolting/nuts/studs	ASTM A-193-59T Gr B7 ASTM A-194-59T Gr 2H
Castings	ASTM A351-61T TP304 ASME-SA-351
Forgings	ASTM A403-60T WP304 and WP304L. ASME SA-182 Grade F 304.
Weld rod	Type 308-AWS-ASTM ER308-ASTM A371-53T Type 308L-AWS-ASTM ER308L-ASTM A371-53T E308-15 AWS-ASTM A-298-55T

a. EG&G Idaho 1988; INEEL 2001.

Table 6.1-2. Specifications of principal Engineered Safety Feature materials exposed to reactor coolant.[a]

Component	Material
Piping/tubing	Seamless per ASTM A376-60T TP304 and TP304L or welded per ASTM A-358-60T TP304 and TP304L. Instrument tubing in accordance with ASTM-A269-60, 1/2-in. OD and smaller 0.035 wall. ASME SA-312 Grade TP304 and TP304L. 0.375-in. Grade TP304 ASTM A269,1961
Fittings/flanges	ASTM A358-60T TP304 and TP304L ASTM A376-60T TP304 AND TP304L ASTM A-240-61T ASTM A181-61T Grade II Flareless fittings, 316 stainless steel ASTM A182-58T type F304 or F304L ASME SA-403 Grade WP-304L Class 1 ASME-SA-182 F304.
Plate	ASME-SA240 TP304 ASTM-A36
Shapes	ASME-SA240 TP304 ASME SA36
Bolts/nuts/studs/pins	ASTM A-193-59T Gr B7 ASTM A-194-59T Gr 2H ASTM-A307
Weld rod	Type 308-AWS-ASTM ER308-ASTM A371-53T Type 308L-AWS-ASTM ER308L-ASTM A371-53T E308-15 AWS-ASTM A-298-55T
Forgings	ASTM A403-60T WP304 and WP304L. ASME SA-182 Grade F 304.
Castings	ASTM A351-61T TP304. ASME-SA-351

a. EG&G Idaho 1988; INEEL 2001.

Table 6.1-3. Organic protective coatings inside the Advanced Test Reactor confinement.

Type	Walkdown location	Surface area from walkdown (ft^2)	Thickness (ft)[a]	Volume (ft^3)[b]
Oil-based enamel	First floor	31,330	0.00075	23.5
	First basement	12,420	0.00075	9.3
	Second basement	10,150	0.00075	7.6
Corrected total volume = 2 (walkdown volume) with an estimated accuracy of ±50%				80.8
Epoxy	First floor	7,200	0.01667	120.0
	First basement			
	Floor	19,900	0.01667	331.7
	Cubicles	21,200	0.00833	176.6
	Second Basement			
	Floor	20,750	0.01667	345.9
	Cubicles	31,340	0.00833	261.1
	Primary HX	3,560	0.00750	26.7
	Secondary piping	2,880	0.00750	21.6
Corrected total volume = 1.5 (walkdown volume) with an estimated accuracy of ±50%				1,925.4
Latex	First floor	2,197	0.00750	16.5
	First basement	655	0.00750	4.9
	Second basement	1,960	0.00750	14.7
Total volume = 1.25 (walkdown volume) with an estimated accuracy of ±25%				45.0

a. The thickness was determined by the number of coats of paint or coating applied since the reactor went into operation.

b. The corrected total volume and accuracy are based on areas available for inspection corrected for areas not accessible during the walkdown.

Table 6.1-4. Other organic materials within the Advanced Test Reactor confinement.

Material	Location	Volume (ft^3)[a]
Plywood	First floor	62.2
	First basement	29.2
	Second basement	60.6
Corrected total volume = 1.10 (walkdown volume) with an estimated accuracy of ± 10%		167.2
Asphalt tile	Control room area	9.0
	First basement	2.1
Corrected total volume = 1.10 (walkdown volume) with an estimated accuracy of ± 10%		12.2
Formica	Second basement	58.3
Corrected total volume = 1.10 (walkdown volume) with an estimated accuracy of ± 10%		64.1
Carpet	Control room area	4.6
Corrected total volume = 1.10 (Walkdown volume) with an estimated accuracy of ± 10%		5.0
Wiring insulation	First basement	1,505.3
	Second basement	904.4
Corrected total volume = 2.0 (walkdown volume) with an estimated accuracy of ± 50%		4,819.0
Oil	Second basement	11.5
Corrected total volume = 1.20 (walkdown volume) with an estimated accuracy of ± 20%		13.8
Pipe insulation	First basement	173.1
	Second basement	680.8
Corrected total volume = 1.20 (walkdown volume) with an estimated accuracy of ± 20%		1,024.7

a. Estimates of total volume and accuracy for areas that were not accessible during the walkdown are based upon values from accessible areas.

6.2 Confinement Systems

The ATR confinement systems include the building confinement structure and the RMSS. The confinement is classified as safety-related (House 1992), and the RMSS is categorized as an ESF. The reactor building structure is described in Chapter 3 (Design of Structures, Components, Equipment, and Systems). Although the confinement has not been categorized as an ESF, it is included in this chapter because the building confinement structure is needed for the RMSS to perform its function, and in the current format, the discussion of the confinement falls most logically in this chapter.

6.2.1 Confinement and RMSS Functional Design Basis

The reactor building is divided into confinement and areas outside of confinement. The confinement is designed to act as a final barrier to delay the release of airborne radioactive contamination resulting from an accidental release of radioactivity from the reactor or irradiation facilities. Confinement has been selected to include all areas where an accidental contaminated release from the reactor or irradiation facilities must be controlled, or where sealed penetrations from such an area to an otherwise "clean" area would be difficult to maintain during normal operation.

The RMSS is an ESF that actuates to shut off the ventilation supply and exhaust fans and to seal the building ventilation ducts when radiation readings in the ventilation offgas reach a predetermined setpoint.

The ATR is a moderate-pressure, low-temperature facility, and its confinement has no energy-removal systems. The energy released to the confinement during design basis accidents, which include little or no steam generation, is included in the evaluation of confinement performance.

The design basis event considered for the confinement and RMSS is the design basis 3-in. break loss of coolant accident (LOCA) that occurs during pressurized operation. During this event, the pressure inside the confinement increases because air in the confinement is displaced by water discharging from the break. The peak pressure occurs during initial depressurization of the primary system. The confinement leakage during this event relieves the pressure buildup at an internal pressure below building yield. For the design basis accident, there is a high (greater than one confinement volume per day) leak rate for approximately two minutes, followed by approximately one hour or possibly more of leakage at the same volume rate as the firewater injection. When firewater injection is shut off, the building's internal pressure (gage) goes to near zero and the leak rate drops to under 51.4% (Lucas 2000) of the confinement volume per day.

6.2.2 System Description

6.2.2.1 Confinement Structure. The ATR reactor building is a complex of enclosed areas approximately 200 ft by 200 ft, extending a maximum of 60 ft both above and below grade. The first floor is located at grade and is divided into the following areas: reactor area, storage-canal area, utility area (including the diesel generator pit), general storage and laydown area, critical facility area, control room, and offices. The first and second mezzanine floors are devoted to offices and heating-and-ventilating (H&V) equipment rooms. The first and second basements are used for experiment cubicles and equipment, electrical equipment, heat exchangers, demineralizer equipment, H&V equipment, and other associated items. The Primary Coolant System is located in the first and second basements except for the top head of the reactor which extends into the first floor reactor area.

The building is divided into confinement and areas outside of confinement. The confinement is designed to act as a final barrier to delay release of radioactive contamination resulting from an accidental release of radioactivity. The confinement volumes have been selected to include all areas where an accidental contaminated release from the reactor or irradiation facilities must be contained, or where sealed penetrations from such an area to an otherwise "clean" area would be difficult to maintain during normal operation.

All fixed penetrations of confinement are sealed, and ventilation penetrations are equipped with gasketed dampers. The RMSS, upon detection of high radiation in the ATR building exhaust, will initiate a confinement seal by closing the penetration dampers and shutting off the ventilation supply and exhaust fans.

The confinement volume of 1.64×10^6 ft^3, which represents approximately 62% of the total building volume, includes the following: reactor area, including freight and passenger elevators; reactor control room (Room 100); instrument-repair room (Room 112); Reactor Data Acquisition System (RDAS) area (Rooms 110 & 111); a lunch room (located north of the reactor control room); first basement, including the ATR Warm Waste Treatment Facility cubicle (located on the first basement level, but outside the basement wall near the SW corner); and the second basement. The doors and the canal structure make up part of the confinement boundary.

The substructure portions of confinement (below grade), encompassing 1,122,900 ft^3, include all first- and second-basement areas (except Stairwell No. 3), the Warm Waste Treatment Facility cubicle, and the reactor exhaust-gas duct out to the isolation damper near the stack. Stairwell No. 3 has been excluded from the confinement area to permit first-floor access to the process-utility control room on the first floor without entry into the confinement area.

The building substructure is of heavily reinforced concrete construction, either resting directly on and keyed into the subsurface lava or supported by concrete piers that extend to the lava level. Shielding requirements are used wherever possible to meet part of the structural requirements of the building. While all load-carrying frames are of reinforced concrete, many partition walls and some shielding walls are of masonry (concrete block) construction. Where required, all masonry walls below grade are reinforced to resist seismic loads.

The superstructure portion of confinement (above grade), encompassing 517,000 ft^3, includes the reactor area, reactor control room (Room 100) with attached lunch room, instrument-repair room (Room 112), the RDAS area (Rooms 110 and 111), freight elevator, passenger elevator, and Stairwell Nos. 1, 2, and 4. The truck airlock (45,760 ft^3) is also part of the confinement superstructure.

In general, the building above grade is of steel frame construction with exterior walls of insulated aluminum sandwich panels supported by steel girders and a reinforced masonry base wall, 3 ft 4 in. high, around the building perimeter.

Roof construction consists of steel decking covered with a vapor barrier, insulation, roofing, and gravel. Generous slopes are provided over the entire area to internally located drains to handle precipitation.

Confinement areas of the superstructure are of seal-welded steel plate, reinforced masonry, or concrete construction. Special provisions have been made to maintain the integrity of the confinement perimeter's penetrations and doors.

Windows, used as a part of the confinement boundary, are located in instrument-repair room (Room 112), RDAS area Rooms 110 and 111, and the offices in the southeast corner of the building. Generally, swing doors are hollow metal, and truck doors bounding the confinement area are of reinforced steel-sheet construction. The two truck doors in the south end of the reactor area are vertical-lift doors of reinforced steel-sheet construction, and the truck access door in the north wall of the reactor area is a horizontal sliding door of reinforced steel-sheet construction. The horizontal sliding truck door at the south end of the truck airlock is reinforced plate-steel construction. A large vertical-lift door made of steel plate is located over the working canal in the north wall of the reactor area. This door is furnished with a stainless-steel bulkhead, mounted on its south face and so arranged that the bulkhead extends to the working canal floor when the door is shut.

Penetrations through the confinement boundary have been minimized. All penetrations are designed to be zero- or low-leakage, and are sealed either by caulking or gasketing.

Table 6.2-1 gives the general types of penetrations and sealing techniques employed for maintaining confinement.

Most confinement leakage is through functional penetrations such as doors and hatch covers. All hatches are caulked and/or gasketed. All swing doors are gasketed and provided with automatic closers. The following ATR confinement doors, which are all located on the first floor of the reactor building, are provided with wedged or inflatable gaskets. Inflatable seals inflate automatically on door closure.

- Truck overhead doors (D-13 and D-15)
- Truck sliding door (D-441)
- Sliding door (D-52)
- Canal overhead door (D-51).

6.2.2.2 ***Truck Airlock.*** The ATR truck airlock allows semi-trucks and smaller vehicular traffic to enter or exit the ATR main floor without breaching confinement, and also provides a weather-protected enclosure for transferring resin.

The airlock is 80 ft long × 26 ft wide × 22 ft high, and extends south of the original main building's west overhead truck door D-15. The two truck doors on the airlock, overhead truck door D-15 and sliding truck door D-441, are controlled from a single station immediately west of door D-15. The truck door to be operated is selected using a key-operated selector switch.

The two airlock truck doors are interlocked to prevent both from being open at the same time. Overhead truck door D-15 must be shut and the seal pressurized before sliding truck door D-441 can be opened. Likewise, sliding truck door D-441 must be shut and the seal pressurized before overhead truck door D-15 can be opened.

Overhead truck door D-15 and sliding truck door D-441 are interlocked with ventilation fans 670 M-539 and 670-M-433, supply damper 670-M-434, and exhaust damper 670-M-435. Selecting "OPEN" on the controller for either truck door D-15 or D-441 will automatically turn off the ventilation fans, shut both dampers, and depressurize the seal on the selected door before the door will open.

The interlock between the two airlock truck doors can be bypassed to allow both doors to open simultaneously. This can be done using a key- operated bypass on the controller. The key bypass will prevent operation of all interlocks associated with the truck doors and ventilation system. Key access is specified by Contractor procedures.

6.2.2.3 Instrument Air/Nitrogen Gas System. Instrument air is the source of air for door seals D-13, D-15, D-51, D-52, and D-441. Two cylinders of nitrogen gas, located on the west wall of the main reactor room floor and connected to the instrument air tubing, provide a redundant gas supply for the door seals D-13, D-15, D-51, D-52, and D-441.

Each door is equipped with an isolation valve, a check valve, a pressure regulating valve, and a solenoid valve. The pressure regulating valves are normally adjusted as follows:

Door	Pressure (PSIG)
D-13	8 - 12
D-15	8 - 12
D-51	25 - 30
D-52	15 - 20
D-441	20 - 30

The backup gas bottles are in parallel to the instrument air supply to the doors (isolation from the remainder of the instrument air system is provided by CK-6-969). The backup gas pressure is regulated below the instrument air pressure to prevent usage of gas when instrument air is in service. The typical setting for this regulator is about 50 psig.

6.2.2.4 Fluid System Penetrations. Fluid systems that penetrate the confinement boundary include:

- Firewater
- Potable water
- Secondary cooling water
- Plant air
- Warm waste water
- Primary coolant recycle system (PCRS)[a]
- Heating and Ventilating (H&V) System supply & exhaust
- Raw water
- Demineralized water

---

[a] The primary coolant recycle system (PCRS) is located in TRA-689 and tied to TRA-670 by pipe. TRA-689 is not in use at this time. The piping between TRA-689 and TRA-670 is isolated by both MOV-32-1 and MOV-1-909. Since the piping connections to TRA-689 are downstream of either a <3-in. orifice or valve, any break is bounded by the analysis in Chapter 15.6.

- Utility cooling water
- Instrument air
- Hot waste water
- Steam (disconnected)
- Cold waste water
- High pressure air.

All of the above systems, except plant air, instrument air, high pressure air, warm waste, hot waste, primary coolant recycle system[a], and the H&V system's supply and exhaust ducts, are closed systems that do not connect directly to the confinement atmosphere. Plant air and instrument air penetrate the confinement area and can be opened into the confinement when in use. These systems do not provide a pathway from the confinement to the environment. The compressors for these systems are screw-type air compressors, and the systems are equipped with check valves to prevent back flow. Manual isolation valves are located inside and outside of confinement. The RMSS isolates the H&V duct penetrations. Because of the location of dampers in the ducting, the duct may become a part of the confinement boundary. However, the amount of ducting involved is small relative to the total confinement boundary; the ducting that is part of the boundary is tested during the normal surveillance. All of the water systems maintain the confinement boundary with a water seal at a low point in the system, and manual and remotely operated isolation valves.

6.2.2.5 ***Radiation Monitoring and Seal System (RMSS).*** The ESF that provides ATR confinement isolation is the RMSS. The RMSS consists of the RMSS actuation system and the isolation dampers and fan controls used to actuate a confinement seal. The RMSS actuation system includes 3-channel radiation monitoring at the inlet to the exhaust gas stack, and an electronic auctioneering system that outputs to isolation dampers and fan controls in the H&V systems. The RMSS actuation system is shown schematically in Figures 6.2-1 through 6.2-3 and is discussed in detail in Chapter 7 (Instrumentation and Controls).

6.2.2.6 ***Isolation Dampers.*** The H&V system penetrations associated with the RMSS are equipped with both primary and backup dampers with gaskets. The RMSS dampers are listed in Table 6.2-2 and are shown schematically in Figure 6.2-4. Additional information and more complete figures of the H&V system can be found in Chapter 9 (Auxiliary Systems). During normal operation, the isolation dampers are maintained open using instrument air. Upon an RMS-1 shutdown, the solenoid valves associated with all dampers except stack dampers BDM-1-5 and BDM-1-5A vent the instrument air, allowing the spring-loaded dampers to shut. Dampers BDM-1-5 and BDM1-5A require instrument air to open or shut. The instrument air has a nitrogen supply backup and a safety feature consisting of a pressure switch that actuates closure of the dampers on low pressure of the instrument air supply. Installed pressure switches on BDM-1-5 and BDM-1-5A actuate at 75 psig decreasing to reposition the solenoids so the valve will shut, therefore, BDM-1-5 and BDM-1-5A fail shut on loss of air and nitrogen pressure. All dampers except BDM-1-5 and BDM-1-5A are designed to fail shut upon loss of power to the solenoid or upon loss of instrument air. The ventilation system containing damper BDM-1-4 is not in operation.

---

[a] The primary coolant recycle system (PCRS) is located in TRA-689 and tied to TRA-670 by pipe. TRA-689 is not in use at this time. The piping between TRA-689 and TRA-670 is isolated by both MOV-32-1 and MOV-1-909. Since the piping connections to TRA-689 are downstream of either a <3-in. orifice or valve, any break is bounded by the analysis in Chapter 15.6.

Damper BDM-1-4 is disabled in the shut position to prevent exhaust of air from the reactor room directly to the atmosphere without passing a radiation detector (the stack exhaust is routinely monitored for radioactivity).

The exhaust duct for BDM-1-4 has been covered with a sealed aluminum plate to ensure the damper does not leak by. The butterfly valves in the Argon Delay Line System are also activated on an RMS-1 shutdown. The Argon Delay Line System supply, return, and condensate return lines will shut, and the bypass valve will open, upon an RMS-1 shutdown. Most of the Argon Delay Line System piping is outside of confinement and is not safety-related.

6.2.2.7 Fan Circuit Breakers. The RMS-1 shutdown deenergizes the relays in the Health Physics Monitoring Panel. The circuit on this panel directly shuts the gasketed dampers and de-energizes fans HVS-1, HVS-5, HVE-4, HVE-9, HVE-17A or HVE-17B, and HVA-2. Due to interlocks with fan HVS-1, the fans HVE-2, HVE-5, HVE-6, and HVE-16 also shut off. The remaining fans HVE-1A, HVE 1B, HVE-7, HVE-8, HVE-18, and HVE-22 shut off due to interlocks with either HVE-17A or HVE 17B.

The fan circuit breakers are part of the ATR original design and do not meet current ESF design requirements. However, these circuit breakers have a history of acceptable performance. Periodic testing and maintenance ensure reliability consistent with the design, and ensure that these components can be relied upon to mitigate the consequences of the release of fission products within the confinement.

6.2.2.8 Power Sources. Four independent PPS dc battery-backed power sources, charged from diesel and commercial sources, supply power to all detectors, signal conditioning, comparators, and logic power supplies. The loss of power to or in a channel is designed to cause the channel to go into a tripped state. Control-room recorders and check-source power supplies are powered from instrument battery-backed power. The actuators for closing dampers and shutting off fans are designed to be fail-safe upon loss of power or instrument air. The actuators to open the dampers do not use the same power source as the channels and logic.

6.2.2.9 Failure Analysis. A failure analysis of the confinement and the RMSS has been performed as documented for the Level 2 ATR probabilistic risk assessment (Thatcher et al. 1994). A fault tree analysis for the confinement isolation system (CIS), the confinement and RMSS considered together as one system, calculated a mean CIS unavailability on demand of 3.3×10^{-2}, or about three in a hundred. This CIS unavailability is dominated by many potential single failures of confinement seal dampers and their controls (84% of the CIS unavailability) and personnel doors (15% of CIS unavailability). The backup confinement seal dampers were conservatively neglected in this analysis since, at the time of the analysis, the backup dampers had not been successfully qualified and preliminary Level 2 and Level 3 PRA analysis results were indicating that CIS failure was not going to be a significant contributor to risk. The backup dampers have been successfully qualified since the PRA analysis was completed. Although most personnel door failures are unlikely to greatly increase confinement leak rate, any failure was treated as if it resulted in a fully open door. This conservative treatment was also retained when it became known that CIS failure was not a significant contributor to total risk. ATR severe fuel damage accident sequences including CIS failure contribute less than 2% to the total public risk. The greater portion of the public risk is associated with higher probability sequences with an intact and successfully sealed confinement, but with the still significant maximum 100% per day leak rate. The remainder of the risk is associated with severe accident confinement failure scenarios (resulting in hydrogen generation and deflagration), sequences associated with open confinement conditions during shutdown operations, or radionuclide releases from the canal area outside confinement.

The confinement failure analysis thus defined the confinement dampers as the principal potential source of CIS failure. Successful operation of the backup dampers will significantly reduce the potential for CIS failure. A truck door airlock has also been added to the confinement since the performance of the failure analysis. However, potential seal failure or inadvertent operation of the truck doors contributed less than 1% to the CIS unavailability. The addition of the truck door airlock is of principal importance for allowing truck ingress and egress during reactor operation without compromising confinement integrity. The confinement serves to limit the rate of radionuclide release and the consequences for the most probable severe ATR fuel damage events (which are beyond design basis severe accident events), but significant releases would still occur even with successful confinement operation. However, the risk to the public or INEEL workers is minimal (see the risk results of the ATR probabilistic risk analysis (Thatcher et al. 1994)).

6.2.3 System Performance Evaluation

6.2.3.1 System Actuation. For confinement of ATR reactor radiation releases, the RMSS is capable of actuating a building seal by shutting off all supply and exhaust fans and closing the gasketed butterfly dampers in the confinement boundary upon detection of high radiation levels in the ATR building exhaust to the stack.

6.2.3.2 System Performance. The effects on confinement of the design basis LOCA are bounded by an evaluation of the confinement response , described as follows. The confinement air volume displaced by the water can be inferred from the building characteristic curves given in the leak rate EDF (Lucas 2000). This rate rapidly falls off after the initial depressurization during the LBLOCA.

An extrapolation of data from the upper bound data fit (Lucas 2000) for the confinement building characteristic curve indicates the leak rate would be 31607 cfm at 7.5 in. of water. Based on a yield pressure of 9.0 in. of water (Close 1988) the building can easily relieve the air displacement pressure due to a LBLOCA (Bayless 1992) volumetric flow of < 5530 cfm. This volumetric flow is the sum of the peak break flow (< 5000 cfm) from Figure 2-2 in Bayless plus the maximum EFIS flow of 530 cfm (~4000 gpm) used in (Lucas 2000). Hence, the building can easily relieve a maximum 5530 cfm volume displacement due to a LBLOCA and EFIS flow.

The design basis LOCA discussed in Chapter 15 (Accident Analyses) does not result in fuel damage and the release of fission products from the fuel to the primary coolant and confinement. Severe beyond-design-basis accidents which do result in fission product release are also discussed in Chapter 15. The analysis was done for a direct damage LOCA resulting in 100% core melt. U.S. Nuclear Regulatory Commission (NRC) Regulatory Guide 1.4 release fractions were used for all fission products but iodine (NRC 1974). Iodine release fractions are based on ATR confinement conditions. Limiting the confinement leakage to 100% per day provides adequate protection to allow evacuation of onsite personnel, and will keep the site-boundary doses within 10 CFR 100 limits.

The confinement building can be threatened by both external and internal floods. In both cases, the floods can be detected early enough to take protective actions (including shutting down the reactor if necessary) so that a radiological release coincident with the flood can be avoided.

The potential for missiles threatening confinement has been evaluated and found not to be a hazard. The refueling port shield blocks are shut during operation. Missile shields are provided above the inpile tubes and the powered axial-locator mechanism (PALM) units. Any other missile event (e.g., diesel flywheel disassembly, planes, tornadoes, etc.) would be independent of a breach of the Primary Coolant System, and protective actions such as shutting down the reactor could be taken.

Some external events, that might threaten confinement, are independent of a breach of the PCS. An external-events analysis for the ATR Probabilistic Risk Assessment (PRA) has shown the probability to be very low for confinement failure by these events (Eide, Khericha, and Thatcher 1991; Thatcher et al. 1994).

6.2.4 Confinement Leakage Testing

Air leakage from the confinement area of the building is a function of the pressure differential between the confined air volume and the surrounding atmosphere. Factors initially considered to affect leakage include changes in barometric pressure, atmospheric temperature changes, and wind pressure acting on the building. A new leak rate measurement system (Lucas and Wagoner 2001) has been installed in the confinement building. This system is independent of the ventilation system in the confinement building. The system uses a fan to pressurize the confinement building. When steady state conditions on the pressure and inflow are obtained the out-leakage is equivalent to the inflow. The analysis discussed in the previous section shows that building over-pressure following an accident decays rapidly. Once water addition in the building is shut off, meteorological conditions are the major contribution to leakage.

Original calculations based on a maximum 24-hour barometric pressure change of 0.5 in. Hg showed a resulting release of 34,000 ft^3 in 24 hours, or 2.1% of the confinement volume, to maintain the differential pressure at zero.

Calculations based on a maximum 24-hour temperature range of 58°F showed a corresponding confined air temperature range (due to heat conduction through the walls) of 24°F in the building. This temperature change then would require a release of 75,000 ft^3 in 24 hours or 4.6% of the confined volume to maintain the differential pressure at zero.

The combined effect of temperature and pressure changes acting concurrently would then require a release of 109,000 ft^3 or 6.7% of the confined volume to maintain a differential pressure of zero.

A new approach (Lucas 2000) for the analysis of the confinement leak rate is used. The new method develops a bounding analysis curve based on the building air-exchange rate characteristic curve of flow versus building differential pressure. The bounding analysis curve is an approximate limit of 100% per day of the confinement volume for the air-exchange rate. This bounding curve is used to calculate the maximum air exchange rate for a maximum leakage area ratio for the building. The results are used for the dose analysis.

The new approach also uses the traditional 11.7 miles per hour maximum seasonal average wind speed. The leakage is computed with the combined effects of pressure and temperature changes, wind, EFIS flow and additional uncertainties due to instrumentation and damper leakage. This results in a confinement building air exchange rate of < 100% per day.

The initial test procedure has been revised to fit the new leak rate measurement. The acceptance criteria is that the measured flow rate in cubic feet per minute be less than the corresponding calculated flow rate based on the pressure change as (Lucas 2000),

$$\text{Leak Rate (cfm)} = \left[6050\sqrt{+\frac{\Delta P}{0.65}} - 1 \right] \qquad (6.2\text{-}1)$$

Where ΔP is the difference between the wind pressure at the face of the building and the building pressure.

Table 6.2-1. General types of confinement area penetrations.

Location	Type of penetration
Substructure	Electrical duct banks containing multiple cables. Each duct is sealed with sealing-fittings for each cable.
	Pipes welded to embedded steel plates.
	Pipes through gasketed sleeves.
	Gasketed hollow metal doors with caulked frames.
	One gasketed H&V exhaust duct sealed by rubber-lined, quick-closing dampers.
First floor	Gasketed hatch covers.
	Gasketed neoprene panels for tubing and cable seals.
	Steam pipes sealed by expansion joints, capped, and abandoned.
	Gasketed H&V ducts sealed by rubber-lined, quick-closing butterfly dampers.
	Miscellaneous tubes, rods, pipes, and conduits, sealed by fittings, or packed as required.
	Electrical bus ducts sealed by sealing fittings.
	Removable floor plugs.
Superstructure	Gasketed hollow metal doors with caulked frames.
	Caulked windows with fixed sash.
	Steel truck doors with inflatable gaskets.
	One vertical-lift door in the north wall of the reactor room over canal. This door is of solid steel plate with inflatable gaskets around the perimeter except for the bottom edge, which extends two ft below canal water level.
	Gasketed H&V ducts and registers sealed by rubber-lined, quick-closing butterfly dampers.
	Steam pipes sealed by expansion joints.
	Four hundred linear feet of gasketed and caulked intersection of steel plate liner with concrete and masonry surfaces.
	Building Leak Rate test system outlet box sealed by a gasketed cover plate.

Table 6.2-2. Radiation Monitoring and Seal System Dampers.

Damper	Equipment number	Function
Butterfly damper	BDM-1-1[a]	HVS-1 reactor operating area supply
	BDM-1-1A	BDM-1-1 backup damper
	BDM-1-2	HVS-1 basement area supply
	BDM-1-2A	BDM-1-2 backup damper
	BDM-1-3	HVS-1 reactor operating area return
	BDM-1-3A	BDM-1-3 backup damper
	BDM-1-4	HVR-1 reactor operating area exhaust
	BDM-1-5	HVE-17A and HVE-17B stack breech
	BDM-1-5A	BDM-1-5 backup damper
	BDM-5-8	HVS-5 basement area supply
	BDM-5-8A	BDM-5-8 backup damper
	BDM-5-9	HVS-5 basement area return
	BDM-5-9A	BDM-5-9 backup damper
	BDM-5-10	HVE-9 exhaust
	BDM-5-10A	BDM-5-10 backup damper
	BDM-4-8	Office 110 return to HVS-4
	BDM-4-8A	BDM-4-8 backup damper
	BDM-1	HVA-2 supply
	BDM-1A	BDM-1 backup damper
	BDM-2	HVA-2 return
	BDM-2A	BDM-2 backup damper
Butterfly Valve	BF-29-1	Argon delay line supply
	BF-29-2	Argon delay line supply
	BF-29-5	Argon delay line return
	BF-29-6	Argon delay line return
	BF-29-12	Argon delay line condensate return
	BF-29-7	Argon delay line bypass

a. The "BDM"' designation includes both the damper and the damper actuator.

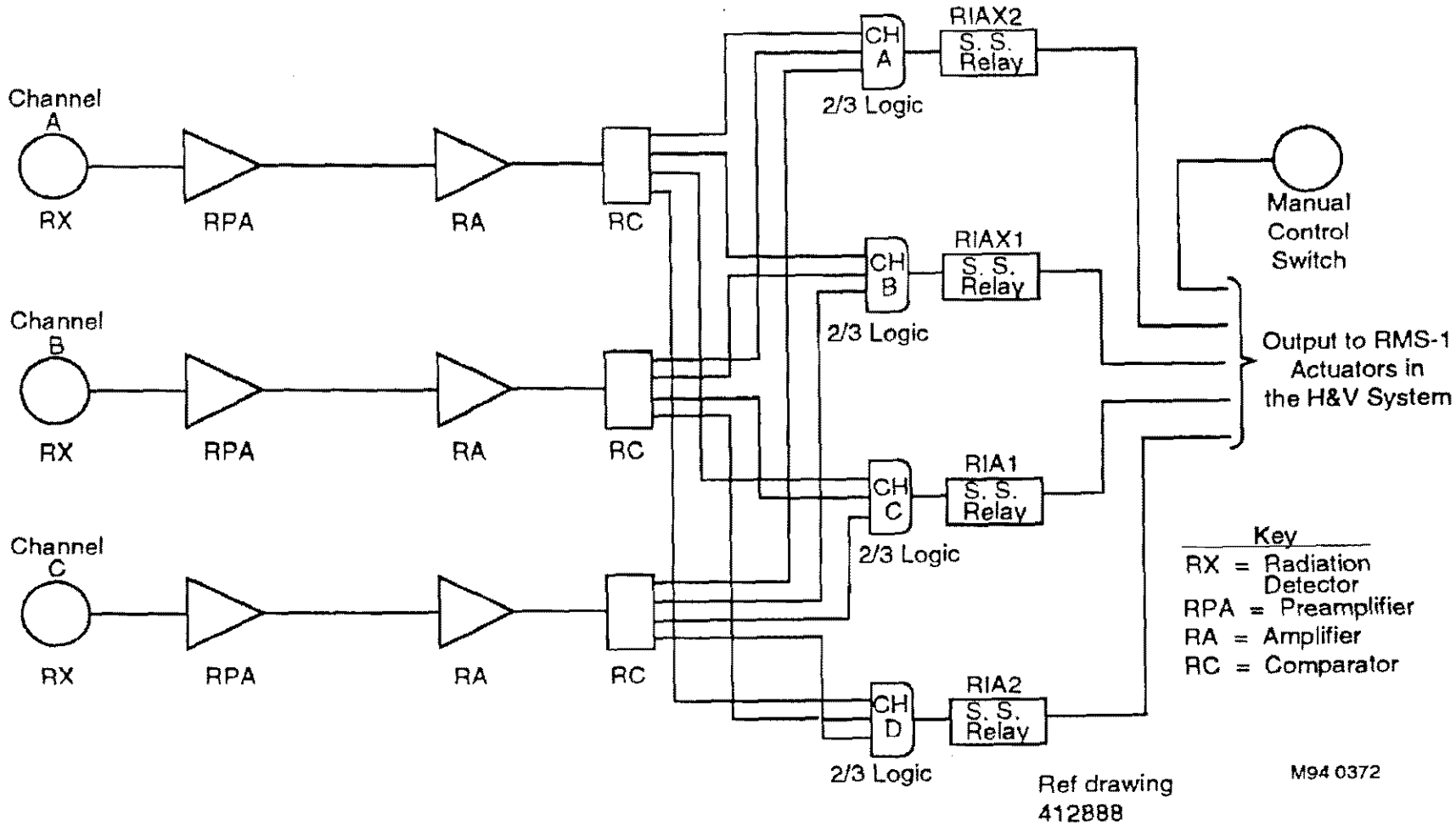

Figure 6.2-1. Stack exhaust radiation logic diagram. **(For Information Only)**

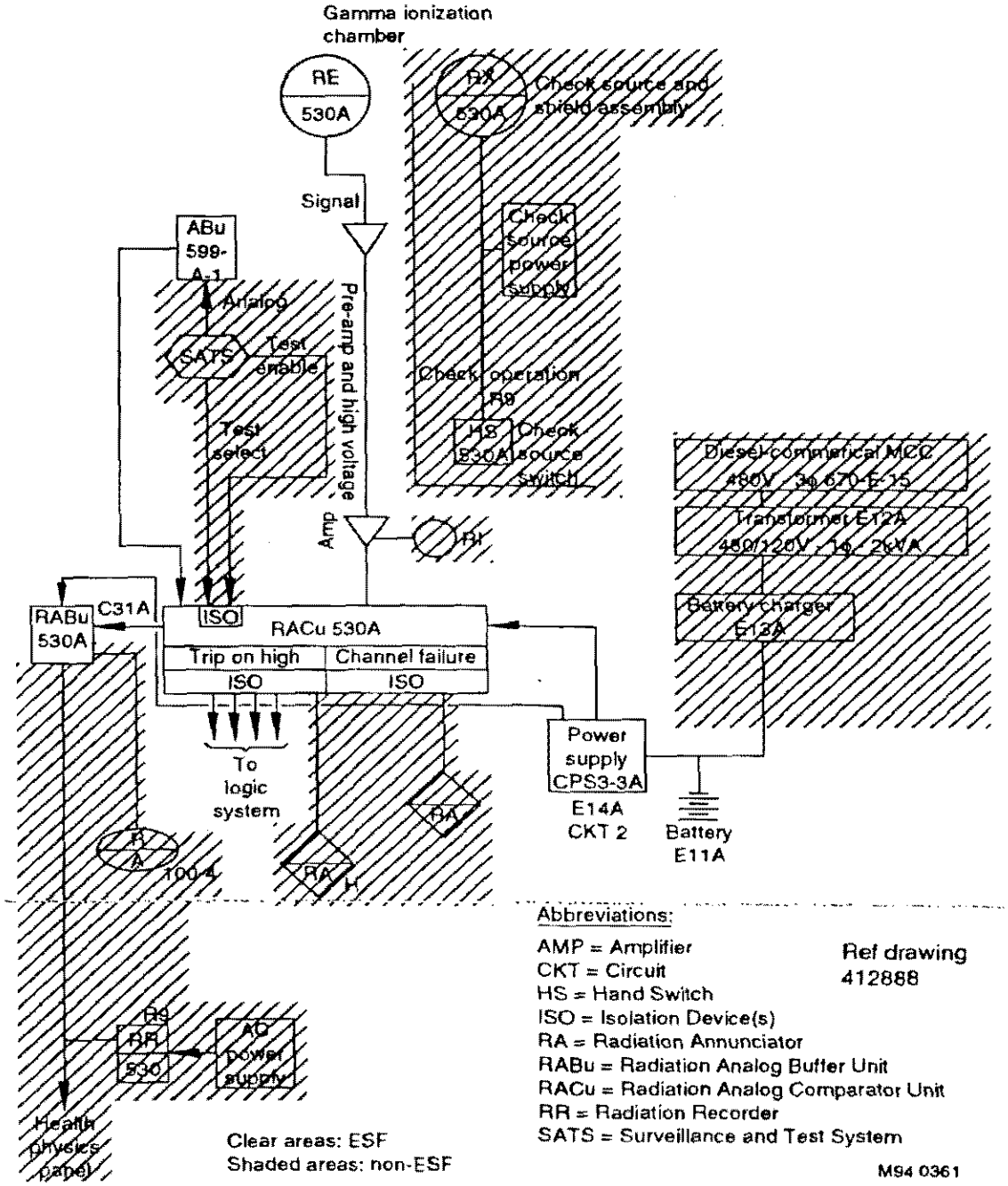

Figure 6.2-2. Radiation Monitoring and Seal System: Part 1. **(For Information Only)**

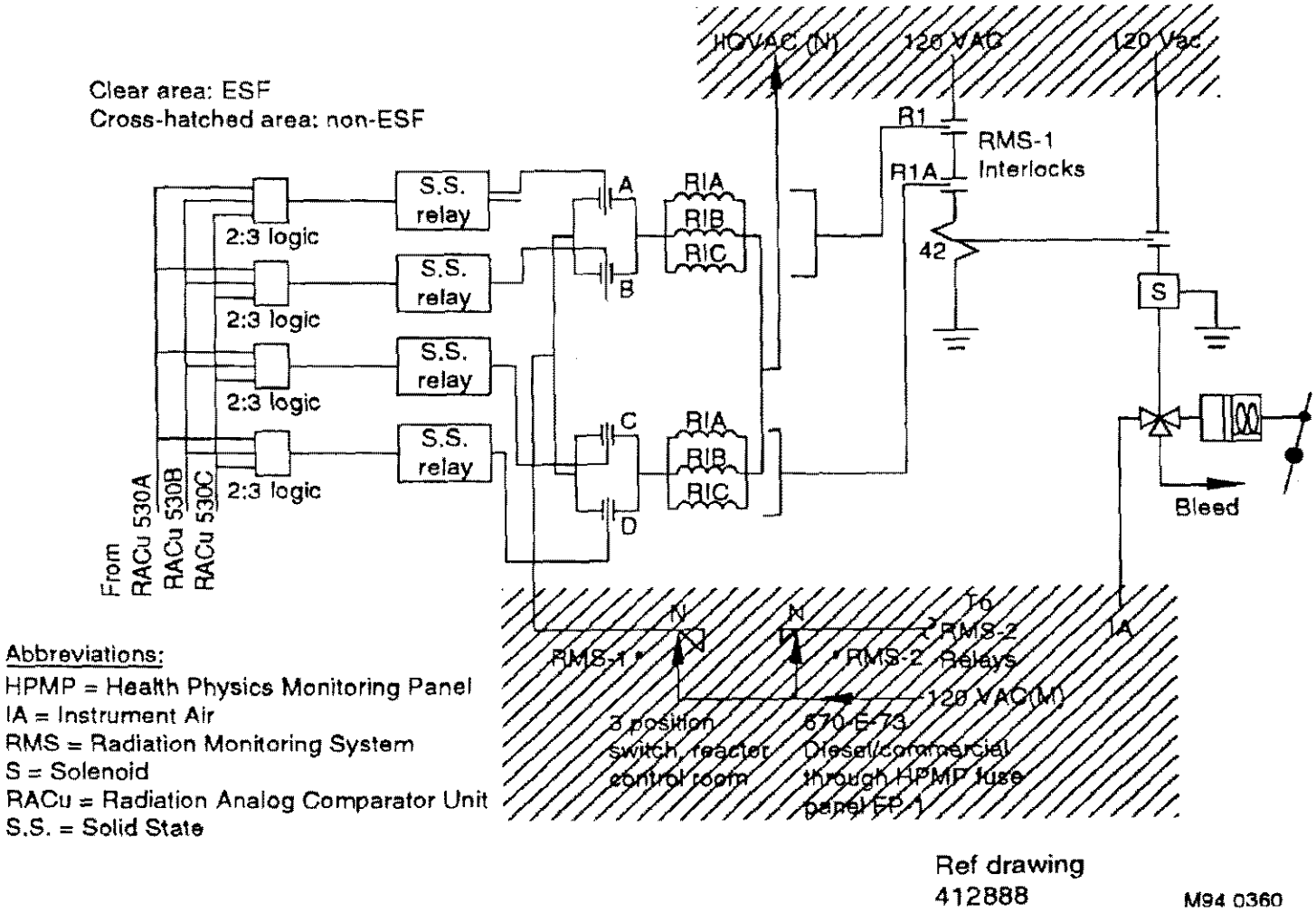

Figure 6.2-3. Radiation Monitoring and Seal System: Part 2. **(For Information Only)**

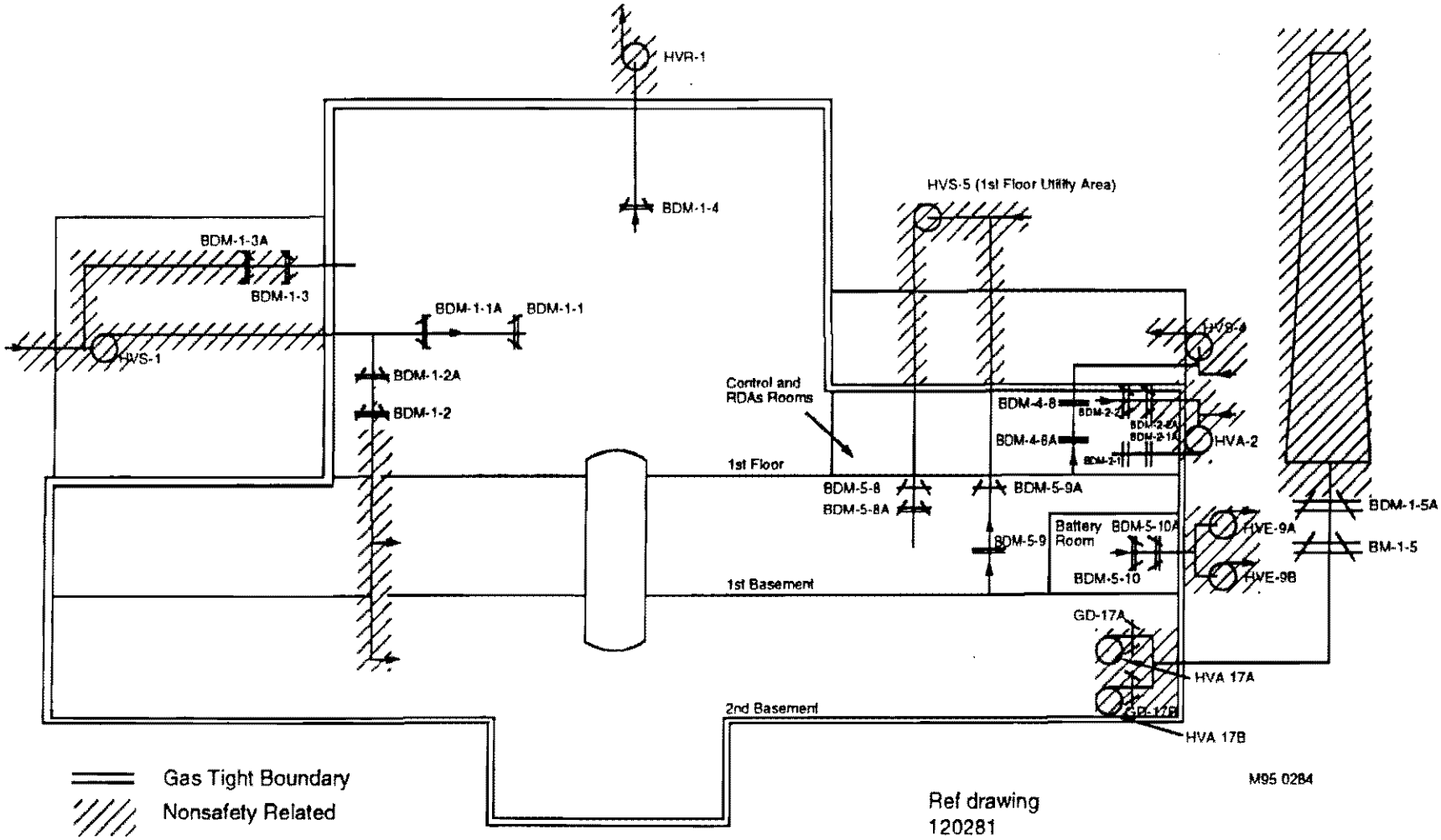

Figure 6.2-4. Radiation Monitoring and Seal System: Dampers. **(For Information Only)**

6.3 Emergency Core Cooling System (Emergency Firewater Injection System)

The EFIS provides emergency reactor core cooling and flooding of the reactor vessel in the event of a major break in the PCS piping. This ESF is designed to activate when the water level lowers to a predetermined height above the top of the reactor core, or at low pressure.

The EFIS is composed of the upper vessel subsystem, the bottom-head subsystem, and the EFIS actuation system [discussed in Chapter 7 (Instrumentation and Controls)]. Figure 6.3-1 shows the ESF portion of the EFIS that is discussed in detail in this chapter.

6.3.1 Design Bases

- The EFIS actuation system provides the required redundancy to ensure that the EFIS is actuated after a LOCA.
- The minimum supply from either the bottom head injection system or the upper head injection system must be adequate to keep the reactor core covered and to mitigate core damage after a design basis LOCA.
- The EFIS is designed so that inadvertent opening of the control valves will not result in depressurization of the Primary Coolant System.
- The design pressure and temperature from the inlet to the reactor vessel (upper vessel and bottom head) to the control valves is 390 psig and 240°F.
- The ATR confinement penetrations for the upper vessel and bottom-head EFIS are sealed such that the confinement gaseous leak rate is not compromised. Penetrations in the ATR shielding are constructed so that the radiation protection is not decreased (INEEL 2003).
- The following external environmental conditions are considered in the design of valves.
    - Normal ambient pressure: 12.3 psia. Maximum accident ambient pressure increase is the pressure head for water to a depth of 3 ft.
    - Ambient temperature: Normal ambient temperature does not exceed 120°F. Accident ambient temperature does not exceed 300°F.
    - Ambient Atmosphere: Normal ambient atmosphere is air. Accident ambient atmosphere: water (flooded). Humidity: 100%.
- The upper vessel EFIS firewater piping is designed and constructed to ASME Section III Class I Code, 1980 Edition with Winter 1980 Addenda (ASME 1980), between the level control valves and the reactor vessel (Miller and Yuan 1986). The ESF piping (between the level control valves and the reactor vessel) is designed to withstand the safe shutdown earthquake (SSE), which meets the requirements of ATR General Design Criterion (GDC) No. 2. The ATR GDCs are presented in Chapter 3 (Design of Structures, Components, Equipment, and Systems). The bottom head EFIS firewater piping is designed and constructed to the Code for Pressure Piping, ASA B31.1-1955 (ASME 1955). The ESF portion of the piping (that portion within the PCS boundary) has been shown to meet the requirements of ASME Section III Division 1. This includes the effects of the safe shutdown earthquake (SSE) (Snow and Hendrickson 1996), which meets the requirements of GDC No. 2.

6.3.2 System Description

The ATR EFIS is composed of: (a) the upper vessel subsystem, (b) the bottom head subsystem, and (c) the EFIS actuation system [discussed in Chapter 7 (Instrumentation and Controls)].

The ATR EFIS differs from a commercial pressurized water reactor's (PWR's) emergency core cooling system (ECCS) in that it does not use borated water. The supply to the ATR EFIS is untreated, raw water obtained from the TRA firewater system, which supplies firewater to the general area. This firewater system is discussed in Chapter 9 (Auxiliary Systems). The VVS (discussed in Section 6.6) vents the reactor vessel so that the EFIS firewater pressure is sufficient to inject firewater into the ATR vessel after transients that do not result in primary system depressurization.

The bottom head EFIS was original ATR equipment installed in 1962. The EFIS piping, instrumentation, and controls were modified in 1983 to include the upper vessel EFIS as a redundant firewater supply.

The upper vessel EFIS can inject emergency firewater coolant through the reactor vessel lower drain piping, while the bottom head EFIS can inject emergency firewater coolant through the reactor vessel bottom head.

From the firewater supply, the upper vessel EFIS piping and the bottom-head EFIS piping penetrate the ATR building concrete through the south and east outside walls of the first basement, respectively. The building wall penetrations are sealed around the pipe to prevent gas leakage. To reach the reactor vessel, the upper vessel EFIS system penetrates the biological shielding surrounding the nozzle trench, and the bottom head EFIS system penetrates the reactor vessel at the bottom head in the subpile room (INEEL 2003).

6.3.2.1 Upper Vessel EFIS. The upper vessel EFIS is an 8-in. firewater line that divides into two 4-in. pipes that are connected to the lower drain for the reactor vessel. The upper vessel EFIS has two actuation valves (LCV-1-615, LCV-1-616), two gate valves (GT-1-619, GT-1-620), and two check valves (CK-1-617, CK-1-618).

The upper vessel EFIS line taps the underground firewater supply line near the southwest corner of the ATR building. The line is routed at an incline to allow it to enter the TRA-670 Building between the freight elevator and the stairs on the first basement level. The line runs north between the 1C cubicle and the pump test loops, and then splits into the two 4-in. lines. These lines continue north through the biological shielding into the nozzle trench corridor, where they connect with the 8-in. vessel lower drain line.

6.3.2.2 Bottom Head EFIS. The bottom head EFIS is an 8-in. firewater line that injects water through four 2-in. nozzles in the bottom head of the reactor vessel. It has two actuation valves (LCV-1-7A, -7B), four check valves (CK-B-1-77, -78, -79, -80), and four gate valves (GT-J-1-150, -151, -152, -153).

The bottom head EFIS line taps the underground firewater supply line east of the ATR building. The line is routed through a penetration in the TRA-670 building first basement near the H&V platform, runs west to the primary pump motor area, then drops vertically to the second basement. The line continues west along the PCS valve corridor, then south into the Second Basement experiment cubicle access area, where it follows the cubicle perimeters south and then east to a position west of the 2C cubicle. It then finally runs north down a stairwell into the rod-access entrance area, and turns west to the primary pipe corridor. There, it rises vertically into an area surrounding the subpile room, and connects to the four 2-in. distribution lines leading into the reactor vessel bottom head.

6.3.2.3 EFIS Components. The EFIS Components are listed in Table 6.3-1.

6.3.2.4 EFIS Actuation System. The EFIS Actuation System [discussed in Chapter 7 (Instrumentation and Controls)] controls the air-operated control valves in the EFIS, allowing emergency cooling water to be injected into the reactor vessel. Air pressure to each of the control valves is supplied through separate solenoid valves. The solenoid valves supply air to the control valves, keeping the control valves shut when the solenoid valves are in the energized condition. A trip to the EFIS actuation system deenergizes the solenoid valves, which dumps the air pressure from the control valves, causing them to open.

6.3.2.5 Instrument Air/Nitrogen Gas System. The instrument air is normally used to maintain the control valves shut. The instrument air is supplied from the plant instrument-air system discussed in Chapter 9 (Auxiliary Systems) in separate lines for each control valve. Two independent bottled nitrogen gas backup systems are provided.

6.3.2.6 Firewater Supply System. The TRA firewater system (discussed in Chapter 9, Auxiliary Systems) supplies raw water to the EFIS. The water and static head for the firewater system are provided by an open supply to a 150,000-gal overhead tank. This supply is supplemented by water from three 375,000-gal ground-level storage tanks. A 500,000-gal minimum supply of water is maintained in the overhead tank and three ground-level tanks. The water level in the overhead tank is maintained by electrically driven feedwater pumps. A backup supply is provided by one safety-related electric motor-driven firewater pump and two safety-related, self-starting diesel-operated firewater pumps. The firewater pumps start automatically on low pressure in the firewater system. The firewater supply piping is arranged with separate paths of delivery so that a failure in one supply line can be isolated without interrupting the normal flow rate of the alternate line (INEEL 2003).

The 1,000,000-gallon firewater storage tank and pumphouse provide a redundant firewater supply. This tank and pumphouse have not been incorporated into the safety-related EFIS.

6.3.2.7 Power Sources. Power is supplied to the EFIS actuation system from the 32-volt PPS battery bank. Commercial/diesel power supplies the electric pump in the TRA firewater supply system.

6.3.3 System Performance Evaluation

6.3.3.1 EFIS Actuation. Automatic and manual actuation of the EFIS is provided by the EFIS actuation system. This system is discussed in Chapter 7 (Instrumentation and Controls).

6.3.3.2 System Performance. Either system can supply sufficient water for credible design basis accidents. With the minimum supply pressure of 43 psig at the upper vessel actuation valves or 60 psig at the bottom head actuation valves, the LOCA analysis performed for Chapter 15 (Accident Analyses) shows that the supply from either system is adequate to flood the reactor vessel and mitigate core damage.

Each 4-in. EFIS piping header in the upper vessel system, and each 2-in. EFIS distribution line in the bottom head system has a check valve between the reactor vessel and the level control valves (LCVs). The check valves prevent the primary coolant from backing up into the firewater system in the event of an inadvertent opening of the LCVs while the reactor is pressurized.

The EFIS piping between the LCVs and the check valves just upstream of the reactor vessel inlet ports in both upper vessel and bottom head systems should normally remain filled with water. Sight glass level indicators are installed on the high points in each of the systems to detect leakage into or out of the filled EFIS piping. LDW tubing is installed to provide makeup, if water leaks out of the EFIS piping. Each makeup and drain path is equipped with double isolation valves to prevent leakage. As a design feature to detect leakage of either firewater through an LCV, or PCS water through a check valve, each EFIS piping header is provided with a pressure alarm and instrumentation. In addition, just upstream of the upper vessel LCVs, a radiation monitor is installed to sense radioactive reactor coolant in the line (INEEL 2003). Monitoring of the bottom head firewater piping is completed on an as needed basis using portable monitors.

Both EFIS piping systems are equipped with fail-safe valving. Deenergizing the solenoid valves or losing instrument-air and nitrogen-gas pressure will result in opening of the control valves.

Each control valve in each circuit has separate valve controls and is operated separately so that failure of one valve control system will not prevent at least one line from operating.

6.3.3.3 Equipment Qualification. Equipment qualification is discussed in Chapter 3 (Design of Structures, Components, Equipment, and Systems).

6.3.3.4 Single Failure Evaluation. The EFIS actuation system includes three independent water-level and three independent pressure channels, and two-out-of-three actuation logic. The EFIS actuation system employs redundancy such that no single failure in the actuation system will result in the failure to deenergize any of the solenoid valves. The upper vessel EFIS and the bottom head EFIS individually provide adequate protection from a design-basis LOCA. No single active failure in the EFIS will result in the loss of safety function, which meets the requirements of GDCs No. 21 and 35.

6.3.4 Tests and Inspection

To the extent practical, all instrumentation and control components are located in areas that are accessible during reactor operation. This configuration meets the requirements of GDC No. 36 with respect to permitting periodic inspection of important components of the system (see Chapter 3, "Design of Structures, Components, Equipment, and Systems").

The EFIS valving and controls are capable of being tested through the control range without injecting firewater into the ATR vessel. A demineralized water line tees with the EFIS piping in each system, allowing flow and valve operation testing by injecting demineralized water into the reactor vessel at a low rate (INEEL 2003). This testing meets the requirements of GDC No. 37.

The ATR Inservice Inspection Plan (INEEL 2002) includes requirements for periodic nondestructive examination, functional testing, and pressure testing of the EFIS.

6.3.5 Instrumentation

See Chapter 7 (Instrumentation and Controls).

Table 6.3-1. Components of the Emergency Firewater Injection System.

Equipment	Description
Upper Vessel EFIS components	
Piping Type	4-in Schedule 40 Grade TP-304L stainless steel
Fittings Type	Stainless-steel butt-weld type, Schedule 40S seamless
Valves	
Control valves Type Valve operators	LCV-1-615 and –616 4-in. carbon steel Pneumatic diaphragm, single acting with spring return Fail open Safe Mode
Check valves Type Flanged ends	CK-1-617 and –618 4-in. horizontal swing-type check Forged or rolled alloy steel
Gate valves Type	GT-1-619 and –620 4-in. outside screw and yoke, stainless steel
Solenoid valves Type	SV-1-626 and –627 5/8-in. orifice, 3-way, normally shut
Bottom Head EFIS components	
Piping Type	8-in. Schedule 20 304 Stainless Steel, 2-in. Schedule 40S 304L
Fittings Type	Butt-weld
Flanges Type	Carbon steel serrated-face lap joint, lap joint stub ends
Valves	
Control valves Type Material Safe Mode	LCV-1-7A and -7B 8-in. self-contained, air-operated diaphragm Carbon steel body, 316 stainless steel plug Fail open
Check valves Type	CK-B-1-77, -78, -79, and –80 3-in., tilting disk type 3-in., swing check (spare valve)
Gate valves Type	GT-J-1-150, -151, -152, and –153 2-in., outside screw and yoke
Solenoid valves Type	SV-1-624 and –625 5/8-in. orifice, 3-way, normally shut

FOIA Exemption 3 UCNI, Exemption 7f (Page 6-34 – emergency firewater injection system details)

6.4 Habitability Systems

The ATR control room is located inside the ATR confinement. The air treatment unit HVA-2 system supplies the reactor control room with 7,000 ft^3/min of air (5,600 ft^3/min recirculated, and 1,400 ft^3/min of fresh air). In the event that high radioactivity is indicated by the stack monitoring system (RMS-1), the ventilation system to the ATR control room is shut down. This is done automatically by closing the HVA-2 butterfly dampers on the control room's air-supply and -return ducts, and the HVA-2 fan is stopped. The habitability of the control room is maintained during normal operation and during incidents when levels of airborne activity are low enough to not require evacuation. In the event of an evacuation, the reactor would be scrammed and the control room evacuated.

The accident sequences requiring operator action are discussed in Chapter 18 (Human Factors Engineering). The limiting events are complete loss of flow accident (CLOFA), complete loss of secondary, large crack or other failure of the storage canal, and shutdown LOCA with irradiated fuel in the core. Successful termination of these events requires that the plant status is correctly identified and successful terminating actions are performed. The first two events require operator actuation of the Vessel Vent System (VVS). The second two events are mitigated by manually opening valves outside the control room. These events do not result in fuel damage, and evacuation would not be required prior to required operator action. Except for the events requiring operator action, the ATR was designed to allow operators to accomplish rapid reactor shutdown and then to leave the control room in an emergency.

6.5 Fission Product Removal and Control Systems

6.5.1 Engineered Safety Feature Filter Systems

The ATR has no ESF filter systems, so this topic is not applicable to the ATR.

6.5.2 Containment Spray System

A spray system is provided in the ATR reactor area. This system is arranged to wash down the walls and air in the reactor area to reduce the concentration of fission products in the event of a severe beyond design basis accident. No credit for this system is taken in the safety analysis of design basis events, and the spray system is not classified as an ESF or safety related system.

Water is supplied to this system by a 3-in. line from the ATR fire water supply. The system is operator-actuated from the reactor control room, or TRA-658. The ATR spray system key is required to actuate the system from TRA-658.

6.5.3 Fission Product Control Systems

The ATR does not have a primary containment, but it does have a confinement equipped with an RMSS designed to detect radiation release and seal the confinement. The confinement and RMSS are covered in Section 6.2.

6.6 Vessel Vent System

The VVS is an ESF that provides depressurization capability for the PCS. Depressurizing the PCS ensures that the EFIS (discussed in Section 6.3) can maintain water over the ATR core during a long-term CLOFA. The mechanical portion of the VVS (including the ESF portion of the supporting bottled nitrogen backup system) is discussed below. The supporting instrument air system is discussed in Chapter 9 (Auxiliary Systems), and the instrument and electrical actuation system is discussed in Chapter 7 (Instrumentation and Controls).

6.6.1 Design Bases

- The VVS is designed to remove steam from the ATR vessel at a design flow rate of 9,140 lbs steam/hr at 43 psig (Wilson 1987a). For redundancy, each of the two VVS system vent valves is capable of venting the required steam flow (Wilson 1988).

- The VVS piping design pressure is 390 psig from the upper vessel drain line to and including the vent valves, and 150 psig from the vent valves to the 8-in. warm-waste drain line. The design temperature is 240°F (Harris 1988).

- The combined flow rate through both vent valves does not exceed the 3-in. equivalent break discussed in Chapter 15 (Accident Analyses).

- The VVS provides the redundancy necessary to ensure that the vent valves can be actuated for reactor core protection (Haroldsen 1989).

- The VVS is designed so that failure results in a fail-safe configuration that does not depressurize the PCS (Golden 1988).

- The VVS piping is designed to withstand the ATR safe shutdown earthquake (SSE) (Harris 1988).

- The VVS piping within the ATR PCS radiographic limits (from the ATR vessel to and including the vent valves) is designed to the ASME Boiler and Pressure Vessel Code, Section III, Division 1, Class 1 Components, "Rules for Construction of Nuclear Power Plant Components," 1986 Edition including 1986 Winter Addenda (ASME 1986a).

- The piping for the bottled nitrogen backup system is designed to the requirements of the American National Standards Institute (ANSI) B31.1 "Power Piping," 1986 Edition without addenda (EG&G Idaho 1988; ASME 1986b).

6.6.2 System Description

The VVS is a system of piping and valves designed to remove decay-heat-generated steam from the upper part of the ATR vessel and exhaust the steam into the reactor's warm-waste system (discussed in Chapter 11, Radioactive and Hazardous Material Waste Management) to reduce the vessel pressure to below 43 psig in the upper plenum (EG&G Idaho 1988). The VVS is manually actuated by causing the opening of two parallel vent valves located in the reactor vessel upper drain line.

The normal procedure for preventing a pressure buildup in the ATR vessel is to establish a purge from the reactor vessel through the reactor vessel's upper drain. However, if the reactor vessel's upper drain valve, GT-D-1-39, is inaccessible or cannot be opened due to mechanical problems, then the VVS would be used to prevent the pressure buildup.

As shown in the system piping and instrumentation diagram (P&ID), (Figure 6.6-1) and piping isometric (Figure 6.6-2), the VVS extends from the reactor vessel flange in the ATR upper vessel drain line downstream to the upper drain valve GT-D-1-39. Upstream of this gate valve, the line tees and goes through vent valves GB-23-1 and GB-23-2, and from there to the ATR Warm Waste System. The ESF boundaries for the VVS are the reactor vessel flange, the outlet of GB-23-1 and GB-23-2, and the inlet to, but not including, GT-D-1-39.

The accident analysis in Chapter 15 shows that the requirement to use the VVS during a long-term CLOFA develops slowly. The operator has ample time to make a conscious and rational decision to activate the system. Therefore, manual activation is used with electrical switches located in both the reactor control room and the Senior Reactor Auxiliary Operator work station.

These switches, one for each vent valve, are located adjacent to each other in the control room. The two switches in the reactor control room are connected by a bar so that if one switch is activated, both switches move in the same direction. The work station has one push-button switch to open both valves and one push-button switch to shut both valves. These switches provide electrical power to solenoid valves. The solenoid valves allow instrument air or backup nitrogen to operate pneumatic actuators that open or shut the vent valves. The electrical power supply, described in Chapter 8 (Electric Power), is a safety-related system. Once the solenoid valves are opened, they remain open even upon loss of electrical power. The vent-valve actuators are spring-loaded (to shut the valves), and the valves fail shut upon loss of air and nitrogen gas.

Plant instrument air is the primary supply for operating the vent valve pneumatic actuators. The instrument air is backed up by an independent bottled nitrogen gas supply system for each actuator.

6.6.2.1 Component Description. ESF components, shown on Figure 6.6-1 as ESF, are described in this section.

6.6.2.1.1 Vessel-Vent Valves—Vessel-vent valves GB-23-1 and GB-23-2 are globe valves with air-operated piston-type actuators. When air is ported to the underside of the actuator piston, the valve opens. Dual springs in the actuator keep the plug down and shut against system pressure. The valves are "N" stamp certified.

Vent-valve data include:

- Inlet: 3-in., 300 psi integral flange.
- Outlet: 4-in., 150 psi integral flange.
- Valve plug is quick-open type with flow under the plug.
- Stroke is 2 in. to full open.
- Plug seat is 2-5/8 in. in diameter (5.41 in.2 area).

- Rated Cv: 123. Calculated steam flow rate capacity for each valve is approximately 11,000 lbs/hr at 40 psi system pressure.
- Valve-actuator data include:
- Air-operated piston, air to open, with 100 in.2 piston.
- Dual springs over the piston holds the valve plug shut.
- Spring rate: 850 lb/in.
- Initial spring force: 3,670 lbs, sufficient to hold the valve shut against a system pressure of 650 psig.

6.6.2.1.2 ***Valve Limit Switches***—Each vessel-vent valve has two limit switches. These switches have contacts that are used to provide information about the position of the valve plug. One limit switch signals when the valve plug is in its most downward position (the plug is seated), and the other switch signals when the valve plug is in its most upward position (the valve is fully open).

6.6.2.1.3 ***Metering Valves***—The plug-seat areas of the vent valves are large enough that fluid transient forces could cause excessive stresses in the vent-valve piping if the valves were to be opened quickly while the upstream piping is at normal reactor operating pressures. Therefore, a metering valve and filter in each line leading to each vent-valve actuator ensures that each vent valve's opening is gradual. Each metering valve is lock-wired so that its setting cannot be changed without breaking the lock-wire.

6.6.2.1.4 ***Solenoid Valves***—The solenoid valves, which provide pneumatic actuation of the vent valves, are pilot-operated, four-way valves with one port plugged. Two coils are on each solenoid valve. When one coil is energized, a port will open to direct air/nitrogen to the vessel-vent valve actuator. The solenoid valve remains open (even if power to the solenoid should fail) until the second coil is energized to open the exhaust port.

Solenoid valve SV-23-10, which opens valve GB-23-1, is located on the reactor main floor near the instrument air connection and nitrogen gas backup supply. Solenoid valve SV-23-11, which opens valve GB-23-2, is located in the ATR first basement near the instrument air connection and nitrogen gas backup supply.

6.6.2.2 ***Instrument Air/Nitrogen Gas System.*** The instrument air used to actuate the vent-valve operators comes from the plant instrument air system discussed in Chapter 9 (Auxiliary Systems). Separate lines from the plant instrument air system are brought to the instrument air nitrogen gas system for each vent valve. The instrument air supply for each vent valve has a pressure regulator, check valve, and strainer within the ESF boundary.

Two independent bottled nitrogen gas backup systems are used. Each nitrogen gas system has a pressure regulator and check valve within the ESF boundary. Pressure relief valves set at 125 psig provide the overpressure protection to prevent the system downstream from the regulator from exceeding the 150 psig design pressure (Pace 1988).

Instrument air is the normal source of power to operate the vent-valve operators. The instrument air pressure regulator is set to provide air at 100 psig while the bottled nitrogen backup system regulator is set at 90 psig. If the instrument air system were to fail, or if the pressure were to drop below 90 psig, then the bottled nitrogen backup system would take over and supply the operating power for the vent-valve operators.

6.6.2.3 Power Sources. Electric power to actuate each of the solenoid valves comes from independent safety-grade PPS battery sources described in Chapter 8 (Electric Power).

6.6.3 System Performance Evaluation

6.6.3.1 System Actuation. Manual activation of the VVS was chosen for two reasons: (1) the required response time to actuate the VVS is calculated as greater than two hours (Ambrosek 1986), and (2) actuation of the VVS depressurizes the PCS. The system design minimizes the likelihood of inadvertent actuation. The solenoid valves will fail in place in the case of loss of electric power. The vent valves will not open in the case of single or multiple failures in the air/nitrogen gas systems. The manual activation switches are placed under a locked plastic cover to prevent accidental bumping. The activation switches are also located on their respective panel boards so as to prevent confusion with other switches.

6.6.3.2 VVS Discharge. Under CLOFA conditions, steam would be vented by the VVS to the ATR warm-waste system, which is capable of handling the amount of steam that would be vented by the VVS (Wilson 1988). In the worst case, steam would escape the warm-waste system through open H&V duct work in the reactor rod access entrance area. This area is within the reactor confinement area, and such venting would be acceptable under accident conditions.

6.6.3.3 Design Evaluation. The VVS piping, and supports for the nitrogen gas bottles, are attached to the ATR building structure to satisfy SSE requirements.

Piping from the reactor pressure vessel through the vent valves meets the seismic requirements of the ASME Boiler and Pressure Vessel Code, Section III, for Class I components, 1986 Edition including Winter 1986 Addenda (Harris 1988; ASME 1986a).

Electrical power required to energize the two solenoid valves in the VVS is provided by independent safety-grade PPS power supplies. If one channel fails, the VVS will still function since each vent valve has the capacity to vent the required steam flow rate.

The actuator of each vent valve is operated with ATR instrument air. If the instrument air supply is lost, each vent valve has an independent bottled nitrogen supply for backup.

6.6.3.4 Equipment Qualification. Equipment qualification is discussed in Chapter 3 (Design of Structures, Components, Equipment, and Systems).

6.6.3.5 Failure Modes and Effects Analysis. Single Failure Analysis (SFA) and Failure Modes and Effects Analysis (FMEA) have been performed for the VVS to evaluate defenses against internal random failures, common-mode failures, and external single events. The analyses demonstrate that the VVS can sustain a single active failure and retain its capability to depressurize the ATR's PCS (Golden 1988). This meets the requirements of GDC No. 21.

6.6.4 Testing and Inspection

The ATR Inservice Inspection Plan includes requirements for periodic nondestructive examination functional testing, and pressure testing of the VVS.

6.6.5 Instrumentation

Instrumentation is discussed in Chapter 7 (Instrumentation and Controls).

CHAPTER 6 – ENGINEERING SAFETY FEATURES - UPGRADED FINAL SAFETY ANALYSIS REPORT FOR THE ADVANCED TEST REACTOR	Identifier: SAR-153 Revision: 9 Page: 6-43 of 6-50 Effective Date: 08/10/04

FOIA Exemption 3 UCNI, Exemption 7f (Page 6-42 - 6-43 – vessel vent system details)

6.7 Reactor Shutdown System Primary Pump Shutoff System

Fluid flow in the ATR PCS is provided by four primary coolant pumps connected in parallel. There are either two or three pumps on line during normal operation, with the other pumps as spares. Pressure drop across the reactor vessel and the reactor core is controlled by adjusting the opening of a butterfly valve located between the pumps and the reactor vessel. The Primary Pump Shutoff System is a subsystem of the RSS and is categorized as an ESF. The purpose of the Primary Pump Shutoff System is to protect the reactor core and internals by providing a limit on high differential pressure (Δp) as a result of high flow.

The Primary Pump Shutoff System consists primarily of the actuation system, which is described in detail in Chapter 7 (Instrumentation and Controls).

6.7.1 Design Bases

The reactor core Δp stresses the core support structure, the gear box support beams, and the core reflector tank. If these structures fail or strain excessively, the proper action of movable core components, including the safety rods, may be inhibited. Also, excessive core/fuel element Δp can cause damage to the fuel elements. The Primary Pump Shutoff System is designed to shut down two primary pumps in the event of a high flow condition during three-pump operation to prevent overstressing the ATR vessel components or fuel elements from high flow, which meets the requirements of GDC No. 20. The design basis events that establishes the Primary Pump Shutoff System requirements is the butterfly-valve opening incident during three-pump operation, and the accidental starting of a third pump during two-pump operation.

6.7.2 System Description

The only components in this system other than the actuation system are the circuit breakers for the motors powering primary pumps 670-M-6, 670-M-7, 670-M-8, and 670-M-9. Surveillance testing and maintenance of these circuit breakers ensure the high probability that ESF performance will be achieved.

6.8 RSS Pressurizing and Gland Seal Pump Shutoff System

The Pressurizing and Gland Seal Pump Shutoff System is a subsystem of the RSS and is categorized as an ESF. The purpose of this system is to protect the PCS by providing a limit on high pressure. The PCS provides a barrier against uncontrolled release of primary coolant and radioactive material to the confinement, and also provides core cooling. The Pressurizing and Gland Seal Pump Shutoff System protects the PCS from undergoing pressure beyond 110% of design pressure (Pace 1990). This protection is provided by sensing the reactor vessel inlet pressure and, if the setpoint pressure is exceeded, the reactor is scrammed and the following pumps are shut down: pressurizing pumps M-14, M-15, and gland-seal pumps M-40 and M-41.

The RSS Pressurizing and Gland Seal Pump Shutoff System is described in detail in Chapter 7 (Instrumentation and Controls).

6.8.1 Design Bases

This subsystem protects the PCS from high pressure by sensing a reactor vessel inlet pressure and providing a pump trip, which meets the requirements of GDC No. 20. The PCS design pressure is discussed in Chapter 5 (Primary Coolant System). A high inlet pressure causes a reactor scram and also trips both pressurizing pumps and both gland-seal pumps.

The design basis event that establishes the pressurizing and gland seal pump shutdown requirements is the loss of instrument air incident.

6.8.2 System Description

The only components in this system other than the actuation system are the circuit breakers for pressurizing pumps 670-M-14 and 670-M-15 and gland-seal-pumps 670-M-40 and 670-M-41. Surveillance testing and maintenance of these circuit breakers ensure the high probability that ESF performance will be achieved.

6.9 Vessel Level Alarm System

The Vessel Level Alarm System actuation is an ESF function provided by the inputs from the RSS Reactor Vessel Water Level Subsytem or by the reactor water level channels of the EFIS. The purpose of the Vessel Level Alarm System actuation is to alert the operators of low vessel liquid level for potential actuation of the EFIS. The RSS Reactor Vessel Water Level Subsystem and the EFIS are described in Chapter 7.

6.9.1 Design Bases

The failure of a bottom head plate penetration during depressurized operation is the limiting accident for the Vessel Level Alarm System. This failure is a maintenance induced event that results in relatively rapid draining of the reactor vessel with elevation head as the driving force. Mitigation for the loss of inventory is the injection of firewater into the reactor vessel.

6.9.2 System Description

The Vessel Level Alarm System alarm is generated on low reactor vessel water level by the RSS Reactor Vessel Water Level Subsystem or by the reactor vessel water level portion of the EFIS.

There are three identical channels of reactor vessel water level indication for the RSS Reactor Vessel Water Level Subsytem. Pressure taps in the upper plenum of the reactor vessel are sensed by the channels transmitters and a signal is sent to the RSS comparator logic. When the signal reaches the pre-set value for the comparator, a window on an annunciator panel in the reactor control room is actuated by the Sequence of Events Recorder (SER). The annunciator panel provides an audible alarm and the lit window provides a visual indication. This actuation of the window/audible alarm is the vessel level alarm. The alarm function is not designed in a two-out-of-three or one-out-of-two logic but will respond to a single comparator tripping. Successive signals for the RSS Reactor Vessel Water Level Subsystem are not separately indicated.

Like the RSS Reactor Vessel Water Level Subsystem, the reactor vessel water level portion of the EFIS has three identical channels of level instrumentation and actuates a separate window of and annunciator panel in the reactor control room. The EFIS level alarm is redundant to the RSS Reactor Vessel Water Level Alarm System.

During reactor shutdown and depressurized operation with irradiated fuel in the reactor vessel, the EFIS is placed in manual. The upper vessel and bottom head injection manual isolation values are shut and are required to be opened manually to cause the injection of firewater into the reactor vessel to replace any loss of inventory. The alarm coupled with the controls on outage activities ensure adequate time to mitigate a loss of inventory.

6.10 LOCA Primary Coolant Pump Shutoff System

The LOCA Primary Coolant Pump (PCP) Shutoff System is an ESF function provided by the inputs from the RSS Vessel Inlet and Outlet Pressure Subsystems. The purpose of the LOCA Primary Coolant Pump Shutoff System is to shutoff all operating primary coolant pumps in the event of a loss-of-coolant-accident (LOCA). Shutoff of the primary coolant pumps needs to occur prior to air being drawn from the surge tank into the primary cooling system (PCS). Air in the PCS could cause a degradation of emergency pump flow.

The LOCA PCP Shutoff System consists of the actuation system described in detail in Chapter 7 (Instrumentation and Controls).

6.10.1 Design Bases

The LOCA Primary Coolant Pump (PCP) Shutoff System actuation ensures adequate thermal margins are maintained following the design basis LOCA by preventing air entering the PCS from the surge tank thereby preventing the degradation of emergency pump flow.

6.10.2 System Description

The LOCA Primary Coolant Pump (PCP) Shutoff System has been designed to trip primary coolant pumps following a loss-of-coolant-accident (LOCA). The LOCA ESF feature is designed to shutoff all running primary cooling pumps on low primary coolant pressure; however, failure of one pump to trip has been analyzed and is tolerated.

The actuation system for the LOCA Primary Coolant Pump (PCP) Shutoff System has components in common with the RSS Vessel Inlet and Outlet Pressure Subsystems. The actuation system utilizes low pressure trip signals from the channel comparators of these subsystems to actuate ESF 2:3 Logic Modules. The inlet pressure and outlet pressure subsystem each have two 2:3 logic devices, LOCA ESF-1 located in PPS Room A and LOCA ESF-4 located in PPS Room D.

When a low pressure condition from either the RSS Vessel Inlet Pressure or Outlet Pressure Subsystem satisfies the 2:3 logic requirements, signals are sent from the ESF 2:3 logic modules to the actuation logic circuits. There are four actuation logic circuits, one for each primary cooling pump. Each actuation logic circuit consists of a time delay circuit and relays configured in a 2:4 relay logic, bypass switches, reset switches, pump test switches and indicators. When two time delay circuits have tripped, the 2:4 relay circuit provides the final actuation of tripping the primary pump breaker.

The actuation system can be bypassed using bypass switches located on panel TMR-LOCA-ESF-1 located in PPS Room A, on panel TMR-LOCA-ESF-4 located in PPS Room D, and on Panel P11 located in the reactor control room. The status of the LOCA PCP Shutoff System is monitored by the process DCS and indicator lights on panels in the PPS rooms and on Panel P11 in the reactor control room.

Surveillance testing and maintenance of these circuits along with those performed on the primary pump breakers ensure high probability that the LOCA ESF performance will be achieved.

6.11 References

Ambrosek, R. G., 1986, *RELAP5 Evaluation of the ATR Primary Coolant System Response during a CLOFA*, PG-T-86-017, EG&G Idaho, Inc., December 1986.

ASME, 1955, *Code for Pressure Piping*, ASA B31.1-1955, American Society of Mechanical Engineers, New York, NY.

ASME, 1980, *Section III, Rules for Construction of Nuclear Power Plant Components, Division 1 - Appendices, 1980 ASME Boiler and Pressure Vessel Code*, ANSI/ASME BPV-III-1-A, The American Society of Mechanical Engineers, New York, NY, July 1, 1980.

ASME, 1986a, *Section III, Rules for Construction of Nuclear Power Plant Components, Division 1 - Subsection NB, Class 1 Components, 1986 ASME Boiler and Pressure Vessel Code*, The American Society of Mechanical Engineers, New York, NY, July 1, 1986.

ASME, 1986b, *Power Piping, ASME Code for Pressure Piping, B31*, ANSI/ASME B31.1-1986, The American Society of Mechanical Engineers, New York, NY, July 1, 1986.

CFR, 2002, *Determination of Exclusion Area, Low Population Zone, and Population Center Distance*, 10 CFR 100.11, *Code of Federal Regulations*, Office of the Federal Register, November 4, 2002.

Close, J. A., 1988, *ATR Hypothetical Accident Description*, PG-T-88-021, EG&G Idaho, Inc., September 1988.

EG&G Idaho, 1988, *ATR Vessel Vent System, System Design Description for the ATR Reactor Vessel Systems*, SDD-7.1.6, September 30, 1988.

Eide, S. A., S. T. Khericha, and T. A. Thatcher, 1991, *Advanced Test Reactor Probabilistic Risk Assessment*, EGG-PRP-8823, Rev. 1, EG&G Idaho, Inc., September 1991.

Golden, R. W., 1988, *ATR Vent Valve System Failure Mode and Effects Analysis (FMEA) and Single Failure Analysis (SFA)*, EDF PRPTS-ATR-234 Rev. 1, EG&G Idaho, Inc., March 23, 1988.

Haroldsen, F. O., 1989, *ATR Vent Valve System Compliance Review*, EDF TRA-ATR-345, EG&G Idaho, Inc., September 19, 1989.

Harris, B. L., 1988, *Design Report for the ATR Vessel Vent System*, PG-T-88-006, Rev. 1, EG&G Idaho, Inc., March 28, 1988.

House, R. K., 1992, *Bases for Designation of Safety-Related Equipment in the ATR*, PG-T-92-114, EG&G Idaho, Inc., July 1992.

INEEL, 2002, "ATR Inservice Inspection Plan Third Inspection Interval June 1994 to May 2004 (PLN-859)," Rev. 4, October 15, 2002.

INEEL, 2003, *ATR Emergency Firewater Injection System, System Design Description for the ATR Plant Protection System (PPS)*, SDD-7.7.1, Rev. 3, December 8, 2003.

Lucas, D.S., 2000, *ATR Confinement Building Leak Rate Calculations*, EDF TRA-ATR-1543, Rev. 1, July 11, 2000

Lucas, D.S., and S.R. Wagoner, 2001, *SAR Addendum for Unreviewed Safety Question (USQ) on the ATR Confinement Leak Rate*, EDF TRA-ATR-1588, Rev. 2, March 1, 2001.

Miller, C. L. and C. Y. Yuan, 1986, *Design Report for the ATR Fire Water Redundant Line*, PR-T-83-001, Rev. 1, EG&G Idaho, Inc., August 28, 1986.

NRC, 1974, *Assumptions Used for Evaluating the Potential Radiological Consequences of a Loss of Coolant Accident for Pressurized Water Reactors*, Regulatory Guide 1.4, Rev. 2, U.S. Nuclear Regulatory Commission, Washington, D.C., June 1974.

Pace, N. E., 1988, *ATR PCS Upper Drain Vent Valves Nitrogen Supply Overpressure Protection Report*, EDF PRPTS-ATR-233, EG&G Idaho, Inc., February 2, 1988.

Pace, N. E., 1990, *ATR Primary Coolant System Overpressure Protection Report*, PG-T-88-005, Rev. 1, EG&G Idaho, Inc., September 1990.

Snow, S. D. and M. B. Hendrickson, 1996, *Analysis of the Complete ATR Fire Water Piping System*, PG-T-90-016, Rev. 2, LMITCO, August 1996.

Thatcher, T. A., et al., 1994, *Update to the Advanced Test Reactor Probabilistic Risk Assessment (Levels 1, 2, and 3, Including Shutdown Operations)*, EGG-PRP-11229, EG&G Idaho, Inc., May 1994.

Wilson, J. E., 1987, *Venting Steam during a CLOFA into the ATR Warm Waste System*, EDF PRPTS-ATR-224, EG&G Idaho Inc., November 6, 1987.

Wilson, J. E., 1988, *Sizing Steam Vent Valves for a CLOFA*, EDF PRPTS-ATR-223, EG&G Idaho, Inc., May 5, 1988.

INTENTIONALLY BLANK